

NUREG/CR-3567

LA-9944-MS

Los Alamos National Laboratory is operated by the University of California for the United States Department of Energy under contract W-7405-ENG-36

*TRAC-PF1:
An Advanced Best-Estimate Computer Program
for Pressurized Water Reactor Analysis*

Los Alamos Los Alamos National Laboratory
Los Alamos, New Mexico 87545

B405220073 B46430
RDR NUREG
CR-3567 R RDR

An Affirmative Action/Equal Opportunity Employer

Edited by Nancy Sheheen, Q Division

NOTICE

This report was prepared as an account of work sponsored by an agency of the United States Government. Neither the United States Government nor any agency thereof, or any of their employees, makes any warranty, expressed or implied, or assumes any legal liability or responsibility for any third party's use, or the results of such use, of any information, apparatus, product or process disclosed in this report, or represents that its use by such third party would not infringe privately owned rights.

**TRAC-PF1:
An Advanced Best-Estimate Computer Program
for Pressurized Water Reactor Analysis**

Safety Code Development Group
Energy Division

Manuscript submitted: November 1983
Date published: February 1984

Prepared for
Division of Accident Evaluation
Office of Nuclear Regulatory Research
US Nuclear Regulatory Commission
Washington, DC 20555

NRC FIN No. A7016

CONTENTS

FIGURES	xi
TABLES	xvi
STANDARD NOMENCLATURE	xviii
CONVERSION TABLE	xxi
ABSTRACT	1
I. COMPUTER PROGRAM OUTLINE	2
A. Program Name	2
B. Computer	2
C. Problem or Function Description	2
D. Solution Method	2
E. Problem Complexity Restrictions	2
F. Typical Running Time	2
G. Unusual Program Features	3
H. Related and Auxiliary Programs	3
I. Status	3
J. References	3
K. Machine Requirements	3
L. Programming Languages	3
M. Operating System or Monitor	3
N. Other Programming, Operating Information, or Restrictions . . .	3
O. Available Materials	3
II. INTRODUCTION	4
A. TRAC Characteristics	5
1. Variable-Dimensional Fluid Dynamics	5
2. Nonhomogeneous, Nonequilibrium Modeling	5
3. Flow-Regime-Dependent Constitutive Equation Package	5
4. Comprehensive Heat-Transfer Capability	5
5. Consistent Analysis of Entire Accident Sequences	6
6. Component and Functional Modularity	6
B. Physical Phenomena Treated	6
C. Planned Improvements	7
D. Scope of TRAC Manual	8

CONTENTS (cont.)

III. BASIC METHODS	9
A. Hydrodynamics	9
1. Field Equations	9
2. Three-Dimensional Finite-Difference Equations	12
3. One-Dimensional Finite-Difference Methods	22
4. Constitutive Equations	32
a. One-Dimensional Wall Shear and Form Losses	32
(1) Homogeneous Model	33
(2) Annular Flow Model	34
(3) Forms Losses	35
b. Three-Dimensional Wall Shear Coefficients	36
c. Interfacial Heat Transfer and Shear	37
d. Interface Sharpener	44
e. Horizontal Stratified Flow	44
f. Subcooled Boiling Model	45
B. Structural Heat Transfer	45
1. Heat-Conduction Models	47
a. Cylindrical Wall Heat Conduction	47
b. Slab Heat Conduction	50
c. Rod Heat Conduction	51
(1) Numerical Model	51
(2) Reflood Algorithm	56
(3) Fuel-Clad Gap Conductance	60
(4) Metal-Water Reaction	63
2. Wall-to-Fluid Heat Transfer	65
a. Wall-to-Fluid HTC Selection Logic	66
b. HTC Correlations	69
(1) Single-Phase Liquid (Heat-Transfer Regimes 1 and 12)	69
(2) Nucleate Boiling HTCs (Heat-Transfer Regime 2)	72
(3) Transition Boiling HTCs (Heat-Transfer Regime 3)	75
(4) Film Boiling HTCs (Heat-Transfer Regime 4)	76
(5) Single-Phase Vapor HTCs (Heat-Transfer Regime 6)	79
(6) Condensation HTCs (Heat-Transfer Regime 11)	79
(7) Two-Phase Mixture HTCs (Heat-Transfer Regime 7)	79
c. Critical Heat Flux (CHF)	81
d. Minimum Stable Film Boiling Temperature, T_{min}	83
e. Steady-State Calculations	84
C. Reactor Kinetics	85
D. Overall Solution Strategy	92
1. Transient Solutions	92
a. Outer Iteration Strategy	92
b. Details of the Solution Method	93
2. Steady-State Solutions	96
a. Generalized Steady-State Calculations	97
b. PWR-Initialization Calculation	98

CONTENTS (cont.)

IV.	COMPONENT MODELS	106
	A. Pipe	106
	B. Accumulator	108
	C. Break and Fill	110
	D. Core	112
	E. Pressurizer	112
	F. Pump	116
	G. Steam Generator	128
	H. Tee	131
	I. Valve	133
	J. Vessel	135
V.	USER INFORMATION	143
	A. Input Organization and Format	143
	B. Signal Variables	145
	C. Trips	150
	D. Controllers	154
	E. Dump/Restart Feature	154
	F. TRAC-PFI Input Specifications	155
	1. Main Control Data	155
	2. Signal-Variable Data	160
	3. Trip Data	162
	4. Controller Data	170
	5. Component Data	170
	a. Accumulator Component (ACCUM)	171
	b. Break Component (BREAK)	172
	c. One-Dimensional Core Component (CORE)	176
	d. Fill Component (FILL)	185
	e. Pipe Component (PIPE)	189
	f. Pressurizer Component (PRIZER)	192
	g. Pump Component (PUMP)	193
	h. Steam-Generator Component (STGEN)	200
	i. Tee Component (TEE)	205
	j. Valve Component (VALVE)	209
	k. Vessel Component (VESSEL)	213
	6. PWR-Initialization Data	226
	7. Time-Step Data	227
	G. LOAD Subroutine	228
	H. Free Format	229
	1. Free-Format Comments, Problem Title Cards, and Hollerith Component Descriptions	231
	2. Free-Format Input-Error Handling	232
	I. NAMELIST Format	232
	J. Output Files	233

CONTENTS (cont.)

VI.	PROGRAMMING DETAILS	235
	A. Overall Code Organization	235
	B. Input Processing	240
	C. Component Initialization	250
	D. Transient Calculation	251
	1. General	251
	2. Time-Step Selection and Output Control	256
	3. Prepass Calculations	257
	4. Outer Iterations	259
	5. Postpass Calculations and Backup	261
	6. Vessel Data Structure	262
	E. Steady-State Calculations	263
	F. Output Processing	266
	G. Storage Requirements	275

CONTENTS (cont.)

APPENDIX A.	THERMODYNAMIC AND TRANSPORT FLUID PROPERTIES	285
I.	THERMODYNAMIC PROPERTIES	286
A.	Saturation Properties	286
1.	Saturation Temperature.	286
2.	Internal Energy	286
3.	Heat Capacity	287
4.	Enthalpy	287
B.	Liquid Properties	288
1.	Internal Energy	288
2.	Density	290
3.	Enthalpy	292
C.	Vapor Properties	293
1.	Superheated Vapor	293
2.	Subcooled Vapor	296
3.	Noncondensable Gas (Air).	296
II.	TRANSPORT PROPERTIES	297
A.	Latent Heat of Vaporization	297
B.	Constant Pressure Specific Heats	298
C.	Fluid Viscosities	298
1.	Liquid	298
2.	Steam	299
D.	Fluid Thermal Conductivities	300
E.	Surface Tension	301
III.	VERIFICATION	301
APPENDIX B.	MATERIAL PROPERTIES	310
I.	INTRODUCTION	310
II.	NUCLEAR FUEL MIXED-OXIDE PROPERTIES	312
A.	Density	312
B.	Specific Heat	314
C.	Thermal Conductivity	314
D.	Spectral Emissivity	315
III.	ZIRCALOY CLADDING PROPERTIES	316
A.	Density	316
B.	Specific Heat	317
C.	Thermal Conductivity	317
D.	Spectral Emissivity	318
IV.	FUEL-CLADDING GAS GAP PROPERTIES	319
V.	ELECTRICAL FUEL-ROD INSULATOR (BN) PROPERTIES	321
A.	Density	321
B.	Specific Heat	321
C.	Thermal Conductivity	321
D.	Spectral Emissivity	321
VI.	ELECTRICAL FUEL-ROD HEATER COIL (CONSTANTAN) PROPERTIES	321
A.	Density	322
B.	Specific Heat	322
C.	Thermal Conductivity	322
D.	Spectral Emissivity	322
VII.	STRUCTURAL MATERIAL PROPERTIES	322

CONTENTS (cont.)

APPENDIX C. CHOKED-FLOW MODEL	329
I. TWO-PHASE-FLOW CHOKING CRITERION	329
II. SUBCOOLED-FLOW CHOKING CRITERION	332
III. TRANSITION REGIME	334
APPENDIX D. SYSTEM CONTROL WITH TRIPS	335
APPENDIX E. SAMPLE PROBLEM	364
I. SEMISCALE MOD-3 SYSTEM DESCRIPTION	364
II. TEST DESCRIPTION	364
III. TRAC ONE-DIMENSIONAL MODEL	366
IV. STEADY-STATE CALCULATION	373
V. INPUT LISTINGS	380
APPENDIX F. TRAC SUBPROGRAMS	446
APPENDIX G. TRAC ERROR MESSAGES	463
I. OVERLAY MAIN	463
II. OVERLAY INPUT	466
III. OVERLAY INIT	480
IV. OVERLAY DUMP	481
V. OVERLAY TWOTIM	481
VI. OVERLAY PWRSS	482
VII. OVERLAY PREP	484
VIII. OVERLAY OUTER	485
IX. OVERLAY POST	486
APPENDIX H. DESCRIPTION OF COMMON BLOCK VARIABLES	487
APPENDIX I. COMPONENT DATA TABLES	514
I. FIXED LENGTH TABLES	514
II. GENERAL POINTER TABLES	515
A. DUALPT	515
B. HYDROPT	518
C. INTPT	520
D. HEATPT	520
III. ACCUMULATOR MODULE	521
A. ACCUM Variable Length Table	521
B. ACCUM Pointer Table	522
IV. BREAK MODULE	522
A. BREAK Variable Length Table	522
B. BREAK Pointer Table	523
V. CORE MODULE	523
A. CORE Variable Length Table	523
B. CORE Pointer Table	529
VI. FILL MODULE	533
A. FILL Variable Length Table	533
B. FILL Pointer Table	534

CONTENTS (cont.)

VII. PIPE MODULE	534
A. PIPE Variable Length Table	534
B. PIPE Pointer Table	536
VIII. PRESSURIZER MODULE	536
A. PRIZER Variable Length Table	536
B. PRIZER Pointer Table	537
IX. PUMP MODULE	538
A. PUMP Variable Length Table	538
B. PUMP Pointer Table	541
X. STEAM-GENERATOR MODULE	542
A. STGEN Variable Length Table	542
B. STGEN Pointer Table	542
XI. TEE MODULE	547
A. TEE Variable Length Table	547
B. TEE Pointer Table	550
XII. VALVE MODULE	550
A. VALVE Variable Length Table	550
B. VALVE Pointer Table	552
XIII. VESSEL MODULE	553
A. VESSEL Variable Length Table	553
B. VESSEL Pointer Table	560
AUTHORS AND ACKNOWLEDGMENTS	572
REFERENCES	573

FIGURES

1.	Three-dimensional mesh-cell velocities	14
2.	Flow-regime map for three-dimensional hydrodynamics	38
3.	Semi-implicit coupling between hydrodynamics and structural heat transfer	46
4.	Cylindrical wall geometry	48
5.	Rod geometry	52
6.	Node located at the interface between two dissimilar materials . .	56
7.	Fine-mesh rezoning	57
8.	Insertion of conduction nodes during reflood	58
9.	Fuel-rod geometry	61
10.	TRAC-PF1 boiling curve	66
11.	Heat-transfer coefficient correlation selection logic	67
12.	TRAC-PF1 heat-transfer regimes	69
13.	Component network with one three-dimensional vessel	95
14.	Primary loop schematic for a PWR-initialization calculation . . .	100
15.	Pipe noding diagram	107
16.	Accumulator noding diagram	109
17.	Break noding diagram	110
18.	FILL noding diagram	111
19.	CORE noding diagram	113
20.	Pressurizer noding diagram	114
21.	Pump noding diagram	116
22.	Semiscale single-phase homologous head curves	125
23.	Semiscale fully degraded homologous head curves	125
24.	Semiscale head degradation multiplier curve	125

FIGURES (cont.)

25.	Semiscale single-phase homologous torque curves	125
26.	Semiscale torque degradation multiplier curve	126
27.	LOFT single-phase homologous head curves	126
28.	LOFT fully degraded homologous head curves.	126
29.	LOFT head degradation multiplier curve	126
30.	LOFT single-phase homologous torque curves	127
31.	LOFT torque degradation multiplier curve	127
32.	Steam generator noding diagram	128
33.	TEE noding diagram	132
34.	Valve noding diagram	133
35.	Cell noding diagram for a typical PWR vessel	136
36.	Vessel geometry, three-dimensional mesh construction with three rings, six angular segments, and seven axial intervals . .	137
37.	Boundaries of a three-dimensional mesh cell	138
38.	Flow restrictions and downcomer modeling	139
39.	Pipe connections to the vessel	139
40.	Core region inside the vessel	141
41.	TRAC input deck organization	143
42.	TRAC input and output files	234
43.	TRAC overlay structure	239
44.	Relationships between SCM and LCM storage areas	241
45.	Signal-variable and trip data	240
46.	PWR-initialization data structure	248
47.	Flow diagram for transient calculations	255

FIGURES (cont.)

48.	Outer iteration flow diagram	260
49.	Flow diagram for steady-state calculation	267
50.	Overall graphics file structure	270
51.	Structure of graphics file general information section	271
52.	Structure of graphics file catalog	272
53.	Structure of graphics file time-edit data section	273
54.	Graphics file catalog and time-edit data correspondence	274
55.	Dump file overall structure	276
56.	Structure of dump file time-edit data section	277
57.	Component dump structure	278
58.	Blank COMMON dynamic storage area organization	280
59.	LCM data organization	284
B-1.	Material properties code organization	311
C-1.	Subcooled choking process at the onset of nucleation at the throat	333
D-1.	LOFT steam-generator secondary-side model	339
D-2.	Coincidence trip for controlling the power-reactivity table . . .	342
D-3.	Blocking trip for controlling the pump speed table	342
D-4.	The controlling trip is based on the signal subrange	343
D-5.	Trips with ON set status for a specific subrange of the signal . .	344
D-6.	Blocking trips for specific subranges of a signal	344
D-7.	Coincidence trip for controlling the component action	345
D-8.	Set point factor tables for trip ID = 1	346
D-9.	Coincidence trip for controlling the component action	346
D-10.	A trip that avoids spurious signals for ON set status	347
D-11.	Trips for defining five subranges to the trip signal.	349

FIGURES (cont.)

D-12.	Coincidence trip which behaves like a trip with five subranges	350
D-13.	The five subranges of the trip signal	288
D-14.	Steam generator secondary-side feedwater mass flow table.	351
D-15.	Trip for controlling the FILL mass flow table	352
D-16.	Trip for controlling the pump speed table	353
D-17.	Pump speed table.	353
D-18.	Rate factor table for the pump speed table's abscissa coordinate.	355
D-19.	Set point factor tables for trip ID = -1.	356
D-20.	Valve flow area adjustment table	357
D-21.	Trip for editing the closure limits of a valve.	357
D-22.	Trip for controlling the valve flow area adjustment table	358
D-23.	Valve flow area adjustment table	358
D-24.	Trip for controlling a regulating valve	359
D-25.	Two valve tables for flow area adjustment	360
D-26.	Control-rod bank programmed reactivity	361
D-27.	Axial power shape table	362
D-28.	Trip for controlling programmed reactivity and axial power shape	363
E-1.	Semiscale Mod-3 system for cold leg break configuration--isometric (Ref. 62)	365
E-2.	TRAC model for Semiscale Mod-3 facility	368
E-3.	One-dimensional downcomer and vessel noding for Semiscale Mod-3 facility	367
E-4.	Three-dimensional VESSEL noding combining all the components shown in Fig. E-3	369
E-5.	Upper-plenum pressure	375
E-6.	Liquid velocity at the pressurizer outlet	375
E-7.	Liquid velocity in the intact-loop hot leg.	376

FIGURES (cont.)

E-8.	Liquid velocity in the intact-loop cold leg	376
E-9.	Liquid velocity in the broken-loop hot leg	377
E-10.	Liquid velocity in the broken-loop cold leg	377
E-11.	Liquid temperature in the intact-loop hot leg	378
E-12.	Liquid temperature in the intact-loop cold leg	378
E-13.	Liquid temperature in the broken-loop hot leg	379
E-14.	Liquid temperature in the broken-loop cold leg	379

TABLES

I.	DELAYED NEUTRON CONSTANTS.	87
II.	DECAY HEAT CONSTANTS	87
III.	REACTIVITY-COEFFICIENT FORMS	89
IV.	VARIABLES CONSIDERED IN EVALUATING THE APPROACH TO STEADY STATE	99
V.	DEFINITIONS OF THE FOUR CURVE SEGMENTS THAT DESCRIBE THE HOMOLOGOUS PUMP HEAD CURVES	119
VI.	SIGNAL-VARIABLE PARAMETERS	146
VII.	TRIP-SIGNAL-RANGE TYPES	151
VIII.	ARITHMETIC-OPERATOR ID NUMBERS	165
IX.	IMPORTANT LOW-LEVEL SUBPROGRAMS	236
X.	TRAC OVERLAYS	239
XI.	FIXED SEGMENT ALLOCATIONS FOR THE BLANK COMMON AREA.	242
XII.	COMPONENT INPUT SUBROUTINES.	247
XIII.	JUNCTION-COMPONENT PAIR ARRAY.	247
XIV.	COMPONENT INITIALIZATION SUBROUTINES	250
XV.	BOUNDARY ARRAY DATA.	252
XVI.	ITERATION SUBROUTINES.	259
XVII.	STEADY-STATE CALCULATION EFFECTS	264
XVIII.	EXAMPLE OF A STEADY-STATE CONVERGENCE EDIT	265
XIX.	COMPONENT EDIT SUBROUTINES	268
XX.	COMPONENT DUMP SUBROUTINES	275
XXI.	TRAC STORAGE ALLOCATIONS	279
XXII.	ONE-DIMENSIONAL COMPONENT ARRAY STORAGE REQUIREMENTS	281
XXIII.	COMPONENT TABLE LENGTHS.	283

TABLES (cont.)

A-I.	POLYNOMIAL CONSTANTS FOR THERMO.	303
A-II.	DERIVED CONSTANTS FOR THERMODYNAMIC PROPERTIES OF WATER AND AIR	305
A-III.	BASIC CONSTANTS FOR TRANSPORT PROPERTIES OF WATER AND AIR. . .	306
A-IV.	LIQUID VISCOSITY CONSTANTS	307
A-V.	VAPOR VISCOSITY CONSTANTS.	308
A-VI.	THERMAL CONDUCTIVITY CONSTANTS	309
A-VII.	SURFACE TENSION CONSTANTS.	309
B-I.	SPECIFIC HEAT VS TEMPERATURE	318
B-II.	STRUCTURAL MATERIAL PROPERTIES STAINLESS STEEL, TYPE 304.	323
B-III.	STRUCTURAL MATERIAL PROPERTIES STAINLESS STEEL, TYPE 316.	324
B-IV.	STRUCTURAL MATERIAL PROPERTIES STAINLESS STEEL, TYPE 347.	325
B-V.	STRUCTURAL MATERIAL PROPERTIES CARBON STEEL, TYPE 508	326
B-VI.	STRUCTURAL MATERIAL PROPERTIES INCONEL, TYPE 718.	327
B-VII.	STRUCTURAL MATERIAL PROPERTIES INCONEL, TYPE 600.	328
E-1.	TRAC MODEL COMPONENTS	370
E-2.	TEST S-SB-P7 INITIAL CONDITIONS	374

STANDARD NOMENCLATURE

Independent Variables

r	Radial coordinate in cylindrical geometry.
t	Time.
θ	Azimuthal coordinate in cylindrical geometry.
x	Coordinate for one-dimensional geometry.
z	Axial coordinate in cylindrical geometry.

Other Variables

A	Area.
c	Shear or friction coefficient in two-fluid equations.
c_p	Specific heat at constant pressure.
c_v	Specific heat at constant volume.
D	Diameter.
e	Specific internal energy.
FA	Flow area.
g	Acceleration caused by gravity.
G	Mass flux ($\rho_m V_m$).
h	Specific enthalpy or heat-transfer coefficient.
h_{fg}	Latent heat of vaporization.
H	Pump head ($\Delta p/\rho$).
k	Thermal conductivity, form-loss coefficient, or pipe roughness.
m	Mass.
Nu	Nusselt number.
p	Pressure.
q	Heat generation rate.
q''	Heat flux.
q'''	Volumetric heat-generation rate.
Q	Pump volumetric flow.
R	Radius.
Re	Reynolds number.
T	Temperature.
V	Velocity.

STANDARD NOMENCLATURE (cont.)

Other Variables

vol	Hydrodynamic cell volume.
We	Weber number.
x	Quality.
α	Vapor volume fraction or absorptivity.
Γ	Net volumetric vapor-production rate caused by phase change.
δ	Mean fuel-surface roughness.
Δ	Increment.
ϵ	Emissivity.
μ	Viscosity.
ρ	Microscopic density.
σ	Surface tension or Stefan-Boltzmann constant.
τ	Shear stress.
ϕ^2	Two-phase friction factor multiplier.
ω	Angular velocity.
Ω	Pump-impeller angular velocity.

Subscripts

a	Noncondensable gas component.
b	Bubble.
c	Cladding.
d	Droplet.
f	Fuel or friction.
g	Gas field or vapor.
h	Hydraulic.
i	Interface (liquid-vapor) quantity or one-dimensional cell index in heat-transfer equations.
j	One-dimensional cell index in hydrodynamics equations.
l	Liquid field.
lg	Liquid to vapor.
m	Mixture quantities.

STANDARD NOMENCLATURE (cont.)

Subscripts

mw	Metal-water reaction.
qf	Quench front.
r	Relative quantities.
r, θ , z	Cylindrical coordinate directions.
$r \pm 1/2$	
$\theta \pm 1/2$	Mesh-cell boundary indices.
$z \pm 1/2$	
s	Saturation quantities.
sp	Single-phase quantities.
ss	Steady-state quantities.
t	Transient quantities.
tp	Two-phase quantities.
v	Water vapor (steam).
w	Wall quantities.

Superscripts

k	Iteration count index.
n, n+1	Time- τ boundary indices.

CONVERSION TABLE^a

Unit	SI Description (x)	English Description (y)	x = f(y)
length	meter (m)	foot (ft)	$x = 3.048\ 000 \cdot 10^{-1} y$
area	square meter (m ²)	square foot (ft ²)	$x = 9.290\ 304 \cdot 10^{-2} y$
volume	cubic meter (m ³)	cubic foot (ft ³)	$x = 2.831\ 685 \cdot 10^{-2} y$
mass	kilogram (kg)	pound (lb _m)	$x = 4.535\ 924 \cdot 10^{-1} y$
time	second (s)	second (s)	$x = y$
	second	hour (h)	$x = 3.600\ 000 \cdot 10^{+3} y$
temperature	kelvin (K)	degree Fahrenheit (°F)	$x = (y + 459.67)/1.8$
pressure	pascal (Pa)	pound force per square inch [(psf) or (lb _f ·in ⁻²)]	$x = 6.894\ 757 \cdot 10^{+3} y$
mass flow	kilogram per second (kg·s ⁻¹)	pound per second (lb _m ·s ⁻¹)	$x = 4.535\ 924 \cdot 10^{-1} y$
velocity	meter per second (m·s ⁻¹)	foot per second (ft·s ⁻¹)	$x = 3.048\ 000 \cdot 10^{-1} y$
density	kilogram per cubic meter (kg·m ⁻³)	pound per cubic foot (lb _m ·ft ⁻³)	$x = 1.601\ 846 \cdot 10^{+1} y$
torque	newton meter (N·m)	pound force foot (lb _f ·ft)	$x = 1.355\ 818 \cdot 10^0 y$
power	joule per second [(J·s ⁻¹) or watt (W)]	British thermal unit per second (Btu·s ⁻¹)	$x = 1.055\ 056 \cdot 10^{+3} y$
	joule per second [(J·s ⁻¹) or watt (W)]	Btu per hour (Btu·h ⁻¹)	$x = 2.930\ 711 \cdot 10^{-1} y$
pump head (Δp/ρ)	square meter per second squared (m ² ·s ⁻²)	foot (ft) (ft·lb _f ·lb _m ⁻¹ actual units)	$x = 2.989\ 066 \cdot 10^0 y$
mass flux	kilogram per second per square meter (kg·s ⁻¹ ·m ⁻²)	pound per second per square foot (lb _m ·s ⁻¹ ·ft ⁻²)	$x = 4.882\ 427 \cdot 10^0 y$
volumetric flow	cubic meter per second (m ³ ·s ⁻¹)	cubic foot per second (ft ³ ·s ⁻¹)	$x = 2.831\ 685 \cdot 10^{-2} y$
heat flux	watt per square meter (W·m ⁻²)	watt per square foot (W·ft ⁻²)	$x = 1.076\ 391 \cdot 10^{+1} y$
	watt per square meter (W·m ⁻²)	Btu per hour per square foot (Btu·h ⁻¹ ·ft ⁻²)	$x = 3.154\ 591 \cdot 10^0 y$
volumetric heat source	watt per cubic meter (W·m ⁻³)	watt per cubic foot (W·ft ⁻³)	$x = 3.531\ 467 \cdot 10^{+1} y$
	watt per cubic meter (W·m ⁻³)	Btu per hour per cubic foot (Btu·h ⁻¹ ·ft ⁻³)	$x = 1.034\ 970 \cdot 10^{+1} y$
moment of inertia	kilogram square meter (kg·m ²)	pound square foot (lb _m ·ft ²)	$x = 4.214\ 011 \cdot 10^{-2} y$
specific heat	joule per kilogram per kelvin (J·kg ⁻¹ ·K ⁻¹)	Btu per pound per degree Fahrenheit (Btu·lb _m ⁻¹ ·°F ⁻¹)	$x = 4.186\ 800 \cdot 10^{+3} y$
thermal conductivity	watt per meter per kelvin (W·m ⁻¹ ·K ⁻¹)	Btu inch per hour per square foot per degree Fahrenheit (Btu·in·h ⁻¹ ·ft ⁻² ·°F ⁻¹)	$x = 1.442\ 279 \cdot 10^{-1} y$
	watt per meter per kelvin (W·m ⁻¹ ·K ⁻¹)	Btu per hour per foot per degree Fahrenheit (Btu·h ⁻¹ ·ft ⁻¹ ·°F ⁻¹)	$x = 1.730\ 734 \cdot 10^0 y$
gap conductance	watt per square meter per kelvin (W·m ⁻² ·K ⁻¹)	Btu per hour per square foot per degree Fahrenheit (Btu·h ⁻¹ ·ft ⁻² ·°F ⁻¹)	$x = 5.678\ 263 \cdot 10^0 y$
heat-transfer coefficient	watt per square meter per kelvin (W·m ⁻² ·K ⁻¹)	Btu per hour per square foot per degree Fahrenheit (Btu·h ⁻¹ ·ft ⁻² ·°F ⁻¹)	$x = 5.678\ 263 \cdot 10^0 y$

^a "Standard for Metric Practice," American Society for Testing and Materials designation E 380-76 (IEEE standard 268-1976), Philadelphia, Pennsylvania (February 1976). The British thermal unit (Btu) used in this table is the Btu unit from the International Table.

TRAC-PF1:
AN ADVANCED BEST-ESTIMATE COMPUTER PROGRAM
FOR PRESSURIZED WATER REACTOR ANALYSIS

by

Safety Code Development Group
Energy Division

ABSTRACT

The Transient Reactor Analysis Code (TRAC) is being developed at the Los Alamos National Laboratory to provide advanced best-estimate predictions of postulated accidents in light water reactors. The TRAC-PF1 program provides this capability for pressurized water reactors and for many thermal-hydraulic experimental facilities. The code features either a one-dimensional or a three-dimensional treatment of the pressure vessel and its associated internals; a two-phase, two-fluid nonequilibrium hydrodynamics model with a noncondensable gas field; flow-regime-dependent constitutive equation treatment; optional reflood tracking capability for both bottom flood and falling-film quench fronts; and consistent treatment of entire accident sequences including the generation of consistent initial conditions. A new numerical algorithm is used in the one-dimensional hydrodynamics that permits this portion of the fluid dynamics to violate the material Courant condition. This technique permits large time steps and, hence, reduced running time for slow transients.

This report describes the thermal-hydraulic models and the numerical solution methods used in the code. Detailed programming and user information also are provided. A second Los Alamos report, "TRAC-PF1 Developmental Assessment," presents the results of the developmental assessment calculations.

I. COMPUTER PROGRAM OUTLINE

A. Program Name

The program name is TRAC-PF1.

B. Computer

The computer for which the code is designed is the CDC 7600. Efforts have been made to make the programming as machine independent as possible.

C. Problem or Function Description

TRAC-PF1 performs best-estimate analyses of loss-of-coolant accidents (LOCAs) and other transients in pressurized light water reactors (LWRs) and of thermal-hydraulic experiments in reduced-scale facilities. Models used include reflood, multidimensional two-phase flow, nonequilibrium thermodynamics, generalized heat transfer, and reactor kinetics. Automatic steady-state and dump/restart capabilities also are provided.

D. Solution Method

The partial differential equations that describe the two-phase flow and the heat transfer are solved by finite differences. The heat-transfer equations are treated using a semi-implicit differencing technique. The fluid-dynamics equations in the one-dimensional components use a multistep procedure that allows the material Courant condition to be violated. The three-dimensional vessel option uses semi-implicit differencing. The finite-difference equations for hydrodynamic phenomena form a system of coupled, nonlinear equations that are solved by a Newton-Raphson iteration procedure.

E. Problem Complexity Restrictions

All storage arrays in the code are allocated dynamically so the only limit on the problem size is the amount of core memory. The number of reactor components in the problem and the manner in which they are coupled are arbitrary. Reactor components in TRAC-PF1 include accumulators, pipes, pressurizers, pumps, steam generators, tees, valves, and vessels with associated internals.

F. Typical Running Time

Running time is highly problem dependent and is a function of the total number of mesh cells, the maximum allowable time-step size, and whether a three-dimensional vessel model is used. For a purely one-dimensional model, very large time steps can be used for slow transients. If a three-dimensional

vessel is employed, a material Courant limit in the vessel may reduce the maximum time-step size allowed and increase the running time. Typical computer times for a CDC 7600 average 2-3 ms per time step per mesh cell.

G. Unusual Program Features

The highly versatile TRAC-PF1 program describes most thermal-hydraulic experiments in addition to the wide variety of LWR system designs. The code's modularity allows better geometric problem descriptions, more detailed models of physical processes, and reduced maintenance costs.

H. Related and Auxiliary Programs

One of the output files written by TRAC contains graphics information that can be used to produce plots and movies. Two auxiliary programs, TRAP and EXCON, are available for this purpose and are documented separately. These programs may require changes to account for differences in graphics software and hardware at various installations.

I. Status

The program is in use at the Los Alamos National Laboratory and at many other installations.

J. References

References are provided in the manual.

K. Machine Requirements

A CDC 7600 computer with 60000 words of small-core memory and 220000 words of large-core memory is required.

L. Programming Languages

The programming language is FORTRAN-IV. (Although COMPASS matrix inversion subroutines are available, they are not mandatory.)

M. Operating System or Monitor

The operating system or monitor that executes the program is a standard CDC 7600 operating system with FTN FORTRAN compiler and loader.

N. Other Programming or Operating Information or Restrictions

None.

O. Available Materials

A source listing, a TRAC-PF1 manual, and sample problems are available.

II. INTRODUCTION

The Transient Reactor Analysis Code (TRAC) is an advanced best-estimate systems code for analyzing LWR accidents. It is being developed at the Los Alamos National Laboratory under the sponsorship of the Reactor Safety Research Division of the US Nuclear Regulatory Commission. A preliminary TRAC version consisting of only one-dimensional components was completed in December 1976. This version was not released publicly nor formally documented. However, it was used in the TRAC-P1 development and formed the basis for the one-dimensional loop-component modules. The first publicly released version was TRAC-P1, completed in December 1977. It is described in the Los Alamos report LA-7279-MS (June 1978).

The TRAC-P1 program was designed primarily for the analysis of large-break LOCAs in pressurized water reactors (PWRs). Because of its versatility, however, it can be applied directly to many analyses ranging from blowdowns in simple pipes to integral LOCA tests in multiloop facilities. A refined version, called TRAC-P1A, was released to the National Energy Software Center (NESC) in March 1979. It is described in the Los Alamos report LA-7777-MS (May 1979). Although it still treats the same class of problems, TRAC-P1A is more efficient than TRAC-P1 and incorporates improved hydrodynamic and heat-transfer models. It also is easier to implement on various computers. TRAC-PD2 contains improvements in reflood, heat-transfer models, and numerical solution methods. Although a large LOCA code, it has been applied successfully to small-break problems and to the Three Mile Island incident.

TRAC-PF1 was designed to improve the ability of TRAC-PD2 to handle small-break LOCAs and other transients. TRAC-PF1 has all of the major improvements of TRAC-PD2; in addition, it uses a full two-fluid model with two-step numerics in the one-dimensional components. The two-fluid model, in conjunction with a stratified-flow regime, handles countercurrent flow better than the drift-flux model previously used. The two-step numerics allow large time steps for slow transients. A one-dimensional core component permits calculations with reduced dimensionality although the three-dimensional vessel option has been retained. A noncondensable gas field has been added to both the one-dimensional and three-dimensional hydrodynamics. Significant improvements also have been made to the trip logic and the input. TRAC-PF1 was publicly released in July 1981.

A. TRAC Characteristics

Some distinguishing characteristics of TRAC-PF1 are summarized below. Within restrictions imposed by computer running times, attempts are being made to incorporate state-of-the-art technology in two-phase thermal hydraulics.

1. Variable-Dimensional Fluid Dynamics. A full three-dimensional (r, θ, z) flow calculation can be used within the reactor vessel; the flow within the loop components is treated one dimensionally. This allows an accurate calculation of the complex multidimensional flow patterns inside the reactor vessel that are important in determining accident behavior. For example, phenomena such as emergency core coolant (ECC) downcomer penetration during blowdown, multidimensional plenum and core flow effects, and upper plenum pool formation and core penetration during reflood can be treated directly. However, a one-dimensional vessel model may be constructed that allows transients to be calculated very quickly because the usual time-step restrictions are removed by the special stabilizing numerical treatment.

2. Nonhomogeneous, Nonequilibrium Modeling. A full two-fluid (six-equation) hydrodynamics model describes the steam-water flow, thereby allowing important phenomena such as countercurrent flow to be treated explicitly. A stratified-flow regime has been added to the one-dimensional hydrodynamics and a seventh field equation (mass balance) describes a noncondensable gas field.

3. Flow-Regime-Dependent Constitutive Equation Package. The thermal-hydraulic equations describe the transfer of mass, energy, and momentum between the steam-water phases and the interaction of these phases with the system structure. Because these interactions are dependent on the flow topology, a flow-regime-dependent constitutive equation package has been incorporated into the code. Although this package undoubtedly will be improved in future code versions, assessment calculations performed to date indicate that many flow conditions can be handled adequately with the current package.

4. Comprehensive Heat-Transfer Capability. The TRAC-PF1 program incorporates detailed heat-transfer analyses of both the vessel and the loop components. Included is a two-dimensional (r, z) treatment of fuel-rod heat conduction with dynamic fine-mesh rezoning to resolve bottom flood and falling-film quench fronts. The heat transfer from the fuel rods and other system structures is calculated using flow-regime-dependent heat-transfer

coefficients obtained from a generalized boiling curve based on local conditions.

5. Consistent Analysis of Entire Accident Sequences. An important TRAC feature is its ability to address entire accident sequences, including computation of initial conditions, with a consistent and continuous calculation. For example, the code models the blowdown, refill, and reflood phases of a LOCA. This modeling eliminates the need to perform calculations using different codes to analyze a given accident. In addition, a steady-state solution capability provides self-consistent initial conditions for subsequent transient calculations. Both a steady-state and a transient calculation can be performed in the same run, if desired.

6. Component and Functional Modularity. The TRAC program is completely modular by component. The components in a calculation are specified through input data; available components allow the user to model virtually any PWR design or experimental configuration. This gives TRAC great versatility in the possible range of applications. It also allows component modules to be improved, modified, or added without disturbing the remainder of the code. TRAC component modules currently include accumulators, pipes, pressurizers, pumps, steam generators, tees, valves, and vessels with associated internals (downcomer, lower plenum, core, upper plenum).

The TRAC program also is modular by function; that is, the major aspects of the calculations are performed in separate modules. For example, the basic one-dimensional hydrodynamics solution algorithm, the wall-temperature field solution algorithm, heat-transfer coefficient selection, and other functions are performed in separate sets of routines that are accessed by all component modules. This modularity allows the code to be upgraded readily as improved correlations and experimental information become available.

B. Physical Phenomena Treated

Because of the detailed modeling in TRAC, most of the physical phenomena important in large- and small-break LOCA analysis can be treated. Included are:

1. ECC downcomer penetration and bypass, including the effects of countercurrent flow and hot walls;
2. lower plenum refill with entrainment and phase separation effects;

3. bottom flood and falling-film reflood quench fronts;
4. multidimensional flow patterns in the core and plenum regions;
5. pool formation and countercurrent flow at the upper core support plate (UCSP) region;
6. pool formation in the upper plenum;
7. steam binding;
8. average-rod and hot-rod cladding temperature histories;
9. alternate ECC injection systems, including hot-leg and upper-head injection;
10. direct injection of subcooled ECC water, without the requirement for artificial mixing zones;
11. critical flow (choking);
12. liquid carryover during reflood;
13. metal-water reaction;
14. water hammer effects; and
15. wall friction losses.

C. Planned Improvements

Although advanced modeling capabilities are provided in TRAC-PF1, there are additions and improvements planned for future Los Alamos versions of the code. Some of the more important are summarized below.

1. Work is in progress on a new version of TRAC, TRAC-PF1/Mod1, which will handle all operational transients. The principal improvements involve adding a proportional-integral-differential controller, turbine and condenser models, and an extra field to track boron.
2. Some development work is proceeding on a final, detailed version, TRAC-PD3. In addition to the options available in TRAC-PF1/Mod1, this version will have another liquid field in the vessel, a detailed gap model for the fuel rods, and a multidimensional neutronics capability.

A boiling water reactor (BWR) version is under development at the Idaho National Engineering Laboratory (INEL). The necessary additional component models (jet pumps, steam separators) are being developed at INEL; the basis for this version is the PWR version and a one-dimensional, two-fluid hydrodynamic package developed at Los Alamos.

One important constraint that must be considered in TRAC applications is the computer running-time requirements. With the release of TRAC-PF1, the user has a great deal of control over the running time of the code. If less detailed, rapid calculations are desired, a full one-dimensional model often will reduce the running time by an order of magnitude over the previous

version, TRAC-PD2. If detail in the vessel is desired, the running time often will be comparable to TRAC-PD2.

D. Scope of TRAC Manual

This manual describes TRAC basic methods and models and provides user information and programming details. Section III describes the basic hydrodynamics and heat-transfer methods and discusses the overall strategies for transient and steady-state solutions. Section III is supplemented by Appendixes A and B that supply, respectively, the fluid and material properties for the thermal-hydraulic analyses.

A standard nomenclature guide is included. Quantities that are not included in the standard nomenclature list are defined in the text. All units are metric as given in National Bureau of Standards Special Publication 330, "The International System of Units (SI)," unless otherwise specified.

Section IV describes the component models. The user should study these descriptions if questions arise when preparing detailed input specifications for a TRAC problem.

Section V provides input specifications and other user information. To provide additional guidance to the user in the area of input preparation, input decks for a PWR sample problem are provided in Appendix C. Error messages that might occur during a calculation are explained in Appendix D.

Section VI discusses the overall code organization, input and output processing, storage requirements, and other programming details associated with both transient and steady-state solutions. Appendix E provides a list of TRAC subprograms; Appendix F, a compilation of COMMON arrays; and Appendix G, component data tables.

An important aspect of the TRAC program involves the developmental assessment of the code through comparisons with measurements obtained from test facilities. Developmental assessment calculations already have been performed with TRAC-PF1. A Los Alamos report entitled "TRAC-PF1 Developmental Assessment," which summarizes the key developmental assessment results, has been published (NUREG/CR-3280, LA-9404-M).

III. BASIC METHODS

A. Hydrodynamics

1. Field Equations. Unlike previous TRAC versions, TRAC-PF1 uses the same two-phase two-fluid model for fluid flow in both one- and three-dimensional components. In addition, a noncondensable gas component has been included in the vapor field, requiring one extra mass continuity equation. Homogeneity and thermal equilibrium are assumed for the combined gas field.

Seven differential equations describe the three-component, two-fluid model.^{1,2}

Liquid Mass Equation

$$\frac{\partial(1 - \alpha)\rho_l}{\partial t} + \nabla \cdot [(1 - \alpha) \rho_l \vec{V}_l] = - \Gamma \quad (1)$$

Combined Vapor Mass Equation

$$\frac{\partial(\alpha\rho_g)}{\partial t} + \nabla \cdot (\alpha\rho_g \vec{V}_g) = \Gamma \quad (2)$$

Noncondensable Gas Mass Equation

$$\frac{\partial(\alpha\rho_a)}{\partial t} + \nabla \cdot (\alpha\rho_a \vec{V}_g) = 0 \quad (3)$$

Combined Vapor Equation of Motion

$$\begin{aligned} \frac{\partial \vec{v}_g}{\partial t} + \vec{v}_g \cdot \nabla \vec{v}_g = & - \frac{c_1}{\alpha \rho_g} (\vec{v}_g - \vec{v}_\ell) |\vec{v}_g - \vec{v}_\ell| - \frac{1}{\rho_g} \nabla p \\ & - \frac{c_{wg}}{\alpha \rho_g} \vec{v}_g |\vec{v}_g| + \vec{g} . \end{aligned} \quad (4)$$

Liquid Equation of Motion

$$\begin{aligned} \frac{\partial \vec{v}_\ell}{\partial t} + \vec{v}_\ell \cdot \nabla \vec{v}_\ell = & \frac{c_1}{(1-\alpha)\rho_\ell} (\vec{v}_g - \vec{v}_\ell) |\vec{v}_g - \vec{v}_\ell| - \frac{1}{\rho_\ell} \nabla p \\ & - \frac{c_{w\ell}}{(1-\alpha)\rho_\ell} \vec{v}_\ell |\vec{v}_\ell| + \vec{g} . \end{aligned} \quad (5)$$

Combined Vapor Energy Equation

$$\begin{aligned} \frac{\partial}{\partial t} (\alpha \rho_g e_g) + \nabla \cdot (\alpha \rho_g e_g \vec{v}_g) \\ = - p \frac{\partial \alpha}{\partial t} - p \nabla \cdot (\alpha \vec{v}_g) + q_{wg} + q_{ig} + \Gamma h_{sg} . \end{aligned} \quad (6)$$

Total Energy Equation

$$\begin{aligned} \frac{\partial [(1-\alpha)\rho_\ell e_\ell + \alpha \rho_g e_g]}{\partial t} + \nabla \cdot [(1-\alpha)\rho_\ell e_\ell \vec{v}_\ell + \alpha \rho_g e_g \vec{v}_g] \\ = - p \nabla \cdot [(1-\alpha)\vec{v}_\ell + \alpha \vec{v}_g] + q_{w\ell} + q_{wg} . \end{aligned} \quad (7)$$

In these equations the vapor densities and energies are sums of the steam and noncondensable components,

$$\rho_g = \rho_s + \rho_a \quad (8)$$

and

$$\rho_g e_g = \rho_s e_s + \rho_a e_a \quad (9)$$

We assume Dalton's law applies; therefore,

$$p = p_s + p_a \quad (10)$$

A subscript, a, is used for the noncondensable gas because the internal thermodynamic properties model air. It would be easy to replace these properties with others describing different noncondensable gases.

In addition to the thermodynamic relations that are required for closure, specifications for the interfacial drag coefficients (c_i), the interfacial heat transfer (q_{ig}), the phase-change rate (Γ), the wall shear coefficients (c_{wg} and c_{wl}), and the wall heat transfers (q_{wg} and q_{wl}) are required. Gamma is evaluated from a simple thermal energy jump relation,

$$\Gamma = \frac{-q_{ig} - q_{il}}{h_{sg} - h_{sl}} \quad (11)$$

where

$$q_{ig} = h_{ig} A_i \frac{(T_{ss} - T_g)}{\text{vol}} \quad (12)$$

and

$$q_{il} = h_{il} A_i \frac{(T_{ss} - T_l)}{\text{vol}} \quad (13)$$

Here, A_i and the h_i terms are the interfacial area and heat-transfer coefficients and T_{ss} is the saturation temperature corresponding to the partial steam pressure.

Wall heat-transfer terms assume the form

$$q_{wg} = h_{wg} A_{wg} \frac{(T_w - T_g)}{\text{vol}} \quad (14)$$

and

$$q_{wl} = h_{wl} A_{wl} \frac{(T_w - T_l)}{\text{vol}} , \quad (15)$$

where A_{wg} and A_{wl} are the actual heated surface areas of the cell, except during reflood, when the average heat-transfer coefficients (HTCs) reflect the fraction of the heated surface area that is quenched.

2. Three-Dimensional Finite-Difference Equations. The momentum equations are separated into the three coordinate components. Only the vapor equation is discussed with the understanding that the liquid-momentum equation is treated in an analogous manner. There are three components of the vapor-momentum differential equation.

Axial (z) Component

$$\frac{\partial v_{gz}}{\partial t} = - \left(v_{gr} \frac{\partial v_{gz}}{\partial r} + \frac{v_{g\theta}}{r} \frac{\partial v_{gz}}{\partial \theta} + v_{gz} \frac{\partial v_{gz}}{\partial z} \right) - \frac{1}{\rho_g} \frac{\partial p}{\partial z} - \frac{c_{1z}}{\alpha \rho_g} (v_{gz} - v_{lz}) |\vec{v}_g - \vec{v}_l| - \frac{\Gamma}{\alpha \rho_g} (v_{gz} - v_{lgz}) - \frac{c_{wgz}}{\alpha \rho_g} v_{gz} |\vec{v}_g| + g . \quad (16)$$

Radial (r) Component

$$\begin{aligned} \frac{\partial v_{gr}}{\partial t} = & - \left(v_{gr} \frac{\partial v_{gr}}{\partial r} + \frac{v_{g\theta}}{r} \frac{\partial v_{gr}}{\partial \theta} - \frac{v_{g\theta}^2}{r} + v_{gz} \frac{\partial v_{gr}}{\partial z} \right) - \frac{1}{\rho_g} \frac{\partial p}{\partial r} \\ & - \frac{c_{ir}}{\alpha \rho_g} (v_{gr} - v_{lr}) |\vec{v}_g - \vec{v}_l| - \frac{\Gamma}{\alpha \rho_g} (v_{gr} - v_{igr}) - \frac{c_{wgr}}{\alpha \rho_g} v_{gr} |\vec{v}_g| . \end{aligned} \quad (17)$$

Azimuthal (θ) Component

$$\begin{aligned} \frac{\partial v_{g\theta}}{\partial t} = & - \left(v_{gr} \frac{\partial v_{g\theta}}{\partial r} + \frac{v_{g\theta}}{r} \frac{\partial v_{g\theta}}{\partial \theta} + \frac{v_{gr} v_{g\theta}}{r} + v_{gz} \frac{\partial v_{g\theta}}{\partial z} \right) - \frac{1}{\rho_g r} \frac{\partial p}{\partial \theta} \\ & - \frac{c_{i\theta}}{\alpha \rho_g} (v_{g\theta} - v_{l\theta}) |\vec{v}_g - \vec{v}_l| - \frac{\Gamma}{\alpha \rho_g} (v_{g\theta} - v_{i\theta}) - \frac{c_{wg\theta}}{\alpha \rho_g} v_{g\theta} |\vec{v}_g| . \end{aligned} \quad (18)$$

In the TRAC staggered scheme^{3,4} the velocities are defined on the mesh-cell surfaces at the locations shown in Fig. 1, where the subscript a stands for either l or g. However, the volume properties p, α , T, e, and ρ are located at the mesh-cell centers. The scalar field equations are written over a given mesh cell, whereas the momentum equations are staggered between mesh cells in the three component directions.

The written difference scheme for each of the momentum equations is lengthy because of the cross-derivative terms. Therefore, only the vapor z-direction finite-difference equations for a typical mesh cell are given to illustrate the procedure used. The time levels are indicated by the superscript n (old time) or n+1 (new time). The subscript g (for vapor) is dropped except where it is needed for clarity.

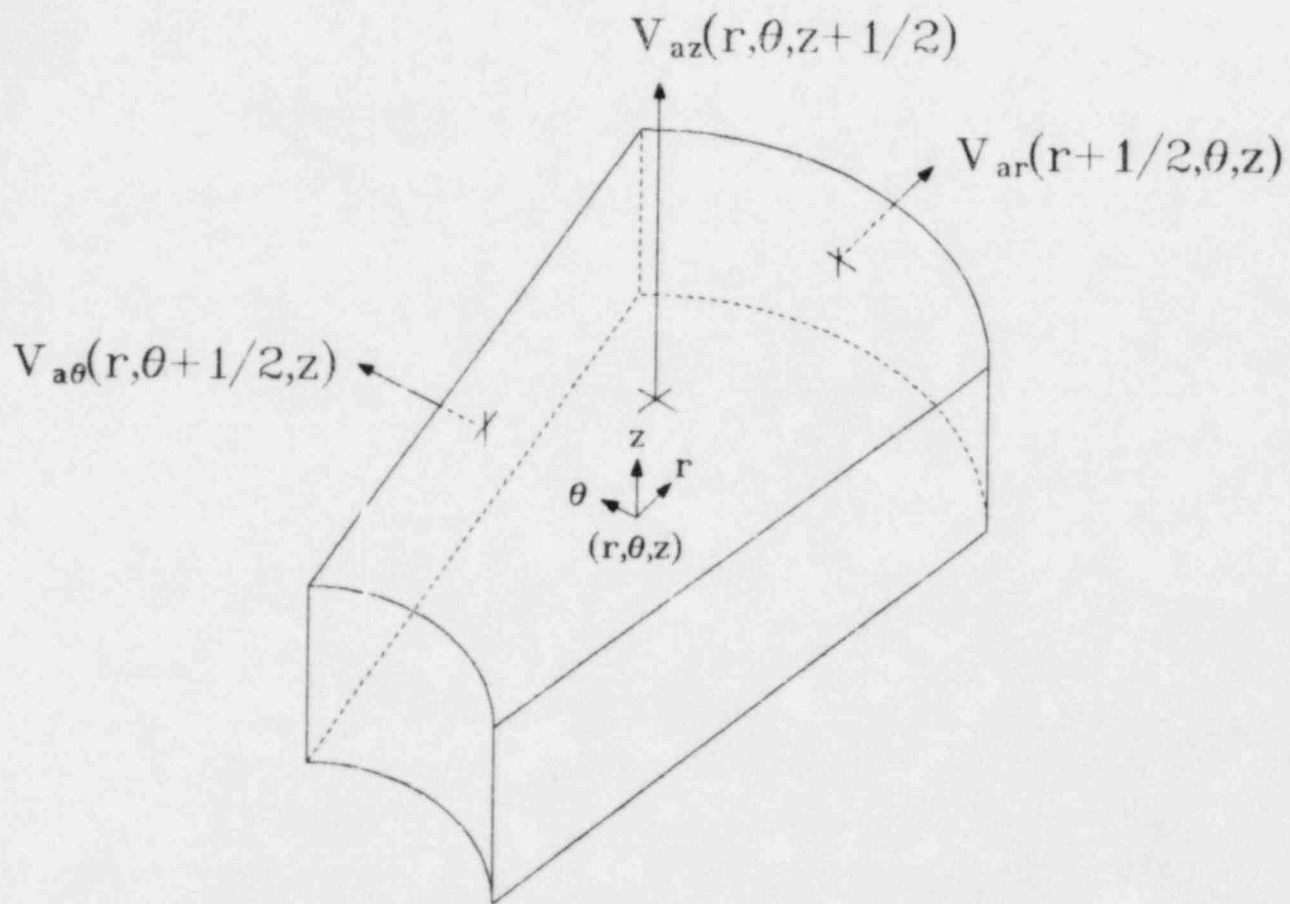


Fig. 1.
Three-dimensional mesh-cell velocities.

Using these conventions, the finite-difference vapor-momentum equation in the z-direction is

$$\begin{aligned}
 v_z^{n+1}(r, \theta, z+1/2) = & v_z^n(r, \theta, z+1/2) \\
 & - \Delta t \left\{ \frac{v_r(r, \theta, z+1/2)}{\Delta r} [v_z(r+1/2, \theta, z+1/2) - v_z(r-1/2, \theta, z+1/2)]^n \right. \\
 & + \frac{v_\theta(r, \theta, z+1/2)}{r \Delta \theta} [v_z(r, \theta+1/2, z+1/2) - v_z(r, \theta-1/2, z+1/2)]^n \\
 & + \frac{v_z(r, \theta, z+1/2)}{\Delta z} [v_z(r, \theta, z+1/2) - v_z(r, \theta, z-1/2)]^n \\
 & - \frac{[p(r, \theta, z+1) - p(r, \theta, z)]^{n+1}}{\rho^n(r, \theta, z+1/2) \Delta z} \\
 & - \frac{c_{iz}^n(r, \theta, z+1/2) [\vec{v}_g(r, \theta, z+1/2) - \vec{v}_l(r, \theta, z+1/2)]^{n+1}}{\alpha^n(r, \theta, z+1/2)} \\
 & \times |v_{gz}(r, \theta, z+1/2) - v_{lz}(r, \theta, z+1/2)| \\
 & - \frac{\Gamma^n(r, \theta, z+1/2) [v_z(r, \theta, z+1/2) - v_{iz}(r, \theta, z-1/2)]^{n+1}}{\alpha^n(r, \theta, z+1/2) \rho^n(r, \theta, z+1/2)} \\
 & \left. - \frac{c_{wz}^n(r, \theta, z+1/2) v_z^{n+1}(r, \theta, z+1/2) |\vec{v}^n(r, \theta, z+1/2)|}{\alpha^n(r, \theta, z+1/2) \rho^n(r, \theta, z+1/2)} \right\}, \tag{19}
 \end{aligned}$$

where Δt is the time-step size.

In any finite-difference scheme, certain quantities are required at locations where they are not defined formally; therefore, additional relations are needed. The volume properties Γ , α , and ρ_g are donor celled depending on the direction of $v_z(r, \theta, z+1/2)$.

For example,

$$\begin{aligned} \alpha(r, \theta, z+1/2) &= \alpha(r, \theta, z), & \text{if } V_z(r, \theta, z+1/2) \geq 0 & ; \\ &= \alpha(r, \theta, z+1), & \text{if } V_z(r, \theta, z+1/2) < 0 & . \end{aligned} \quad (20)$$

The radial component of the velocity at the axial location $(z+1/2)$ is obtained from

$$\begin{aligned} V_r(r, \theta, z+1/2) &= \frac{1}{4} [V_r(r+1/2, \theta, z) + V_r(r-1/2, \theta, z) + V_r(r+1/2, \theta, z+1) \\ &\quad + V_r(r-1/2, \theta, z+1)] ; \end{aligned} \quad (21)$$

a similar expression applies to $V_\theta(r, \theta, z+1/2)$. The spatial differences for V_z are, in the r -direction,

$$\begin{aligned} V_z(r+1/2, \theta, z+1/2) - V_z(r-1/2, \theta, z+1/2) &= V_z(r, \theta, z+1/2) - V_z(r-1, \theta, z+1/2) \\ &\text{if } V_r(r, \theta, z+1/2) \geq 0 \text{ , or} \\ V_z(r+1/2, \theta, z+1/2) - V_z(r-1/2, \theta, z+1/2) &= V_z(r+1, \theta, z+1/2) - V_z(r, \theta, z+1/2) \\ &\text{if } V_r(r, \theta, z+1/2) < 0 \text{ .} \end{aligned} \quad (22)$$

In the θ -direction,

$$\begin{aligned} V_z(r, \theta+1/2, z+1/2) - V_z(r, \theta-1/2, z+1/2) &= V_z(r, \theta, z+1/2) - V_z(r, \theta-1, z+1/2) \\ &\text{if } V_\theta(r, \theta, z+1/2) \geq 0 \text{ , or} \\ V_z(r, \theta+1/2, z+1/2) - V_z(r, \theta-1/2, z+1/2) &= V_z(r, \theta+1, z+1/2) - V_z(r, \theta, z+1/2) \\ &\text{if } V_\theta(r, \theta, z+1/2) < 0 \text{ .} \end{aligned} \quad (23)$$

In the z-direction,

$$V_z(r, \theta, z+1) - V_z(r, \theta, z) = V_z(r, \theta, z+1/2) - V_z(r, \theta, z-1/2)$$

if $V_z(r, \theta, z+1/2) \geq 0$, or

$$V_z(r, \theta, z+1) - V_z(r, \theta, z) = V_z(r, \theta, z+3/2) - V_z(r, \theta, z+1/2)$$

if $V_z(r, \theta, z+1/2) < 0$.

(24)

The convective terms in the finite-difference relations for the scalar field equations are written in conservative form. The finite-difference form of the overall mixture mass equation is

$$\begin{aligned} \rho_m^{n+1} = & \rho_m^n + \left[\frac{\Delta t}{\text{vol}} \right] \{ FA_{z-1/2} [[(1-\alpha)\rho_\ell]^{n_{V_\ell^{n+1}}} + (\alpha\rho_g)^{n_{V_g^{n+1}}}]_{z-1/2} \\ & - FA_{z+1/2} [[(1-\alpha)\rho_\ell]^{n_{V_\ell^{n+1}}} + (\alpha\rho_g)^{n_{V_g^{n+1}}}]_{z+1/2} \\ & + FA_{r-1/2} [[(1-\alpha)\rho_\ell]^{n_{V_\ell^{n+1}}} + (\alpha\rho_g)^{n_{V_g^{n+1}}}]_{r-1/2} \\ & - FA_{r+1/2} [[(1-\alpha)\rho_\ell]^{n_{V_\ell^{n+1}}} + (\alpha\rho_g)^{n_{V_g^{n+1}}}]_{r+1/2} \\ & + FA_{\theta-1/2} [[(1-\alpha)\rho_\ell]^{n_{V_\ell^{n+1}}} + (\alpha\rho_g)^{n_{V_g^{n+1}}}]_{\theta-1/2} \\ & - FA_{\theta+1/2} [[(1-\alpha)\rho_\ell]^{n_{V_\ell^{n+1}}} - (\alpha\rho_g)^{n_{V_g^{n+1}}}]_{\theta+1/2} \} , \end{aligned} \quad (25)$$

where vol is the hydrodynamic cell volume and FA is the flow area at the mesh-cell edge. The other scalar equations are differenced similarly.

All of the field equations [Eqs. (1)-(7)] have additional source terms to allow piping to be connected anywhere in the mesh. The source terms appearing in the mass and energy equations are given below. The subscripts p and v refer to pipe and vessel quantities, respectively.

Overall Mass Continuity Source Term

$$\{\alpha \rho_g^{n+1} V_g^{n+1} FA + [(1 - \alpha) \rho_l]^{n+1} V_l^{n+1} FA\}_p \cdot$$

Vapor Mass Continuity Source Term

$$[(\alpha \rho_g)^n FA V_g^{n+1}]_p \cdot$$

Overall Energy Source Term

$$[(1 - \alpha) \rho_l e_l^n FA V_l^{n+1}]_p + [(\alpha \rho_g e_g)^n FA V_g^{n+1}]_p \\ + p_v [\alpha^n FA V_g^{n+1} + (1 - \alpha)^n FA V_l^{n+1}]_p \cdot$$

Vapor Energy Source Term

$$[(\alpha \rho_g e_g)^n FA V_g^{n+1}]_p + p_v (\alpha^n FA V_g^{n+1})_p \cdot$$

The momentum source terms are complicated because of the staggered differencing and the fact that pipes may enter at arbitrary angles. For TRAC-PF1, we have assumed that the pipes enter normal to the vessel mesh-cell face. The basic forms for the liquid- and vapor-momentum source terms are:

Liquid-Momentum Source Term

$$\left(\frac{V_l V_{lv}}{\Delta x_v} \right)_p^n \cdot$$

Vapor-Momentum Source Term

$$\left(\frac{V_g V_{gv}}{\Delta x_v} \right)_p^n \cdot$$

The existence of the momentum source terms is dependent on the sign of the velocities in the vessel to keep the vessel donor-cell momentum equations consistent. For example, if the nearest vessel liquid velocity indicates that the flow is into the pipe from the vessel, then the source term is set equal to zero.

If structure exists in the mesh cell, the hydrodynamic flow areas (FA) and volumes (vol) are reduced from their geometric mesh-cell values. Thus, FA may be less than or equal to the geometric mesh-cell area and vol may be less than or equal to the geometric mesh-cell volume. Flow areas also may be set equal to zero. If this is the case, all fluxes across that plane are suppressed, as are the individual velocities of each phase. This procedure allows large obstacles such as the downcomer walls to be modeled properly. The user specifies the flow and volume restrictions.

The finite-difference equations thus formed are semi-implicit, because the pressure gradient terms in the vapor- and liquid-momentum equations are treated at the new time. A Courant stability criterion,

$$\frac{|V|}{L} = \max \left(\frac{V_{gz}}{\Delta z}, \frac{V_{g\theta}}{r\Delta\theta}, \frac{V_{gr}}{\Delta r}, \frac{V_{lz}}{\Delta z}, \frac{V_{l\theta}}{r\Delta\theta}, \frac{V_{lr}}{\Delta r} \right) , \quad (26)$$

is necessary, where

$$\frac{|V|\Delta t}{L} < 1 . \quad (27)$$

To solve the system of finite-difference equations, a linearization procedure is necessary. All of the scalar equations are reduced to a linear system in V_l , V_g , T_l , T_g , α , and p . This is accomplished by using the thermal equations of state,

$$\rho_l = \rho_l(p, T_l)$$

and

$$\rho_g = \rho_g(p, T_g) ;$$

the caloric equations of state,

$$e_l = e_l(p, T_l)$$

and

$$e_g = e_g(p, T_g) ;$$

and the definitions for ρ_m and e_m .

A further system reduction is accomplished by observing that the finite-difference vapor- and liquid-momentum equations yield equations of the form,

$$v^{n+1} = v^n + (\text{conv}^n + \frac{1}{\rho_l} \nabla p^{n+1} + \text{FRIC})\Delta t , \quad (28)$$

where conv designates the explicit convection terms and FRIC includes both the wall and the interfacial shears. Equation (28) indicates that changes in V are linearly dependent (after an explicit pass on the explicit parts of the momentum equations) on changes in pressure. Therefore, the system of variables may be reduced further to T_l , T_g , p , and α and can be solved by a Block Gauss-Seidel method. Reference 5 provides a much more detailed description of the basic Newton Block Gauss-Seidel numerical technique.

An improvement to the method proposed in Ref. 5 has been implemented to reduce the computing cost. The linear system that results from this method is a block seven-stripe matrix. In performing the Gauss-Seidel operation, if the nonlinear terms are not updated, the matrix coefficients remain constant for the time step. In this case a Gauss elimination technique can be applied once at each time step to the seven-stripe block array that allows its reduction to a seven-stripe single-element array. This results in a much faster iteration (after the first iteration) for the pressure. The actual iteration is performed in subroutine ITR1. When the vessel pressures are obtained for a specified convergence criterion, a back-substitution in subroutine FF3D is performed to unfold T_l , T_g , α , and the velocities for each phase. A call to

THERMO in FF3D then updates all of the thermodynamic properties and their derivatives in preparation for the next time step.

Two features have been added since version TRAC-PIA to improve mass conservation and to reduce running time. The first is a direct inversion of the pressure solution matrix when the number of vessel cells is sufficiently small (≤ 80). The second feature is a coarse-mesh rebalance method for other cases where Gauss-Seidel iteration is required. During the iteration the pressure solution is scaled nonuniformly to reduce the overall iteration error. Such scaling can be represented by

$$P^{(i)} = S^{(i)} P^{(1)} \quad ,$$

where $P^{(i)}$ is the pressure solution vector after i iterations and $S^{(i)}$ is its scaling matrix that is diagonal with scalar elements s_j . We define a coarse-mesh region as those vessel regions having the same scale factor. The scaled pressure solution vector is then

$$P' = s_1 P_1 + s_2 P_2 + \dots \quad ,$$

where P is a vector of pressures belonging to coarse-mesh region i . Using this equation in the vessel pressure equation

$$A \cdot P = B$$

and requiring that the least-squares error in P' be a minimum yield an equation for the scale factors,

$$U \cdot S = V \quad ,$$

where $U_{ij} = (P_i, AP_j)$, $V_i = (P_i, B)$, and the notation (X, Y) means the inner product of the vectors X and Y . The matrix size of U is equal to the number of

coarse-mesh regions and normally is small enough to be solved by direct inversion.

The choice of coarse-mesh regions is extremely important. We have selected a scheme that follows the flow path in the vessel so that coarse-mesh regions are coupled in the flow direction. We use the facts that the vessel matrix A is a seven-stripe matrix for a three-dimensional vessel and that coupling occurs only between nearest neighbors (there is no coupling if neighbors are separated by a wall such as a downcomer boundary). Based on these facts we select coarse-mesh regions as follows. All mesh cells on a level in the downcomer form a single coarse-mesh region and all other mesh cells on a level form another coarse-mesh region. Hence, the total number of coarse-mesh regions is equal to the number of downcomer levels plus the total number of vessel levels. Although this choice of coarse-mesh regions is not unique, we have found it to be very effective in reducing the number of vessel iterations (typically a factor of 10).

The three-dimensional hydrodynamics package has a water-packing algorithm that is similar in function to the one-dimensional algorithm but somewhat different in construction. In subroutine TF3DI, after the initial block matrix inversion, the center diagonal δP is calculated. If the resulting predicted pressure is either very low or very high and the mesh cell has a large liquid fraction, then the surrounding region is scanned for additional information. If an adjoining cell has a liquid fraction less than 0.9, the momentum derivative $\delta V_L / \delta P_L$ (derived from the momentum equation) is multiplied by a large constant wherever it appears in terms within the offending mesh cell. This reduces the liquid inertia and consequently allows the resultant velocity to adjust during the time step to ameliorate the effects of the sudden pressure change. The matrix is then re-evaluated and the calculation continues.

3. One-Dimensional Finite-Difference Methods. Spatial differencing is the same in one-dimensional and three-dimensional components. However, a new approach to time integration has been applied. This stability-enhancing two-step (SETS) method^{6,7} eliminates the material Courant stability limit from all one-dimensional components. This limit applies only in vessels and at junctions between vessels and one-dimensional components.

The stability-enhancing two-step method consists of a basic step (that is almost identical to the standard semi-implicit method used in the vessel) and a stabilizing step. For homogeneous flow, the order of these steps does not matter. However, for two-fluid flow with noticeable relative velocity, it is necessary to do the stabilizing step for the equations of motion before the basic step. When this stabilizing step precedes the basic step, an initial explicit prediction of velocities gives strong coupling through the interfacial drag terms without requiring direct communication between the stabilizing equations for liquid and vapor motion. To provide improved conservation and to minimize machine storage required by TRAC, the stabilizing steps for mass and energy equations are done as the final portion of the calculation.

The spatial mesh used for the finite-difference equations is staggered with thermodynamic properties evaluated at the cell centers and velocities evaluated at the cell edges. For stability, flux terms at cell edges require donor-cell averages of the form,

$$\begin{aligned} \langle YV \rangle_{j+1/2} &= Y_j V_{j+1/2}, & \text{if } V_{j+1/2} \geq 0 ; \\ &= Y_{j+1} V_{j+1/2}, & \text{if } V_{j+1/2} < 0 . \end{aligned} \quad (29)$$

Here, Y can be any cell-center state variable or a combination of such variables and V may be either liquid or vapor velocity. With this notation the finite-difference divergence operator for one-dimensional calculations is

$$\nabla_j \cdot (YV) = \frac{(A_{j+1/2} \langle YV \rangle_{j+1/2} - A_{j-1/2} \langle YV \rangle_{j-1/2})}{\text{vol}_j} . \quad (30)$$

where A is the local cross-sectional area and vol_j is the volume of the j^{th} cell. For the equations of motion, the donor-cell form of any $V \cdot \nabla V$ term is

$$\begin{aligned}
 v_{j+1/2} \nabla_{j+1/2} v &= \frac{v_{j+1/2} (v_{j+1/2} - v_{j-1/2})}{\Delta x_{j+1/2}}, \text{ if } v_{j+1/2} \geq 0 ; \\
 &= \frac{v_{j+1/2} (v_{j+3/2} - v_{j+1/2})}{\Delta x_{j+1/2}}, \text{ if } v_{j+1/2} < 0 ; \quad (31)
 \end{aligned}$$

where $\Delta x_{j+1/2}$ is half the sum of Δx_j and Δx_{j+1} .

The following finite-difference equations (roughly in order of their calculation) currently are used.

Predictors for Equations of Motion

Vapor

$$\begin{aligned}
 \frac{(\hat{v}_g^{n+1} - v_g^n)}{\Delta t} + v_g^n \nabla_{j+1/2} \tilde{v}_g^n + \beta (\hat{v}_g^{n+1} - v_g^n) \nabla_{j+1/2} \tilde{v}_g^n \\
 + \frac{c_1^n}{(\bar{\rho}_g^n)_{j+1/2}} [2(\hat{v}_g^{n+1} - \hat{v}_l^{n+1}) - (v_g^n - v_l^n)] |v_g^n - v_l^n| \\
 + \frac{1}{(\bar{\rho}_g^n)_{j+1/2}} \frac{(p_{j+1}^n - p_j^n)}{\Delta x_{j+1/2}} \\
 + \frac{c_{wg}}{(\bar{\rho}_g^n)_{j+1/2}} (2\hat{v}_g^{n+1} - v_g^n) |v_g^n| + g \cos \theta = 0, \quad (32)
 \end{aligned}$$

where

$$\beta = 0, \text{ if } v_{j+1/2}^n \leq 0;$$

$$= 1, \text{ if } v_{j+1/2}^n > 0.$$

Liquid

$$\begin{aligned} & \frac{(\hat{v}_k^{n+1} - v_k^n)}{\Delta t} + v_k^n v_{j+1/2} \bar{v}_k^n + \beta (\hat{v}_k^{n+1} - v_k^n) v_{j+1/2} \bar{v}_k^n \\ & + \frac{c_i^n}{[(1-\alpha)\rho_k]_{j+1/2}^n} [2(\hat{v}_k^{n+1} - \hat{v}_g^{n+1}) - (v_k^n - v_g^n)] |v_g^n - v_k^n| \\ & + \frac{1}{(\bar{\rho}_k)_{j+1/2}^n} \frac{(p_{j+1}^n - p_j^n)}{\Delta x_{j+1/2}} \\ & + \frac{c_{wl}}{[(1-\alpha)\rho_k]_{j+1/2}^n} (2\hat{v}_k^{n+1} - v_k^n) |v_k^n| + g \cos \theta = 0. \quad (33) \end{aligned}$$

Stabilizer Equations of Motion

Vapor

$$\begin{aligned}
 & \frac{(\tilde{v}_g^{n+1} - v_g^n)}{\Delta t} + v_g^n \nabla_{j+1/2} \tilde{v}_g^{n+1} + \beta(\tilde{v}_g^{n+1} - v_g^n) \nabla_{j+1/2} \tilde{v}_g^n \\
 & + \frac{c_1^n}{(\bar{\alpha}_g)_j^{n+1/2}} [2(\hat{v}_g^{n+1} - \hat{v}_g^{n+1}) - (v_g^n - v_g^n)] |v_g^n - v_g^n| \\
 & + \frac{1}{(\bar{\rho}_g)_j^{n+1/2}} \frac{(p_{j+1}^n - p_j^n)}{\Delta X_{j+1/2}} \\
 & + \frac{c_{wg}}{(\bar{\alpha}_g)_j^{n+1/2}} (2\tilde{v}_g^{n+1} - v_g^n) |v_g^n| + g \cos \theta = 0 \quad . \quad (34)
 \end{aligned}$$

Liquid

$$\begin{aligned}
 & \frac{(\tilde{v}_\ell^{n+1} - v_\ell^n)}{\Delta t} + v_\ell^n \nabla_{j+1/2} \tilde{v}_\ell^{n+1} + \beta(\tilde{v}_\ell^{n+1} - v_\ell^n) \nabla_{j+1/2} \tilde{v}_\ell^n \\
 & + \frac{c_1^n}{[(1 - \alpha)\rho_\ell]_j^{n+1/2}} [2(\hat{v}_\ell^{n+1} - \hat{v}_\ell^{n+1}) - (v_\ell^n - v_\ell^n)] |v_\ell^n - v_\ell^n| \\
 & + \frac{1}{(\bar{\rho}_\ell)_j^{n+1/2}} \frac{(p_{j+1}^n - p_j^n)}{\Delta X_{j+1/2}} \\
 & + \frac{c_{w\ell}}{[(1 - \alpha)\rho_\ell]_j^{n+1/2}} (2\tilde{v}_\ell^{n+1} - v_\ell^n) |v_\ell^n| + g \cos \theta = 0 \quad . \quad (35)
 \end{aligned}$$

Basic Equations of Motion

Vapor

$$\begin{aligned}
 & \frac{(v_g^{n+1} - v_g^n)}{\Delta t} + v_g^n \nabla_{j+1/2} \tilde{v}_g^{n+1} + \beta(v_g^{n+1} - v_g^n) \nabla_{j+1/2} \tilde{v}_g^n \\
 & + \frac{c_i^n}{(\bar{\alpha}\rho_g)_j^{n+1/2}} [2(v_g^{n+1} - v_\ell^{n+1}) - (v_g^n - v_\ell^n)] |v_g^n - v_\ell^n| \\
 & + \frac{1}{(\bar{\rho}_g)_j^{n+1/2}} \frac{(\tilde{p}_{j+1}^{n+1} - \tilde{p}_j^{n+1})}{\Delta X_{j+1/2}} \\
 & + \frac{c_{wg}}{(\bar{\alpha}\rho_g)_j^{n+1/2}} (2v_g^{n+1} - v_g^n) |v_g^n| + g \cos \theta = 0 \quad . \quad (36)
 \end{aligned}$$

Liquid

$$\begin{aligned}
 & \frac{(v_\ell^{n+1} - v_\ell^n)}{\Delta t} + v_\ell^n \nabla_{j+1/2} \tilde{v}_\ell^{n+1} + \beta(v_\ell^{n+1} - v_\ell^n) \nabla_{j+1/2} \tilde{v}_\ell^n \\
 & + \frac{c_i^n}{[(1 - \alpha)\rho_\ell]_j^{n+1/2}} [2(v_\ell^{n+1} - v_g^{n+1}) - (v_\ell^n - v_g^n)] |v_\ell^n - v_g^n| \\
 & + \frac{1}{(\bar{\rho}_\ell)_j^{n+1/2}} \frac{(\tilde{p}_{j+1}^{n+1} - \tilde{p}_j^{n+1})}{\Delta X_{j+1/2}}
 \end{aligned}$$

$$+ \frac{c_{w\ell}}{[(1-\alpha)\rho_\ell]_{j+1/2}^n} (2V_\ell^{n+1} - V_\ell^n) |V_\ell^n| + g \cos \theta = 0 \quad (37)$$

Basic Mass Equations

Vapor

$$\frac{[(\tilde{\alpha}\tilde{\rho}_g)^{n+1} - (\alpha\rho_g)^n]}{\Delta t} + \nabla_j \cdot (\alpha\rho_g V_g^{n+1}) = \tilde{\Gamma}^{n+1} \quad (38)$$

Noncondensable Gas

$$\frac{[(\tilde{\alpha}\tilde{\rho}_a)^{n+1} - (\alpha\rho_a)^n]}{\Delta t} + \nabla_j \cdot (\alpha\rho_a V_g^{n+1}) = 0 \quad (39)$$

Liquid

$$\frac{[(1-\tilde{\alpha})^{n+1} \tilde{\rho}_\ell^{n+1} - (1-\alpha)^n \rho_\ell^n]}{\Delta t} + \nabla_j \cdot [(1-\alpha)\rho_\ell V_\ell^{n+1}] = -\tilde{\Gamma}^{n+1} \quad (40)$$

Basic Energy Equations

Vapor

$$\frac{[(\tilde{\alpha}\tilde{\rho}_g \tilde{e}_g)^{n+1} - (\alpha\rho_g e_g)^n]}{\Delta t} + \nabla_j \cdot (\alpha\rho_g e_g V_g^{n+1}) + \tilde{p}^{n+1} \left[\frac{(\tilde{\alpha}^{n+1} - \alpha^n)}{\Delta t} + \nabla_j \cdot (\alpha^n V_g^{n+1}) \right]$$

$$= \tilde{q}_{wg}^{n+1} + \tilde{q}_{ig}^{n+1} + \tilde{\Gamma}^{n+1} \tilde{h}_{sg}^{n+1} . \quad (41)$$

Liquid

$$\frac{\{[\tilde{\alpha} \tilde{\rho}_g \tilde{e}_g + (1 - \tilde{\alpha}) \tilde{\rho}_l \tilde{e}_l]^{n+1} - [\alpha \rho_g e_g + (1 - \alpha) \rho_l e_l]^n\}}{\Delta t}$$

$$+ v_j \cdot [(\alpha \rho_g e_g) v_g^{n+1} + (1 - \alpha) \rho_l e_l v_l^{n+1}]$$

$$+ \tilde{p}^{n+1} v_j \cdot [(1 - \alpha)^n v_l^{n+1} + \alpha^n v_v^{n+1}] = \tilde{q}_{wg}^{n+1} + \tilde{q}_{wl}^{n+1} . \quad (42)$$

Stabilizing Mass Equations

Vapor

$$\frac{[(\alpha \rho_g)^{n+1} - (\alpha \rho_g)^n]}{\Delta t} + v_j \cdot [(\alpha \rho_g)^{n+1} v_g^{n+1}] = \tilde{\Gamma}^{n+1} . \quad (43)$$

Noncondensable Gas

$$\frac{[(\alpha \rho_a)^{n+1} - (\alpha \rho_a)^n]}{\Delta t} + v_j \cdot [(\alpha \rho_a)^{n+1} v_g^{n+1}] = 0 . \quad (44)$$

Liquid

$$\frac{[(1 - \alpha)^{n+1} \rho_l^{n+1} - (1 - \alpha)^n \rho_l^n]}{\Delta t} + v_j \cdot [(1 - \alpha)^{n+1} \rho_l^{n+1} v_l^{n+1}]$$

$$= - \tilde{\Gamma}^{n+1} . \quad (45)$$

Stabilizing Energy Equations

Vapor

$$\begin{aligned}
 & \frac{[(\alpha \rho_g e_g)^{n+1} - (\alpha \rho_g e_g)^n]}{\Delta t} + v_j \cdot [(\alpha \rho_g e_g)^{n+1} v_g^{n+1}] \\
 & + \tilde{p}^{n+1} \left[\frac{(\tilde{\alpha}^{n+1} - \alpha^n)}{\Delta t} + v_j \cdot (\alpha^n v_g^{n+1}) \right] \\
 & = \tilde{q}_{ig}^{n+1} + \tilde{q}_{wg}^{n+1} + \tilde{\Gamma}^{n+1} \tilde{h}_{sg}^{n+1} .
 \end{aligned} \tag{46}$$

Liquid

$$\begin{aligned}
 & \frac{[(1 - \alpha) \rho_l e_l]^{n+1} - [(1 - \alpha) \rho_l e_l]^n}{\Delta t} + v_j \cdot \{[(1 - \alpha) \rho_l e_l]^{n+1} v_l^{n+1}\} \\
 & + \tilde{p}^{n+1} \left\{ \frac{(\alpha^n - \tilde{\alpha}^{n+1})}{\Delta t} + v_j \cdot [(1 - \alpha)^n v_l^{n+1}] \right\} \\
 & = \tilde{q}_{wl}^{n+1} - \tilde{q}_{ig}^{n+1} - \tilde{\Gamma}^{n+1} \tilde{h}_{sg}^{n+1} .
 \end{aligned} \tag{47}$$

A caret above velocities denotes explicit predictor values. A tilde above a variable indicates that it is the result of an intermediate step and not a final value for the end of the time step. A horizontal line above a quantity indicates that it is obtained with a 50% average between values at adjacent cells. If there are no subscripts denoting cell location, we assume subscript j for mass and energy equations and subscript $j+1/2$ for equations of motion. Finally, theta is the angle between a vector from the center of cell j to the center of cell $j+1$ and a vector directed against gravity.

Time levels were omitted from some flux terms in Eqs. (38)-(42) because these terms contain both old and new time quantities. If X is a combination of state variables without a time superscript, then the correct definition for the divergence term in which it appears is

$$\begin{aligned} \nabla_j(XV_j^{n+1}) = & \{A_{j+1/2} v_{j+1/2}^{n+1} [f_{j+1/2} X_j^m + (1 - f_{j+1/2}) X_{j+1}^n] \\ & - A_{j-1/2} v_{j-1/2}^{n+1} [f_{j-1/2} X_{j-1}^n + (1 - f_{j-1/2}) X_j^m]\} / \text{vol}_j, \end{aligned} \quad (48)$$

where

$$X_j^m = g^{\sim} X_j^n + (1 - g^{\sim}) X_j^{n+1}. \quad (49)$$

The weighting function used to obtain donor-cell averaging [Eq. (29)] is f , and g^{\sim} is a weighting factor that depends on the rate of phase change, which goes to unity as the phase change disappears and to zero as the phase change approaches the total outflow of the phase created in the cell. For nonzero g^{\sim} , this form of the divergence operator is nonconservative but total conservation is maintained by the stabilizer step.

Equations (32) and (33) do not involve any implicit coupling between cells and can be solved rapidly for each cell. Because Eqs. (34) and (35) do not couple, each one requires only the solution of a tridiagonal linear system. Equations (36)-(42), combined with the necessary thermodynamic and constitutive equations, form a coupled system of nonlinear equations. Equations (36) and (37) are solved directly to obtain v_g^{n+1} and v_ℓ^{n+1} as dependent variables. After substituting these equations for velocity into Eqs. (38)-(42), the resulting system is solved for the independent variables \tilde{p}^{n+1} , \tilde{p}_a^{n+1} , \tilde{T}_b^{n+1} , \tilde{T}_ℓ^{n+1} , and $\tilde{\alpha}^{n+1}$ with a standard Newton iteration, including all coupling between cells. In practice, the linearized equations solved during this iteration can be reduced easily to a tridiagonal system involving only total pressures. The final five stabilizing equations [Eqs. (43)-(47)] also are simple tridiagonal linear systems because v_g^{n+1} and v_ℓ^{n+1} are known after solving Eqs. (36)-(42).

4. Constitutive Equations. The field equations [Eqs. (1)-(7)] require certain auxiliary or constitutive equations to effect closure. Thermal and caloric equations of state for each phase are required and these are discussed in Appendix A. In addition, the liquid and vapor wall shear, interfacial drag, wall heat transfer, interfacial heat transfer, and the net vaporization rate are necessary.

In TRAC-PF1, the vaporization thrust terms in the momentum equations are neglected. The wall heat transfers, q_{wg} and q_{wl} , are accounted for in the standard way [see Eqs. (14)-(15)]. The total wall surface area wetted by each phase is represented, whereas h_{wl} and h_{wg} are based on heat-transfer correlations from the literature. In many two-phase flow situations the walls are totally wetted by the liquid phase, in which case wall heat transfer to the vapor is zero.

a. One-Dimensional Wall Shear and Form Losses. The total pressure gradient calculated in the momentum equations is expressed as the sum of the frictional dissipation, acceleration head, and potential head terms. Subroutine FWALL calculates coefficients both for the frictional dissipation terms and for losses associated with abrupt area changes. Under single-phase flow conditions, pressure drops associated with frictional losses are correlated as functions of fluid velocity, fluid density, fluid viscosity, channel hydraulic diameter, and surface roughness of the channel wall. When a two-phase mixture is flowing in a channel, a correction to the single-phase frictional loss is necessary to account for added dissipation between phases and interactions with the channel walls. This correction factor is the two-phase flow multiplier.

The wall shear coefficients, c_{wg} and c_{wl} , are defined as

$$c_{wg} = \alpha \rho_g \frac{c_{fg}}{2D_h}$$

and

$$c_{wl} = (1 - \alpha) \rho_l \frac{c_{fl}}{2D_h},$$

where c_{fg} and c_{fl} are the vapor and liquid friction factors. The options available to calculate the wall friction are:

NFF = 0, constant value (user input);

NFF = 1, homogeneous model; and

NFF = 2, annular model;

where NFF is the user-supplied index. Use of a negative index value results in an automatic calculation of an appropriate form-loss coefficient in addition to the selected two-phase flow friction factor if there are abrupt area changes. This option is not available for the accumulator component, where a constant value for the friction factor is used.

(1) Homogeneous Model. The homogeneous friction-factor model alters the single-phase value by using a two-phase viscosity ($\bar{\mu}$) defined in terms of the flow quality (x),⁸

$$\frac{1}{\bar{\mu}} = \frac{x}{\mu_g} + \frac{(1-x)}{\mu_l} \quad . \quad (50)$$

The homogeneous friction factor⁹ then is given by

$$f = 0.046 (Re)^{-0.2} \quad , \quad \text{if } Re \geq 5000 \quad ; \quad (51a)$$

$$f = 0.032 \quad , \quad \text{if } Re \leq 500 \quad ; \quad (51b)$$

$$f = 0.032 - 5.25 \times 10^{-6}(Re - 500) \quad , \quad \text{if } 500 < Re < 5000 \quad ; \quad (51c)$$

where $Re = GD_h/\bar{\mu}$ and $G = \rho_m V_m$.

Equations (51a)-(51c) represent a constant friction factor for $Re \leq 500$ and a linear interpolation between $500 < Re < 5000$, where the friction factor is given by Eq. (51a).

The two-phase friction multiplier is

$$\phi^2 = [1.0 + x \left(\frac{\mu_l}{\mu_v} - 1.0 \right)]^{-0.2} \quad (52)$$

The coefficient of friction for the liquid is

$$c_{f_l} = 2.0 f \phi^2 \quad (53)$$

and, if the void fraction is greater than 0.90, the vapor coefficient of friction is

$$c_{f_g} = (10.0\alpha - 9.0)^2 (21.0 - 20.0\alpha) c_{f_l} \quad (54)$$

The purpose of this function is to ensure a smooth transition from zero vapor wall friction at $\alpha = 0.9$ to the single-phase vapor value at $\alpha = 1.0$.

(2) Annular Flow Model. The annular-flow friction-factor method from Ref. 10 is adopted with a modification at high vapor fractions. The single-phase friction factor (f_{sp}) from Ref. 11 is

$$f_{sp} = a + bRe^{-c} \quad (55)$$

where

$$a = 0.026 \left(\frac{k}{D} \right)^{0.225} + 0.133 \left(\frac{k}{D} \right) \quad (56)$$

$$b = 22.0 \left(\frac{k}{D} \right)^{0.44} \quad (57)$$

$$c = 1.62 \left(\frac{k}{D} \right)^{0.134} \quad (58)$$

and k/D is the relative pipe wall roughness. A value of $k = 5.0 \times 10^{-6}$ m, corresponding to drawn tubing, currently is used for the absolute pipe roughness. The annular flow friction factor is then

$$f = f_{sp} \phi^2 , \quad (59)$$

where

$$\phi^2 = \frac{\rho_l V_l^2}{\rho_m V_m^2} . \quad (60)$$

At vapor fractions above 0.90, the annular-flow friction factor is merged linearly into the homogeneous model with full transition occurring at $\alpha = 0.9995$. As discussed in Sec. III.A.1, the wall friction is partitioned between the liquid and vapor phases for a void fraction greater than 0.90.

(3) Form Losses. The finite-difference equations yield the correct pressure loss for an abrupt expansion. However, this is not true for an abrupt contraction or for an orifice. Form-loss corrections can be included in a TRAC calculation in two ways. The simplest method is to specify a negative value for the input friction option variable NFF (see Sec. V.F) at the location of any abrupt area change. This triggers logic in the code that examines the local pipe geometry, the flow direction, and the implicitness level of the difference equations to determine an appropriate loss correction. An extra term in the Bernoulli equation of the form,

$$\Delta p = \frac{k_p V^2}{2} , \quad (61)$$

where k is a form-loss coefficient, accounts for these corrections. The values used for k are

$$k = \left(1 - \frac{A_1}{A_2}\right)^2 \quad (62)$$

for an abrupt expansion or zero-length orifice, and

$$k = 0.5 - 0.7\left(\frac{A_1}{A_2}\right) + 0.2\left(\frac{A_1}{A_2}\right)^2 \quad (63)$$

for an abrupt contraction, where A_1 and A_2 are the smaller and larger flow areas, respectively. Equation (63) is a curve that was fitted to the values reported in Ref. 12.

The other way to account for form losses is through the use of the FRIC input array. Losses computed using this array are added to those specified with the NFF option. The pressure loss that results from FRIC is

$$\Delta p_j = \frac{(\Delta x_j + \Delta x_{j-1})}{2D_{h,j}} \text{FRIC}_j \rho_m V_m |V_m| \quad , \quad (64)$$

where j is the mesh-cell index.

An input option allows standard k (Refs. 13,14) factors to be input.

b. Three-Dimensional Wall Shear Coefficients. The wall shear coefficients, c_{wg} and c_{wl} , are defined similarly to the one-dimensional wall friction. The standard homogeneous correlation is used to provide the wall friction factors for two-phase flow. These factors approach the appropriate single-phase values for $\alpha = 0$ and $\alpha = 1$.

The velocity used by the correlations is determined from the average mesh-cell porosity; therefore, at locations where orifice plates exist and velocities are high, the wall friction is calculated using V_{avg} determined by

continuity considerations. This prevents excessive losses at major flow restrictions. A total friction factor is calculated from the information above and is ascribed completely to the liquid-momentum equation until a vapor fraction of 0.75 is reached. If $0.75 < \alpha < 0.95$, the shear is assigned with linear weighting (in α) to both the liquid and vapor. If $\alpha > 0.95$, the entire skin friction is assigned to the vapor.

A single friction coefficient is generated from this procedure for both the outer radial and upper axial cell face. However, the hydraulic diameter used in the radial and axial directions, in general, will vary depending on the geometry. If nonzero hydraulic diameters are specified in the problem input, these are used. If the hydraulic diameters are zero in the input, then TF3DE calculates, where $i = (\theta, z, r)$ and the wetted perimeter (P_i) normal to direction i includes the surface area of any rods, wall heat slabs, or flow boundaries. If there is no solid material in a mesh cell, the wall shear is zero. A similar procedure is used to calculate a wall shear in the theta direction. In this case, however, vector velocities and properties on the appropriate theta face (rather than the cell-centered averages) are used to achieve theta symmetry where such symmetry should exist.

The basic finite-difference scheme properly calculates classical Bourda form losses at an expansion but overpredicts the losses at a contraction [see discussion in Sec. III.A.4.a.(3)]. The user can specify an additional constant hydraulic loss factor in any of the coordinate directions to account for geometric details whose scale is smaller than the mesh-cell size.

c. Interfacial Heat Transfer and Shear. The interfacial constitutive equations basically are identical for the one-dimensional and three-dimensional portions of TRAC-PF1. A generic description of these relations will be given and any differences between the one-dimensional and three-dimensional sections will be noted. The interfacial heat transfer during boiling and the interfacial shear are calculated in conjunction with a simple flow-regime map.¹⁵ This flow-regime map, although originally developed for vertical pipe flow, is the simplest prescription that provides a rational means for defining the constitutive equations. Figure 2 illustrates how the flow map is implemented in the code.

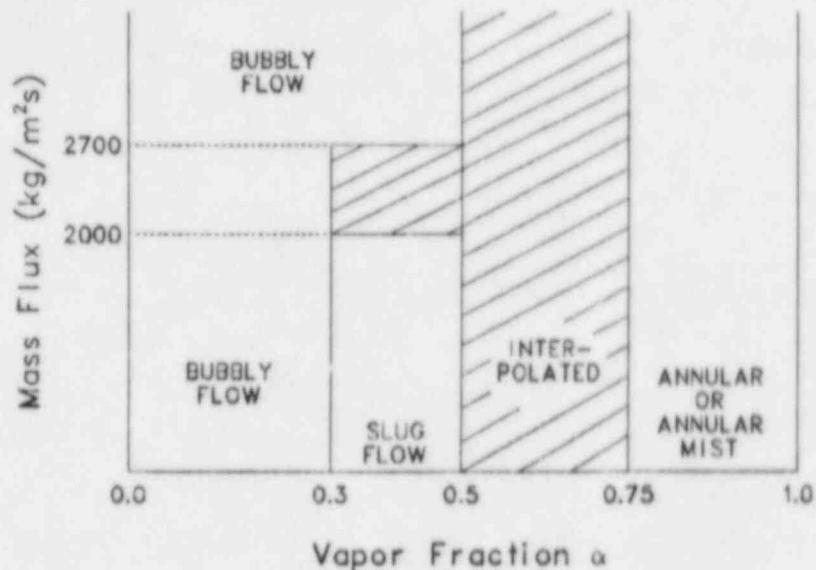


Fig. 2.
Flow-regime map for three-dimensional hydrodynamics.
(Cross-hatched regions are transition zones.)

If the void fraction is less than or equal to 0.3 (or $\alpha \leq 0.5$ if $G \geq 2700 \text{ kg/m}^2\text{s}$), a bubbly flow is assumed. The interfacial surface area in this regime is calculated in conjunction with a critical bubble Weber number, We_b . A value of $We_b = 7.5$ is used in TRAC-PF1. This value was chosen based on comparisons between the TRAC predictions and the experimental results for low subcooling (that is, shear-dominated) downcomer tests performed by Creare, Inc.¹⁶ The expression relating interfacial surface area to We_b is

$$\frac{\rho_l V_r^2 D_b}{\sigma} = We_b$$

or

$$D_b = \frac{We_b \sigma}{\rho_l V_r^2}, \quad (65)$$

where D_b is the bubble diameter. The bubble diameter must lie between the mesh-cell hydraulic diameter and 10^{-3} m. For this diameter and assuming a uniform bubble distribution within the mesh-cell vol, the number of bubbles is

$$CNB = \frac{6\alpha \text{ vol}}{\pi D_b^3} \quad (66)$$

and the interfacial area is

$$A_I = 6\alpha \text{ vol } \rho_L \frac{v^2 r}{We_b \sigma} \quad (67)$$

If the relative velocity is very small, this area can become small enough to allow significant nonequilibrium. Another surface area,

$$A = 4.83\alpha^{2/3} (N_B)^{1/3} \text{ vol} \quad (68)$$

based on a minimum number density ($N_B = 10^{10}$ bubbles/m³), is computed and the actual surface area used is the larger of the two.

The liquid-side interfacial heat-transfer coefficient is the larger of an approximate formulation of the Plesset-Zwicky bubble growth model,¹⁷

$$Nu = \frac{12}{\pi} (T_L - T_B) \rho_L \frac{\frac{\partial e_L}{\partial T_L}}{[\rho_g (h_{sg} - h_{sL})]} \quad (69)$$

and a sphere convection coefficient,¹⁸

$$Nu = 2.0 + 0.74 Re_b^{0.5} \quad (70)$$

where

$$Re_b = \rho_l V_r \frac{D_b}{\mu_l} .$$

The interfacial shear coefficient is provided by a standard set of formulas for a sphere,¹¹

$$c_i = \frac{3c_b \alpha \rho_l}{4D_b} , \quad (71)$$

where

$$c_b = 240 , \quad \text{if } Re_b < 0.1 ;$$
$$= \frac{24}{Re_b} , \quad \text{if } 0.1 \leq Re_b \leq 2 ;$$

or

$$= \frac{18.7}{Re_b^{0.68}} , \quad \text{if } Re_b > 2 .$$

If the cell-average mass flux is less than $2000 \text{ kg/m}^2\text{s}$ and the vapor fraction is between 0.3 and 0.5, the flow enters the slug regime. At the maximum alpha of 0.5, 40% of the vapor is assumed to exist in the form of trailing bubbles, with the remainder contained in the slug. These bubbles probably contribute to the majority of the interfacial heat transfer and the liquid-side coefficient is calculated from the heat-transfer relations for the entrained bubbles. If the mass flux is greater than $2700 \text{ kg/m}^2\text{s}$, all of the vapor is assumed to exist in bubbly form. Linear interpolation in mass flux is used in the range of 2000 to $2700 \text{ kg/m}^2\text{s}$. In the slug regime the bubble diameter is determined by a linear weighting in α between the Weber number criterion and the channel hydraulic diameter such that the value is the

hydraulic diameter at a void fraction of 0.5 and the Weber number size at an α of 0.3.

In the vapor-fraction range of 0.75 to 1.0, an annular or annular-mist regime is assumed. A simple s-shaped entrainment correlation based on the critical Weber number is used. Thus,

$$E = 1 - \exp [(-V_g - V_E) 0.23] \quad , \quad (72)$$

where

$$V_E = 2.3 \left[\frac{(\rho_l - \rho_g) \sigma We_d}{2 \rho_g} \right]^{1/4} .$$

This method appears to provide reasonable results for the FLECHT reflood tests. The remainder of the liquid is in a film or sheet. The interfacial shear and heat transfer are volume averages of the film and droplet relations in the annular-mist regime. The wetted surface area of the mesh cell is determined from the rod or slab heat-transfer area in the cell and the portion of the geometric flow area that is blocked off. If the cell is in a region devoid of any structure, the geometric surface area is used as a scaling factor. This, of course, is artificial; but in a realistic PWR simulation very few, if any, of the mesh cells are completely free of metal structure. The total interfacial surface area is determined by the sum of the areas contained in the wetted film and the droplets. A critical Weber number equal to four for the drops is used with a calculation procedure similar to that for bubbly flow. This value of the Weber number is appropriate for accelerating drops. For those cases where sensitivity to We_d was tested, the results were not influenced strongly by We_d in the range of $2 \leq We_d \leq 12$. The liquid-side heat-transfer coefficient is simply

$$h_{l\ell} = \frac{ck_\ell}{D_d} \quad , \quad (73)$$

where c , a constant, has been adjusted to drive the drops to equilibrium under a variety of flow conditions. In TRAC-PF1, $c = 11300$, which implies a thermal boundary layer in the drops that is about a thousandth of the drop diameter. In the film, a correlation,

$$\text{Nu} = 0.02 \text{ Re} \quad , \quad (74)$$

is employed to predict $h_{i\ell}$. The Dukler annular-flow model¹⁹ determines the shear for a wavy film, whereas the same drag correlations used for a bubble are employed if droplets exist. The Dukler model has a gas Reynolds number dependence and is of the form

$$\frac{1}{f_i} = C_1 \log \left(\frac{D}{S} \text{Re}_g \right) + C_2 \quad . \quad (75)$$

From the graphical data reported in Ref. 18, we obtain

$$\begin{aligned} C_1 &= 3.04 \text{ and } C_2 = -16.16 \text{ in countercurrent flow and} \\ C_1 &= 6.73 \text{ and } C_2 = -40.61 \text{ in cocurrent flow.} \end{aligned}$$

To avoid the discontinuity that occurs as Re_g becomes small (the correlation is for turbulent flow anyway), smoothing is employed in a transition region. The droplet Reynolds number is defined as

$$\text{Re}_d = \frac{\rho_g V_{rd} D_d}{\mu_g} \quad . \quad (76)$$

Because the actual relative velocity calculated is based on a shear that has been averaged between the film and drop correlations, a separate function²⁰ is used for V_{rd} ,

$$v_{rd} = 2.33 \left[\frac{(\rho_l - \rho_g) \sigma We_b}{\rho_l} \right]^{1/4} \quad (77)$$

For the regime between droplet and bubbly slug flow, a cubic spline interpolation in the vapor fraction is made between the conditions that would exist if the vapor fraction were at 0.75 in the annular or annular-mist topology and the conditions that would exist if the flow were in the bubbly slug regime at a void fraction of 0.5. This interpolation assures that the correlation for the interfacial shear, interfacial heat transfer, and surface area is a continuous function of the vapor fraction, the relative velocity, the mass flux, and the various fluid thermodynamic and transport properties.

We now discuss the vapor-side heat-transfer coefficient and the liquid heat-transfer coefficient during condensation. The vapor heat-transfer coefficient is a constant, $h_{ig} = 1 \times 10^4$. This implies that the rate for boiling or condensation is determined mainly by the liquid-side coefficient with a vapor coefficient designed to drive the vapor toward the saturation temperature. The formulation for the total liquid heat-transfer coefficient during condensation is based on the following model. If a pipe enters a given three-dimensional mesh cell and the liquid flows into that cell, then a jet is assumed with an α -weighted diameter, a surface area for condensation based on a right circular cylinder is provided, and h_{il} is given by Eq. (74) multiplied by $(\Delta X/D_{jet})^2$. If the jet model is not activated, the surface area is a constant times the mesh-cell volume. The h_{il} again is given by Eq. (74).

If the noncondensable gas is present, the condensation rate is reduced according to the prescription,

$$\frac{h_{nc}}{h_{il}} = 0.168 \left[\frac{\alpha \rho_s^2}{\rho_a (1 - \alpha) \rho_l} \right]^{0.1} \quad (78)$$

where h_{nc} is the liquid interfacial heat-transfer coefficient with noncondensable gas present. Small cutoffs on $(1 - \alpha)$ and ρ_a prevent the denominator from ever becoming so close to zero as to cause difficulties. This

model is based on Russian jet data²¹ and can dramatically reduce condensation when a vapor other than steam is in a region.

d. Interface Sharpener. An interface sharpener is used in the lower plenum and core of the three-dimensional vessel to improve the liquid distribution during reflood. Simple void fraction tests are employed to sense the presence of a sharp mixture density discontinuity. The entrainment model then is used to predict the void fraction to be used for convection out of the mesh cell's positive face. This void fraction will always be greater than or equal to the actual void fraction in the cell. The interfacial shear constitutive relations are calculated based on this void fraction, and the scalar field equations use this new value in the z-direction convective terms. A cubic spline is used to merge the sharpened alpha as the mesh cell fills.

e. Horizontal Stratified Flow. In TRAC-PF1 the one-dimensional components have an additional flow regime if the angle from the horizontal is less than 30°. A stratification criterion based on a modified Froude number analysis developed by Y. Taitel and A. E. Dukler²² is used to determine if the flow is stratified.

The critical velocity U_{crit} is calculated as

$$U_{crit} = C_2 \left[\frac{(\rho_l - \rho_g)g \cos \beta A_g}{\rho_g \frac{dA_l}{dh_l}} \right]^{1/2}, \quad (79)$$

$$C_2 = 1 - \frac{h_l}{D},$$

$$\frac{dA_l}{dh_l} = [D^2 - (2h_l - D)^2]^{1/2},$$

where h_l is the collapsed liquid height (determined by a standard mensuration formula) and D is the pipe inside diameter. If the absolute value of the vapor velocity is above U_{crit} , the standard flow map is used. As the vapor velocity goes to zero, the interfacial and wall shear coefficients are calculated by the Blasius relation (but based on a minimum turbulent Reynolds number). A cubic

spline employing the independent variable $\text{abs}(V_g)$ connects the two end points. This form of interpolation is necessary to prevent oscillations in the flow pattern with the large time steps often used by the code.

In addition, the hydraulic approximation for the difference in gravitational head caused by collapsed liquid height variations is added explicitly into the liquid equation of motion. Because this calculation is explicit, horizontal manometer oscillations can occur at larger time-step sizes. To prevent this difficulty, the magnitude of this added term is reduced as the time-step size is increased beyond the basic stability limit. This reduction eliminates the undesired oscillations.

f. Subcooled Boiling Model. If hot metal surfaces are present in a region, then the flashing rate Γ is modified to include the effects of subcooled boiling. If rods or slabs exist and $T_w > T_s$, the $h_{w\ell}$ is compared to the Dittus-Boelter liquid convective coefficient. If $h_{w\ell}$ is larger, the difference in wall flux (q_{sb}) is attributed to subcooled boiling and

$$\Gamma = \frac{q_{i\ell} + q_{ig} + q_{sb}}{h_{\ell g}} .$$

In both the vapor continuity equation and the vapor thermal-energy equation, the potentials $(T_s - T_g)$ and $(T_s - T_\ell)$ are evaluated at the new time level, whereas $h_{ig}A_i$ and $h_{i\ell}A_i$ are evaluated at the old time.

B. Structural Heat Transfer

Three fundamental heat-transfer mechanisms are modeled by the TRAC code. They include the interfacial heat transfer between the vapor and liquid phases, conduction within the reactor's structural components, and the heat transfer between the structures and the fluid. Interfacial heat transfer has been addressed in Sec. III.A.1.c. The remaining two mechanisms are discussed here.

The thermal history of the structural reactor materials is obtained from a solution of the heat-conduction equation. The energy exchange between the structures and the fluid is modeled using Newton's law. The coupling algorithm (Fig. 3) is semi-implicit. For each new time step, the fluid-dynamics equations are solved based on previous values for the wall heat-transfer coefficients (h) and surface wall temperatures (T_w); that is,

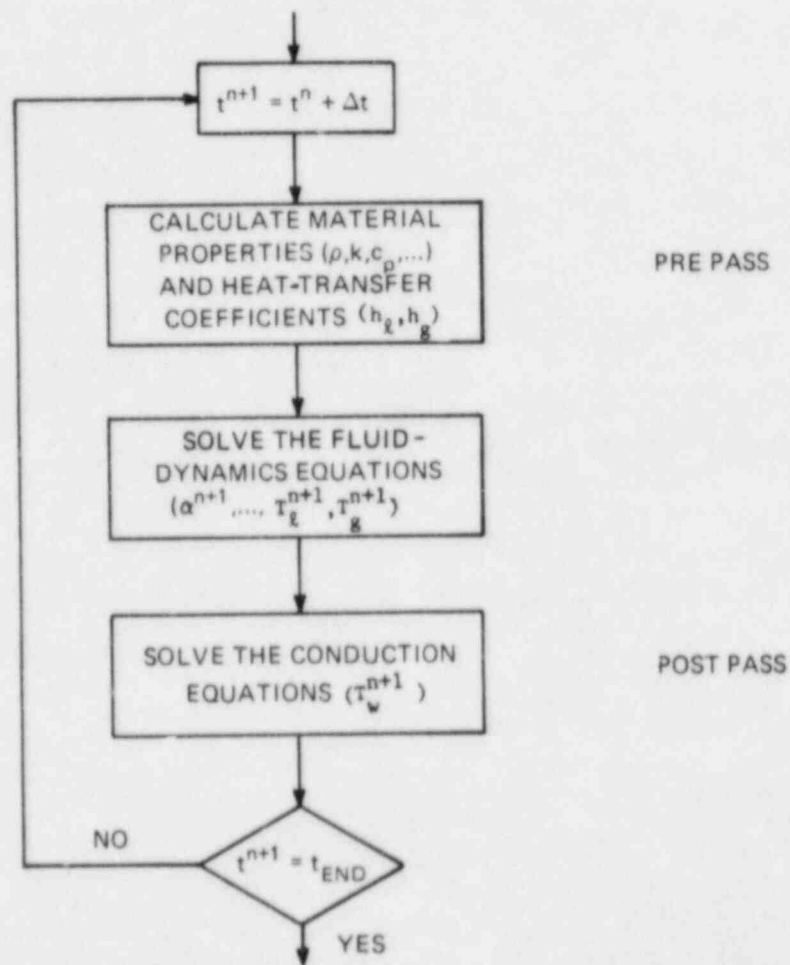


Fig. 3.

Semi-implicit coupling between hydrodynamics and structural heat transfer.

$$q_w^{n+1} = h^n (T_w^n - T_f^{n+1}) \quad (80)$$

Once the fluid-dynamics equations are solved, the wall temperature distributions are deduced from the conduction equation.

1. Heat-Conduction Models. For simplicity as well as computing efficiency, the conduction models are separated according to their geometric function. They include conduction within cylindrical walls, slabs, and core rods. The first model analyzes heat conduction within the walls of the one-dimensional loop components, such as the pipe walls. The latter two are associated with heat transfer within structural components of the vessel. Each of these models will be discussed in detail.

a. Cylindrical Wall Heat Conduction. The temperature distribution within the walls of the one-dimensional components is determined by subroutine CYLHT. A solution is obtained from a finite-difference approximation to the one-dimensional conduction equation,

$$\rho c_p \frac{\partial T}{\partial t} = \frac{1}{r} \left[\frac{\partial}{\partial r} \left(r k \frac{\partial T}{\partial r} \right) \right] + \dot{q}'''' \quad (81)$$

The finite-difference equations are derived by applying an integral method²³ to the elemental volumes shown in Fig. 4. The general form for the i^{th} volume ($1 < i < N$) is

$$\begin{aligned} & \frac{r_{i-1/2} k_{i-1/2}}{\Delta r_{i-1}} T_{i-1}^{n+1} - \left\{ \frac{r_{i-1/2} k_{i-1/2}}{\Delta r_{i-1}} + \frac{r_{i+1/2} k_{i+1/2}}{\Delta r_i} \right. \\ & + \frac{1}{2\Delta t} \left[(r_i \Delta r_{i-1} - \frac{\Delta r_{i-1}^2}{4}) (\rho c_p)_{i-1/2} + (r_i \Delta r_i + \frac{\Delta r_i^2}{4}) (\rho c_p)_{i+1/2} \right] \left. \right\} T_i^{n+1} \\ & + \frac{r_{i+1/2} k_{i+1/2}}{\Delta r_i} T_{i+1}^{n+1} = - \frac{1}{2} \left\{ (r_i \Delta r_i - \frac{\Delta r_i^2}{4}) \left[\frac{(\rho c_p)_{i-1/2}}{\Delta t} T_i^n + \dot{q}'''' \right] \right. \\ & \left. + (r_i \Delta r_i + \frac{\Delta r_i^2}{4}) \left[\frac{(\rho c_p)_{i+1/2}}{\Delta t} T_i^n + \dot{q}'''' \right] \right\} \quad (82) \end{aligned}$$

where

$$f_i^n \equiv f(t^n, r_i).$$

The boundary conditions applied to the inner ($i=1$) and outer ($i=N$) surfaces are:

$$-k \frac{\partial T}{\partial r} \Big|_{i=1,N} = \pm [h_\ell(T_\ell - T_i) + h_g(T_g - T_i)] \quad (83)$$

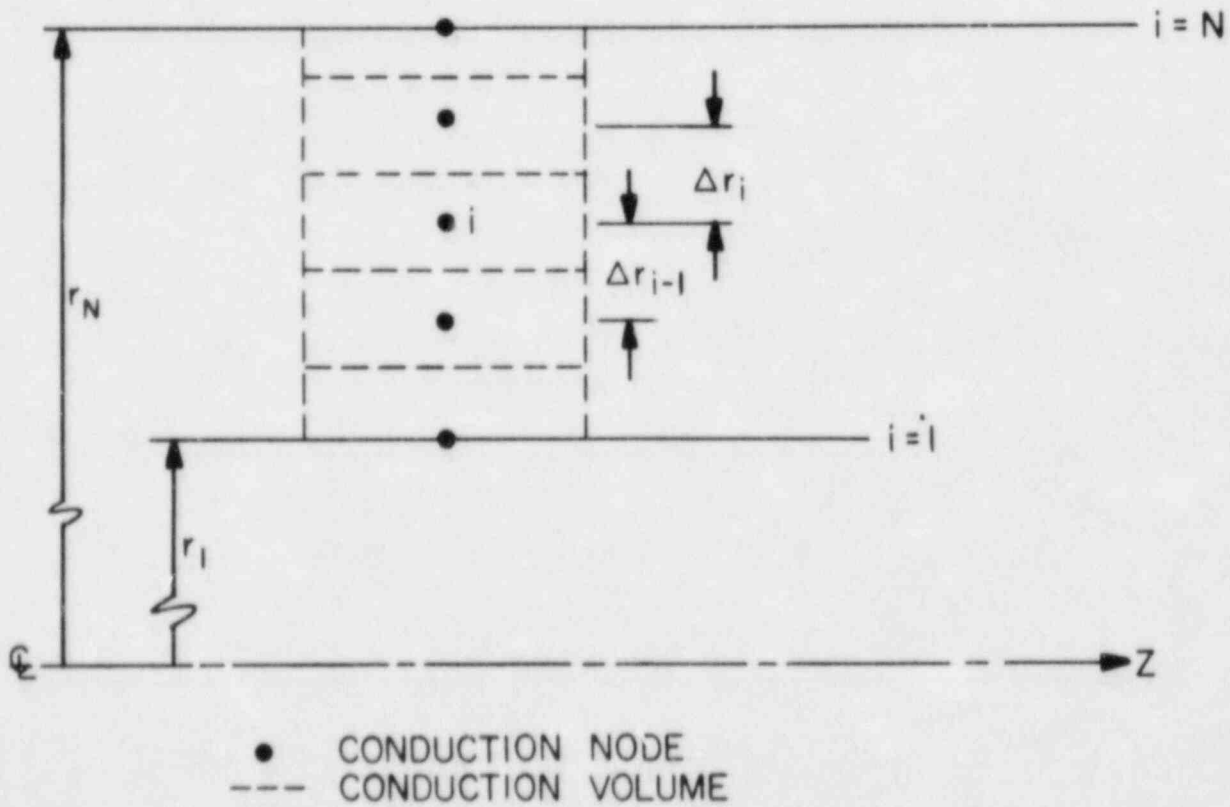


Fig. 4.
Cylindrical wall geometry.

Application of this boundary condition to the inner surface ($i=1$) yields, for example,

$$\begin{aligned}
 & - \left\{ \frac{r_{3/2} k_{3/2}}{\Delta r_1} + \frac{1}{2} \left[r_1 \Delta r_1 + \frac{\Delta r_1^2}{4} \right] \frac{(\rho c_p)_{3/2}}{\Delta t} + f_{ss} r_1 (h_\ell + h_g) \right\} T_1^{n+1} + \frac{r_{3/2} k_{3/2}}{\Delta r_1} T_2^{n+1} \\
 & = - \frac{1}{2} \left(r_1 \Delta r_1 + \frac{\Delta r_1^2}{4} \right) \left[\frac{(\rho c_p)_{3/2}}{\Delta t} T_1^n + \dot{q}'' \right] \\
 & + r_1 [h_\ell (f_t T_1^n - T_\ell^{n+1}) + h_g (f_t T_1^n - T_g^{n+1})] \quad . \quad (84)
 \end{aligned}$$

Because of the semi-implicit coupling with the fluid equations, f_{ss} and f_t take on the values of 0 and 1, respectively, for transient calculations. This ensures that both sets of equations use identical surface heat fluxes as boundary conditions for each time step. When a steady-state solution is required, however, large time steps are desirable. For this case, the conduction equation is written in a fully implicit form, and $f_{ss} = 1$ and $f_t = 0$.

Note that the above formulation conveniently positions nodal points on material interfaces. Material properties are evaluated between nodes.

The resulting linear equations are solved sequentially in the axial (z) direction. For each axial position a solution is achieved using Gaussian elimination.

A lumped-parameter solution is available to the user if the number of nodes equals 1. For this option the wall temperature is obtained from the equation,

$$\begin{aligned}
 T^{n+1} = & \left\{ \frac{1}{2} (2\Delta r + \frac{\Delta r^2}{R_i}) \left(\frac{\rho c_p}{\Delta t} T^n + \dot{q} \right) + h_{\ell_i} (T_{\ell_i}^{n+1} - f_t T^n) \right. \\
 & + h_{g_i} (T_{g_i}^{n+1} - f_t T^n) - \left(1 + \frac{\Delta r}{R_i} \right) [h_{\ell_o} (f_t T^n - T_{\ell_o}^{n+1}) + h_{g_o} (f_t T^n - T_{g_o}^{n+1})] \left. \right\} \\
 & / \left\{ \frac{1}{2} (2\Delta r + \frac{\Delta r^2}{R_i}) \left(\frac{\rho c_p}{\Delta t} \right) + f_{ss} [h_{\ell_i} + h_{g_i} + \left(1 + \frac{\Delta r}{R_i} \right) (h_{\ell_o} + h_{g_o})] \right\} \quad (85)
 \end{aligned}$$

The subscripts i and o refer to the inner and outer radii, respectively.

b. Slab Heat Conduction. Heat conduction within vessel structures (such as downcomer walls and support plates) is modeled in subroutine SLABHT. Only one slab is allowed in each fluid-dynamic cell. The number of nodes used to determine the temperature distributions is identical for all slabs within the vessel. The model includes the ability to account for the temperature effects in the slab properties (ρ , c_p , k , etc.). The temperature distribution is obtained from the one-dimensional conduction equation,

$$\rho c_p \frac{\partial T}{\partial t} = \frac{\partial}{\partial x} \left(k \frac{\partial T}{\partial x} \right) + \dot{q} \quad (86)$$

The appropriate finite-difference equations are derived by applying an integral method to the elemental volumes in a manner similar to that used for the cylindrical wall heat-conduction solution technique (Sec. IVI.B.1.a).

At the first surface ($i=1$), a symmetry boundary condition ($\partial T / \partial x|_{i=1} = 0$) is applied. The boundary condition applied to the remaining surface ($i=N$) is

$$-k \frac{\partial T}{\partial x} \Big|_{i=N} = [h_{\ell} (T_{\ell} - T_1) + h_g (T_g - T_1)] \quad (87)$$

Within the vessel slabs, \dot{q}''' is assumed to be zero.

An arbitrary number of interfaces between dissimilar materials also can be considered in the slab conduction model. The technique used is identical to the method used in the rod conduction solution [Sec. III.B.1.c.(1)].

Heat slabs of arbitrary thickness and surface areas can be defined in any mesh cell (including core regions) to model the heat capacity of structures within the vessel. One HTC is computed for each slab using the local fluid conditions. For vessel cells without structural material, input the slab area as 0.0; the remaining input arrays describing the slab should have values that the code can recognize (filling the arrays with zeros is an error).

c. Rod Heat Conduction. Subroutine RODHT analyzes the conduction of the reactor rods on a rod-by-rod basis. The formulation can model diverse rod geometries. Both nuclear and electrically heated rods can be analyzed. The effects of internal heat generation, gap conduction, metal-water reaction, and variable rod properties are included.

The numerical procedures can model the entire LOCA scenario in a consistent and mechanistic fashion. The model also can resolve large axial (z) gradients characteristic of the reflood phase.

One computational rod is associated with each segment (that is, for each r,θ region) within the core. This "average" rod is coupled to the fluid by Newton's law of cooling. Any number of additional user-specified rods may be included in each segment. The rod power factors (that is, relative to the average rod located within each segment) are also user specified. The supplemental rods allow the user to include hot rods in the reactor vessel. Such rods do not influence the fluid-dynamics calculations.

(1) Numerical Model. The thermal response of the vessel rods is modeled using the two-dimensional (r,z) cylindrical conduction equation. Azimuthal symmetry has been assumed.

$$\rho c_p \frac{\partial T}{\partial t} = \dot{q}''' + \frac{1}{r} \frac{\partial}{\partial r} \left(rk \frac{\partial T}{\partial r} \right) + \frac{\partial}{\partial z} \left(k \frac{\partial T}{\partial z} \right) \quad (88)$$

The effects of internal heat generation resulting from nuclear fission, electrical current, or the metal-water reaction may be included.

Appropriate finite-difference equations are obtained by applying an integral method²³ to appropriate differential volumes. The noding within the rods is staggered with respect to the nodes used in the fluid-dynamics calculations (Fig. 5). This noding scheme is necessary to simplify the algorithm that generates the fine mesh required by the reflood calculations. The staggered mesh gives the further advantage of providing axial numerical smoothing.

Differencing, in the radial (r) direction is implicit. Therefore, large radial power variations do not create any numerical difficulties. Differencing in the axial (z) direction is explicit to simplify the computations and to

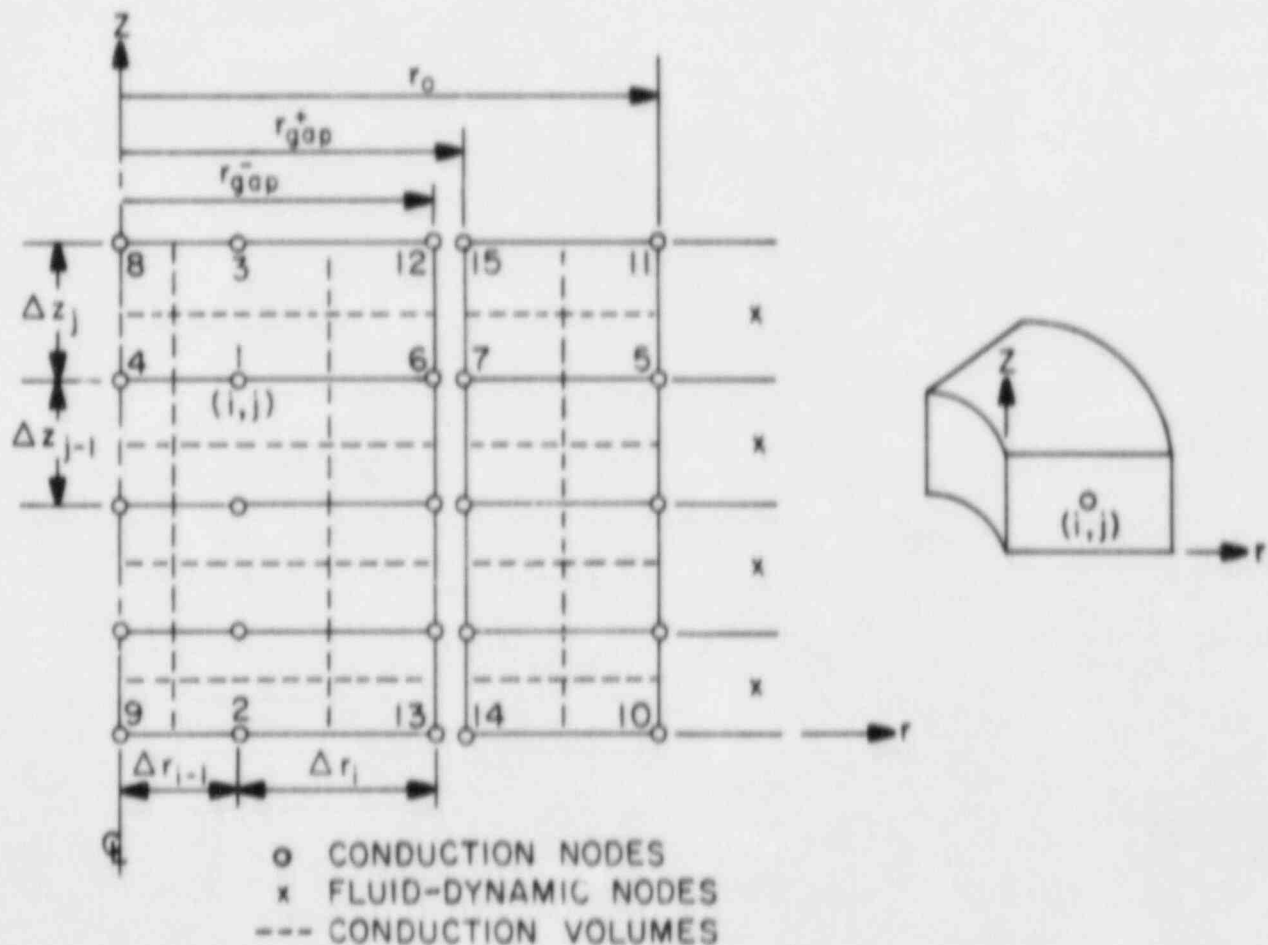


Fig. 5.
Rod geometry.

reduce computer costs. The explicit differencing does limit the minimum axial spacing between nodes for a given time increment. However, this spacing is orders of magnitude less than that used by the fluid-dynamics calculations. The resulting finite-difference equations form a tridiagonal matrix for each row (z fixed) within the rod. The temperature distribution is obtained by using Gaussian elimination on each row in a sequential manner.

Consider a general differential volume (that is, the volume labeled l in Fig. 5). The finite-difference equation for this volume is

$$\begin{aligned}
 & [(\rho c_p)_{lj}] \frac{T_{lj}^{n+1} - T_{lj}^n}{\Delta t} - \dot{q}_{lj}^{\prime\prime} \frac{1}{2} \left[(r_l \Delta r_l + \frac{\Delta r_l^2}{4}) + (r_l \Delta r_l - \frac{\Delta r_{l-1}^2}{4}) \right] \times \left[\frac{\Delta z_j + \Delta z_{j-1}}{2} \right] \\
 & = [r_{l+1/2} k_{l+1/2, j}] \left(\frac{T_{l+1, j}^{n+1} - T_{lj}^{n+1}}{\Delta r_l} \right) + [r_{l-1/2} k_{l-1/2, j}] \left(\frac{T_{l-1, j}^{n+1} - T_{lj}^{n+1}}{\Delta r_{l-1}} \right) \\
 & \times \left(\frac{\Delta z_j + \Delta z_{j-1}}{2} \right) + [k_{l, j+1/2}] \left(\frac{T_{l, j+1}^n - T_{lj}^n}{\Delta z_j} \right) + [k_{l, j-1/2}] \left(\frac{T_{l, j-1}^n - T_{lj}^n}{\Delta z_{j-1}} \right) \\
 & \times \frac{1}{2} \left[(r_l \Delta r_l + \frac{\Delta r_l^2}{4}) + (r_l \Delta r_{l-1} - \frac{\Delta r_{l-1}^2}{4}) \right] , \tag{89}
 \end{aligned}$$

where

$$f_{lj}^n \equiv f(t^n, r_l, z_j).$$

It should be observed that the locations of nodes within the volumes located at the boundaries differ (Fig. 5). This difference should be considered when assigning values for the relative power densities at each node.

The boundary conditions applied to the vessel rods are:

- the top ($z = z_u$) and bottom ($z = z_l$) of the rods are assumed to be insulated,

$$k \frac{\partial T}{\partial z} \Big|_{z = z_l, z_u} = 0 ;$$

- the rod center line ($r = 0$) is a line of symmetry,

$$\frac{\partial T}{\partial r} \Big|_{r = 0} = 0 ; \text{ and}$$

- heat transfer at the inner and outer gap surfaces ($r = r_{\text{gap}}^-, r_{\text{gap}}^+$) and at the clad surface ($r = r_o$) is specified using Newton's law,

$$k \frac{\partial T}{\partial r} \Big|_{r = r_{\text{gap}}^{\pm}} = - h_{\text{gap}}^{\pm} (T_{r_{\text{gap}}^-} - T_{r_{\text{gap}}^+}) \text{ and}$$

$$k \frac{\partial T}{\partial r} \Big|_{r = r_o} = - h_{\text{fluid}} (T_{r_o} - T_{\text{fluid}}) ,$$

where $h_{\text{gap}}^+ = h_{\text{gap}}^- (r_{\text{gap}}^- / r_{\text{gap}}^+)$ to conserve energy.

All properties (that is, ρ , c_p , and k) required by the difference equations are stored at the node locations. Linear interpolation is used to obtain properties between nodes (that is, at cell surfaces). A node located at the interface between two dissimilar materials requires two sets of properties. Consider the differential volume provided in Fig. 6. Application of an integral technique to this volume results in the differential equation (after dividing through by the volume),

$$\begin{aligned}
 \overline{(\rho c_p)}_{ij} \left(\frac{T_{ij}^{n+1} - T_{ij}^n}{\Delta t} \right) - \dot{q}_{ij} = & [r_{i+1/2} k_{i+1/2,j} \left(\frac{T_{i+1,j}^{n+1} - T_{ij}^{n+1}}{\Delta r_i} \right) \\
 & + r_{i-1/2} k_{i-1/2,j} \left(\frac{T_{i-1,j}^{n+1} - T_{ij}^{n+1}}{\Delta r_{i-1}} \right)] \left[\frac{(r_i \Delta r_i + \frac{\Delta r_i^2}{4}) + (r_i \Delta r_{i-1} + \frac{\Delta r_i^2}{4})}{2} \right]^{-1} \\
 & + [k_{i,j+1/2} \left(\frac{T_{i,j+1}^n - T_{ij}^n}{\Delta z_j} \right) + k_{i,j-1/2} \left(\frac{T_{i,j-1}^n - T_{ij}^n}{\Delta z_{j-1}} \right)] \left[\frac{\Delta z_j + \Delta z_{j-1}}{2} \right]^{-1}, \quad (90)
 \end{aligned}$$

where

$$\overline{(\rho c_p)}_{ij} \equiv \frac{[(\rho c_p)_{i^+,j} R^+ + (\rho c_p)_{i^-,j} R^-]}{R^+ + R^-}$$

and

$$\overline{k}_{i,j+1/2} \equiv \frac{[k_{i^+,j+1/2} R^+ + k_{i^-,j+1/2} R^-]}{(R^+ + R^-)}.$$

In the above equations,

$$R^+ \equiv \left(r_i + \frac{\Delta r_i}{4} \right) \frac{\Delta r_i}{2} \quad \text{and} \quad R^- \equiv \left(r_i - \frac{\Delta r_{i-1}}{4} \right) \frac{\Delta r_{i-1}}{2}. \quad (91)$$

The superscript + (-) refers to the material to the right (left) of the interface.

(2) Reflood Algorithm. The reflood phase of a postulated LOCA is characterized by a sequence of heat-transfer and two-phase flow regimes advancing rapidly through the vessel core. A correct prediction of the thermal response of the rods during reflood requires a numerical technique that can model the rewetting phenomena associated with the quench-front motion.

The leading edge of the rewetting region is characterized by large variations of temperatures and heat fluxes within small axial distances ($\Delta z \sim 1 \text{ mm}$).²⁴ The front advancement is controlled by two heat removal mechanisms, the first being axial conduction from the dry region ahead of the quenched region to the wetted region behind the advancing film. The second is the precursory rod cooling associated with heat transfer to the droplets entrained in the advancing vapor field. The rod conduction model contains the necessary physics to analyze such phenomena. The need remains to define an algorithm capable of resolving the large gradients.

When reflood begins, supplemental rows of conduction nodes (Fig. 7) are inserted in the rod. The number of rows inserted within each fluid level is user specified. The rows are uniformly spaced (that is, z is constant) within

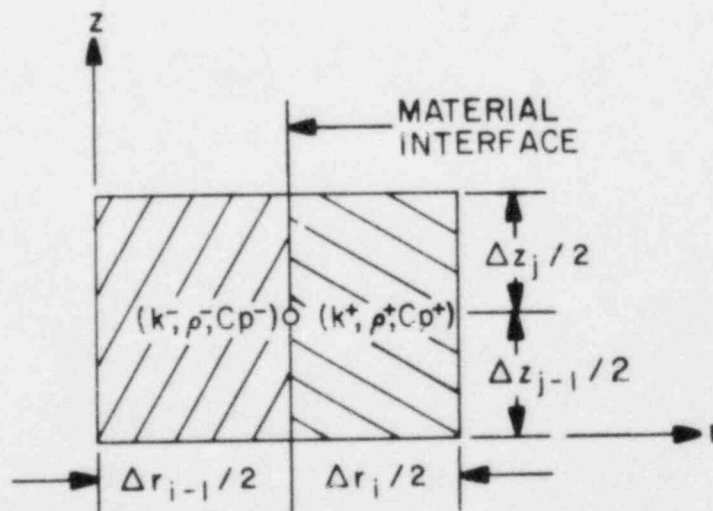
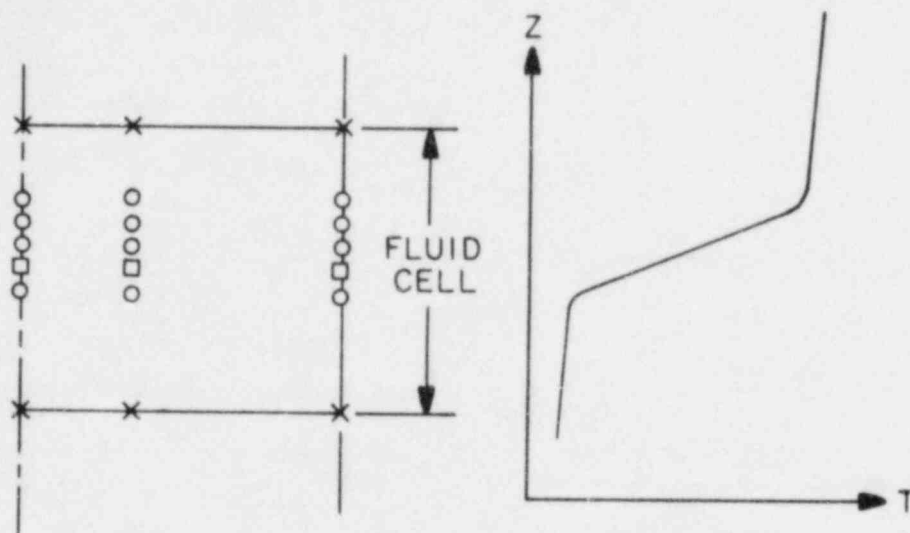


Fig. 6.

Node located at the interface between two dissimilar materials.



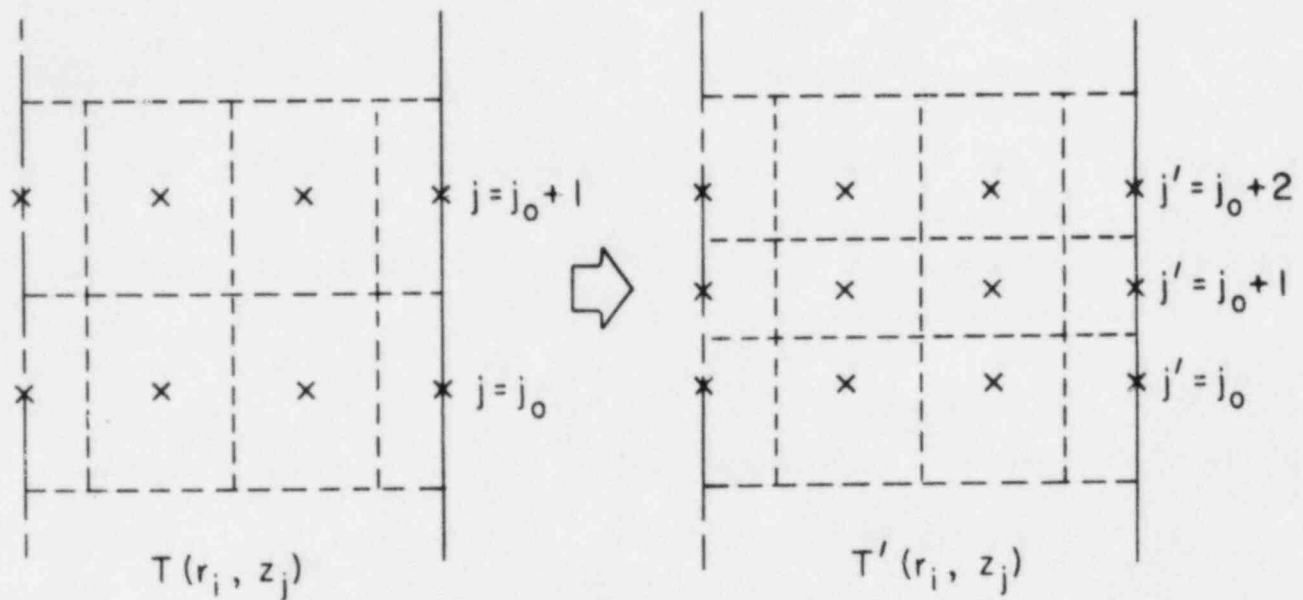
- × ORIGINAL CONDUCTION NODES (PERMANENT)
- NODES ADDED AT THE START OF REFLOOD (PERMANENT)
- NODES ADDED TO RESOLVE THE QUENCH FRONT (TRANSITORY)

Fig. 7.
Fine-mesh rezoning.

each fluid level. The temperature values at the supplemental nodes are determined from a three-point Lagrangian interpolation technique. The interpolation is normalized to conserve the total energy of the rod. The nodes added in this fashion remain during the entire reflood phase.

To model the inherently nonstationary, Lagrangian quench-front motion and to resolve the related thermal gradients, a fine-mesh rezoning technique²⁵ is used during the reflood conduction calculations. The axial gradients encountered within the rewetting region are resolved by the insertion of rows of stationary nodes (Fig. 7). These additional transitory nodes are added whenever the temperature difference between adjacent rod surface nodes exceeds a user-specified value (T_{\max}). The temperatures assigned to the nodes are required to conserve energy (Fig. 8),

$$\sum_{j=j_0}^{j_0+2} \rho_{ij} c_{p_{ij}} T_{ij} V_{ij} = \sum_{j=j_0}^{j_0+1} \rho_{ij} c_{p_{ij}} T_{ij} V_{ij}; \quad i = 1, \dots, \text{nodes} \quad (92)$$



x CONDUCTION NODES
 --- CONDUCTION VOLUMES

Fig. 8.
 Insertion of conduction nodes during reflood.

The primed quantities denote rod properties after the nodes have been added. The values of ρ' , c_p' , and T' at the original node locations are set equal to their original values. After the quench front has progressed beyond the location of the inserted rows and the surface temperature difference falls below a prescribed value (ΔT_{\min}), the transitory nodes are eliminated. Temperatures at nodes axially adjacent to those deleted retain their original values. For small ΔT_{\min} , this results in a negligible effect on the total energy of the rod.

Two values for ΔT_{\max} are specified by the user. The first and smaller value is applied to the part of the rewetting region that is in a nucleate or transitional boiling regime. The largest wall heat fluxes occur in these heat-transfer regimes. The second ΔT_{\max} value is applied to all other heat-transfer regimes. The ΔT_{\min} values are computed internally based on the specified values for ΔT_{\max} .

The above algorithm can analyze multiple quench fronts simultaneously. Both quenching and dryout are modeled automatically.

During the reflood phase, a number of surface conduction nodes are located within each fluid-dynamics cell. Therefore, it is necessary to calculate an effective wall-temperature and heat-transfer coefficient for use in the fluid-dynamics computations. These values are obtained by ensuring the conservation of the total energy transferred to the fluid within each cell. Values applied to the liquid phase that satisfy this criteria are

$$h_{\ell} \equiv \frac{\sum_j h_{\ell j} A_j}{\sum_j A_j}$$

and

$$T_{w\ell} \equiv \frac{\sum_j h_{\ell j} A_j T_j}{\sum_j h_{\ell j} A_j},$$

where the sum is taken over all surface nodes in each fluid cell. Similar values are used in the vapor phase.

It already has been pointed out that for a given time step (Δt) a minimum spacing (Δz) between rows of conduction nodes exists because of the explicit axial differencing. For reflood calculations this axial spacing can be violated, resulting in stability problems. To avoid such problems, the time step is limited internally by a diffusion number. The user also can specify minimum spacing (Δz_{\min}) beyond which supplemental rows of conduction nodes will not be added. This additional advantage can prevent excessively large computer costs.

Computing costs are reduced further by calculating material properties only at those nodes located at the edges of the fluid cells. Linear interpolation is used to obtain the properties at any additional locations required by the reflood calculations. Heat-transfer coefficients, however, are obtained directly from the boiling curve for all rod surface nodes.

(3) Fuel-Clad Gap Conductance. Two options are available in TRAC-PF1 for the fuel-clad gap conductance. If the input variable NFCI = 0, a constant input value for the gap conductance is used throughout the entire calculation. If the input variable NFCI = 1, the input value for the gap conductance becomes the initial value and a thermal-expansion model is used to calculate the transient gap conductance.

Subroutine GAPHT calculates the gap heat-transfer coefficient (h_{gap}) as a function of three components: gap gas conductance, fuel-clad interfacial contact, and fuel-clad thermal radiation;

$$h_{\text{gap}} = h_{\text{gas}} + h_{\text{contact}} + h_{\text{radiation}} \quad , \quad (93)$$

where

$$h_{\text{gas}} = \frac{k_{\text{gas}}}{\Delta r_{\text{gap}} + \delta} \quad , \quad (94)$$

$$h_{\text{radiation}} = \frac{\sigma F(T_f^4 - T_c^4)}{(T_f - T_c)} \quad , \quad (95)$$

and

$$F = \frac{1}{\frac{1}{\epsilon_f} + \frac{R_f}{R_c} \left(\frac{1}{\epsilon_c} - 1 \right)} \quad . \quad (96)$$

Subscripts f and c refer to fuel and clad, respectively, and σ is the Stefan-Boltzmann constant. A value of 4.4×10^{-6} m is used for δ , which includes the mean fuel surface roughness of the fuel and clad and the temperature jump distances.^{26,27} The contact conductance, h_{contact} , is zero in the present code.

The fuel-clad radial gas gap, Δr_{gap} , is found by using the uncoupled, quasi-static approximation.²⁸ In this approximation the mechanical coupling term in the energy equation and the inertial term in the mechanical force balance are omitted. Neglect of these terms assumes that the influence of the

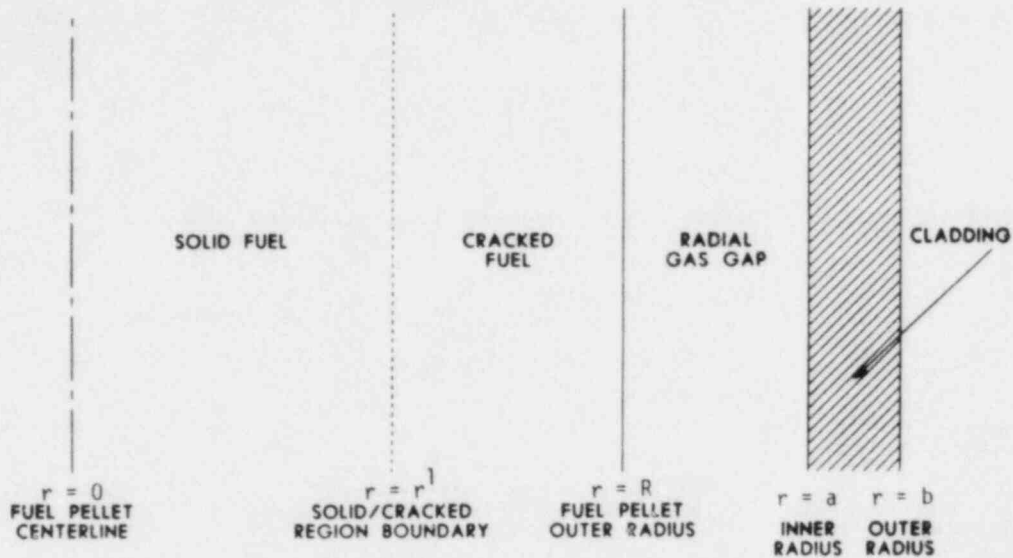


Fig. 9.
Fuel-rod geometry.

strains in the fuel and clad on the temperature distribution is small and that displacements are instantaneous. Figure 9 shows the fuel-clad gap system modeled in three regions: solid fuel, cracked fuel, and clad. Gap changes are found by calculating the radial displacement of each region caused by thermal expansion.

The calculations for the deformation of a hollow or solid circular cylindrical body of outer radius b and of height h are given in Ref. 28 for the case of plane strain where the ratio h/b is large compared to unity. Other assumptions are made that the cylindrical surfaces are free of forces and that axial displacement is allowed. Because the uncoupled, quasi-static approximation is used, the temperature distributions are assumed to be known from the energy balance. The radial displacement u is given by

$$u(r) = \frac{\alpha}{r(1-\nu)} \left[(1+\nu) \int_a^r T r \, dr + \frac{(1-3\nu)r^2 + a^2(1+\nu)}{b^2 - a^2} \int_a^b T r \, dr \right], \quad (97)$$

where a is the inner radius of a cylindrical shell, ν is Poisson's ratio, and α is the linear thermal-expansion coefficient. Equation (97) is used to

calculate the radial displacement of the clad inner radius and solid fuel radius, $r = a$ and $r = r'$, respectively. The results are

$$u(a) = \frac{2\alpha_c a}{b^2 - a^2} \int_a^b T_c r \, dr \quad (98)$$

and

$$u(r') = \frac{2\alpha_f}{r'^2} \int_0^{r'} T_i r \, dr \quad (99)$$

The clad inner radius and solid fuel radius after thermal expansion will be

$$a_{\text{new}} = a + u(a) \quad (100)$$

and

$$r'_{\text{new}} = r' + u(r') \quad (101)$$

A parabolic radial temperature distribution is assumed across the fuel pellet,

$$T_f = T_{cl} + \frac{(T_{\text{surf}} - T_{cl})r^2}{R^2}, \quad (102)$$

where T_{cl} is the fuel center-line temperature and T_{surf} is the fuel surface temperature. A linear temperature profile is assumed across the clad,

$$T = \frac{(T_{co} - T_{cl})(r - a)}{b - a} + T_{cl}, \quad (103)$$

where T_{co} and T_{ci} are the clad outside and inside temperatures, respectively, and a and b are the clad inside and outside radii.

The following equation is used for the cracked fuel thickness;

$$t = t_0 \left(1 + \frac{\alpha_f}{R - r'} \int_{r'}^R T_f dr \right) , \quad (104)$$

where t_0 is the initial undeformed radial thickness of the cracked fuel,

$$t_0 = R - r' . \quad (105)$$

The radial gap width after thermal expansion will be

$$\text{gap width} = a_{\text{new}} - (r'_{\text{new}} + t) , \quad (106)$$

or

$$\begin{aligned} \text{gap width} = & (a - r') + \frac{2\alpha_c a}{b^2 - a^2} \int_a^b T_c r dr - \frac{2\alpha_f}{r'} \int_0^{r'} T_f r dr \\ & - t_0 \left[1 - \frac{\alpha_f}{R - r'} \int_{r'}^R T_f dr \right] . \end{aligned} \quad (107)$$

The fuel-clad radial spacing is evaluated in subroutine DELTAR.

(4) Metal-Water Reaction. When sufficiently high temperatures are reached by Zircaloy in a steam environment, an exothermic reaction may occur that will influence the peak cladding temperatures. The zirconium-steam reaction equation is



Given sufficient steam, the reaction rate equation^{29,30} is assumed valid:

$$\tau \frac{d\tau}{dt} = A \exp\left(-\frac{B}{T}\right), \quad (109)$$

where τ = total oxygen consumed (kg/m^2), $A = 16.8 \text{ kg}^2/\text{m}^4\text{s}$, and $B = 2.007 \times 10^4 \text{ K}$.

The kinetic parameter τ is converted to an effective zirconium-oxide layer thickness according to

$$1.5(R_o - r) = \frac{\tau}{0.26\rho_{\text{ZrO}_2}}, \quad (110)$$

where

r = reacting surface radius (m),

R_o = clad outer radius (m), and

ρ_{ZrO_2} = density of zirconium oxide (kg/m^3).

Equation (110) is based on a reacted material volume expansion of 50% in the radial direction. This assumption leads to $\rho_{\text{ZrO}_2} = 0.90\rho_{\text{Zr}}$. Equation (110) allows Eq. (109) to be rewritten as

$$\tau \frac{d\tau}{dt} = -C(R_o - r) \frac{dr}{dt},$$

where $C = (0.351\rho_{\text{Zr}})^2$.

The method outlined in Ref. 29 is used to calculate the zirconium-oxide penetration depth and associated heat source. The mass per unit length of zirconium (m_{ZR}') consumed by the reaction in one time step is

$$m_{Zr}^{\dot{}} = \pi \rho_{Zr} [(r^n)^2 - (r^{n+1})^2] \quad (111)$$

Equation (109) is used to calculate r^{n+1} , yielding

$$r^{n+1} = R_o - [(R_o - r^n)^2 + 2 \frac{A}{C} \Delta t \exp(-\frac{B}{T})]^{1/2} \quad (112)$$

Assuming a one-region clad, the heat source ($\dot{q}_{mw}^{\dot{}}$) added to the conduction equations is

$$\dot{q}_{mw}^{\dot{}} = 6.45 \times 10^6 m_{Zr}^{\dot{}} [\Delta t (R_o^2 - R_i^2)\pi]^{-1} \quad (113)$$

where R_i is the inner clad radius and 6.45×10^6 J/kg corresponds to the energy released per kilogram of oxidized zirconium.

2. Wall-to-Fluid Heat Transfer. The wall-to-fluid HTC's are obtained from a generalized boiling curve constructed within subroutine HTCOR. The HTC correlations in HTCOR are used by all TRAC components under all conditions. Figure 10 shows a portion of the boiling curve, which is not dependent on the flow regime. The single-phase vapor and condensation regimes are not shown in this figure.

The individual correlations used for each heat-transfer regime and the method of partitioning the energy between the two phases are discussed in this section. We have tried to make the boiling curve continuous between regimes; thus, we also discuss our methods to smooth the boiling curve.

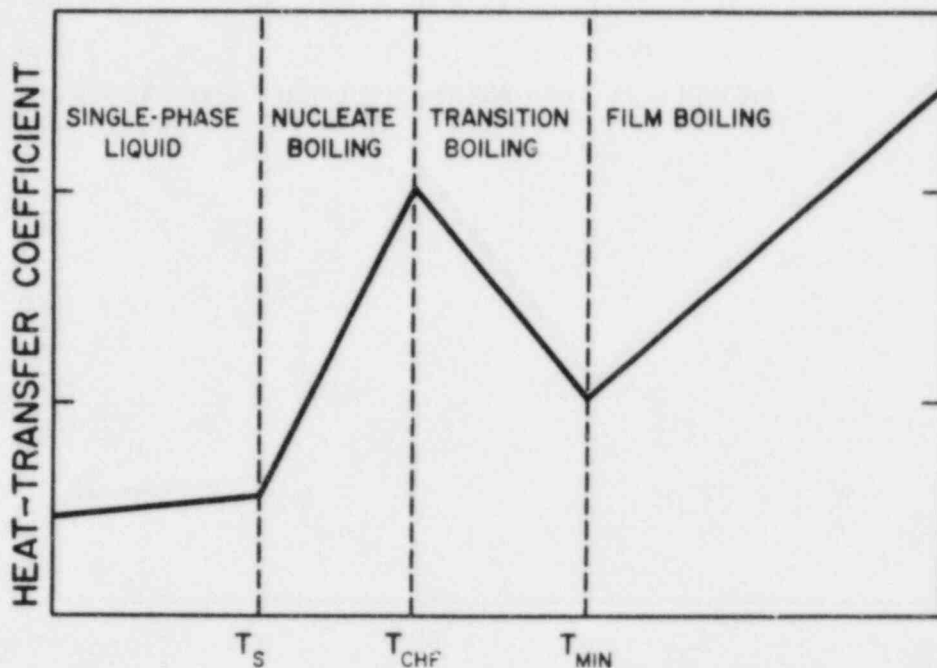


Fig. 10.
TRAC-PF1 boiling curve.

a. Wall-to-Fluid HTC Selection Logic. The HTC selection logic is outlined in the flow chart shown in Fig. 11. The following sequence, corresponding to the numbers on the left side of Fig. 11, is used. If one step is not satisfied, then the next step is examined.

Step 1. Initialize subroutine HTCOR by calculating absolute values, the slip, and the flow and equilibrium qualities. If the slip is less than or equal to zero in HTCOR, it is set equal to 1.0.

Step 2. If $T_w < T_\ell$, $T_w < T_s$ and the void fraction is greater than 0.05, the heat transfer is in the condensation regime. The Chen correlation,³¹ discussed in Sec. III.B.2.b.(2), is used in this regime with the suppression factor S set equal to zero. If the equilibrium quality, $x \equiv x_e$, is greater than 0.71, the limit of Chen's data base, then the Chen correlation is evaluated at $x = 0.71$. This gives h_ℓ , with $h_g = 0$. Linear interpolation is used between these values and the single-phase vapor HTCs ($h_g = 0$).

Step 3. If $x_e \geq 1$, a single-phase vapor HTC is calculated.

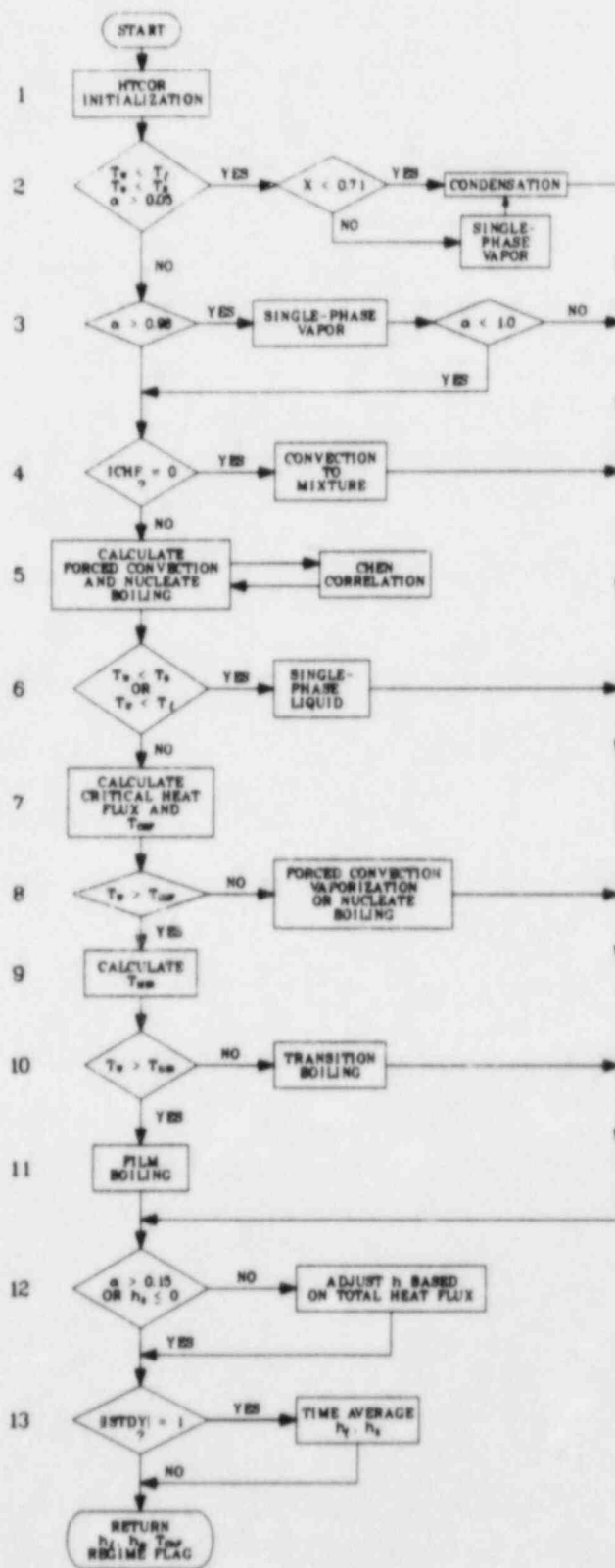


Fig. 11.
Heat-transfer coefficient correlation selection logic.

Step 4. When the void fraction, α , is greater than 0.98, linear interpolation is used between the HTC's from the appropriate heat-transfer regime and the single-phase vapor values. The h_ℓ is interpolated between $0.98 \leq \alpha \leq 0.999$; the h_g is interpolated between $0.98 \leq \alpha \leq 1.0$.

Step 5. When the input variable $ICHF = 0$, the boiling curve is not used to determine the liquid and vapor HTC's. These values are obtained from the two-phase mixture equations only (heat-transfer regime 7), as described in Sec. III.B.2.b.(7).

Step 6. The forced convection and nucleate boiling HTC's are calculated by using the Chen correlation. At this point the heat-transfer regime has not been determined.

Step 7. If $T_w < T_\ell$ or $T_w < T_s$, the heat-transfer regime is single-phase liquid.

Step 8. The input variable $ISTDY$ determines whether a steady-state or a transient calculation is being made. For steady-state conditions, $ISTDY = 1$; otherwise, $ISTDY = 0$. When a steady-state calculation is being made, the only heat-transfer regimes available are single-phase liquid, nucleate boiling, single-phase vapor, or condensation. Critical heat flux is not allowed during steady state.

Step 9. The critical heat flux (CHF) and the corresponding temperature, T_{CHF} , are calculated next.

Step 10. If $T_w < T_{CHF}$, nucleate boiling exists.

Step 11. The minimum stable film boiling temperature, T_{min} , is calculated by using the homogeneous nucleation model ($ITMIN = 0$) or by using the maximum of the homogeneous nucleation and the Iloeje T_{min} values ($ITMIN = 1$). These correlations are discussed in Sec. III.B.2.d.

Step 12. If $T_w < T_{min}$, transition boiling exists. It previously has been determined that T_w is greater than the temperature at CHF conditions (Step 10).

Step 13. If $T_w > T_{min}$, film boiling is occurring.

Step 14. The HTC's are restricted to zero or to positive values. (For $\alpha > 0.999$, extrapolation occurs and a negative h_ℓ could result. See Step 4.) For $\alpha < 0.15$, the vapor heat flux is interpolated linearly from its value at $\alpha = 0.15$ to a value of 0.0 at $\alpha = 0.01$. The liquid heat flux is adjusted so that the total heat flux remains unchanged. Then h_ℓ and h_g are recalculated

from the adjusted heat fluxes and the known temperature differences. This prevents an extremely small mass of vapor from becoming superheated to an unrealistic value.

Step 15. The HTC's are averaged between the current time step and the previous time step.

b. HTC Correlations. In this section we discuss the HTC correlations used in the construction of the boiling curve. In addition, the correlation used for $ICHF = 0$ is discussed. Because TRAC is a nonequilibrium code, HTC's are needed for the liquid and the vapor phases; this partitioning of energy between the phases is discussed also. The heat-transfer regimes available in TRAC are shown in Fig. 12.

(1) Single-Phase Liquid (Heat-Transfer Regimes 1 and 12). Either forced convection (regime 1) or natural convection (regime 12) can occur when single-phase liquid is present. Forced convection correlations are used when the ratio of the Grashof number to the Reynolds number squared is less than or

IDREG (IHTE)	WALL-TO-FLUID HEAT-TRANSFER REGIME
1	FORCED CONVECTION TO SINGLE-PHASE LIQUID
2	NUCLEATE BOILING
3	TRANSITION BOILING
4	FILM BOILING
6	CONVECTION TO SINGLE-PHASE VAPOR
7	CONVECTION TO TWO-PHASE MIXTURE
11	CONDENSATION
12	LIQUID NATURAL CONVECTION

Fig. 12.
TRAC-PF1 heat-transfer regimes.

equal to 1.0. Laminar or turbulent forced convection correlations are available. These equations are contained in subroutine CHEN because they constitute one part of the Chen correlation. The laminar equation⁹ is

$$h_{\ell} = 4.0 \frac{k_{\ell}}{D_h} \quad (114)$$

The turbulent HTC is found from the Dittus-Boelter equation,²⁶

$$h_{\ell} = 0.023 \frac{k_{\ell}}{D_h} Re_{\ell}^{0.8} Pr_{\ell}^{0.4} \quad (115)$$

where the liquid Reynolds number is

$$Re = \frac{\rho_{\ell} V_{\ell} D_h}{\mu_{\ell}} \quad (116)$$

and the liquid Prandtl number is

$$Pr_{\ell} = \left(\frac{u_c p}{k} \right)_{\ell} \quad (117)$$

Note that all the properties are evaluated at T_{ℓ} . The maximum of Eqs. (114) and (115) is set equal to the single-phase-liquid forced convection heat-transfer coefficient, HFORC. In heat-transfer regime 1, the Chen F factor is set equal to 1.0.

In heat-transfer regime 12, natural convection to single-phase liquid, the maximum of the laminar and turbulent correlations for vertical flat plates and cylinders is used.³² For laminar flow, the equation is

$$\text{Nu} = 0.59 (\text{Gr Pr})^{0.25} ; \quad (118a)$$

for turbulent flow,

$$\text{Nu} = 0.10 (\text{Gr Pr})^{0.3333} ; \quad (118b)$$

where the Grashof number is

$$\text{Gr} = \frac{g\beta|T_w - T_\ell|\rho_f^2 D_h^3}{\mu^2} , \quad (119)$$

the Prandtl number is

$$\text{Pr} = \left(\frac{\mu c_p}{k}\right)_\ell , \quad (120)$$

and the Nusselt number is

$$\text{Nu} = \frac{h_\ell D_h}{k_\ell} . \quad (121)$$

The maximum of the laminar and turbulent Nusselt numbers is used. To avoid extra calls to the thermodynamic property subroutine, THERMO, all the properties are evaluated at T_ℓ except the density, ρ_f , and the volume coefficient of expansion, β ; these are evaluated by using a Taylor series expansion about T_ℓ ,

$$\rho_f = \rho_l + \frac{\partial \rho_l}{\partial T} (T_f - T_l) , \quad (122)$$

$$\beta = - \frac{\partial \rho_l}{\partial T} \frac{1}{\rho_f} , \quad (123)$$

and

$$T_f = \frac{1}{2} (T_w + T_l) . \quad (124)$$

Two points should be noted about heat-transfer regimes 1 and 12. First, because only single-phase liquid is assumed present, the vapor heat-transfer coefficient, h_g , is set equal to zero. Second, in Eq. (118a) the hydraulic diameter, D_h , is used for the characteristic length even though the axial distance would be more appropriate. This was done because the axial length would approach zero near the bottom of a channel. The characteristic length drops out of Eq. (118b) and appears only to the -0.25 power in Eq. (118a). Thus, the choice of the characteristic length has a small effect on the HTC.

(2) Nucleate Boiling HTCs (Heat-Transfer Regime 2). The Chen correlation³¹ is used in heat-transfer regime 2, nucleate boiling. In addition, the nucleate-boiling HTC correlation affects the transition boiling regime through the interpolation between the CHF and the minimum stable film boiling points.

The Chen correlation is composed of two parts, a forced convection term multiplied by the Reynolds F factor and a nucleate boiling term that contains the suppression factor, S; here,

$$h_l = h_{forc} + \min \left(1, \frac{T_w - T_s}{T_w - T_l} \right) h_{nucb} , \quad (125)$$

where h_{forc} (HFORC in the code), with the F factor equal to 1.0, was discussed in the previous section, and the nucleate boiling term is given by

$h_{nucb} =$

$$0.00122 \frac{k_l^{0.79} c_{pl}^{0.45} \rho_l^{0.49}}{\sigma^{0.5} \mu^{0.29} h_{lg}^{0.24} \rho_g^{0.24}} (T_w - T_s)^{0.24} (p_w - p)^{0.75} S, \quad (126)$$

where p_w is the saturation pressure corresponding to the wall temperature and F and S are functions that are given in graphical form by Chen. The Reynolds number factor, F , can be expressed³³ as

$$F = 1.0, \quad \text{for } \chi_{TT}^{-1} \leq 0.10; \quad (127)$$

and

$$F = 2.35 (\chi_{TT}^{-1} + 0.213)^{0.736}, \quad \text{for } \chi_{TT}^{-1} > 0.10; \quad (128)$$

where χ_{TT}^{-1} , the Lockhart-Martinelli factor, is

$$\chi_{TT}^{-1} = \left(\frac{x}{1-x} \right)^{0.9} \left(\frac{\rho_c}{\rho_g} \right)^{0.5} \left(\frac{\mu_g}{\mu_l} \right)^{0.1}. \quad (129)$$

The value of χ_{TT}^{-1} is restricted to a value less than 100.0.

The suppression factor, S ,³³ can be expressed as

$$S = [1 + 0.12 (\text{Re}_{tp})^{1.14}]^{-1}, \quad \text{for } \text{Re}_{tp} < 32.5;$$

or

$$S = [1 + 0.42 (\text{Re}_{tp})^{0.78}]^{-1}, \quad \text{for } 32.5 \leq \text{Re}_{tp} \leq 70.0; \quad (130)$$

where

$$Re_{tp} = \frac{10^{-4} |V_\ell| \rho_\ell (1 - \alpha)}{\mu_\ell} D_h F^{1.25} \quad . \quad (131)$$

The value of Re_{tp} is restricted to a value less than 70.0.

The above correlations for the suppression factor do not approach the correct limit (zero) as the void fraction approaches one. In the above equations, $S \rightarrow 1.0$ as $\alpha \rightarrow 1.0$. The following procedure is used to ensure that S approaches the correct limit. For $\alpha > 0.70$, S is calculated at $\alpha_s = 0.70$ and at the current value of α and the minimum value of the two suppression factors, S_{min} , is saved. Linear interpolation is then used between S_{min} and $S = 0$ at $\alpha = \alpha_c$,

$$S = \frac{S_{min} (\alpha_c - \alpha)}{\alpha_c - \alpha_s} \quad .$$

In TRAC-PF1, $\alpha_c = 0.98$ and $\alpha_s = 0.70$. For $\alpha > \alpha_c$, $S = 0.0$.

The properties are evaluated at the liquid and vapor temperatures; x is the equilibrium quality and V_ℓ is the liquid velocity parallel to the surface. Because the nucleate boiling contribution to the Chen correlation was developed for saturated conditions,³¹ h_{nucb} is multiplied by a temperature ratio to adjust the HTC to the actual T_ℓ , Eq. (125). Because TRAC can calculate superheated liquids, the adjustment factor is restricted to a maximum of 1.0 so that the adjustment is made for subcooled liquid only.

The vapor HTC goes from zero at $T_w = T_s$ to the transition boiling value at $T_w = T_{CHF}$ [Sec. III.B.2.b.(3)]; thus,

$$h_g = \left(\frac{T_w - T_s}{T_{CHF} - T_s} \right)^2 \max (h_{fbb}, h_{nc}, h_{dr}) \quad ,$$

where h_{fbb} , h_{nc} , and h_{dr} are the Bromley, natural convection, and Dougall-Rohsenow HTCs, respectively. The vapor HTC is calculated in subroutine

HVFILM. For a void fraction greater than a cutoff value, α_c , linear interpolation is used between the current values of h_l and h_g and the values that are calculated for single-phase vapor; that is, $h_l = 0$ and h_g , calculated as discussed in Sec. III.B.2.b.(5). This linear interpolation ensures that the boiling curve is smooth between heat-transfer regimes.

(3) Transition Boiling HTC's. (Heat-Transfer Regime 3). Transition boiling may be considered as a combination of nucleate and film boiling. A given spot on the wall surface is wet part of the time and dry during the remainder of the time. Therefore, contributions to the liquid and vapor HTC's exist for all conditions.

The total wall-to-fluid heat flux is obtained from a quadratic interpolation between the CHF and the minimum stable film boiling points,³³

$$q_{\text{trans}} = \delta q_{\text{CHF}}'' + (1.0 - \delta) q_{\text{min}}'' , \quad (132)$$

where q_{CHF}'' is the heat flux at CHF conditions, found from the Biasi correlation (Sec. III.B.2.c), and q_{min}'' is the heat flux at the minimum stable film boiling point; that is, the intersection of the transition and the film boiling points. This point is found from the homogeneous nucleation correlation, as discussed in Sec. III.B.2.d. Delta is a function of the wall temperature and the temperatures corresponding to q_{CHF}'' and q_{min}'' ,

$$\delta = \left(\frac{T_w - T_{\text{min}}}{T_{\text{CHF}} - T_{\text{min}}} \right)^2 . \quad (133)$$

The vapor HTC is

$$h_g = \max (h_{\text{fbb}}, h_{\text{nc}}, h_{\text{DR}}) ,$$

These correlations are discussed in the next section.

As in the nucleate boiling heat-transfer regime, linear interpolation is used for $\alpha > \alpha_c$. The liquid HTC is

$$h_\ell = \frac{q_{\text{trans}} - h_g (T_w - T_g)}{T_w - T_\ell} .$$

(4) Film Boiling HTCs (Heat-Transfer Regime 4). In the film boiling heat-transfer regime, radiative heat transfer and dispersed-flow heat transfer occur between the surface and the liquid; convective heat transfer occurs between the wall and the adjacent vapor. The liquid HTC is given by

$$h_\ell = h_r \left(\frac{T_w - T_s}{T_w - T_\ell} \right) + h_{df} ,$$

where h_{df} is the dispersed flow HTC.

The radiative contribution is

$$h_r = (1 - \alpha)\sigma\epsilon \left(\frac{T_w^4 - T_s^4}{T_w - T_s} \right) , \quad (134)$$

where σ is the Stefan-Boltzmann constant and ϵ is the wall emissivity. In Eq. (134) the liquid absorptivity is 1.0.

The dispersed flow HTC, h_{df} , uses the Forslund and Rohsenow equation,³⁴ modified by multiplying $(1 - \alpha)$ by the fraction of liquid entrained, E ; thus,

$$h_{df} = 0.2 c_1 [(1 - \alpha)E]^{0.6667} \text{BRAC}^{0.25} \left(\frac{T_w - T_s}{T_w - T_\ell} \right) , \quad (135)$$

where c_1 is a constant equal to 1.2760 and

$$\text{BRAC} = \frac{g \rho_l \rho_g h_l k^3}{|T_w - T_s| \mu_g d_{\text{drop}}} .$$

The dispersed flow HTC is set equal to zero if $(1 - \alpha)E > 0.05$.

Equation (135) is multiplied by the temperature ratio to change the base of the HTC from T_s to T_l . The droplet diameter, d_{drop} , is found from a Weber number criterion of 4.0.

$$d_{\text{drop}} = \frac{We \sigma}{\rho_g (V_g - V_l)^2} .$$

The droplet diameter is restricted to the range,

$$1.0 \times 10^{-4} \leq d_{\text{drop}} \leq 3.0 \times 10^{-3} .$$

The fraction of liquid entrained is found in the following manner;

$$E = 0 , \quad \text{if } |V_g| \leq V_E ;$$

or

$$E = 1.0 - \exp 0.23 [- (|V_g| - V_E)] , \text{ if } |V_g| > V_E ,$$

where the entrainment velocity is

$$V_E = 3.65 \left[\frac{(\rho_l - \rho_g) \sigma}{2 \rho_g} \right]^{1/4}$$

and E is restricted to values between 0.07 and 1.0.

The vapor HTC is the maximum of the Bromley, natural convection, and Doughall-Rohsenow values,

$$h_g = \max (h_{fbb}, h_{nc}, h_{DR}) \quad (136)$$

The Bromley³⁵ film boiling HTC is h_{fbb} .

$$h_{fbb} = 0.62 \left[\frac{\rho_g k_g^3 (\rho_l - \rho_g) g \tilde{h}_{lg}}{\mu_g (T_w - T_s) \lambda} \right]^{1/4} \quad (137)$$

where the characteristic length, λ , is

$$\lambda = 2\pi \left[\frac{\sigma}{g(\rho_l - \rho_g)} \right]^{1/2} .$$

The latent heat of vaporization is modified as suggested in Ref. 36 to

$$\tilde{h}_{lg} = h_{lg} + 0.5 (c_p)_g (T_w - T_s) .$$

The turbulent natural convection equation³⁷ used in this heat-transfer regime is

$$h_{nc} = 0.13 k_g \left(\frac{\rho_g^2 g |T_w - T_g|}{\mu_g^2 T_g} \right)^{0.333} Pr_g^{0.333} \quad (138)$$

The forced convection equation is based on Dougall and Rohsenow's modification³⁸ to the Dittus-Boelter equation:

$$h_{fc} = 0.023 \frac{k_g}{D_h} \left\{ \frac{\rho_g [\alpha |v_g| + (1 - \alpha) |v_l|] D_h}{\mu_g} \right\}^{0.8} \left[\frac{\mu_g (c_p)_g}{k_g} \right]^{0.4} ,$$

where the Reynolds number is modified to reflect the volumetric flow rate of the two-phase mixture. As in the previous heat-transfer regimes, linear interpolation is used for $\alpha > \alpha_c$.

(5) Single-Phase Vapor HTC (Heat-Transfer Regime 6). For the single-phase vapor heat-transfer regime, $h_l = 0$ and h_g is the maximum of Eq. (138), of turbulent natural convection, and of the Dittus-Boelter Eq. (115) evaluated by using vapor properties and flow conditions.

(6) Condensation HTCs (Heat-Transfer Regime 11). The Chen correlation³¹ is used to calculate the wall-to-liquid HTC when condensation occurs. The suppression factor, S , is set equal to zero. The Chen correlation is based upon data taken up to an equilibrium quality, $x = 0.71$. For $x > 0.71$, the Chen correlation is evaluated at $x = 0.71$; then h_l is found by linear interpolation between the value of h_l found from the correlation and the single-phase vapor value, $h_l = 0.0$. Similarly, h_g is found by interpolation between zero and the single-phase vapor value.

(7) Two-Phase Mixture HTCs (Heat-Transfer Regime 7). This heat-transfer regime is unique because it is not part of the boiling curve discussed above. Regime 7 is used only when the input flag $ICH? = 0$. When $ICF = 0$, h_l and h_g are calculated from regime 7 only. Critical heat flux cannot occur in this case.

If the void fraction is less than or equal to the cutoff void fraction, $h_g = 0$ and h_l is the maximum of the laminar and turbulent values,

$$h_l = \max (h_{l\text{lam}}, h_{l\text{turb}}) , \quad (139)$$

where

$$h_{l\text{lam}} = \frac{4k_l}{D_h} , \quad (140)$$

$$h_{\ell\text{turb}} = \frac{0.023k_{\ell} \text{Re}_m^{0.8} \text{Pr}_{\ell}^{0.4}}{D_h} , \quad (141)$$

and

$$\text{Re}_m = \frac{GD_h}{\mu_m} . \quad (142)$$

The two-phase viscosity is calculated by using McAdam's equation,³⁷

$$\mu_m = \frac{1}{\frac{x_f}{\mu_g} + \frac{1-x_f}{\mu_{\ell}}} , \quad (143)$$

where x_f is the flow quality.

If the void fraction is greater than the cutoff void fraction, h_g is the maximum of the Dittus-Boelter value for vapor and the turbulent natural convection value,

$$h_g = \max (h_{\text{vnc}}, h_{\text{vturb}}) , \quad (144)$$

where the natural convection value³⁷ is

$$h_{\text{vnc}} = 0.13k_g \left(\frac{\rho_g^2 |T_w - T_g|}{\mu_g^2 T_g} \right)^{0.333} \text{Pr}_g^{0.333} , \quad (145)$$

and the forced convection HTC is given by the Dittus-Boelter equation,

$$h_{vturb} = \frac{0.023 k_g Re_g^{0.8} Pr_g^{0.333}}{D_h} \quad (146)$$

The Reynolds and Prandtl numbers in Eq. (146) are calculated by using vapor properties evaluated at the vapor temperature.

For $\alpha > \alpha_c$, linear interpolation is used between the current values of h_2 and h_g and the single-phase values.

c. Critical Heat Flux (CHF). The CHF point has two purposes in relation to the TRAC boiling curve. First, the CHF point indicates the change from nucleate boiling (heat-transfer regime 2) to transition boiling (regime 3). Second, the CHF point is used in the quadratic interpolation that gives the transition boiling liquid HTC. If the input variable ICHF = 1, the Biasi forced flow CHF correlation³⁹ is used. For ICHF = 0 and for steady-state calculations (ISTDY = 1), no CHF calculation is performed. In the vessel ICHF = 1 is always used and it also is recommended for other components.

The Biasi correlation has a data base that covers the mass flux range, G, between 100 kg/m²s and 6000 kg/m²s. For mass flux values between 0 and 200 kg/m²s, the Biasi correlation is evaluated at 200 kg/m²s. For negative values of G, the absolute value of G is used.

The Biasi CHF correlation consists of two equations for q_{CHF}'' and the maximum CHF value calculated by the two equations is used,

$$q_{CHF}'' = \frac{1.883 \times 10^7}{D_h^n G^{1/6}} \left[\frac{f_p}{G^{1/6}} - x \right] \quad (147)$$

and

$$q_{CHF}'' = \frac{3.78 \times 10^7}{D_h^n G^{0.6}} h_p (1 - x) \quad (148)$$

where

$$n = 0.4, \quad \text{for } D_h \geq 1 \text{ cm};$$

$$n = 0.6, \quad \text{for } D_h < 1 \text{ cm};$$

$$f_p = 0.7249 + 0.099 p \exp(-0.032 p);$$

$$h_p = -1.159 + 0.149 p \exp(-0.019 p) + \frac{8.99 p}{10 + p^2};$$

D_h = hydraulic diameter (cm);

G = mass flux ($\text{g}/\text{cm}^2\text{s}$);

p = pressure (bar); and

x = equilibrium quality.

Note that the Biasi correlation uses cgs units, but the constants in Eqs. (147) and (148) have been changed so that $q_{\text{CHF}}^{\prime\prime}$ is in W/m^2 .

Predictions made with earlier versions of TRAC show that the Biasi correlation sometimes fails to predict CHF at high void fraction, even though the data indicate that CHF has occurred. To correct this problem, the Biasi correlation is used for a void fraction less than 0.97 and linear interpolation is used between the HTC at this void fraction and the one at 0.98 assuming that the T_{CHF} is one-half degree above T_s . For a void fraction greater than 0.98, the T_{CHF} is fixed at one-half degree above T_s .

Once $q_{\text{CHF}}^{\prime\prime}$ is obtained, the temperature corresponding to the CHF point, T_{CHF} , is calculated by using a Newton-Raphson iteration⁴⁰ to determine the intersection of the heat flux found by using the nucleate boiling HTC and the CHF. An iteration is required because $T_w = T_{\text{CHF}}$ must be known to evaluate the Chen correlation; and, in turn, the Chen HTC must be known to calculate the wall temperature,

$$q_{\text{CHF}}^{\prime\prime} = h(T_w - T_s) \quad . \quad (149)$$

The equation for T_{CHF} is

$$T_{CHF}^{n+1} = T_{CHF}^n - \frac{(T_{CHF}^n - T_s - \frac{q_{CHF}^n}{h})}{[1 + (\frac{q_{CHF}^n}{h^2} \frac{dh}{dT_w})]} , \quad (150)$$

where T_{CHF}^n is the CHF temperature for the n^{th} iteration, h is the HTC evaluated by using the Chen correlation, and dh/dT_w is the derivative of the HTC with respect to the wall temperature.

Convergence occurs if $|T_{CHF}^{n+1} - T_{CHF}^n| < 1.0$. A maximum of ten iterations is allowed; if convergence does not occur, a message is printed and a fatal error occurs.

The CHF temperature is restricted to the range, $T_s + 0.5 \leq T_{CHF} \leq T_s + 100$. The CHF calculations are done in subroutines CHF and CHF1.

d. Minimum Stable Film Boiling Temperature, T_{min} . The minimum stable film boiling point is the intersection point between the transition and film boiling heat-transfer regimes (Fig. 10). In addition, this point is one of the points used in the interpolation scheme for the calculation of the transition boiling heat flux.

The homogeneous nucleation minimum stable film boiling temperature correlation⁴¹ is

$$T_{min} = T_{nh} + (T_{nh} - T_\ell)R^{0.5} , \quad (151)$$

where

$$R = \frac{(k\rho c)_\ell}{(k\rho c)_w} , \quad (152)$$

and T_{nh} is the homogeneous nucleation temperature. In Eq. (152) the subscript ℓ indicates liquid properties and the subscript w indicates wall properties.

The homogeneous nucleation temperature is given by Fauske and a curve fit to these results, from the COBRA-TF code,* is used in TRAC-PF1.

$$T_{nh} = 705.44 - (4.722 \times 10^{-2})DP \\ + (2.3907 \times 10^{-5}) DP^2 \\ - (5.8193 \times 10^{-9}) DP^3 ,$$

where $DP = 3203.6 - P$. The pressure P is in psia units and T_{nh} is in degrees Fahrenheit. In TRAC-PF1, P is converted to a temporary variable in British units and T_{nh} is converted to degrees Kelvin after the equation is evaluated.

Once T_{min} is evaluated, the corresponding heat flux, q'_{min} , which is used in the transition boiling HTC interpolation, can be calculated,

$$q'_{min} = h_{lmin} (T_{min} - T_l) + h_{gmin} (T_{min} - T_g) ,$$

where h_{lmin} and h_{gmin} are the liquid and vapor HTCs, respectively, evaluated at the minimum stable film boiling temperature. Thus,

$$h_{lmin} = h_r \left(\frac{T_{min} - T_s}{T_{min} - T_l} \right) + h_{df}$$

and

$$h_{gmin} = \max (h_{fbb}, h_{nc}, h_{DR})$$

If $\alpha > \alpha_c$, linear interpolation again is used between the values of the HTCs at alpha and the single-phase vapor values.

e. Steady-State Calculations. The steady-state (ISTDY = 1) and transient (ISTDY = 0) wall-to-fluid HTC code logics differ. The entire boiling curve is not available during steady state; only that part of the heat transfer before CHF is calculated (Sec. III.B.2.a).

C. Reactor Kinetics

Subroutine RKIN evaluates power generation in the reactor core by one of two methods. In the first method the user specifies power to be a constant or defined by a signal-variable-dependent power table supplied as input. Values between entries in the table are determined by linear interpolation. Power can be trip-controlled by evaluating the power table when the power trip is ON and by holding the power constant when the power trip is OFF. In the second method the user determines power from the solution of the point-reactor-kinetics equations. These equations specify the time behavior of the core power level with total reactivity (R), the sum of programmed (R_{prog}) and feedback (R_{fdbk}) reactivities, the controlling parameter. The user defines programmed reactivity with the same forms that define power in the first method. Subroutine RFDBK evaluates feedback reactivity based on changes in the core-averaged fuel temperature, coolant temperature, and coolant vapor fraction.

The point-reactor kinetics equations define the combined power from prompt fission and decay of fission products. These equations are

$$\frac{dP}{dt} = \frac{(R - \beta)}{\Lambda} P + \sum_{i=1}^I \lambda_i C_i \quad , \quad (153)$$

$$\frac{dC_i}{dt} = -\lambda_i C_i + \frac{\beta_i}{\Lambda} P \quad (i = 1, 2, \dots, I) \quad , \quad (154)$$

and

$$\frac{dH_j}{dt} = -\lambda_j^H H_j + E_j P \quad (j = 1, 2, \dots, J) \quad , \quad (155)$$

* M. J. Thurgood and J. M. Kelley, Battelle Pacific Northwest Laboratories (December 1979).

where

- P = instantaneous total power (W),
 t = problem time (s),
 $R = \text{total reactivity} = R_{\text{prog}} + R_{\text{fdbk}} = k - 1$,
 R_{prog} = programmed reactivity,
 R_{fdbk} = feedback reactivity,
 k = reactor multiplication constant,
 $\beta = \text{total effective delayed neutron fraction} \left(\sum_{i=1}^I \beta_i \right)$,
 I = number of delayed neutron groups,
 β_i = effective delayed neutron fraction of delayed neutron group i ,
 Λ = prompt neutron generation time (s),
 λ_i = decay constant of delayed neutron group i (s^{-1}),
 C_i = decay power of delayed neutron group i (W),
 H_j = decay energy of decay heat group j (W • s),
 λ_j^H = decay constant of decay heat group j (s^{-1}),
 E_j = effective energy fraction of decay heat group j , and
 J = number of decay heat groups.

The solution of these three coupled first-order differential equations is used to evaluate the effective energy generation rate (P_{eff}) in the reactor core; that is, the power being deposited in the core at the current time,

$$P_{\text{eff}} = \left(1 - \sum_{j=1}^J E_j \right) P + \sum_{j=1}^J \lambda_j^H H_j \quad (156)$$

The right-hand expression sums the power released from the fuel by prompt fission and fission product decay.

The user inputs the number of delayed neutron groups, I ; the delayed neutron parameters, λ_i and β_i ; the delayed neutron group initial decay powers, $C_i(0)$; the number of decay heat groups, J ; the decay heat parameters, λ_j^H and E_j ; and the decay heat group initial decay energies, $H_j(0)$. If $I \leq 0$ is input, TRAC sets I to 6 and defines λ_i and β_i with the values in Table I. If $J \leq 0$ is input, TRAC sets J to 11 and defines λ_j^H and E_j with the values in Table II. The RELAP⁴² and RETRAN⁴³ computer programs set these default values internally. The power decay that these parameters evaluate closely approximates the

TABLE I
 DELAYED NEUTRON CONSTANTS

<u>Group i</u>	<u>Decay Constant λ_i (s⁻¹)</u>	<u>Neutron Fraction β_i</u>
1	0.012 7	0.000 247
2	0.031 7	0.001 38
3	0.115	0.001 22
4	0.311	0.002 64
5	1.40	0.000 832
6	3.87	0.000 169

TABLE II
 DECAY HEAT CONSTANTS

<u>Group j</u>	<u>Decay Energy λ_j^H (s⁻¹)</u>	<u>Energy Fraction E_j</u>
1	1.772	0.002 99
2	0.577 4	0.008 25
3	0.067 43	0.015 50
4	0.006 214	0.019 35
5	4.739×10^{-4}	0.011 65
6	4.810×10^{-5}	0.006 45
7	5.344×10^{-6}	0.002 31
8	5.726×10^{-7}	0.001 64
9	1.036×10^{-7}	0.000 85
10	2.959×10^{-8}	0.000 43
11	7.585×10^{-10}	0.000 57

standard American Nuclear Society (ANS) decay heat curve.⁴³ If $I \leq 0$ or $C_i(0) \leq 0$ is input and/or if $J \leq 0$ or $H_j(0) \leq 0$ is input, an initial steady-state condition is assumed to exist in order to initialize $C_i(0)$ and/or $H_j(0)$ in TRAC. This requires the initial power $P(0)$ that is specified as input. Setting dC_i/dt and dH_j/dt to zero at the initial time in Eqs. (154) and (155) gives

$$C_i(0) = \frac{\beta_i}{\lambda_i \Lambda} P(0) \quad (i = 1, 2, \dots, I) \quad (157)$$

and

$$H_j(0) = \frac{E_j}{\lambda_j} P(0) \quad (j = 1, 2, \dots, J) \quad (158)$$

Subroutine RFDBK evaluates feedback reactivity. The reactivity feedback model is based on the assumption that only changes in the core-averaged fuel temperature (T_f), coolant temperature (T_c), and coolant vapor fraction (α) affect the neutron multiplication reactivity of the reactor. TRAC determines core-averaged values by applying mass and power weighting factors to the temperatures and a power weighting factor to the vapor fraction. These factors approximate the product of the adjoint flux, neutron flux, and volume. Perturbation theory uses this product to weight spatially the change in reaction-rate cross sections for estimating reactivity-change.

The user defines a reactivity coefficient for each of the independent variables, $x = T_f, T_c,$ or α , by choosing one of the forms from Table III. We assume that the reactivity-coefficient form for each independent variable has second-order polynomial dependence in x without dependence on the other two independent variables. The user specifies through input the form number and the polynomial coefficients, $A_x, B_x,$ and C_x , for each independent variable x . The polynomial coefficients can be obtained by performing a second-order-polynomial least-squares fit to the reactivity coefficient vs temperature or vapor fraction data in a reactor-safety analysis report or from a detailed neutronics calculation. The coolant-temperature reactivity

TABLE III
REACTIVITY-COEFFICIENT FORMS

<u>Form Number</u>	<u>Reactivity Coefficient Form</u>	<u>Assumed Dependence</u>
0	$\frac{\partial k}{\partial x}$	
1	$\frac{1}{k} \frac{\partial k}{\partial x}$	$= A_x + B_x x + C_x x^2$
2	$x \frac{\partial k}{\partial x}$	
3	$\frac{x}{k} \frac{\partial k}{\partial x}$	

coefficient needs to include the reactivity effect from temperature changes in soluble boron and burnable poison because the coolant temperature closely approximates their temperatures. Based on these assumptions, feedback reactivity during the time step from time t_0 to time t_n is defined by

$$\Delta R_{fdbk_n} = R_{fdbk_n} - R_{fdbk_0} = k(T_{f_n}, T_{c_n}, \alpha_n) - k(T_{f_0}, T_{c_0}, \alpha_0) \quad (159)$$

$$\begin{aligned}
 &= \exp \left(\left[A_x \left\{ \frac{x_n - x_0}{\ln x_n / x_0} \right\} + B_x \left\{ \frac{1}{2} \frac{(x_n^2 - x_0^2)}{x_n - x_0} \right\} \right. \right. \\
 &\quad \left. \left. + C_x \left\{ \frac{1}{3} \frac{(x_n^3 - x_0^3)}{x_n^2 - x_0^2} \right\} \right] \right) * (k(T_{f_0}, T_{c_0}, \alpha_0)) \\
 &+ \left[A_x \left\{ \frac{x_n - x_0}{\ln x_n / x_0} \right\} + B_x \left\{ \frac{1}{2} \frac{(x_n^2 - x_0^2)}{x_n - x_0} \right\} \right. \\
 &\quad \left. + C_x \left\{ \frac{1}{3} \frac{(x_n^3 - x_0^3)}{x_n^2 - x_0^2} \right\} \right] - k(T_{f_0}, T_{c_0}, \alpha_0)
 \end{aligned}$$

where \bullet = summation over x variables with reactivity coefficient forms $\begin{Bmatrix} 1 \\ 3 \end{Bmatrix}$;
 $\#$ = summation over x variables with reactivity coefficient forms $\begin{Bmatrix} 0 \\ 2 \end{Bmatrix}$;
 $x = T_f, T_c, \text{ or } \alpha$; and
 $0 = n - 1$.

One needs to know the end-of-time-step values for T_{f_n} , T_{c_n} , and α_n to evaluate ΔR_{fdbk_n} using Eq. (159). To evaluate that reactor state, one needs to know the average effective energy generation rate,

$$P_{eff} = \frac{1}{2} (P_{eff_0} + P_{eff_n}) \quad , \quad (160)$$

during time step $\Delta t_n = t_n - t_0$. The value of P_{eff_n} is known only after solving the point-reactor-kinetics equations knowing the average reactivity during the time step,

$$R = \frac{1}{2} (R_0 + R_n) = \frac{1}{2} (R_{prog_0} + R_{prog_n}) + R_{fdbk_0} + \frac{1}{2} \Delta R_{fdbk_n} \quad . \quad (161)$$

Before performing the time-step solution to evaluate ΔR_{fdbk_n} by Eq. (159), TRAC estimates ΔR_{fdbk_n} for Eq. (161) by assuming the feedback reactivity rate is the same as in the previous time step, Δt_0 .

$$\Delta R_{fdbk_n}^{est} = \Delta R_{fdbk_0} * \left(\frac{\Delta t_n}{\Delta t_0} \right) \quad . \quad (162)$$

After evaluating the time-step solution, TRAC compares the feedback reactivity (ΔR_{fdbk_n}) from Eq. (159) and the estimated feedback reactivity ($\Delta R_{\text{fdbk}_n}^{\text{est}}$) from Eq. (162). Any discrepancy is corrected by applying the difference,

$$\Delta R_{\text{fdbk}_n}^{\text{cor}} = (\Delta R_{\text{fdbk}_n} - \Delta R_{\text{fdbk}_n}^{\text{est}}) * \min \left(\frac{\Delta t_n}{\Delta t_{n+1}}, 2 \right) \quad (163)$$

during the next time step, Δt_{n+1} . To prevent a significant reactivity correction from being applied when $\Delta t_n \gg \Delta t_{n+1}$, the reactivity correction in Eq. (163) is limited to twice its amount during time step Δt_n . A similar estimate and correction procedure is applied to power in the first method and programmed reactivity in the second method because the signal variable for interpolating the power table is defined by the end-of-time-step state.

The point-reactor-kinetics equations [Eqs. (153)-(155)] are solved by numerical integration using a fourth-order accurate Runge-Kutta technique⁴⁴ including Gill's modifications.⁴⁵ This technique is fast, accurate, and has excellent round-off, error-limiting characteristics. However, because this technique is explicit, the stability condition

$$\Delta t_{\text{max}} = \frac{0.8\Lambda}{\max(\beta f, \beta^f)}, \quad (164)$$

where $f = 1 - R/\beta$, limits the maximum numerical integration time-step size, Δt_{max} . To ensure that Δt_{max} does not limit the problem time-step size, Δt_n , when $\Delta t_{\text{max}} < \Delta t_n$, the kinetics equations are integrated over ℓ equal time-step subintervals Δt_{ℓ} during each problem time step, where

$$l = \text{INT} \left(\frac{\Delta t_n}{\Delta t_{\max}} \right) + 1 \quad (165)$$

and

$$\Delta t_l = \frac{\Delta t_n}{l} . \quad (166)$$

Only one time-step subinterval of Δt_n is evaluated where Δt_{\max} exceeds Δt_n .

D. Overall Solution Strategy

Overall solution strategies for both transient and steady-state calculations are described in this section. Each time step in the transient calculation consists of several sweeps through all the components in the system. The purpose of these sweeps is to converge to the solution of the nonlinear finite-difference equations. Two types of steady-state calculations are available in TRAC. The first type has general applicability, whereas the second type is used to obtain initial steady-state conditions for a PWR. Both steady-state calculations utilize the transient fluid-dynamics and heat-transfer routines.

1. Transient Solutions.

a. Outer Iteration Strategy. The solution of the thermal-hydraulic flow equations for all components is controlled by subroutines TRANS, PREP, OUTER, and POST. Subroutine TRANS controls the overall strategy, whereas the others call each component in turn.

At least six passes are made through each component. Subroutine PREP makes two passes through all components. During the first pass, HTCs are evaluated by calls to subroutine HTCOR and the matrices for the stabilizer motion equations are obtained and reduced by subroutine FEMOM. The second pass in overlay PREP is for a back-substitution on the motion equation done in routine BKSMOM. The next two or more passes call the basic hydrodynamic routines until a solution is found within the convergence criterion or the maximum number of iterations is exceeded. This stage of the calculation is done by a call to subroutine OUTER, which performs both a forward elimination

and a backward substitution pass. The recommended convergence criterion (EPSO) is 10^{-4} and the maximum outer iteration count (OUTMAX) generally should range between 6 and 10. The order in which subroutine OUTER calls the given components is determined by the IORDER array that is set after input by subroutine SRTLPL.

If the OUTER iteration process converges, a final pair of passes is made by subroutine POST. The first of these sets up and reduces the stabilizer equations for mass and energy using subroutine STBME. The second calls BKSSTB to compile the solution of these equations, updates the wall, slab, or rod heat conduction, and generates the information required to begin the next time step. If the OUTER iteration fails to converge, the time-step size is halved (subject to the constraint that Δt must be greater than or equal to the minimum time-step size indicated in the input); then, another attempt to converge the OUTER iteration cycle begins. After six unsuccessful attempts, the code produces a dump, an edit, and then shuts down.

Programming details of the iteration procedure for transient solutions are given in Sec. VI.D. A flow schematic for the TRANS routine is given in that section.

b. Details of the Solution Method. Solution of the fluid flow difference equations is broken into phases. First the stabilizing motion equations are solved, then the basic equation set is solved, and finally the stabilizing mass and energy equations are solved.

Solution of the stabilizing motion equations is a relatively simple process because they are linear equations in \tilde{V}_g and \tilde{V}_ℓ , with no coupling between the \tilde{V}_g and \tilde{V}_ℓ terms. First, the motion equations interior to all components are solved to obtain the interior velocities as linear functions of the junction velocities (done in subroutine FEMOM) in the form,

$$\tilde{V}_j = a_j + b_j \tilde{V}_L + c_j \tilde{V}_R + d_j \tilde{V}_T , \quad (167)$$

where the subscripts L, R, and T indicate the cell faces at the left, right, and tee (where applicable) component junctions. Next, the motion equations at component junctions are applied and Eq. (167) is substituted into them where necessary to obtain a closed set of equations in the velocities at component

junctions. This linear system is solved directly, using lower-upper (LU) decomposition. Finally, a back-substitution through all components is done using the known junction velocities and Eq. (167) to obtain values for the interior velocities (subroutine BKSMOM).

To solve the basic equation set (Secs. III.A.3 and III.A.4), a special junction variable and equation are defined,

$$\Delta P = \delta p_+ - \delta p_- , \quad (168)$$

where δp_+ is the linearized variation in pressure on one side of the junction and δp_- the variation on the other. When the basic equation set is linearized within each one-dimensional component, Eq. (168) is substituted into the pressure gradient term of the motion equations at the component junctions. This linearized set of equations is solved in subroutine TFIDS to obtain the variations of independent variables (δp , δp_a , δT_e , δT_g , and $\delta \alpha$) as linear functions of the ΔP junction terms. For example,

$$\delta p_j = a_j' + b_j' \Delta P_L + c_j' \Delta P_R + d_j' \Delta P_T . \quad (169)$$

After this has been done, Eq. (169) is substituted whenever applicable into the defining Eq. (168) at all junctions and the solution proceeds with the stabilizing velocities.

When one or more three-dimensional components are present, the situation is slightly more complicated. For the network illustrated in Fig. 13, a linear set of equations in ΔP_i results after all possible substitutions are made. The equations have the form,

$$\begin{bmatrix} X & X & 0 & 0 & 0 & 0 \\ X & X & X & 0 & X & 0 \\ 0 & X & X & X & X & 0 \\ 0 & 0 & X & X & 0 & 0 \\ 0 & X & X & 0 & X & X \\ 0 & 0 & 0 & 0 & X & X \end{bmatrix} \begin{bmatrix} \Delta P_1 \\ \Delta P_2 \\ \Delta P_3 \\ \Delta P_4 \\ \Delta P_5 \\ \Delta P_6 \end{bmatrix} = \begin{bmatrix} X \\ X \\ X \\ X \\ X \\ X \end{bmatrix} + \begin{bmatrix} X \\ 0 \\ 0 \\ 0 \\ 0 \\ 0 \end{bmatrix} \delta p_{v1} + \begin{bmatrix} 0 \\ 0 \\ 0 \\ X \\ 0 \\ 0 \end{bmatrix} \delta p_{v4} , \quad (170)$$

where X indicates nonzero matrix and vector elements, and p_{v1} and p_{v4} are the linear pressure variations in the vessel cells adjacent to junctions 1 and 4, respectively. This system is solved directly to obtain,

$$\Delta P_1 = A_1 + B_1 \delta p_{v1} + C_1 \delta p_{v4} \quad (171)$$

The combination of these equations with the remaining linearized ones in the three-dimensional vessel region provides a closed set of linear equations that is solved in one of two ways. If the input variable IITMAX is set to zero, then the system is solved directly using calls to subroutines STDIR, SOLVE, and BACIT. If this variable is greater than zero, an iterative solution procedure is used. This iteration is a combination of a Gauss-Seidel and a coarse-mesh rebalance as described in Sec. III.A.2. The recommended convergence criterion for this iteration (EPSI) is 10^{-5} , and the maximum allowed number of iterations (IITMAX) is 30-50. Back-substitution through the one-dimensional components again completes the solution of the full linear system.

A single, complete pass through this solution procedure provides the solution for the linearized finite-difference equations. Subsequent passes

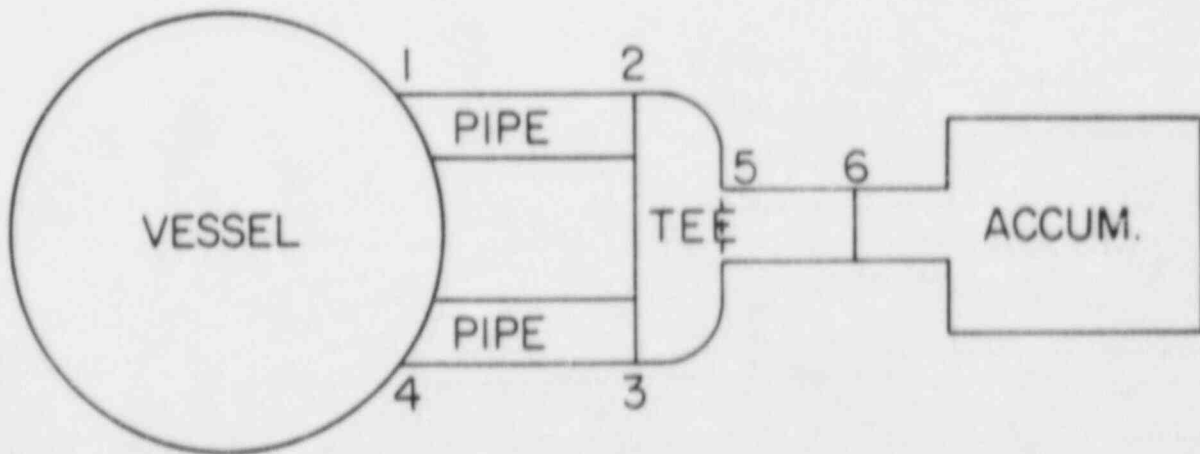


Fig. 13.
Component network with one three-dimensional vessel.

through the procedure for the same time step produce a Newton iteration on the nonlinear difference equations, with quadratic convergence.

Solution of the stabilizing mass and energy equations is quite similar to that for the stabilizing motion equations. Because the unknown quantities are all cell centered, it is necessary to define the junction variables as those in a cell adjacent to the junction that occurs first in the calculational sequence. Special logic is provided to avoid conflicts when this criterion is applied to one cell components.

2. Steady-State Solutions. The TRAC steady-state capability provides time-independent solutions that may be of interest in their own right or as initial conditions for transient calculations. Two distinct calculations are available within the steady-state capability: the generalized steady-state calculation and the PWR-initialization calculation. The first finds the time-independent conditions of a system for arbitrary, but fixed, geometry and parameters. The second adjusts certain loop parameters to match a set of user-specified flow conditions, but only for the fixed geometry typical of current PWR systems.

Both calculations use the transient fluid-dynamics and heat-transfer routines to search for time-independent conditions. The search is terminated when the normalized rates of change for the fluid and thermal variables are reduced below a user-specified criterion throughout the system.

Although the same subroutines are used in the transient and the steady-state calculations, there are important ways in which their behaviors differ between the two calculations. The most crucial differences are:

- The time-step size used by the heat-transfer and fluid-flow calculations are not required to be equal during a steady-state calculation. The ratio of these time-step sizes is fixed through user-specified input. This permits compensation for the difference between the natural time scales of the two processes. (Caution should be taken not to exceed the diffusion limit in axial rod conduction by using too large a time-step ratio.)
- The occurrence of critical heat flux (CHF) is inhibited during the steady-state calculation. This results in an HTC that cannot undergo a rapid reduction caused by burnout.
- Pressurizers are modeled as pressure boundary conditions during steady-state calculations. Therefore, each pressurizer's energy and mass inventory, as well as

pressure, remain constant regardless of the flow rate between it and the remainder of the system.

- Trips are inhibited during steady-state calculations. Thus, even though conditions may exist that would cause a trip during a transient, the trip will not be activated during the steady-state calculation.
- The reactor power is set to zero for a period at the beginning of the steady-state calculation. It is increased to its nominal value once the fluid velocity has approached its equilibrium value.
- During the steady-state calculation, the pump momentum source is averaged to prevent oscillations.
- The reactor-kinetics calculation is not performed.

a. Generalized Steady-State Calculation. The generalized steady-state calculation consists of a simple normalized rate of change based on the numerical first derivative of the void fraction, pressure, liquid and vapor temperatures, and velocities. The rate of change of variable x for time step $(n+1)$ at cell i is given by

$$\delta x_i^{n+1} = \frac{x_i^{n+1} - x_i^n}{|x_i^{n+1}|(t^{n+1} - t^n)} \quad (172)$$

Thus, δx_i^{n+1} is the fractional rate of change for the variable x_i^{n+1} in 1 s. This rate of change is checked every 50 time steps during the steady-state run. When the maximum absolute value of δx_i^n for all cells in the system is less than a user-specified convergence criterion for all variables, the steady-state calculation is ended. An edit, including the maximum rates of change and the component and cell number where it occurs for each variable, is printed every 50 time steps and at every long edit, dump, or time domain change. Logic is included to limit change rate checking only to those cells where the variable being checked is important. For example, liquid temperature change rates are not calculated in cells where the void fraction is above 0.9999 because the liquid temperature in this cell is not a meaningful value.

The variables that are considered in evaluating the approach to steady state are listed in Table IV.

b. PWR-Initialization Calculation. The PWR-initialization calculation provides a convenient way for the user to match important PWR operating conditions by adjusting certain operating parameters. The conditions that this calculation attempts to match are reactor power, pressurizer pressure, primary loop flow rates, and vessel inlet temperatures. This matching is accomplished by adjusting the pump speed and steam generator fouling factor in each loop of the reactor system. This idea was first developed by Sharp,⁴⁶ although the implementation method in TRAC is somewhat different.

As implied by its name, the PWR-initialization calculation is limited to systems whose geometry is characteristic of a PWR. The system must have one and only one VESSEL component. Although the number of primary coolant flow loops is arbitrary, each loop must satisfy the following criteria.

- There must be a single STGEN component in each loop. This component must be located between the VESSEL hot-leg junction for that loop and the loop pump or pumps.
- There must be either one or two pumps in each loop. These must be located between the STGEN and the VESSEL cold-leg junctions. If there are two pumps, they must operate in parallel and both must be connected to the VESSEL through a distinct junction.
- The secondary side of the steam generator must be connected to a BREAK on one side and to a FILL on the other. Only pipes may be located between the STGEN and the FILL or BREAK.
- The primary coolant flow loops must not connect directly to one another, but they are connected to the VESSEL.

The values of the operating parameters are determined by an iterative process that begins with the execution of a sequence of transient time steps. These should bring the system close to a steady state for the current value of the operating parameters. The VESSEL inlet temperatures and loop flow rates are compared to their desired values for each primary loop. Once these agree within a user-specified criterion, the calculation is complete. If the

TABLE IV

VARIABLES CONSIDERED IN EVALUATING THE APPROACH TO STEADY STATE

One-Dimensional Fluid-Flow Variables

<u>Dependent Variable</u>	<u>Generalized Forces</u>
Mixture velocity	Wall friction Pressure gradients Gravity Momentum fluxes
Mixture mass	Sources Mass fluxes
Mixture energy	Sources Energy fluxes
Vapor mass	Sources Phase exchange Mass fluxes
Vapor energy	Sources Phase exchange Energy fluxes

Three-Dimensional Fluid-Flow Variables

<u>Dependent Variable</u>	<u>Generalized Forces</u>
Vapor velocity	Wall friction Interphase friction Pressure gradients Gravity Momentum fluxes
Liquid velocity	Wall friction Interphase friction Pressure gradients Gravity Momentum fluxes
Mixture mass	Sources Mass fluxes
Mixture energy	Sources Energy fluxes
Vapor mass	Sources Phase exchange Mass fluxes
Vapor energy	Sources Phase exchange Mass fluxes

Heat-Transfer Variables

<u>Dependent Variable</u>	<u>Generalized Forces</u>
Temperature	Energy sources Heat fluxes

calculation is incomplete, the state of the system at the conclusion of this sequence is used to evaluate new values of the operating parameters.

In the evaluation of operating parameters, each primary coolant flow loop is treated independently. The coupling between loops is treated implicitly by the method used to evaluate VESSEL characteristics for each loop. Because the transient routines force the PRIZER pressure and the VESSEL power to their prescribed values, only variations in the loop flow rates and VESSEL inlet temperatures must be considered. The TRAC program uses only information from the current state of the system (as derived from the transient calculation) in evaluating a new set of operating parameters; no information is stored from previous iterations. The new loop parameters are relaxed by the input relaxation factor (RELX) before the calculation is resumed.

Neglecting components not in the primary coolant flow path (such as pressurizers and accumulators), each loop can be depicted schematically as shown in Fig. 14. Loops with only one pump are treated similarly. The evaluation of new operating parameters for this primary coolant flow loop is based on the solution of the pressure and energy balance equations written

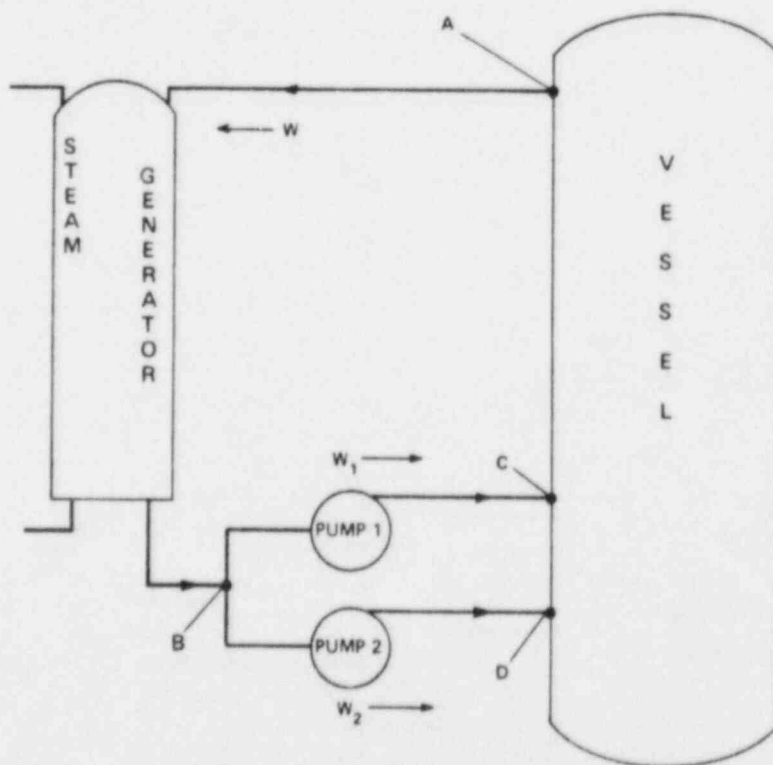


Fig. 14.
Primary loop schematic for a PWR-initialization calculation.

around this loop. Mass balance is satisfied automatically as a result of the transient calculation.

The steady-state pressure and energy balance equations may be written

$$\Delta p_{v1} + \Delta p_s = \Delta p_{p1} \quad , \quad (173)$$

$$\Delta p_{v2} + \Delta p_s = \Delta p_{p2} \quad , \quad (174)$$

and

$$\Delta H_s + \Delta H_{p1} + \Delta H_{p2} = \Delta H_{v1} + \Delta H_{v2} \quad , \quad (175)$$

where the subscripts s, p, and v refer to the steam generator, pumps, and vessel, respectively; Δp stands for a pressure difference; and ΔH stands for a change in the flow rate of enthalpy. Referring to Fig. 14, the pressure and enthalpy flow-rate differences may be written

$$\Delta p_{v1} = p(C) - p(A) \quad ,$$

$$\Delta p_{v2} = p(D) - p(A) \quad ,$$

$$\Delta p_s = p(A) - p(B) \quad ,$$

$$\Delta p_{p1} = p(C) - p(B) \quad ,$$

$$\Delta p_{p2} = p(D) - p(B) \quad ,$$

$$\Delta H_{v1} = \left(\frac{W_1}{W}\right)H(A) - H(C) \quad ,$$

$$\Delta H_{v2} = \left(\frac{W_2}{W}\right)H(A) - H(D) \quad ,$$

$$\Delta H_s = H(A) - H(B) \quad ,$$

$$\Delta H_{p1} = \left(\frac{W_1}{W}\right)H(B) - H(C) \quad ,$$

and

$$\Delta H_{p2} = \left(\frac{W_2}{W}\right)H(B) - H(D) \quad , \quad (176)$$

where the W terms are mass flows, as indicated in Fig. 14.

To solve these equations for new pump speeds and steam generator fouling factors, these variables must be related to the pressure and enthalpy flow-rate differences and to the desired flow rates and the vessel inlet temperatures. This is accomplished by assuming specific forms for the pressure rise across each pump, the enthalpy difference across each pump, and the enthalpy loss across the steam generator. The pressure rise across each pump is composed of two components: a pump head (PH), which depends on the pump speed, fluid density, and mass flow; and a flow resistance (R) pressure loss, which is proportional to the square of the mass flow. This results in the expressions

$$\Delta p_{p1} = PH_1 - W_1^2 R_{p1} \quad .$$

and

$$\Delta p_{p2} = PH_2 - W_2^2 R_{p2} \quad . \quad (177)$$

Similarly, the enthalpy difference across the pump is composed of two components; the first, caused by the pump head, and the second, which is proportional to the mass flow, result in the expressions

$$\Delta H_{p1} = W_1 \delta h_{p1} - \frac{PH_1}{\rho_{p1}} \quad ,$$

and

$$\Delta H_{p2} = W_2 \delta h_{p2} - \frac{PH_2}{\rho_{p2}} \quad . \quad (178)$$

The enthalpy change across the steam generator is expressed in terms of the overall heat-transfer coefficient, U ; the mean temperature difference, $\overline{\Delta T}$; the heat-transfer area, A ; plus a residual loss term caused by the flow rate,

$$\Delta H_s = W \delta h_s + W A U \overline{\Delta T} . \quad (179)$$

Using the definitions of Eq. (176) and the state of the system at the conclusion of the transient calculation, Eqs. (177)-(179) are solved for the flow resistances, R_{p1} and R_{p2} ; the specific enthalpy differentials, δh_{p1} , δh_{p2} , and δh_s ; and the overall heat-transfer coefficient, U . These characteristics are assumed to be independent of the loop operating parameters, which will be adjusted.

To characterize fully the response of the loop to changes in the operating parameters, we must be able to evaluate the remaining terms in Eqs. (173)-(175). These may be written in terms of the steam generator flow resistance,

$$\Delta p_g = W^2 R_s ; \quad (180)$$

and the vessel flow resistances and specific enthalpy differentials,

$$\Delta p_{v1} = W_1^2 R_{v1} ,$$

$$\Delta p_{v2} = W_2^2 R_{v2} ,$$

$$\Delta H_{v1} = W_1 \delta h_{v1} ,$$

and

$$\Delta H_{v2} = W_2 \delta h_{v2} . \quad (181)$$

The steam generator flow resistance may be evaluated by using Eq. (180) directly; however, the vessel characteristics are defined somewhat differently

to account for the effects of other loops and for the possibility of nonequilibrium thermal conditions in that component. Therefore, we use the definitions

$$R_{v1} = WR^2 \frac{p(C) - p(A)}{W_1^2} , \quad (182)$$

$$R_{v2} = WR^2 \frac{p(D) - p(A)}{W_2^2} , \quad (183)$$

$$\delta h_{v1} = \left(\frac{QR}{WR}\right) \left[\frac{H(A)}{W} - \frac{H(C)}{W_1} \right] , \quad (184)$$

and

$$\delta h_{v2} = \left(\frac{QR}{WR}\right) \left[\frac{H(A)}{W} - \frac{H(D)}{W_1} \right] , \quad (185)$$

where WR is the ratio of the desired total mass flow through the vessel to the current total mass flow, and QR is the ratio of the desired total energy transfer rate in the vessel to the current total energy transfer rate in the vessel. Note that as the problem converges to the desired solution, Eqs. (182)-(185) reduce to the solutions of Eq. (181) because both QR and WR approach unity.

Given the flow resistance values as calculated above, we immediately solve Eqs. (173) and (174) for the new pump heads in the loop under consideration. Using the pump curves, the fluid densities in the pumps, and the desired flow rates, we can determine iteratively new pump speeds that should produce the desired pump heads. Once the pump heads have been determined, we can use Eq. (175) to estimate a new value of the steam generator area. All terms of Eq. (175) are known except the steam generator area and the mean temperature difference between the steam generator primary and secondary sides, $\overline{\Delta T}$. We attempt to match the desired vessel inlet temperature by modifying $\overline{\Delta T}$ by the difference between the desired and current values of the

vessel inlet temperature. Solution of the resulting equation for the steam generator area drives the ensuing steady state to the desired condition.

The pump speeds and steam generator areas calculated in this manner may be relaxed by supplying RELX on the time-step input cards. The values actually used for the next iteration are then

$$\omega_{\text{new}} = \omega_{\text{old}} + \text{RELX} (\omega - \omega_{\text{old}})$$

and

$$A_{\text{new}} = A_{\text{old}} + \text{RELX} (A - A_{\text{old}}) .$$

IV. COMPONENT MODELS

Descriptions of the various component models that are included in TRAC-PF1 are given in this section. A physical description of each component is presented, along with a typical TRAC noding diagram showing the conventions used to model the component. Mathematical models, including finite-difference approximations, are given only for those aspects of the component that are not covered in the basic hydrodynamics and heat-transfer descriptions (Sec. III). User options, restrictions on the use of the component, subroutines used by the component, and input/output information also are given. Detailed input specifications for each component are given in Sec. V.

A. Pipe

The PIPE component models the flow in a one-dimensional duct or pipe. A PIPE can be used alone in a problem or it can be used as a connector between components to model a reactor system. The capability is provided to model area changes, wall heat sources, and heat transfer across the inner and outer wall surfaces. A wide selection of pipe materials is available to represent the wall material in the wall conduction calculation.

Figure 15 shows a typical noding diagram for a PIPE containing a venturi tube and an abrupt area change. The numbers within the PIPE indicate cell numbers and those above indicate cell boundary numbers. The geometry is specified by providing a volume and length for each cell and a flow area and hydraulic diameter at each cell boundary. The junction variables, JUN1 and JUN2, provide reference numbers for connecting a pipe to other components. The numerical methods used to treat the thermal hydraulics in a PIPE are described in Sec. III.A.3.

Input options are available to allow for wall heat transfer and to select correlations for CHF and wall friction factors. Wall heat transfer can be omitted by setting the number of heat-transfer nodes (NODES) to zero. The CHF calculation can be bypassed by setting the input parameter ICHF to zero. Wall friction and losses caused by abrupt area changes are chosen by setting values of the input arrays, NFF and FRIC, at each cell interface. The choices for these arrays are described in the input specifications in Sec. V.D.5.e.

By setting NPOWTB to a nonzero number and NODES to zero, heat can be provided to a PIPE by a table of power vs time. The table provides total power, which is evenly distributed among all of the cells.

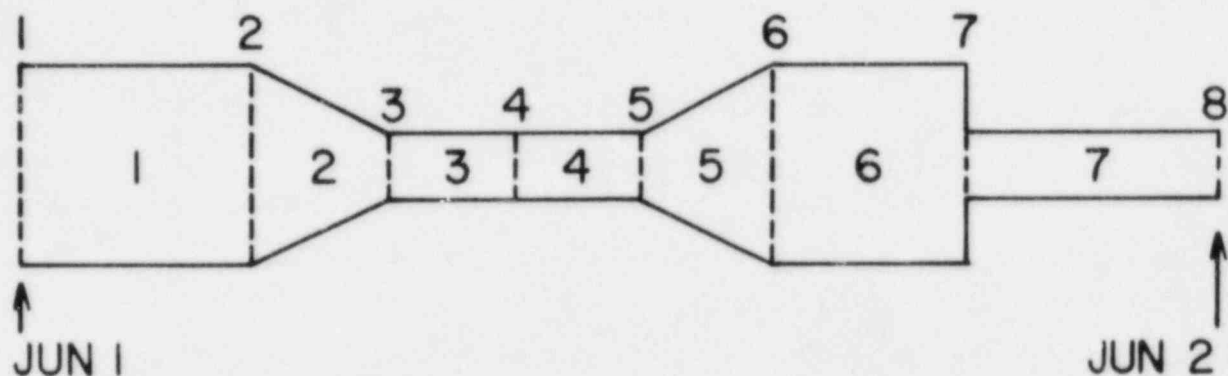


Fig. 15.
Pipe noding diagram.

By setting parameter IACC to 1 or 2 (see PIPE input, Sec. V.F.5.e), a PIPE can be used to model an accumulator (ACCUM) component, discussed in Sec. IV.B. Although a PIPE can be connected to any other component, including another PIPE, the user should keep the number of components to a minimum.

Detailed input for a PIPE module is processed by subroutines RPIPE and REPIPE. Subroutine RPIPE reads input data from the card input file. Subroutine REPIPE reads the corresponding data from the restart file. Initialization of the remaining variables is performed with subroutine IPIPE. This subroutine establishes the noding for wall heat transfer, sets the remaining fluid properties by calls to THERMO and FPROP, and initializes the boundary data by a call to J1D.

During problem execution, the solution procedure is controlled by routines PIPE1, PIPE2, and PIPE3. At the beginning of each time step, PIPE1 calls PREPER that in turn calls FWALL for wall friction and orifice loss coefficients, MPROP for wall metal properties, HTPipe for wall HTC's, and FEMOM to set up the stabilizer motion equations. Routine PIPE1 also calls BKMOM for a final back-substitution on the motion equations. During the iterations for a time step, PIPE2 calls TFLD for the numerical hydrodynamics solution (see Sec. III.A.3) and J1D to update boundary arrays. After a time step is

completed successfully, PIPE3 calls CONSTB to set up the stabilizer mass and energy equations. Routine PIPE3 also calls POSTER that updates the wall temperatures with a call to CYLHT, computes new fluid properties (viscosity, heat capacity, and surface tension) with a call to FPROP, performs back-substitution on the stabilizer mass and energy equations, and resets the boundary arrays with a call to JLD. If the time step fails to converge, THERMO is called to restore variables to their old values.

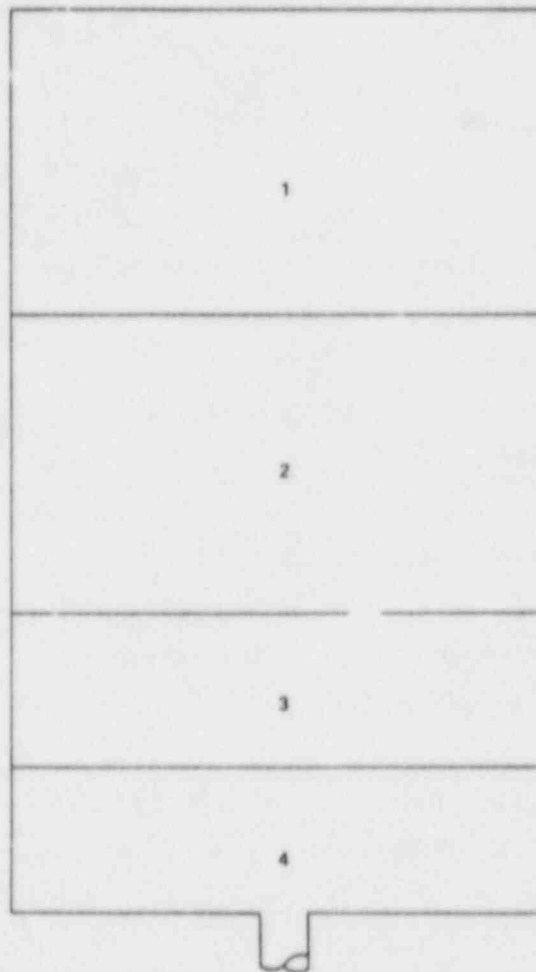
Output for a PIPE is managed by subroutine WPIPE. This subroutine prints the component number, junction numbers, iteration count, pressures, vapor fractions, saturation temperatures, liquid and vapor temperatures, liquid and vapor densities, liquid and vapor velocities, and wall friction factors. If wall heat transfer is included (NODES \neq 0), then information on the heat-transfer regime, liquid and vapor wall HTCs, interfacial HTC, heat-transfer rate from the wall, wall temperature for critical heat flux, and wall temperature profiles also are provided.

B. Accumulator

An accumulator is a pressure vessel filled with ECC water and pressurized with nitrogen gas. During normal operation each accumulator is isolated from the reactor primary coolant system by a check valve. If the reactor-coolant-system pressure falls below the accumulator pressure, the check valves open and ECC water is forced into the reactor coolant system.

An accumulator component may be simulated by an ACCUM module in TRAC. This module can be connected only at one junction to other TRAC components. This connection is at the highest numbered cell. It is assumed that cell 1 is closed, as shown in the typical noding diagram in Fig. 16, and that the accumulator is not connected to a nitrogen pressure source. Therefore, the nitrogen pressure results from the expansion of the initial gas volume.

The procedures for data input, for initialization of arrays, for advancement of time-dependent variables, and for editing are similar to those given for a PIPE component (see Sec. IV.A). A sharp liquid-vapor interface is maintained by neglecting interfacial shear. In an accumulator, the vapor-phase properties are those for nitrogen gas; so interphase mass transfer cannot occur. The vapor-phase temperature minimum is not limited. Additionally, there is a phase separator at the accumulator discharge to ensure that pure liquid is discharged. The accumulator walls are assumed to be adiabatic.



● - JUNCTION

Fig. 16.

Accumulator noding diagram.

The output edit is similar to that for a PIPE one-dimensional component with the addition of three variables specific to an accumulator. These are: (1) the discharge volumetric flow rate, (2) the total liquid volume discharge, and (3) the collapsed liquid level.

An accumulator also may be modeled with a PIPE component by setting the air partial pressures to the desired values. Thus, wall heat transfer can be included by setting NODES to a nonzero value. The air-steam vapor-phase temperature minimum is limited to 280 K by routine THERMO. An input switch activates the interface sharpener, phase separator (optional) at the discharge and the additional edit as described above for the ACCUM component. The edit logic assumes that the component is vertical with the lowest numbered cell at the top.

C. Break and Fill

The BREAK and FILL modules are used to impose boundary conditions at the terminal junction of any one-dimensional component. Consequently, these modules differ from the others in that they do not model any system component per se and they do not perform any hydrodynamic or heat-transfer calculations. However, they are treated the same as any other component for input, initialization, and identification procedures.

The BREAK module imposes a pressure boundary condition one cell away from its adjacent component, as shown in Fig. 17. The pressure boundary condition, as well as the fluid properties associated with the BREAK, may be specified as functions of time by using the optional BREAK table cards. This module commonly is used to model the containment system in LOCA calculations.

A FILL module imposes a velocity boundary condition at the junction with its adjacent component, as shown in Fig. 18. For example, the ECC injection may be modeled with a FILL.

The velocity boundary condition and the fluid properties associated with a FILL are specified in one of three basic ways according to the control option selected. For the first type of FILL, only the homogeneous fluid velocity and

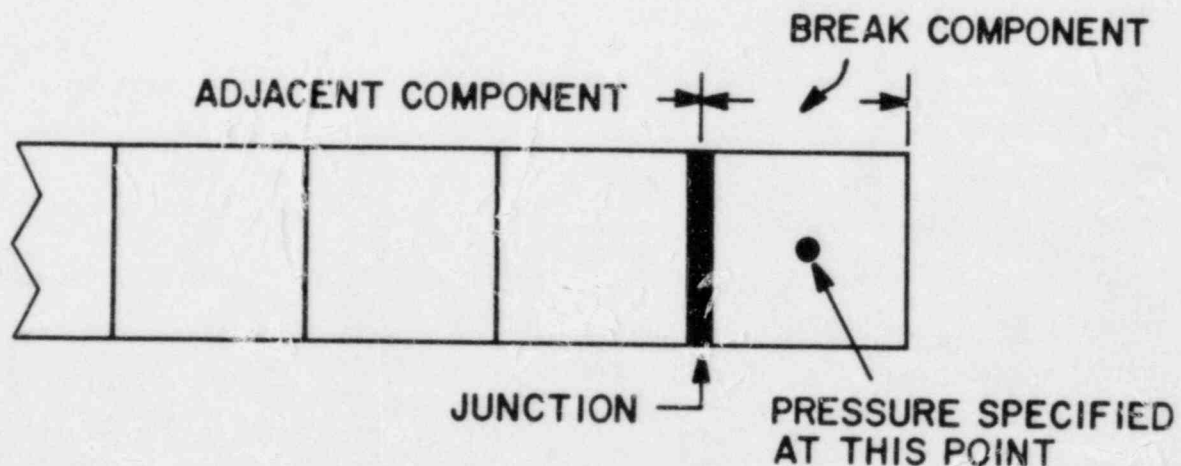


Fig. 17.
Break noding diagram.

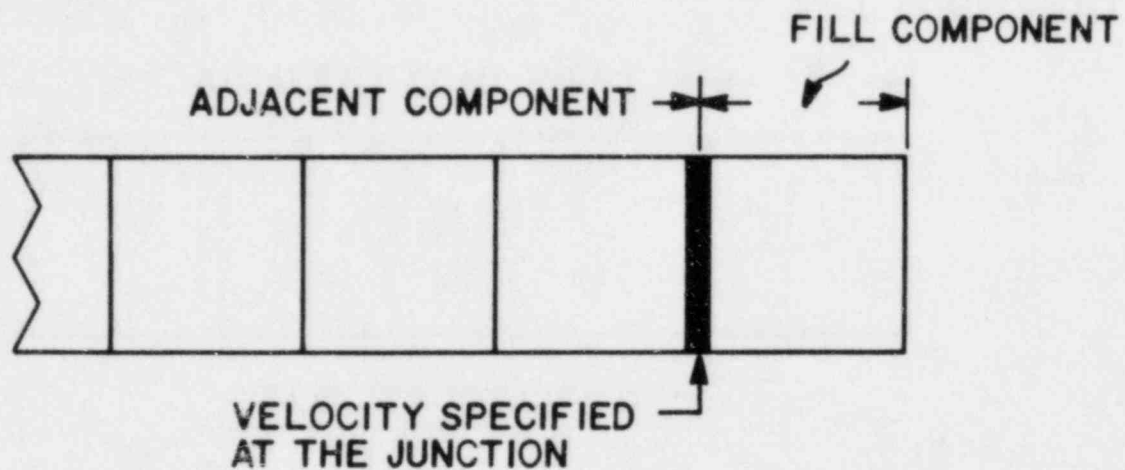


Fig. 18.
FILL noding diagram.

fluid properties are specified; for the second type, the mass flow and homogeneous fluid properties are specified; and for the third type, nonhomogeneous fluid velocities and fluid properties are specified. For each type of FILL, the relevant parameters may be constant, interpolated from a table, or constant until a trip and then interpolated from a table. The independent variable for the tables may depend on almost any system parameter (signal variable) as discussed in Sec. V.B. If use of the table is not trip initiated, the independent variable is always the absolute value of the signal variable. If use of the table is trip initiated, the independent variable may be either the absolute value of the signal variable or the difference between the signal-variable value and its value at trip initiation. This latter option requires a rate-factor table as discussed in Sec. V.C. When the signal variable varies rapidly or is strongly coupled to the FILL velocity, direct use of the tabulated values for the velocities or mass flow may lead to hydrodynamic instabilities. This situation may be avoided by using a weighted average of the previous and current tabular values (see Sec. V.F.5.b).

The parameters needed to specify a FILL or a BREAK are described in Secs. V.F.5.b and V.F.5.d. It is suggested that the cell volume and length in a BREAK be identical to those for the neighboring cell of the adjacent component. The pressure, void fraction, fluid temperatures, and air partial pressure specified in FILL and BREAK determine the properties of fluid convected into the adjacent component if an inflow condition should occur. (By convention, inflow corresponds to a positive FILL velocity and a negative BREAK velocity.) These components may not be connected directly to the VESSEL component.

D. Core

A CORE component is available in TRAC to analyze the reactor core in situations that do not demand a three-dimensional fluid-dynamics characterization. It has several advantages. First, this one-dimensional treatment can significantly reduce computer running time for a wide range of problems. Second, the CORE component is a hybrid that incorporates the coding characteristic to the PIPE and VESSEL components.

The fluid-dynamics and exterior-wall conduction models are identical to those used by a PIPE component. Both are one dimensional. In addition, any number of fuel rods may be introduced into the CORE component. The rod heat-transfer model is identical to that used by the VESSEL component.

A typical noding diagram for a CORE component is shown in Fig. 19. Presently, connections can be made only at the first and last cells. Therefore, it has been necessary to model the upper and lower plenums using a TEE component. The vessel downcomer has been modeled by attaching a PIPE to the CORE component. Therefore, bypass effects are difficult to model with this component. Detailed input specifications for a CORE component are provided in Sec. V.F.5.c. Input and output information is similar to that for the PIPE and VESSEL components.

E. Pressurizer

A PWR pressurizer is a large fluid reservoir that maintains the pressure within the reactor primary-coolant system and compensates for changes in the coolant volume caused by system transients. During normal operation this reservoir contains the hottest fluid in the primary system. It is usually maintained ~50-60% full of saturated liquid that is pressurized by the saturated steam above it. The pressurizer pressure is the controlling source

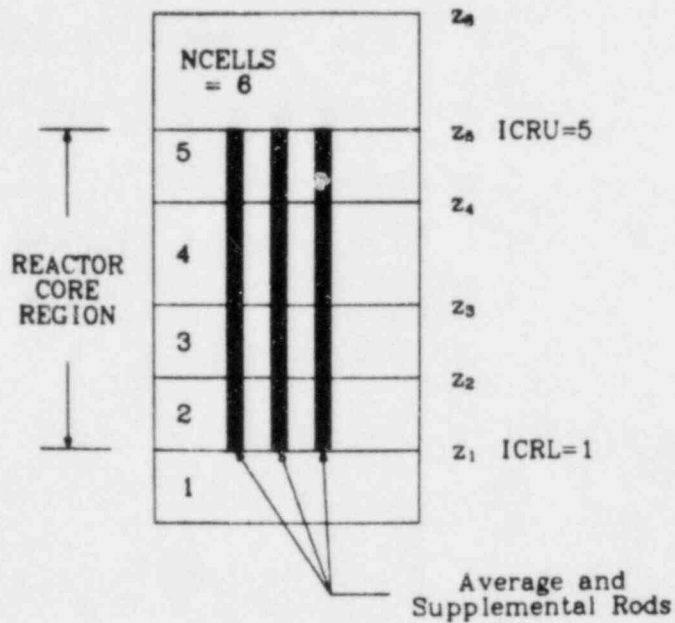


Fig. 19.
CORE noding diagram.

of the primary-coolant-loop pressure and is transmitted by a long surge line connected to one of the hot legs. (For steady-state calculations, the PRIZER module is replaced by a break equivalent.)

The PRIZER module simulates the pressurizer component. This module normally models the pressurizer itself with the surge line represented by a PIPE component. Figure 20, a typical noding diagram, shows that a PRIZER component may be connected at both junctions to other components. To calculate the collapsed liquid level, we assume that cell 1 is at the upper end, which may be closed by connecting it to a zero-velocity FILL.

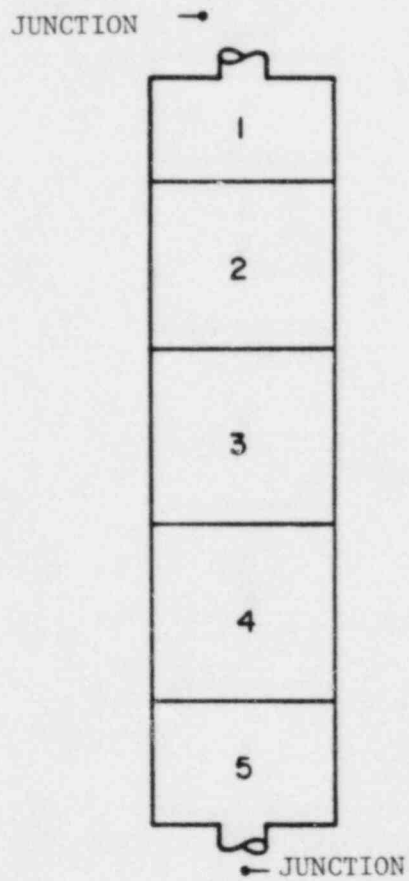


Fig. 20.
Pressurizer noding diagram.

The procedures for data input, initialization of arrays, advancement of time-dependent variables, and for editing are similar to those given for a PIPE component (see Sec. IV.A).

In the PRIZER component the walls are assumed to be adiabatic, but energy transfer from a heater/sprayer can be simulated. The primary purpose of this heater/sprayer logic is to serve as a system pressure controller, not to account for the added energy. The user specifies a desired pressure set point, PSET, and the pressure deviation, DPMAX, at which the heater sprayers add or remove a maximum power of QHEAT. The power that is input to the pressurizer fluid is directly proportional to the difference between PSET and P(1), the pressure in cell 1; that is,

$$Q_{\text{input}} = QHEAT \left[\frac{PSET - P(1)}{DPMAX} \right] ,$$

with the maximum value limited to $\pm QHEAT$. This power is distributed over all fluid cells in the pressurizer and the fraction of power input to each cell is equal to the fraction of total liquid mass in that cell. Power is not added if the collapsed liquid level is less than the input parameter ZHTR. (The collapsed liquid level is calculated assuming a cylindrical geometry with a cross-sectional area equal to the minimum of the flow areas input for the two faces of cell 1.) If pressure control is not desired, then QHEAT is set to zero.

Wall friction coefficients are calculated in routine FWALL by specifying a friction correlation option, NFF, along with the additive friction factors, FRIC, for each cell edge. The homogeneous flow friction correlation option (NFF = 1) is suggested for a pressurizer.

The output edit for a PRIZER component is similar to a PIPE component with the addition of four variables specific to the pressurizer. They are: (1) the discharge volumetric flow rate, (2) total liquid volume discharged, (3) collapsed liquid level, and (4) heater/sprayer power input to the pressurizer fluid.

F. Pump

The PUMP module describes the interaction of the system fluid with a centrifugal pump. The model calculates the pressure differential across the pump and its angular velocity as a function of the fluid flow rate and properties. The model can treat any centrifugal pump and allows for the inclusion of two-phase effects.

The pump model is represented by a one-dimensional component with N cells ($N > 1$). Figure 21 shows a typical noding diagram for the pump component. The pump momentum is modeled as a source between cells 1 and 2. The source is positive for normal operation so that a pressure rise occurs from cell 1 to cell 2. Therefore, it is necessary to construct the cell noding such that the cell number increases in the normal flow direction.

The following considerations were important in creating the PUMP module:

1. compatibility with adjacent components should be maximized,
2. choking at the pump inlet or outlet should be predicted automatically, and
3. the calculated pressure rise across the pump should agree with that measured at steady-state conditions.

The first two criteria precluded the use of a lumped-parameter model. The PUMP module, therefore, combines the PIPE module with pump correlations.

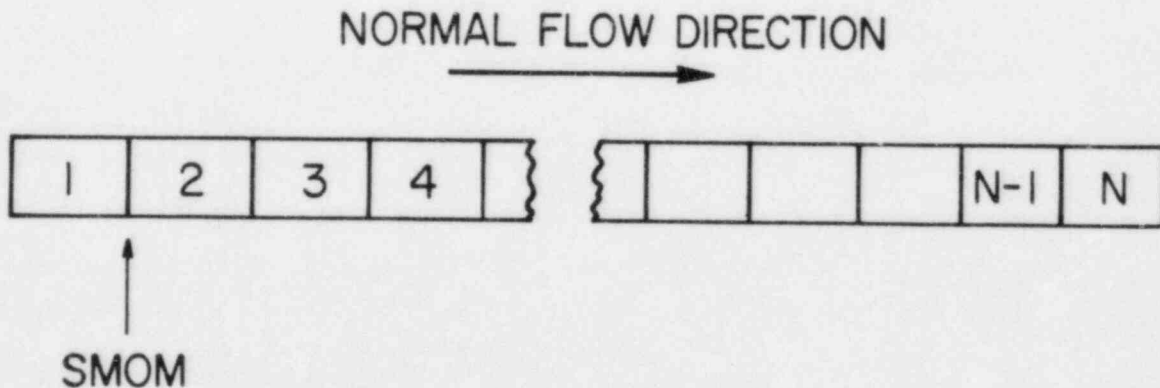


Fig. 21.
Pump noding diagram.

The pump model is identical to the one-dimensional pipe model except that the momentum equations between cells 1 and 2 are rewritten as:

$$\frac{V_{\ell}^{n+1} - V_{\ell}^n}{\Delta t} = \frac{[P_1^{n+1} - P_2^{n+1} + \Delta P^n + (\frac{\partial \Delta P}{\partial V})^n (V_{\ell}^{n+1} - V_{\ell}^n)]}{(\langle \rho_m \rangle \bar{\Delta x})} - g \cos \theta \quad (186)$$

and

$$V_g = V_{\ell} \quad , \quad (187)$$

where ΔP is the pressure rise through the pump evaluated from the pump correlation. The steady-state solution of Eq. (186) is

$$\Delta P = P_2 - P_1 + g \cos \theta \quad ,$$

which is the desired result. Friction does not enter explicitly into the pump motion equation. Therefore, additive friction is not allowed between cells 1 and 2 [FRIC (2) = 0.0].

It is necessary to evaluate ΔP and its derivative with respect to velocity for a pump cell only once each time step. The source is needed only in routines FEMOM and TF1DS1. This evaluation is performed by subroutine PUMPSR.

The pump correlation curves describe the pump head and torque response as a function of fluid volumetric flow rate and pump speed. Homologous curves (one curve segment represents a family of curves) are used for this description because of their simplicity. These curves describe, in a compact manner, all operating states of the pump obtained by combining positive or negative impeller velocities with positive or negative flow rates.

The following definitions are used in the subsequent development:

$H =$ the pump head $= \frac{\Delta P}{\rho}$,

$Q =$ the pump volumetric flow rate, and

$\Omega =$ the pump impeller angular velocity,

where ΔP is the pump differential pressure and ρ is the pump upstream mixture density. To allow one set of curves to be used for a variety of pumps, the following normalized quantities are used:

$$h \equiv \frac{H}{H_R} ,$$

$$q \equiv \frac{Q}{Q_R} , \text{ and}$$

$$\omega \equiv \frac{\Omega}{\Omega_R} ,$$

where H_R is the rated head (RHEAD) for the pump, Q_R is the rated volumetric flow (RFLOW), and Ω_R is the rated pump speed (ROMEGA). The pump similarity relations⁴⁷ show that

$$\frac{h}{\omega^2} = f \left(\frac{q}{\omega} \right) . \quad (188)$$

For lower case ω this correlation is not satisfactory and the following combination of variables is used;

$$\frac{h}{q} = f \left(\frac{\omega}{q} \right) . \quad (189)$$

Correlation (183) is used in the range $0 \leq |q/\omega| \leq 1$ and results in two separate curves, one for $\omega > 0$ and one for $\omega < 0$. Correlation (184) is used in the range $0 \leq |\omega/q| < 1$ and yields two separate curves, one for $q > 0$ and one for $q < 0$. The four resulting curve segments, as well as the curve selection logic used in TRAC, are shown in Table V.

To account for two-phase effects on pump performance, the pump curves are divided into two separate regimes. Data indicate that two-phase pump performance in the vapor-fraction range of 20-80% is degraded significantly in comparison to its performance at vapor fractions outside this range. One set of curves describes the pump performance for single-phase fluid (0 or 100% vapor fraction) and another set describes the two-phase, fully degraded performance at some void fraction between 0 and 100%. For single-phase conditions the curve segments for correlation (183) are input as HSP1 for $\omega > 0$ and HSP4 for $\omega < 0$, and correlation (184) curve segments are input as HSP2 for $q > 0$ and HSP3 for $q < 0$. The fully degraded version of correlation (183) is input as curve HTP1 for $\omega > 0$ and HTP4 for $\omega < 0$. The fully degraded version of correlation (184) is input as HTP2 for $q > 0$ and HTP3 for $q < 0$.

TABLE V

DEFINITIONS OF THE FOUR CURVE SEGMENTS THAT DESCRIBE THE
HOMOLOGOUS PUMP HEAD CURVES

<u>Curve Segment</u>	$\frac{ q }{\omega}$	ω	q	<u>Correlation^a</u>
1	≤ 1	> 0		$[\frac{h}{\omega^2} = f(\frac{q}{\omega})]$
4	≤ 1	< 0		
2	> 1		> 0	
3	> 1		< 0	$[\frac{h}{q^2} = f(\frac{\omega}{q})]$

^aFor the special case of both $\omega = 0.0$ and $q = 0.0$, the code sets $h = 0.0$.

The pump head at any vapor fraction is calculated from the relationship,

$$H = H_1 - M(\alpha) (H_1 - H_2) \quad , \quad (190)$$

where

H = the total pump head,

$H_1 = h_1 H_R$ = the single-phase pump head (h_1 is the nondimensional head from the single-phase homologous head curves),

$H_2 = h_2 H_R$ = the fully degraded pump head (h_2 is the nondimensional head from the fully degraded homologous head curves),

M = the pump degradation multiplier (input as HDM), and

α = the vapor fraction.

To this point, no knowledge of density is required to calculate H from the homologous head curves. The upstream mixture density is always used to convert the total pump head H to ΔP , the pressure rise through the pump.

The development of homologous torque curves parallels the previous development for homologous head curves. The dimensionless hydraulic torque is defined by

$$\beta \equiv \frac{T_{hy}}{T_R} \quad ,$$

where T_{hy} is the hydraulic torque and T_R is the rated torque (RTORK). The convention used is that a positive T_{hy} works to retard positive pump angular velocity. The dimensionless torque β is correlated as either β/ω or β/q , just as the dimensionless head was correlated. For single-phase conditions the correlations yield the corresponding four curve segments TSP1, TSP2, TSP3, and TSP4. The fully degraded correlations produce four corresponding curves TTP1, TTP2, TTP3, and TTP4. The homologous torque curve segments are correlated in the same manner as the head curve segments shown in Table V (replace h with β). For the special case of $\omega = q = 0.0$, the code sets $\beta_1 = \beta_2 = 0.0$.

The single-phase torque T_1 is dependent upon the fluid density and is calculated from

$$T_1 = \beta_1 T_R \left(\frac{\rho}{\rho_R} \right) , \quad (191)$$

where β_1 is the dimensionless hydraulic torque from the single-phase homologous torque curves, ρ is the pump upstream mixture density, and ρ_R is the rated density (RRHO). The density ratio is needed to correct for the density difference between the pumped fluid and the rated condition. Similarly, the fully degraded torque T_2 is obtained from

$$T_2 = \beta_2 T_R \left(\frac{\rho}{\rho_R} \right) ,$$

where β_2 is the dimensionless hydraulic torque from the fully degraded homologous torque curves. For two-phase conditions the impeller torque is calculated from

$$T = T_1 - N(\alpha) (T_1 - T_2) , \quad (192)$$

where T is the total impeller torque and $N(\alpha)$ is the torque degradation multiplier (input as TDM).

In addition to the homologous head and torque curves, the head and torque degradation multipliers defined in Eqs. (190) and (192) are required. These functions of void fraction are nonzero only in the vapor-fraction range where the pump head and torque are either partially or fully degraded.

The pump module treats the pump angular velocity as a constant (input) while the motor is energized. After a drive motor trip, the time rate of change for the pump angular velocity Ω is proportional to the sum of the moments acting on it and is calculated from the equation,

$$I \frac{d\Omega}{dt} = - \sum_i T_i = - (T + T_f + T_b) \quad , \quad (193)$$

where I is the combined impeller, shaft, and motor assembly moment of inertia (EFFMI); T_f is the torque caused by friction; and T_b is the bearing and windage torque. We assume that T_f and T_b are

$$T_f = C_1 \frac{\Omega |\Omega|}{\Omega_R^2} \quad (194)$$

and

$$T_b = C_2 \frac{\Omega |\Omega|}{\Omega_R^2} \quad , \quad (195)$$

where C_1 and C_2 are input constants (TFR1 and TFR2, respectively). The hydraulic torque T is evaluated using the homologous torque curves and Eq. (192); it is a function of the volumetric flow, the upstream void fraction, the upstream density, and the pump angular velocity. For time step $(n+1)$, Eq. (193) is evaluated explicitly,

$$\Omega^{n+1} = \Omega^n - \frac{\Delta t}{I} [T(Q, \alpha, \rho, \Omega) + (C_1 + C_2) \frac{\Omega^n |\Omega^n|}{\Omega_R^2}] \quad . \quad (196)$$

The wall heat transfer, wall friction, and CHF calculation options are the same for the PUMP module as for the PIPE module. In addition, the following options are specified: pump type (IPMPTY), motor action (IPMPTR), reverse speed option (IRP), degradation option (IPM), and pump curve option (OPTION). The input variables IPMPTR and NPMPTX specify, respectively, the trip identifier for the pump trip initiation and the number of pairs of points in the pump-speed table (array SPTBL). If IPMPTR = 0, no pump trip action occurs and the pump runs for the entire calculation at the constant speed (OMEGAN) specified in the input.

If the pump motor is energized (trip IPMPTR set OFF), the angular velocity is assumed to be the constant value (OMEGAN). Otherwise (trip IPMPTR set ON), the pump speed is allowed to vary.

Two types of pumps are available. For pump type 1 (IPMPTY = 1), the pump-speed variation is specified by the input table. The pump is energized initially at a constant speed specified by input (OMEGAN). Trip IPMPTR may initiate a pump trip, after which the pump speed is taken from a pump-speed table (array SPTBL). The independent variable for the pump-speed table may be the time elapsed after trip initiation or any other signal variable, as discussed in Sec. V.3. For pump type 1 the torque calculation is not used. Pump type 2 (IPMPTY = 2) is similar to option 1 except that a speed table is not inserted. Instead, the pump speed is calculated from Eq. (196) after a trip has occurred.

If the reverse speed option is specified [(IRP) = 1], the pump is allowed to rotate both forward and in reverse. Otherwise (IRP = 0), the pump will rotate in the forward direction only. For this case, if negative rotation is calculated (after trip with pump type 2), the speed will be set to zero. The variable IRP is checked only for IPMPTY = 2.

If the degradation option is turned on (IPM = 1), the degraded pump head and torque are calculated from Eqs. (190) and (192). Otherwise (IPM = 0), only the single-phase head and torque homologous curves are used [equivalent to setting $M(\alpha)$ and $N(\alpha)$ to zero in Eqs. (190) and (192)].

The user may specify pump homologous curves in the input (OPTION = 0) or alternatively may use the built-in pump curves (OPTION = 1 or 2). The first set (OPTION = 1) of built-in pump curves is based on the Semiscale Mod-1 system pump.^{42,48-50} The Semiscale pump curves for single-phase homologous head

(HSP), fully degraded two-phase homologous head (HTP), head degradation multiplier (HDM), single-phase homologous torque (TSP), and torque degradation multiplier (TDM) are provided in Figs. 22-26, respectively. The second set (OPTION = 2) of built-in pump curves is based on the Loss-of-Fluid Test (LOFT) system pump.⁵¹ The LOFT pump curves for HSP, HTP, HDM, TSP, and TDM are shown in Figs. 27-31, respectively. For lack of data, the fully degraded two-phase homologous torque curves (TTP) for both Semiscale and LOFT are zero. Where applicable, the curve numbers correspond to the conditions provided in Table V.

Because these homologous curves are dimensionless, they can describe a variety of pumps by specifying the desired rated density, head, torque, volumetric flow, and angular velocity as input. We recommend that for full-scale PWR analyses, plant-specific pump curves be inserted; however, if such data are unavailable, the LOFT pump curves (OPTION = 2) generally should be used.

There are several restrictions and limitations in the current version of the PUMP module. Because there is no model portraying pump motor torque vs speed, the pump speed is the assumed input if the motor is energized. Pump noding is restricted such that the cell numbers increase in the direction of normal flow (NCELLS \geq 2), the pump momentum source is located between cells 1 and 2 of the pump model, and the additive friction (loss coefficient) between cells 1 and 2 is 0.0 [FRIC(2) = 0.0]. A flow area change should not be modeled between cells 1 and 2. Finally, the head degradation multiplier $M(\alpha)$ and the torque degradation multiplier $N(\alpha)$ are assumed to apply to all operating states of the pump.

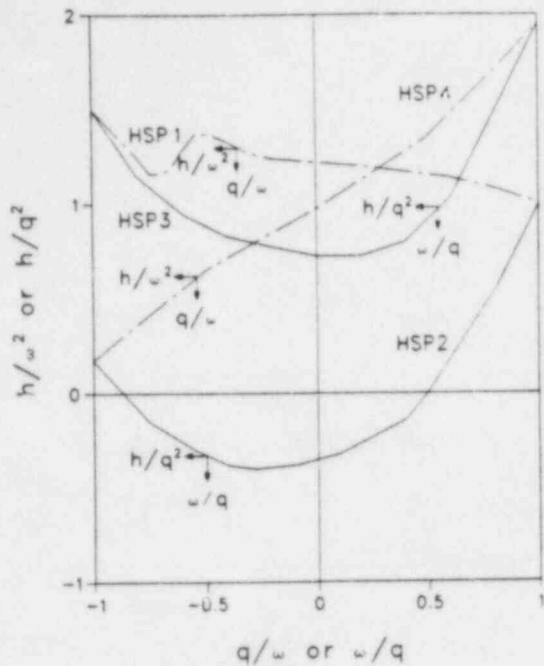


Fig. 22.

Semiscale single-phase homologous head curves.

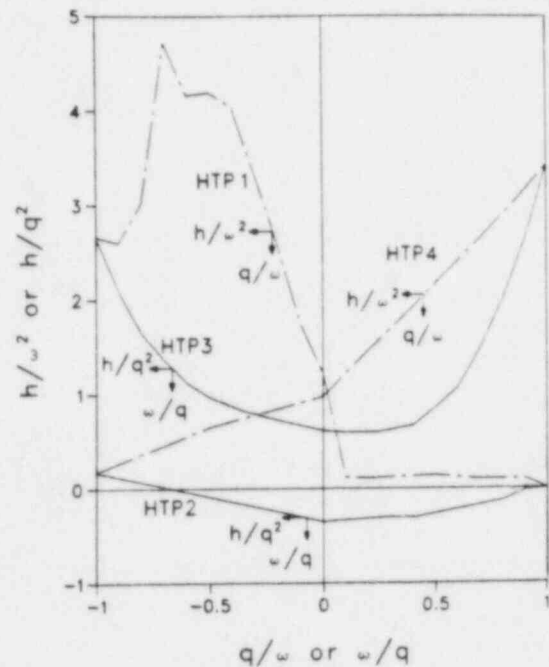


Fig. 23.

Semiscale fully degraded homologous head curves.

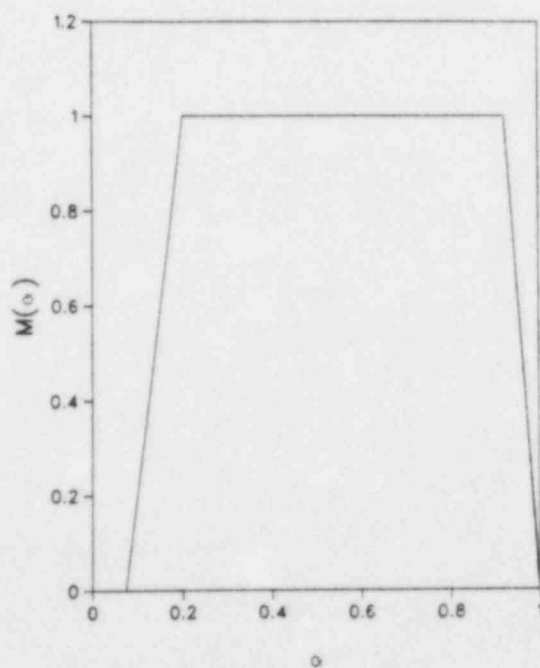


Fig. 24.

Semiscale head degradation multiplier curve.

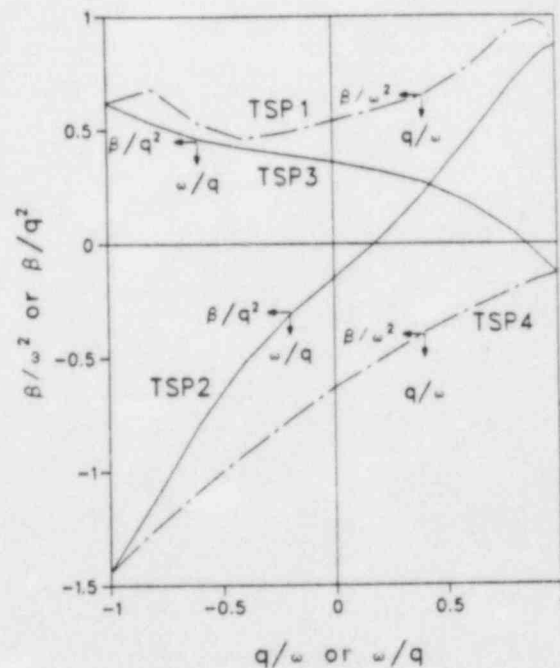


Fig. 25.

Semiscale single-phase homologous torque curves.

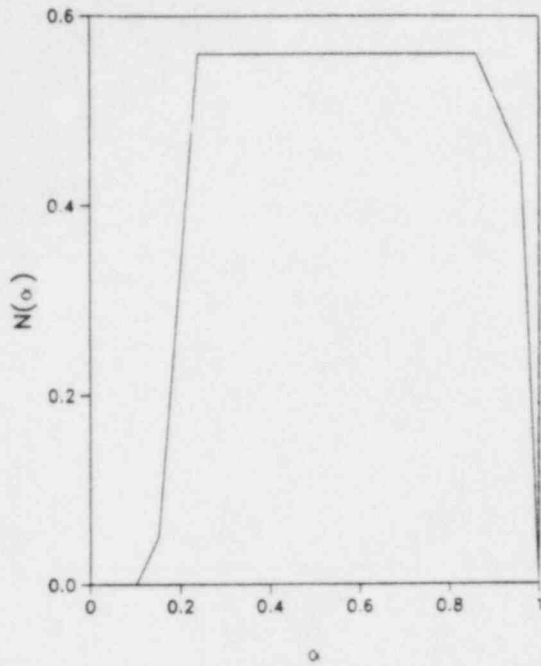


Fig. 26.
Semiscale torque degradation multiplier curve.

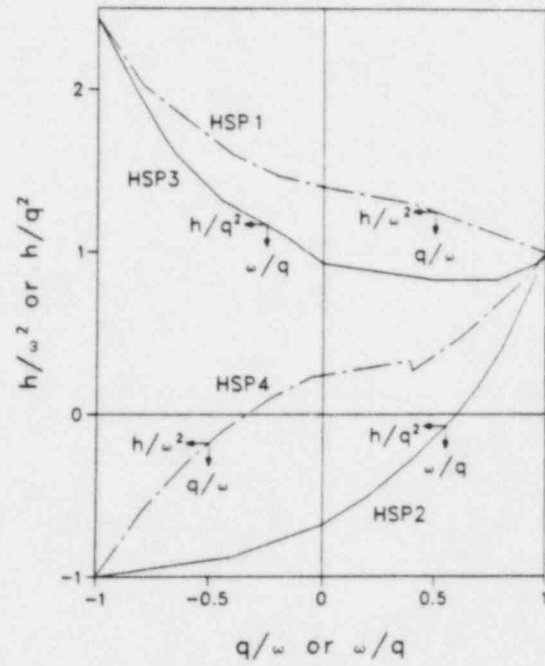


Fig. 27.
LOFT single-phase homologous head curves.

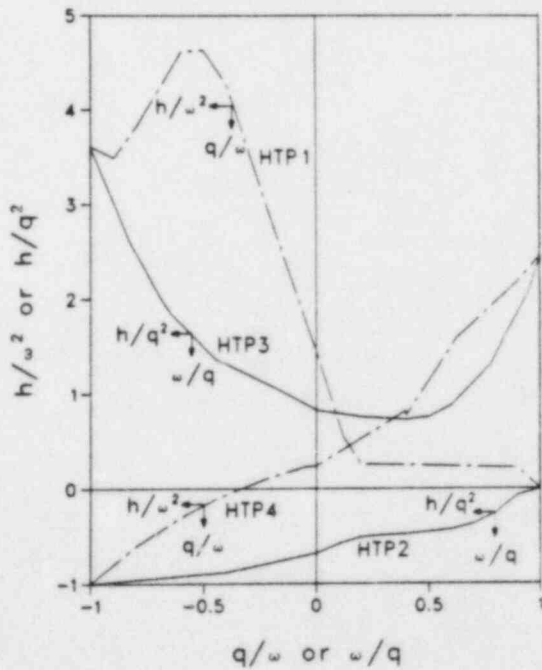


Fig. 28.
LOFT fully degraded homologous head curves.

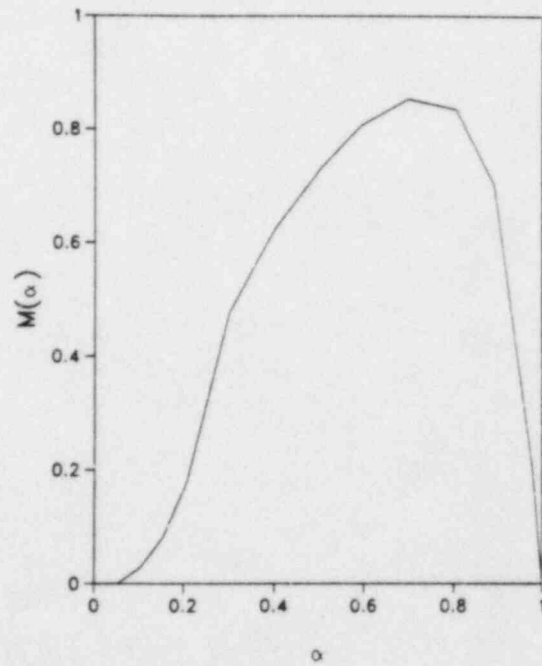


Fig. 29.
LOFT head degradation multiplier curve.

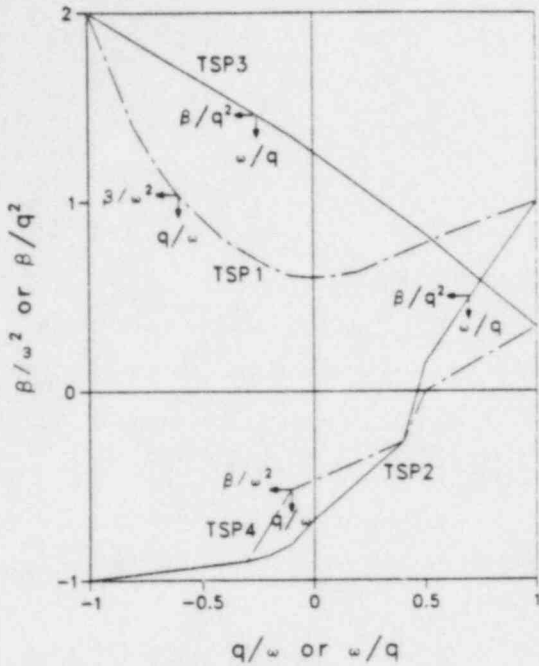


Fig. 30.

LOFT single-phase homologous torque curves.

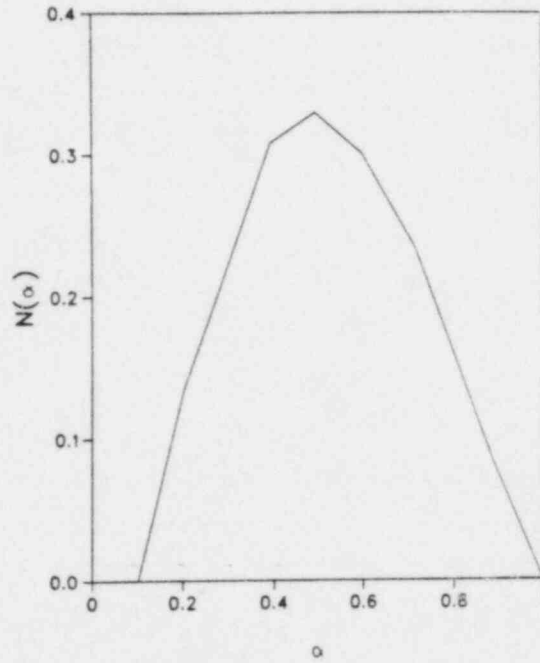


Fig. 31.

LOFT torque degradation multiplier curve.

The PUMP module input consists of the same geometric and hydrodynamic data and initial conditions that are required for the PIPE module. In addition, information specific to the PUMP is required, as described in the input specifications (Sec. V.F.5). The speed table (SPTBL) and the homologous pump curve arrays must be inserted in the following order:

$x(1), y(1), x(2), y(2), \dots, x(n), y(n)$.

Here, x is the independent variable and y is the dependent variable. Furthermore, the independent variables must increase monotonically on input; that is,

$x(1) < x(2) < \dots < x(n-1) < x(n)$.

Linear interpolation is used within the arrays.

G. Steam Generator

In a PWR the steam generators transfer energy from the primary to the secondary coolant loop to produce steam. The STGEN module can model either "U-tube" or "once-through" steam generators. The user specifies the type of generator through the input variable KIND (1 = U-tube and 2 = once-through). Although there are two different steam generator types, the basic operation is similar. That is, primary coolant enters an inlet plenum, flows through a tube bank in which the primary coolant exchanges heat with a secondary coolant that flows over the exterior of the tube bank, and finally discharges into an outlet plenum. Figure 32 provides typical noding diagrams for the STGEN components and illustrates that there is an inlet plenum (cell 1) and an outlet plenum (last cell) on the primary side; these two cells are assumed adiabatic. The tube bank, however, is represented by a single "effective" tube that has heat-transfer characteristics such that it is representative of the entire tube bank.

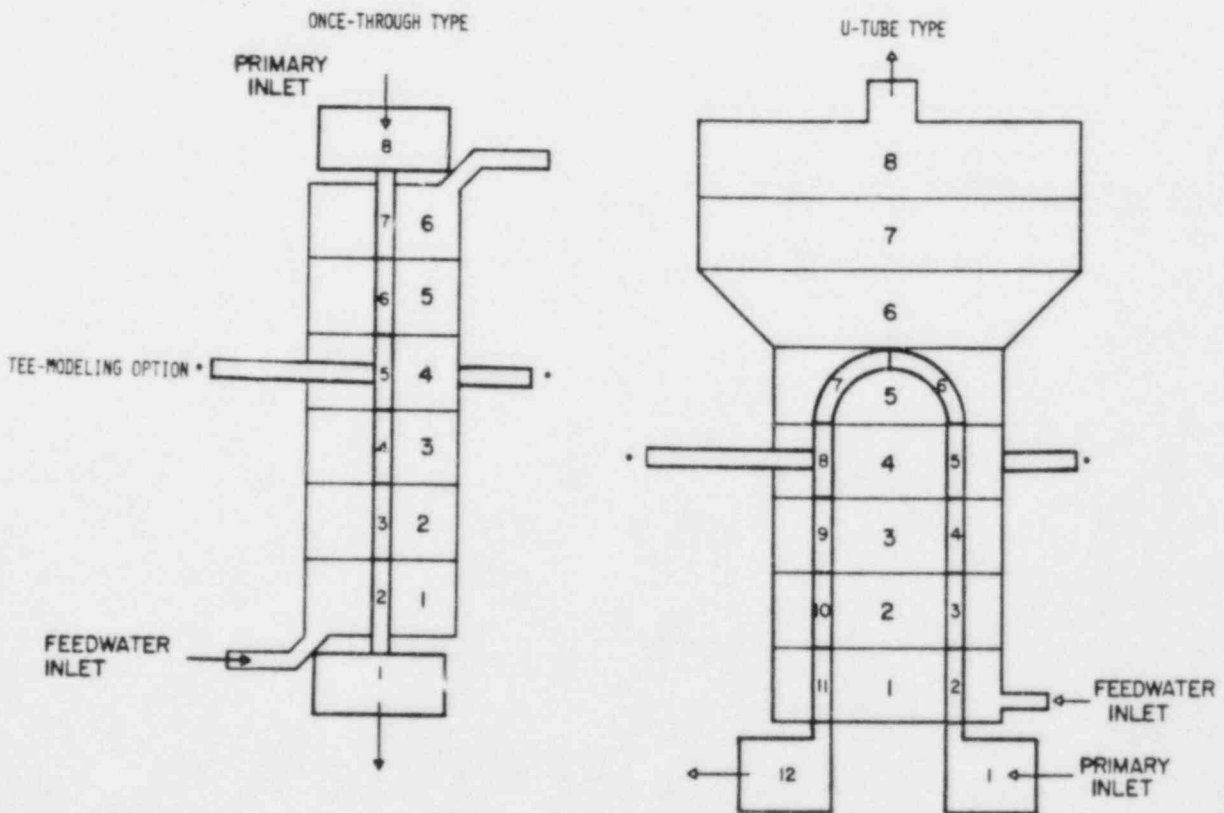


Fig. 32.
Steam generator noding diagram.

In the STGEN module the primary- and the secondary-side hydrodynamics are treated separately. Coupling between the two sides is achieved through wall heat transfer, which is modeled semi-implicitly. The hydrodynamics are solved by calling the one-dimensional, two-fluid routine TR1DS.

The procedures for reading input, for initialization of arrays, for advancement of the time step, and for editing are similar to those described for the PIPE module (see Sec. IV.A). The calculational sequence for the STGEN module is identical to that for PIPE (or TEE) except that the sequence of calls is performed twice, once for the primary side and once for the secondary side.

Although the procedure for reading input data is similar to that for a PIPE module, there are some differences. The most obvious difference is the specification of four junction numbers (Fig. 32), two for the primary-side and two for the secondary-side connections. Although it is possible to connect the secondary-side junctions to any TRAC component, the most common arrangement is to connect the inlet to a FILL, specifying the secondary-side fluid inlet conditions and the flow rate, and to a BREAK at the discharge, specifying the steam-generator-secondary discharge pressure. Because there is no provision for modeling the downcomer on the steam generator secondary, the fluid conditions for this FILL should be those for the water entering the tube bank and not those for the feedwater.

The number of fluid mesh cells on the primary side is specified by NCELL1 and that on the secondary side by NCELL2. There are some constraints imposed on the possible values for (NCELL1, NCELL2) combinations. For a once-through type (KIND = 2), it is required that $NCELL2 = NCELL1 - 2$. For a U-tube type (KIND = 1), it is assumed that there is a one-to-one correspondence between two active primary cells and one active secondary cell (see Fig. 32). Thus, for the fluid cells on the secondary side to reach the U-tube bundle top, it is required that $NCELL2 \geq (NCELL1 - 2)/2$. The secondary-side cells that are greater than $(NCELL1 - 2)/2$ are treated adiabatically and are used to model possible area changes and volumes above the tube bank. In Fig. 32, these are cells 6-8 on the secondary side.

The STGEN module also includes a TEE-modeling option where side tubing can be added to a main pipe, as in the TEE module. This feature is available on both the secondary and primary pipes. It may be used to model either a separate feedwater inlet or a tube-rupture break, or it may be used for other

purposes. When this option is exercised, the steam generator input, calculational sequences, and thermal-hydraulic modeling are similar to that for the TEE module except that the side tubing can only be adiabatic with no heat-transfer capability. The input parameters that invoke the TEE-modeling option are JCELL3 and JCELL4, the TEE junction cell (see the TEE module description, Sec. IV.H) for the secondary side and primary sides, respectively. The TEE junction cell may be any of the primary and secondary cells. To model a separate feedwater inlet, use only the TEE option on the secondary side. To model a tube-rupture break, use the TEE option on both the secondary and primary sides. The end junctions of both tees may be connected directly to each other to model the break flow between the primary and secondary sides. If only the primary TEE option is used, the secondary TEE still must be specified. It may be connected to a zero mass flow or a zero-velocity FILL.

At least one wall temperature nodes (NODES) must be specified. Three nodes are suggested, one at each tube surface and one at the tube wall center. The tube material is specified by the variable MAT. Available material options are given in the input specifications (Sec. V.F.5). Two flags, ICHF1 and ICHF2, determine if a CHF calculation is to be performed on the primary and secondary sides, respectively. If CHF calculations are desired, these flags are set equal to one; otherwise, they are set equal to zero. It should be noted that, if a CHF calculation is not performed, boiling heat-transfer calculations are precluded. Thus, stagnant fluid on the secondary side would have a low HTC, which is typical of natural convection. Therefore, we suggest that the combination $ICHF1 = 0$ and $ICHF2 = 1$ be used.

Geometrical input data for the tubes must be determined cautiously. As stated earlier, it is necessary to model the heat-transfer characteristics of the entire tube bundle with a single effective tube. This can best be achieved as follows: the inner tube radius, RADIN, and tube wall thickness, TH, should be those of a single tube in the bundle. The user specifies the heat-transfer surface area in each cell for both the primary and secondary sides. These two sets of areas are checked against RADIN and TH for consistency. If these numbers are inconsistent, the secondary areas are adjusted. The steam generator can be made adiabatic by specifying zero heat-transfer areas.

Specification of the heat-transfer area for the once-through type is straightforward; it is the total heat-transfer area for the steam generator multiplied by the fraction of the total tube length in each mesh cell. For the U-tube type, however, caution must be used. On the primary side, the heat-transfer area is the interior area for all the tubes in each mesh cell. The total heat transfer to a secondary-side fluid cell is the sum of the heat transfer from the up and the down tubes in the cell. In the TRAC calculation, the heat-transfer areas for the up and the down tubes are assumed equal. Therefore, the user should insert an area that is equal to one-half the surface area on the tube exteriors of both the up and the down tubes in that fluid cell.

The volumes and the flow areas on the primary side are determined by considering all the tubes in the bank. However, the hydraulic diameter is that of a single tube. The volumes and the flow areas on the secondary side are the actual geometric values for each mesh cell. The secondary hydraulic diameter is determined by standard methods used in heat transfer over tube bundles.

Tube wall initial temperatures also must be specified; the required number is the product of NCELL1 and NODES. Thus, even though cell 1 and cell NCELL1 are adiabatic, tube wall temperatures must be given for both cells to simplify indexing. The numbering convention is that temperatures begin with cell 1 and are specified from interior (primary side) to exterior (secondary side) for each mesh cell.

Friction-factor correlation options (NFF) and additive friction losses (FRIC) are input separately for the two sides. The possible options for NFF are described in Sec. III.A.4.1. The homogeneous option (NFF = 1) is suggested for both the primary and the secondary sides.

The output edit for a steam generator component is similar to that given for a PIPE component, with the primary-side variables input first and then the secondary-side variables. Heat-transfer variables always are provided. Tube wall temperatures are printed for each active mesh cell on a nodal basis.

H. Tee

The TEE module models the thermal hydraulics of three piping branches, two of which lie along a common line and the third enters at some angle β from the main axis of the other two (Fig. 33). In TRAC-PF1, the tee is treated as two PIPES, as indicated in Fig. 33. Beta is defined as the angle from the

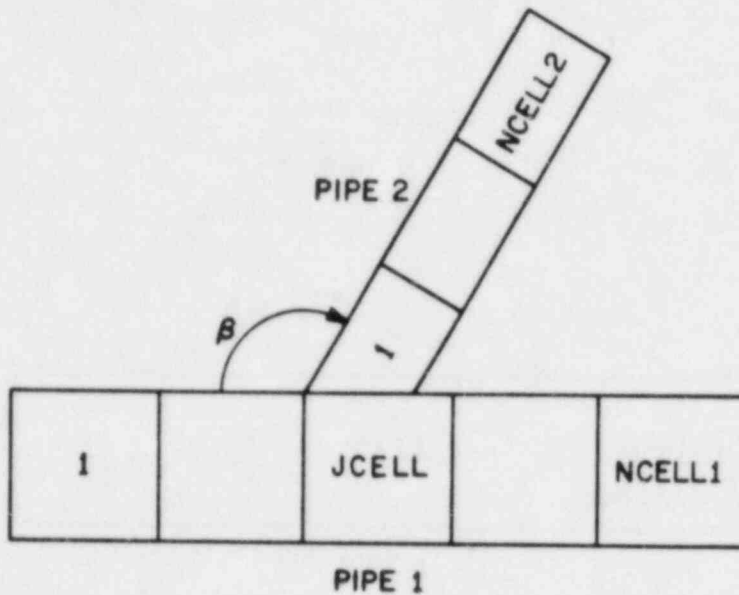


Fig. 33.
TEE noding diagram.

low-numbered end of PIPE 1 to PIPE 2. The low-numbered end of PIPE 2 always connects to PIPE 1. The first PIPE extends from cell 1 to cell NCELL1 and connects to PIPE 2 at cell JCELL. The second PIPE begins at cell 1 and ends at cell NCELL2.

The connection is effected through mass, momentum, and energy source terms in PIPE 1. PIPE 2 sees the connection as boundary conditions from cell JCELL in PIPE 1. Liquid may be prevented from entering the TEE secondary by setting the value of FRIC at that junction to 1.E30. However, no generalized separation model has been implemented.

Because the TEE is modeled essentially as two interconnected PIPES, the PIPE model description in Sec. IV.A should be referenced for additional information on the calculational sequence. Naturally, the sequence for a TEE includes separate calculations of the primary and secondary sides.

Detailed input specifications for a TEE component are given in Sec. V.F.5.1. Input and output information is very similar to that for a PIPE component except that two PIPES are involved in a TEE component.

I. Valve

The VALVE module is used to model various types of valves associated with light water reactors. The valve action is modeled by controlling the flow area and the hydraulic diameter at one cell face of a one-dimensional component as shown in Fig. 34. The valve action may not be located at a valve component junction unless that junction is connected to a BREAK.

Two methods are provided for specifying the valve flow area. The flow area can be computed directly from a flow area fraction (FAVLVE) according to

$$\text{flow area} = \text{FAVLVE} \times \text{AVLVE} ,$$

where AVLVE is the input value for the fully open valve flow area. Alternatively, the flow area may be computed from the relative position (XPOS) of the valve stem assuming a guillotine-type cut of circular cross section. The relative position of the valve stem, XPOS = 1, corresponds to a fully open valve with flow area AVLVE. In either case, the corresponding hydraulic diameter HD is computed from

$$\text{hydraulic diameter} = \frac{4 \text{ AVLVE}}{P} \text{ HVLVE} ,$$

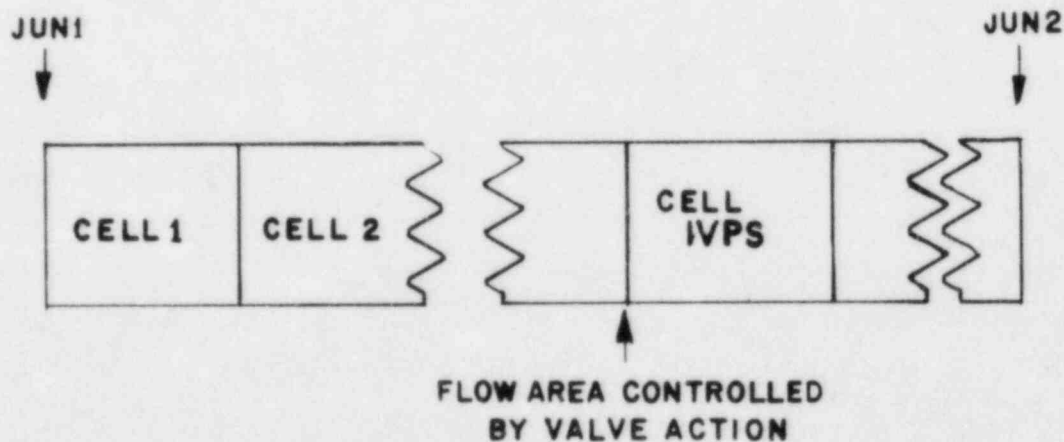


Fig. 34.
Valve noding diagram.

where P is the flow perimeter and HVLVE is the input value for the fully open valve hydraulic diameter.

The flow area fractions or valve stem positions are inserted as tables. Use of a table may be trip initiated according to the control option selected. To increase the flexibility to model various types of valves, two valve tables may be inserted for trip-controlled valves. The second table is used when the trip set status is in the ON_{reverse} position (see Sec. V.C). The independent variable for the tables may be a signal variable that is dependent upon almost any system parameter, as discussed in Sec. V.B.

Many different types of valves can be modeled because of the flexibility to choose both the independent variable for the valve action tables and the signal variable and associated set points that initiate trips and the possible use of a rate factor table, as discussed in Sec. V.C.

Simple valves that either open or close on a trip may be modeled using an OFF-ON or ON-OFF type trip and a table that has elapsed time as the independent variable to obtain the desired rate of opening or closing. (See Sec. V.C for a discussion of the rate-factor table input needed to flag the use of elapsed time rather than problem time for the independent variable.) Valve leakage can be simulated by restricting the minimum table value for flow area fraction or valve stem position to a value greater than zero. Simple valves can be used to model pipe breaks or the opening of rupture disks.

A simple check valve can be modeled by using a valve table with the appropriate pressure gradient as the independent variable. Alternatively, a check valve can be modeled as a trip-controlled valve with pressure gradients used as the trip set points and the valve table used to control the rate of action, as described previously in this section.

A steam flow control valve (or power-operated relief valve) can be modeled using an ON_{reverse}-OFF-ON_{forward} trip (see Sec. V.C) with the beginning closing pressure, ending closing pressure, ending opening pressure, and beginning opening pressure as the respective trip set points. The rate of opening (ON_{forward} state) can be determined by the first table and the rate of closing (ON_{reverse} state) by the second table.

A relief valve can be modeled by using a table with pressure as the independent variable and a step-like function for the flow area fraction or valve stem position. In this case, it is important that the step function not

be too steep or the valve flow area may oscillate because of the coupling between the flow through the valve and the pressure variable. A bank of relief valves can be modeled with a single valve component in a similar manner by using a multistep function to simulate the multiple set points corresponding to the various valves. The input parameters for the VALVE module are defined in Sec. V.F.5.j.

J. Vessel

The VESSEL module models a PWR vessel and its associated internals. The component is three dimensional and uses a six-equation, two-fluid model to evaluate the flow through and around all internals of a PWR vessel including the downcomer, core, and upper and lower plenums. Models incorporated into the VESSEL module are designed mainly for LOCA analysis, but the VESSEL module can be applied to other transient analyses as well. A mechanistic reflood model that can model quenching or dryout for an arbitrary number of quench fronts is included. The reactor power is modeled using point-reactor kinetics or by providing a power table in the problem input. Most of the detailed discussion of the fluid-dynamics, heat-transfer, and point-reactor kinetics equations and solution methods for the three-dimensional VESSEL module can be found in Sec. III. In this section, we discuss the VESSEL geometry and other important considerations.

A three-dimensional, two-fluid, thermal-hydraulic model in cylindrical coordinates describes the VESSEL flow. A regular cylindrical mesh, with variable mesh spacings in all three directions, encompasses the downcomer, core, and upper and lower plenums of the VESSEL, as shown in Fig. 35. The user describes the mesh by specifying the radial, angular, and axial coordinates of the mesh-cell boundaries:

$$r_i \quad i = 1, \dots, \text{NRSX} ;$$

$$\theta_j \quad j = 1, \dots, \text{NTSX} ;$$

and

$$z_k \quad k = 1, \dots, \text{NASX} ;$$

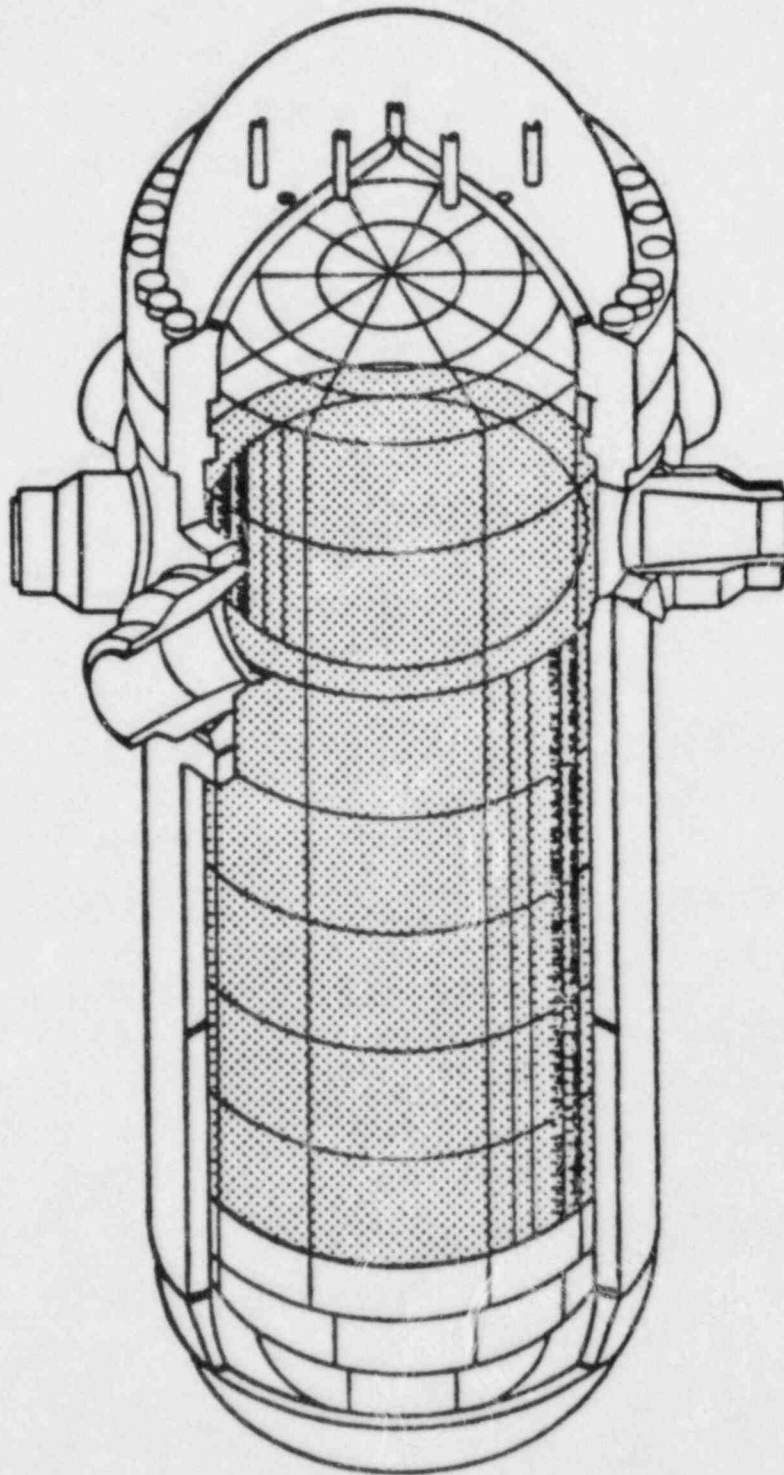


Fig. 35.
Cell noding diagram for a typical PWR vessel.

where NRSX is the number of rings, NTSX is the number of angular segments, and NASX is the number of axial levels. The point (r_i, θ_j, z_k) is a vertex in the

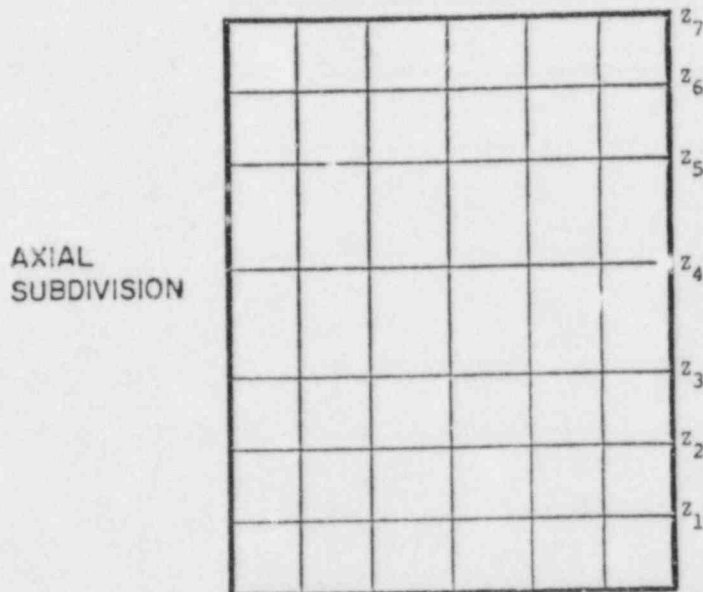
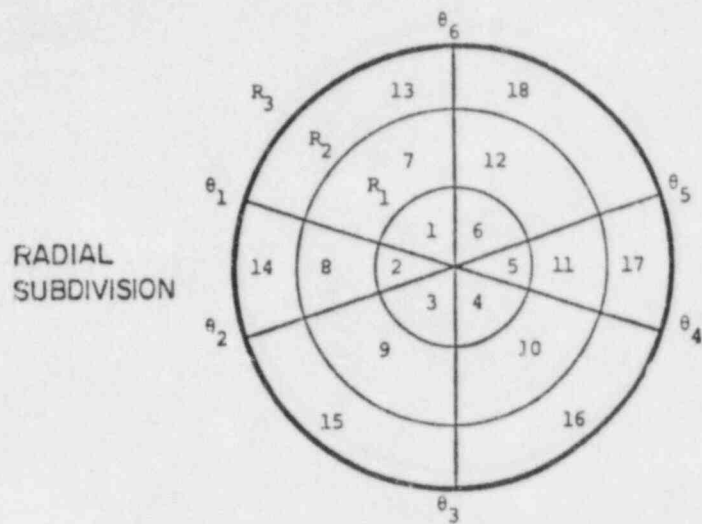


Fig. 36.

Vessel geometry, three-dimensional mesh construction with three rings, six angular segments, and seven axial intervals.

coordinate mesh. Figure 36 illustrates the mesh construction. Mesh cells are formed as shown in Fig. 37 and identified by an axial level number and a cell number. For each axial level, the cell number is determined by counting the cells radially outward starting with the first angular segment and the innermost ring of cells, as shown in Fig. 36. Figure 37 also shows the relative face-numbering convention that is used in connecting other components to the vessel. Note that only three faces per mesh cell must be identified because the other faces will be defined by neighboring cells.

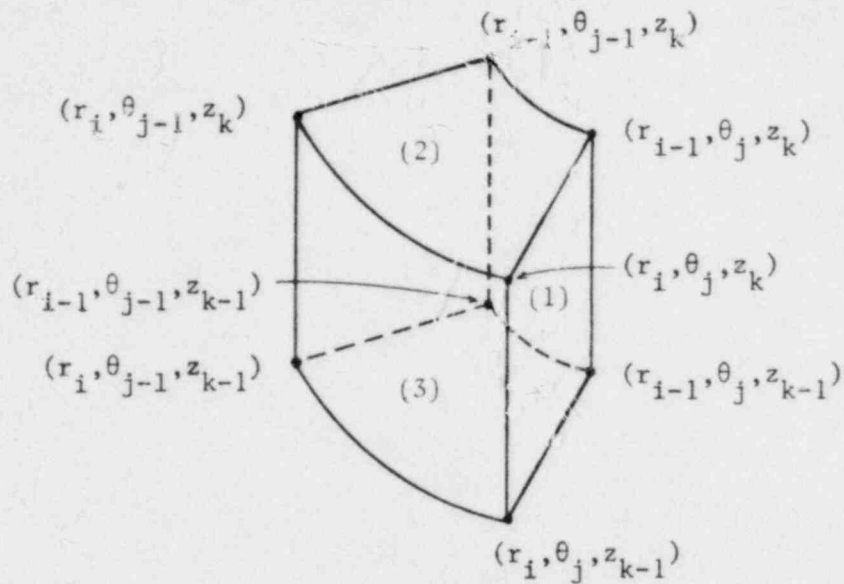


Fig. 37.

Boundaries of a three-dimensional mesh cell. The-face numbering convention also is shown. Faces 1, 2, and 3 are in the θ , z , and r directions, respectively.

All fluid flow areas (on cell faces) and all fluid volumes are dimensioned so that the internal structure within the vessel can be modeled. Flow areas and fluid volumes are computed based on the geometric mesh spacings and are scaled according to factors supplied as input. The scaled volumes and flow areas then are used in the fluid-dynamics and heat-transfer calculations.

Flow restrictions and the volume occupied by the structure within each mesh cell are modeled through the use of these scale factors. For example, the downcomer walls are modeled by setting the appropriate flow area scale factors to zero. A feature is provided to do this automatically in the code if the upper, lower, and radial downcomer position parameters (IDCU, IDCL, and IDCR) are specified as described in the input section (Sec. V.D.3.k). Flow restrictions such as the top and bottom core support plates require scale factors between zero and one. Fig. 38 shows the cell faces that are scaled to model the downcomer and core support plate flow restrictions.

Plumbing connections from other components to the VESSEL are made on the faces of the mesh cells. Only one connection per VESSEL cell is allowed, and all mesh cells in the VESSEL can have a component connected to it. Four input parameters are used to describe a connection: ISRL, ISPC, ISRF, and JUNS. The parameter ISRL defines the axial level in which the connection is made; ISRC is

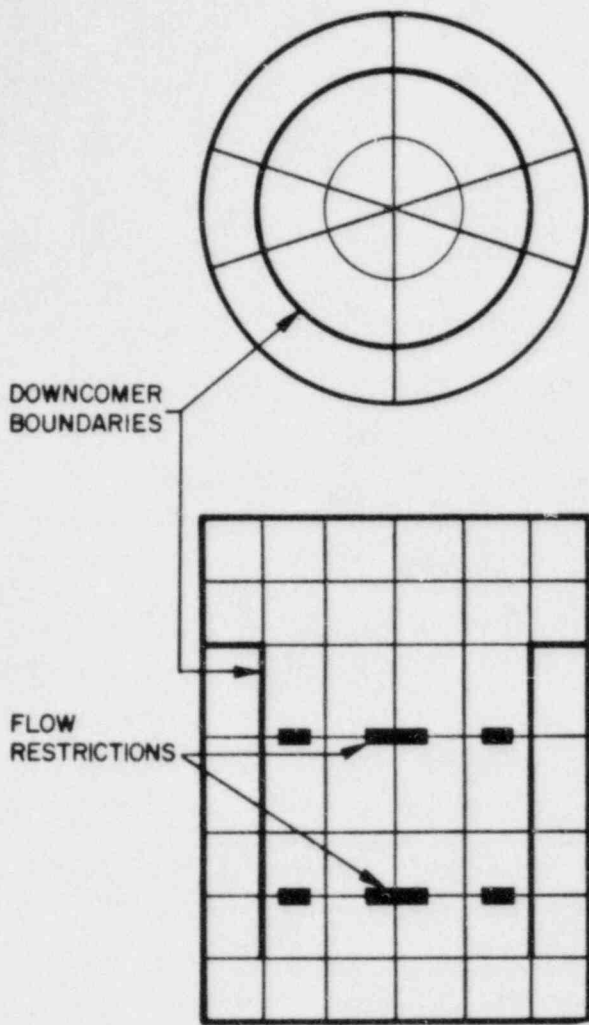


Fig. 38.

Flow restrictions and downcomer modeling.

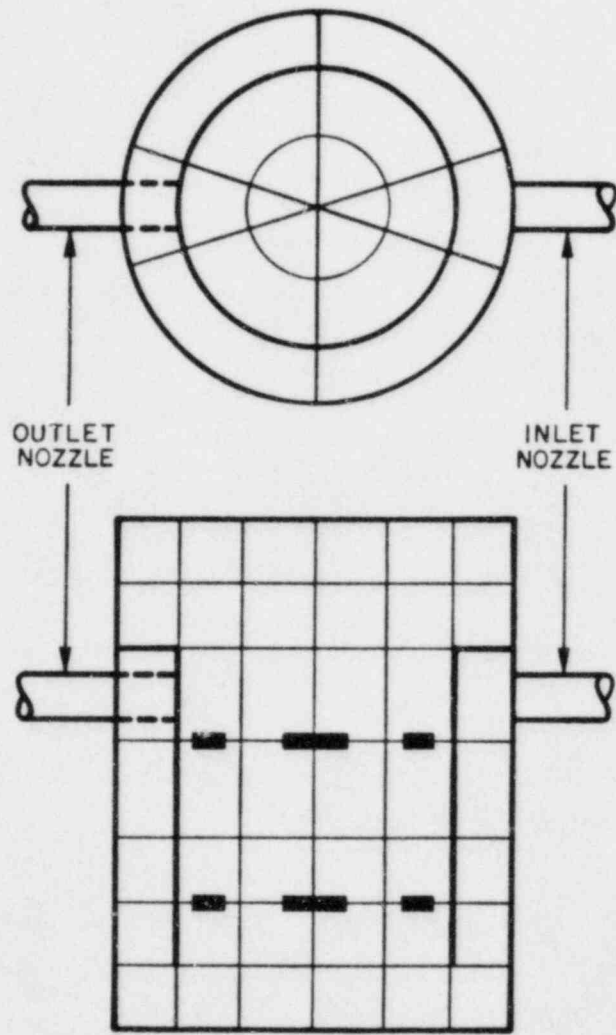


Fig. 39.

Pipe connections to the vessel.

the mesh-cell number, as defined above; and ISRF is the face number, as defined in Fig. 37. If ISRF is positive, the connection is made on the face shown in the figure with the direction of positive flow inward into the cell. If ISRF is negative, the connection is made on the opposite face shown in the figure with the direction of positive flow also inward into the cell. (Face 1 is the azimuthal face at θ , and face -1 is the azimuthal face at θ_{j-1} . Face 2 is the axial face at z_k , and face -2 is the axial face at z_{k-1} . Face 3 is the radial face at r_i , and face -3 is the radial face at r_{i-1} .) The parameter JUNS is the system junction number used to identify this junction. Figure 39 shows two VESSEL pipe connections. Note that internal as well as external connections

are allowed. The user is cautioned against connecting to the VESSEL any component with a flow area that differs greatly from the flow area of the mesh-cell face to which it is connected because this can cause anomalous pressure gradients. Such a situation can be avoided by proper adjustment of the VESSEL geometry coordinate spacings.

A VESSEL option models the Babcock & Wilcox vent valves that are located in the wall between the upper plenum and downcomer. These vent valves permit flow directly from the upper plenum to the downcomer and out the cold leg for a cold-leg break. They are modeled as fixed areas in the outer radial surface of a vessel cell with a variable FRIC term to model opening and closing.

The user specifies the cells that have vent valves by giving the axial level, cell number, and total area of vent valves for each cell with vent valves in the outer radial surface. The user also specifies for each cell with vent valves: (1) the pressure drop for the valves to be closed, DPCVN; (2) the pressure drop for the valves to be open, DPOVN; (3) the FRIC value when the valves are closed to model leakage, FRCVN; and (4) the FRIC value when the valves are open, FROVN. The pressure drop is defined as the pressure of the inner radial cell minus the pressure of the outer radial cell. The code uses FRCVN when the pressure drop is less than DPCVN, uses FROVN when the pressure drop is greater than DPOVN, and interpolates for pressure drops between DPCVN and DPOVN.

The reactor core region in the VESSEL is specified by the upper, lower, and radial core positional parameters (ICRU, ICRL, and ICRR). These parameters define, respectively, the upper, lower, and radial boundaries of the cylindrical core region. The example provided in Fig. 40 shows a possible configuration in which ICRU = 4, ICRL = 2, and ICRR = 2. Each mesh cell in the core region can contain an arbitrary number of fuel rods. One average rod represents the average of the ensemble of rods in each mesh cell, and its thermal calculation couples directly to the fluid dynamics. The thermal analysis of any supplemental rods does not feed back or couple directly to the fluid-dynamics analysis. However, the local fluid conditions in the mesh cell are used to obtain rod temperature history for the additional rods. A fuel-clad interaction treatment and a reflood treatment are available for these calculations and are described in Sec. III.B.

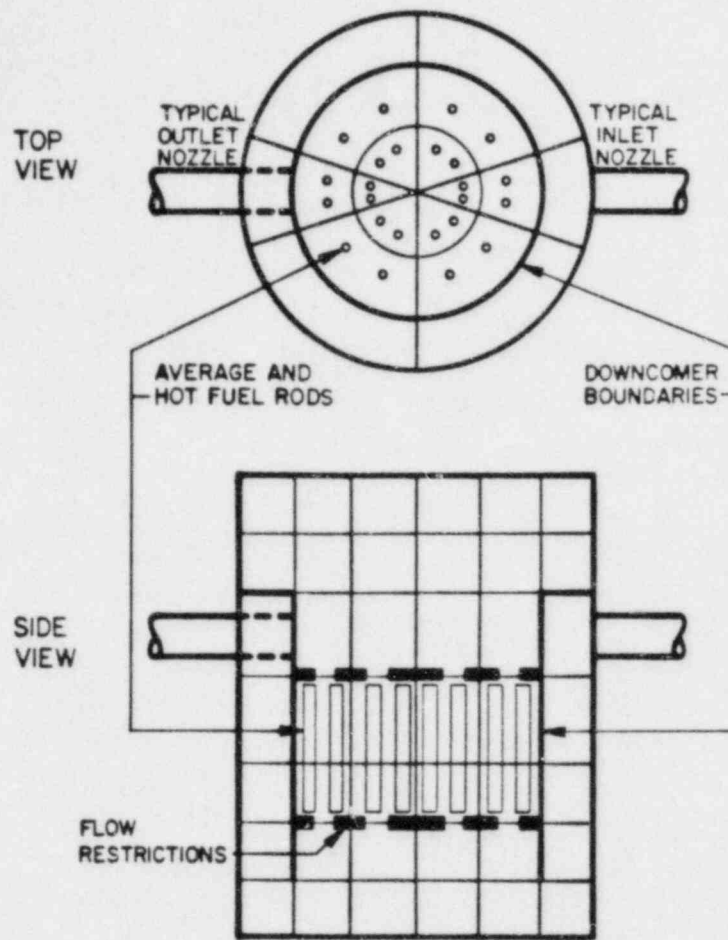


Fig. 40.
Core region inside the vessel.

Heat slabs of arbitrary thicknesses and surface areas can be defined in any mesh cell (including core regions) to model the heat capacity of structures within the vessel. An HTC is computed for each slab using the local fluid conditions. The temperature distribution is calculated based on a one-dimensional conduction model (refer to Sec. III. B.1.b). The thermal response of the slab properties is included. Furthermore, the code can account for an arbitrary number of interfaces between dissimilar materials.

The total power level in the core may be specified in terms of either power or reactivity with optional reactivity feedback. The solution of the point-reactor kinetics equations used in the latter case is described in Sec. III.C. The power or reactivity can be constant, determined from a table, or constant until a trip and then determined from a table. The table independent variable may be any signal-variable form as described in Sec. V.B.

For trip-initiated table use, the table independent variable can be modified by a rate factor that is a tabular function of the departure of the trip signal from the set point that turns off the trip. Consequently, override control of the core power level can be simulated. The flexibility that is available for the selection of the trip signal, trip set points, and delay times, as well as for the choice of the power or reactivity table independent variable and associated rate factor, permits accurate modeling of a large class of transient conditions.

The spatial power distribution in the core is specified by separate axial- and horizontal-plane power shapes, plus a radial power distribution across the fuel rods. These spatial distributions are specified in relative units when inserted and are held constant throughout a problem except for the axial power shape. Through input, one or more axial power shapes may be employed with any signal variable used to interpolate among them.

The power density in fuel rod node i in cell j on core level k is given by the expression,

$$P(i,j,k) = S \cdot P_{\text{tot}} \cdot \text{RDPWR}(i) \cdot \text{CPOWER}(j) \cdot \text{ZPOWER}(k) \quad , \quad (197)$$

where S is the scale factor that normalizes the three input relative power distributions, P_{tot} is the total core power level, $\text{RDPWR}(i)$ is the relative power in fuel node i , $\text{CPOWER}(j)$ is the relative power in cell j , and $\text{ZPOWER}(k)$ is the relative power at core elevation k . The scale factor S is given by the expression,

$$S = \left[\sum_{i,j,k} [\text{AREA}(i) \cdot \text{RDPWR}(i) \cdot \text{NRDX}(j) \cdot \text{CPOWER}(j) \cdot \Delta z(k) \cdot \text{ZPOWER}(k)] \right]^{-1} \quad , (198)$$

where $\text{AREA}(i)$ is the cross-sectional area of fuel rod node i , $\text{NRDX}(j)$ is the number of fuel rods in cell j , and $z(k)$ is the height of core axial level k . For the analyses of user-specified supplemental rods, the power density in Eq. (198) is multiplied by an input power factor $\text{RPKF}(j)$ to obtain the power density for each additional fuel rod.

V. USER INFORMATION

This chapter describes how to set up a problem input data deck, how to obtain restart dumps, how to restart problems from those dumps, and how to produce printer and graphics output files. Detailed descriptions of the signal-variable, trip, and controller features are presented.

A. Input Organization and Format

The input deck is divided into seven major sections: control, signal-variable, trip, controller, component, PWR-initialization, and time-step data. These data blocks are contained in a file named TRACIN and are read in the order shown in Fig. 41. The control data block contains general control parameters including title cards for problem identification, restart and dump control information, transient and steady-state control information, problem size information, and problem convergence criteria. This data block must be present in TRACIN.

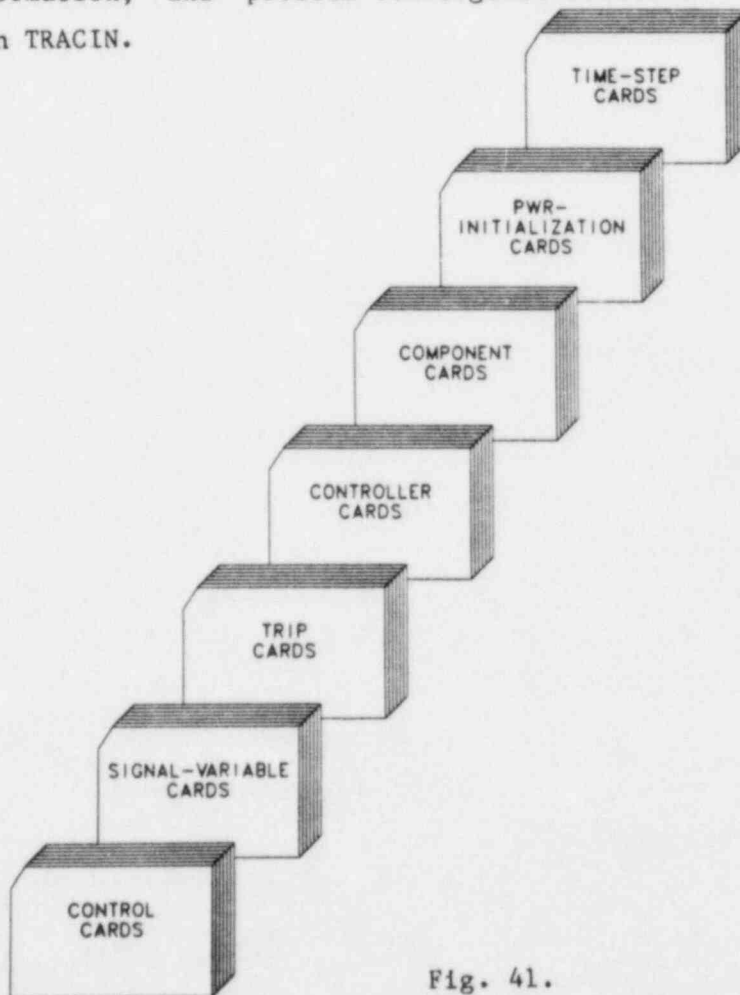


Fig. 41.
TRAC input deck organization.

Signal-variable data define signal parameters for trips and controllers and the independent variable for tables defining component actions. This data block is specified only if the control block parameter NTSV > 0. Part or all of the signal-variable data can come from the restart dump file TRCRST.

Trip control information is provided in the third data block. This data block is present only if NTRP > 0 in the control data block. Part or all of these trip input data also can come from the restart dump file.

Controller data are provided in the fourth data block. Controllers differ from the ON-OFF switch control of trips in that they directly convert a signal-variable input signal to an output signal for controlling a defined action. This data block is present only if the control block parameter NTCN > 0. Part or all of these input data can come from the restart dump file. This feature is not operational at present.

The main body of the input deck is contained in the component data block. This block contains a detailed description of every component in the problem unless the problem is reinitiated from a restart dump. For restart problems, only those components that are added or modified are included in the component block. The rest of the component data is obtained from the restart file. There is a component data block in the TRACIN file unless all the component data are obtained from the restart file.

A PWR-initialization data block is required only if STDYST = 2 or 3 has been specified in the control block data. This block contains several user-specified steady-state operating conditions that the code tries to match by adjusting certain operating parameters.

The time-step data block must be present in TRACIN. It specifies maximum and minimum time-step sizes, edit frequencies, and the end of the problem. All numeric input data are read into the code with either an E14.6 or I14 format statement, by the LOAD subroutine, or as NAMELIST data. Standard FORTRAN statements are used for formatted and NAMELIST reads. The LOAD subroutine provides additional flexibility to input array data.

The user is given the choice either to prepare his TRACIN input deck in strict accordance with the input specifications described in Sec. V.F (formatted input) or to prepare the deck in free format. If the user chooses formatted input, care must be taken to enter all data and array loading operations in the card columns specified in Sec. V.F. If free format is

chosen, the input cards and the data on each card must adhere to the order specified in Sec. V.F, but the data need not be entered in the specified columns. Besides the obvious convenience of not counting columns, free format gives the user greater flexibility in using comments to document his input deck and provides better diagnostics for input errors. The free format option is described in detail in Sec. V.H.

The following sections describe the signal-variable, trip, and controller capabilities; the dump/restart feature; the input data in detail; the LOAD subroutine read formats; the free-format option; the NAMELIST format; and the TRAC output files. A sample input deck is provided in Appendix C. Part of this deck, modified to illustrate various free-format possibilities, also is shown in Appendix C.

B. Signal Variables

Signal variables are parameters in the simulation model whose values provide input signals that control various actions within the system. Their values determine trip status, controller output signals, and component actions defined by tabular input. Signal variables are evaluated at the beginning of each time step where they undergo a step change in value. Their new value is assumed constant over the time step and defines the action during the time step.

Table VI lists 40 system parameters that define signal variables. The signal-variable parameter number ISVN defines the signal-variable parameter. Parameters with $1 \leq \text{ISVN} \leq 15$ come from the control panel vector, CPV(J), which the code evaluates and edits to simulate signals that are instrumented in the operator control room. Control actions initiated automatically or by the operator often are based on these signals. Their evaluation is not operational at present. Parameters with ISVN = 16 or 17 are specially defined parameters that the user may program into the PREP evaluation stage of TRAC. They are stored in and obtained from array DSV(I), $1 \leq I = \text{ISVN} - 15 \leq 2$, in common block SIGNAL where CPV(J) also is stored. Parameters with $20 \leq \text{ISVN} \leq 39$ are location-dependent; that is, both the component number and the mesh cell number(s) where the parameter is defined must be input for the component. Whereas all of the control-panel-vector parameters are location-dependent as well, their locations will be defined elsewhere in input when this feature

TABLE VI
SIGNAL-VARIABLE PARAMETERS

<u>Signal- Variable Parameter Number</u>	<u>Parameter Description</u>	<u>Additional Location Data</u>
0	Problem time (s)	
1	Primary pressure (Pa)	
2	Pressurizer-relief-tank pressure (Pa)	
3	Containment pressure (Pa)	
4	Containment temperature (K)	
5	Pressurizer water level (m)	
6	Refueling-storage-tank water level (m)	
7	Hot-leg temperature (K)	Coolant loop number
8	Cold-leg temperature (K)	Coolant loop number
9	Primary-coolant mass flow (kg/s)	Coolant loop number
10	Emergency-core-coolant (ECC) mass flow (kg/s)	Coolant loop number
11	Letdown-coolant mass flow (kg/s)	Coolant loop number
12	Steam-generator pressure (Pa)	Coolant loop number
13	Steam-generator-primary coolant flow (kg/s)	Coolant loop number
14	Steam-generator-secondary coolant flow (kg/s)	Coolant loop number
15	Steam-generator-secondary liquid level (m)	Coolant loop number
16	Dummy storage variable number 1	
17	Dummy storage variable number 2	
18	Reactor power (W)	Component number
19	Reactor period (s)	Component number

TABLE VI (cont.)

<u>Signal- Variable Parameter Number</u>	<u>Parameter Description</u>	<u>Additional Location Data</u>
20	Liquid water level (m)	Component, cell ₁ , and cell ₂ numbers
21	Cell pressure (Pa)	Component, cell ₁ , and cell ₂ numbers
22	Cell vapor temperature (K)	Component, cell ₁ , and cell ₂ numbers
23	Cell liquid temperature (K)	Component, cell ₁ , and cell ₂ numbers
24	Cell slab outer-surface temperature (K)	Component, cell ₁ , and cell ₂ numbers
25	Cell fuel-rod outer-surface temperature (K)	Component, cell ₁ , and cell ₂ numbers
26	Cell fuel-rod centerline temperature (K)	Component, cell ₁ , and cell ₂ numbers
27	Cell vapor volume fraction	Component, cell ₁ , and cell ₂ numbers
28	θ -interface vapor mass flow (kg/s)	Component, cell ₁ , and cell ₂ numbers
29	z-interface vapor mass flow (kg/s)	Component, cell ₁ , and cell ₂ numbers
30	r-interface vapor mass flow (kg/s)	Component, cell ₁ , and cell ₂ numbers
31	θ -interface liquid mass flow (kg/s)	Component, cell ₁ , and cell ₂ numbers
32	z-interface liquid mass flow (kg/s)	Component, cell ₁ , and cell ₂ numbers
33	r-interface liquid mass flow (kg/s)	Component, cell ₁ , and cell ₂ numbers
34	θ -interface vapor velocity (m/s)	Component, cell ₁ , and cell ₂ numbers
35	z-interface vapor velocity (m/s)	Component, cell ₁ , and cell ₂ numbers
36	r-interface vapor velocity (m/s)	Component, cell ₁ , and cell ₂ numbers
37	θ -interface liquid velocity (m/s)	Component, cell ₁ , and cell ₂ numbers
38	z-interface liquid velocity (m/s)	Component, cell ₁ , and cell ₂ numbers
39	r-interface liquid velocity (m/s)	Component, cell ₁ , and cell ₂ numbers

becomes operational. These parameters are included in Table VI for the user's convenience. Their use is more efficient because they are evaluated at each time step. Parameters with ISVN = 18, 19, 25, or 26 apply only to the CORE and VESSEL components when fuel rods are present.

The liquid water level, ISVN = 20, is the height of the liquid above the bottom interface of mesh cell, $|cell_1|$, and is defined by

$$\sum_{i=|cell_1|}^{I \pm 1} \Delta x_i + f \Delta x_I ,$$

where Δx_i is the height of mesh cell i and the liquid-vapor interface is at a distance $f \Delta x_I$ above the lower interface of mesh cell I . The values of f and I are defined by requiring that the volume of liquid between mesh cells $|cell_1|$ and $|cell_2|$ fill the fluid volume of mesh cells $|cell_1|$ to $I \pm 1$ below mesh cell I and the fraction f of the volume of mesh cell I ,

$$\sum_{i=|cell_1|}^{|cell_2|} (1 - \alpha_i) V_i \equiv \sum_{i=|cell_1|}^{I \pm 1} V_i + f V_I ,$$

where α_i is the volume fraction of the vapor fluid in mesh cell i and V_i is the volume of fluid in mesh cell i . If either $cell_1$ or $cell_2$ is zero, TRAC internally redefines $cell_1$ equal to 1 and $cell_2$ equal to the total number of mesh cells in the component.

The signal variables for the location-dependent parameters, $21 \leq |IVSN| \leq 39$, take one of five different forms. The signal-variable value is:

1. the parameter value in mesh cell $|cell_1|$ or $|cell_2|$ of the component number when $cell_2 = 0$ or $cell_1 = 0$, respectively;
2. the maximum value of the parameter between mesh cells $|cell_1|$ and $|cell_2|$ in the component when $cell_1$ and $cell_2$ are both positive;
3. the minimum value of the parameter between mesh cells $|cell_1|$ and $|cell_2|$ in the component when $cell_1$ and $cell_2$ are both negative;
4. the volume-averaged value of the parameter between mesh cells $|cell_1|$ and $|cell_2|$ in the component number when $cell_1$ and $cell_2$ are of opposite signs; and
5. the difference between the parameter values in mesh cells $|cell_1|$ and $|cell_2|$ when ISVN is negative (the signal-variable value equals the parameter value in $|cell_1|$ minus the parameter value in $|cell_2|$ when $-39 \leq ISVN \leq -21$).

For the three-dimensional VESSEL component, $cell_1$ and $cell_2$ are defined as composites of the relative cell number in the horizontal plane and the axial level number.

$$\begin{pmatrix} cell_1 \\ cell_2 \end{pmatrix} = (\text{horizontal plane relative cell number}) * 1000 + (\text{axial level number}).$$

When $20 \leq ISVN \leq 39$, the summation over vessel mesh cells includes all cells between the minimum and maximum relative cell numbers (defined by $cell_1$ and $cell_2$) for all axial levels between the minimum and maximum axial level numbers (also defined by $cell_1$ and $cell_2$).

The $cell_1$ and $cell_2$ numbers for the $28 \leq |ISVN| \leq 39$ mass flow and velocity signal-variable parameters are associated with the mesh-cell interface(s). In the three-dimension VESSEL, the second aximuthal interface, the outer radial interface, and the upper axial interface of a mesh cell are associated with the mesh-cell number. In one-dimensional components, the I^{th} mesh-cell interface lies between mesh cells $I-1$ and I . Specification of the r-interface or θ -interface for one-dimensional components prompts a default to the z-interface definition.

For mesh cells on the secondary side of TEE and STGEN components, $cell_1$ and $cell_2$ are defined as composites of the total number of mesh cells on the primary side, NCELL1, and the secondary mesh-cell number, N2.

$$\begin{pmatrix} cell_1 \\ cell_2 \end{pmatrix} = NCELL1 + 1 + N2 .$$

Similar considerations apply when STGEN components have TEEs on the primary or secondary sides. When $cell_1$ or $cell_2$ is in the secondary-side TEE then

$$\begin{pmatrix} cell_1 \\ cell_2 \end{pmatrix} = NCELL1 + NCELL2 + 2 + N2T ,$$

where NCELL2 is the number of cells in the steam-generator secondary and N2T is the cell number in the secondary TEE-side leg.

If one of the cells is in a primary TEE-side leg, then

$$\left(\begin{array}{l} \text{cell}_1 \\ \text{cell}_2 \end{array} \right) = \text{NCELL1} + \text{NCELL2} + \text{NCELL3} + 3 + \text{N1T} ,$$

where NCELL3 is the number of cells in the steam-generator secondary TEE-side leg and N1T is the cell number in the primary TEE-side leg. Signal-variable value forms 2, 3, or 4, spanning cell₁ to cell₂, should not be used when cell₁ and cell₂ are located on the primary and secondary sides. In spanning across cell number NCELL1 + 1, which is a dummy buffer cell between the primary and secondary mesh cells in storage, a nonphysical parameter cell would be incorporated in determining the maximum, minimum, or volume-averaged parameter value.

C. Trips

Trips are used to simulate operator and plant protective system response to transient or abnormal conditions. An ON-OFF switch type of control initiates and terminates action. Trip control can be applied to the following actions: the fluid condition in a FILL component; the pump rotational speed in a PUMP component; the opening and closing of the flow area in a VALVE component; and the variation of the reactor power or reactivity, the axial power shape, and the reflood fine axial mesh in the fuel rods of CORE and VESSEL components. Trips also can be used to implement special time-step data, to generate restart dumps, and to terminate problem execution.

The decision to switch the set status of a trip to ON or OFF and, thus, to initiate or terminate trip-controlled action, respectively, is based on a signal value defined to the trip. Trip-signal set points are defined over the trip-signal value range to delimit subranges with an ON or OFF set status for the trip. Thus, the set status of the subrange wherein the trip signal value lies defines the set status for the trip. Table VII shows the five trip-signal-range types defined by the trip-signal-range type number. For IPOS = 1 or 2, there are two subranges delimited by set points S₁ and S₂. In going from the left to the right subrange, the trip-signal value increases and must equal or exceed set point S₂ to change the trip-set-status condition. However, in going from the right to the left subrange, the trip-signal value must equal or be less than set point S₁ to change the trip-set-status

TABLE VII

TRIP-SIGNAL-RANGE TYPES

Trip-Signal-Range Type Number	Trip-Signal-Range Diagram With Subrange Trip Set Status		Trip Signal
1	ON	OFF	Trip Signal
2	OFF	ON	Trip Signal
3	ON _{reverse}	OFF	Trip Signal
4	ON _{forward}	OFF	Trip Signal
5	OFF	ON	Trip Signal

Trip-Signal-Range Type Number	Description of How the Trip-Set Status Is Changed
1	Trip to be set to ON when the trip signal $\leq S_1$ Trip to be set to OFF when the trip signal $\geq S_2$
2	Trip to be set to ON when the trip signal $\geq S_2$ Trip to be set to OFF when the trip signal $\leq S_1$
3	Trip to be set to ON _{reverse} when the trip signal $\leq S_1$ Trip to be set to OFF when the trip signal $\geq S_2$ or $\leq S_3$ Trip to be set to ON _{forward} when the trip signal $\geq S_4$
4	Trip to be set to ON _{forward} when the trip signal $\leq S_1$ Trip to be set to OFF when the trip signal $\geq S_2$ or $\leq S_3$ Trip to be set to ON _{reverse} when the trip signal $\geq S_4$
5	Trip to be set to ON when the trip signal $\geq S_2$ or $\leq S_3$ Trip to be set to OFF when the trip signal $\leq S_1$ or $\geq S_4$

condition. To ensure that the criterion for changing subranges is unique, S_1 must be less than S_2 . For IPOS = 3, 4, or 5, there are three subranges with four set points. Again, the trip-signal value increases to the right and $S_1 < S_2 < S_3 < S_4$. In cases where IPOS = 3 or 4, set status ON is either $ON_{forward}$ or $ON_{reverse}$. In $ON_{reverse}$, the action occurs in the opposite direction from $ON_{forward}$ when the trip-controlled component action table has as its independent variable the signal-variable value difference form. For the signal-variable value form, however, the same action will be interpolated from the table for both $ON_{forward}$ and $ON_{reverse}$. For IPOS = 5, there are two subranges with an OFF set status. Action occurs only in the ON set-status subrange.

Each trip-signal set point can be specified as a constant or as a tabular function of a signal variable. In the latter situation, the tabular form is interpolated each time step (based on the value of its signal variable) and applied as a factor to the set-point value. The criteria that $S_1 < S_2$ for IPOS = 1 or 2 and $S_1 < S_2 < S_3 < S_4$ for IPOS = 3, 4, or 5 must be satisfied after the factors are applied.

Each trip-signal set point has a defined delay time. After a set-point criterion is satisfied by the trip-signal value, its delay time must pass before the set status of the trip is changed. The delay time simulates the time necessary to process the signal and initiate trip action in the actual system hardware or by the control room operator. Delay times are nonnegative. A negative delay time is replaced by zero.

There are three forms for defining the trip signal: a signal variable, a signal expression that combines signal-variable values with arithmetic operations, or a trip-controlled trip signal that sums the set status value of other trips. A signal expression consists of 1 to 10 subexpressions, each having an arithmetic operator and 2 argument values. The arithmetic operators are addition, subtraction, multiplication, division, exponentiation, the maximum value, the minimum value, and the absolute value. Argument values are defined by signal-variable values, by input constants, or by an earlier evaluated subexpression in the list of subexpressions. The value of the last subexpression in the list defines the signal-expression value. Any signal variable that defines a subexpression argument can be flagged for evaluation either initially or at the end of each time step when the trip using this

signal expression is set to ON. This allows the argument values in a signal expression to be defined at different times. Also, signal parameters located in different components of the modeled system define the trip signal because the signal variables are combined through arithmetic operations in a signal expression.

The signal value for a trip-controlled trip is the sum of the set status values of two or more trips. The values for the different trip set status are: -1 for ON_{reverse}, 0 for OFF, and 1 for ON and ON_{forward}. All the trips defining the signal must occur earlier in the list of trips if their set-status value is to be for the current rather than previous time step. Note that trips obtained from the restart file will follow the list the trips that are specified. The logic operators AND or OR are implemented through the set-point values of trip-controlled trips and through the use of multiple trip-controlled trips. Set-point values specify how many trips assigned to the trip-controlled trip signal need to be set ON before the trip-controlled set-point criterion is met and its set status is changed. Multiple trip-controlled trips are used to evaluate an expression signal having logical subexpressions.

Component actions that vary and are trip controlled are specified through tabular input. A signal variable defines the component-action-table independent variable. It can have either of two forms: the absolute signal-variable value or the difference between the current signal-variable value and its value when the controlling trip was set ON. The signal-variable difference form is used when a separate rate-factor table is required; otherwise, the absolute signal-variable value form is used.

The rate-factor table for a trip-controlled component-action table is defined as a function of the difference between the current trip-signal value and the set-point value that turns the trip off. As stated above, when a rate-factor table is defined, the component-action-table independent variable defaults to the signal-variable difference form. The rate factor is applied as a factor to that difference. By including unit rate factors, the table only serves to flag the signal-variable difference form for the component-action-table independent variable. By including nonunit rate factors, the component action table is made dependent not only on the change in its signal variable but also on the departure of the current trip-signal value from the set-point value that turns the trip off. This allows modeling with

rate factors the override control on component actions by the control room hardware or operator. A rate factor can be used to supplement component action control with direct feedback from the controlling trip. Component action can be accelerated when the departure of the trip signal becomes too large or it can be decelerated to approach a preset limit more closely.

Rate factors are applied at the beginning of each time step to the incremental change in the signal variable of the component action table. The sum of these weighted incremental changes from trip initiation determines the integral value of the signal-variable difference used to interpolate in the component action table. For programming convenience, the values of the component-action-table independent variable are shifted each time step after interpolation so that the interpolation point has a zero abscissa coordinate. Consequently, the abscissa value for interpolation is the product of the rate factor and the change in the signal-variable value during each time step.

D. Controllers

This feature is not operational.

E. Dump/Restart Feature

TRAC automatically generates a dump/restart data file named TRCDMP, which contains snapshots of the state of the system at various times during problem execution. Any one of these snapshots, called dumps, may be used to initialize all or part of the system for subsequent calculations. The times when dumps are generated are determined by several criteria. The user may specify a dump interval on the time-step cards, and a dump will be created after this interval. These dumps are added sequentially to the end of the TRCDMP file. A dump with one or more trips also may be initiated by the user. When the set status of any of those trips is set ON, a dump is added to the end of the TRCDMP file. This permits the restart of a problem when particular events of interest occur.

In addition to these user-specified dumps, TRAC automatically will generate dumps at various times. A dump is generated at the end of the initialization stage. Another dump is generated at the end of the steady-state or transient calculation and at intermediate points in the calculation based upon the central processor unit (CPU) time utilized by the job.

To use a dump file to initialize a subsequent calculation, the name of the file must be changed from TRCDMP to TRCRST. The time-step number of the particular dump desired must be specified on Main Control Card 1. (A message containing this dump time-step number is sent to the print file TRCOUT whenever a dump is written.) If the time-step number has been specified as a negative value, TRAC will use the dump with the largest time-step number and overwrite the initial time (specified on Main Control Card 1) with the time taken from that dump.

Data retrieved from the selected dump depend on the information that already has been found in the TRACIN file. Any component not defined by the input deck (as determined from the component numbers listed in the IORDER array), is initialized from the restart dump. Also, any signal variable, trip, and controller found in the dump that has not been defined by input will be initialized at the state found on the dump.

F. TRAC-PF1 Input Specifications

The TRAC input data may be classified into seven general data types:

1. main control,
2. signal variable,
3. trip,
4. controller,
5. component,
6. PWR initialization, and
7. time step.

1. Main Control Data. The main control parameters are listed below in the order of entry. This data block must be supplied at the start of the input deck.

Card Number 1. (Free Format) The first card of a TRACIN deck serves as the free format ON-OFF switch, indicating whether the following cards are in free format or TRAC format. It must be present, containing either the string FREE (free format), TRAC (TRAC format), or both strings (FREE overrides TRAC). This card is in free format. Up to 80 columns may be used. The control string(s) and any other documentation may appear anywhere on the card.

Card Number 2. (Format 3I14) NUMTCR, IEOS, INOPT

<u>Columns</u>	<u>Variable</u>	<u>Description</u>
1-14	NUMTCR	Number of title cards to be read. Note: At least one title card must be supplied.
15-28	IEOS	Air-water option. 0 = gas phase treated as steam-air mixture throughout system; 1 = gas phase treated as air throughout system. Evaporation and condensation are inhibited.
29-42	INOPT	Specification for including or excluding NAMELIST group INOPTS data after the title cards. 0 = NAMELIST group INOPTS data omitted after the title cards or 1 = NAMELIST group INOPTS data inserted after the title cards.

Title Card(s). (Format 20A4) NUMTCR Cards

<u>Columns</u>	<u>Variable</u>	<u>Description</u>
1-80		Problem title information.

NAMELIST Data Cards for Group INOPTS. (NAMELIST format)

This section is included only if the variable INOPT = 1. In this case one or more of the special input options described below may be specified. The format of this data is not checked during preprocessing and, therefore, should be entered carefully to avoid fatal input errors. The data are entered in columns 2-80 on one or more cards, beginning with "\$INOPTS" in column 2 and are terminated with "\$." A more detailed discussion of the format for NAMELIST input data is included in Sec. V.I (also see local FORTRAN manual). The following variables are included in the NAMELIST group INOPTS, and one or more of them can be included in the NAMELIST data to select desired options. Variables omitted from the data retain their default status.

<u>Variable</u>	<u>Description</u>
IELV	Switch that determines whether gravity (GRAV) terms or cell-centered elevations (ELEV), in meters, are to be input in the component data. When this option is selected, ELEV (dimensioned NCELLS) or cell-centered elevations should be input for GRAV array data cards in all components. In addition, a break elevation BELV (see BREAK component data,

<u>Variable</u>	<u>Description</u>
	card 4) and a VESSEL elevation shift SHELV (see VESSEL component data, card 6) are required. 0 = gravity terms must be input (default condition) or 1 = cell-centered elevations must be input.
IKFAC	Switch that determines whether additive loss coefficients (FRIC) or K factors are to be input in the component data. When this option is selected, K factors (dimensioned NCELLS + 1) must replace the FRIC array input cards in all components. 0 = additive loss coefficients will be input or 1 = K factors will be input.
ICFLOW	Choked flow model controller. 0 = model turned off or 1 = model turned on (default condition).
NOAIR	Controls calculation of air partial pressure in one-dimensional components. 0 = air partial pressures solved for (less efficient when no air in system) or 1 = air partial pressures set automatically to zero (default condition).
ISTOPT	Steady-state option that allows the user to specify only once certain parameters or default values that are used to initialize data arrays for other components. The default parameters also are inserted through the NAMELIST group INOPTS and are described below. The variables that can be assigned default values are ALP, VL, VV, TL, TV, TW, P, PA, QPPP, and HSTN. When ISTOPT is nonzero, the values of these variables are used to fill the corresponding arrays in all components except accumulators, pressurizers, valves, and steam-generator secondary sides. This option also can be used for transient calculations. 0 = option off (default condition). 1 = option on. Those component arrays (excluding accumulators, pressurizers, valves, and steam-generator secondary sides), for which default values are included in the NAMELIST data, are filled with the default value. All cards that would contain data for defaulted arrays must be omitted from the input deck. 2 = option on. Those component arrays (excluding accumulators, pressurizers, valves, and steam-generator secondary sides), for which default values are included in the NAMELIST data, are filled with the default value. Cards containing data for defaulted arrays must remain in the input deck but are overridden by the default value.
ALP	Default value for initial void fractions. Used when ISTOPT is nonzero. (Real format.)

<u>Variable</u>	<u>Description</u>
VL	Default value for initial liquid velocities. Used when ISTOPT is nonzero. (Real format.)
VV	Default value for initial vapor velocities. Used when ISTOPT is nonzero. (Real format.)
TL	Default value for initial liquid temperatures. Used when ISTOPT is nonzero. (Real format.)
TV	Default value for initial vapor temperatures. Used when ISTOPT is nonzero. (Real format.)
TW	Default value for initial wall temperatures. Used when ISTOPT is nonzero. (Real format.)
P	Default value for initial pressures. Used when ISTOPT is nonzero. (Real format.)
PA	Default value for initial air partial pressures. Used when ISTOPT is nonzero. (Real format.)
QPPP	Default value for volumetric heat sources in pipe wall in one-dimensional components. Used when ISTOPT is nonzero. (Real format.)
HSTN	Default value for heat-slab temperatures in three-dimensional components. Used when ISTOPT is nonzero. (Real format.)

Main Control Card 1. (Format I14,E14.6) DSTEP, TIMET

<u>Columns</u>	<u>Variable</u>	<u>Description</u>
1-14	DSTEP	Time-step number of dump to be used for restart. If DSTEP is less than zero, the last dump found will be used for restart.
15-28	TIMET	Problem start time. If DSTEP or TIMET is less than zero, the initial time will be overridden by the time specified for the retrieved dump.

Main Control Card 2. (Format 5I14) STDYST, TRANSI, NCOMP, NJUN, IPAK

<u>Columns</u>	<u>Variable</u>	<u>Description</u>
1-14	STDYST	Steady-state calculation indicator. 0 = no steady-state calculation; 1 = generalized steady-state calculation; 2 = PWR-initialization calculation; 3 = PWR-initialization calculation with initial

<u>Columns</u>	<u>Variable</u>	<u>Description</u>
		evaluation of operating parameters; or 5 = static balance calculation; checks to see if zero flow can be achieved with pumps off and no heat transfer.
15-28	TRANSI	Transient calculation indicator. 0 = no transient calculation; 1 = transient to be calculated.
29-42	NCOMP	Number of components.
43-56	NJUN	Number of junctions.
57-70	IPAK	Water packing option. 0 = off; 1 = on.

Main Control Card 3. (Format 4E14.6) EPSO, EPSI, EPSS, EPSP

<u>Columns</u>	<u>Variable</u>	<u>Description</u>
1-14	EPSO	Convergence criterion for outer iteration (suggested value = 1.0×10^{-3}).
15-28	EPSI	Convergence criterion for vessel iteration (suggested value = 1.0×10^{-5}).
29-42	EPSS	Convergence criterion for steady-state calculation (suggested value = 1.0×10^{-4}).
43-56	EPSP	PWR-initialization convergence criterion (suggested value = 1.0×10^{-3}).

Main Control Card 4. (Format 3I14) OITMAX, IITMAX, SITMAX

<u>Columns</u>	<u>Variable</u>	<u>Description</u>
1-14	OITMAX	Maximum number of outer iterations (suggested value = 10).
15-28	IITMAX	Maximum number of vessel iterations (suggested value = 50). Set to zero for direct inversion of the vessel matrix.
29-42	SITMAX	Maximum number of outer iterations for steady-state calculation (suggested value = 10).

Main Control Card 5. (Format 3I14) NTSV, NTRP, NTCN

<u>Columns</u>	<u>Variable</u>	<u>Description</u>
1-14	NTSV	The number of signal variables from input and the restart file ($0 \leq \text{NTSV}$).
15-28	NTRP	The number of trips from input and the restart file ($0 \leq \text{NTRP}$).
29-42	NTCN	The number of controllers from input and the restart file. (The controller is not operational at this time; input NTCN = 0.)

Component List Card(s). (Format 5(3X,I11)) IORDER(i), $i = (1, \text{NCOMP})$, read by routine LOAD.

<u>Columns</u>	<u>Variable</u>	<u>Description</u>
4-14	IORDER(1)	First component number.
18-28	IORDER(2)	Second component number.
29-42	IORDER(3)	Etc.

2. Signal-Variable Data. Signal-variable data are defined when $\text{NTSV} > 0$ (word 1 on Main Control Card 5). Signal variables define the signal parameters for trips and controllers and the independent variable for tabular input that define component action. Either NTSV or fewer signal variables are input. When fewer than NTSV are input, conclude the data with a card having a negative integer in columns 1-14. The remaining signal variables (for a total of NTSV) are obtained from the restart file. They are the signal variables on the restart file whose IDSV identification numbers differ from those defined when inserted. Each signal variable is defined by the following card:

<u>Columns</u>	<u>Variable</u>	<u>Description</u>
1-14	IDSV	The signal-variable ID number ($1 \leq \text{IDSV} \leq 399$).

<u>Columns</u>	<u>Variable</u>	<u>Description</u>
15-28	ISVN	The signal-variable parameter number ($-39 \leq \text{ISVN} \leq -21$ or $0 \leq \text{ISVN} \leq 39$). See Table VI for a list of the signal-variable parameter numbers vs their parameter descriptions. The sign of ISVN (for $ \text{ISVN} > 20$) specifies how the parameter is defined. When $0 \leq \text{ISVN} \leq 39$, the signal variable is the parameter value; when $-39 \leq \text{ISVN} \leq -21$, the signal variable is the difference between the parameter values at two locations. The control-panel vector parameters ($1 \leq \text{ISVN} \leq 15$) are not to be used at this time because their evaluation is not operational.
29-42	ILCN	The coolant loop number ($7 \leq \text{ISVN} \leq 15$) or the component number ($18 \leq \text{ISVN} \leq 39$) where the signal variable parameter is defined. The variable ILCN is not used when $ \text{ISVN} < 7$ or $\text{ISVN} = 16$ or 17 .
43-56	ICN1	The cell number of the first location in component ILCN where the signal-variable parameter is defined. Input ICN1 when $ \text{ISVN} > 19$.
57-70	ICN2	The cell number of the second location in component ILCN where the signal-variable parameter is defined. Input ICN2 when $ \text{ISVN} > 19$.

For the VESSEL component, $|\text{ICN1}|$ and $|\text{ICN2}|$ are defined as composites of the relative cell number in the horizontal plane and the axial level number.

$$\begin{pmatrix} |\text{ICN1}| \\ |\text{ICN2}| \end{pmatrix} = (\text{horizontal plane relative cell number}) * 1000 + (\text{axial level number}).$$

Further information is provided by the signs of ICN1 and ICN2 for defining the signal-variable value. For $21 \leq \text{ISVN} \leq 39$, the signal variable is:

1. the parameter value in cell $|\text{ICN1}|$ when $\text{ICN2} = 0$ or in cell $|\text{ICN2}|$ when $\text{ICN1} = 0$;
2. the maximum parameter value between cells $|\text{ICN1}|$ and $|\text{ICN2}|$ when $\text{ICN1} > 0$ and $\text{ICN2} > 0$;
3. the minimum parameter value between cells $|\text{ICN1}|$ and $|\text{ICN2}|$ when $\text{ICN1} < 0$ and $\text{ICN2} < 0$; and

4. the volume-averaged parameter value between cells |ICN1| and |ICN2| when ICN1 and ICN2 are of opposite sign.

For $-39 \leq \text{ISVN} \leq -21$, the signal variable is the difference between the parameter values in cells |ICN1| and |ICN2|.

3. Trip Data. Trip data are defined when $\text{NTRP} > 0$ (word 2 on Main Control Card 5). There are seven categories of trip input data. The first category, Trip-Dimension Variables Card, is always input when $\text{NTRP} > 0$. The five variables on this card and NTRP define the variable storage required for the remaining six data categories. In each of these categories, none, part, or all of the data can be input. Any data that are not input are obtained from the restart file.

Trip-Dimension Variables Card. (Format 5I14) NTSE, NTCT, NTSF, NTDP, NTSD

<u>Columns</u>	<u>Variable</u>	<u>Description</u>
1-14	NTSE	The number of signal-expression trips from input and the restart file ($0 \leq \text{NTSE}$).
15-28	NTCT	The number of trip-controlled trips from input and the restart file ($0 \leq \text{NTCT}$).
29-42	NTSF	The number of set-point factor tables referenced by trips from input and the restart file ($0 \leq \text{NTSF}$).
43-56	NTDP	The number of trips from input and the restart file where the trips generate a restart dump and possible problem termination when they are set ON ($0 \leq \text{NTDP}$).
57-70	NTSD	The number of trip time-step data sets that are to be used when their defined trips are set ON ($0 \leq \text{NTSD}$).

Trip-Defining Variables Cards. Input from 0 to NTRP (word 2 on Main Control Card 5) of the following card set. If fewer than NTRP card sets are input, conclude these data with a card having a -1 in columns 13 and 14. The remaining trips, having trip IDTP identification numbers different from those input will be obtained from the restart file.

Card Number 1. (Format 5I14) IDTP, IPOS, ISET, ITYP, IDSG

<u>Columns</u>	<u>Variable</u>	<u>Description</u>
1-14	IDTP	The trip ID number ($-9999 \leq IDTP \leq -2$ or $1 \leq IDTP \leq 9999$).
15-28	IPOS	The trip-signal-range type number. Over the trip-signal value range, the trip-signal-range type number IPOS defines either two (IPOS = 1 or 2) or three (IPOS = 3, 4, or 5) subranges with different set status (ON _{reverse} , OFF, ON, or ON _{forward}). See Table VII for a description of these subranges and their delimiting set-point values for the five values of IPOS ($1 \leq IPOS \leq 5$).
29-42	ISET	The initial trip set-status number (only used for steady state). -1 = ON _{reverse} , 0 = OFF, or 1 = ON or ON _{forward} .
43-56	ITYP	The trip-signal type number. 1 = signal-variable trip, 2 = signal-expression trip, or 3 = trip-controlled trip.
57-70	IDSG	The ID number for the trip signal variable (for ITYP = 1, IDSG corresponds to IDSV in the signal-variable data), the trip signal expression (for ITYP = 2, IDSG corresponds to IDSE in the trip-signal-expression data), or the trip-controlled trip signal (for ITYP = 3, IDSG corresponds to IDTN in the trip-controlled-trip data).

Card Number 2. (Format 4E14.6) SETP(I), I = (1,NSP)

<u>Columns</u>	<u>Variable</u>	<u>Description</u>
1-14 through 43-56	SETP(I)	The I th trip-signal set-point value shown as S# (where # = I) in the Table VII definition of IPOS (word 2 on Trip-Defining Variables Card 1). For IPOS = 1 or 2, NSP = 2; for IPOS = 3, 4, or 5, NSP = 4. The set-point values must satisfy SETP(1) < SETP(2) when IPOS = 1 or 2 or SETP(1) < SETP(2) < SETP(3) < SETP(4) when IPOS = 3, 4, or 5.

Card Number 3. (Format 4E14.6) DTSP(I), I = (1,NSP)

<u>Columns</u>	<u>Variable</u>	<u>Description</u>
1-14 through 43-56	DTSP(I)	The I th set-point delay time (s) after the trip signal crosses the set-point value to when the trip set status is changed. For IPOS = 1 or 2, P = 2; for IPOS = 3, 4, or 5, NSP = 4.

Card Number 4. (Format 4I14) IFSP(I), I = (1,NSP)

<u>Columns</u>	<u>Variable</u>	<u>Description</u>
1-14 through 43-56	IFSP(I)	The I th set-point factor-table ID number. The variable IFSP(I) corresponds to IDFT defined on the Trip Set-Point Factor-Table Card Number 1 that follows. Input IFSP(I) = 0 when no factor table is to be applied to SETP(I); that is, the set point value remains constant during the problem. For IPOS = 1 or 2, NSP = 2; for IPOS = 3, 4, or 5, NSP = 4.

If none of the above trips have ITYP = 2 (Trip-Defining Variables Card 1), skip the Trip Signal-Expression Cards.

Trip Signal-Expression Cards. Input the following card data for each of the above trips having ITYP = 2.

Card Number 1. (Format 3I14) IDSE, INSE, INCN

<u>Columns</u>	<u>Variable</u>	<u>Description</u>
1-14	IDSE	The trip signal-expression ID number. This number corresponds to IDSG (word 5 on Trip Defining Variables Card 1) for one of the above trips having ITYP = 2.
15-28	INSE	The number of subexpressions defining the signal-expression ($1 \leq INSE \leq 10$).
29-42	INCN	The number of different constants referenced in the subexpressions defining the signal expression ($0 \leq INCN \leq 5$).

Input INSE cards of the following card to define the J = (1,INSE) arithmetic subexpressions.

Card Number 2. (Format 3I14) ISE(I,J), I = (1,3)

1-14	ISE(I,J)	The arithmetic-operator ID number of the J th arithmetic subexpression. (See Table VIII.)
------	----------	--

<u>Columns</u>	<u>Variable</u>	<u>Description</u>
15-28	ISE(2,J)	The first argument ID number of the J th arithmetic subexpression.
29-42	ISE(3,J)	The second argument ID number of the J th arithmetic subexpression.

The first and second argument ID numbers define values that, when operated on by the arithmetic operator, give a value to their Jth arithmetic subexpression. There are four forms for the value of the first and second argument ID numbers. Their value is:

1. a signal-variable value evaluated each time step when their ID number is a signal-variable ID number IDSV (word 1 of Signal-Variable Data) [0 < IDSV < 400];

TABLE VIII
ARITHMETIC-OPERATOR ID NUMBERS

<u>Arithmetic- Operator ID Number</u>	<u>Arithmetic Operator</u>	<u>Arithmetic Subexpression</u>
1	Addition	(First argument ID number value) + (Second argument ID number value)
2	Subtraction	(First argument ID number value) - (Second argument ID number value)
3	Multiplication	(First argument ID number value) * (Second argument ID number value)
4	Division	(First argument ID number value) / (Second argument ID number value)
5	Exponentiation	(First argument ID number value) ** (Second argument ID number value)
6	Maximum value	MAX[(First argument ID number value) (Second argument ID number value)]
7	Minimum value	MIN[(First argument ID number value) (Second argument ID number value)]
8	Absolute value	ABS(First argument ID number value)

2. a signal-variable value evaluated initially and at time steps when the trip controlled by this signal expression is set to ON^{reverse}, ON, or ON^{forward} when their ID number is a signal-variable ID number $IDSV$ plus 400 ($400 < IDSV + 400 < 800$);
3. a constant input on Card Number 3 that follows when their ID number is the I^{th} subscript of $SCN(I)$ plus 800 ($800 < I + 800 < 806$); or
4. the value of an earlier subexpression j ($0 < j < J \leq INSE$) when their ID number is j plus 900 ($900 < j + 900 < 910$).

For example, the signal expression,

$$\max [\sqrt{(IDSV = 5) + (IDSV = 33)}, 1.0 \times 10^{-10}] ,$$

would be input as

1	2	3	4	5
1234567890123456789012345678901234567890123456789012...				
1		5		33
5		901		801
6		902		802

where $SCN(1) = 0.5$, $SCN(2) = 1.0 \times 10^{-10}$, $INCN = 2$, and $INSE = 3$.

Skip Card Number 3 if $INCN = 0$.

Card Number 3. (Format 5E14.6) $SCN(I)$, $I = (1, INCN)$

<u>Columns</u>	<u>Variable</u>	<u>Description</u>
1-14 through 57-70	$SCN(I)$	The I^{th} constant with argument ID number $800 + I$ in a subexpression used to evaluate the signal expression.

If none of the above trips have $ITYP = 3$ (word 4 on Trip-Defining Variables Card 1), skip the Trip-Controlled Trip Cards.

Trip-Controlled Trip Cards. Input the following card data for each of the above trips having $ITYP = 3$.

Card Number 1. (Format 2I14) $IDTN$, $INTN$

<u>Columns</u>	<u>Variable</u>	<u>Description</u>
1-14	$IDTN$	The trip-controlled trip ID number. This number corresponds to $IDSG$ (word 5 on Trip-Defining Variables Card 1) for one of the above trips having $ITYP = 3$.

<u>Columns</u>	<u>Variable</u>	<u>Description</u>
15-28	INTN	The number of trip ID numbers whose set-status values defined by variable ISET (word 3 on Trip-Defining Variables Card 1) are summed to evaluate the signal value of this trip-controlled trip ($2 \leq \text{INTN} \leq 10$).

Card Number 2. (Format 5I14) ITN(I), I = (1,INTN)

<u>Columns</u>	<u>Variable</u>	<u>Description</u>
1-14 through 57-70	ITN(I)	The I th trip ID number whose set-status value defined by variable ISET is summed to the ISET values of the other trips to determine the signal value for this trip-controlled trip. When $\text{INTN} > 5$, a second card is needed.

If all the above trips have constant trip-signal set points because $\text{IFSP}(I) = 0$ (Trip-Defining Variables Card 4), skip the Trip Set-Point Factor-Table Cards.

Trip Set-Point Factor-Table Cards. Input the following card data for each different set-point factor-table ID number, $\text{IFSP}(I)$, in the above trips.

Card Number 1. (Format 3I14) IDFT, IDSG, INFT

<u>Columns</u>	<u>Variable</u>	<u>Description</u>
1-14	IDFT	The set-point factor-table ID number. This number corresponds to $\text{IFSP}(I)$ (Trip-Defining Variables Card 4) with the same value for one or more trip set points.
15-28	IDSG	The signal-variable ID number defining the set-point factor-table independent variable. This number corresponds to one of the ID numbers in the list of signal variables.
29-42	INFT	The number of set-point factor-table pair entries ($1 \leq \text{INFT} \leq 10$).

Card Number 2. (Format 5E14.6) FTX(I), FTY(I), I = (1,INFT)

<u>Columns</u>	<u>Variable</u>	<u>Description</u>
1-14	FTX(1)	The signal-variable ID number IDSG value for the first pair entry in the set-point factor table.
15-28	FTY(1)	The value of the set-point factor for the first pair entry in the set-point factor table.

<u>Columns</u>	<u>Variable</u>	<u>Description</u>
29-42	FTX(2)	The signal-variable ID number IDSG value for the second pair entry in the set-point factor table.
43-56	FTY(2)	Etc.

Card Number 2 requires one to four cards to input the set-point factor table.

If NTDP = 0 (word 4 on the Trip-Dimension Variables Card), skip the Trip-Initiated Restart Dump and Problem Termination card set.

Trip-Initiated Restart Dump and Problem Termination Cards.

Card Number 1. (Format I14) NDMP

<u>Columns</u>	<u>Variable</u>	<u>Description</u>
1-14	NDMP	The number of trip ID numbers that generate a restart dump and possible problem termination when they are set to ON _{reverse} , ON, or ON _{forward} (NDMP ≤ NTDP).

If NDMP < 1, skip card 2; all NTDP trip ID numbers will be obtained from the restart file.

Card Number 2. (Format 5I14) IDMP(I), I = (1,NDMP)

<u>Columns</u>	<u>Variable</u>	<u>Description</u>
1-14 through 57-70	IDMP(I)	The I th trip ID number that generates a restart dump when the trip is set to ON _{reverse} , ON, or ON _{forward} . If IDMP(I) is given a negative sign, problem termination will occur after the restart dump is generated.

Card Number 2 requires (NDMP - 1)/5 + 1 input cards.

If NTSD = 0 (word 5 on the Trip-Dimension Variables Card), skip the Trip-Initiated Time-Step Data card set.

Trip-Initiated Time-Step Data Cards. Input from 0 to NTSD of the following card set. If fewer than NTSD sets are input, conclude these data with a card having a negative integer in columns 1-14.

Card Number 1. (Format 2I14) NDID, NTID

<u>Columns</u>	<u>Variable</u>	<u>Description</u>
1-14	NDID	The ID number for the following set of trip-initiated time-step data.
15-28	NTID	The number of trip ID numbers that initiates the use of these time-step data when any one of the trips is set to ON _{reverse} , ON, or ON _{forward} ($1 \leq NTID \leq 5$).

Card Number 2. (Format 5I14) ITID(I), I = (1,NTID)

<u>Columns</u>	<u>Variable</u>	<u>Description</u>
1-14 through 57-70	ITID(I)	The I th trip ID number that initiates the use of these time-step data on Cards 3 and 4 that follow when the trip is set to ON _{reverse} , ON, or ON _{forward} .

Card Number 3. (Format 4E14.6) DTMIN, DTMAX, DTEND, DTSOF

<u>Columns</u>	<u>Variable</u>	<u>Description</u>
1-14	DTMIN	The minimum time-step size (s).
15-28	DTMAX	The maximum time-step size (s).
29-42	DTEND	The problem time interval (s) during which these time-step data are used.
43-56	DTSOF	The new time step (s) (DTSOF > 0) or the factor DTSOF to be applied to the existing time step (DTSOF < 0).

Card Number 4. (Format 4E14.6) EDINT, GFINT, DMPIT, SEDINT

<u>Columns</u>	<u>Variable</u>	<u>Description</u>
1-14	EDINT	Print edit interval (s).
15-28	GFINT	Graphics edit interval (s).
29-42	DMPIT	Restart dump edit interval (s).
43-56	SEDINT	Short print edit interval (s).

Time-step data on cards 3 and 4 replace the time-step data defined later in Sec. V.F.7 for a time interval DTEND (word 3 on Card Number 3) after any one of its trips is set to ON_{reverse}, ON, or ON_{forward}.

4. Controller Data. The controller feature is not operational in TRAC at this time. By setting NTCN = 0 (word 3 on Main Control Card 5), no controller data are read.

5. Component Data. Either NCOMP or fewer sets of component cards are input. The sets may be input in any order. If less than NCOMP sets are input, the end of the component data is marked by a single card containing the characters END in columns 1-3. In this case the remaining components are initialized from the TRCRST file. The format of each set depends on the component type. The following is the input format for the components. All velocities are positive in the direction of ascending cell number. Most of the subscripted component data variables are processed by the LOAD subroutine described in Sec. V.G. Additional information on preparing component input data can be found in Sec. IV, where the component models are described. All tables that are entered as pairs of numbers (x,y) must be supplied in ascending order of the independent variable x.

Each component requires a junction number, JUN, for each of its connecting points. A junction is the connection point between two components. A pipe requires two junction numbers, one for each end. A unique junction number must be assigned to each connecting point and referenced by both components to be connected. For example, if two pipes are joined, then the junction numbers of the connecting end of each pipe must be the same. No component may "wrap around" and connect to itself and no junction may have only one component connected to it. Any of the single-ended components (BREAK, FILL, or ACCUM) may be used to complete a junction.

In the following input descriptions, the asterisk (*) indicates units of the signal variable and the hyphen (-) indicates dimensionless quantities.

a. Accumulator Component (ACCUM).

Card Number 1. (Format A10,4X,2I14,A30) TYPE, NUM, ID, CTITLE

<u>Columns</u>	<u>Variable</u>	<u>Description</u>
1-5	TYPE	Component type (ACCUM left justified).
15-28	NUM	Component ID number (must be unique for each component, $1 \leq \text{NUM} \leq 99$).
29-42	ID	User ID number (arbitrary).
43-72	CTITLE	Hollerith component description.

Card Number 2. (Format 2I14) NCELLS, JUN2

<u>Columns</u>	<u>Variable</u>	<u>Description</u>
1-14	NCELLS	Number of fluid cells.
15-28	JUN2	Junction number for junction adjacent to cell NCELLS. This must be the accumulator discharge.

ACCUM Array Cards. Fourteen sets of cards, one set for each of the following variables. Use LOAD format.

<u>Variable</u>	<u>Dimension</u>	<u>Description</u>
DX	NCELLS	Cell lengths (m).
VOL	NCELLS	Cell volumes (m ³).
FA	NCELLS+1	Cell-edge flow areas (m ²).
FRIC	NCELLS+1	Additive loss coefficients.
GRAV	NCELLS+1	Gravity terms. (See PIPE, Sec. V.F.5.e.)
HD	NCELLS+1	Hydraulic diameters (m).

<u>Variable</u>	<u>Dimension</u>	<u>Description</u>
NFF	NCELLS+1	Friction-factor correlation options: 0 = constant friction factor, user input; 1 = homogeneous flow friction factor; -1 = homogeneous flow friction factor plus automatic form-loss computation (see Sec. III.A.1.d); 2 = annular flow friction factor; -2 = annular flow friction factor plus automatic form-loss computation; or -100 = form-loss computation only.
ALP	NCELLS	Initial void fractions (-).
VL	NCELLS+1	Initial liquid velocities (m/s).
VV	NCELLS+1	Initial vapor velocities (m/s).
TL	NCELLS	Initial liquid temperatures (K).
TV	NCELLS	Initial vapor temperatures (K).
P	NCELLS	Initial pressures (Pa).
PA	NCELLS	Initial air partial pressures (Pa).

b. Break Component (BREAK).

Card Number 1. (Format A10,4X,2I14,A30) TYPE, NUM, ID, CTITLE

<u>Columns</u>	<u>Variable</u>	<u>Description</u>
1-5	TYPE	Component type (BREAK left justified).
15-28	NUM	Component ID number (must be unique for each component, $1 \leq \text{NUM} \leq 99$).
29-42	ID	User ID number (arbitrary).
43-72	CTITLE	Hollerith component description.

Card Number 2. (Format 4I14) JUN1, IBROP, NBTB, ISAT

<u>Columns</u>	<u>Variable</u>	<u>Description</u>
1-14	JUN1	Junction number where break is located.

<u>Columns</u>	<u>Variable</u>	<u>Description</u>
15-28	IBROP	Break table read options: 0 = no tables read; 1 = read pressure table; 2 = read pressure and temperature tables; 3 = read pressure, temperature, and void-fraction tables; or 4 = read pressure, temperature, void-fraction, and air-partial-pressure tables.
29-42	NBTB	Number of pairs for each break table.
43-56	ISAT	Break temperature table use options (make consistent with IBROP): 0 = use TIN or single table for liquid and vapor temperatures (K), 1 = use TIN or table for liquid and set vapor to T_{sat} , 2 = use TIN or table for vapor and set liquid to T_{sat} , 3 = set liquid and vapor to T_{sat} , or 4 = use separate tables for liquid and vapor.
57-70	IVDV	Momentum transport during flow in from the break (VVV term). 0 = the velocity outside the break must be set to the velocity at the break junction (VVV = 0). 1 = the velocity outside the break must be set to zero when computing VVV. This is recommended for breaks that model connections to pressure suppression tanks or the atmosphere.

Card Number 3. (Format 5E14.6) DXIN, VOLIN, ALPIN, TIN, PIN

<u>Columns</u>	<u>Variable</u>	<u>Description</u>
1-14	DXIN	Break-cell length (m), generally the same as its neighboring cell in the adjacent component. Used only when the flow is from the break into the the system and for stratified-flow calculations.
15-28	VOLIN	Break-cell volume (m ³), generally the same as its neighboring cell in the adjacent component. Used only for stratified-flow calculations.
29-42	ALPIN	Mixture void fraction (-) at break.
43-56	TIN	Mixture temperature (K) at break.
57-70	PIN	Pressure (Pa) at break.

Card Number 4. (Format 1E14.6) PAIN, BELV

<u>Columns</u>	<u>Variable</u>	<u>Description</u>
1-14	PAIN	Air partial pressure (Pa) at break.
15-28	BELV	Break elevation (m). Used to compute GRAV array only when IELV = 1.

BREAK-Table Scale Factors and BREAK-Table Input. Input the table scale factor only if associated BREAK table is required based on input values for IBROP and ISAT.

Pressure Scale Factor. (Format E14.6) PSCL

<u>Columns</u>	<u>Variable</u>	<u>Description</u>
1-14	PSCL	Pressure scale factor. The dependent variable in the pressure table PTB is multiplied by this factor to obtain absolute pressure. Input PSCL only if table PTB is input.

Pressure Table. LOAD format (input only if NBTB > 0 and IBROP \geq 1).

<u>Table</u>	<u>Dimension</u>	<u>Description</u>
PTB	2*NBTB	Pressure vs time table; input [time (s), pressure (Pa)] pairs.

Liquid-Temperature Scale Factor. (Format E14.6) TLSCl

<u>Columns</u>	<u>Variable</u>	<u>Description</u>
1-14	TLSCl	Liquid-temperature scale factor. The dependent variable in the liquid-temperature table TLTB is multiplied by this factor to obtain the absolute liquid temperature (K). Input TLSCl only if table TLTB is input.

Liquid-Temperature Table. LOAD format (input only if NBTB > 0 and IBROP \geq 2).

<u>Table</u>	<u>Dimension</u>	<u>Description</u>
TLTB	2*NBTB	Liquid-temperature vs time table; input [time (s), temperature (K)] pairs. For ISAT = 2, this table is used for vapor temperature.

Vapor-Temperature Scale Factor. (Format E14.6) TVSCL

<u>Columns</u>	<u>Variable</u>	<u>Description</u>
1-4	TVSCL	Vapor-temperature scale factor. The dependent variable in the vapor-temperature table TVTB is multiplied by this scale factor to obtain the absolute vapor temperature (K). Input TVSCL only if table TVTB is input.

Vapor-Temperature Table. LOAD format (input only if NBTB > 0, IBRO^W ≥ 2, and ISAT = 4).

<u>Table</u>	<u>Dimension</u>	<u>Description</u>
TVTB	2*NBTB	Vapor-temperature vs time table; input [time (s), temperature (K)] pairs.

Void-Fraction Table. LOAD format (input only if NBTB > 0 and IBROP ≥ 3).

<u>Table</u>	<u>Dimension</u>	<u>Description</u>
ALPTB	2*NBTB	Void-fraction vs time table; input [time (s), void fraction (-)] pairs.

Air-Partial-Pressure Scale Factor. (Format E14.6) PASCL

<u>Columns</u>	<u>Variable</u>	<u>Description</u>
1-14	PASCL	Air-partial-pressure scale factor. The dependent variable in the air-partial-pressure table PATB is multiplied by this scale factor to obtain the absolute air partial pressure (Pa).

Air-Partial-Pressure Table. LOAD format (input only if NBTB > 0 and IBROP = 4).

<u>Table</u>	<u>Dimension</u>	<u>Description</u>
PATB	2*NBTB	Air-partial-pressure vs time table; input [time (s), pressure (Pa)] pairs.

c. One-Dimensional Core Component (CORE).

Card Number 1. (Format A10,4X,2I14,A30) TYPE, NUM, ID, CTITLE

<u>Columns</u>	<u>Variable</u>	<u>Description</u>
1-14	TYPE	Component type (CORE, left justified).
15-28	NUM	Component ID number (must be unique for each component, $1 \leq \text{NUM} \leq 99$).
29-42	ID	User ID number (arbitrary).
43-72	CTITLE	Hollerith component description.

Card Number 2. (Format 5I14) NCELLS, JUN1, JUN2, MAT, ICHF

<u>Columns</u>	<u>Variable</u>	<u>Description</u>
1-14	NCELLS	Number of fluid cells.
15-28	JUN1	Junction number for junction adjacent to cell 1 (assumed to be at the bottom of the component).
29-42	JUN2	Junction number for junction adjacent to cell NCELLS (assumed to be at the top of the component).
43-56	MAT	Material ID of core wall. (See PIPE input description, Sec. V.F.5.e.)
57-70	ICHF	CHF calculation flag. 0 = no; 1 = yes.

Card Number 3. (Format 5I14) IHYDRO, NDGX, NDHX, NRTS, IRPSV

<u>Columns</u>	<u>Variable</u>	<u>Description</u>
1-14	IHYDRO	Variable not used.
15-28	NDGX	The number of delayed-neutron groups (NDGX ≤ 0 defaults to six delayed-neutron groups with the delayed-neutron constants defined internally in TRAC).
29-42	NDHX	The number of decay heat groups (NDHX ≤ 0 defaults to 11 decay heat groups with the decay heat constants defined internally in TRAC).

<u>Columns</u>	<u>Variable</u>	<u>Description</u>
43-56	NRTS	The number of time steps the reactivity feedback changes are summed over for printout.
57-70	IRPSV	The signal-variable ID number that defines the independent variable in the reactor power-reactivity table.

Card Number 4. (Format 5I14) ICRU, ICRL, NPWX, IRPOP, IRPTR

<u>Columns</u>	<u>Variable</u>	<u>Description</u>
1-14	ICRU	Power-region upper-boundary fluid cell number (NCELLS if boundary is at JUN2).
15-28	ICRL	Power-region lower-boundary fluid cell number (zero if boundary is at JUN1).
29-42	NPWX	Number of signal-variable form, power, or reactivity pairs in reactor power-reactivity table.
43-56	IRPOP	Reactor-kinetics option (input parameters required for each option are shown in parentheses). Add 10 to the option value of IRPOP if a reactivity feedback evaluation is to be performed.

<u>IRPOP</u>	<u>Option</u>
1	Constant power (RPOWRI).
2	Reactor kinetics with constant programmed reactivity (RPOWRI, REACT).
3	Reactor kinetics with table lookup of programmed reactivity (RPOWRI, NPWX, PWTB).
4	Reactor kinetics with trip-initiated constant programmed reactivity insertion (RPOWRI, IRPTR, REACT).
5	Reactor kinetics with trip-initiated table lookup of programmed reactivity (RPOWRI, IRPTR, NPWX, PWTB).
6	Table lookup of power (NPWX, PWTB).
7	Constant initial power with trip-initiated table lookup of power (RPOWRI, IRPTR, NPWX, PWTB).

57-70	IRPTR	Power or reactor-kinetics trip ID number.
-------	-------	---

Card Number 5. (Format 5I14) NPSZ, IPSTR, IPSSV, NPSRF, NRPRF

<u>Columns</u>	<u>Variable</u>	<u>Description</u>
1-14	NPSZ	The number of axial power shapes defined in the axial-power-shape table ($NPSZ \geq 1$).
15-28	IPSTR	The axial-power-shape trip ID number. (Currently not used.)
29-42	IPSSV	The signal-variable ID number that defines the independent variable in the axial-power-shape table.
43-56	NPSRF	The number of rate-factor table pairs where the rate factor is dependent on the axial-power-shape trip signal difference from its trip OFF set point. The rate factor is to be applied to changes in the axial-power-shape-table independent variable defined by IPSSV. (Currently not used.)
57-70	NRPRF	The number of rate-factor table pairs where the rate factor is dependent on the power-reactivity trip signal difference from its trip OFF set point. The rate factor is to be applied to changes in the reactor power-reactivity table independent variable defined by IRPSV.

Card Number 6. (Format 5I14) NRFDT, NMWRX, NFCI, NFCIL, NZMAX

<u>Columns</u>	<u>Variable</u>	<u>Description</u>
1-14	NRFDT	Reflood rod fine-mesh calculation trip ID number (no fine-mesh calculation is performed if $NRFDT = 0$).
15-28	NMWRX	Metal-water reaction option. 0 = off; 1 = on.
29-42	NFCI	Fuel-clad interaction (FCI) option. Option 1 performs the dynamic gap conductance calculation. 0 = off; 1 = on.
43-56	NFCIL	Limit on FCI calculations per time step (set $NFCIL = 1$).
57-70	NZMAX	Maximum number of rows of nodes used in the fuel-rod conduction calculation.

Card Number 7. (Format 5I14) NRODS, NSLBS, NODES, NDRDS, NDSLBS

<u>Columns</u>	<u>Variable</u>	<u>Description</u>
1-14	NRODS	Number of calculational fuel rods.
15-28	NSLBS	Variable not used.
29-42	NODES	Number of nodes in the core walls.
43-56	NDRDS	Number of nodes in the fuel rods.
57-70	NDSLBS	Variable not used.

Card Number 8. (Format 5E14.6) RPOWRI, REACT, PLDR, PDRAT, FUCRAC

<u>Columns</u>	<u>Variable</u>	<u>Description</u>
1-14	RPOWRI	Initial reactor power (W).
15-28	REACT	Initial programmed reactivity (IRPOP options 2 and 4 only).
29-42	PLDR	Pellet dish radius (m). (No calculation of pellet dishing is performed if PLDR = 0.0).
43-56	PDRAT	Fuel-rod pitch-to-diameter ratio.
57-70	FUCRAC	Fraction of fuel <u>not</u> cracked. Use only if NFCI = 1 on Card Number 6.

Card Number 9. (Format 5E14.6) RADIN, TH, HOUTL, HOUTV, TOUTL

<u>Columns</u>	<u>Variable</u>	<u>Description</u>
1-14	RADIN	Inner radius (m) of core wall.
15-28	TH	Core wall thickness (m).
29-42	HOUTL	HTC ($W/m^2/K$) between outer boundary of core wall and liquid outside pipe.
43-56	HOUTV	HTC ($W/m^2/K$) between outer boundary of core wall and vapor outside pipe.
57-70	TOUTL	Liquid temperature (K) outside core wall.

Card Number 10. (Format 2E14.6) TOUTV, POWSCL

<u>Columns</u>	<u>Variable</u>	<u>Description</u>
1-14	TOUTV	Vapor temperature (K) outside core wall.
15-28	POWSCL	Power-reactivity-table (variable PWTB) scale factor. The dependent variable in PWTB is multiplied by POWSCL to obtain its absolute value.

Card Number 11. (FORMAT 5E14.6) DTXHT(1), DTXHT(2), DZNHT, HGAPO, TNEUT

<u>Columns</u>	<u>Variable</u>	<u>Description</u>
1-14	DTXHT(1)	Maximum ΔT (K) above which rows of nodes are inserted in the fuel-rod conduction calculation during reflood for the nucleate and transition boiling regimes (suggested value = 3.0).
15-28	DTXHT(2)	Maximum ΔT (K) above which rows of nodes are inserted in the fuel-rod conduction calculation during reflood for all boiling regimes except nucleate and transition (suggested value = 10.0).
29-42	DZNHT	Minimum ΔZ (m) below which no additional rows are inserted in the fuel-rod conduction calculation during the reflood calculation (this value comes from the diffusion number).
43-56	HGAPO	Fuel-rod gap conductance coefficient (constant for NFCI = 0 on Card Number 6; initial value otherwise) ($W/m^2/K$).
57-70	TNEUT	The prompt neutron lifetime (s) ($TNEUT \leq 0.0$ defaults to the value 1.625×10^{-5} s set internally in TRAC).

(If IRPOP < 11 on Card Number 4, skip Card Number 112.)

Card Number 12. (Format 4E14.6) RCFORM(I), RCA(I), RCB(I), RCC(I), I = (1,3)

<u>Columns</u>	<u>Variable</u>	<u>Description</u>
1-14	RCFORM(I)	The form number for the reactivity coefficient type [0.0 = $\delta k/\delta x$, 1.0 = $(1/k)(\delta k/\delta x)$, 2.0 = $x(\delta k/\delta x)$, 3.0 = $(x/k)(\delta k/\delta x)$ for independent variables $x = T_{fuel}$ for $I = 1$, $T_{coolant}$ for $I = 2$, and $\alpha_{coolant}$ for $I = 3$].
15-28	RCA(I)	The coefficient for the zero th power polynomial term defining the I^{th} independent-variable reactivity coefficient.

<u>Columns</u>	<u>Variable</u>	<u>Description</u>
29-42	RBC(I)	The coefficient for the first power polynomial term defining the I^{th} independent-variable reactivity coefficient.
43-56	RCC(I)	The coefficient for the second power polynomial term defining the I^{th} independent-variable reactivity coefficient.

(The above card consists of three records, one for each of the independent variables $x = T_{\text{fuel}}, T_{\text{coolant}},$ and $\alpha_{\text{coolant}}.$)

CORE Array Cards. Sixteen sets of cards, one set for each of the following variables. Use LOAD format.

<u>Variable</u>	<u>Dimension</u>	<u>Description</u>
DX	NCELLS	Cell lengths (m).
VOL	NCELLS	Cell volumes (m^3).
FA	NCELLS+1	Cell-edge flow areas (m^2).
FRIC	NCELLS+1	Additive loss coefficients.
GRAV	NCELLS+1	The ratio of the elevation difference to the flow length between the centers of cell i and cell $i-1$ (positive GRAV indicates increasing elevation with increasing cell number). Gravity terms must be greater than zero for the required orientation of a CORE component.
HD	NCELLS+1	Hydraulic diameters (m).
NFF	NCELLS+1	Friction-factor correlation options. (See ACCUM input description, Sec. V.F.5.a.)
ALP	NCELLS	Initial void fractions (-).
VL	NCELLS+1	Initial liquid velocities (m/s).
VV	NCELLS+1	Initial vapor velocities (m/s).
TL	NCELLS	Initial liquid temperatures (K).
TV	NCELLS	Initial vapor temperatures (K).
P	NCELLS	Initial pressures (Pa).

<u>Variable</u>	<u>Dimension</u>	<u>Description</u>
PA	NCELLS	Initial air partial pressures (Pa).
QPPP	NCELLS	Volumetric heat sources (W/m^3) in pipe wall. (Eliminate this card set if NODES = 0.)
TW	NODES*NCELLS	Initial wall temperatures (K). (Eliminate this card set if NODES = 0.)

CORE COMMON Rod Array Cards. One set of cards for each of the following variables. Use LOAD format.

<u>Variable</u>	<u>Dimension</u>	<u>Description</u>
Z	NCELLS	Cumulative flow length (m) to the end of the cell.
RDPWR	NDRDS	Relative radial power density at the node positions.
CPOWR	1	Relative power density for the average rod.
RPKF	NRODS-1	Rod power peaking factors (relative to the cell average rod) for the additional rods.
ZPOWR	(ICRU-ICRL+2)*NPSZ	Axial-power-shape table; input [signal variable form defined by IPSSV and NPSRF on Card Number 5, axial-power-shape densities (ICRU-ICRL+1 values)] pairs. The relative axial power densities defining the axial power shape are specified at the axial segment level interfaces from one end of the fuel rod to the other. There are NPSZ axial power shapes, each having (ICRU-ICRL+1) values.
PSRF	NPSRF*2	Rate factor table for the trip-controlled axial-power-shape table independent variable defined by IPSSV on Card Number 5; input (trip signal minus the set point that turns the trip OFF, rate factor to be applied to the axial-power-shape table independent variable) pairs.
NRDX	1	Number of fuel rods in the core.
RADR	NDRDS	Rod node radii (m) (cold).

<u>Variable</u>	<u>Dimension</u>	<u>Description</u>																										
MATRD	NDRDS-1	Rod material ID numbers.																										
		<table border="1"> <thead> <tr> <th><u>ID</u></th> <th><u>Material Type</u></th> </tr> </thead> <tbody> <tr><td>1</td><td>Mixed oxide fuel</td></tr> <tr><td>2</td><td>Zircaloy</td></tr> <tr><td>3</td><td>Fuel-clad gap gases</td></tr> <tr><td>4</td><td>Boron nitride insulation</td></tr> <tr><td>5</td><td>Constantan/Nichrome heater wire</td></tr> <tr><td>6</td><td>Stainless steel, type 304</td></tr> <tr><td>7</td><td>Stainless steel, type 316</td></tr> <tr><td>8</td><td>Stainless steel, type 347</td></tr> <tr><td>9</td><td>Carbon steel, type A508</td></tr> <tr><td>10</td><td>Inconel, type 718</td></tr> <tr><td>11</td><td>Zircaloy dioxide</td></tr> <tr><td>12</td><td>Inconel, type 600</td></tr> </tbody> </table>	<u>ID</u>	<u>Material Type</u>	1	Mixed oxide fuel	2	Zircaloy	3	Fuel-clad gap gases	4	Boron nitride insulation	5	Constantan/Nichrome heater wire	6	Stainless steel, type 304	7	Stainless steel, type 316	8	Stainless steel, type 347	9	Carbon steel, type A508	10	Inconel, type 718	11	Zircaloy dioxide	12	Inconel, type 600
<u>ID</u>	<u>Material Type</u>																											
1	Mixed oxide fuel																											
2	Zircaloy																											
3	Fuel-clad gap gases																											
4	Boron nitride insulation																											
5	Constantan/Nichrome heater wire																											
6	Stainless steel, type 304																											
7	Stainless steel, type 316																											
8	Stainless steel, type 347																											
9	Carbon steel, type A508																											
10	Inconel, type 718																											
11	Zircaloy dioxide																											
12	Inconel, type 600																											

Only one MATRD may have the value 3 and MATRD(1) and MATRD(NDRDS - 1) cannot be 3.

PWTB	NPWX*2	Power or reactivity table; input (signal-variable form defined by IRPSV on Card Number 3 and NRPRF on Card Number 5, power or reactivity) pairs.
------	--------	--

RPRF	NRPRF*2	Rate factor table for the trip-controlled power or reactivity table independent variable defined by IRPRF on Card Number 3; input (trip signal minus the set point that turns the trip OFF, rate factor to be applied to the power or reactivity table independent variable) pairs.
------	---------	---

(Omit the next three variables if $NDGX \leq 0$ is input; the default 6 group delayed-neutron constants are defined internally in TRAC.)

<u>Variable</u>	<u>Dimension</u>	<u>Description</u>
BETA	NDGX	The effective delayed-neutron fraction.
LAMDA	NDGX	The delayed-neutron decay constant (1/s).
CDGN	NDGX	The delayed-neutron concentrations. If 0.0 is input, steady-state values are evaluated internally based on BETA, LAMDA, RPOWRI, and TNEUT.

(Omit the next three variables if NDHX \leq 0 is input; the default 11 group decay heat constants are defined internally in TRAC.)

<u>Variable</u>	<u>Dimension</u>	<u>Description</u>																
LAMDH	NDHX	The decay-heat decay constant (1/s).																
EDH	NDHX	The effective decay-heat energy fraction.																
CDHN	NDHX	The decay-heat concentrations. If 0.0 is input, steady-state values are evaluated internally based on LAMDH, EDG, and RPOWRI.																
NFAX	ICRU-ICRL	Number of permanent fine-mesh intervals per coarse-mesh interval added at the start of the reflood calculation. (The total number of heat-transfer rows per fuel rod must be less than NZMAX.)																
FPUO2	1	Fraction of plutonium dioxide (PuO ₂) in mixed oxide fuel.																
FTD	1	Fraction of theoretical fuel density.																
GMIX	7	Mole fraction of gap gas constituents. Array is not used if NFCI = 0 but still must be inserted. Enter data for each gas in the order indicated.																
		<table border="1"> <thead> <tr> <th><u>Index</u></th> <th><u>Gas</u></th> </tr> </thead> <tbody> <tr> <td>1</td> <td>Helium</td> </tr> <tr> <td>2</td> <td>Argon</td> </tr> <tr> <td>3</td> <td>Xenon</td> </tr> <tr> <td>4</td> <td>Krypton</td> </tr> <tr> <td>5</td> <td>Hydrogen</td> </tr> <tr> <td>6</td> <td>Air/nitrogen</td> </tr> <tr> <td>7</td> <td>Water vapor</td> </tr> </tbody> </table>	<u>Index</u>	<u>Gas</u>	1	Helium	2	Argon	3	Xenon	4	Krypton	5	Hydrogen	6	Air/nitrogen	7	Water vapor
<u>Index</u>	<u>Gas</u>																	
1	Helium																	
2	Argon																	
3	Xenon																	
4	Krypton																	
5	Hydrogen																	
6	Air/nitrogen																	
7	Water vapor																	
GMLFS	1	Moles of gap gas per fuel rod (not used).																
PGAPT	1	Average gap gas pressure (Pa) (not used if NFCI = 0).																
PLVOL	1	Plenum volume (m ³) in each fuel rod above the pellet stack (not used).																
PSLEN	1	Pellet-stack length (m) (not used).																
CLENN	1	Total cladding length (m) (not used).																

CORE Rod Array Cards. Two sets of cards, one for each of the following variables for each rod including the average rod and each additional rod.

<u>Variable</u>	<u>Dimension</u>	<u>Description</u>
BURN	ICRU-ICRL+1	Fuel burnup, MWD/MTU.
RFTN	NDRDS*(ICRU-ICRL+1)	Initial rod node temperatures (K).

d. Fill Component (FILL).

Card Number 1. (Format A10,4X,2I14,A30) TYPE, NUM, ID, CTITLE

<u>Columns</u>	<u>Variable</u>	<u>Description</u>
1-4	TYPE	Component type (FILL left justified).
15-28	NUM	Component ID number (must be unique for each component, $1 \leq \text{NUM} \leq 99$).
29-42	ID	User ID number (arbitrary).
43-72	CTITLE	Hollerith component description.

Card Number 2. (Format 5I14) JUN1, IFTY, IFSV, IFTR, NFTX

<u>Columns</u>	<u>Variable</u>	<u>Description</u>
1-14	JUN1	Junction number where fill is located.
15-28	IFTY	FILL-type options: 1 = constant velocity, 2 = constant mass flow, 3 = constant generalized state, 4 = velocity vs signal-variable form, 5 = mass flow vs signal-variable form, 6 = generalized state vs signal-variable form, 7 = constant velocity until trip then velocity vs signal-variable form, 8 = constant mass flow until trip then mass flow vs signal-variable form, or 9 = constant generalized state until trip then generalized state vs signal-variable form.
29-42	IFSV	The signal-variable ID number that defines the independent variable in the IFTY = 4 to 9 tables.

<u>Columns</u>	<u>Variable</u>	<u>Description</u>
43-56	IFTR	Trip ID number for FILL-type options IFTY = 7, 8, or 9.
57-70	NFTX	Number of FILL table pairs for FILL-type options IFTY = 4 to 9.

Card Number 3. (Format I14,E14.6) NFRF, TWTOLD

<u>Columns</u>	<u>Variable</u>	<u>Description</u>
1-14	NFRF	The number of rate-factor-table pairs where the rate factor is dependent on the trip signal difference from its trip OFF set point. The rate factor is to be applied to changes in the FILL-table independent variable defined by IFSV for FILL-type options IFTY = 7, 8, or 9.
15-28	TWTOLD	The fraction of the previous FILL fluid- dynamic state that is averaged with the FILL- table-defined state to define the FILL fluid- dynamic state for this time step ($0.0 \leq \text{TWTOLD} < 1.0$). (A value of 0.9 is recommended to avoid hydrodynamic instabilities when the FILL-table signal variable depends on a parameter, such as adjacent component pressure, that may couple strongly to the FILL velocity or a parameter that varies rapidly with time.)

Card Number 4. (Format 5E14.6) DXIN, VOLIN, ALPIN, VLIN, TLIN

<u>Columns</u>	<u>Variable</u>	<u>Description</u>
1-14	DXIN	Cell length (m), generally the same as its neighboring cell in the adjacent component. Currently not used.
15-28	VOLIN	Cell volume (m^3) (generally the same as that of its neighboring cell in the adjacent component). Currently not used.
29-42	ALPIN	Fluid void fraction (-) for positive flow (out of the FILL).
43-56	VLIN	Liquid velocity (m/s); a positive value indicates flow into the adjacent component; a negative value indicates flow from the adjacent component.
57-70	TLIN	Liquid temperatures (K) for positive flow.

Card Number 5. (Format 5E14.6) PIN, PAIN, FLOWIN, VVIN, TVIN

<u>Columns</u>	<u>Variable</u>	<u>Description</u>
1-14	PIN	Fill pressure (Pa).
15-28	PAIN	Fill air partial pressure (Pa).
29-42	FLOWIN	Initial mass flow (kg/s); a positive value indicates flow into the adjacent component; a negative value indicates flow from the adjacent component (only used for FILL-type options IFTY = 2 or 8).
43-56	VVIN	Vapor velocity (m/s); a positive value indicates flow into the adjacent component; a negative value indicates flow from the adjacent component (only used for FILL-type options IFTY = 3 or 9).
57-70	TVIN	Vapor temperature (K) for positive flow (only used for FILL-type options IFTY = 3 or 9).

FILL Liquid-Velocity or Mass-Flow Table Scale Factor. (Format E14.6) VMSCl

<u>Columns</u>	<u>Variable</u>	<u>Description</u>
1-14	VMSCl	The dependent variable in table VMTB is multiplied by this variable to obtain the absolute liquid velocity or absolute mass flow. Input only if table VMTB is input.

FILL-Table Cards. LOAD format (omit if IFTY < 4).

<u>Variable</u>	<u>Dimension</u>	<u>Description</u>
VMTB	NFTX*2	FILL liquid velocity or mass flow table; input (signal-variable form defined by IFSV on Card Number 2, velocity or mass flow) pairs (*,m/s) or (*,kg/s). Velocity is input for generalized state options, IFTY = 6 or 9.

Include the following scale factors and six tables only if IFTY = 6 or 9. The five scale factors should appear on a single card before table VVTB.

Remaining FILL-Table Scale Factors. (Format 5E14.6) VVSCL, TLSCL, TVSCL, PSCL, PASCL

<u>Columns</u>	<u>Variable</u>	<u>Description</u>
1-14	VVSCL	Vapor velocity scale factor. The dependent variable in table VVTB is multiplied by this factor to obtain absolute vapor velocity.
15-28	TLSCL	Liquid-temperature scale factor. The dependent variable in table TLTB is multiplied by this factor to obtain absolute liquid temperature.
29-42	TVSCL	Vapor-temperature scale factor. The dependent variable in table TVTB is multiplied by this factor to obtain absolute vapor temperature.
43-56	PSCL	Pressure scale factor. The dependent variable in table PTB is multiplied by this factor to obtain absolute pressure.
57-70	PASCL	Air-partial-pressure scale factor. The dependent variable in table PATB is multiplied by this factor to obtain absolute air partial pressure.

FILL-Table Cards. LOAD format.

<u>Variable</u>	<u>Dimension</u>	<u>Description</u>
VVTB	NFTX*2	Vapor-velocity vs signal-variable-form table (*,m/s).
TLTB	NFTX*2	Liquid-temperature vs signal-variable-form table (*,K).
TVTB	NFTX*2	Vapor-temperature vs signal-variable-form table (*,K).
ALPTB	NFTX*2	Void-fraction vs signal-variable-form table (*,-).
PTB	NFTX*2	Pressure vs signal-variable-form table (*,Pa).
PATB	NFTX*2	Air-partial-pressure vs signal-variable-form table (*,Pa).

Rate-Factor-Table Cards. LOAD format (omit if NFRF = 0 on Card Number 3).

<u>Variable</u>	<u>Dimension</u>	<u>Description</u>
RFTB	NFRF*2	Rate-factor table for the trip-controlled FILL-table independent variable defined by IFSV on Card Number 2; input (trip signal minus the set point that turns the trip OFF, rate factor to be applied to the FILL-table independent variable) pairs.

e. Pipe Component (PIPE).

Card Number 1. (Format A10,4X,2I14,A30) TYPE, NUM, ID, CTITLE

<u>Columns</u>	<u>Variable</u>	<u>Description</u>
1-14	TYPE	Component type (PIPE left justified).
15-28	NUM	Component ID number (must be unique for each component, $1 \leq \text{NUM} \leq 99$).
29-42	ID	User ID number (arbitrary).
43-72	CTITLE	Hollerith component description.

Card Number 2. (Format 5I14) NCELLS, NODES, JUN1, JUN2, MAT

<u>Columns</u>	<u>Variable</u>	<u>Description</u>
1-14	NCELLS	Number of fluid cells in the pipe.
15-28	NODES	Number of radial heat-transfer nodes in the pipe wall. (Zero implies no wall heat transfer.)
29-42	JUN1	Junction number for junction adjacent to cell 1.
43-56	JUN2	Junction number for junction adjacent to cell NCELLS.
57-70	MAT	Material ID number of the pipe wall: 6 = stainless steel, type 304; 7 = stainless steel, type 316; 8 = stainless steel, type 347, 9 = carbon steel, type A508; 10 = Inconel, type 718; or 12 = Inconel, type 600.

Card Number 3. (Format 4I14, E14.6) ICHF, IHYDRO, NPOWTB, IACC, POWSCL

<u>Columns</u>	<u>Variable</u>	<u>Description</u>
1-14	ICHF	CHF calculation flag. 0 = no; 1 = yes.
15-28	IHYDRO	Variable not used.
29-42	NPOWTB	Number of power table pairs.
43-56	IACC	Accumulator model flag. (See ACCUMULATOR, Sec. IV.B.) 0 = no accumulator logic; 1 = calculation of water level, volumetric flow, liquid volume discharge, and addition of interface sharpener; or 2 = same as (1) plus the phase separator at JUN2.
57-70	POWSCL	Power-table (variable POW) scale factor. The dependent variable in POW is multiplied by POWSCL to obtain absolute power.

Card Number 4. (Format 5E14.6) RADIN, TH, HOUTL, HOUTV, TOUTL

<u>Columns</u>	<u>Variable</u>	<u>Description</u>
1-14	RADIN	Inner radius (m) of the pipe wall
15-28	TH	Pipe wall thickness (m).
29-42	HOUTL	HTC ($W/m^2 \cdot K$) between outer boundary of pipe wall and liquid outside pipe.
43-56	HOUTV	HTC ($W/m^2 \cdot K$) between outer boundary of pipe wall and vapor outside pipe.
57-70	TOUTL	Liquid temperature (K) outside pipe.

Card Number 5. (Format E14.6) TOUTV, TDPOW

<u>Columns</u>	<u>Variable</u>	<u>Description</u>
1-14	TOUTV	Vapor temperature (K) outside pipe.
15-28	TDPOW	Time delay (s) for pipe power table. (The time abscissa coordinate in the table is the transient time minus TDPOW.)

Note: The four parameters, HOUTL, HOUTV, TOUTL, and TOUTV, allow flexibility in calculating possible heat losses from the outside of pipes. Typically, such heat losses are not important for fast transients or large breaks and HOUTL and HOUTV are set equal to zero. When heat losses are significant, they often can be described by a single HTC and a single external temperature (K).

PIPE Array Cards. Seventeen sets of cards, one set for each of the following variables. Use LOAD format.

<u>Variable</u>	<u>Dimension</u>	<u>Description</u>
DX	NCELLS	Cell lengths (m).
VOL	NCELLS	Cell volumes (m ³).
FA	NCELLS+1	Cell-edge flow areas (m ²).
FRIC	NCELLS+1	Additive loss coefficients.
GRAV	NCELLS+1	The ratio of the elevation difference to the distance between the center of cell i and the center of cell i-1. Positive GRAV indicates increasing elevation with increasing cell number.
HD	NCELLS+1	Hydraulic diameters (m).
NFF	NCELLS+1	Friction-factor correlation options. (See ACCUM input description, Sec. V.F.5.a.)
ALP	NCELLS	Initial void fractions (-).
VL	NCELLS+1	Initial liquid velocities (m/s).
VV	NCELLS+1	Initial vapor velocities (m/s).
TL	NCELLS	Initial liquid temperatures (K).
TV	NCELLS	Initial vapor temperatures (K).
P	NCELLS	Initial pressures (Pa).
PA	NCELLS	Initial air partial pressures (Pa).
QPPP	NCELLS	Volumetric heat sources (W/m ³) in pipe wall. (Eliminate this card set if NODES = 0.)
TW	NODES*NCELLS	Initial wall temperatures (K). (Eliminate this card set if NODES = 0.)

<u>Variable</u>	<u>Dimension</u>	<u>Description</u>
POW	NPOWTB*2	Power vs time table; input [time (s), power (W)] pairs. Power is input directly to the fluid in the pipe and distributed evenly among the cells. The variable NODES must be zero.

f. Pressurizer Component (PRIZER).

Card Number 1. (Format A10,4X,2I14,A30) TYPE, NUM, ID, CTITLE

<u>Columns</u>	<u>Variable</u>	<u>Description</u>
1-6	TYPE	Component type (PRIZER left justified).
15-28	NUM	Component ID number (must be unique for each component, $1 \leq \text{NUM} \leq 99$).
29-42	ID	User ID number (arbitrary).
43-72	CTITLE	Hollerith component description.

Card Number 2. (Format 2I14) NCELLS, JUN1, JUN2

<u>Columns</u>	<u>Variable</u>	<u>Description</u>
1-14	NCELLS	Number of fluid cells in pressurizer component.
15-28	JUN1	Junction number for junction adjacent to cell 1.
29-42	JUN2	Number of the junction adjacent to cell NCELL. This must be the pressurizer discharge.

Card Number 3. (Format 4E14.6) QHEAT, PSET, DPMAX, ZHTR

<u>Columns</u>	<u>Variable</u>	<u>Description</u>
1-14	QHEAT	Total heater power (W).
15-28	PSET	Pressure set point (Pa) for heater/sprayer controller.
29-42	DPMAX	Pressure differential (Pa) at which heater/sprayer has maximum power.
43-56	ZHTR	Water level (m) for heater cutoff.

PRIZER Array Cards. Fourteen sets of cards, one set for each of the following variables. Use LOAD format.

<u>Variable</u>	<u>Dimension</u>	<u>Description</u>
DX	NCELLS	Cell lengths (m).
VOL	NCELLS	Cell volumes (m ³).
FA	NCELLS+1	Cell-edge flow areas (m ²).
FRIC	NCELLS+1	Additive loss coefficients.
GRAV	NCELLS+1	Gravity terms. (See PIPE, Sec. V.F.5.e.)
HD	NCELLS+1	Hydraulic diameters (m).
NFF	NCELLS+1	Friction-factor correlation options. See ACCUM input description, Sec. V.F.5.a. The value NFF = 1 is suggested for this component.
ALP	NCELLS	Initial void fractions (-).
VL	NCELLS+1	Initial liquid velocities (m/s).
VV	NCELLS+1	Initial vapor velocities (m/s).
TL	NCELLS	Initial liquid temperatures (K).
TV	NCELLS	Initial vapor temperatures (K).
P	NCELLS	Initial pressures (Pa).
PA	NCELLS	Initial air partial pressures (Pa).

g. Pump Component (PUMP).

Card Number 1. (Format A10,4X,2I14,A30) TYPE, NUM, ID, CTITLE

<u>Columns</u>	<u>Variable</u>	<u>Description</u>
1-4	TYPE	Component type (PUMP left justified).
15-28	NUM	Component ID number (must be unique for each component, $1 \leq \text{NUM} \leq 99$).
29-42	ID	User ID number (arbitrary).
43-72	CTITLE	Hollerith component description.

Card Number 2. (Format 5I14) NCELLS, NODES, JUN1, JUN2, MAT

<u>Columns</u>	<u>Variable</u>	<u>Description</u>
1-14	NCELLS	Number of fluid cells in pump component (must be at least two).
15-28	NODES	Number of radial heat-transfer nodes in wall. (Zero implies no wall heat transfer.)
29-42	JUN1	Junction number for junction adjacent to cell 1.
43-56	JUN2	Junction number for junction adjacent to cell NCELLS.
57-70	MAT	Material ID of wall. See PIPE input description, Sec. V.F.5.e.

Card Number 3. (Format 5I14) ICHF, IHYDRO, IPMPTY, IRP, IPM

<u>Columns</u>	<u>Variable</u>	<u>Description</u>
1-14	ICHF	CHF calculation flag. 0 = no; 1 = yes.
15-28	IHYDRO	Variable not used.
29-42	IPMPTY	Pump type. 1 = pump rotational speed when trip set ON specified by table SPTBL; 2 = pump rotational speed when trip set ON calculated from Eq. (196).
43-56	IRP	Reverse speed option. 0 = reverse rotation not allowed; 1 = reverse rotation allowed. (Checked only for IPMPTY = 2.)
57-70	IPM	Degradation option. 0 = use single-phase homologous curves or 1 = use combined single-phase and fully degraded two-phase homologous curves.

Card Number 4. (Format 4I14) IPMPSV, IPMPTR, NPMPTX, NPMPRF

<u>Columns</u>	<u>Variable</u>	<u>Description</u>
1-14	IPMPSV	The signal-variable ID number that defines the independent variable in the IPMPTY = 1 pump-speed table.

<u>Columns</u>	<u>Variable</u>	<u>Description</u>
15-28	IPMPTR	Pump trip ID number (zero implies a constant speed pump).
29-42	NPMPTX	Number of pairs of points in the pump-speed table.
43-56	NMPPRF	Number of pairs of points in the rate-factor table to be applied to the trip-controlled pump-speed-table independent variable defined by IPMPSV on Card Number 4.

Card Number 5. (Format 5E14.6) RADIN, TH, HOUTL, HOUTV, TOUTL

<u>Columns</u>	<u>Variable</u>	<u>Description</u>
1-14	RADIN	Inner radius (m) of pump wall.
15-28	TH	Pump wall thickness (m).
29-42	HOUTL	HTC ($W/m^2 \cdot K$) between outer boundary of pump wall and liquid outside pump.
43-56	HOUTV	HTC ($W/m^2 \cdot K$) between outer boundary of pump wall and vapor outside pump.
57-70	TOUTL	Liquid temperature (K) outside pump wall.

Card Number 6. (Format E14.6) TOUTV

<u>Columns</u>	<u>Variable</u>	<u>Description</u>
1-14	TOUTV	Vapor temperature (K) outside pump wall.

(See PIPE module description, Sec. IV.A, for further comments on these heat-transfer parameters.)

Card Number 7. (Format 5E14.6) RHEAD, RTORK, RFLOW, RRHO, ROMEGA

<u>Columns</u>	<u>Variable</u>	<u>Description</u>
1-14	RHEAD	Rated head ($Pa \cdot m^3/kg$ or m^2/s^2).
15-28	RTORK	Rated torque ($N \cdot m$).
29-42	RFLOW	Rated volumetric flow (m^3/s).
43-56	RRHO	Rated density (kg/m^3).
57-70	ROMEGA	Rated pump speed (rad/s).

Card Number 8. (Format 5E14.6) EFFMI, TFR1, TFR2, OMEGAN, OMGSC

<u>Columns</u>	<u>Variable</u>	<u>Description</u>
1-14	EFFMI	Effective moment of inertia ($\text{kg} \cdot \text{m}^2$).
15-28	TFR1	Frictional torque coefficient [Eq. (194)] ($\text{N} \cdot \text{m}$).
29-42	TFR2	Bearing and windage torque coefficient [(Eq. 195)] ($\text{N} \cdot \text{m}$).
43-56	OMEGAN	Initial pump speed (rad/s).
57-70	OMGSC	Pump-speed-table (variable SPTBL) scale factor (-). The dependent variable in table SPTBL is multiplied by OMGSC to obtain absolute rotational speed.

Card Number 9. (Format I14) OPTION

<u>Columns</u>	<u>Variable</u>	<u>Description</u>
1-14	OPTION	Pump curve option number. 0 = user-specified pump, input following; 1 = use built-in Semiscale pump; or 2 = use built-in LOFT pump.

Card Set 10 and pump curve cards are needed only if OPTION = 0. If OPTION = 1 or 2, skip to the pump array cards. The user is referred to the pump model description in Sec. IV.F for definitions of the terms used below. Each homologous curve is divided into four curve segments. Each curve segment is denoted by the number appended to the curve name. The segments are defined by Table V in Sec. IV.F.

Under certain conditions for OPTION = 0, some curves do not need to be entered. However, to avoid confusion, we recommend that all curves be entered when OPTION = 0. For IPMPTY = 1 and IPM = 0, curves HSP1 through HSP4 are required, and the remaining curves can be dummies. For IPMPTY = 1 and IPM = 1, curves HSP1 through HSP4, HTP1 through HTP4, and HDM are required, and the remaining curves can be dummies. For IPMPTY = 2 and IPM = 0, curves HSP1 through HSP4 and TSP1 through TSP4 are required, and the remaining curves can be dummies. For IPMPTY = 2 and IPM = 1, all curves are required. The foregoing indication of potential dummy curves does not imply that curve I may be left out by specifying NDATA(I) = 0 in Card Set 10. Future code changes may

restrict those curves that can be represented by dummy curves under various conditions.

Card Set 10. (Format 5114) NDATA(I) (I = 1,16), NHDM, NTDM

First Card.

<u>Columns</u>	<u>Variable</u>	<u>Description</u>
1-14	NDATA(1)	Number of pairs of points on the HSP1 curve.
15-28	NDATA(2)	Number of pairs of points on the HSP2 curve.
29-42	NDATA(3)	Number of pairs of points on the HSP3 curve.
43-56	NDATA(4)	Number of pairs of points on the HSP4 curve.
57-70	NDATA(5)	Number of pairs of points on the HTP1 curve.

Second Card.

<u>Columns</u>	<u>Variable</u>	<u>Description</u>
1-14	NDATA(6)	Number of pairs of points on the HTP2 curve.
15-28	NDATA(7)	Number of pairs of points on the HTP3 curve.
29-42	NDATA(8)	Number of pairs of points on the HTP4 curve.
43-56	NDATA(9)	Number of pairs of points on the TSP1 curve.
57-70	NDATA(10)	Number of pairs of points on the TSP2 curve.

Third Card.

<u>Columns</u>	<u>Variable</u>	<u>Description</u>
1-14	NDATA(11)	Number of pairs of points on the TSP3 curve.
15-28	NDATA(12)	Number of pairs of points on the TSP4 curve.
29-42	NDATA(13)	Number of pairs of points on the TTP1 curve.
43-56	NDATA(14)	Number of pairs of points on the TTP2 curve.
57-70	NDATA(15)	Number of pairs of points on the TTP3 curve.

Fourth Card.

<u>Columns</u>	<u>Variable</u>	<u>Description</u>
1-14	NDATA(16)	Number of pairs of points on the TTP4 curve.

<u>Columns</u>	<u>Variable</u>	<u>Description</u>
15-28	NHDM	Number of pairs of points on the HDM curve.
29-42	NTDM	Number of pairs of points on the TDM curve.

PUMP Curve Cards. Up to 18 sets of cards. One set for each curve listed in card set 10 that has nonzero data points. Use LOAD format. Data are entered in pairs $(x,y)_i$, $i = (1, NDATA)$ where x is the independent variable and y is the dependent variable. The x_i values must increase monotonically from -1.0 to 1.0 for the homologous curves and from 0.0 to 1.0 for the multiplier curves. If information for a particular curve does not exist or if you desire to input a simple dummy curve, we suggest that the four points (-1.0, 0.0, 1.0, 0.0) be used. [The suggested dummy for HDM and TDM is (0.0, 0.0, 1.0, 0.0).]

<u>Variable</u>	<u>Dimension</u>	<u>Description</u>
HSP1	2*NDATA(1)	HSP1 curve
HSP2	2*NDATA(2)	HSP2 curve
HSP3	2*NDATA(3)	HSP3 curve
HSP4	2*NDATA(4)	HSP4 curve
HTP1	2*NDATA(5)	HTP1 curve
HTP2	2*NDATA(6)	HTP2 curve
HTP3	2*NDATA(7)	HTP3 curve
HTP4	2*NDATA(8)	HTP4 curve
TSP1	2*NDATA(9)	TSP1 curve
TSP2	2*NDATA(10)	TSP2 curve
TSP3	2*NDATA(11)	TSP3 curve
TSP4	2*NDATA(12)	TSP4 curve

single-phase homologous head curves.

fully degraded homologous head curves.

single-phase homologous torque curves.

<u>Variable</u>	<u>Dimension</u>	<u>Description</u>
TTP1	2*NDATA(13)	TTP1 curve
TTP2	2*NDATA(14)	TTP2 curve
TTP3	2*NDATA(15)	TTP3 curve
TTP4	2*NDATA(16)	TTP4 curve
HDM	2*NHDM	Head degradation multiplier.
TDM	2*NTDM	Torque degradation multiplier.

fully degraded homologous torque curves

PUMP Array Cards. Eighteen sets of cards. One set for each of the following variables. Use LOAD format.

<u>Variable</u>	<u>Dimension</u>	<u>Description</u>
SPTBL	2*NPMP TX	Pump-speed vs signal-variable-form table. Input as signal-variable form defined by IPMP SV and NPMP RF on Card Number 4, pump speed pairs [$*$,rad/s].
RFTBL	2*NPMP RF	Rate-factor table for the trip-controlled pump-speed-table independent variable defined by IPMP SV on Card Number 4; insert pairs (trip signal minus the set point that turns the trip OFF, rate factor to be applied to the pump-speed-table independent variable).
DX	NCELLS	Cell lengths (m).
VOL	NCELLS	Cell volumes (m^3).
FA	NCELLS+1	Cell-edge flow areas (m^2).
FRIC	NCELLS+1	Additive loss coefficients [FRIC(2) must be 0.0].
GRAV	NCELLS+1	Gravity terms. (See PIPE, Sec. V.F.5.e.)
HD	NCELLS+1	Hydraulic diameters (m).
NFF	NCELLS+1	Friction-factor correlation options. (See ACCUM input description, Sec. V.F.5.a.)
ALP	NCELLS	Initial void fractions (-).
VL	NCELLS+1	Initial liquid velocities (m/s).

<u>Variable</u>	<u>Dimension</u>	<u>Description</u>
VV	NCELLS+1	Initial vapor velocities (m/s).
TL	NCELLS	Initial liquid temperatures (K).
TV	NCELLS	Initial vapor temperatures (K).
P	NCELLS	Initial pressures (Pa).
PA	NCELLS	Initial air pressures (Pa).
QPPP	NCELLS	Volumetric heat sources (W/m^3) in pump wall. (Eliminate this card set if NODES = 0.)
TW	NODES*NCELLS	Initial wall temperatures (K). (Eliminate this card set if NODES = 0.)

h. Steam-Generator Component (STGEN).

Card Number 1. (Format A10,4X,2I14,A30) TYPE, NUM, ID, CTITLE

<u>Columns</u>	<u>Variable</u>	<u>Description</u>
1-14	TYPE	Component type (STGEN left justified).
15-28	NUM	Component ID number (must be unique for each component, $1 \leq NUM \leq 99$).
29-42	ID	User ID number (arbitrary).
43-72	CTITLE	Hollerith component description.

Card Number 2. (Format 5I14) NCELL1, NODES, JUN11, JUN12, MAT

<u>Columns</u>	<u>Variable</u>	<u>Description</u>
1-14	NCELL1	Number of fluid cells on primary side.
15-28	NODES	Number of radial heat-transfer nodes in wall (<u>must</u> be greater than or equal to 1).
29-42	JUN11	Junction number for junction adjacent to cell 1 on primary side.
43-56	JUN12	Junction number adjacent to cell NCELL1 on primary side.
57-70	MAT	Material ID number of tube. (See PIPE input description, Sec. V.F.5.e.)

Card Number 3. (Format 4I14) KIND, IHYDRO, ICHF1, ICHF2

<u>Columns</u>	<u>Variable</u>	<u>Description</u>
1-14	KIND	Steam-generator type. 1 = U-tube; 2 = once-through.
15-28	IHYDRO	Variable not used.
29-42	ICHF1	Indicator for CHF calculation on primary side. 0 = no; 1 = yes.
43-56	ICHF2	Indicator for CHF calculation on secondary side. 0 = no; 1 = yes.

Card Number 4. (Format 2E14.6) RADIN, TH

<u>Columns</u>	<u>Variable</u>	<u>Description</u>
1-14	RADIN	Inner radius of tube wall.
15-28	TH	Tube wall thickness (m).

Card Number 5. (Format 5I14) NCELL2, JUN21, JUN22, JCELLS, JCELLP

<u>Columns</u>	<u>Variable</u>	<u>Description</u>
1-14	NCELL2	Number of fluid cells on secondary side.
15-28	JUN21	Junction number for junction adjacent to cell 1 on secondary side.
29-42	JUN22	Junction number for junction adjacent to cell NCELL2 on secondary side.
43-56	JCELLS	Junction cell for secondary tee (optional).
57-70	JCELLP	Junction cell for primary tee (optional, if JCELLP > 0, then JCELLS > 0).

Card Number 6. (Format 3I14, E14.6) IHYD3, NCELL3, JUN3, COSTS

(Card 6 is read only if JCELLS > 0 on Card Number 5.)

<u>Columns</u>	<u>Variable</u>	<u>Description</u>
1-14	IHYD3	Variable not used.
15-28	NCELL3	Number of cells in secondary tee.

<u>Columns</u>	<u>Variable</u>	<u>Description</u>
29-42	JUN3	Junction number for the free end of the secondary tee.
43-56	COSTS	Cosine of the angle from the low-numbered side of the secondary tube to the secondary tee tube.

Card Number 7. (Format 3114, E14.6) IHYD4, NCELL4, JUN4, COSTP

(Card 7 is read only if JCELLP > 0 on Card Number 5.)

<u>Columns</u>	<u>Variable</u>	<u>Description</u>
1-14	IHYD4	Variable not used.
15-28	NCELL4	Number of cells in primary tee.
29-42	JUN4	Junction number for the free end of the primary tee.
43-56	COSTP	Cosine of the angle from the low-numbered side of the primary tube to the primary tee tube.

STGEN Array Cards. Thirty-one sets of cards, one set for each of the following variables. Use LOAD format.

<u>Variable</u>	<u>Dimension</u>	<u>Description</u>
DX	NCELL1	Cell lengths (m) on primary side.
VOL	NCELL1	Cell volumes (m^3) on primary side for all tubes.
FA	NCELL1+1	Cell-edge flow areas (m^2) on primary side for all tubes.
FRIC	NCELL1+1	Additive loss coefficients on primary side.
GRAV	NCELL1+1	Gravity terms. (See PIPE, Sec. V.F.5.e.)
HD	NCELL1+1	Primary-side hydraulic diameters (m) for a single tube.
NFF	NCELL1+1	Primary side friction-factor correlation options. (See ACCUM input description, Sec. V.D.3.a.)
ALP	NCELL1	Primary-side initial void fractions (-).

<u>Variable</u>	<u>Dimension</u>	<u>Description</u>
VL	NCELL1+1	Primary-side initial liquid velocities (m/s).
VV	NCELL1+1	Primary-side initial vapor velocities (m/s).
TL	NCELL1	Primary-side initial liquid temperatures (K).
TV	NCELL1	Primary-side initial vapor temperatures (K).
P	NCELL1	Primary-side initial pressures (Pa).
PA	NCELL1	Primary-side initial air partial pressures (Pa).
TW	NODES*NCELL1	Initial tube-wall temperatures (K).
DX	NCELL2	Cell lengths (m) on secondary side.
VOL	NCELL2	Cell volumes (m ³) on secondary side.
FA	NCELL2+1	Cell-edge flow areas (m ²) on secondary side.
FRIC	NCELL2+1	Additive loss coefficients on secondary side.
GRAV	NCELL2+1	Gravity terms. (See PIPE, Sec. V.F.5.e.)
HD	NCELL2+1	Secondary-side hydraulic diameters (m).
NFF	NCELL2+1	Friction-factor correlation option for secondary side. (See ACCUM input description, Sec. V.F.5.a.)
ALP	NCELL2	Secondary-side initial void fractions (-).
VL	NCELL2+1	Secondary-side initial liquid velocities (m/s).
VV	NCELL2+1	Secondary-side initial vapor velocities (m/s).
TL	NCELL2	Secondary-side initial liquid temperatures (K).
TV	NCELL2	Secondary-side initial vapor temperatures (K).
P	NCELL2	Secondary-side initial pressures (Pa).
PA	NCELL2	Secondary-side initial air partial pressures (Pa).
WA	NCELL1	Primary side wall areas for all tubes.
WA	NCELL2	Secondary side wall areas for all tubes {WA(SECONDARY) = WA(PRIMARY) * [1. + (TH/RADIN)]}.

Secondary Tee Array. Fourteen sets of cards, one set for each of the following variables. Use LOAD format.

(These cards are read only if JCELLS > 0 on Card Number 5.)

<u>Variable</u>	<u>Dimension</u>	<u>Description</u>
DX	NCELL3	Tee-tube cell lengths (m).
VOL	NCELL3	Tee-tube cell volumes (m ³).
FA	NCELL3+1	Tee-tube cell-edge flow areas (m ²).
FRIC	NCELL3+1	Tee-tube additive loss coefficients.
GRAV	NCELL3+1	Tee-tube gravity terms. (See PIPE, Sec. V.F.5.e.)
HD	NCELL3+1	Tee-tube hydraulic diameters (m).
NFF	NCELL3+1	Friction-factor correlation options for secondary tee tube. (See ACCUM input description (Sec. V.D.a).)
ALP	NCELL3	Tee-tube initial void fractions (-).
VL	NCELL3+1	Tee-tube initial liquid velocities (m/s).
VV	NCELL3+1	Tee-tube initial vapor velocities (m/s).
TL	NCELL3+1	Tee-tube initial liquid temperatures (K).
TV	NCELL3	Tee-tube initial vapor temperatures (K).
P	NCELL3	Tee-tube initial pressures (Pa).
PA	NCELL3	Tee-tube initial air partial pressures (Pa).

Primary Tee Array. Fourteen sets of cards, one set for each of the following variables. Use LOAD format.

(These cards are read only if JCELLP > 0 on Card 5.)

<u>Variable</u>	<u>Dimension</u>	<u>Description</u>
DX	NCELL4	Tee-tube cell lengths (m).
VOL	NCELL4	Tee-tube cell volumes (m ³).
FA	NCELL4+1	Tee-tube cell-edge flow areas (m ²).

<u>Variable</u>	<u>Dimension</u>	<u>Description</u>
FRIC	NCELL4+1	Tee-tube additive loss coefficients.
GRAV	NCELL4+1	Tee-tube gravity terms. (See PIPE, Sec. V.F.5.e.)
HD	NCELL4+1	Tee-tube hydraulic diameters (m).
NFF	NCELL4+1	Friction-factor correlation options for primary tee tube. (See ACCUM input description (Sec. V.D.a.)
ALP	NCELL4	Tee-tube initial void fractions (-).
VL	NCELL4+1	Tee-tube initial liquid velocities (m/s).
VV	NCELL4+1	Tee-tube initial vapor velocities (m/s).
TL	NCELL4+1	Tee-tube initial liquid temperatures (K).
TV	NCELL4	Tee-tube initial vapor temperatures (K).
P	NCELL4	Tee-tube initial pressures (Pa).
PA	NCELL4	Tee-tube initial air partial pressures (Pa).

i. Tee Component (TEE).

Card Number 1. (Format A10,4X,2I14,A30) TYPE, NUM, ID, CTITLE

<u>Columns</u>	<u>Variable</u>	<u>Description</u>
1-14	TYPE	Component type (TEE left justified).
15-28	NUM	Component ID number (must be unique for each component, $1 \leq \text{NUM} \leq 99$).
29-42	ID	User ID number (arbitrary).
43-72	CTITLE	Hollerith component description.

Card Number 2. (Format 3I14, E14.6, I14) JCELL, NODES, MATID, COST, ICHF

1-14	JCELL	Junction cell number.
15-28	NODES	Number of radial heat-transfer nodes in the tee wall. (Zero implies no wall heat transfer.)
29-42	MATID	Material ID number of tee wall. (See PIPE input description, Sec. V.F.5.e.)

<u>Columns</u>	<u>Variable</u>	<u>Description</u>
43-56	COST	Cosine of the angle from the low-numbered side of the primary tube to the secondary tube.
57-70	ICHF	CHF calculation flag. 0 = no; 1 = yes.

Card Number 3. (Format 5I14) IHYD1, NCELL1, JUN1, JUN2

<u>Columns</u>	<u>Variable</u>	<u>Description</u>
1-14	IHYD1	Variable not used.
15-28	NCELL1	Number of fluid cells in the primary tee tube.
29-42	JUN1	Junction number for the junction adjacent to cell 1.
43-56	JUN2	Junction number for the junction adjacent to cell NCELL1.

Card Number 4. (Format 5E14.6) RADIN1, TH1, HOUTL1, HOUTV1, TOUTL1

<u>Columns</u>	<u>Variable</u>	<u>Description</u>
1-14	RADIN1	Inner radius (m) of the primary tube wall.
15-28	TH1	Wall thickness (m) of the primary tube.
29-42	HOUTL1	HTC ($W/m^2 \cdot K$) between outer boundary of the primary tube wall and liquid outside the primary tube wall.
43-56	HOUTV1	HTC ($W/m^2 \cdot K$) between outer boundary of the primary tube wall and vapor outside the primary tube wall.
57-70	TOUTL1	Liquid temperature (K) outside the primary tube wall.

Card Number 5. (Format E14.6) TOUTV1

1-14	TOUTV1	Vapor temperature (K) outside the primary tube wall.
------	--------	--

(See PIPE module description, Sec. IV.A, for further comments on these heat-transfer parameters.)

Card Number 6. (Format 3I14) IHYD2, NCELL2, JUN3

<u>Columns</u>	<u>Variable</u>	<u>Description</u>
1-14	IHYD2	Variable not used.
15-28	NCELL2	Number of fluid cells in the secondary tee tube.
29-42	JUN3	Junction number at the free end of the secondary tube adjacent to cell NCELL2.

Card Number 7. (Format 5E14.6) RADIN2, TH2, HOUTL2, HOUTV2, TOUTL2

<u>Columns</u>	<u>Variable</u>	<u>Description</u>
1-14	RADIN2	Inner radius (m) of the secondary tube wall.
15-28	TH2	Wall thickness (m) of the secondary tube.
29-42	HOUTL2	HTC ($W/m^2 \cdot K$) between outer boundary of the secondary tube wall and liquid outside the secondary tube wall.
43-56	HOUTV2	HTC ($W/m^2 \cdot K$) between boundary of the secondary tube wall and vapor outside the secondary tube wall.
57-70	TOUTL2	Liquid temperature (K) outside the secondary tube wall.

Card Number 8. (Format E14.6) TOUTV2

<u>Columns</u>	<u>Variable</u>	<u>Description</u>
1-14	TOUTV2	Vapor temperature (K) outside the secondary tube wall.

(See comment on Card 5.)

TEE Array Cards. Thirty-two sets of cards, one for each of the following variables. Use LOAD format.

<u>Variable</u>	<u>Dimension</u>	<u>Description</u>
DX	NCELL1	Primary-tube cell lengths (m).
VOL	NCELL1	Primary-tube cell volumes (m^3).
FA	NCELL1+1	Primary-tube cell-edge flow areas (m^2).
FRIC	NCELL1+1	Primary-tube additive loss coefficients.

<u>Variable</u>	<u>Dimension</u>	<u>Description</u>
GRAV	NCELL1+1	Primary-tube gravity terms (see PIPE input description, Sec. V.F.5.e.)
HD	NCELL1+1	Primary-tube hydraulic diameters (m).
NFF	NCELL1+1	Friction-factor correlation options for primary tube. (See ACCUM input description, Sec. V.F.5.a.)
ALP	NCELL1	Primary-tube initial void fractions (-).
VL	NCELL1+1	Primary-tube initial liquid velocities (m/s).
VV	NCELL1+1	Primary-tube initial vapor velocities (m/s).
TL	NCELL1	Primary-tube initial liquid temperatures (K).
TV	NCELL1	Primary-tube initial vapor temperatures (K).
P	NCELL1	Primary-tube initial pressures (Pa).
PA	NCELL1	Primary-tube initial air partial pressures (Pa).
QPPP	NCELL1	Volumetric heat sources (W/m^3) in tee wall for primary tube. (Eliminate this card set if NODES = 0.)
TW	NODES*NCELL1	Primary-tube initial wall temperatures (K). (Eliminate this card set if NODES = 0.)
DX	NCELL2	Secondary-tube cell lengths (m).
VOL	NCELL2	Secondary-tube cell volumes (m^3).
FA	NCELL2+1	Secondary-tube cell-edge flow areas (m^2).
FRIC	NCELL2+1	Secondary-tube additive loss coefficients.
GRAV	NCELL2+1	Secondary-tube gravity terms (see PIPE input description, Sec. V.F.5.e.)
HD	NCELL2+1	Secondary-tube hydraulic diameters (m).
NFF	NCELL2+1	Friction-factor correlation options for secondary tube. (See ACCUM input description, Sec. V.F.5.a.)
ALP	NCELL2	Secondary-tube initial void fractions (-).
VL	NCELL2+1	Secondary-tube initial liquid velocities (m/s).

<u>Variable</u>	<u>Dimension</u>	<u>Description</u>
VV	NCELL2+1	Secondary-tube initial vapor velocities (m/s).
TL	NCELL2	Secondary-tube initial liquid temperatures (K).
TV	NCELL2	Secondary-tube initial vapor temperatures (K).
P	NCELL2	Secondary-side initial pressures (Pa).
PA	NCELL2	Secondary-tube initial air partial pressures (Pa).
QPPP	NCELL2	Volumetric heat sources (W/m^3) in tee wall (secondary tube). (Eliminate this card set if NODES = 0.)
TW	NODES*NCELL2	Secondary-tube initial wall temperatures (K). (Eliminate this card set if NODES = 0.)

j. Valve Component (VALVE).

Card Number 1. (Format A10,4X,2I14,A30) TYPE, NUM, ID, CTITLE

<u>Columns</u>	<u>Variable</u>	<u>Description</u>
1-14	TYPE	Component type (VALVE left justified).
15-28	NUM	Component ID number (must be unique for each component, $1 \leq NUM \leq 99$).
29-42	ID	User ID number (arbitrary).
43-72	CTITLE	Hollerith component description.

Card Number 2. (Format 5I14) NCELLS, NODES, JUN1, JUN2, MAT

<u>Columns</u>	<u>Variable</u>	<u>Description</u>
1-14	NCELLS	Number of fluid cells (must be at least two unless a BREAK is attached to JUN2).
15-28	NODES	Number of radial heat-transfer nodes in valve wall. (Zero implies no wall heat transfer.)
29-42	JUN1	Junction number for junction adjacent to cell 1.
43-56	JUN2	Junction number for junction adjacent to cell NCELLS.
57-70	MAT	Material ID of wall. (See PIPE input description, Sec. V.F.5.e.)

Card Number 3. (Format 5I14) ICHF, IHYDRO, IVTY, IVSV, IVTR

<u>Columns</u>	<u>Variable</u>	<u>Description</u>
----------------	-----------------	--------------------

1-14	ICHF	CHF calculation flag. 0 = no; 1 = yes.
------	------	--

15-28	IHYDRO	Variable not used.
-------	--------	--------------------

<u>Columns</u>	<u>Variable</u>	<u>Description</u>
----------------	-----------------	--------------------

29-42	IVTY	Valve-type option. 0 = constant flow area; 1 = flow area fraction vs the signal-variable form; 2 = relative position of the valve stem (0.0 = fully closed, 1.0 = fully opened) vs the signal-variable form; 3 = constant flow area until trip then flow area fraction vs the signal-variable form; or 4 = constant flow area until trip then relative position of the valve stem vs the signal-variable form.
-------	------	---

43-56	IVSV	The signal-variable ID number that defines the independent variable in the valve-type option IVTY = 1 to 4 tables.
-------	------	--

57-70	IVTR	The trip ID number for valve-type option IVTY = 3 or 4.
-------	------	---

Card Number 4. (Format 4I14) IVPS, NVOTB, NVCTB, NVRF .

<u>Columns</u>	<u>Variable</u>	<u>Description</u>
----------------	-----------------	--------------------

1-14	IVPS	The mesh-cell interface number where the valve flow area is adjusted ($1 < IVPS < NCELLS+1$ unless a BREAK component is at the VALVE component junction JUN2; then IVPS can equal NCELLS+1).
------	------	---

15-28	NVOTB	The number of pairs of points in the first valve table. (When IVTY = 0, NVOTB = 0; when IVTY = 1 to 4, NVOTB \geq 1.)
-------	-------	---

29-42	NVCTB	The number of pairs of points in the second valve table. (When IVTY = 0 to 2, NVCTB = 0. If NVCTB = 0 when IVTY = 3 or 4, the first valve table is used when the trip is set to ON _{reverse} , ON, or ON _{forward} . If NVCTB \geq 1 when IVTY = 3 or 4, the first valve table is
-------	-------	---

<u>Columns</u>	<u>Variable</u>	<u>Description</u>
		used when the trip is set to ON or ON _{forward} and the second valve table is used when the trip is set to ON _{reverse} .)
43-56	NVRF	The number of the rate-factor-table pairs where the rate factor is dependent on the trip-signal difference from its trip OFF set point. The rate factor is to be applied to changes in the valve-table independent variable defined by IVSV for valve-type options IVTY = 3 or 4.

Card Number 5. (Format 5E14.6) RADIN, TH, HOUTL, HOUTV, TOUTL

<u>Columns</u>	<u>Variable</u>	<u>Description</u>
1-14	RADIN	Inner radius (m) of valve wall.
15-28	TH	Valve wall thickness (m).
29-42	HOUTL	HTC ($W/m^2 \cdot K$) between outer boundary of valve wall and liquid outside valve.
43-56	HOUTV	HTC ($W/m^2 \cdot K$) between outer boundary of valve wall and vapor outside valve.
57-70	TOUTL	Liquid temperature (K) outside valve.

Card Number 6. (Format 5E14.6) TOUTV, AVLVE, HVLVE, FAVLVE, XPOS

<u>Columns</u>	<u>Variable</u>	<u>Description</u>
1-14	TOUTV	Vapor temperature (K) outside pipe.
15-28	AVLVE	Valve adjustable interface flow area when the valve is fully open.
29-42	HVLVE	Valve adjustable interface hydraulic diameter when the valve is fully open.
43-56	FAVLVE	Initial flow area fraction at mesh-cell interface IVPS (word 1 on Card Number 4).
57-70	XPOS	Initial fraction of valve stem withdrawal at mesh-cell interface IVPS (0.0 = no flow area, valve closed; 1.0 = AVLVE flow area, valve fully opened).

If $0.0 \leq FAVLVE \leq 1.0$ is input, a consistent value for XPOS is evaluated in TRAC based on the valve stem controlling a guillotine closure of a circular

flow-area cross section. Otherwise, a consistent value of FAVLVE is evaluated in TRAC based on $0.0 \leq XPOS \leq 1.0$ that is input.

(See PIPE module description, Sec. IV.A, for further comments on the heat-transfer parameters, HOUTL, HOUTV, TOUTL, and TOUTV.)

VALVE Array Cards. Nineteen sets of cards, one set for each of the following variables. Use LOAD format.

<u>Variable</u>	<u>Dimension</u>	<u>Description</u>
DX	NCELLS	Cell lengths (m).
VOL	NCELLS	Cell volumes (m ³).
FA	NCELLS+1	Cell-edge flow areas (m ²).
FRIC	NCELLS+1	Additive loss coefficients.
GRAV	NCELLS+1	Gravity terms. (See PIPE, Sec. V.F.5.e.)
HD	NCELLS+1	Hydraulic diameters (m).
NFF	NCELLS+1	Friction-factor correlation options. (See ACCUM input description, Sec. V.F.5.a.)
ALP	NCELLS	Initial void fractions (-).
VL	NCELLS+1	Initial liquid velocities (m/s).
VL	NCELLS+1	Initial vapor velocities (m/s).
TL	NCELLS	Initial liquid temperatures (K).
TV	NCELLS	Initial vapor temperatures (K).
P	NCELLS	Initial pressures (Pa).
PA	NCELLS	Initial air partial pressures (Pa).
QPPP	NCELLS	Volumetric heat sources (W/m ³) in valve wall. (Eliminate this card set if NODES = 0.)
TW	NODES*NCELLS	Initial wall temperatures (K). (Eliminate this card set if NODES = 0.)
VLOTB	NVOTB*2	First valve table; input pairs (signal-variable form defined by IVSV on Card Number 3 and NVRF on Card Number 4, flow-area fraction or valve-stem fraction). When IVTY = 1 to 4, VLOTB is defined.

<u>Variable</u>	<u>Dimension</u>	<u>Description</u>
VLCTB	NVCTB*2	Second valve table; input pairs (signal-variable defined by IVSV on Card Number 3 and NVRF on Card Number 4, flow-area fraction or valve-stem fraction). Eliminate this card set if NVCTB = 0. If NVCTB \geq 1 when IVTY = 3 or 4, define the flow-area fraction or valve-stem fraction values in the second valve table to vary in the same direction as they do in the first valve table; that is, if the flow-area fraction or valve-stem fraction increases in going from left to right in the first valve table, define them to increase in going from left to right in the second valve table as well.
VRFTB	NVRF*2	Rate-factor table for the trip-controlled first and second valve-tables independent variable defined by IVSV on Card Number 3; input pairs (trip-signal minus the set point that turns the trip OFF, rate factor to be applied to the valve-table independent variable). (Eliminate this card set if NVRF = 0.)

k. Vessel Component (VESSEL).

Card Number 1. (Format A10,4X,I14,A30) TYPE, NUM, ID, CTITLE

<u>Columns</u>	<u>Variable</u>	<u>Description</u>
1-14	TYPE	Component type (VESSEL left justified).
15-28	NUM	Component ID number (must be unique for each component, $1 \leq \text{NUM} \leq 99$).
29-42	ID	User ID number (arbitrary).
43-72	CTITLE	Hollerith component description.

Card Number 2. (Format 4I14) NASX, NRSX, NTSX, NCSR

<u>Columns</u>	<u>Variable</u>	<u>Description</u>
1-14	NASX	Number of axial (z) segments (levels).
15-28	NRSX	Number of radial (r) segments (rings).
29-42	NTSX	Number of azimuthal (θ) segments (sectors).
43-56	NCSR	Number of cell sources (component connections).

Card Number 3. (Format 5I14) IDCU, IDCL, IDCR, ICRU, ICRL

<u>Columns</u>	<u>Variable</u>	<u>Description</u>
1-14	IDCU	Axial segment level at which the upper elevation is the downcomer upper boundary elevation.
15-28	IDCL	Axial segment level at which the upper elevation is the downcomer lower boundary elevation.
29-42	IDCR	Radial segment ring at which the outer radius forms the downcomer inner radial boundary.
43-56	ICRU	Axial segment level at which the upper elevation is the core upper boundary elevation.
57-70	ICRL	Axial segment level at which the upper elevation is the core lower boundary elevation.

Card Number 4. (Format 4I14) ICRR, ILCSP, IUCSP, IUHP

<u>Columns</u>	<u>Variable</u>	<u>Description</u>
1-14	ICRR	Radial segment ring at which the outer radius forms the core outer radial boundary.
15-28	ILCSP	Axial segment level at which the upper elevation is the lower core-support-plate elevation as used for graphics output. (Defaults to ICRL on Card Number 3) if ILCSP = 0.)
29-42	IUCSP	Axial segment level at which the upper elevation is the upper core-support-plate elevation as used for graphics output. (Defaults to ICRU on Card Number 3 if IUCSP = 0.)
43-56	IUHP	Axial segment level at which the upper elevation is the upper head-support-plate elevation as used for graphics output. (Defaults to IDCU on Card Number 3 if IUHP = 0.)

Card Number 5. (Format 5I14) NFFA, NFFR, NFFT, NRODS, NVENT

<u>Columns</u>	<u>Variable</u>	<u>Description</u>
1-14	NFFA	Axial friction-factor correlation option. (Set NFFA = 0.)
15-28	NFFR	Radial friction-factor correlation option. (Set NFFR = 0.)
29-42	NFFT	Azimuthal friction-factor correlation option. (Set NFFT = 0.)

<u>Columns</u>	<u>Variable</u>	<u>Description</u>
43-56	NRODS	Total number of computational rods within the vessel (greater than or equal to the number of core mesh cells in the horizontal plane, ICRR*NTSX).
57-70	NVENT	Number of vent valves in the VESSEL component. There is one vent valve per connection between cells, so lump actual ones for each cell.

Card Number 6. (Format 3E14.6) DTXHT(1), DTXHT(2), DZNHT

<u>Columns</u>	<u>Variable</u>	<u>Description</u>
1-14	DTXHT(1)	Maximum ΔT (K) above which rows of nodes are inserted in the fuel-rod conduction calculation during reflood for the nucleate and transitional boiling regimes (suggested value = 3.0).
15-28	DTXHT(2)	Maximum ΔT (K) above which rows of nodes are inserted in the fuel-rod conduction calculation during reflood for all boiling regimes except nucleate and transitional (suggested value = 10.0).
29-42	DZNHT	Minimum ΔZ (m) below which no additional rows are inserted in the fuel-rod conduction calculation during the reflood calculation (this value comes from the diffusion number).

Card Number 7. (Format 3E14.6) HGAPO, PDRAT, FUCRAC, SHELV

<u>Columns</u>	<u>Variable</u>	<u>Description</u>
1-14	HGAPO	Fuel-rod gap conductance coefficient ($W/m^2/K$) (constant for NFCI = 0 on Card Number 10; otherwise, initial value).
15-28	PDRAT	Fuel-rod pitch-to-diameter ratio.
29-42	FUCRAC	Fraction of fuel <u>not</u> cracked. Use only if NFCI = 1 on Card Number 10.
43-56	SHELV	The shift added to the cell-centered axial elevations (m) based on the vessel z-input (see VESSEL Geometry Cards) when computing GRAV for one-dimensional components (used when IELV = 1).

Card Number 8. (Format 5I14) NODES, NPWX, IRPOP, IRPTR, NODHS

<u>Columns</u>	<u>Variable</u>	<u>Description</u>
1-14	NODES	Number of fuel-rod radial heat-transfer nodes must be greater than or equal to four if a core region is specified).
15-28	NPWX	Number of pairs in reactor power-reactivity table (signal-variable form, power, or reactivity).
29-42	IRPOP	Reactor kinetics option (input parameters required for each option are shown in parentheses). Add 10 to the option value of IRPOP if a reactivity feedback evaluation is to be performed.

IRPOP

Option

1	Constant power (RPOWRI)
2	Reactor kinetics with constant programmed reactivity (RPOWRI, REACT)
3	Reactor kinetics with table lookup of programmed reactivity (RPOWRI, NPWX, PWTB)
4	Reactor kinetics with trip-initiated constant programmed reactivity insertion (RPOWRI, IRPTR, REACT)
5	Reactor kinetics with trip-initiated table lookup of programmed reactivity (RPOWRI, IRPTR, NPWX, PWTB)
6	Table lookup of power (NPWX, PWTB)
7	Constant initial power with trip-initiated table lookup of power (RPOWRI, IRPTR, NPWX, PWTB)

43-56	IRPTR	Power or reactor-kinetics trip ID number.
57-70	NODHS	The number of heat-transfer nodes used in all of the vessel slabs. A value of 1 defaults to the lumped-parameter model.

Card Number 9. (Format 5I14) INHSMX, NPSZ, IPSTR, IPSSV, NPSRF

<u>Columns</u>	<u>Variable</u>	<u>Description</u>
1-14	INHSMX	The maximum number of interfaces between dissimilar materials. An internal check is made and an error message results for inconsistent values (INHSMX \geq 1).
15-28	NPSZ	The number of axial power shapes in the axial-power-shape table (NPSZ \geq 1 when NRODS \geq 1; otherwise, NPSZ = 0).
29-42	IPSTR	The axial-power-shape trip ID number. (Currently not used.)
43-56	IPSSV	The signal-variable ID number that defines the independent variable in the axial-power-shape table.
57-70	NPSRF	The number of the rate-factor table pairs where the rate factor is dependent on the axial-power-shape trip signal difference from its trip OFF set point. The rate factor is to be applied to changes in the axial-power-shape-table independent variable defined by IPSSV. (Currently not used.)

Card Number 10. (Format 5I14) NRFDT, NMWRX, NFCI, NFCIL, NZMAX

<u>Columns</u>	<u>Variable</u>	<u>Description</u>
1-14	NRFDT	Reflood rod fine-mesh calculation trip ID number (if zero, no fine-mesh calculation is performed if NRFDT = 0).
15-28	NMWRX	Metal-water reaction option. 0 = off; 1 = on.
29-42	NFCI	FCI option. Option 1 performs the dynamic gap conductance calculation. 0 = off; 1 = on.
43-56	NFCIL	Limit on FCI calculations per time step (set NFCIL = 1).
57-70	NZMAX	Maximum number of rows of nodes used in the fuel-rod conduction calculation.

Card Number 11. (Format 5I14) NDGX, NDHX, NRTS, IRPSV, NRPRF

<u>Columns</u>	<u>Variable</u>	<u>Description</u>
1-14	NDGX	The number of delayed-neutron groups (NDGX \leq 0 defaults to six delayed-neutron groups with the delayed-neutron constants defined internally in TRAC).
15-28	NDHX	The number of decay heat groups (NDHX \leq 0 defaults to 11 decay heat groups with the decay heat constants defined internally in TRAC).
29-42	NRTS	The number of time steps the reactivity feedback changes are summed over for printout (NRTS \leq 0 defaults to 10).
43-56	IRPSV	The signal-variable ID number that defines the independent variable in the reactor power-reactivity table.
57-70	NRPRF	The number of rate-factor table pairs where the rate factor is dependent on the power-reactivity trip-signal difference from its trip OFF terminating set point. The rate factor is to be applied to changes in the reactor power-reactivity table independent variable defined by IRPSV.

Card Number 12. (Format 5E14.6) RPOWRI, REACT, PLDR, TNEUT, POWSCL

<u>Columns</u>	<u>Variable</u>	<u>Description</u>
1-14	RPOWRI	Initial reactor power (W).
15-28	REACT	Initial programmed reactivity (IRPOP options 2 and 4 only).
29-42	PLDR	Pellet dish radius (m). (No calculation of pellet dishing is performed if PLDR = 0.0.)
43-56	TNEUT	The prompt neutron lifetime (s) [TNEUT \leq 0.0 defaults to the value 1.625×10^{-5} s set internally in TRAC].
57-70	POWSCL	Power-reactivity-table (variable PWTB) scale factor. The dependent variable in PWTB is multiplied by POWSCL to obtain its absolute value.

(If IRPOP < 11 on Card Number 8, skip Card Number 13.)

Card Number 13. (Format 4E14.6) RCFORM(I), RCA(I), RCB(I), RCC(I), I = (1,3)

<u>Columns</u>	<u>Variable</u>	<u>Description</u>
1-14	RCFORM(I)	The form number for the reactivity coefficient type [0.0 = $\delta k/\delta x$, 1.0 = $(1/k)(\delta k/\delta x)$, 2.0 = $x(\delta k/\delta x)$, 3.0 = $(x/k)(\delta k/\delta x)$ for independent variables $x = T_{\text{fuel}}$ for I = 1, T_{coolant} for I = 2, and α_{coolant} for I = 3].
15-28	RCA(I)	The coefficient for the zero th power polynomial term defining the I th independent-variable reactivity coefficient.
29-42	RCB(I)	The coefficient for the first power polynomial term defining the I th independent-variable reactivity coefficient.
43-56	RCC(I)	The coefficient for the second power polynomial term defining the i th independent-variable reactivity coefficient.

(The above card consists of three records, one for each of the independent variables $x = T_{\text{fuel}}$, T_{coolant} , and α_{coolant}).

VESSEL Geometry Cards. Three sets of cards, one set for each of the following variables. Use LOAD format.

<u>Variable</u>	<u>Dimension</u>	<u>Description</u>
Z	NASX	Upper elevations (m) of axial segment levels. (Referenced to zero elevation at the bottom interface of the first axial segment level in the vessel.)
RAD	NRSX	Outer radii (m) of radial segment rings.
TH	NTSX	Theta angles (rad) at azimuthal segment ends. For NTSX = 1, the VESSEL component is two-dimensional and x-y slab geometry applies.

If NVENT = 0 on Card Number 5, skip the next two card types.

VESSEL Vent-Valve Location and Area Cards. (Format 2I14,E14.6) IZV, KV, AVENT

One card per cell with the vent valves on the outer radial surface.

<u>Columns</u>	<u>Variable</u>	<u>Description</u>
1-14	IZV	Axial segment level in the vessel.
15-28	KV	Horizontal plane relative cell number.
29-42	AVENT	Total area (m ²) of vent valves in outer radial wall of cell.

VESSEL Vent-Valve Pressure Drop and Friction-Loss Cards. (Format 4E14.6))

DPCVN, DPOVN, FRCVN, FROVN

One card per cell with the vent valves on the outer radial surface.

<u>Columns</u>	<u>Variable</u>	<u>Description</u>
1-14	DPCVN	Maximum pressure drop (Pa) between the inner and outer radial cells for vent valve to be closed.
15-28	DPOVN	Minimum pressure drop (Pa) between the inner and outer radial cells for vent valve to be opened.
29-42	FRCVN	Additive friction loss coefficient for vent valve in closed position.
43-55	FROVN	Additive friction loss coefficient for vent valve in open position.

VESSEL Source Cards. (Format 4I14) LISRL, LISRC, LISRF, LJUNS

One card per component connection source. See vessel description, Sec. IV.I.

<u>Columns</u>	<u>Variable</u>	<u>Description</u>
1-14	LISRL	Axial segment level number associated with the source.
15-28	LISRC	Horizontal plane relative cell number associated with the source. (See Sec. IV.I.)
29-42	LISRF	Face number associated with the source. 1 = azimuthal direction; 2 = axial direction; 3 = radial direction. A positive number indicates a connection into the top, outer radius, or second azimuthal face of the cell whereas a negative number indicates a connection into the bottom, inner radius, or first azimuthal face of the cell.
43-56	LJUNS	Junction number associated with the component source.

VESSEL Core Cards. Twenty-six sets of cards, one for each of the following variables. Omit these cards if there is no core.
Use LOAD format.

Note: See Sec. IV.I for precise definitions of the following parameters and the ordering conventions used for reading in the data. Many parameters are read in with dimension (ICRR*NTSX). These parameters are supplied for each (r,θ) mesh cell in the horizontal plane core region. Each such cell constitutes one of the axial channels in the core formed by a stack of mesh cells with the same (r,θ) mesh boundaries. Each (r,θ) mesh cell encloses a number of fuel rods and their associated coolant channels.

<u>Variable</u>	<u>Dimension</u>	<u>Description</u>
RDPWR	NODES	Relative radial power density at the node positions.
CPOWR	ICRR*NTSX	Average fuel-rod relative power density in each (r,θ) mesh cell.
IDROD	NRODS-ICRR*NTSX	Definition of the cells in which the additional fuel rods are placed.
RPKF	NRODS-ICRR*NTSX	Fuel-rod power peaking factors (relative to the average fuel rod) in the additional rods.
ZPOWR	(ICRU-ICRL+2)*NPSZ	Axial-power-shape table; input [signal-variable form defined by IPSSV and NPSRF on Card Number 9, relative axial-power-shape densities (ICRU-ICRL+1 values)] pairs. The relative axial-power-shape densities defining the axial power shape are specified at the axial segment level interfaces from one end of the fuel rod to the other. There are NPSZ axial power shapes, each having (ICRU-ICRL+1) values.
PSRF	NPSRF*2	Rate factor table for the trip-controlled axial-power-shape-table independent variable defined by IPSSV on Card Number 9; input pairs (trip signal minus the set point that turns the trip OFF, rate factor to be applied to the axial-power-shape table independent variable).

<u>Variable</u>	<u>Dimension</u>	<u>Description</u>
RDX	ICOR*NCXS	Number of rods in each (r,θ) mesh cell of the core.
RARDR	NRDRS	Fuel-rod node radii (m) (cold).
MATRD	NQDES-1	Fuel-rod material ID numbers.

<u>ID</u>	<u>Material Type</u>
1	Mixed oxide fuel
2	Zircaloy
3	Fuel-clad gap gases
4	Boron nitride insulation
5	Constantan/Nichrome heater chrome
6	Stainless steel, type 304
7	Stainless steel, type 316
8	Stainless steel, type 347
9	Carbon steel, type A508
10	Inconel, type 718
11	Zircaloy dioxide
12	Inconel, type 600

PWTB NPWX*2 Power or reactivity table; input (signal-variable form defined by IRPSV and NRPRF on Card Number 11, power or reactivity pairs.

RPRF NRPRF*2 Rate-factor table for the trip-controlled power or reactivity table independent variable defined by IRPSV on Card Number 11; input pairs (trip signal minus the set point that turns the trip OFF, rate factor to be applied to the power or reactivity table independent variable).

(Omit the next three variables if NDGX ≤ 0 is input; the default 6 group delayed neutron constants are defined internally in TRAC.)

<u>Variable</u>	<u>Dimension</u>	<u>Description</u>
BETA	NDGX	The effective delayed-neutron fraction.
LAMDA	NDGX	The delayed-neutron decay constant (1/s).
CDGN	NDGX	The delayed-neutron concentrations. If 0.0 is input, steady-state values are evaluated internally based on BETA, LAMDA, RPOWRI, and TNEUT.

(Omit the next three variables if NDHX \leq 0 is input; the default 11 group decay heat constants are defined internally in TRAC.)

<u>Variable</u>	<u>Dimension</u>	<u>Description</u>																
LAMDH	NDHX	The decay-heat decay constant (s^{-1}).																
EDH	NDHX	The effective decay-heat energy fraction.																
CDHN	NDHX	The decay-heat concentrations. If 0.0 is input, steady-state values are evaluated internally based on LAMDH, EDG, and RPOWRI.																
NFAX	ICRU-ICRL	Number of permanent fine-mesh intervals per coarse-mesh interval added at the start of the reflood calculation. (The total number of heat-transfer rows per fuel rod must be less than NZMAX).																
FPUO2	ICRR*NTSX	Fraction of plutonium dioxide (PuO_2) in mixed oxide fuel.																
FTD	ICRR*NTSX	Fraction of theoretical fuel density.																
GMIx	ICRR*NTSX*7	Mole fraction of gap gas constituents. Array is not used if NFCI = 0 but still must be input. Enter data for each gas in the order indicated.																
		<table border="1"> <thead> <tr> <th><u>Index</u></th> <th><u>Gas</u></th> </tr> </thead> <tbody> <tr> <td>1</td> <td>Helium</td> </tr> <tr> <td>2</td> <td>Argon</td> </tr> <tr> <td>3</td> <td>Xenon</td> </tr> <tr> <td>4</td> <td>Krypton</td> </tr> <tr> <td>5</td> <td>Hydrogen</td> </tr> <tr> <td>6</td> <td>Air/nitrogen</td> </tr> <tr> <td>7</td> <td>Water vapor</td> </tr> </tbody> </table>	<u>Index</u>	<u>Gas</u>	1	Helium	2	Argon	3	Xenon	4	Krypton	5	Hydrogen	6	Air/nitrogen	7	Water vapor
<u>Index</u>	<u>Gas</u>																	
1	Helium																	
2	Argon																	
3	Xenon																	
4	Krypton																	
5	Hydrogen																	
6	Air/nitrogen																	
7	Water vapor																	
GMLES	ICRR*NTSX	Moles of gap gas per fuel rod (not used).																
PGAPT	ICRR*NTSX	Average gap gas pressure (Pa) (not used if NFCI = 0).																
PLVOL	ICRR*NTSX	Plenum volume (m^3) in each fuel rod above the pellet stack (not used).																
PSLEN	ICRR*NTSX	Pellet stack length (m) (not used).																
CLENN	ICRR*NTSX	Total cladding length (m) (not used).																

VESSEL Level Cards. Twenty-eight sets of cards, one for each of the following variables for each axial segment level. Use LOAD format. If desired, an entire level can be repeated by a single REPEAT LEVEL card. (See description after the level data description.)

Note: The following parameters (dimensioned NRSX*NTSX) are read in for each (r,θ) mesh cell at each axial segment level. Here they extend over the entire vessel horizontal plane for each axial segment level. Because a separate data set is read for each axial segment level, these parameters are supplied for all mesh cells in the vessel.

<u>Variable</u>	<u>Dimension</u>	<u>Description</u>
HSA	NRSX*NTSX	Heat-slab area (m ²). If no slab is desired in a cell, input 0.0 for the area.
HSX	NODHS*NRSX*NTSX	Heat-slab node position (m). For each cell, HSX should increase monotonically; the first node sees the adiabatic boundary; and node NODHS sees the fluid-heat-transfer boundary.
CFZL-T	NRSX*NTSX	Liquid additive friction loss coefficients (θ-direction).
CFZL-Z	NRSX*NTSX	Liquid additive friction loss coefficients (z-direction).
CFZL-R	NRSX*NTSX	Liquid additive friction loss coefficients (r-direction).
CFZV-T	NRSX*NTSX	Vapor additive friction loss coefficients (θ-direction).
CFZV-Z	NRSX*NTSX	Vapor additive friction loss coefficients (z-direction).
CFZV-R	NRSX*NTSX	Vapor additive friction loss coefficients (r-direction).
VOL	NRSX*NTSX	Cell fluid volume fractions.
FA-T	NRSX*NTSX	Cell fluid-edge average area fractions (θ-direction).
FA-Z	NRSX*NTSX	Cell fluid-edge average area fractions (z-direction).

<u>Variable</u>	<u>Dimension</u>	<u>Description</u>
FA-R	NRSX*NTSX	Cell fluid edge average area fractions (r-direction).
HD-T	NRSX*NTSX	Hydraulic diameters (m) (θ -direction).
HD-Z	NRSX*NTSX	Hydraulic diameters (m) (z-direction).
HD-R	NRSX*NTSX	Hydraulic diameters (m) (r-direction).
HSTN	NODHS*NRSX*NTSX	Heat-slab temperatures (K). Do not input 0.0 temperatures.
MATHS	(NODHS-1)*NRSX*NTSX	Heat-slab material ID numbers. All material ID numbers must be defined (see Sec. V.F.5.e--card 2).
ALPN	NRSX*NTSX	Vapor fraction (-).
VVN-T	NRSX*NTSX	Vapor velocity (m/s) (θ -direction).
VVN-Z	NRSX*NTSX	Vapor velocity (m/s) (z-direction).
VVN-R	NRSX*NTSX	Vapor velocity (m/s) (r-direction).
VLN-T	NRSX*NTSX	Liquid velocity (θ -direction).
VLN-Z	NRSX*NTSX	Liquid velocity (z-direction).
VLN-R	NRSX*NTSX	Liquid velocity (r-direction).
TVN	NRSX*NTSX	Vapor temperature (K).
TLN	NRSX*NTSX	Liquid temperature (K).
PN	NRSX*NTSX	Pressure (Pa).
PAN	NRSX*NTSX	Air partial pressure (Pa).

REPEAT LEVEL Card. (Format A12,2x,I14) This card can be used to repeat the data from one level to another. As many of these cards can be used as needed. Each REPEAT LEVEL card should be placed after the data for the preceding level and before the data for the next level. These cards may be used consecutively.

<u>Columns</u>	<u>Variable</u>	<u>Description</u>
1-14	AREP	The character string: "REPEAT.LEVEL."

<u>Columns</u>	<u>Variable</u>	<u>Description</u>
15-18	NLEV	The number of the level to be repeated. The value of NLEV must be greater than one but less than the number of the level that results from the repeat.

VESSEL Fuel-Rod Cards. Two sets of cards, one for each of the following variables for each fuel rod. Omit these cards if there is no core. Use LOAD format.

<u>Variable</u>	<u>Dimension</u>	<u>Description</u>
BURN	(ICRU-ICRL+1)	Fuel burnup (MWD/MTU).
RDTN	NODES*(ICRU-ICRL+1)	Fuel-rod temperatures (K).

6. PWR-Initialization Data. The following cards are required only if a PWR-initialization calculation is to be performed. (This is indicated by setting STDYST = 2 or 3 on Main Control Card 1.)

Card Number 1. (Format I14) NLOOP

<u>Columns</u>	<u>Variable</u>	<u>Description</u>
1-14	NLOOP	Number of primary coolant loops.

Cards 2-4 are repeated for each primary coolant loop.

Card Number 2. (Format I14, E14.6) NLPMP, TILPC1

<u>Columns</u>	<u>Variable</u>	<u>Description</u>
1-14	NLPMP	Number of pumps in this loop (must be 1 or 2).
15-28	TILPC1	Desired coolant temperature (K) at the vessel junction connected to the outlet side of the first primary-loop coolant pump.

Card Number 3. (Format I14, E14.6) JNLPC1, WLPC1

<u>Columns</u>	<u>Variable</u>	<u>Description</u>
1-14	JNLPC1	Identification number of the vessel junction connected to the outlet side of the first primary-loop coolant pump.
15-28	WLPC1	Desired mass flow (kg/s) through the first primary-loop coolant pump.

Card Number 4. (Format I14, E14.6) JNLPC2, WLPC2

(Omit this card if NLPMP = 1.)

<u>Columns</u>	<u>Variable</u>	<u>Description</u>
1-14	JNLPC2	Identification number of the vessel junction connected to the outlet side of the second primary-loop coolant pump.
15-28	WLPC2	Desired mass flow (kg/s) through the second primary-loop coolant pump.

7. Time-Step Data. The last data block of input information is the time-step cards for directing the calculation and output edit. The problem time span is separated into domains. Each domain (specified by two cards) may have different minimum and maximum time-step sizes and edit intervals. Any number of time domains may be input. The end of the calculation is specified by making the minimum time-step size a negative number. An exception to this rule occurs if a PWR-initialization calculation is done. See Sec. III.D.2 for a detailed description of the steady-state calculations. The format of each set of two time-step cards is as follows.

Card Number 1. (Format 5E14.6) DTMIN, DTMAX, TEND, RTWFP, RELX

<u>Columns</u>	<u>Variable</u>	<u>Description</u>
1-14	DTMIN	Minimum allowable time-step size (s) for this time domain.
15-28	DTMAX	Maximum allowable time-step size (s) for this time domain.
29-42	TEND	End time (s) of this time domain.
43-56	RTWFP	Ratio between heat-transfer and fluid-dynamics time-step sizes. (Used only for steady-state calculations, suggested value = 1000.0.)
57-70	RELX	PWR-initialization relaxation factor (suggested value = 1.0).

Card Number 2. (Format 4E14.6) EDINT, GFINT, DMPINT, SEDINT

<u>Columns</u>	<u>Variable</u>	<u>Description</u>
1-14	EDINT	Print edit interval (s) for this time domain.
15-28	GFINT	Graphics edit interval (s) for this time domain.
29-42	DMPINT	Restart dump interval (s) for this time domain.
43-56	SEDINT	Short print edit interval (s) for this time domain.

G. LOAD Subroutine

The TRAC program uses the LOAD subroutine to read most subscripted array variables. The arrays may be read in floating point or integer format. The input card images for subscripted variables consist of up to six fields. The first five fields consist of an (A1), a repeat count (I2) (for operations R, M, and I), and a floating point or integer data constant (E11.2 or I11) (except for operatives E and S). The sixth field can be used for operation E only if the array data end in the fifth field. In formatted input decks, cards with an asterisk in column 1 are ignored and may be used as spacers or for comments.

Seven operations are defined. These operations and an explanation of each are listed below.

<u>Operation</u>	<u>Description</u>
F	Fill array starting at current data index with data constant
BLANK	No action
R	Repeat data constant I2 times
M	Multiple repeat. Repeat data constant 10*I2 times
I	Interpolate between data constant and succeeding data constant with I2 points
E	End of data array (<u>must</u> be followed by at least one blank)
S	Skip to next card

Some restrictions in the use of the LOAD format are:

1. end of data for an array must be signaled by E,
2. overstore or partial fill of an array is not allowed,
3. integer interpolation is not allowed, and
4. data for different arrays must be on different records.

Following are examples of the use of the options listed above to fill an array of dimension 11 with data.

EXAMPLE 1. Fill an integer array with a value of 61.

F.....61E

EXAMPLE 2. Use of the repeat option to fill an array with a value of 1.2.

R11.....1.2....E

EXAMPLE 3. Use of the skip option.

R.2.....15.....16S

R.5.....17.....18.....19.....20E

EXAMPLE 4. Use of the multiple repeat option to fill an array with 101 values.

M10.....1.56E-2......0156E

EXAMPLE 5. Use of the interpolation option to get points 1.0, 2.0, 3.0, ..., 11.0.

I.9.....1.....11.E

H. Free Format

Appendix C shows part of a TRACIN deck in free format that illustrates the points discussed here. Section V.F gives the TRAC-PF1 input specifications for formatted input. When the free-format option is chosen, TRAC-PF1 internally converts a free-format TRACIN deck to a new deck in TRAC format that is written to a file called TRCINP. File TRCINP is subsequently and automatically read by the standard input routines. Therefore, to use the free-format option, all cards must be kept in the same order as shown in Sec. V.F and all variables must stay in the same order on those cards. Input records may be up to 80 columns long. All data not to be read by the LOAD routine must be delimited by at least one blank column. (However, data may start in column 1 or end in column 80.) Array data to be read by the LOAD routine may be blank delimited: delimited by any of the LOAD control characters, F, R, S, I, M, or E; or delimited by a control-character repeat count.

Note the following examples, all of which will run in free-format mode.

F^1.OE+07E

also TRAC format

F^1.OE+07E

F^^1.OE+07E

F1.OE+07E

F^^^^^^^^1.OE+07^E

etc.

free format

R10^1.OE+07R^2^1.1E+07

also TRAC format; both modes read 10 repeats, 2 repeats

R1^1.OE+07

free-format reads 1 repeat; TRAC format (I2) reads 10 repeats

R^10^1.OE+07^^R^2^1.1E+07

R^^10^^1.OE+07R2^^1.1E+07

R^^101.OE+07^^R^2^1.1E+07

etc.

free format; all three read 10 repeats, 2 repeats

Note the R^^101.OE+07 example. The free-format parser scans to the first character after the R; it includes the next character in the repeat count if that character is a nonblank numeric. There is one exception to this rule: a situation such as R^112.3456E+07, where the control character is followed by one space, a two-digit repeat count, and a nonblank column. To facilitate conversion of existing TRAC-format decks, this field is assumed to indicate 1 repeat of 12.3456E+07, not 11 of 2.3456E+07. The following examples will give 11 repeats:

R11^2.3456E+07

R^11^2.3456E+07

R^^112.3456E+07

R112.3456E+07

The E character of the LOAD subroutine is recognized as part of the string 'E^^^' so the three columns after the E should be blank. The E can appear in column 78, 79, or 80 with any remaining columns blank.

The LOAD data must be 11 characters or less; non-LOAD data, 14 or less.

The requirement to blank-delimit data carries with it the requirements that embedded and significant trailing blanks be punched explicitly as zero. The user of the free-format option also should note that to run previously formatted decks that have all-blank 14-column fields meant to represent zero, the zero must be entered explicitly. Of course, this is not necessary for trailing fields. In this regard, note, for example, the one-dimensional component variable IHYDRO that presently is not used by TRAC-PF1. A dummy value must be input for this variable. The NAMELIST input is presently implemented using CDC-FTN-FORTRAN. The format is essentially free but there are a few restrictions that are discussed in Sec. V.I.

1. Free-Format Comments, Problem Title Cards, and Hollerith

Component Descriptions. Free-format TRACIN decks may be annotated with user comments. These comments must be delimited by asterisks (*) in unbroken strings of any length. The first card of the deck is an exception to this requirement. Comments and their delimiters are equivalent to blank columns. Should an input record have an odd number of comment delimiters (where *, **, ***, ****, etc. are all considered to be a single delimiter), everything on the record to the right of the last delimiter is considered a comment. Entire records may be comments, for example, by making the first nonblank character an asterisk. Comments and comment cards may appear anywhere in the deck except

1. in and immediately before the problem title cards,
2. before Main Control Card Number 1,
3. within NAMELIST group records (see additional comments on NAMELIST in Sec. V.I).

The NUMTCR title cards immediately following Main Control Card Number 2 (from which NUMTCR is read) are written to TRCINP exactly as they are read: asterisks, blank cards, and all. Blank and comment cards may appear between the first two main control cards and immediately after the NUMTCR title cards. Hollerith descriptions of individual components (the CTITLE information) are written to TRCINP, left justified, starting in column 43. Asterisk strings in component descriptions are treated as comment delimiters.

2. Free-Format Input-Error Handling. The free-format option provides advantages over formatted runs in handling of many types of input errors. Free-format input-error handling occurs during two stages, first as TRACIN is being converted to TRCINP, and later as TRCINP is being read. In the first stage, when an error is detected (such as detectable errors that might arise from failure to blank-delimit data properly, for example, using 1.0E-07 instead of 1.0E07 or 1.0E+07) processing of the record in question is immediately halted, subroutine ERROR is called to send warning messages, and the record is flagged before it is written to TRCINP. In the second stage, under most circumstances a fatal FORTRAN input error will not force an immediate program abort; the entire deck will be processed and appropriate error messages issued before program termination. An exception to this situation occurs in the case of fatal NAMELIST errors. In situations where there are no errors detected but input problems are suspected, the user should inspect the file TRCINP, where faulty records may be readily apparent.

I. NAMELIST Format

The NAMELIST statement is an extremely useful--but nonstandard--FORTRAN statement that can be used to input selectively values to subsets of groups of variables named in a program. The user-convenience features in TRAC available through NAMELIST input options are described in Sec. V.F, "TRAC-PF1 Input Specifications." The TRAC NAMELIST options are implemented using NAMELIST as described in the CDC-FTN-FORTRAN manual. (A somewhat more flexible NAMELIST is available at Los Alamos.) The reader is referred to the FTN manual for details. Here we point out that, although NAMELIST is essentially in free format, there are certain restrictions. At present these restrictions apply to all TRAC input decks, whether the TRAC free-format option is selected. The restrictions include the following (Los Alamos-available extensions are indicated in parentheses):

1. Hollerith constants are not allowed (allowed).
2. The first column of all physical records is ignored [terminating dollar sign (\$) can appear in any column].
3. There must be no embedded blanks in the string \$NAME; where NAME is a NAMELIST group name, there must be at least one trailing blank. The initial \$ must appear in column 2.

4. Free-format *-delimited user comments are not allowed on NAMELIST cards. Also, free-format comment cards are not allowed among the physical records of a NAMELIST group record, although all-blank cards are allowed.

As an example, the following five cards might be used to input data for the NAMELIST group INOPTS (described in Sec. V.F).

```
123456789...
^$INOPTS^IELV=1,^^IKFAC^=^1,
^^^ISTOPT=2,
^ALP=0.,VL=0.,VV=0.,TL=550.,TV=550.,
^^P=1.55E+07,PA=0.,QPPP=0.,^TW=5.5E+02,HSTN=550.,
^$END
```

J. Output Files

Figure 42 shows the files read and written by TRAC during a problem. We discussed the two input files, TRACIN and TRCRST, in Sec. V.A, the free-format option output-input file TRCINP in Sec. V.H, and the dump output file, TRCDMP, in Sec. V.E. This section describes the remaining three output files, TRCOUT, TRCGRF, and TRCMMSG.

The TRCOUT file contains printer output. This file is produced with standard FORTRAN write statements contained in the various component module output subroutines. Included are complete descriptions of the problem input file that was read by the code and the time edits that are produced with a frequency specified on the time-step cards. Each time edit includes a printout of results from each component in a problem. The component output includes pressures, temperatures, and other important results. The TRAC error messages, if any, also are written in the TRCOUT file. Appendix D describes these messages. Section IV gives a more complete description of individual component output.

The TRCGRF file contains graphics output and is a structured binary file produced with unformatted write statements. This file structure is discussed in Sec. VI.F. A Livermore Time Sharing System (LTSS) library computer code, GRIT, generates plots of the problem calculation from the TRCGRF file. A versatile graphics package TRAP/EXCON also has been developed to produce high-quality plots and movies from the TRCGRF file. This package is designed for the Los Alamos National Laboratory CDC 7600 computer and is documented separately (to be published).

The TRCMSG file contains warning messages that are sometimes produced by various computational modules within TRAC. These warnings, written with formatted input/output (I/O), indicate difficulty with the progress of the problem.

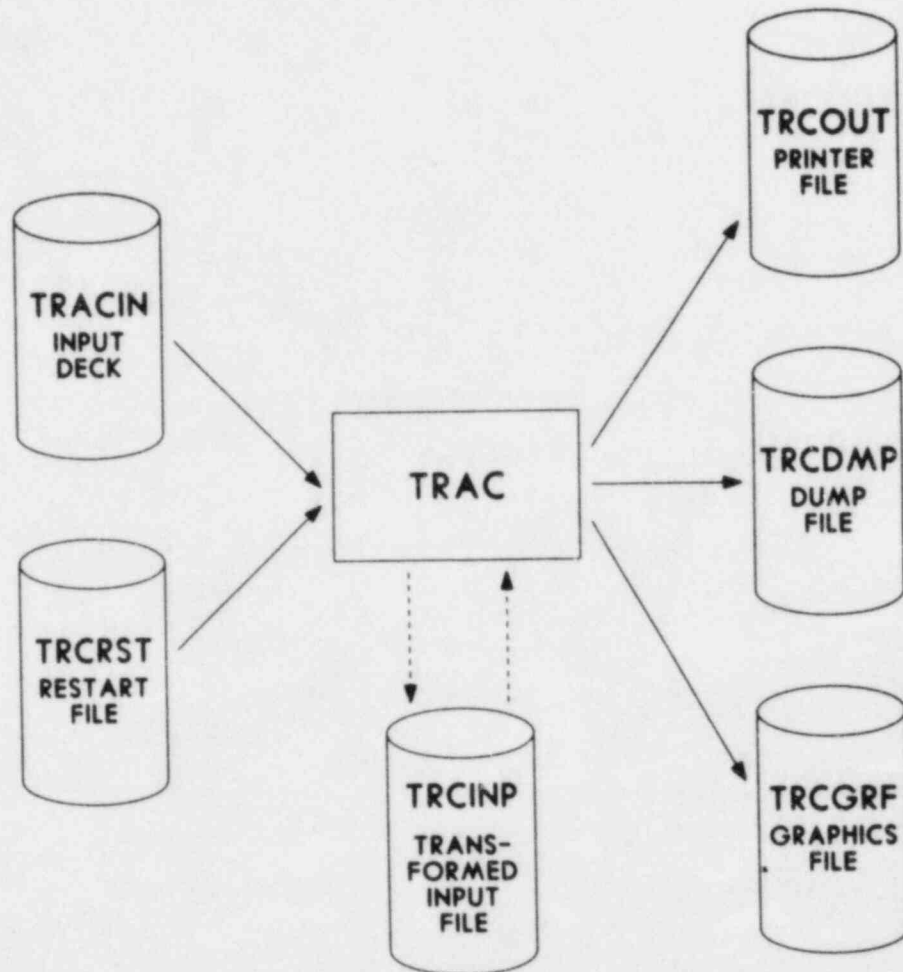


Fig. 42.
TRAC input and output files.

VI. PROGRAMMING DETAILS

A. Overall Code Organization

During TRAC development, much attention was paid to the programming techniques. The decision was made to strive for a code structure that minimizes the problems of maintaining and extending the code. In addition, we attempted to program in a manner that is understandable to knowledgeable persons in the LWR safety field and that reduces the difficulties of implementing TRAC at other sites and/or computers. We also recognized that we should take advantage of the Laboratory's efficient computing facility. In this case, the system is a CDC 7600 computer running on LTSS. In conflict situations, we ranked the importance of these goals in the order presented. Whenever possible, we segregated specialized coding to subprograms that perform specific, low-level service functions.

To attain these goals, modularity is the best approach. The TRAC program is modular in two important ways. Because it analyzes reactor systems that consist of specific types of components, the program contains subroutines that treat each component type. The TRAC components are described in Sec. IV. This modularity simplifies both the subroutine programming and the data associated with particular components. For example, because fuel rods are associated only with the VESSEL component, no fuel-rod data are referenced, nor are fuel-rod calculations performed by the subroutines that treat any other component.

Second, the TRAC program is functionally modular; that is, each TRAC subprogram performs a specific function. If the performance of a function requires modification, only those routines that perform that function must be altered. For example, if the dump/restart capability needs modification, only those routines that perform the dump/restart for the affected components require changes. Some low-level subprograms are used by all components, thereby strengthening this modularity. The most important low-level routines and a brief description of their functions are listed in Table IX. All TRAC subroutines are described in Appendix E.

Functional modularity within TRAC is taken a step further by its division into overlays. The use of an overlay structure originally was mandated by computer size limitations because the small CDC 7600 core memory, where all executable instructions must reside, is limited to 65 536 60-bit words. This division isolates functional subunits within TRAC. Figure 43 displays a

TABLE IX
IMPORTANT LOW-LEVEL SUBPROGRAMS

<u>Subprogram</u>	<u>Function</u>
BKMOM	Initiates back-substitution for stabilizing momentum equations.
BKSSTB	Initiates back-substitution for stabilizing mass and energy equations.
CHEN	Uses Chen correlation to evaluate the forced-convection nucleate-boiling HTC.
CHF	Evaluates the critical heat flux based on a local-conditions formulation.
CLEAR	Sets an array to a constant value.
CYLHT	Calculates temperature fields in a cylinder.
ERROR	Processes error conditions.
FEMOM	Sets up stabilizing momentum equations.
FF3D	Makes final pass update for all variables in three-dimensional vessel.
FLUX	Calculates mass flow at boundary of one-dimensional components for use in mass inventory.
FPROP	Calculates values for fluid enthalpy, transport properties, and surface tension.
FWALL	Computes a two-phase friction factor.
HTCOR	Computes HTCs from material surfaces to vapor and liquid.
HTPIPE	Averages velocities and generates HTCs for one-dimensional components.
HTVSSL	Averages velocities and generates HTCs for the vessel.
INNER	Performs an inner iteration for a one-dimensional component.
J1D	Fills boundary array at component junctions.
JUNSOL	Determines junction parameters for connecting and sequencing components.

TABLE IX (cont.)

<u>Subprogram</u>	<u>Function</u>
MFRD	Orders fuel-rod property selection and evaluates an average temperature for property evaluation.
MPROP	Orders structure property selection and evaluates an average temperature for property evaluation.
POSTER	Performs postpass calculation for a one-dimensional component.
PREPER	Performs prepass calculation for a one-dimensional component.
RDLCM	Transfers data from LCM into SCM.
RKIN	Integrates the neutron point-kinetics equations.
RODHT	Calculates the fuel-rod temperature field.
SAVBD	Moves boundary information into component arrays.
SCMLCM	Transfers the fixed-length, variable-length, and pointer tables to LCM.
SETBD	Stores component information into boundary arrays.
SLABHT	Calculates the slab temperatures.
STBME	Sets up stabilizing mass and energy equations.
TF1D	Controls solution of the hydrodynamic equations for one-dimensional components.
TF3DE	Evaluates constitutive relations for interfacial heat transfer and shear; makes an initial evaluation of new time velocities.
TF3DI	Sets up the linearized three-dimensional finite-difference equations.
THERMO	Calculates thermodynamic properties of water.
TRIP	Returns status of a TRIP.
TRPSET	Sets up trip status flags.
VOLV	Calculates cell average phase velocities for one-dimensional components.

TABLE IX (cont.)

WARRAY	Writes a real array to TRCOUT.
WIARR	Writes an integer array to TRCOUT.
WRLCM	Transfers a given number of words from SCM to LCM.

calling tree of the TRAC overlays. Table X briefly describes the function of each overlay.

The TRAC component modularity can be seen in the data structure as well as in the program structure. We used the data modularity in a manner that efficiently utilizes the CDC 7600 computer. The CDC 7600 central memory is divided into two segments: small-core memory (SCM) and large-core memory (LCM). The CPU must retrieve the instruction stream from SCM, which is limited in size, but may retrieve data from either segment. Single-word accesses to SCM require between 27.5 and 275 ns to complete. Single-word accesses to the 512 000-word LCM require 1 760 ns to complete. For transfers of large data blocks between SCM and LCM, the transfer time per word is as low as 27.5 ns.

To take advantage of this feature, TRAC divides the data for each component into four blocks. These are the fixed-length table, the variable-length table, the pointer table, and the array data. The first three of these blocks are stored in SCM in the COMMON blocks, FLTAB, VLTAB, and PTAB, respectively. The structure of the FLTAB COMMON area is the same for all components. The variables in the VLTAB and PTAB COMMON areas differ from one component to another. Appendix F describes the fixed-length, variable-length, and pointer tables for each component.

The array data are stored in SCM within the dynamic storage array. The location of individual arrays is determined by the value of variables in the pointer table. Dynamic storage of data arrays permits effective use of space for many different problems. The array data for all components are contained in the SCM blank COMMON dynamic area. The pointer tables for all one-dimensional components have a common structure. The first 111 pointers locate the basic hydrodynamic, thermodynamic, and heat-transfer information and have the same interpretation for all one-dimensional components. The next 12 pointers locate data for wall heat transfer in those components that support

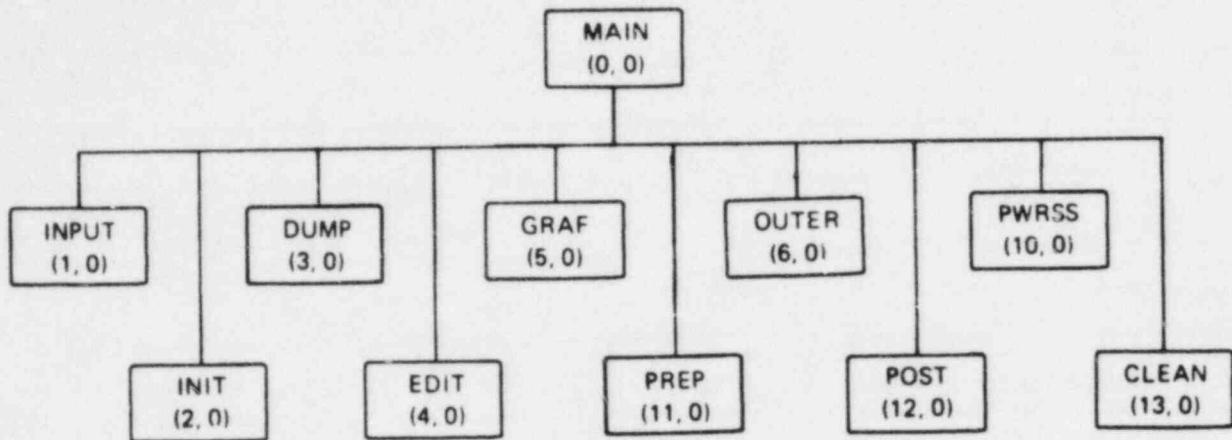


Fig. 43.
TRAC overlay structure.

TABLE X
TRAC OVERLAYS

<u>Overlay</u>	<u>Function</u>
MAIN	Controls overall flow of calculation. (The MAIN overlay also contains many service routines used throughout the code.)
INPUT	Reads input and restart files, assigns LCM storage space and saves input data there, and analyzes PWR loops for PWR-initialization calculations.
INIT	Initializes component data and graphics tables.
OUTER	Performs one complete outer iteration for all components.
PREP	Performs prepass for all components.
POST	Performs postpass for all components.
PWRSS	Evaluates new parameter values for the PWR-initialization option.
DUMP	Adds a dump at the current time to the TRCDMP file.
EDIT	Adds an edit at the current time to the TRCOUT file.
GRAF	Adds a graphics edit at the current time to the TRCGRF file.
CLEAN	Closes all output files.

the calculation. This common structure permits construction of low-level subroutines that can manipulate data for any one-dimensional component, for example, subroutine INNER in overlay OUTER.

Data for a particular component are stored in the dynamic SCM areas only while TRAC processes that component. At other times the data are retained in LCM. Two service subroutines, RDLCM and WRLCM, use the efficient block-transfer capability to transfer data to and from SCM as required. Processing of a component by TRAC begins with the transfer of its component data from LCM to SCM and the computation of the pointer variables based on the available space in the dynamic storage array. The processing of this component ends with the reverse data transfer from SCM to LCM. Figure 44 shows the relationship between SCM and LCM storage areas.

In addition to the data that refer to a particular component, TRAC uses many variables to describe the overall state of the calculation. These variables are grouped according to their use into several other COMMON areas. Appendix G describes the structure of these COMMON areas, which are identical throughout TRAC.

The overall sequence of calculations is directed by the main program. Overlay INPUT always is invoked at the start of each TRAC execution to read component and control input data. The component data are initialized by overlay INIT. The reactor power level is set to zero at this point. The steady-state calculation (if requested) is performed by subroutine STEADY. Output operations are performed using the EDIT, GRAF, and DUMP overlays as required. During the steady-state calculation, the reactor power is turned on after the fluid flow rates have been established. This is to prevent high rod temperatures early in the steady-state calculation when the flow rates are small. If no steady-state calculation is performed, the reactor power is turned on by subroutine STEADY in preparation for the transient calculation, which is performed by subroutine TRANS. Overlays EDIT, GRAF, and DUMP are invoked by TRANS to generate output as required. Overlay CLEAN is invoked to close all output files at the end of the problem or when a fatal error occurs.

B. Input Processing

The processing of all TRAC input information is performed by the INPUT overlay. This information is of two types: input data cards retrieved from the input file, TRACIN, and restart information from the problem restart file,

RELATIONSHIPS BETWEEN SCM AND LCM STORAGE AREAS

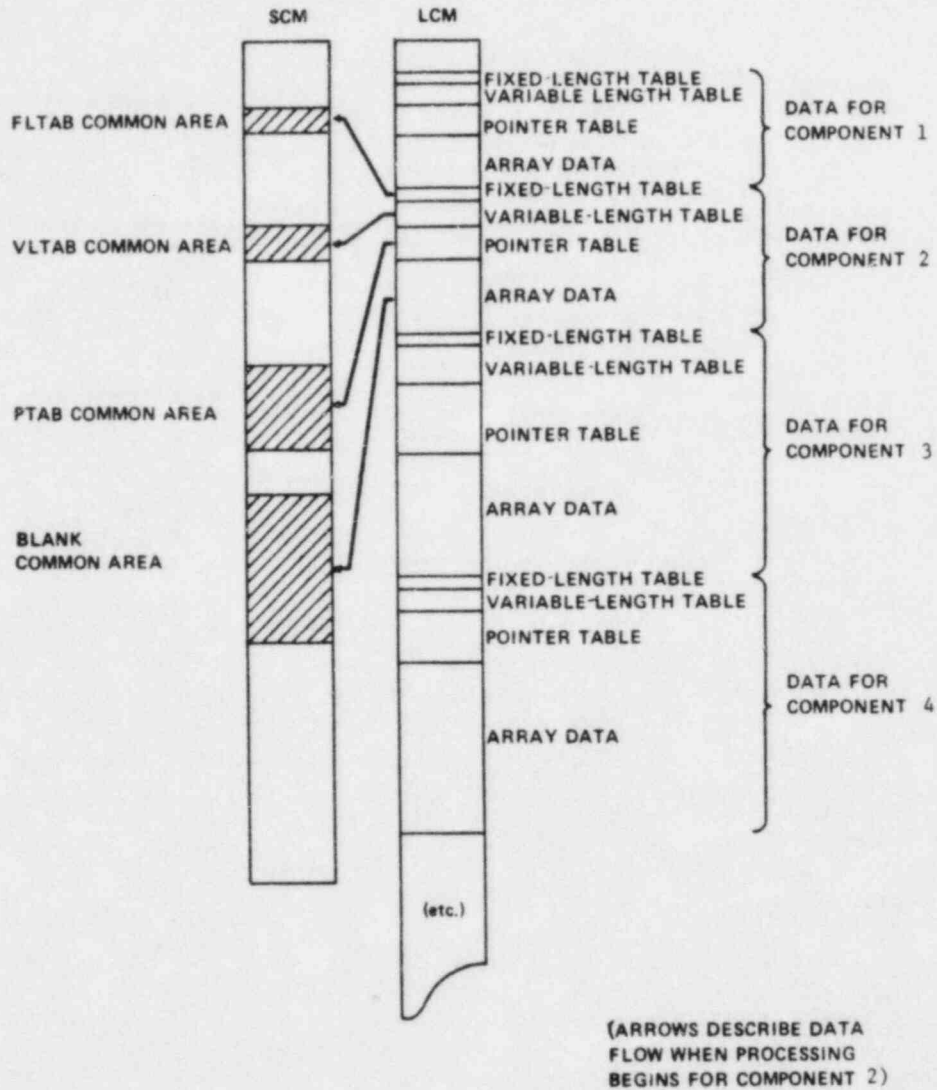


Fig. 44.
Relationships between SCM and LCM storage areas.

TRCRST. In addition to obtaining the input data from the appropriate location, overlay INPUT also organizes the component data in LCM, assigns the array pointer variables for every component, allocates one fixed segment of the blank COMMON area, and analyzes the problem loop structure.

Subroutine INPUT is the entry point for this overlay and controls the input process. The main control parameters (see Sec. V.F.1) are read from the TRACIN file by subroutine INPUT. Using this information, INPUT allocates one

TABLE XI

FIXED-SEGMENT ALLOCATIONS FOR THE BLANK COMMON AREA

<u>Pointer</u>	<u>Dimension</u>	<u>Array Description</u>
LTITLE	20*(NUMTCR+2)	Problem title and version information (stored using only the first four bytes of each word).
LORDER	NCOMP	Component numbers stored in the order used for iteration.
LILCMP	NCOMP	Component LCM pointers stored in the order in which components were read.
LNBR	NCOMP	Component numbers stored in the order in which components were read.
LCOMPT	NCOMP	Component LCM pointers stored in the order used for iteration.
LIITNO	NCOMP	Number of inner iterations during the last outer iteration for each component (in the order used for iteration).
LLCON	NCOMP	Number of times each component was the last to converge since last edit.
LJUN	8*NJUN	Junction-component pair array.
LJSEQ	NJUN	Junction numbers in the order in which junctions occur in the junction-component array.
LVSI	NJUN	Junction flow reversal indicators in the order in which junctions occur in the junction-component array.
LBD	38*NJUN	Boundary data array.
LCNTL	KPTT ^a	Signal-variable, trip, and controller data array described in Fig. 45.
LMSCT	NVCON	Temporary storage for vessel pressure changes adjacent to sources.
LMCMSH	NVCON	Storage for coarse-mesh number of vessel source cells or absolute cell index if direct vessel solution is used.

TABLE XI (cont.)

<u>Pointer</u>	<u>Dimension</u>	<u>Array Description</u>
LIVCON	NVCON+1	Pointer to network junction numbers that connect to a vessel.
LJOUT	IT+1 ^b	Storage area for pointers that locate the beginning of each system loop within data for IOU.
LNBCNL	IT+1	IA(LNBCNL+IL-1) points to the elements of IVCON and IVLJN that begin the IL th loop.
LLOOPN	IT+1	IA(LLOOPN+IL-1) gives the element of the IORDER array that begins the IL th loop.
LNSIGP	IT	NSIGP(IL) is NSIG(IL) plus the number of steam generators in loop IL.
LNSIG	IT	NSIG(IL) is the total number of components excluding breaks and fills in a loop.
LNJN	IT	NJN(IL) is the number of network junctions in loop IL.
LIVLJN	NVCON+1	IVLJN(I) is the vessel junction number corresponding to the network junction number given by IVCON(I).
LIJU	IT ^{2c}	Network junction numbers for the junctions of all components excluding breaks and fills.
LLOOP	LENPCL ^d	Loop data for PWR-initialization calculations.
LVJN	4*NCSR	Vessel junction data area within loop data area for PWR-initialization calculation.
LVRH	NJNT	Storage for explicit information to evaluate equations of motion at network junctions.
LDVB	NJNT	Storage for the right-hand side of the network junction equations or the changes in junction velocities.
LDREV	NJNT	Storage for right-hand side of the vapor stabilizer equation.

TABLE XI (cont.)

<u>Pointer</u>	<u>Dimension</u>	<u>Array Description</u>
LDREL	NJNT	Storage for right side of the liquid stabilizer equation.
LDRA	NJNT	Storage for right side of the air stabilizer equation.
LIDPCV	NVCON	Pointers to coefficients stored in DPCV.
LDPVC	J ^e	Locator that shows the beginning of coefficients to evaluate the derivatives of junction velocities with respect to vessel pressures.
LAOU	JC ^f	Network junction coefficient matrix.
LOD	4*NJNMX	Temporary storage for intercomponent coupling information.

$${}^a\text{KPTT} = 7*\text{NTSV} + 80*\text{NTRP} + 38*\text{NTSE} + 12*\text{NTCT} + 23*\text{NTSF} + \text{NTDP} + 15*\text{NTSD} + 10.$$

$${}^b\text{IT} = (\text{NVCON} + \text{the number of BREAKS} + \text{the number of FILLS})/2 + 2.$$

$${}^c\text{IT2} = \text{MAXO}\{3, 3*[\text{IA}(\text{LJOUT} + \text{NLOOPS}) - 1]\}.$$

$${}^d\text{LENPCL} = \text{the amount of storage needed for all the primary coolant loops} + 2.$$

$${}^e\text{J} = \text{Product of the number of junctions in each loop and the number of vessel connections in each loop summed over all loops.}$$

$${}^f\text{JC} = \text{MAXO}[\text{NVCON}*2*(\text{JNVSSL}+1), \text{NJNMX}*(\text{NJNMX}+2)].$$

fixed segment of the SCM blank COMMON area, as described in Table XI. The remainder of the fixed segment of SCM is allocated by subroutine INIT. At the end of each of the overlays, INPUT and INIT, these fixed segments are moved to the end of the dynamic SCM area. (This is done to facilitate special handling of this area on the Laboratory computer.) The signal-variable and trip data from the TRACIN file are read and processed by subroutine RCNTL, which creates the CNTL array described in Fig. 45. Subroutine RDCOMP reads the component data from the TRACIN file, assigns pointer values to the data, and then stores the data in LCM. Signal-variable, trip, and component data are retrieved from the restart file TRCRST by subroutine RDREST. This subroutine is analogous to

RDCOMP, as described below. Finally, INPUT utilizes the subroutines, ASIGN, SRTLTP, and RDLOOP, to fill the component LCM pointer array; to sort system components; and to process the PWR-initialization input, respectively.

Subroutine RDCOMP invokes a component input routine to process each component. Table XII lists these routines. Input routines for one-dimensional components utilize subroutine RCOMP to read data that are common to all one-dimensional components. Subroutine RDCOMP determines each component type by reading the first input card. When a component type "END" is encountered, RDCOMP knows that all component input has been read. The component input routines perform the following functions: read input cards for a component, store data in the component data tables and write them to LCM, assign relative pointers for the component array data, and fill in the JUN array, as described in Table XIII.

If not all components have been read from the TRACIN file, subroutine RDREST reads the remaining components from the restart file, TRCRST. This file is opened and the dump corresponding to the requested time-step number (input on Main Control Card 1) is located. (If the requested time step is negative, RDREST uses the last dump.) This dump then is used to initialize the components and trips that were not found in the TRACIN file, using the component restart subroutines listed in Table XII. Restart subroutines for one-dimensional components utilize subroutine RECOMP to read data that are common to all one-dimensional components. The detailed structure of the restart file is described in Sec. VI.F in conjunction with the dump capability.

The subroutine SRTLTP sorts through the components of the system and groups them by loops that are isolated from one another by a vessel component. The IORDER array is rearranged to reflect this grouping and to provide a convenient order within each group for the flow network solution procedure.

The PWR-initialization input data are read and the reactor structure analyzed by subroutine RDLOOP, if a PWR-initialization calculation was requested on Main Control Card 2. The analysis of the reactor loop geometry results in the creation of a PWR-initialization data area, which also resides in the fixed segment of the blank COMMON area. Figure 46 shows this data structure. The overall prologue, loop prologues, and VESSEL junction data area are created by subroutine RDLOOP. The data structure for each loop is generated by subroutine FNDLP.

KPTT	Length of trip data array
NTSV	Number of signal variables
NTRP	Number of trips
NTCN	Number of controllers (currently not used)
NTSE	Number of signal-expression trips
NTCT	Number of trip-controlled trips
NTSF	Number of set-point factor tables
NTDP	Number of trips that generates restart dumps and possible problem termination
NTSD	Number of trip time-step data sets
Signal-Variable Data	7*NTSV entries
General Trip Data	80*NTRP entries
Signal-Expression Trip Data	38*NTSE entries
Trip-Controlled Trip Data	12*NTCT entries
Trip Set-Point Factor Tables	23*NTSF entries
Trip, Dump, and Termination Data	NTDP+1 entries
Trip Time-Step Data	15*NTSD entries

Fig. 45.
Signal-variable and trip data.

TABLE XII
COMPONENT INPUT SUBROUTINES

<u>Component Type</u>	<u>Card Input</u>	<u>Restart Input</u>
ACCUM	RACCUM	REACCM
BREAK	RBREAK	REBRK
CORE	RCORE	RECORE
FILL	RFILL	REFILL
PIPE	RPIPE	REPIPE
PRIZER	RPRIZR	REPRZR
PUMP	RPUMP	REPUMP
STGEN	RSTGEN	RESTGN
TEE	RTEE	RETEE
VALVE	RVLVE	REVLVE
VESSEL	RVSSL	REVSSL

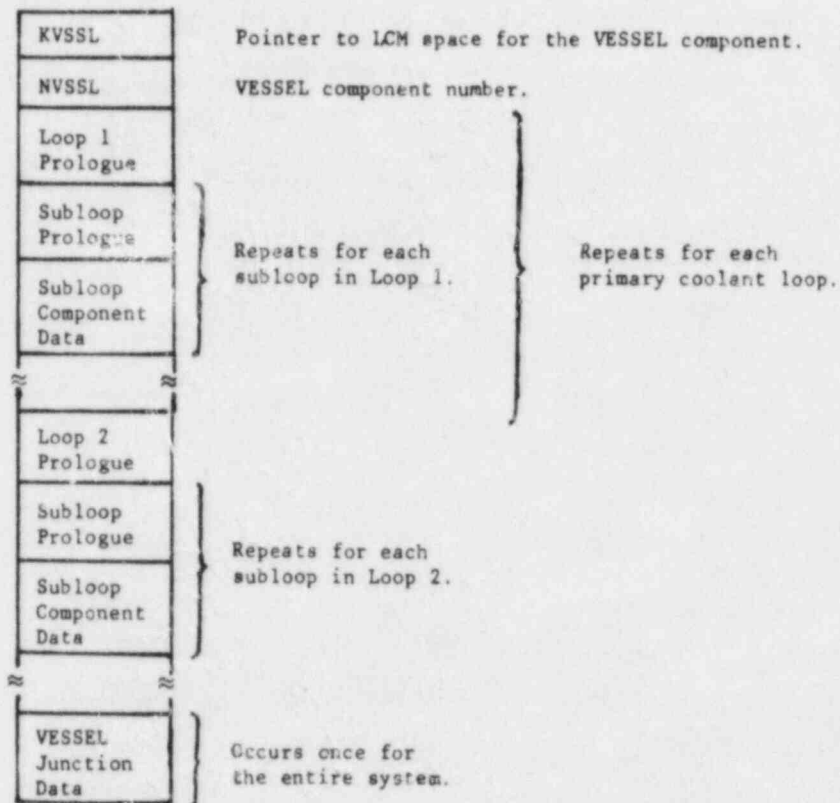
TABLE XIII
JUNCTION-COMPONENT PAIR ARRAY

The JUN array is doubly subscripted, JUN(4,2*NJUN). The second index indicates the order in which the junction-component pair was encountered during input. The four values of the first index correspond to:

<u>Index</u>	<u>Description</u>
1	Junction number.
2	Component number.
3	Component type.
4	Junction direction flag. = 0, if positive flow in this component is into the component at this junction, or = 1, if positive flow in this component is out of the component at this junction.

The data area shown in Fig. 46 describes the geometry of PWR systems from a specific point of view. Of principal interest in the PWR-initialization calculations are the components through which the primary coolant flows during steady-state conditions. To isolate these components, the components in each primary-coolant flow loop are grouped into subloops of three kinds indicated by

Overall Structure



Loop Prologue Structure

ILOOP	Loop index.
KNLOOP	Pointer to next loop.
JNLPC1	First vessel cold-leg junction.
JNLPC2	Second vessel cold-leg junction.
JNLPCH	Vessel hot-leg junction.
TILPC1	Desired temperature at JNLPC1.
WLPC1	Desired flow rate through JNLPC1.
WLPC2	Desired flow rate through JNLPC2.
NSLP	Number of subloops in this loop.
KTEE	Pointer to tee that joins loop pumps.

Fig. 46.
PWR-initialization data structure.

Subloop Prologue Structure

ISL	Subloop index.
KNSL	Pointer to next subloop.
ISLTP	Subloop type index.
NSLCMP	Number of subloop components.
KSLP	Pointer to subloop pump.
KSLS	Pointer to subloop steam generator.
SCAREA	Steam-generator area.
PMSPD	Pump speed.

Subloop Component Data Structure (Repeats for each component in the subloop.)

KCOMP	Pointer to LCM data.
NUM	Component number.
TYPE	Component type.

VESSEL Junction Data Structure

Repeats for each VESSEL junction.	NCSR	Number of vessel junctions.
	JN	Junction number.
	P	Pressure inside vessel.
	H	Enthalpy flow rate at junction.
	W	Mass flow rate at junction..

Fig. 46. (cont.)

the associated value of ISLTP. The components through which the primary coolant normally flows are identified by ISLTP = 1 and constitute one or two principal subloops (depending on the number of pumps). Subloops with ISLTP = 0 are called passive; they are connected to the principal flow loop by a TEE and have zero flow at steady-state conditions (for example, a pressurizer). Secondary-loop components (identified by ISLTP = 2) are connected to the steam-generator-secondary side. For the system to be processed by the PWR-initialization calculation, the secondary loops must be quite simple. One side of the steam generator must be connected by a sequence of pipes to a FILL component and the other side to a BREAK. (The first sequence is identified by ISLTP = 2 and the second by ISLTP = -2.)

C. Component Initialization

The transient or steady-state calculation cannot be initiated directly from the input data. Many arrays and variables for each component are required that are not read by overlay INPUT. Overlay INIT initializes these data based on the values of the input information. It also creates a table that supplies information to the graphics routines. The entry point subroutine, INIT, controls the initialization process by calling ICOMP and IGRAF. Subroutine ICOMP completes the component data tables and IGRAF initializes the graphics capability.

Subroutine ICOMP checks the junction input data (stored in the junction component pair array, JUN, to ensure that the system is configured properly, then fills in the JSEQ and VSI arrays in the fixed segment of the blank COMMON area (Table XI). Then, ICOMP initializes the data for each one-dimensional component by transferring the component data from LCM to SCM, adjusting the array pointers to reflect the origin of the array data, invoking the appropriate component initialization subroutine (listed in Table XIV), and then returning the initialized data to LCM. For each three-dimensional component, ICOMP invokes subroutine CIVSSL. Subroutine CIVSSL transfers the component data from LCM to SCM; adjusts the array pointers; calls the initialization routine, IVSSL; and then returns the initialized data to LCM.

TABLE XIV

COMPONENT INITIALIZATION SUBROUTINES

<u>Component Type</u>	<u>Initialization Routine</u>	<u>Graphics Initialization Routine</u>
ACCUM	IACCUM	IGACUM
BREAK	IBRK	IGBRAK
CORE	ICORE	IGCORE
FILL	IFILL	IGFILL
PIPE	IPIPE	IGPIPE
PRIZER	IPRIZR	IGPRZR
PUMP	IPUMP	IGPUMP
STGEN	ISTGEN	IGSTGN
TEE	ITEE	IGTEE
VALVE	IVLVE	IGVLVE
VESSEL	IVSSL	IGVSSL

Using subroutine JID, the component initialization routines originate geometric and heat-transfer arrays; fluid properties (by calling subroutines THERMO and FPROP); and the junction data array, as described in Table XV. Other individual and array variables are initiated for specific components. Most of these one-dimensional routines use COMPI and IPROP to initialize the data that are common among one-dimensional components.

The subroutine SETNET provides information to the individual components through the IOU array that is passed on to the network junction matrix described in Sec. III.D. The graphics initialization subroutine, IGRAF, creates the TRCGRF file; writes the header, catalog, and geometric data onto the file; and places the catalog in a LCM storage area. The catalog, which contains information about the data to be written on the TRCGRF file during the course of a problem, is constructed by the component graphics initialization routines. The data to be edited for each component are specified in these routines. Each data type adds one entry to the catalog. This entry describes the data location and identifies it with the variable name containing the data and a three-word Hollerith field. The catalog stored in LCM is interrogated later by subroutine GRAF to create each graphics edit.

D. Transient Calculation

1. General. The transient calculation is directed by subroutine TRANS. The system state is advanced through time by a sequence of prepass, outer iteration, and postpass calculations that TRANS requests by invoking overlay PREP, subroutine HOUT, and overlay POST, respectively. In these calculations one or more sweeps are made through all the components in the system. To provide the output requested by the user, TRANS invokes the EDIT, DUMP, and GRAF overlays by calling subroutine PSTEPQ.

Subroutine TRANS is structured as shown in Fig. 47. The major control variables within the time-step loop are: NSTEP, the current time-step number; TIMET, the time since the transient began; DELT, the size of the current time step; and OITNO, the current outer iteration number. The time-step loop begins with the selection of the time-step size, DELT, by subroutine TIMSTP. A prepass is performed for each component by overlay PREP. At this point, if the current time step is zero, TRANS calls in the EDIT overlay to print the system state at the beginning of the transient. Subroutine TRANS then calls subroutine HOUT that performs one or more outer iterations to solve the basic

TABLE XV

BOUNDARY ARRAY DATA*

The specific elements of the array are:

<u>Index</u>	<u>Description</u>
1	Width of the adjacent mesh cell.
2	Volume of the adjacent mesh cell.
3	Old mixture density at space point 2.
4	Product of new vapor density and void fraction ($\alpha\rho_g$) at space point 2.
5	Product of liquid density and liquid fraction $[(1 - \alpha)\rho_l]$ at space point 2.
6	Sign multiplier used on velocities in the adjacent component for consistency.
7	Old void fraction at space point 2.
8	Old vapor density at space point 2.
9	Old liquid density at space point 2.
10	New liquid velocity at space point 3.
11	New vapor velocity at space point 3.
12	Contribution to liquid momentum at space point 1 if there is a tee junction at point 2.
13	Contribution to vapor momentum at space point 1 if there is a tee junction at point 2.

*The boundary array data are stored in a doubly dimensioned array, BD(54,NJUN), whose second index indicates the order in which the junctions occur in the input data. The data in this array indicate the current condition of the adjacent component. Because both components connected to the junction use the same storage space, the JUN array reflects the state of the last of these components processed. The fluid properties are evaluated at one of three space points:

1. at the edge of the mesh cell closest to the junction,
2. at the mid-point of that mesh cell, or
3. at the other edge of that mesh cell.

TABLE XV (cont.)

<u>Index</u>	<u>Description</u>
14	Old pressure at space point 2.
15	New void fraction at space point 2.
16	New vapor density at space point 2.
17	New liquid density at space point 2.
18	New stabilizer liquid velocity at space point 3.
19	New stabilizer vapor velocity at space point 3.
20	Further contribution to liquid momentum at point 1 if there is a tee junction at space point 2.
21	Further contribution to vapor momentum at point 1 if there is a tee junction at space point 2.
22	New pressure at space point 2.
23	New liquid velocity at space point 1.
24	New vapor velocity at space point 1.
25	Surface tension at space point 2.
26	Derivative of liquid velocity at point 1 with respect to pressure at space point 2.
27	Derivative of vapor velocity at point 1 with respect to pressure at space point 2.
28	New macroscopic liquid energy density $[(1 - \alpha)\rho_l e_l]$ at space point 2.
29	New macroscopic vapor energy density $(\alpha\rho_g e_g)$ at space point 2.
30	Vapor viscosity at space point 2.
31	Liquid viscosity at space point 2.
32	Flow area at space point 1.
33	Hydraulic diameter at space point 1.
34	Old stabilizer liquid velocity at space point 3.
35	Old stabilizer vapor velocity at space point 3.
36	Component type of last component to enter data into this array.
37	Component number of last component to enter data into this array.
38	Old bit flags for donor-cell logic and detecting crossings of the saturation line.
39	Old air density (ρ_a) at space point 2.

TABLE XV (cont.)

<u>Index</u>	<u>Description</u>
40	New macroscopic air density ($\alpha\rho_a$) at space point 2.
41	Old macroscopic vapor density ($\alpha\rho_g$) at space point 2.
42	Old macroscopic liquid density $[(1 - \alpha)\rho_l]$ at space point 2.
43	Old macroscopic vapor energy density ($\alpha\rho_g e_g$) at space point 2.
44	Old macroscopic liquid energy density $[(1 - \alpha)\rho_l e_l]$ at space point 2.
45	Void fraction at the beginning of the previous time step at space point 2.
46	Old macroscopic air density ($\alpha\rho_a$) at space point 2.
47	Old partial pressure of air at space point 2.
48	Old vapor temperature at space point 2.
49	Old liquid temperature at space point 2.
50	Vapor velocity averaged for space point 2.
51	Liquid velocity averaged for space point 2.
52	Droplet interfacial drag coefficient for space point 3.
53	New bit flag information for space point 2.

hydrodynamic equations. Each outer iteration is performed by overlay OUTER and corresponds to one iteration in a Newton solution procedure for the fully coupled difference equations for the flow network (see Sec. III.D.). The outer iteration loop normally completes when the outer iteration convergence criterion (EPSO on Main Control Card 3) is met. This criterion is applied to the maximum fractional change in the pressures throughout the system during the last iteration.

The outer iteration loop alternatively may terminate when the number of outer iterations reaches a user-specified limit (OITMAX on Main Control Card 4). In this case, TRAC restores the state of all components to that at the beginning of the time step, halves the time-step size (with the constraint that DELT be greater than or equal to DTMIN), and continues the calculation with the new time-step size.

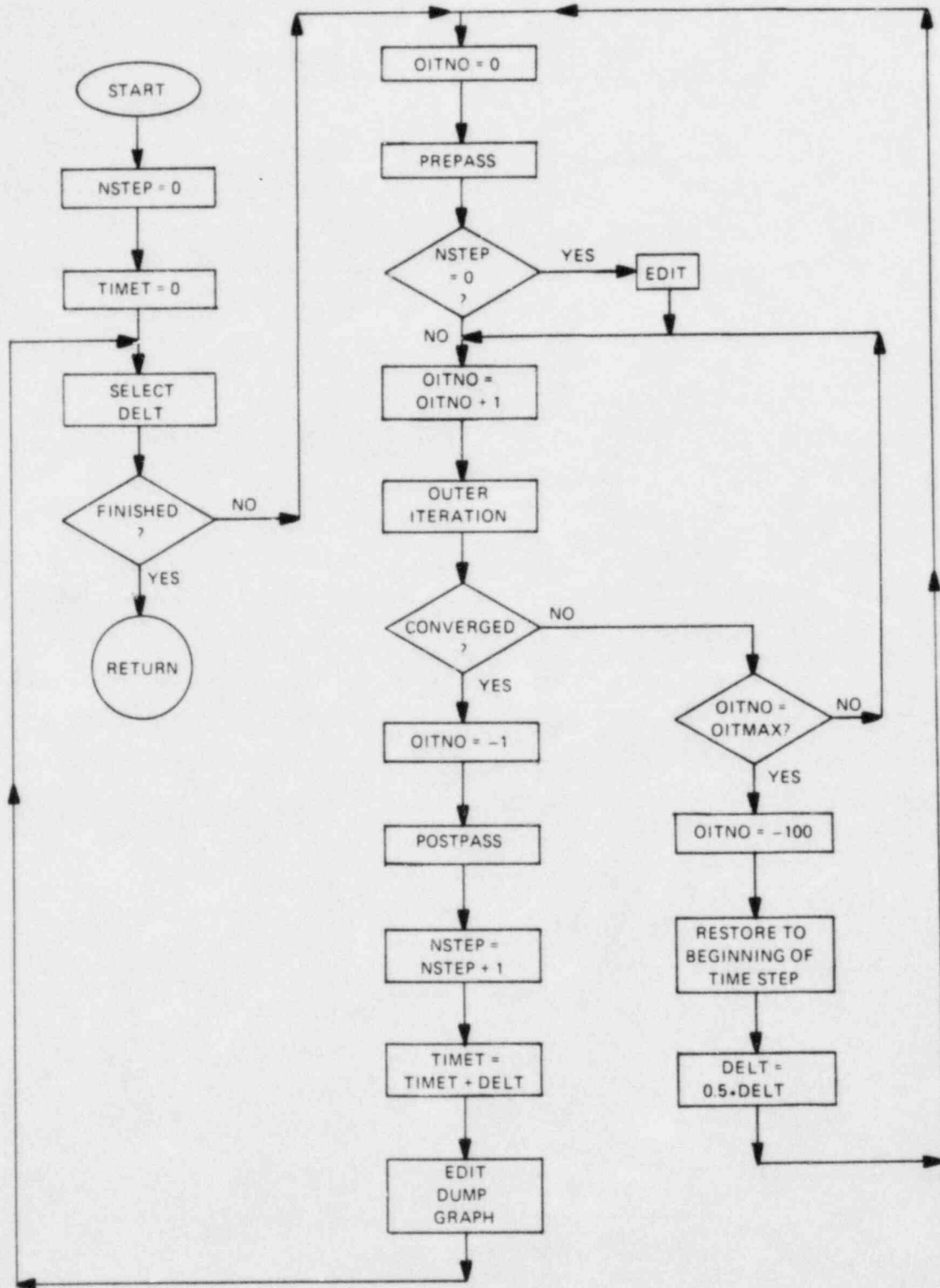


Fig. 47.
Flow diagram for transient calculations.

When the outer iteration converges, TRANS calls in the POST overlay to perform a postpass. The time-step number then is incremented and TIMET is increased by DELT. A calculation is complete when TIMET reaches the last time specified on the time-step input cards.

2. Time-Step Selection and Output Control. The transient calculation interval is a sequence of time domains specified by the user on the time-step input cards. During each of these domains, the minimum and maximum time-step sizes and the edit, dump, and graphics intervals are fixed. When the EDIT, DUMP, and GRAF overlays are invoked, they calculate the time when the next output of the associated type is to occur. When TRANS finds that TIMET has reached or exceeded the indicated time, the corresponding output overlay is invoked again. When a new time domain is reached, the output indicators are set to the requested time plus the new value of the appropriate interval.

Subroutine TIMSTP reads the time-step control cards and evaluates the size of the next time step. At the beginning of the transient, DELT is set to the minimum size specified for the first time domain. At other times, TIMSTP applies several algorithms, implemented in subroutine NEWDLT, to evaluate the size of the next time step. Subroutine TIMSTP then limits DELT to values between the minimum and maximum specified for this time step, unless the minimum time-step size is greater than the computed Courant limit in three-dimensional regions. In this case, DELT is set equal to the Courant limit.

Two types of algorithms, inhibitive and promotional, are implemented in subroutine NEWDLT to evaluate the next time step. The inhibitive algorithms limit the new time-step size to ensure stability and to reduce errors. The promotional algorithm increases the time-step size to improve computational efficiency.

Iteration counts are used by both the inhibitive and promotional algorithms. Both the number of outer iterations (MAXIT) and the number of vessel iterations (IIBIG) required for the previous time step are utilized. If MAXIT is less than four and IIBIG is below 70% of the maximum allowed number of vessel iterations (input as IITMAX), the promotional algorithm increases the time-step size (DELT) by 5%. If MAXIT exceeds five, DELT is reduced by the factor $5/\text{MAXIT}$; if IIBIG exceeds $0.7 \cdot \text{IITMAX} + 1$, DELT is reduced by $(7 \cdot \text{IITMAX} + 10) / (10 \cdot \text{IIBIG})$.

If a new time-step size was estimated in this manner, NEWDLT then invokes the remaining inhibitive algorithms to reduce DELT, if needed for stability or accuracy. The Courant condition in three forms is applied to ensure stability. The three forms use the new, old, and extrapolated fluid velocities to evaluate the limit. The accuracy limits are based on the fractional changes in pressure and void fraction and the calculated error in the new total vessel mass.

During the last outer iteration calculation of the previous time step, the maximum changes in the pressure and void fraction over all fluid cells are evaluated. (Cells in which the void fraction is below 1% are not considered in evaluating the maximum fractional change of the void fraction.) The fractional pressure change ordinarily is limited by the outer convergence criterion, EPSO. If the maximum number of outer iterations is input as one, however, this is not the case. In this instance NEWDLT compares the maximum fractional pressure change (VARERM) to 0.1. If the change exceeds 10%, a maximum time-step size of $0.1 \cdot \text{DEL T} / \text{VARERM}$ is imposed. Similarly, if the maximum void-fraction change (DAMX) exceeds 0.5, a maximum time-step size of $0.5 \cdot \text{DEL T} / \text{DAMX}$ is used.

The error in the vessel mass inventory caused by the previous time step is evaluated by subtracting the mass at the previous time step and the net mass flow into the vessel from the new mass inventory. If the fractional mass error exceeds 0.01%, another maximum time-step size is evaluated as $10^{-4} \cdot \text{DEL T}$ divided by the mass error.

Another maximum time-step size calculation is based on the maximum liquid, vapor, slab, and rod temperature changes during the last time step. For temperature changes that exceed 20 K, the smallest value of $\text{DEL T} \cdot 20. / \Delta T$ is used.

The diffusion number for the rod conduction calculation, DIFMIN, also is used to evaluate a maximum time-step size. It is evaluated as DIFMIN if DIFMIN is nonzero or 1×10^8 if DIFMIN is zero.

3. Prepass Calculations. The prepass calculation uses the system state at the completion of the previous time step to evaluate numerous quantities to be used during the outer iteration. The prepass begins by evaluating trip signal variables and by determining the set position of all trips. The prepass then loops over all components in the system and performs an extra loop over all one-dimensional components. Each component begins the prepass by moving the values calculated during the last time step into the

storage area for old time values. (See Appendix G for a variables list.) Next, wall and interfacial friction coefficients are calculated and an initial forward elimination on the stabilizer equations is performed. For components that require heat-transfer calculations, the prepass also evaluates material properties and HTC's. A second pass through all one-dimensional components is required to do the back-substitution on the stabilizer equations of motion.

The prepass for vessel components can be more complex. Besides calculating material properties and HTC's for both average and hot rods, the prepass evaluates quench-front positions and fine-mesh properties if the reflood segment is under way, as indicated by the reflood flag NRFD.

The prepass calculation is controlled by overlay PREP, whose entry point routine has the same name. Subroutine PREP first processes all one-dimensional components by calling PREP1D, which loads data for each component into SCM, invoking the appropriate component prepass subroutine (see Table XVI), then transfers the component data back to LCM. The prepass for all three-dimensional components is performed by PREP3D, which is called once by PREP after all one-dimensional components have been processed.

The one-dimensional component prepass routines utilize the common low-level routines SAVBD, PREPER, SVSET, TRPSET, and SETBD to avoid redundant coding. Subroutine SAVBD retrieves boundary data from adjacent components, stores it in the appropriate array locations, and moves data for the last completed time step into the old time arrays. Subroutine PREPER evaluates wall friction by calling FWALL, evaluates interfacial friction coefficients and begins solution of the stabilizer equations of motions by calling FEMOM, and uses subroutines MPROP and HTPPIPE to evaluate material properties and HTC's. For a specific component, any or all of these steps may occur under the control of the PREPER argument list.

Subroutine SVSET uses current values of system state variables to evaluate trip signal variables. Subroutine TRPSET uses the current signal-variable values to set the status of trips. (This is in contrast to subroutine TRIP that interrogates the trip status in preparation for specific consequences of trips.) Subroutine SETBD uses the information in the component data arrays to reset the boundary data at both ends of a component.

TABLE XVI

ITERATION SUBROUTINES

<u>Component Type</u>	<u>Prepass</u>	<u>Outer</u>	<u>Postpass</u>
ACCUM	ACCUM1	ACCUM2	ACCUM3
BREAK	BREAK1	BREAK2	BREAK3
CORE	COREC1	COREC2	COREC3
FILL	FILL1	FILL2	FILL3
PIPE	PIPE1	PIPE2	PIPE3
PRIZER	PRIZR1	PRIZR2	PRIZR3
PUMP	PUMP1	PUMP2	PUMP3
STGEN	STGEN1	STGEN2	STGEN3
TEE	TEE1	TEE2	TEE3
VALVE	VLVE1	VLVE2	VLVE3
VESSEL	VSSL1	VSSL2	VSSL3

Each three-dimensional component is processed by subroutine VSSL1, which PREP3D calls between loading and unloading the appropriate data areas. Subroutine VSSL1 uses subroutine RKIN to solve the reactor-kinetics problem; subroutine HTVSSL to evaluate fluid cell HTCs; and CORE1 to evaluate rod HTCs, fine-mesh properties, and quench-front positions.

4. Outer Iterations. The hydrodynamic state of the system is analyzed in TRAC by a sequence of Newton iterations that use full inversion of the linearized equations for each external loop and vessel at each iteration (see Sec. III.D). Throughout the sequence of iterations that constitute a time step (each called an outer iteration within TRAC), the properties evaluated during the prepass and the previous postpass remain fixed. These include wall and rod temperatures, HTCs, wall friction factors, relative velocities, and quench-front positions. The remaining fluid properties are varied to obtain hydrodynamic model solutions.

Each call to overlay OUTER completes a single outer (Newton) iteration. Subroutine OUTER, which is the entry point routine of this overlay, controls the overall structure of an outer iteration, as presented in Fig. 48. Both the forward-elimination and back-substitution sweeps through the external loops are performed by subroutine OUT1D and the associated outer iteration routines. The calculations that these routines perform are controlled by the common variable IBKS, which is set by subroutine OUTER. Subroutine OUT3D solves the

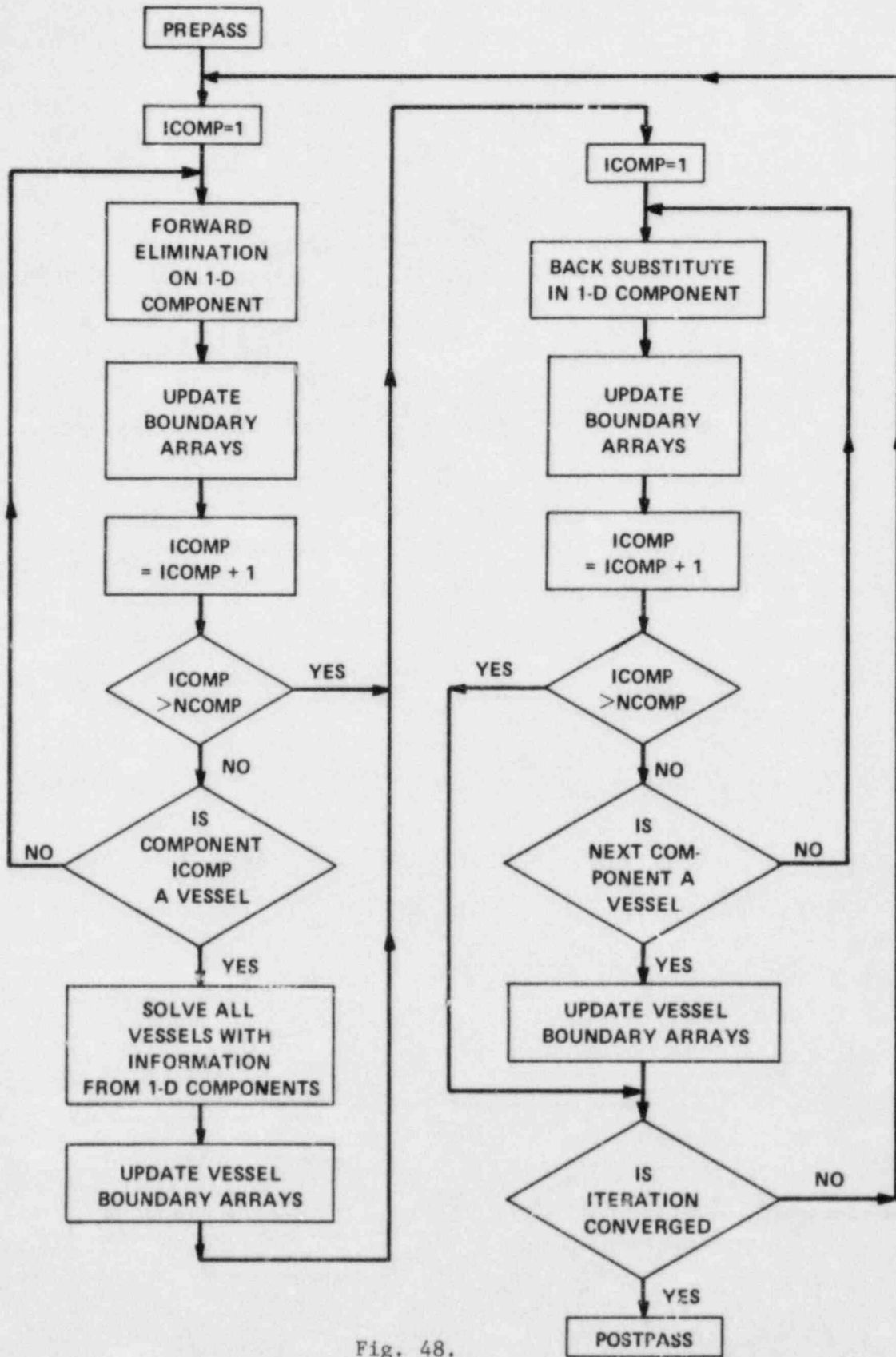


Fig. 48.
Outer iteration flow diagram.

hydrodynamic equations for all vessel components (IBKS = 0) or updates boundary data (IBKS = 1).

All one-dimensional components in a particular external loop are handled by a single call to subroutine OUT1D. This routine loads the data blocks for a component into SCM, then invokes the appropriate component outer iteration subroutine (as listed in Table XVI), and returns the data to LCM. Subroutine OUT3D works in a similar manner, except that all three-dimensional components use the single subroutine VSSL2.

The outer iteration subroutines for one-dimensional components utilize subroutine INNER to perform common functions. Subroutine INNER retrieves boundary information from the boundary arrays, tests other boundary information for consistency, calls subroutine TF1D to perform the appropriate hydrodynamic calculation, and resets the boundary data arrays by calling subroutine J1D. Subroutine TF1D invokes subroutines TF1DS1, TF1DS, and TF1DS3 to solve the basic semi-implicit equation.

Subroutine VSSL2 solves the appropriate problem (depending on the value of IBKS) for a single vessel component. Subroutines TF3DE and TF3DI are invoked to linearize the hydrodynamic equations. The linear system then is solved by one of two methods depending on the value of the input variable IITMAX. A value of IITMAX = 0 causes direct inversion of the vessel matrix. If IITMAX > 0, the system is solved by Gauss-Seidel iteration with coarse-mesh acceleration. Subroutine VELCK then is utilized to check for velocity sign changes. If any are found, TF3DI is called for the appropriate cells.

Subroutine STDIR sets up the vessel matrix for direct inversion when IITMAX = 0. Subroutine SOLVE is called to solve the linear system and then subroutine BACIT stores the new time pressures that were calculated. Subroutine ITR1 is utilized to solve the system by Gauss-Seidel iteration when IITMAX > 0. Subroutines SREBAL and SOLVE are called to set up and solve the coarse-mesh equations for coarse-mesh rebalance. Next, subroutine BREBAL is invoked to apply the coarse-mesh scaling factor to the new time pressures.

5. Postpass Calculations and Backup. After the system hydrodynamic state has been evaluated by a sequence of outer iterations, TRAC performs a postpass to solve the stabilizer mass and energy equations and to determine both mixture properties and wall and rod temperatures. These are based on the new fluid conditions. Overlay POST performs this postpass. The same overlay

also implements the time-step backup procedure. Time-step backup is caused by failure of the outer iteration process or extreme changes in void fraction. When failure occurs, the outer iteration counter, OITNO, is set equal to -100 and overlay POST is invoked. Under these conditions, POST returns the component data arrays to their state at the beginning of the time step.

Subroutine POST is the entry point for this overlay. Subroutine POST first processes all one-dimensional components by loading the proper data into SCM, calling the appropriate component postpass subroutine (see Table XVI), and then returning the data to LCM. Then POST invokes subroutine POST3D to handle all three-dimensional components. Subroutine POST3D loads the vessel data areas, calls VSSL3, and returns the vessel data to LCM for each vessel in the problem.

The one-dimensional component postpass subroutines use the low-level routines SAVBD, POSTER, and SETBD to retrieve boundary conditions; to evaluate the stabilizer equations, wall temperatures, mixture properties, and transport properties; and to reset the boundary arrays, respectively. The vessel processor, VSSL3, first must invoke subroutine FF3D to complete the hydrodynamic calculation, then call subroutine CORE3 to evaluate rod temperatures. When in the backup mode, the postpass subroutine for each component moves data as necessary within the time-dependent array area, then uses subroutine THERMO to reinitialize the thermodynamic property arrays.

6. Vessel Data Structure. All array data for any one-dimensional component are loaded into the core when that component is processed. Because the amount of array data is much larger for the three-dimensional VESSEL component, this is not possible for components of this type. Therefore, the array data for the VESSEL component are subdivided. There are three categories of VESSEL array data: component, level, and rod.

The component data arrays describe the overall VESSEL state. These arrays are loaded into SCM before VESSEL processing begins and remain there throughout the VESSEL calculation.

The level data arrays contain fluid-dynamics and wall-temperature data organized by axial level within the VESSEL. A data management subroutine, MANAGE, is used by all VESSEL subroutines to load single levels into SCM and to replace them in LCM. There are never more than three levels of data in SCM at

one time. These arrays are rotated through the SCM area during the fluid-dynamics calculation by the VESSEL iteration subroutines.

The rod data arrays contain detailed information about the heat-transfer calculation in the fuel rods. These data are organized by fuel rod so that only data pertaining to the rod under study are in SCM at once. These data arrays are loaded into (and unloaded from) the blank COMMON area by calls to the MANAGE subroutine. Subroutines CORE1 and CORE3 coordinate the rod heat-transfer calculations including the management of rod data.

In addition to solving the data space problem, the organization of the VESSEL array data improves the calculation efficiency by grouping data by their use. However, it introduces a communication problem between the fluid-dynamics and heat-transfer calculations because some data must be in both the rod and the level arrays. This problem is resolved by a data transfer between the rod and the level data arrays. This transfer is performed by direct LCM to LCM copies using subroutine LCMOVE during the prepass calculation.

E. Steady-State Calculations

Subroutine STEADY directs steady-state calculations. The calculation sequence of this subroutine is similar to that of the transient driver subroutine TRANS. Both STEADY and TRANS use subroutine HOUT to perform a group of outer iterations. The same sequence of iterations used for transient calculations also is used to advance the steady-state calculation. The main difference is the addition of steady-state convergence tests and PWR-initialization calculations to STEADY. To provide output requested by the user, STEADY invokes the EDIT, DUMP, and GRAF overlays by calling subroutine PSTEPQ. These overlays are described in Sec. VI.F. If the calculation includes PWR initialization, overlay PWRSS is called by STEADY to evaluate new PWR operating parameters. Subroutine STEADY is called by the main program even if a steady-state calculation has not been requested. If no calculation is required, STEADY simply initializes the VESSEL power and returns control to the main program.

The steady-state calculation is determined by the value of the input variable STDYST on Main Control Card 1, as described in the input specifications in Sec. V.F.1. The code sets the steady-state indication flag, ISTDY, to 1 and the transient calculation time, TIMET, to -1 to begin the steady-state calculations. (In steady-state calculations the time variable is

TABLE XVII
STEADY-STATE CALCULATION EFFECTS

<u>Subroutine</u>	<u>Effects</u>
CYLHT	Causes implicit treatment of the convective boundary conditions.
HTCOR	Eliminates CHF calculation.
RODHT	Causes implicit treatment of the convective boundary conditions.
PRIZER	Bypasses calculation of fluid and thermal conditions. Causes cataloging of mass flow through the system junctions.
PUMP2	Causes momentum source to be time averaged.
TIMSTP	Multiplies time-step size for heat transfer by RTWFP.
TRPSET	Causes trips not to be activated.

STIME instead of TIMET.) These values of ISTDY and TIMET have the effects indicated in Table XVII.

The time-step control in STEADY is identical to that implemented in TRANS. This includes the selection of the time-step size, the output timing, and the restarting of time steps if the outer iteration limit is exceeded. (In STEADY the input variable SITMAX, from Main Control Card 4, is used as a delimiter in place of OITMAX.) The maximum normalized rates of change are calculated by subroutines TF1DS3 and FF3D. These rates and their locations in the system are transmitted to STEADY through the variables FMX and LOK in COMMON block SCON. Tests for steady-state convergence are performed every 50 time steps and before every edit. The maximum normalized rates of change and their locations are included in the printed output, as shown in Table XVIII. The maximum normalized rate of change for the axial velocity in the vessel (FMXLVZ) determines when the reactor power should be turned on. Once this value falls below 0.5, the reactor power is set to the input value, RPOWRI (specified on card 12 of the vessel input data or card 8 of the core input data). The generalized steady state completes when all normalized rates of change are below the user-specified convergence criterion, EPSS (on Main

TABLE XVIII

EXAMPLE OF A STEADY-STATE CONVERGENCE EDIT

Steady-State Time-Step Number 114, Converged in 2 Iterations.

TIME = 5.187×10^{-2} DELT = 2.480×10^{-3}

<u>Variable</u>	<u>Maximum Change Ratio</u>	<u>Component</u>	<u>Cell</u>
Pressure	-5.228985×10^{-1}	1	43
Liquid velocity	3.85848×10^1	14	1
Vapor velocity	0	0	0
Void fraction	0	0	0
Liquid temperature	-2.00387×10^{-2}	6	2
Vapor temperature	2.12964×10^{-2}	0	0
Air pressure	0	0	0

Control Card 3) or when STIME reaches the end of the last time domain specified in the steady-state time-step input cards.

Both steady-state and transient calculations may be performed in one computer run. The end of the generalized steady-state time-step cards is signified by a single card containing a -1.0 in columns 11-14. The transient time-step input cards should follow immediately. If the generalized steady state converges before reaching the end of the last time domain, the remaining steady-state time-step input cards are read so that the transient calculation proceeds correctly.

Control of the PWR-initialization calculation necessarily is more complex. The time domains are divided into groups delimited by negative DTMIN values. The completion of each group of time-step cards or convergence to a steady state causes a re-evaluation of the loop parameters. The last group of time domains is marked by a card containing negative values for both DTMIN and DTMAX. As in the generalized calculation, a transient calculation may follow the PWR initialization. The time-step cards for the transient calculation follow those for the PWR initialization.

The PWR-initialization calculation completes when the relative errors in the flow rates and inlet temperatures fall below a user-specified criterion, EPSP (on Main Control Card 3) for all loops. Figure 49 is a flow diagram for the steady-state calculation.

Overlay PWRSS uses the system state, as represented in the LCM component data tables, to evaluate new pump speeds and steam-generator fouling factors for the PWR-initialization calculation. The reactor loop data area (Fig. 46) is used by this overlay for data storage and calculation control.

Subroutine LPSET is the entry point and controlling subroutine for the PWRSS overlay. It calls subroutine VSCON to evaluate the VESSEL pressures as well as mass and energy flow rates at all VESSEL junctions. These data are retrieved from the boundary data arrays. Each primary coolant loop is considered in turn by LPSET. The loop flow resistances, specific enthalpy differentials, and the steam-generator overall HTC are evaluated by subroutine LPCON. The PMPP, TEEP, and STGNP subroutines provide LPCON with data derived from the PUMP, TEE, and STGEN component data tables, respectively. The equations presented in Sec. III.D.2 are solved for the pump heads and steam-generator area by subroutine SLVLP. Finally, LPSET calls subroutine LPRPL to convert these parameters to pump speeds and fouling factors, to relax them as required, and to store them into the appropriate component data tables.

F. Output Processing

The TRAC program produces five output files: TRCOUT, TRCMSG, TRCGRF, TRCDMP, and TRCINP. The first of these files is in printer format and contains a user-oriented analysis of the calculation. During the input process, an input data description is placed in this file. At selected times during the calculation, overlay EDIT is invoked to add to this file a description of the current system state. The TRCGRF and TRCDMP files are binary files designed to allow analysis by graphics postprocessing programs and problem restart by TRAC, respectively. The TRCGRF file is created and the header, catalog, and geometric data are written into it during the initialization phase. File TRCDMP is created immediately thereafter by overlay DUMP. The TRCMSG file is in printer format and contains diagnostic messages concerning the progress of the calculation. File TRCINP is created only when the TRACIN input file is in free format. The data from TRACIN is written into file TRCINP in a form that

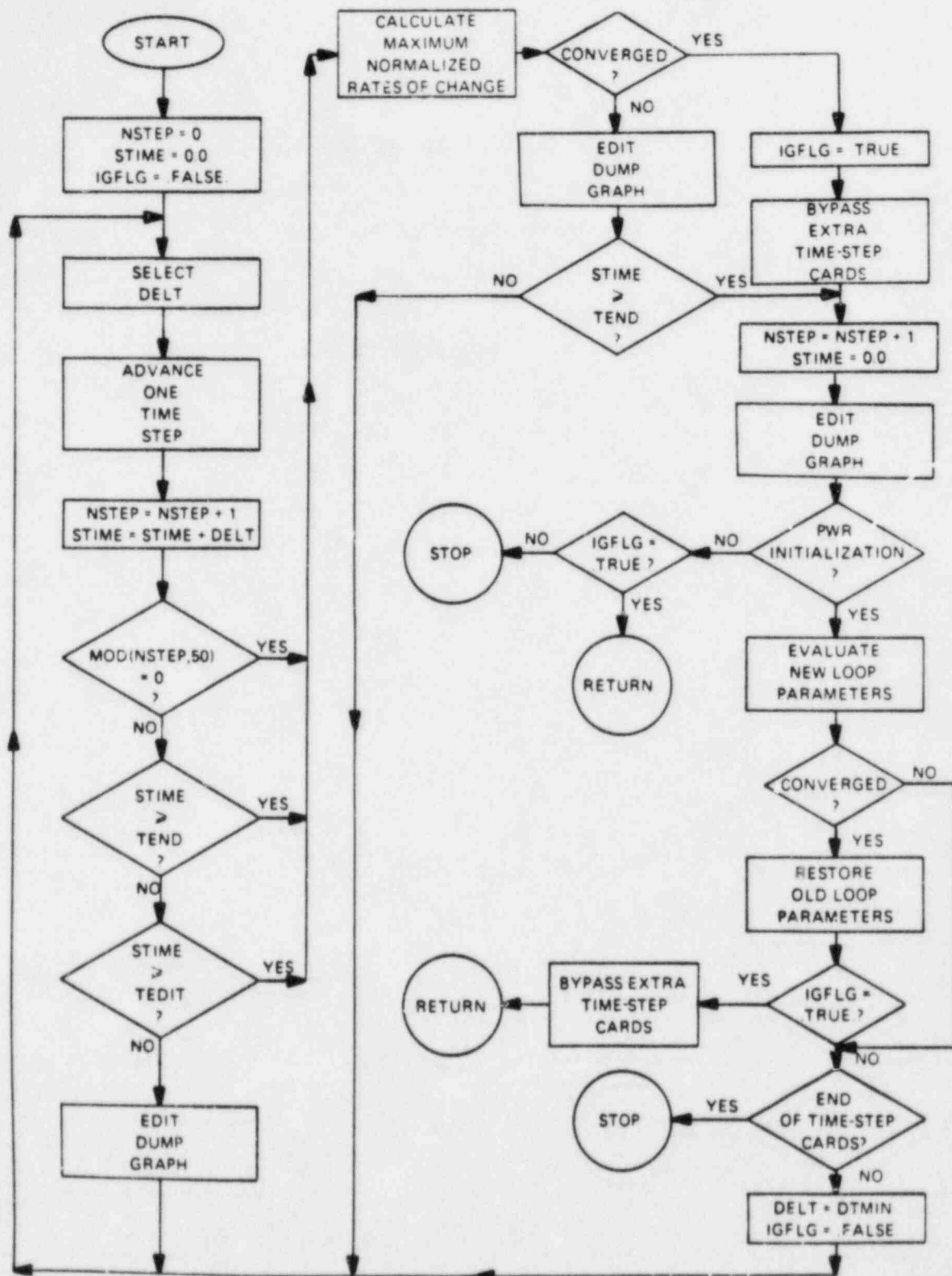


Fig. 49.
Flow diagram for steady-state calculation.

can be read by the TRAC input routines. TRCINP then is used as the input file to TRAC.

Subroutine WCOMP, which is called by the entry-point routine EDIT, directs the addition of a time-step edit to the TRCOUT file. Subroutine WCOMP writes general overall data first, then invokes lower level routines to describe the state of each component. For one-dimensional components, WCOMP directly calls the appropriate component edit subroutine. Table XIX lists the component edit subroutines. These routines invoke subroutine ECOMP to write the data common between one-dimensional components. For three-dimensional components, WCOMP calls subroutine CWSSSL, which loads the component data tables into SCM and then invokes the component-edit-subroutine WVSSL. The component edit routines add the data that are important for that component to the TRCOUT file in an appropriate format.

After initialization by IGRAF, the time-edit data are added to the TRCGRF file by overlay GRAF. This overlay contains the single subroutine, GRAF, which uses the LCM graph data area. The TRCGRF file is a structured binary file written with unformatted write statements and containing information for graphics processing.

TABLE XIX
COMPONENT EDIT SUBROUTINES

<u>Component Type</u>	<u>First-Level Subroutine</u>	<u>Lower-Level Subroutine</u>
ACCUM	--	WACCUM
BREAK	--	WBREAK
CORE	--	WCORE
FILL	--	WFILL
PIPE	--	WPIPE
PRIZER	--	WPRIZR
PUMP	--	WPUMP
STGEN	--	WSTGEN
TEE	--	WTEE
VALVE	--	WVLVE
VESSEL	CWSSSL	WVSSL

Data contained on the TRCGRF file may be divided into four sections:

1. general information,
2. catalog information,
3. geometric information, and
4. time-edit data.

These data appear on the file in the above order, as shown in Fig. 50. The structure of the general information section of the file is given in Fig. 51. This section contains title cards for problem identification and size information needed to describe the problem and the remainder of the file. The catalog section (Fig. 52) contains information that is used to describe the data stored in the time-edit section. The geometric section contains information relating to the cell structure of components. The time-edit section is made up of blocks of data as shown in Fig. 53. Individual arrays within each block are packed to save space. A block is written at each graphics edit taken during the course of a problem. The number of time-edit blocks written on the file is determined by the graphics edit frequency specified on the time-step cards. The last block is followed by the acronym "EOF" to signify the "end of file."

The structure and lengths of the time-edit blocks are identical, minimizing the required catalog information. The catalog is made up of NCTX data entries with one catalog entry for each data type in a block. This relationship is displayed in Fig. 54. Each catalog entry contains six words that provide a data description and a pointer, relative to the beginning of the block, to a specific section in each block. A catalog entry may describe a single variable or a data array. The word count also is included in the catalog. The data types stored are pressures, temperatures, void fractions, and other important system parameters.

The TRCDMP file is a structured binary file written with unformatted write statements. It contains sufficient data to restart the calculation from the current state, as described in Sec. VI.B. This file is created by a sequence of calls to overlay DUMP. The entry point subroutine, DMPIT, writes the dump header data and calls the component dump subroutines, which are listed in Table XX.

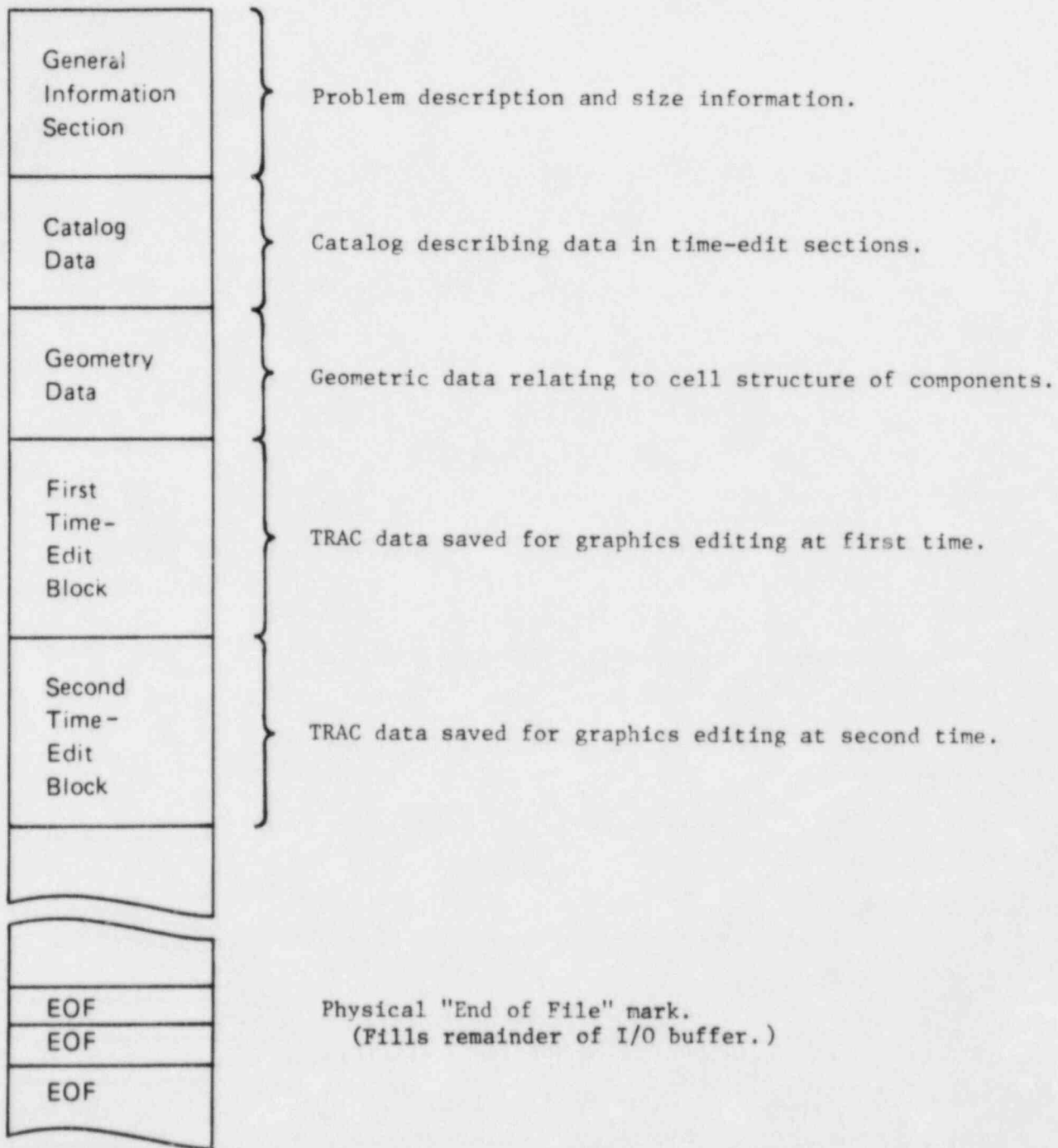


Fig. 50.
Overall graphics file structure.

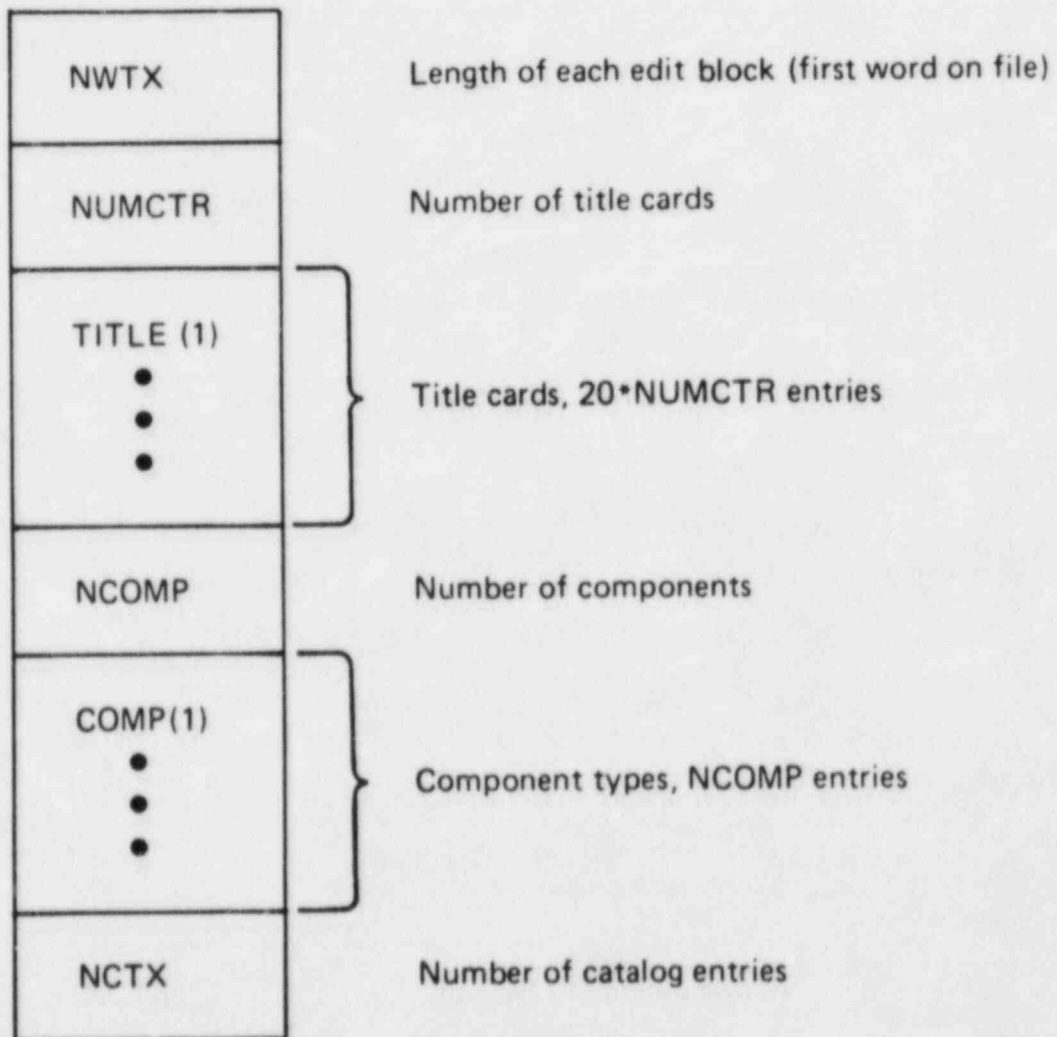
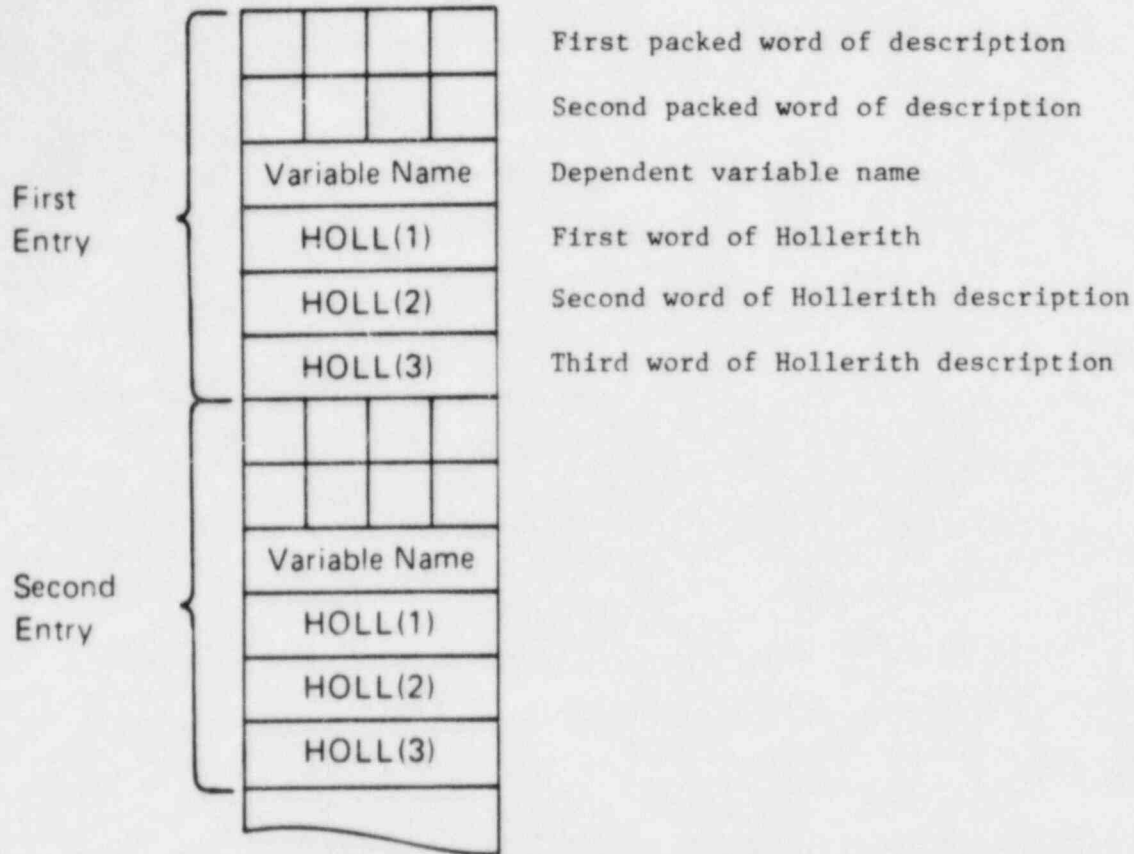
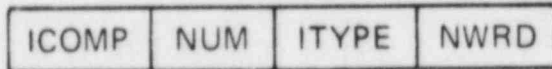


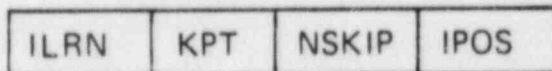
Fig. 51.
Structure of graphics file general information section.



FIRST PACKED WORD OF DESCRIPTION



SECOND PACKED WORD OF DESCRIPTION



- ICOMP -- TRAC-assigned component number
- NUM -- User-assigned component number
- ITYPE -- Data type
- NWRD -- Number of unpacked words stored
- ILRN -- Level or rod number
- KPT -- Relative pointer to data in TRCGRF
- NSKIP -- Data skip frequency
- IPOS -- Relative pointer to where data were extracted from TRAC data base

Fig. 52.
Structure of graphics file catalog.

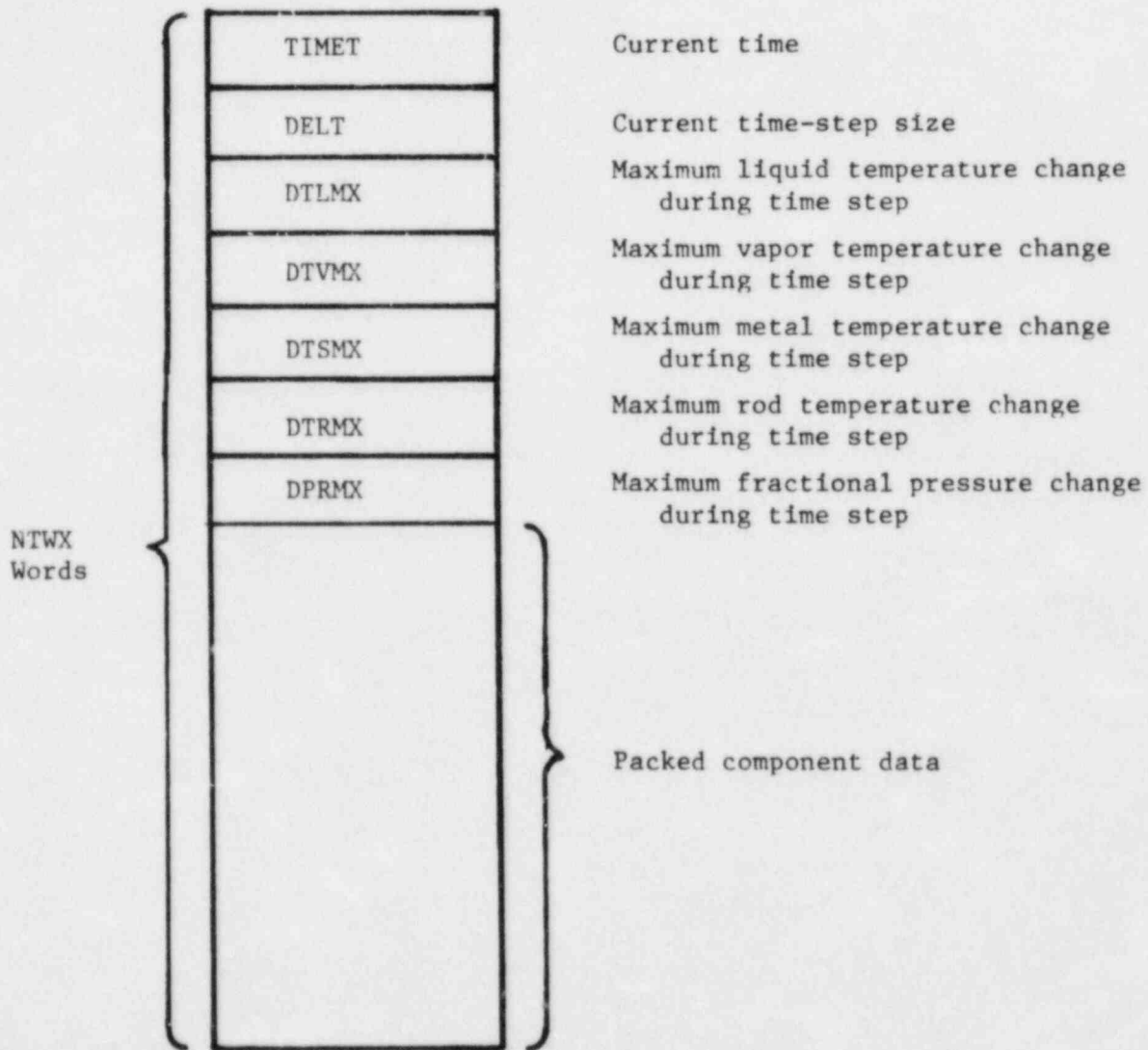


Fig. 53.
Structure of graphics file time-edit data section.

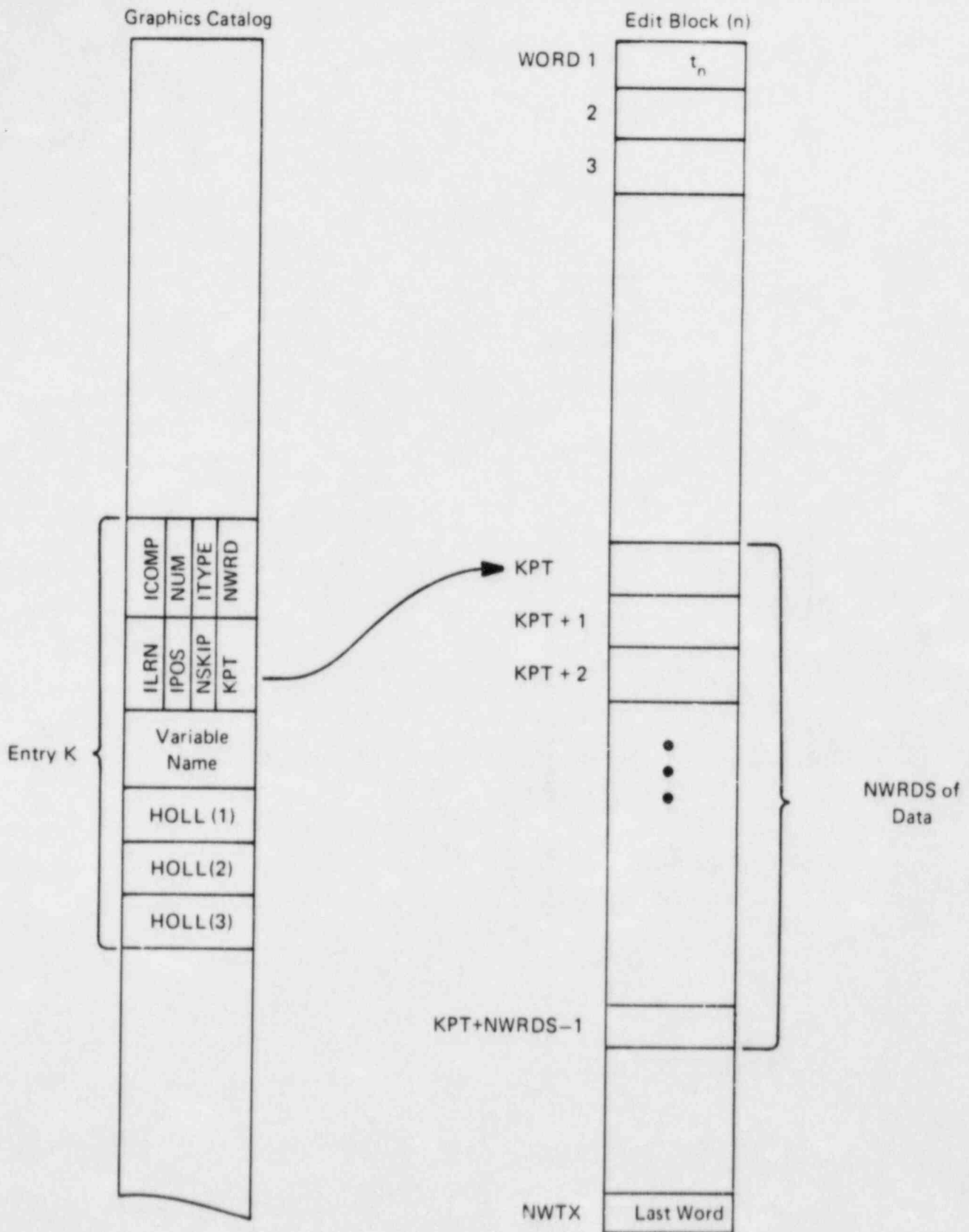


Fig. 54.
Graphics file catalog and time-edit data correspondence.

TABLE XX
COMPONENT DUMP SUBROUTINES

<u>Component Type</u>	<u>Subroutine</u>
ACCUM	DCOMP
BREAK	DBRK
CORE	DCORE
FILL	DFILL
PIPE	DCOMP
PRIZER	DCOMP
PUMP	DPUMP
STGEN	DCOMP
TEE	DCOMP
VALVE	DVLVE
VESSEL	DVSSL

The resulting file is structured as shown in Figs. 55-57. This structure permits easy location of specific dumps and specific components within each dump. This reduces the effort required to restart the problem.

Figure 55 shows the overall dump file structure with a general information section at the beginning followed by a series of time-edit blocks. A block is written at each dump edit taken during a problem. The number of time-edit blocks written on the file is determined by the dump-edit frequency specified on the time-edit cards. The last block is followed by the acronym "EOF".

The structure of each time-edit block in the dump file is illustrated in Fig. 56. Data from each component is included in the component dump section shown at the bottom of the figure. Figure 57 shows a more detailed structure of the component dump section.

G. Storage Requirements

Although maximum use is made of dynamic storage allocation within TRAC, there are limitations on the complexity of problems that may be simulated. These limitations arise from the finite extent of the component data storage areas, as listed in Table XXI. These limitations are imposed on the complexity of single components as well as on the system as a whole.

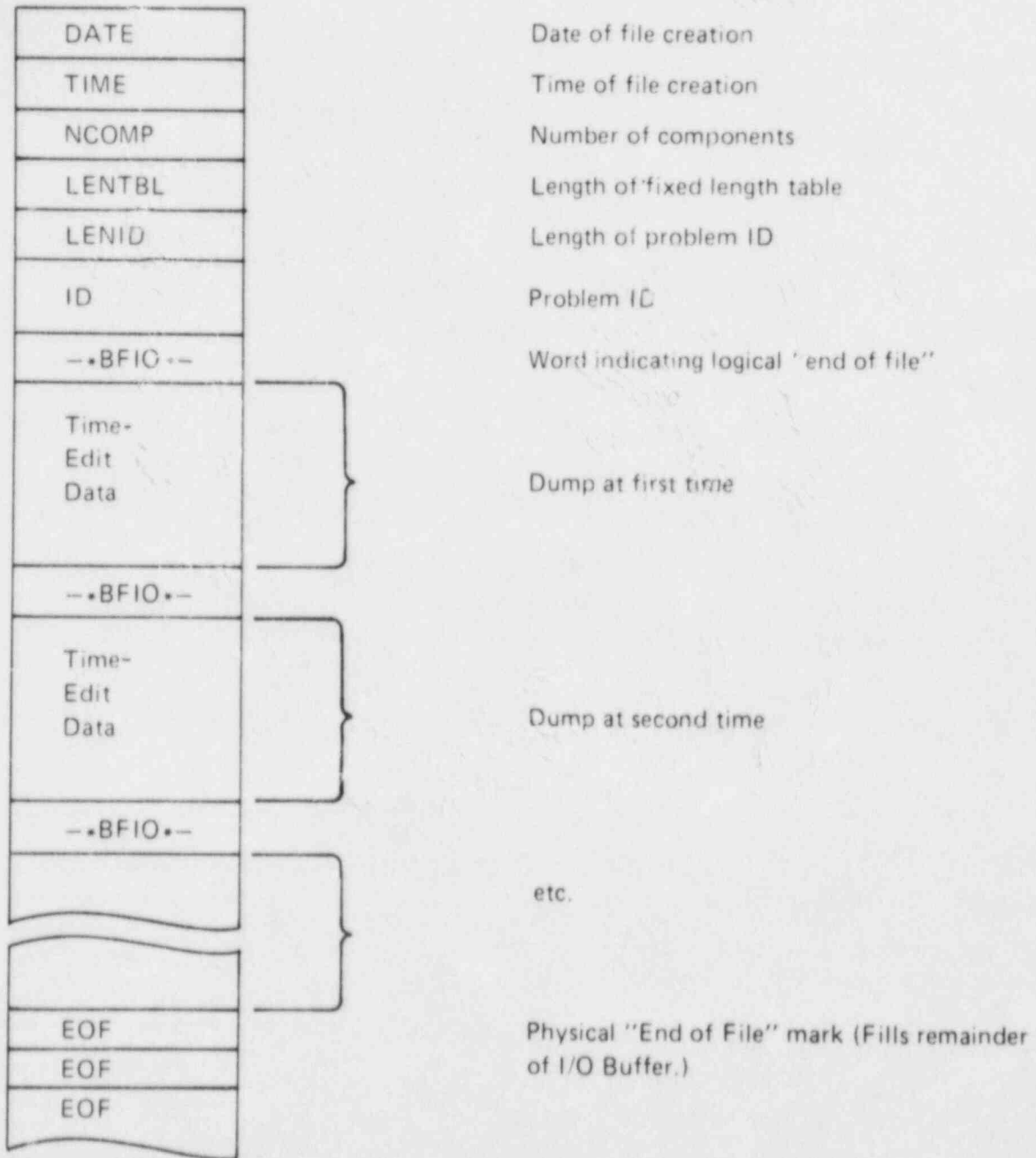


Fig. 55.
Dump file overall structure.

ETIME	Current time
NSTEP	Time-step number
DELT	Time-step size
OITNO	Outer iteration number
VMAXT	Maximum Courant number
VMAXO	Maximum Courant number found during current time step
VMNEW	Vessel water mass (liquid and vapor) at t^{n+1}
VMOLD	Vessel water mass (liquid and vapor) at t^n
VMCON	Net water mass convected into vessel during the interval $t^{n+1} - t^n$
DAMX	Error caused by relative change in void fraction
DAU	Maximum increase in void fraction
DAL	Maximum decrease in void fraction
OAU	Maximum increase in void fraction after a decrease
OAL	Maximum decrease in void fraction after an increase
VERERM	Maximum variable error
IIBIG	Maximum number of inner iterations per outer iteration
ISOLUT	Interactive control-panel vector (optional)
NTRX	Number of trips
Signal-Variable, Trip, and Controller Data	Signal-variable, trip, and controller data array
	Component dump

Fig. 56.
Structure of dump file time-edit data section.

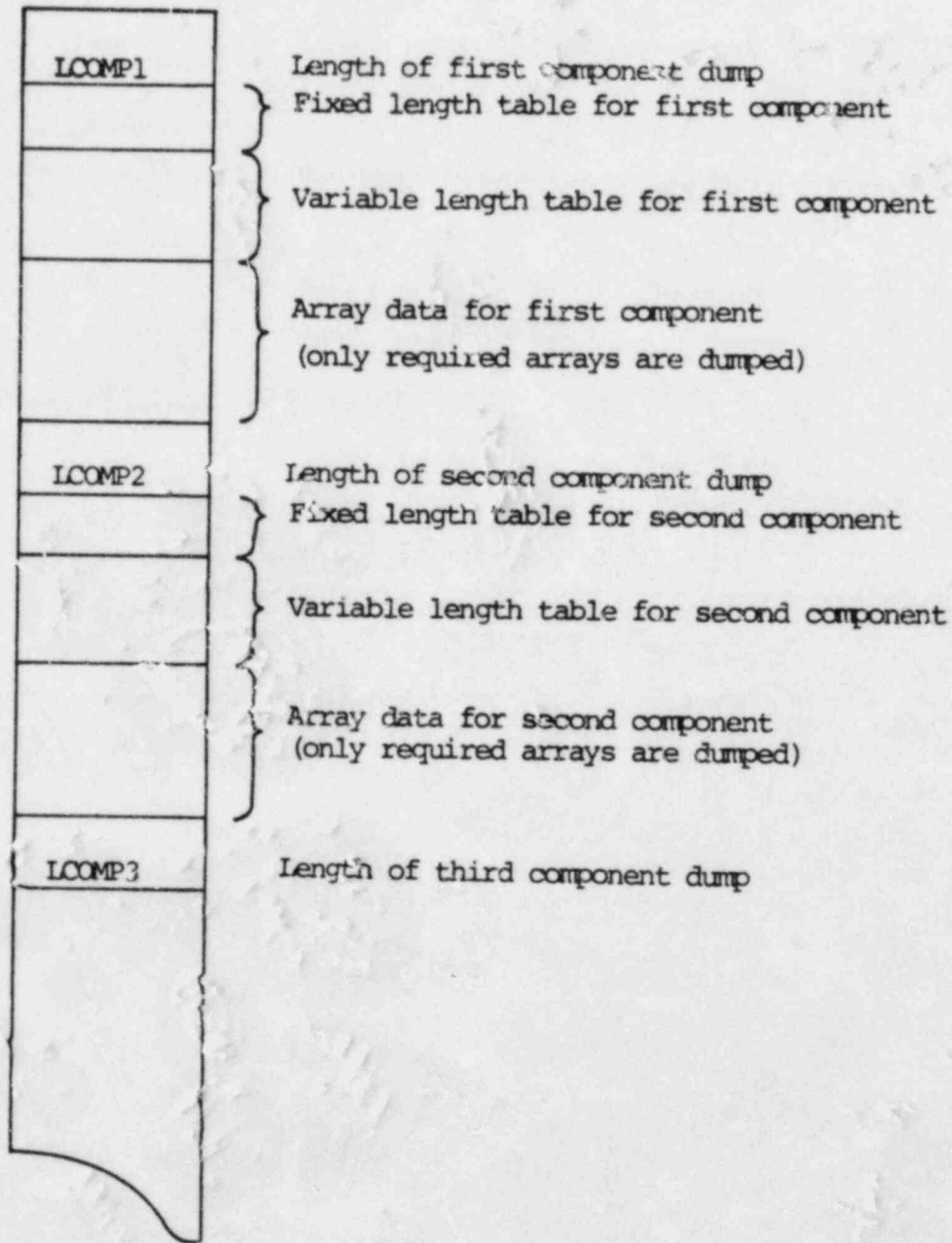


Fig. 57.
Component dump structure.

TABLE XXI

TRAC STORAGE ALLOCATIONS

<u>Storage Area</u>	<u>Size (Words)</u>
COMMON/LCMSP/	131 071
BLANK COMMON	20 000

Figure 58 displays the organization of the blank COMMON dynamic storage area in SCM. The fixed segment, which is described in Table XI, contains information that is used by all system component subroutines and, therefore, must remain in SCM throughout the calculation. The PWR-initialization data area, shown in Fig. 46, is required only during PWR-initialization calculations. Thus, this area does not affect storage requirements when no PWR initialization is performed.

The area that remains, marked as the component data area in Fig. 58, is available to each component when its data are in SCM. Each component type requires varying amounts of array space. Other than CORE, the required space for component types that are modeled with one-dimensional fluid dynamics is linear in the number of fluid cells, the number of heat-transfer nodes, and the product of these numbers. Table XXII lists the coefficients of these three quantities for each component type along with the constant requirement.

The CORE component requires

$$127*NCELLS+5*NODES*(NCELLS+1)+NRODS+2*NPWX+2*NRPRF+2*NPSRF+4*NDGX+4*NDHX$$

$$+7*NZMAX+3*NINT+NDRDS*(NZMAX+8)+(3*NINT+5*NDRDS+NPSZ+22)*(ICRU-ICRL)+79$$

words of space in the component data area. In addition,

$$NDRDS*NZMAX+ICRU-ICRL+1$$

words are required for each rod. The definitions of all the individual variables except NINT that are used in these expressions are given in the CORE

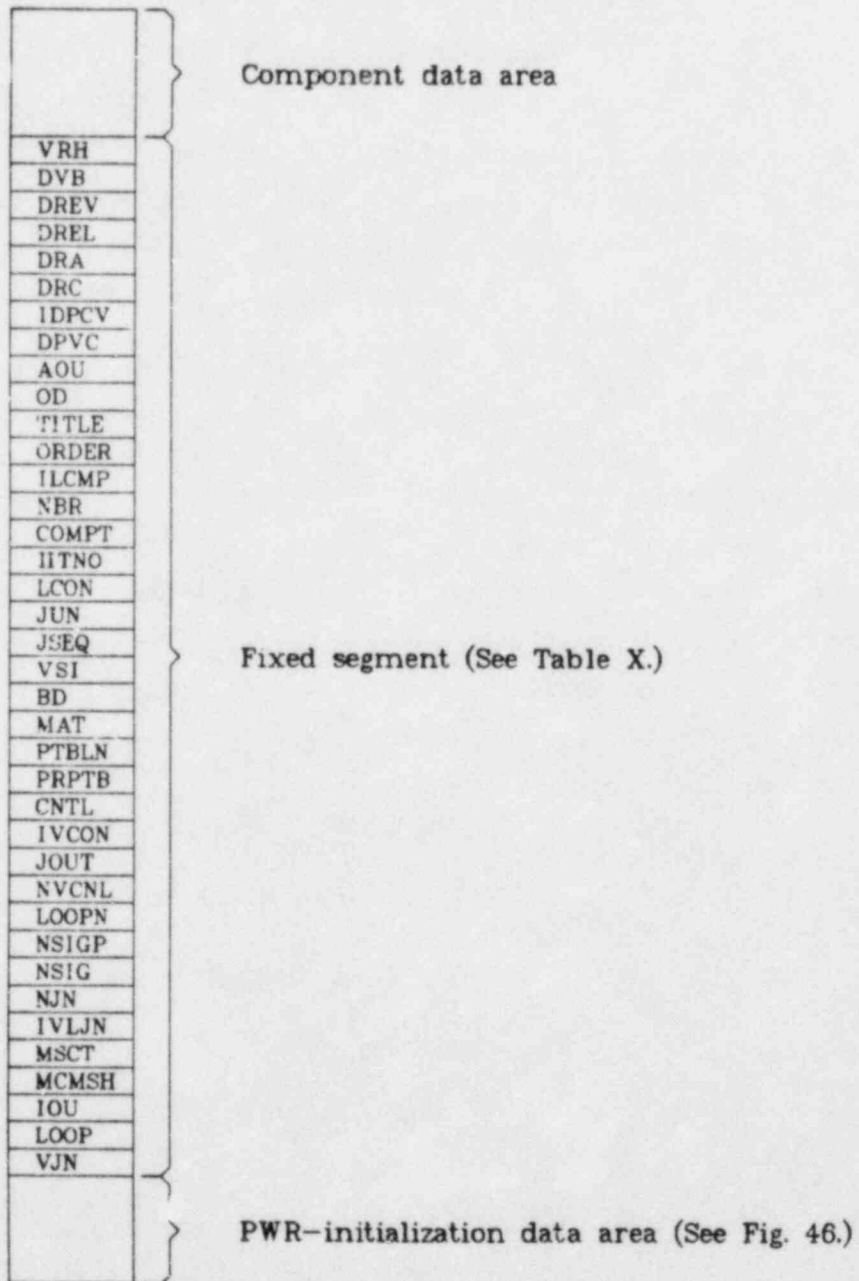


Fig. 58.
Blank COMMON dynamic storage area organization.

TABLE XXII

ONE-DIMENSIONAL COMPONENT ARRAY STORAGE REQUIREMENTS

Component Type	Coefficients for Total Array Requirements			
	Fixed	NCELLS	NODES	NCELLS*NODES
ACCUM	112	117	0	0
BREAK ^a	57	115	0	0
FILL ^b	57	115	0	0
PIPE ^c	55	120	4	5
PRIZER	112	116	0	0
PUMP ^d	141	120	4	5
STGEN ^e	158	122, 120, 117	4	5, 2, 2
TEE ^f	231	120	8	5
VALVE ^g	55	120	4	5

^aFor BREAKs, NCELLS \equiv 1 and NODES \equiv 0.

An additional $2 * [IBROP + \text{MAXO}(0, ISAT - 3)] * NBTB$ words are required for the BREAK tables.

^bFor FILLS, NCELLS \equiv 1 and NODES \equiv 0. An additional $2 * NFTX$ words are required when $IFTY > 3$. For $IFTY = 6$ and $IFTY = 9$, an additional $12 * NFTX$ words are required.

^cAn additional $2 * NPOWTB$ words are required for the PIPE power table.

^dEach PUMP also requires room for pump curves. The built-in Semiscale pump requires 332 additional words, whereas the built-in LOFT pump requires an additional 304 words. An additional $(NPMPTX + NPMPRF) * 2$ words are required for the pump-speed table.

^eThe STGENs can have up to four sets of cells: primary side, secondary side, primary tee, and secondary tee. The number of cells is denoted by NCELL1, NCELL2, NCELL3, and NCELL4, respectively. For the table, $NCELTT = NCELL3 + NCELL4$ (the total number of cells in the primary and secondary tees). The coefficients listed for expressions with NCELLS are for NCELL1, NCELL2, and NCELTT, respectively. Primary and secondary tees require an additional $(NODES + 117)$ words each.

^fThe TEES have two sets of cells but space is allocated in a uniform manner with $NCELLS = NCELL1 + NCELL2$.

^gThe VALVES also require $(NVOTB + NVCTB + NVRF) * 2$ words for the valve tables.

input data description (Sec. V.F.5.c). Variable NINT is the total number of interfaces between dissimilar materials in the rods.

The array data for the VESSEL component are subdivided into three categories: component, level, and rod. The component data arrays describe the overall VESSEL state and remain in SCM throughout the VESSEL calculation. These arrays require

$$4*NASX+2*NRSX+2*NTSX+36*NCSR+3*NODES+2*NRODS+2*NPWX+17*NTSX*ICRR+(NPSZ+1) \\ *(ICRU-ICRL)+6*NVENT+2*NPSZ+2*NPSRF+2*NRPRF+66$$

words of space in the component data area. The definitions of the individual variables used in this expression are given in the VESSEL input data description in Sec. V.F.5.k.

The VESSEL component data arrays remain in SCM throughout the VESSEL calculation; however, the level and rod data arrays are transferred to SCM only when they are needed. The hydrodynamic variables for each axial level in the VESSEL are transferred between SCM and LCM as a unit. At certain points in the calculation, three distinct levels of data must be in SCM simultaneously. Therefore, the maximum size of the data associated with a single level is one-third of the available space in SCM. Each level of data requires

$$143*NRSX*NTSX+8*NODHS*NRSX*NTSX+4*INHSM*NPSX*NTSX+NCSR+7*(ICRR*NSTX)$$

words of space.

In a similar manner, the heat-transfer data for each fuel rod are transferred between SCM and LCM as a unit. Because the data for only one rod must be in SCM at any point in the calculation, the rod data may extend over the available space in SCM. Each rod requires

$$(48+6*NODES+3*NINT)*(ICRU-ICRL)+7*NODES+3*NINT+(7+2*NODES) \\ *MAXO(NZMAX,ICRU-ICRL+1)+71$$

words of space, where NINT is the number of interfaces between dissimilar materials in the rods.

In addition to the component, level, and rod data arrays, an additional $NVCELL*(NVCELL+2)$ words of SCM space are needed for VESSEL components. This space is needed either for direct inversion of the vessel matrix when IITMAX = 0 or for solving the system by Gauss-Seidel iteration with coarse-mesh acceleration when IITMAX > 0. If IITMAX = 0, then NVCELL is the total number of vessel cells. If IITMAX > 0, NVCELL is the total number of vessel coarse-mesh regions.

The finite extent of the LCM component storage area (COMMON block LCMS) limits the total amount of component data that can be handled in a calculation. This amount is found by summing the SCM array requirements including all VESSEL levels and rods and adding the space required for the fixed-length, variable-length, and pointer tables for each component, as listed in Table XXIII. The graphics catalog, discussed in Sec. VI.F, also is stored in this LCM block. This area requires one word for each component plus six words for every catalog entry. Figure 59 shows the organization of LCMS.

TABLE XXIII
COMPONENT TABLE LENGTHS

<u>Component Type</u>	<u>Fixed Length Table</u>	<u>Variable Length Table</u>	<u>Pointer Table</u>
ACCUM	20	18	113
BREAK	20	13	113
CORE	20	132	199
FILL	20	17	116
PIPE	20	35	123
PRIZER	20	28	113
PUMP	20	62	146
STGEN	20	90	134
TEE	20	59	124
VALVE	20	41	126
VESSEL	20	169	238

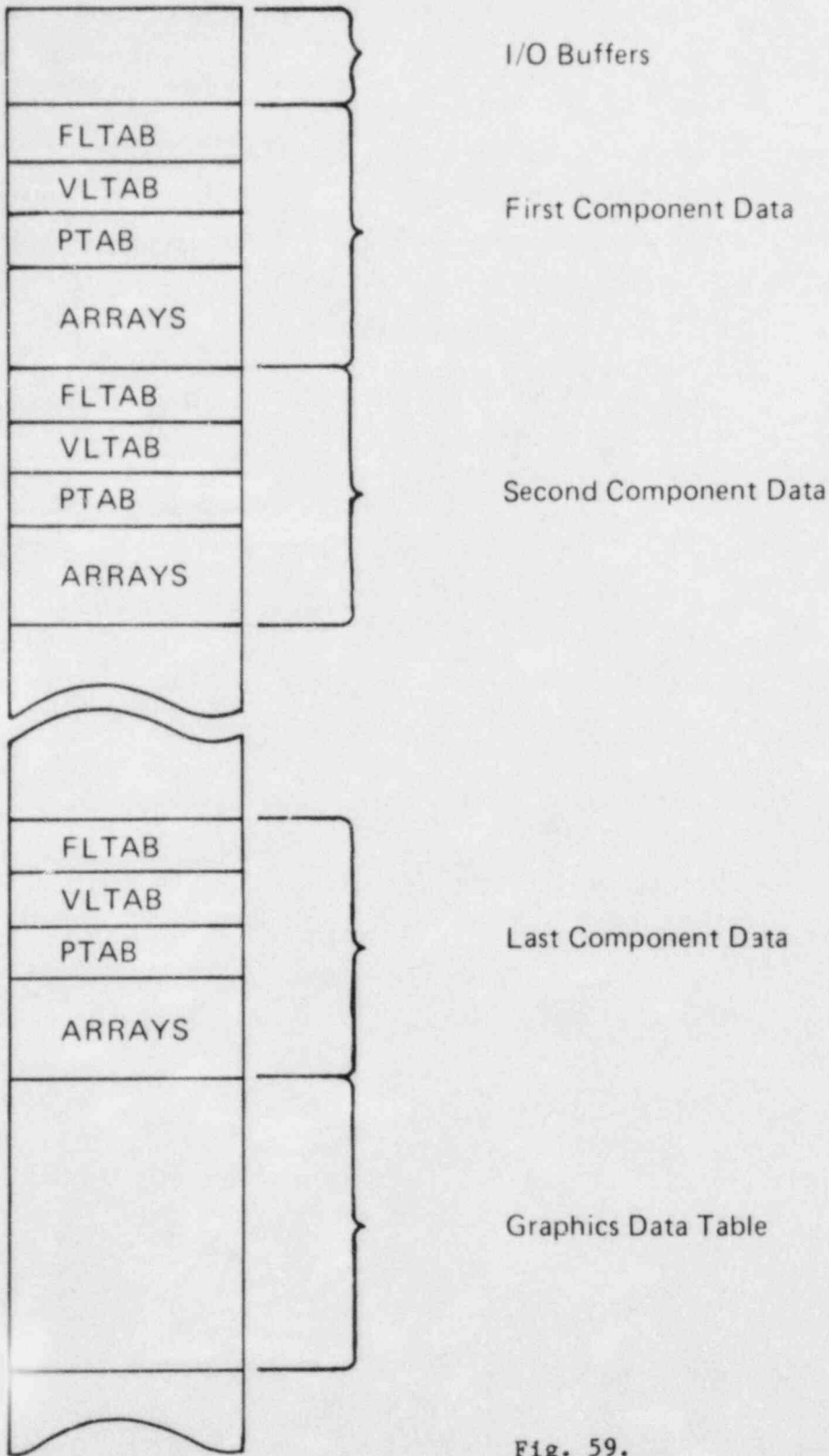


Fig. 59.
LCM data organization.

APPENDIX A

THERMODYNAMIC AND TRANSPORT FLUID PROPERTIES

The thermodynamic and transport properties subroutines used in TRAC are based on polynomial fits to steam table data for water and ideal gas behavior for the noncondensable gas component. Transport property fits were obtained from Ref. 52. The thermodynamic property routines are used by all TRAC component modules. Tables A-I through A-VII, which list the values of the constants, are given at the end of this appendix.

I. THERMODYNAMIC PROPERTIES

Subroutine THERMO supplies thermodynamic properties for TRAC. The input variables are the total pressure, the partial pressure of the noncondensable gas component, and the liquid and gas-phase temperatures. The output variables include the saturation temperature corresponding to total pressure; the saturation temperature corresponding to the partial pressure of steam; the specific internal energies of liquid, gas phase, and noncondensable; the saturated liquid and steam enthalpies corresponding to the partial pressure of steam; the liquid, gas-phase, and noncondensable densities; the derivatives of saturation temperatures and saturation enthalpies with respect to pressure; and, finally, the partial derivatives of liquid, steam, and noncondensable internal energies and densities with respect to pressure (at constant temperature) and with respect to temperature (at constant pressure).

The range of validity for the thermodynamic properties supplied by THERMO is:

$$280.0 \text{ K} \leq T_l \leq 647 \text{ K} ,$$

$$280.0 \text{ K} \leq T_g \leq 3000 \text{ K} ,$$

and

$$1.0 \times 10^3 \text{ Pa} \leq p \leq 190 \times 10^5 \text{ Pa} .$$

If THERMO is provided with data outside this range, it adjusts the data to the corresponding limit and issues a warning message.

Polynomial equations for the various properties used in THERMO are given below. Values of the constants are given in Tables A-I and A-II.

A. Saturation Properties

1. Saturation Temperature Corresponding to a Given Pressure.

$$T_s = C_1(A_{14}P)^{C_2} + C_3 \quad \text{for } T_s \leq C_{23} \quad , \quad (\text{higher saturation temperatures cause THERMO to abort}),$$

and

$$\frac{dT_s}{dp} = A_1(A_{14}P)^{A_2} \quad .$$

2. Internal Energy of Steam.

$$e_{vs} = C_6 + \frac{C_7}{C_8 + p_v} \quad ,$$

and

$$\frac{de_{vs}}{dp_v} = - \frac{C_7}{(C_8 + p_v)^2} \quad , \quad \text{for } p_v \leq C_{21} \quad ;$$

$$e_{vs} = C_{12} + (C_{14}p_v + C_{13})p_v \quad , \quad \text{and}$$

$$\frac{de_{vs}}{dp_v} = C_{13} + A_{17}p_v \quad , \quad \text{for } p_s > C_{21} \quad ;$$

where p_v is the partial pressure of steam.

3. Heat Capacity of Steam at Constant Pressure. Although the heat capacity of steam is not an output variable from THERMO, it is required in subsequent subcooled and superheated steam internal energy calculations.

$$c_{pvs} = C_{52} + T_1(C_{53}T_1 + C_{54}) + \frac{(\frac{C_{55}}{T_1} + C_{56})}{T_1} ;$$

and

$$\frac{dc_{pvs}}{dp_v} = -A_{15} \frac{dT_s}{dp_v} [C_{54} + 2C_{53}T_1 - \frac{(\frac{2C_{55}}{T_1} + C_{56})}{T_1^2}] ,$$

where T_s is the saturation temperature corresponding to the partial pressure of steam and $T_1 = 1.0 - A_{15} \cdot T_s$.

4. Enthalpy.

$$h_{vs} = e_{vs}\gamma_s$$

and

$$\frac{dh_{vs}}{dp_v} = \frac{de_{vs}}{dp_v} \gamma_s ,$$

where

$$\gamma_s = C_9 + (C_{11}p_v + C_{10})p_v , \quad \text{for } p_v \leq C_{21} ;$$

and

$$\gamma_s = C_{15} + (C_{17}p_v + C_{16})p_v, \quad \text{for } p_v > C_{21} .$$

$$h_{\ell s} = e_{\ell s} + \frac{p}{\rho_{\ell s}}$$

and

$$\frac{dh_{\ell s}}{dp} = \frac{de_{\ell s}}{dT_s} \frac{dT_s}{dp} + \frac{1}{\rho_{\ell s}} - \frac{p}{\rho_{\ell s}^2} \left[\left(\frac{\partial \rho_{\ell s}}{\partial p} \right)_T + \left(\frac{\partial \rho_{\ell s}}{\partial T} \right)_p \frac{dT_s}{dp} \right],$$

where $e_{\ell s}$, $\rho_{\ell s}$, and their derivatives are evaluated using the liquid equations given below.

B. Liquid Properties

1. Internal Energy. We define

$$TLC = T_\ell - 273.15 ,$$

$$PSL = \frac{\left[\frac{(T_\ell - C_3)}{C_1} \right]^{1/C_2}}{A_{14}} \quad (\text{saturation pressure corresponding to } T_\ell),$$

$$ELP = (p - PSL) \cdot (C_{k0} + C_{k2}PSL^2) ,$$

and

$$ERT = \frac{-C_{k0} + C_{k2} \cdot (2 \cdot PSL \cdot p - 3 \cdot PSL^2)}{A_1 \cdot (A_{14} \cdot PSL)^{A_2}} .$$

There are three temperature domains used in evaluating the liquid internal energy.

a. $T_\ell < 548.15 \text{ K}$.

$$e_\ell = \text{ELC0} + \text{ELC1} \cdot \text{TLC} + \text{ELC2} \cdot \text{TLC}^2 + \text{ELC3} \cdot \text{TLC}^3 + \text{ELC4} \cdot \text{TLC}^4 + \text{ELP} .$$

$$\left(\frac{\partial e_\ell}{\partial T_\ell}\right)_p = \text{DELCO} + \text{DELCl} \cdot \text{TLC} + \text{DELc2} \cdot \text{TLC}^2 + \text{DELc3} \cdot \text{TLC}^3 + \text{ERT} .$$

b. $548.15 \text{ K} \leq T_\ell \leq 611.15 \text{ K}$.

$$e_\ell = \text{ELD0} + \text{ELD1} \cdot \text{TLC} + \text{ELD2} \cdot \text{TLC}^2 + \text{ELD3} \cdot \text{TLC}^3 + \text{ELD4} \cdot \text{TLC}^4 + \text{ELP} .$$

$$\left(\frac{\partial e_\ell}{\partial T_\ell}\right)_p = \text{DELDO} + \text{DELD1} \cdot \text{TLC} + \text{DELD2} \cdot \text{TLC}^2 + \text{DELD3} \cdot \text{TLC}^3 + \text{ERT} .$$

c. $T_\ell > 611.15 \text{ K}$.

$$e_\ell = \text{ELE0} + \text{ELE1} \cdot \text{TLC} + \text{ELE2} \cdot \text{TLC}^2 + \text{ELE3} \cdot \text{TLC}^3 + \text{ELE4} \cdot \text{TLC}^4 + \text{ELP} .$$

$$\left(\frac{\partial e_\ell}{\partial T_\ell}\right)_p = \text{DELE0} + \text{DELE1} \cdot \text{TLC} + \text{DELE2} \cdot \text{TLC}^2 + \text{DELE3} \cdot \text{TLC}^3 + \text{ERT} .$$

For all three domains

$$\left(\frac{\partial e_\ell}{\partial p}\right)_{T_\ell} = c_{k0} + c_{k2} \cdot \text{PSL}^2 .$$

2. Density.

Define $PBAR = 1.0 \times 10^{-5} p$ and $TLC = T_{\ell} - 273.15$. There are three temperature domains.

a. $T_{\ell} > 525.15 \text{ K}$.

$$\rho_{\ell} = 1.43 + \frac{1000}{(CVH1 + CVH2 \cdot PBAR + CVH3 \cdot PBAR^2 + \beta_1 \cdot TLC + \gamma_1 \cdot TLC^2)} ,$$

$$\left(\frac{\partial \rho_{\ell}}{\partial p} \right)_{T_{\ell}} = - (\rho_{\ell} - 1.43)^2 \cdot 1.0 \times 10^{-8} [CVH2 + 2 \cdot CVH3 \cdot PBAR + TLC(CVH5 + 2 \cdot CVH6 \cdot PBAR) + TLC^2(CVH8 + 2 \cdot CVH9 \cdot PBAR)] ,$$

and

$$\left(\frac{\partial \rho_{\ell}}{\partial T_{\ell}} \right)_p = - (\rho_{\ell} - 1.43)^2 \cdot 1.0 \times 10^{-3} (\beta_1 + 2 \cdot \gamma_1 \cdot TLC) ,$$

where

$$\beta_1 = CVH4 + CVH5 \cdot PBAR + CVH6 \cdot PBAR^2$$

and

$$\gamma_1 = CVH7 + CVH8 \cdot PBAR + CVH9 \cdot PBAR^2 .$$

b. $T_\ell < 521.15 \text{ K} .$

$$\rho_\ell = \frac{1000}{(\text{CVL1} + \text{CVL2} \cdot \text{PBAR} + \text{CVL3} \cdot \text{PBAR}^2 + \beta_1 \cdot \text{TLC} + \gamma_1 \cdot \text{TLC}^2)} - 2.01 ,$$

$$\left(\frac{\partial \rho_\ell}{\partial p}\right)_{T_\ell} = -(\rho_\ell + 2.01)^2 \cdot 1.0 \times 10^{-8} [\text{CVL2} + 2 \cdot \text{CVL3} \cdot \text{PBAR} \\ + \text{TLC}(\text{CVL5} + 2 \cdot \text{CVL6} \cdot \text{PBAR}) + \text{TLC}^2(\text{CVL8} + 2 \cdot \text{CVL9} \cdot \text{PBAR})] .$$

$$\left(\frac{\partial \rho_\ell}{\partial T_\ell}\right)_p = -(\rho_\ell + 2.01)^2 \cdot 1.0 \times 10^{-3} (\beta_1 + 2 \cdot \gamma_1 \cdot \text{TLC}) ,$$

where

$$\beta_1 = \text{CVL4} + \text{CVL5} \cdot \text{PBAR} + \text{CVL6} \cdot \text{PBAR}^2$$

and

$$\gamma_1 = \text{CVL7} + \text{CVL8} \cdot \text{PBAR} + \text{CVL9} \cdot \text{PBAR}^2 .$$

c. $521.15 \text{ K} \leq T_\ell \leq 525.15 \text{ K} .$

An average of the functions in (a) and (b) above is used in this range.

Call the two values $\rho_{\ell a}$ and $\rho_{\ell b}$, then

$$\rho_\ell = \left(\frac{525.15 - T_\ell}{4.0}\right)\rho_{\ell b} + \left(\frac{T_\ell - 521.15}{4.0}\right)\rho_{\ell a} ,$$

$$\left(\frac{\partial \rho_\ell}{\partial p}\right)_{T_\ell} = \left(\frac{525.15 - T_\ell}{4.0}\right) \left(\frac{\partial \rho_{\ell b}}{\partial p}\right)_{T_\ell} + \left(\frac{T_\ell - 521.15}{4.0}\right) \left(\frac{\partial \rho_{\ell a}}{\partial p}\right)_{T_\ell} ,$$

and

$$\left(\frac{\partial \rho_\ell}{\partial T_\ell}\right)_p = \left(\frac{525.15 - T_\ell}{4.0}\right) \left(\frac{\partial \rho_{\ell b}}{\partial T_\ell}\right)_p + \left(\frac{T_\ell - 521.15}{4.0}\right) \left(\frac{\partial \rho_{\ell a}}{\partial T_\ell}\right)_p + \frac{\rho_{\ell a} - \rho_{\ell b}}{4.0} .$$

d. Residual Void Correction. After evaluation in sections (a) through (c), ρ_ℓ and its derivatives are corrected to reflect a residual void fraction. In the following, the values calculated by (a) through (c) above are denoted by a tilde (\sim).

$$(1) \quad p \geq 4.0 \times 10^5 \text{ Pa} .$$

$$\left(\frac{\partial \rho_\ell}{\partial T_\ell}\right)_p = \left(1 - \frac{1000}{p}\right) \left(\frac{\partial \tilde{\rho}_\ell}{\partial T_\ell}\right)_p ,$$

$$\left(\frac{\partial \rho_\ell}{\partial p}\right)_{T_\ell} = \left(1 - \frac{1000}{p}\right) \left(\frac{\partial \tilde{\rho}_\ell}{\partial p}\right)_{T_\ell} + \frac{1000 \tilde{\rho}_\ell}{p^2} ,$$

and

$$\rho_\ell = \left(1 - \frac{1000}{p}\right) \tilde{\rho}_\ell .$$

$$(2) \quad p < 4.0 \times 10^5 \text{ Pa} .$$

$$\left(\frac{\partial \rho_\ell}{\partial T_\ell}\right)_p = (0.995 + 6.25 \times 10^{-9} p) \left(\frac{\partial \tilde{\rho}_\ell}{\partial T_\ell}\right)_p ,$$

$$\left(\frac{\partial \rho_\ell}{\partial p}\right)_{T_\ell} = (0.995 + 6.25 \times 10^{-9} p) \left(\frac{\partial \tilde{\rho}_\ell}{\partial p}\right)_{T_\ell} + 6.25 \times 10^{-9} \tilde{\rho}_\ell ,$$

$$\rho_\ell = (0.995 + 6.25 \times 10^{-9} p) \tilde{\rho}_\ell .$$

3. Enthalpy. Enthalpy is not evaluated by the water property routines, but may be evaluated easily through

$$h_\ell = e_\ell + \frac{p}{\rho_\ell} .$$

C. Vapor Properties

1. Superheated Steam. $(T_g - T_s) > 0$, where T_s is the saturation temperature corresponding to partial pressure of steam.

a. Internal Energy.

$$e_v = e_{vs} + A_{12} \left[(T_g - T_s) + (T_g^2 - \beta)^{1/2} - \frac{T_s}{(A_{11}c_{pvs} - 1.0)} \right] ,$$

where

$$\beta = T_s^2 \left[1.0 - \frac{1.0}{(A_{11}c_{pvs} - 1.0)^2} \right] .$$

The internal energy derivatives are calculated as

$$\left(\frac{\partial e_v}{\partial T_g} \right)_{P_v} = \left[\frac{A_{13}}{2} \left(1.0 - \frac{\beta}{k^2} \right) \right]^{-1.0} ,$$

$$\left(\frac{\partial e_v}{\partial P_v} \right)_{T_g} = -\frac{1}{2} \left(\frac{\partial e_v}{\partial T_g} \right)_{P_v} \left[\left(1.0 - \frac{\beta}{k^2} \right) k'_p + \frac{1}{k} \frac{d\beta}{dP_v} \right] ,$$

where

$$k = A_{13}(e_v - e_s) + T_s \left[1.0 + \frac{1.0}{(A_{11}c_{pvs} - 1.0)} \right] ,$$

$$k'_p = -A_{13} \frac{de_{vs}}{dP_v} + \left[1.0 + \frac{1.0}{(A_{11}c_{pvs} - 1.0)} \right] \frac{dT_s}{dP_v}$$

$$- T_s A_{11} \left[\frac{1.0}{(A_{11}c_{pvs} - 1.0)^2} \right] \frac{dc_{pvs}}{dP_v} ,$$

and

$$\frac{d\beta}{dp} = \frac{2.0}{T_s} \left[\beta \left(\frac{dT_s}{dp_v} \right) + \frac{T_s^3 A_{11}}{(A_{11} c_{pvs} - 1.0)^3} \left(\frac{dc_{pvs}}{dp_v} \right) \right] .$$

b. Density.

$$\rho_v = \frac{p_v}{(\gamma_s - 1.0)e_{vs} + C_{26}(e_v - e_{vs})} ,$$

$$\left(\frac{\partial \rho_v}{\partial T_g} \right)_{p_v} = - \left(\frac{\partial e_v}{\partial T_g} \right)_{p_v} \left[\frac{C_{26} \rho_v}{(\gamma_s - 1.0)e_{vs} + C_{26}(e_v - e_{vs})} \right] ,$$

and

$$\begin{aligned} \left(\frac{\partial \rho_v}{\partial p_v} \right)_{T_g} &= \rho_v \left\{ \frac{1.0}{p_v} - \left[e_{vs} \left(\frac{d\gamma_s}{dp_v} \right) + (\gamma_s - 1.0 - C_{26}) \frac{de_{vs}}{dp_v} \right] \right. \\ &\quad \left. \cdot \left[\frac{1.0}{(\gamma_s - 1.0)e_{vs} + C_{26}(e_v - e_{vs})} \right] \right\} + \left(\frac{\partial \rho_v}{\partial e_v} \right) \left(\frac{\partial e_v}{\partial p_v} \right)_{T_g} , \end{aligned}$$

where

$$\frac{d\gamma_s}{dp_v} = C_{10} + A_{16} p_v \quad \text{for } p_v \leq C_{21} ,$$

$$\frac{d\gamma_s}{dp_v} = C_{16} + A_{18} p_v \quad \text{for } p_v > C_{21} ,$$

and

$$\frac{\partial \rho_v}{\partial e_v} = \frac{-C_{26} \rho_v}{[(\gamma_s - 1.0)e_{vs} + C_{26}(e_v - e_{vs})]} .$$

If ρ_v exceeds $0.9 \rho_l$ or is less than zero, the above is superceded by

$$\rho_v = 0.9 \rho_l ,$$

$$\left(\frac{\partial \rho_v}{\partial T_g}\right)_{P_v} = 0.9 \left(\frac{\partial \rho_l}{\partial T_l}\right)_P ,$$

and

$$\left(\frac{\partial \rho_v}{\partial P_v}\right)_{T_g} = 0.9 \left(\frac{\partial \rho_l}{\partial P}\right)_{T_l} .$$

c. Enthalpy. Enthalpy is not evaluated by the water property routines, but may be calculated easily through

$$h_v = e_v + \frac{P_v}{\rho_v} .$$

2. Subcooled Vapor. $(T_g - T_s) \leq 0$

a. Internal Energy.

$$e_v = e_{vs} + (T_g - T_s) \frac{c_{pvs}}{C_{24}} ,$$

$$\left(\frac{\partial e_v}{\partial T_g}\right)_{p_v} = \frac{c_{pvs}}{C_{24}} ,$$

$$\left(\frac{\partial e_v}{\partial p_v}\right)_{T_g} = - \left(\frac{\partial e_v}{\partial T_g}\right)_{p_v} \left\{ \frac{dT_s}{dp_v} - \left(\frac{C_{24}}{c_{pvs}}\right) \left[\frac{de_{vs}}{dp_v} + \frac{(e_v - e_{vs})}{c_{pvs}} \left(\frac{dc_{pvs}}{dp_v}\right) \right] \right\} .$$

b. Density. The formulas are identical to the superheated vapor case above, but the subcooled vapor energy is used in this case.

c. Enthalpy. Enthalpy is not evaluated by the water property routines, but may be calculated easily through

$$h_v = e_v + \frac{p_v}{\rho_v} .$$

3. Noncondensable Gas (Air).

a. Internal Energy.

$$e_a = c_{va} T_g ,$$

$$\left(\frac{\partial e_a}{\partial T_g}\right)_{p_a} = c_{va} ,$$

and

$$\left(\frac{\partial e_a}{\partial p_a}\right)_{T_g} = 0.0 .$$

b. Density.

$$\rho_a = \frac{P_a}{R_a T_g} ,$$

$$\left(\frac{\partial \rho_a}{\partial P_a}\right)_{T_g} = \frac{1.0}{R_a T_g} ,$$

and

$$\left(\frac{\partial \rho_a}{\partial T_g}\right)_{P_a} = -R_a \rho_a \left(\frac{\partial \rho_a}{\partial P_a}\right)_{T_g} ,$$

where R_a is the gas constant for air.

II. TRANSPORT PROPERTIES

Subroutine FPROP is used to obtain transport properties for water and the noncondensable gas. The input variables for this routine are the saturation temperature, pressure, enthalpies of each phase, vapor density, and the vapor temperature. The output transport variables include the latent heat of vaporization, surface tension, constant pressure specific heat, viscosity, and thermal conductivity of steam, the liquid, and the noncondensable gas. The transport property calls are function calls within the FPROP subroutine. The polynomial equation fits for the transport properties used in FPROP are described. Note that the curve fits for σ and c_{pl} have been updated since TRAC-PlA. Values of the constants are given in Tables A-III through A-VII.

A. Latent Heat of Vaporization

The latent heat of vaporization is calculated as

$$h_{lv} = h_{vs} - h_{ls} ,$$

where h_{vS} and h_{lS} are calculated according to Appendix A, Sec. I. A.

B. Constant Pressure Specific Heats

Constants used in this section are given in Table A-III.

$$c_{pl} = \{h_l[h_l(D_{0l} + D_{1l}p) + (C_{0l} + C_{1l}p)] + B_{0l} + B_{1l}p\}^{-1}$$

and

$$c_{pv} = C_{1g} + C_{2g}T_g + \frac{C_{3g}p}{(C_{5g}T_g - C_{6g})^{2.4}} + \frac{C_{4g}p^3}{(C_{5g}T_g - C_{6g})^9} .$$

Because these values are used only for calculating heat-transfer coefficients, these fits were chosen for simplicity and smoothness and are not necessarily consistent with those derivable from the thermodynamic routines.

The specific heat of the noncondensable gas is 1037.

C. Fluid Viscosities

1. Liquid. Constants used in this section are given in Table A-IV. The evaluation of liquid viscosity is divided into three different enthalpy ranges. For $h_l \leq h_1$,

$$\mu_l = (A_{0l} + A_{1l}x + A_{2l}x^2 + A_{3l}x^3 + A_{4l}x^4) - (B_{0l} + B_{1l}\eta + B_{2l}\eta^2 + B_{3l}\eta^3)(p - p_f) ,$$

where

$$x = (h_l - c_{0n})h_0$$

and

$$\eta = (h_l - e_{c0n})e_{h0} .$$

In the range $h_1 < h \leq h_2$,

$$\mu_l = (E_{0l} + E_{1l}h_l + E_{2l}h_l^2 + E_{3l}h_l^3) \\ + (F_{0l} + F_{1l}h_l + F_{2l}h_l^2 + F_{3l}h_l^3)(p - p_1) .$$

For $h_l > h_2$,

$$\mu_l = (D_{0l} + D_{1l}z + D_{2l}z^2 + D_{3l}z^3 + D_{4l}z^4) ,$$

where

$$z = (h_l - c_n)h_{00} .$$

2. Steam. Constants used in this section are given in Table A-V. Three vapor temperature ranges are used to represent the data.

a. $T_g \leq T_1$.

$$\mu_v = [B_{1g}(T_g - 273.15) + C_{1g}] - \rho_v[D_{1g} - E_{1g}(T_g - 273.15)] .$$

If $\mu_v < 10^{-7}$, it is set to that value.

b. $T_1 < T_g < T_2$.

$$\mu_v = B_{1g}(T_g - 273.15) + C_{1g} + \rho_v[F_{1g} + F_{2g}(T_g - 273.15) \\ + F_{3g}(T_g - 273.15)^2 + F_{4g}(T_g - 273.15)^2] \\ + \rho_v[G_{1g} + G_{2g}(T_g - 273.15) + G_{3g}(T_g - 273.15)^2 \\ + G_{4g}(T_g - 273.15)^3] (A_{0g} + A_{1g}\rho_v + A_{2g}\rho_v^2) .$$

c. $T_g \geq T_2$.

$$\mu_v = B_{1g}(T_g - 273.15) + C_{1g} + \rho_v(A_{0g} + A_{1g}\rho_v + A_{2g}\rho_v^2) .$$

d. Noncondensable Gas. For the noncondensable gas, two ranges of T_g are used.

$$(1) \quad \underline{T_g \leq 502.15 \text{ K} .}$$

$$\mu_a = H_{\ell 1} + H_{\ell 2}(T_g - 273.15) + H_{\ell 3}(T_g - 273.15)^2 .$$

$$(2) \quad \underline{T_g > 502.15 \text{ K} .}$$

$$\mu_a = H_{u1} + H_{u2}(T_g - 273.15) + H_{u3}(T_g - 273.15)^2 .$$

D. Fluid Thermal Conductivities

The liquid thermal conductivity is given by

$$k_{\ell} = A_{\ell 0} + A_{\ell 1}x_k + A_{\ell 2}x_k^2 + A_{\ell 3}x_k^3 ,$$

where

$$x_k = \frac{h_{\ell}}{h_0} ,$$

and the constants are given in Table A-VI.

The steam thermal conductivity is given by

$$k_v = x_1 + \rho_v \left[x_2 + \frac{C_{p_v}}{(T_g - 273.15)^{4.2}} \right] ,$$

where

$$x_1 = A_{g0} + A_{g1}(T_g - 273.15) + A_{g2}(T_g - 273.15)^2 + A_{g3}(T_g - 273.15)^3$$

and

$$x_2 = B_{g0} + B_{g1}(T_g - 273.15) + B_{g2}(T_g - 273.15)^2 .$$

However, the minimum permitted value for k_v is 1.0×10^{-4} .

The thermal conductivity of the noncondensable gas is 0.0228.

E. Surface Tension

Above 647.3 K the surface tension is zero. Below this temperature it is given by

$$\sigma = C_{21}T_R^2 + A_3T_R^3 + A_4T_R^4 + A_5T_R^5 ,$$

where

$$C_{21} = A_2 + \frac{A_1}{1.0 + B \cdot T_R} ,$$

$$T_R = 647.3 - T_g ,$$

and the constants are given in Table A-VII.

III. VERIFICATION

The thermodynamic and transport property fits¹⁸ used in TRAC have been compared with steam table data over a wide range of parameters. The agreement is satisfactory in the saturation region and in the superheated steam region for $1.0 \times 10^5 \text{ Pa} < p < 100.0 \times 10^5 \text{ Pa}$ and $423.0 \text{ K} < T^g < 823.0 \text{ K}$. The agreement also is good in the subcooled water region for $373.0 \text{ K} < T_l < 523.0 \text{ K}$ and $0.4178 \times 10^6 \text{ J/kg} < e_l < 1.0808 \times 10^6 \text{ J/kg}$.

Further verification was performed by comparing the TRAC polynomial fits with the WATER package⁵² over a wider range of nonequilibrium (99 K of both superheat and subcooling) for a pressure variation of $1.0 \times 10^5 \text{ Pa}$

to 2.0×10^7 Pa. The comparisons showed good agreement for both the thermodynamic and transport properties throughout the saturation and nonequilibrium regions except for very extreme cases. For instance, the vapor specific-heat-equation fit used in TRAC diverges to infinity at saturation conditions above 1.8×10^7 -Pa pressure. Also, at high degrees of subcooling or superheat, some inconsistencies are noticed. Because no data exist for comparison in these extreme cases, it is impossible to compare TRAC and the WATER package adequately.

In conclusion, for most TRAC applications, the thermodynamic and transport property routines provide realistic values over a wide range. The simplified polynomial fits provide an efficient and low-cost method compared to other approaches such as steam table interpolation.

TABLE A-I
POLYNOMIAL CONSTANTS FOR THERMO

C_1	= 117.8	C_{24}	= 1.3
C_2	= 0.223	C_{26}	= 0.3
C_3	= 255.2	C_{28}	= 1.0×10^5
C_4	= 958.75	C_{40}	= 273.0
C_5	= -0.856 6	C_{41}	= 239.36
C_6	= 2.619 410 618 $\times 10^6$	C_{42}	= 2.786 7
C_7	= -4.995×10^{10}	C_{43}	= -5.776 26
C_8	= 3.403×10^5	C_{44}	= 3.938
C_9	= 1.066 554 48	C_{45}	= 1.0×10^{-6}
C_{10}	= 1.02×10^{-8}	C_{47}	= 1.0×10^3
C_{11}	= -2.548×10^{-15}	C_{48}	= -0.15×10^3
C_{12}	= 2.589 600 $\times 10^6$	C_{49}	= -20.0
C_{13}	= 6.350×10^{-3}	C_{51}	= 0.657×10^{-6}
C_{14}	= $-1.058 2 \times 10^{-9}$	C_{52}	= 2.996 018 036 $\times 10^3$
C_{15}	= 1.076 4	C_{53}	= 9.700 016 602 $\times 10^3$
C_{16}	= 3.625×10^{-10}	C_{54}	= $-8.448 077 393 \times 10^3$
C_{17}	= -9.063×10^{-17}	C_{55}	= 8.349 824
C_{20}	= 461.7	C_{56}	= 3.495 194 44 $\times 10^2$
C_{21}	= 2.0×10^6	C_{k0}	= $-8.335 44 \times 10^{-4}$
C_{23}	= 647.3	C_{k2}	= $-2.247 45 \times 10^{-17}$

TABLE A-I (cont.)

ELC0 = $1.758\ 80 \times 10^4$
 ELC1 = $3.740\ 2 \times 10^3$
 ELC2 = 4.024 35
 ELC3 = -0.015 729 4
 ELC4 = $3.130\ 1 \times 10^{-5}$

ELD0 = $6.185\ 27 \times 10^6$
 ELD1 = $-8.145\ 47 \times 10^4$
 ELD2 = $4.465\ 98 \times 10^2$
 ELD3 = -1.041 16
 ELD4 = $9.260\ 22 \times 10^{-4}$

CVH1 = 1.002 136 23
 CVH2 = $-5.632\ 785 \times 10^{-5}$
 CVH3 = $-8.971\ 304\ 77 \times 10^{-9}$
 CVH4 = $-2.282\ 874\ 59 \times 10^{-5}$
 CVH5 = $4.765\ 967\ 87 \times 10^{-7}$
 CVH6 = $5.021\ 318 \times 10^{-10}$
 CVH7 = $4.101\ 156\ 58 \times 10^{-6}$
 CVH8 = $-3.803\ 989\ 08 \times 10^{-9}$
 CVH9 = $-1.421\ 997\ 52 \times 10^{-12}$

ELE0 = $2.283\ 789\ 029 \times 10^9$
 ELE1 = $-2.622\ 156\ 77 \times 10^7$
 ELE2 = $1.129\ 486\ 67 \times 10^5$
 ELE3 = $-2.162\ 339\ 85 \times 10^2$
 ELE4 = 0.155 283 438

C_{va} = 714.9
 R_a = 287.12

CVL1 = 2.252 62
 CVL2 = 0.014 859 4
 CVL3 = $-7.154\ 88 \times 10^{-5}$
 CVL4 = 0.010 458 8
 CVL5 = $-1.029\ 62 \times 10^{-4}$
 CVL5 = $5.091\ 35 \times 10^{-7}$
 CVL7 = $2.592\ 66 \times 10^{-5}$
 CVL8 = $1.724\ 1 \times 10^{-7}$
 CVL9 = $-8.984\ 19 \times 10^{-10}$

TABLE A-II

DERIVED CONSTANTS FOR THERMODYNAMIC PROPERTIES OF WATER AND AIR

A_1	$= C_1 \cdot C^2 / C_{28}$	A_{11}	$= 2 \cdot C_{26} / (C_{24} \cdot C_{20})$
A_2	$= C_2 - 1.0$	A_{13}	$= A_{11} \cdot (1.0 + C_{26})$
A_3	$= -C_4 \cdot C^5 / C_{23}$	A_{12}	$= 1.0 / A_{13}$
A_4	$= C_5 - 1.0$	A_{14}	$= 1.0 / C_{28}$
A_5	$= C_{45} \cdot C_{49}$	A_{15}	$= 1.0 / C_{23}$
A_6	$= 2 \cdot C_{45} \cdot C_{48}$	A_{16}	$= 2 \cdot C_{11}$
A_7	$= 4 \cdot C_{44} \cdot C_{45}$	A_{17}	$= 2 \cdot C_{14}$
A_8	$= 3 \cdot C_{43} \cdot C_{45}$	A_{18}	$= 2 \cdot C_{17}$
A_9	$= 2 \cdot C_{42} \cdot C_{45}$	A_{19}	$= 2 \cdot C_{48} \cdot C_{45}$
A_{10}	$= C_{41} \cdot C_{45}$	A_{20}	$= C_{45} \cdot C_{49}$
$DELCO$	$= ELC1$	$DELDO$	$= ELD1$
$DELC1$	$= 2 \cdot ELC2$	$DELD1$	$= 2 \cdot ELD2$
$DELC2$	$= 3 \cdot ELC3$	$DELD2$	$= 3 \cdot ELD3$
$DELC3$	$= 4 \cdot ELC4$	$DELD3$	$= 4 \cdot ELD4$
$DELE0$	$= ELE1$		
$DELE1$	$= 2 \cdot ELE2$		
$DELE2$	$= 3 \cdot ELE3$		
$DELE3$	$= 4 \cdot ELE4$		

TABLE A-III

BASIC CONSTANTS FOR TRANSPORT PROPERTIES OF WATER AND AIR

$$\begin{aligned} H_{g0} &= 2.739\ 623\ 397 \times 10^6 \\ H_{g1} &= 3.758\ 844\ 554 \times 10^{-2} \\ H_{g2} &= -7.163\ 990\ 945 \times 10^{-9} \\ H_{g3} &= 4.200\ 231\ 947 \times 10^{-16} \\ H_{g4} &= 9.850\ 752\ 122 \times 10^{-24} \end{aligned}$$

$$\begin{aligned} B_{0l} &= 2.394\ 907 \times 10^{-4} & B_{1l} &= -5.196\ 250 \times 10^{-13} \\ C_{0l} &= 1.193\ 203 \times 10^{-11} & C_{1l} &= 2.412\ 704 \times 10^{-18} \\ D_{0l} &= -3.944\ 067 \times 10^{-17} & D_{1l} &= -1.680\ 771 \times 10^{-24} \end{aligned}$$

$$\begin{aligned} C_{1g} &= 1.688\ 359\ 68 \times 10^3 \\ C_{2g} &= 0.602\ 985\ 6 \\ C_{3g} &= 4.820\ 979\ 623 \times 10^2 \\ C_{4g} &= 2.953\ 179\ 05 \times 10^7 \\ C_{5g} &= 1.8 \\ C_{6g} &= 4.60 \times 10^2 \end{aligned}$$

TABLE A-IV

LIQUID VISCOSITY CONSTANTS

$$\begin{aligned}
 A_{0l} &= 1.299\ 470\ 229 \times 10^{-3} \\
 A_{1l} &= -9.264\ 032\ 108 \times 10^{-4} \\
 A_{2l} &= 3.810\ 470\ 61 \times 10^{-4} \\
 A_{3l} &= -8.219\ 444\ 458 \times 10^{-5} \\
 A_{4l} &= 7.022\ 437\ 984 \times 10^{-6}
 \end{aligned}$$

$$\begin{aligned}
 B_{0l} &= -6.595\ 9 \times 10^{-12} \\
 B_{1l} &= -6.763 \times 10^{-12} \\
 B_{2l} &= -2.888\ 25 \times 10^{-12} \\
 B_{3l} &= 4.452\ 5 \times 10^{-13}
 \end{aligned}$$

$$\begin{aligned}
 D_{0l} &= 3.026\ 032\ 306 \times 10^{-4} \\
 D_{1l} &= -1.836\ 606\ 896 \times 10^{-4} \\
 D_{2l} &= 7.567\ 075\ 775 \times 10^{-5} \\
 D_{3l} &= -1.647\ 878\ 879 \times 10^{-5} \\
 D_{4l} &= 1.416\ 457\ 633 \times 10^{-6}
 \end{aligned}$$

$$\begin{aligned}
 E_{0l} &= 1.452\ 605\ 261\ 2 \times 10^{-3} \\
 E_{1l} &= -6.988\ 008\ 498\ 5 \times 10^{-9} \\
 E_{2l} &= 1.521\ 023\ 033\ 4 \times 10^{-14} \\
 E_{3l} &= -1.230\ 319\ 494\ 6 \times 10^{-20}
 \end{aligned}$$

$$\begin{aligned}
 F_{0l} &= -3.806\ 350\ 753\ 3 \times 10^{-11} \\
 F_{1l} &= 3.928\ 520\ 767\ 7 \times 10^{-16} \\
 F_{2l} &= -1.258\ 579\ 929\ 2 \times 10^{-21} \\
 F_{3l} &= 1.286\ 018\ 078\ 8 \times 10^{-27}
 \end{aligned}$$

$$\begin{aligned}
 h_0 &= 8.581\ 289\ 699 \times 10^{-6} \\
 c_{0n} &= 4.265\ 884 \times 10^4 \\
 p_f &= 6.894\ 575\ 293 \times 10^5
 \end{aligned}$$

$$\begin{aligned}
 h_{00} &= 3.892\ 077\ 365 \times 10^{-6} \\
 e_{c0n} &= 5.575\ 88 \times 10^4 \\
 h_1 &= 2.76 \times 10^5
 \end{aligned}$$

$$\begin{aligned}
 e_{h0} &= 6.484\ 503\ 981 \times 10^{-6} \\
 c_n &= 4.014\ 676 \times 10^5 \\
 h_2 &= 3.94 \times 10^5
 \end{aligned}$$

TABLE A-V
VAPOR VISCOSITY CONSTANTS

$$\begin{aligned} A_{0g} &= 3.53 \times 10^{-8} \\ A_{1g} &= 6.765 \times 10^{-11} \\ A_{2g} &= 1.021 \times 10^{-14} \end{aligned}$$

$$\begin{aligned} B_{1g} &= 0.407 \times 10^{-7} \\ C_{1g} &= 8.04 \times 10^{-6} \\ D_{1g} &= 1.858 \times 10^{-7} \\ E_{1g} &= 5.9 \times 10^{-10} \end{aligned}$$

$$\begin{aligned} F_{1g} &= -0.2885 \times 10^{-5} \\ F_{2g} &= 0.2427 \times 10^{-7} \\ F_{3g} &= -0.6789333 \times 10^{-10} \\ F_{4g} &= -0.6317037037 \times 10^{-13} \end{aligned}$$

$$\begin{aligned} G_{1g} &= 176.0 \\ G_{2g} &= -1.6 \\ G_{3g} &= 0.0048 \\ G_{4g} &= -0.474074074 \times 10^{-5} \end{aligned}$$

$$\begin{aligned} H_{\ell 1} &= 1.708 \times 10^{-5} \\ H_{\ell 2} &= 5.927 \times 10^{-8} \\ H_{\ell 3} &= 8.14 \times 10^{-11} \end{aligned}$$

$$\begin{aligned} H_{u1} &= 1.735 \times 10^{-5} \\ H_{u2} &= 4.193 \times 10^{-8} \\ H_{u3} &= 1.09 \times 10^{-11} \end{aligned}$$

$$\begin{aligned} T_1 &= 573.15 \\ T_2 &= 648.15 \end{aligned}$$

TABLE A-VI

THERMAL CONDUCTIVITY CONSTANTS

$$\begin{aligned}
 h_0 &= 5.815 \times 10^5 \\
 A_{\ell 0} &= 0.573\ 738\ 622 \\
 A_{\ell 1} &= 0.253\ 610\ 355\ 1 \\
 A_{\ell 2} &= -0.145\ 468\ 269 \\
 A_{\ell 3} &= -0.013\ 874\ 724\ 85
 \end{aligned}$$

$$C = 2.148\ 2 \times 10^5$$

$$\begin{aligned}
 A_{g0} &= 1.76 \times 10^{-2} \\
 A_{g1} &= 5.87 \times 10^{-5} \\
 A_{g2} &= 1.04 \times 10^{-7} \\
 A_{g3} &= -4.51 \times 10^{-11}
 \end{aligned}$$

$$\begin{aligned}
 B_{g0} &= 1.035\ 1 \times 10^{-4} \\
 B_{g1} &= 0.419\ 8 \times 10^{-6} \\
 B_{g2} &= -2.771 \times 10^{-11}
 \end{aligned}$$

TABLE A-VII

SURFACE TENSION CONSTANTS

$$\begin{aligned}
 A_1 &= 1.160\ 936\ 807 \times 10^{-4} \\
 A_2 &= 1.121\ 404\ 68 \times 10^{-6} \\
 A_3 &= -5.752\ 805\ 18 \times 10^{-9} \\
 A_4 &= 1.286\ 274\ 65 \times 10^{-11} \\
 A_5 &= -1.149\ 719\ 29 \times 10^{-14} \\
 B &= 0.83
 \end{aligned}$$

APPENDIX B
MATERIAL PROPERTIES

I. INTRODUCTION

An extensive library of temperature-dependent material properties is incorporated in TRAC. The entire library is accessible by the vessel component; however, the ex-vessel components have access to structural material property sets only. Twelve sets of material properties comprise the library; each set supplies values for thermal conductivity, specific heat, density, and spectral emissivity for use in the heat-transfer calculations. The first 5 sets and set 11 contain properties for nuclear-heated or electrically heated fuel-rod simulation. Included are: nuclear fuels, Zircaloy cladding, fuel-cladding gap gases, electrical heater rod filaments, electrical heater rod insulating material, and Zircaloy dioxide. Sets 6-10 and 12 are for structural materials including stainless steels, carbon steel, and Inconels. In addition, fuel and clad coefficients of thermal expansion, obtained from MATPRO (Ref. 53) subroutines FTHEX and CDTHEX, are available when the gap conductance thermal expansion model is used.

Figure B-1 illustrates the calling tree for obtaining the property values. The subroutines MFROD and MPROP are simple processors for calculating the average temperature and calling the appropriate subroutine based on the user-specified material index. Subroutine FROD controls the fuel-clad gap conductance and fuel-rod thermal conduction calculations. The material indexes in the library are:

- 1 -- mixed oxide fuel;
- 2 -- Zircaloy;
- 3 -- gap gases;
- 4 -- boron nitride insulation;
- 5 -- Constantan/Nichrome heater;
- 6 -- stainless steel, type 304;
- 7 -- stainless steel, type 316;
- 8 -- stainless steel, type 347;
- 9 -- carbon steel, type A508;
- 10 -- Inconel, type 718;

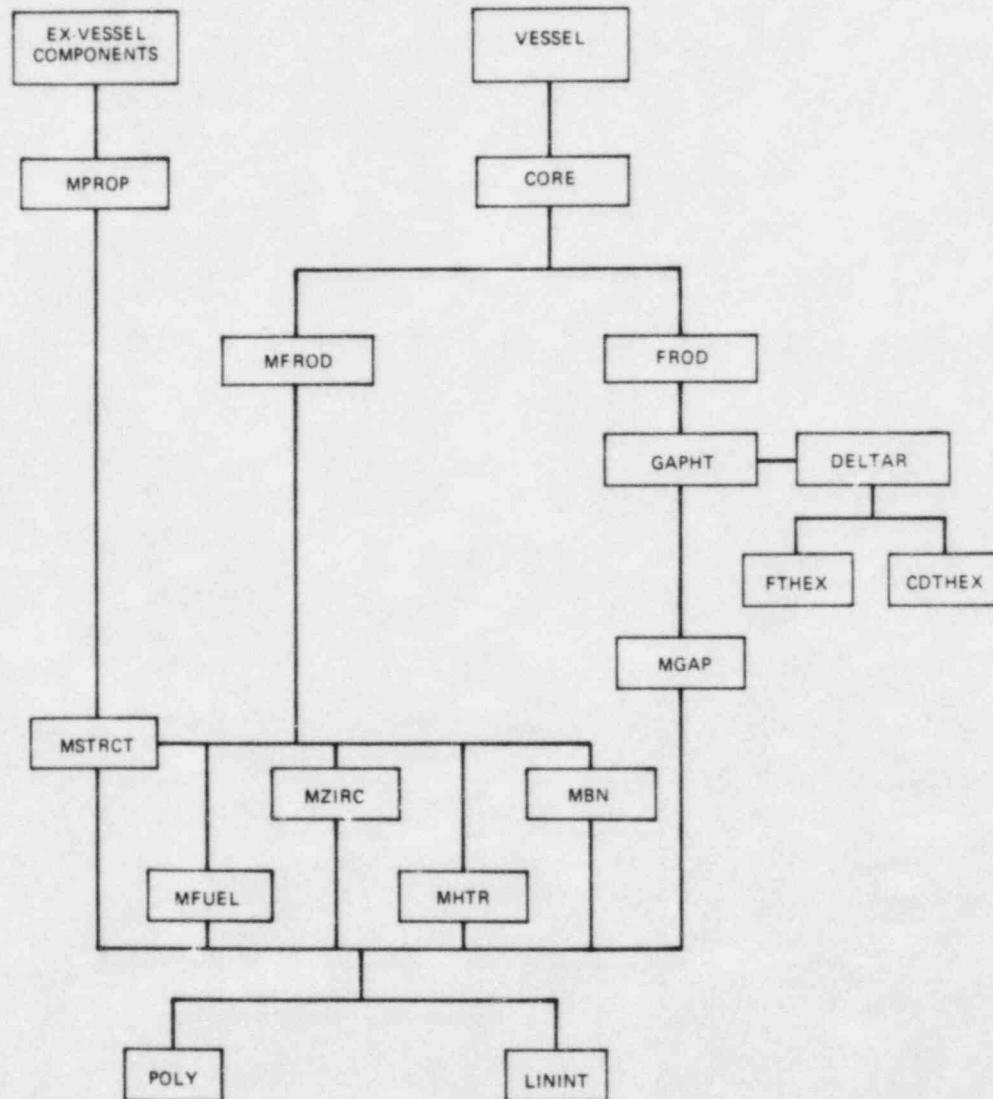


Fig. B-1.
Material properties code organization.

- 11 -- Zircaloy dioxide; and
- 12 -- Inconel, type 600.

Gap gas properties are calculated only when the dynamic fuel-clad gap HTC option is used (NFCI = 1).

II. NUCLEAR FUEL MIXED-OXIDE PROPERTIES

Subroutine MFUEL calculates the properties for mixed-oxide (UO_2 and PuO_2) nuclear fuels. Values obtained are influenced by three user-specified input variables: the fraction of theoretical density, the fraction of plutonium oxide in the fuel, and the fuel burnup. Property changes upon melting are not included in this code version.

A. Density

The mixed-oxide fuel density is calculated with a correction factor to account for thermal expansion, which is assumed to be axisymmetric,

$$\rho = \frac{d}{\left(1 + 3 \frac{\Delta L}{L}\right)},$$

where

$$\rho = \text{density (kg/m}^3\text{)},$$

$$d = f_{TD} \left[(1 - f_{PuO_2}) \rho_{UO_2} + f_{PuO_2} \rho_{PuO_2} \right],$$

$$f_{TD} = \text{fraction of theoretical fuel density},$$

$$f_{PuO_2} = \text{weight fraction of } PuO_2 \text{ in the fuel},$$

$$\rho_{UO_2} = 1.097 \times 10^4,$$

$$\rho_{PuO_2} = 1.146 \times 10^4,$$

and

$$\frac{\Delta L}{L} = \text{linear thermal expansion.}$$

The value calculated for the linear thermal expansion is based on the MATPRO formulation,⁵³

$$\frac{\Delta L}{L_0} = K_1 T - K_2 + K_3 \exp(-E_D/kT) ,$$

where

$$\frac{\Delta L}{L_0} = \text{linear strain caused by thermal expansion (equal to 300 K)(unitless) ,}$$

T = temperature (K) ,

k = Boltzmann's constant (1.38×10^{-23} J/K) ,

and

<u>Constant</u>	<u>Uranium Dioxide</u>	<u>Plutonium Dioxide</u>	<u>Units</u>
K ₁	1.0×10^{-5}	9.0×10^{-6}	K ⁻¹
K ₂	3.0×10^{-3}	2.7×10^{-3}	Unitless
K ₃	4.0×10^{-2}	7.0×10^{-2}	Unitless
E _D	6.9×10^{-20}	7.0×10^{-20}	J

B. Specific Heat

The mixed oxide fuel specific heat correlations are taken from the MATPRO reports,^{53,54}

$$c_p = 15.496 \frac{b_1 b_4^2 \exp(b_4/T)}{T^2 [\exp(b_4/T) - 1]^2} + 2b_2 T + \frac{b_3 b_5}{b_6 T^2} \exp(-b_5/b_6 T) ,$$

where

c = specific heat capacity (J/kg · K) ,

T = fuel temperature (K) ,

and

	<u>Uranium Dioxide</u> (Ref. 53)	<u>Mixed Oxides</u> (Ref. 54)
$b_1 =$	19.145	19.53
$b_2 =$	7.8473×10^{-4}	9.25×10^{-4}
$b_3 =$	5.6437×10^6	6.02×10^6
$b_4 =$	535.285	539.0
$b_5 =$	37 694.6	40 100.0
$b_6 =$	1.987	1.987

C. Thermal Conductivity

The mixed-oxide fuel thermal conductivity correlations are taken from the MATPRO report⁵³ and include porosity and density correction factors. For $T_c \leq T_1$,

$$k = c \left[\frac{c_1}{c_2 + T_c} + c_3 \exp(c_4 T_c) \right] ;$$

and for $T_c > T_1$,

$$k = c[c_5 + c_3 \exp(c_4 T_c)] ,$$

where

T_c = temperature ($^{\circ}\text{C}$) ,

$$c = 100.0 \left[\frac{1 - \beta (1 - f_{TD})}{1 - 0.05} \right] ,$$

$$\beta = c_6 + c_7 T_c ,$$

f_{TD} = fraction of theoretical density ,

and

	<u>Uranium Dioxide</u>	<u>Mixed Oxides</u>
c_1 =	40.4	33.0
c_2 =	464.0	375.0
c_3 =	1.216×10^{-4}	1.54×10^{-4}
c_4 =	1.867×10^{-3}	1.71×10^{-3}
c_5 =	0.019 1	0.017 1
c_6 =	2.58	1.43
c_7 =	-5.8×10^{-4}	0.0
T_1 =	1 650.0	1 550.0

D. Spectral Emissivity

The mixed-oxide spectral emissivity is calculated as a function of temperature based on the MATPRO correlations. The values for uranium dioxide and mixed-oxide fuels are assumed equivalent:

$$\epsilon = 0.870 7 \quad \text{for } T \leq 1\ 000 \text{ C} ,$$

$$\epsilon = 1.311 - 4.404 \times 10^{-4} T \quad \text{for } 1\ 000 < T \leq 2\ 050 \text{ C} ,$$

and

$$\epsilon = 0.4083$$

for $T > 2050^{\circ}\text{C}$.

III. ZIRCALLOY CLADDING PROPERTIES

Subroutine MZIRC calculates the properties for Zircaloy and oxidized Zircaloy cladding. The values obtained are for Zircaloy-4. Zircaloy-2 properties are assumed to be identical. The equations used are based on the correlations in the MATPRO report.⁵³

A. Density

Zircaloy cladding exhibits an asymmetric thermal expansion behavior. Thermal expansion is calculated in the radial and axial directions and these effects are included in the density calculation,

$$\rho = \frac{6.5514}{1 + [2(\frac{\Delta L}{L})_r + (\frac{\Delta L}{L})_z]} ,$$

where

$$(\frac{\Delta L}{L})_r = -2.373 \times 10^{-4} + 6.721 \times 10^{-6} T_c$$

and

$$(\frac{\Delta L}{L})_z = -2.506 \times 10^{-5} + 4.441 \times 10^{-6} T_c ,$$

for $T \leq 1073.15$;

$$(\frac{\Delta L}{L})_r = 5.1395 \times 10^{-3} - 1.12 \times 10^{-5} (T_c - 1073.15)$$

and

$$\left(\frac{\Delta L}{L}\right)_z = 3.527.7 \times 10^{-3} - 1.063\ 85 \times 10^{-5}(T_c - 1\ 073.15) ,$$

for $1\ 073.15 < T \leq 1\ 273.15$;

$$\left(\frac{\Delta L}{L}\right)_r = -6.8 \times 10^{-3} + 9.7 \times 10^{-6} T_c$$

and

$$\left(\frac{\Delta L}{L}\right)_z = -8.3 \times 10^{-3} + 9.7 \times 10^{-6} T_c ,$$

for $T_c > 1\ 273.15$; and $T_c =$ temperature ($^{\circ}\text{C}$).

B. Specific Heat

Because Zircaloy undergoes a phase change (alpha to beta) from 1 090 to 1 248 K, with a resultant sharp spike in the specific heat value during the transition, the specific heat is calculated by linear interpolation. Table B-I is used for $T \leq 1\ 248$ K. For $T > 1\ 248$ K, $c_p = 356$ J/kg \cdot K.

C. Thermal Conductivity

Four-term polynomials are used to calculate the Zircaloy and oxidized Zircaloy thermal conductivities. The Kelvin temperature is the independent variable; the polynomial constants are

	<u>Zirconium</u>	<u>Zirconium Dioxide</u>
a_0	7.51	1.96
a_1	2.09×10^{-2}	-2.41×10^{-4}
a_2	-1.45×10^{-5}	6.43×10^{-7}
a_3	7.67×10^{-9}	-1.95×10^{-10}

The form of the polynomial used in this section and in the subsequent material properties sections is

$$y = a_0 + a_1x + a_2x^2 + \cdot \cdot \cdot + a_mx^m .$$

TABLE B-I
SPECIFIC HEAT VS TEMPERATURE

<u>T (K)</u>	<u>c_p (J/kg · K)</u>
300	281
400	302
640	381
1 090	375
1 093	502
1 113	590
1 133	615
1 153	719
1 173	816
1 193	770
1 213	619
1 233	469
1 248	356

D. Spectral Emissivity

The emissivity of Zircaloy is temperature dependent and the emissivity of Zircaloy oxide is temperature and time dependent. For simplicity, a constant value of $\epsilon = 0.75$ is used.

IV. FUEL-CLADDING GAP GAS PROPERTIES

Subroutine MGAP calculates values for the gap gas mixture thermal conductivity that are used in predicting gap HTC's. The method is taken from the MATPRO report⁵³ and is based on calculating mixture values for seven possible constituent gases:

$$k_{\text{gap}} = \sum_{i=1}^n \left(\frac{k_i x_i}{x_i + \sum_{\substack{j=1 \\ j \neq i}}^n \psi_{ij} x_j} \right),$$

where k_{gap} = gap mixture thermal conductivity (W/m · K),

$$\psi_{ij} = \phi_{ij} \left[1 + 2.41 \frac{(M_i - M_j)(M_i - 0.142 M_j)}{(M_i + M_j)^2} \right],$$

$$\phi_{ij} = \frac{\left[1 + \left(\frac{k_i}{k_j} \right)^{1/2} \left(\frac{M_i}{M_j} \right)^{1/4} \right]^2}{2^{3/2} \left(1 + \frac{M_i}{M_j} \right)^{1/2}},$$

k_i = constituent gas thermal conductivity (W/m · K), M_i = constituent gas molecular weight, and x_i = constituent gas mole fraction.

The seven constituent gases considered are helium, argon, xenon, krypton, hydrogen, air/nitrogen, and water vapor. Except for water vapor, their thermal conductivities are defined as:

$$k = aT^b,$$

where

T = temperature (K) ,

and

Gas	a	b
helium	3.36×10^{-3}	0.668
argon	3.421×10^{-4}	0.701
xenon	4.0288×10^{-5}	0.872
krypton	4.726×10^{-5}	0.923
hydrogen	1.6355×10^{-3}	0.8213
air/nitrogen	2.091×10^{-4}	0.846

For water vapor the following correlation is used:

$$k_{\text{steam}} = (-2.8516 \times 10^{-8} + 9.424 \times 10^{-10} T - 6.004 \times 10^{-14} T^2) \frac{p}{T} \\ + \frac{1.009 p^2}{T^2 (T - 273)^{4.2}} - 8.4083 \times 10^{-3} - 1.19998 \times 10^{-5} T \\ - 6.706 \times 10^{-8} T^2 - 4.51 \times 10^{-11} T^3 ,$$

where p is the gap gas pressure (N/m^2).

When the gap dimension shrinks to the order of the gas mean-free path, a correction factor is applied to the light-gas thermal conductivities to account for the change in energy exchange between the gas and the surface. Once again, using the MATPRO recommendations,⁵³ the correction factor for hydrogen and helium is

$$k = \frac{k_1}{1 + f k_1} ,$$

where

$$f = \frac{0.2103 T_g}{p_g \lambda} ,$$

T_g is the average gap gas temperature (K), and λ is the characteristic fuel root mean square roughness equal to 4.389×10^{-6} m.

V. ELECTRICAL FUEL-ROD INSULATOR (BN) PROPERTIES

Subroutine MBN calculates values for boron nitride insulators that are used in electrically heated nuclear fuel-rod simulators. Magnesium oxide insulators are assumed to have roughly equivalent values.

A. Density

A constant value of $2\ 002\ \text{kg/m}^3$ from Ref. 55 is used.

B. Specific Heat

A four-term polynomial is used to calculate the specific heat. The independent variable is temperature in degrees Fahrenheit and the constants are modifications of those reported in an EPRI report:⁵⁶

$$\begin{array}{cccc} \frac{a_0}{760.59} & \frac{a_1}{1.795\ 5} & \frac{a_2}{-8.670\ 4 \times 10^{-4}} & \frac{a_3}{1.589\ 6 \times 10^{-7}} \end{array}$$

C. Thermal Conductivity

The boron nitride thermal conductivity calculation is based on a conversion to SI units of a curve fit reported in Ref. 57:

$$k = 25.27 - 1.365 \times 10^{-3} T_f \quad ,$$

where k is the thermal conductivity (W/m · K), and T_f is the temperature ($^{\circ}\text{F}$).

D. Spectral Emissivity

A constant value of unity is used for the boron nitride spectral emissivity.

VI. ELECTRICAL FUEL-ROD HEATER COIL (CONSTANTAN) PROPERTIES

Subroutine MHTR calculates property values for Constantan heater coils as used in electrically heated nuclear fuel-rod simulators. Nichrome coils, used in some installations in place of Constantan, are assumed to have similar properties. The correlations used are from Ref. 57.

A. Density

A constant value of $8\,393.4 \text{ kg/m}^3$ is used.

B. Specific Heat

The specific heat is

$$c_p = 110 T_f^{0.2075} ,$$

where c_p is the specific heat ($\text{J/kg} \cdot \text{K}$) and T_f is the temperature ($^{\circ}\text{F}$).

C. Thermal Conductivity

The thermal conductivity is

$$k = 29.18 + 1.683 \times 10^{-3} (T_f - 100) ,$$

where k is the thermal conductivity ($\text{W/m} \cdot \text{K}$) and T_f is the temperature ($^{\circ}\text{F}$).

D. Spectral Emissivity

A constant value of unity is used.

VII. STRUCTURAL MATERIAL PROPERTIES

Subroutine MSTRCT supplies property values for six types of structural materials normally used in LWRs: stainless steel, type 304; stainless steel, type 316; stainless steel, type 347; carbon steel, type A508; and Inconel, types 600 and 718. These properties were obtained from Refs. 57-59. A tabulation of the correlations used is given in Tables B-II through B-VII.

TABLE B-II
 STRUCTURAL MATERIAL PROPERTIES
 STAINLESS STEEL, TYPE 304

<u>Property</u>	<u>Independent Variable</u>	<u>Polynomial Constants</u>	<u>Reference Number</u>
ρ	T	$a_0 = 7\ 984.0$	58
		$a_1 = -2.651 \times 10^{-1}$	
		$a_2 = -1.158 \times 10^{-4}$	
c_p	T_f	$a_0 = 426.17$	58
		$a_1 = 0.438\ 16$	
		$a_2 = -6.375\ 9 \times 10^{-4}$	
		$a_3 = 4.480\ 3 \times 10^{-7}$	
		$a_4 = -1.072\ 9 \times 10^{-10}$	
k	T	$a_0 = 8.116$ $a_1 = 1.618 \times 10^{-2}$	58
ϵ	-	$a_0 = 0.84$	

ρ = density (kg/m^3)

c_p = specific heat ($\text{J/kg} \cdot \text{K}$)

k = thermal conductivity ($\text{W/m} \cdot \text{K}$)

T = temperature (K)

T_f = temperature ($^{\circ}\text{F}$)

$y = a_0 + a_1x + a_2x^2 + \dots + a_mx^m$

TABLE B-III
 STRUCTURAL MATERIAL PROPERTIES
 STAINLESS STEEL, TYPE 316

<u>Property</u>	<u>Independent Variable</u>	<u>Polynomial Constants</u>	<u>Reference Number</u>
ρ	T	$a_0 = 8\ 084.0$	59
		$a_1 = -4.269 \times 10^{-1}$	
		$a_2 = -3.894 \times 10^{-5}$	
c_p	T_f	$a_0 = 426.17$	59
		$a_1 = 0.438\ 16$	
		$a_2 = -6.375\ 9 \times 10^{-4}$	
		$a_3 = 4.480\ 3 \times 10^{-7}$	
		$a_4 = -1.072\ 9 \times 10^{-10}$	
k	T		59
β	-	$a_1 = 1.571 \times 10^{-2}$	59
		$a_0 = 0.84$	

ρ = density (kg/m^3)

c_p = specific heat ($\text{J}/\text{kg} \cdot \text{K}$)

k = thermal conductivity ($\text{W}/\text{m} \cdot \text{K}$)

T = temperature (K)

T_f = temperature ($^{\circ}\text{F}$)

$y = a_0 + a_1x + a_2x^2 + \dots + a_mx^m$

TABLE B-IV

STRUCTURAL MATERIAL PROPERTIES
STAINLESS STEEL, TYPE 347

<u>Property</u>	<u>Independent Variable</u>	<u>Polynomial Constants</u>	<u>Reference Number</u>
ρ	-	$a_0 = 7\ 913.0$	57
		$a_0 = 502.416$	
c_p	$(T_f - 240)$	$a_1 = 0.098\ 4$	57
		$a_0 = 14.192\ 6$	
k	T_f	$a_1 = 7.269 \times 10^{-3}$	57
ϵ	-	$a_0 = 0.84$	57

ρ = density (kg/m^3)

c_p = specific heat ($\text{J}/\text{kg} \cdot \text{K}$)

k = thermal conductivity ($\text{W}/\text{m} \cdot \text{K}$)

T = temperature (K)

T_f = temperature ($^{\circ}\text{F}$)

$y = a_0 + a_1x + a_2x^2 + \dots + a_mx^m$

TABLE B-V
STRUCTURAL MATERIAL PROPERTIES
CARBON STEEL, TYPE 508

<u>Property</u>	<u>Independent Variable</u>	<u>Polynomial Constants</u>	<u>Reference Number</u>
ρ	T_f	$a_0 = 7\ 859.82$	5
		$a_1 = -2.642\ 8 \times 10^{-2}$	
		$a_2 = -4.547\ 1 \times 10^{-4}$	
		$a_3 = 3.311 \times 10^{-7}$	
c_p	T_f	$a_0 = 400.48$	58
		$a_1 = 0.458\ 2$	
		$a_2 = 6.553\ 2 \times 10^{-4}$	
		$a_3 = 5.370\ 6 \times 10^{-7}$	
k	T_f	$a_0 = 66.155\ 8$	58
		$a_1 = -1.438\ 6 \times 10^{-2}$	
		$a_2 = -2.698\ 7 \times 10^{-4}$	
		$a_3 = 1.830\ 6 \times 10^{-6}$	
ϵ	-	$a_4 = -6.067\ 3 \times 10^{-9}$	58
		$a_5 = 1.052\ 4 \times 10^{-11}$	
		$a_6 = -9.160\ 3 \times 10^{-15}$	
		$a_7 = 3.159\ 7 \times 10^{-18}$	
ϵ	-	$a_0 = 0.84$	58

ρ = density (kg/m^3)
 c_p = specific heat ($\text{J/kg} \cdot \text{K}$)
 k = thermal conductivity ($\text{W/m} \cdot \text{K}$)
 T = temperature (K)
 T_f = temperature ($^{\circ}\text{F}$)
 $y = a_0 + a_1x + a_2x^2 + \dots + a_mx^m$

TABLE B-VI
STRUCTURAL MATERIAL PROPERTIES
INCONEL, TYPE 718

<u>Property</u>	<u>Independent Variable</u>	<u>Polynomial Constants</u>	<u>Reference Number</u>
ρ	T_f	$a_0 = 8\ 233.4$	58
		$a_1 = -1.835\ 1 \times 10^{-1}$	
		$a_2 = -9.841\ 5 \times 10^{-6}$	
		$a_3 = -6.534\ 3 \times 10^{-9}$	
c_p	T_f	$a_0 = 418.18$	58
		$a_1 = 0.120\ 4$	
		$a_0 = 10.804\ 6$	
k	T_f	$a_1 = 8.829 \times 10^{-3}$	58
ρ	-	$a_0 = 0.84$	58

ρ = density (kg/m^3)

c_p = specific heat ($\text{J/kg} \cdot \text{K}$)

k = thermal conductivity ($\text{W/m} \cdot \text{K}$)

T = temperature (K)

T_f = temperature ($^{\circ}\text{F}$)

$y = a_0 + a_1x + a_2x^2 + \dots + a_mx^m$

TABLE B-VII
STRUCTURAL MATERIAL PROPERTIES
INCONEL, TYPE 600^a

<u>Property</u>	<u>Independent Variable</u>	<u>Polynomial Constants</u>	<u>Reference Number</u>
ρ	T_f	$a_0 = 5.261\ 008 \times 10^{-2}$	58
		$a_1 = -1.345\ 453 \times 10^{-2}$	
		$a_2 = -1.194\ 367 \times 10^{-7}$	
		$a_3 = 0.101\ 445\ 6$	
		$a_4 = 4.378\ 952 \times 10^{-5}$	
		$a_5 = -2.046\ 138 \times 10^{-8}$	
c_p	T_f	$a_6 = 3.418\ 111 \times 10^{-11}$	58
		$a_7 = -2.060\ 318 \times 10^{-13}$	
		$a_8 = 3.682\ 836 \times 10^{-16}$	
		$a_9 = -2.458\ 648 \times 10^{-19}$	
		$a_{10} = 5.597\ 571 \times 10^{-23}$	
		$a_{11} = 8.011\ 332$	
		$a_{12} = 4.643\ 719 \times 10^{-3}$	
k	T_f	$a_{13} = 1.872\ 857 \times 10^{-6}$	58
		$a_{14} = -3.914\ 512 \times 10^{-9}$	
		$a_{15} = 3.475\ 513 \times 10^{-12}$	
		$a_{16} = -9.936\ 696 \times 10^{-16}$	
		$a_{17} = 0.84$	
ρ	-	$a_{18} = 0.84$	58

ρ = density (kg/m³)

c_p = specific heat (J/kg · K)

k = thermal conductivity (W/m · K)

T = temperature (K)

T_f = temperature (°F)

$y = a_0 + a_1x + a_2x^2 + \dots + a_mx^m$

^aInconel, type 600 coefficients are in British units; then ρ is multiplied by 16.018 46; c_p , by $4.186\ 8 \times 10^{-3}$; and k , by 1.729 577.

APPENDIX C

CHOKED-FLOW MODEL

The TRAC choking model originally was developed by Ramson and Trapp⁶⁰ using the characteristic analysis approach. A simplified version of this model has been implemented in RELAP5 (Ref. 61) computer code.

I. TWO-PHASE-FLOW CHOKING CRITERION

The model is based on thermal equilibrium assumption between the phases because the frozen (adiabatic phases without phase change) assumption was found to be in poor agreement with the data as compared to the equilibrium assumption.

The two-fluid model under thermal equilibrium is described by the overall continuity equation, two phasic momentum equations, and the mixture energy equation. Omitting the nondifferential source terms (as they do not enter into characteristic analysis), the equations are

$$\frac{\partial \rho_m}{\partial t} + \frac{\partial}{\partial x} (\rho_m v_m) = 0 \quad , \quad (C-1)$$

$$\begin{aligned} \alpha \rho_g \left(\frac{\partial v_g}{\partial t} + v_g \frac{\partial v_g}{\partial x} \right) + \alpha \frac{\partial p}{\partial x} \\ + C \alpha (1-\alpha) \rho_m \left(\frac{\partial v_g}{\partial t} + v_g \frac{\partial v_g}{\partial x} - \frac{\partial v_l}{\partial t} - v_l \frac{\partial v_l}{\partial x} \right) = 0 \quad , \end{aligned} \quad (C-2)$$

$$\begin{aligned} (1-\alpha) \rho_l \left(\frac{\partial v_l}{\partial t} + v_l \frac{\partial v_l}{\partial x} \right) + (1-\alpha) \frac{\partial p}{\partial x} \\ + C \alpha (1-\alpha) \rho_m \left(\frac{\partial v_l}{\partial t} + v_l \frac{\partial v_l}{\partial x} - \frac{\partial v_g}{\partial t} - v_g \frac{\partial v_g}{\partial x} \right) = 0 \quad , \end{aligned} \quad (C-3)$$

and

$$\frac{\partial}{\partial t} (\rho_m s_m) + \frac{\partial}{\partial x} [\alpha \rho_g v_g s_g + (1-\alpha) \rho_l v_l s_l] = 0 \quad . \quad (C-4)$$

The last terms in Eqs. (C-2) and (C-3) represent interphasic force terms caused by relative acceleration with the virtual mass coefficient given by $C\alpha(1 - \alpha)\rho_m$. For dispersed flow, the constant $C = 0.5$; whereas, for separated flow, $C \sim 0$. The energy equation is written in the form of mixture specific entropy, which is conserved for adiabatic flow (neglecting irreversibilities associated with interphasic mass transfer and relative phase acceleration).

In the thermal equilibrium case, ρ_g , ρ_l , s_g , and s_l are known functions of pressure. Thus, Eqs. (C-1)-(C-4) can be written in terms of the four unknowns α , p , V_g , and V_l . The matrix representation of these equations is

$$A(\bar{U}) \frac{\partial \bar{U}}{\partial t} + B(\bar{U}) \frac{\partial \bar{U}}{\partial x} + C(\bar{U}) = 0 \quad , \quad (C-5)$$

where \bar{U} is a vector consisting of α , p , V_g , and V_l ; and A and B are fourth-order square coefficient matrices. Because the source terms in the governing equations were neglected, the coefficient $C(\bar{U})$ for this system of equations is zero.

The characteristic roots, λ_1 , of the above system of equations are defined as the roots of the fourth-order polynomial,

$$\det (A\lambda + B) = 0 \quad . \quad (C-6)$$

The first two roots for λ are calculated between V_g and V_l , ^{C-1, C-2} and therefore, are not of any consequence for choked-flow calculations. The remaining two roots are

$$\lambda_{3,4} = V_m + D (V_g - V_l) \pm a \quad , \quad (C-7)$$

where

$$a = a_{HE} \left\{ \frac{C\rho_m^2 + \rho_m [\alpha\rho_\ell + (1-\alpha)\rho_g]}{C\rho_m^2 + \rho_g \rho_\ell} \right\}^{1/2}, \quad (C-8)$$

and

$$D = 0.5 \left\{ \frac{\alpha\rho_\ell - (1-\alpha)\rho_g}{\rho_m C + \alpha\rho_g + (1-\alpha)\rho_\ell} + \frac{\rho_g \rho_\ell [(1-\alpha)\rho_\ell - \alpha\rho_g]}{\rho_m(\rho_g \rho_\ell + C\rho_m^2)} \right. \\ \left. - a_{HE}^2 \frac{\rho [\alpha\rho_g^2 \frac{ds_g}{dp} + (1-\alpha)\rho_\ell^2 \frac{ds_\ell}{dp}]}{\rho_g \rho_\ell (S_g - S_\ell)} \right\}. \quad (C-9)$$

The quantity, a_{HE} , is the homogeneous equilibrium speed of sound. Choking will occur when the signal propagating with the largest velocity relative to the fluid is just stationary, that is, $\lambda_{real,max} = 0$. (The real part of λ represents the speed of the disturbance, and the imaginary part its rate of growth or attenuation.) Thus, the choking criterion is established from Eq. (C-7) as

$$V_m + D(V_g - V_\ell) = \pm a, \quad (C-10)$$

as $\lambda_{3,4}$ have only real values.

The calculation sequence for the two-phase choking in TRAC-PF1 is as follows:

1. At each time step the choking criterion is checked from Eq. (C-10) using the previous time-step values. If the flow is choked, steps (2) and (3) are followed.
2. An estimate of either an intermediate value of the relative velocity between the phases $(V_g - V_\ell)^{n+1/2}$ or an intermediate liquid velocity $(V_\ell)^{n+1/2}$ is made depending upon whether the void fraction is low or high, respectively. (At low α the new relative velocity is assumed equal to the old time-step value, and at high α the liquid velocity is assumed unchanged. A linear interpolation is used for intermediate α).

Equation (C-10) and the above estimate thus give intermediate values of the velocities $v_g^{n+1/2}$ and $v_l^{n+1/2}$.

- Using the above values of the velocities, the TRAC hydrodynamic equations are solved. This gives the new time-step values v_g^{n+1} and v_l^{n+1} .

II. SUBCOOLED-FLOW CHOKING CRITERION

During the subcooled blowdown phase, the fluid undergoes a phase change at the break because the containment pressure is much below the saturation pressure corresponding to the system fluid temperature. The transition from single- to two-phase flow is accompanied by discontinuous change in the fluid bulk modulus. This gives rise to a large discontinuity in the speed of sound at the break.

To understand the physical process during the subcooled blowdown, consider a converging-diverging nozzle shown in Fig. C-1. The pressure downstream is such that the throat pressure is just equal to the local saturation pressure, p_g . The flow upstream of the throat is subsonic. However, because the speed of sound is discontinuous when the fluid becomes saturated and because mass conservation dictates that the velocity just upstream of the throat must be equal to the velocity just downstream of the throat (just downstream of the throat the fluid has only miniscule void fraction), the flow is supersonic throughout the diverging section. Thus, there is no point in the nozzle where the Mach number $M = 1$. The velocity profile and the speeds of sound for this situation also are presented in Fig. C-1.

The velocity at the throat is calculated from the Bernoulli's equation,

$$v_t = \left[v_o^2 + \frac{2(p_o - p_t)}{\rho_m} \right]^{1/2}, \quad (C-11)$$

where subscripts o and t refer to the upstream and the throat conditions, respectively. Clearly, $p_t = p_g$ as discussed above.

Any further reduction in the downstream pressure has no effect on the flow, as the disturbance cannot move upstream because the flow is supersonic in the diverging section. Thus, for a containment pressure lower than this value

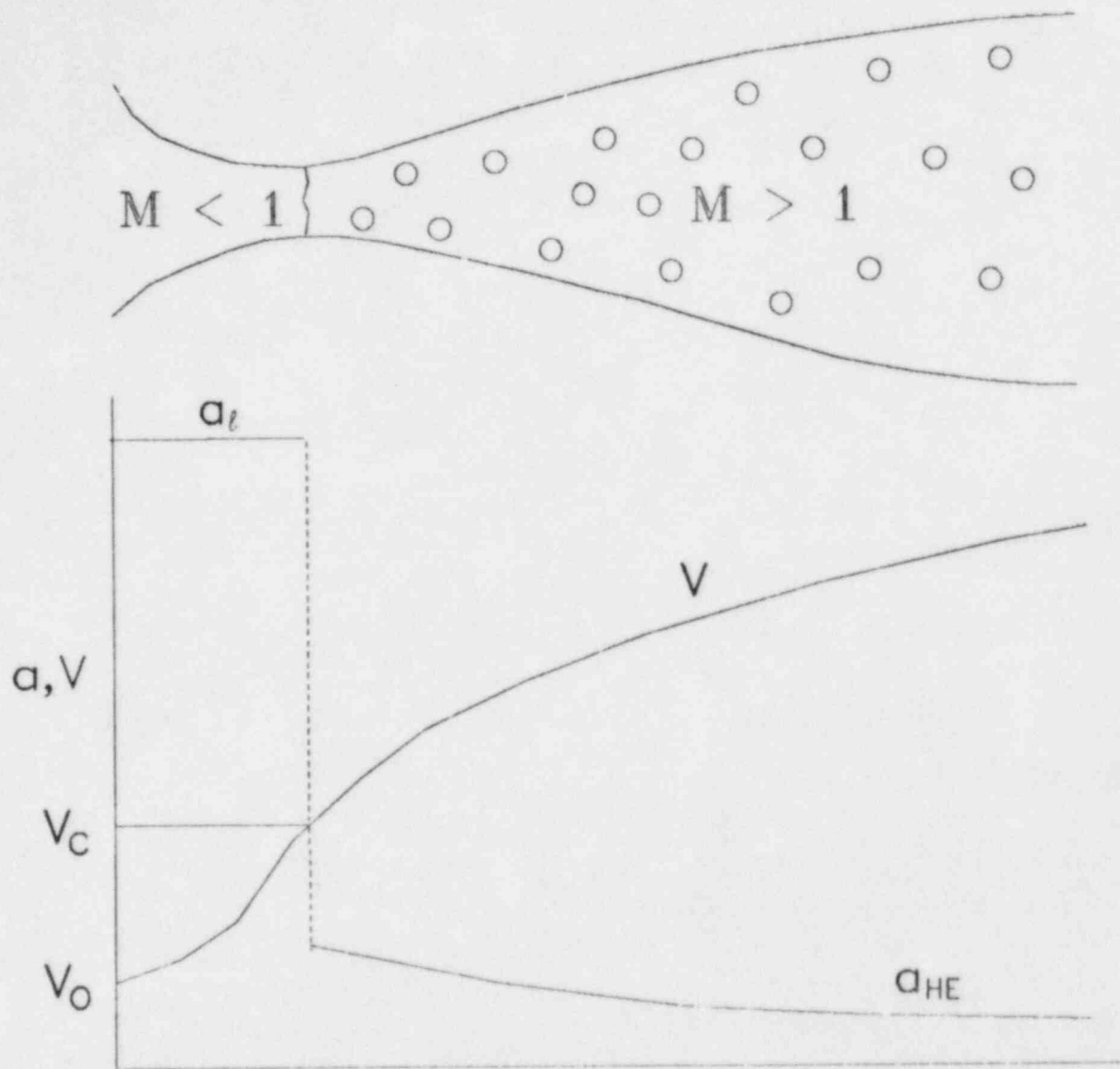


Fig. C-1

Subcooled choking process at the onset of nucleation at the throat.

of the pressure (which is the case for most problems of interest in LWR applications), the throat velocity is given by Eq. (C-11).

Now consider the situation when the subcooled choked flow, as described above, initially exists, and the upstream pressure is lowered. As the upstream pressure decreases, the pressure at the throat still remains p_g and the throat velocity can still be calculated using Eq. (C-11). However, the throat velocity decreases because the upstream pressure decreases. If the upstream pressure is lowered further, a point is reached when $V_t = a_{HE}$. Any further

reduction in the upstream pressure moves the point where $p = p_s$ upstream. In this case, the flow is subsonic in the subcooled zone and in the two-phase zone upstream of the throat. The flow at the throat is sonic with $V_t = a_{HE}$ and that in the diverging portion is supersonic. If the upstream pressure is reduced still further, the p_s point moves upstream until the flow becomes completely two phase.

Thus, based on the foregoing physical process, the choking velocity, V_c , is

$$V_c = \text{Max} \left\{ a_{HE}, \left[v_o^2 + \frac{2(p_o - p_t)}{\rho_m} \right]^{1/2} \right\}, \quad (C-12)$$

where $p_t = p_s$. However, for fast transients, nonequilibrium can result, in which case, p_t can be much lower than p_s . A nucleation delay model is required to account for such a discrepancy; however, the model has not yet been implemented in TRAC-PF1.

The calculation sequence is similar to that for the two-phase model. The only unknown in this case is the liquid-phase choking velocity that is explicitly set using Eq. (C-12) and gives $v_l^{n+1/2}$.

III. TRANSITION REGIME

Because there is a discontinuity in the speed of sound during liquid- to two-phase transition, care must be exercised in analyzing the flow during the transition regime. In TRAC-PF1, this transition is handled by linear interpolation between the subcooled ($\alpha < 0.01$) and the two-phase ($\alpha > 0.1$) regimes.

APPENDIX D

SYSTEM CONTROL WITH TRIPS

TRIP AND TRIP-CONTROLLED COMPONENT ACTION EXAMPLES

TRAC-PF1 has an enhanced trip control procedure for modeling the more complex control logic required for operational transients. The control model is general in nature to allow users the ability to model a spectrum of foreseen as well as unforeseen control scenarios. It is the code user through input and not the code programmer through internal control options who sets up a specific control procedure for TRAC-PF1 to follow. While internal control options are easier to use when a specific control procedure is spelled out in detail, they severely restrict the user only to those options programmed. A control scenario that differs from the available options requires that it be programmed as another option or that it be modeled approximately with the closest available option. The route of specific control options has not been followed in TRAC-PF1 to gain flexibility and generality. In the process, the user pays a penalty in having to think through the modeling details when constructing a desired control model. This is difficult initially because the capabilities of the building blocks (signal variables, trips, controllers, and component action tables) are unfamiliar. With experience, however, these tools enable the user to construct a desired control model with the ease of setting up a hardware component model. The frustration of not having the desired control option capability is avoided.

To gain this experience, some examples are given now for defining trips and the component action tables they control. It is assumed the reader has read the TRAC-PF1 manual sections on signal variables, trips, and the input data for signal variables, trips, and components with trip-controlled actions. The examples to be given are by no means complete or representative of the spectrum of control procedures that can be modeled. They contain some modeling considerations that might commonly be used but that may not be obvious from the manual's description of trips. The very simple and the very complex examples of control models that a user might wish to construct for a problem are somewhat under represented in this set. The examples are complicated only to

illustrate how a user might set up the model to perform a certain control function. By seeing how the modeling tools are used to construct a specific control capability, it is hoped the reader will gain the insight to use these tools creatively to construct the control capabilities that are needed.

The first five examples to be considered involve the definition of a trip signal. There are three types of trip signals: signal variables, signal-variable expressions, and the combined set status of trips assigned to a trip-controlled trip. The description of signal variables in the manual is complete and straightforward. A signal variable defines the local, maximum, minimum, average, or difference value of a parameter within a component at the beginning-of-time-step time or it describes the change in the parameter's value over the last time step. The point to keep in mind is that a signal variable is a parameter value local to a specific component and current problem time.

To extend that definition to the combination of several parameters, several components, or to a larger interval of problem time, the user must use the second type of trip signal, a signal-variable expression. The following signal-variable expression involves a problem time interval with a combination of several signal-variable parameters.

Example 1. Define as a trip signal the average time derivative of a parameter f . Consider doing it for each of the following intervals: (a) previous time step, (b) time since the trip involved was last set ON, and (c) time since the start of the problem.

a. Define $(f_t - f_{t-\Delta t})/\Delta t$ as a trip signal.

Signal variables Δt and $(f_t - f_{t-\Delta t})$ equivalent to $\Delta_t f$ are parameters defining their value change over the last time step. Define the following signal variables:

<u>ID</u>	<u>Signal Variable</u>
1	$\Delta_t f$
2	Δt

Then define the following signal-variable expression for the trip signal:

Subexpression J	Operator ISE(1,J)	1st Argument ISE(2,J)	2nd Argument ISE(3,J)	Subexpression
1	6	2	801	$\max(\Delta t, 10^{-9})$
2	4	1	901	$\Delta_t f / \max(\Delta t, 10^{-9})$,

where $SCN(1) = 1.0E-09$. To avoid division by $\Delta t = 0$ during the first time step, the maximum of Δt and 10^{-9} defines the divisor. The time derivative is evaluated to be zero during the first time step.

b. Define $(f_t - f_{ON}) / (t - t_{ON})$ as a trip signal.

Signal variables f_{ON} and t_{ON} are the values of f and problem time at the start of the problem or at the time when the trip involved was last set ON. Define the following signal variables:

ID	Signal Variable
1	f_t
2	t
3	f_{ON}
4	t_{ON}

Define the following signal-variable expression:

Subexpression J	Operator ISE(1,J)	1st Argument ISE(2,J)	2nd Argument ISE(3,J)	Subexpression
1	2	2	404	$t - t_{ON}$
2	6	901	801	$\max(t - t_{ON}, 10^{-9})$
3	2	1	403	$f_t - f_{ON}$
4	4	903	902	$(f_t - f_{ON}) / \max(t - t_{ON}, 10^{-9})$,

where $SCN(1) = 1.0 E 10^{-9}$. Signal variable IDs 1 and 3 for parameter f and 2 and 4 for problem time are defined identically. It is through the definition of signal variable IDs 3 and 4 as 400-series IDs in the signal-variable expression that they are flagged for re-evaluation only during time steps that the trip is set ON. $t - t_{ON} = 0$ with the maximum function is avoided only for

the first time step. During time steps when the trip is set ON, the signal-variable expression is evaluated before the trip is set ON and thereafter t_{ON} is defined the beginning-of-time-step time of that step. The next evaluation of the signal-variable expression is at the start of the next time step when t is greater than t_{ON} by the previous time step size.

c. Define $(f_t - f_o)/(t - t_o)$ as a trip signal.

Signal variables f_o and t_o are the values of f and problem time at the start of the problem. They are known quantities and are to be input as constants. Define the following signal variables:

<u>ID</u>	<u>Signal Variable</u>
1	f_t
2	t

Define the following signal-variable expression:

<u>Subexpression</u> <u>J</u>	<u>Operator</u> <u>ISE(1,J)</u>	<u>1st Argument</u> <u>ISE(2,J)</u>	<u>2nd Argument</u> <u>ISE(3,J)</u>	<u>Subexpression</u>
1	2	2	801	$t-t_o$
2	6	901	802	$\max(t-t_o, 10^{-9})$
3	2	1	803	f_t-f_o
4	4	903	902	$(f_t-f_o)/\max(t-t_o, 10^{-9})$,

where $SCN(1)$ equals the value of $TIMET$ in the input data, $SCN(2) = 1.0E-09$, and $SCN(3)$ equals the value of f_o in the input data.

The next example of a signal-variable expression involves the combination of parameters from several components.

Example 2. Define as a trip signal the liquid water level in the LOFT steam generator secondary-side downcomer of Fig. D-1.

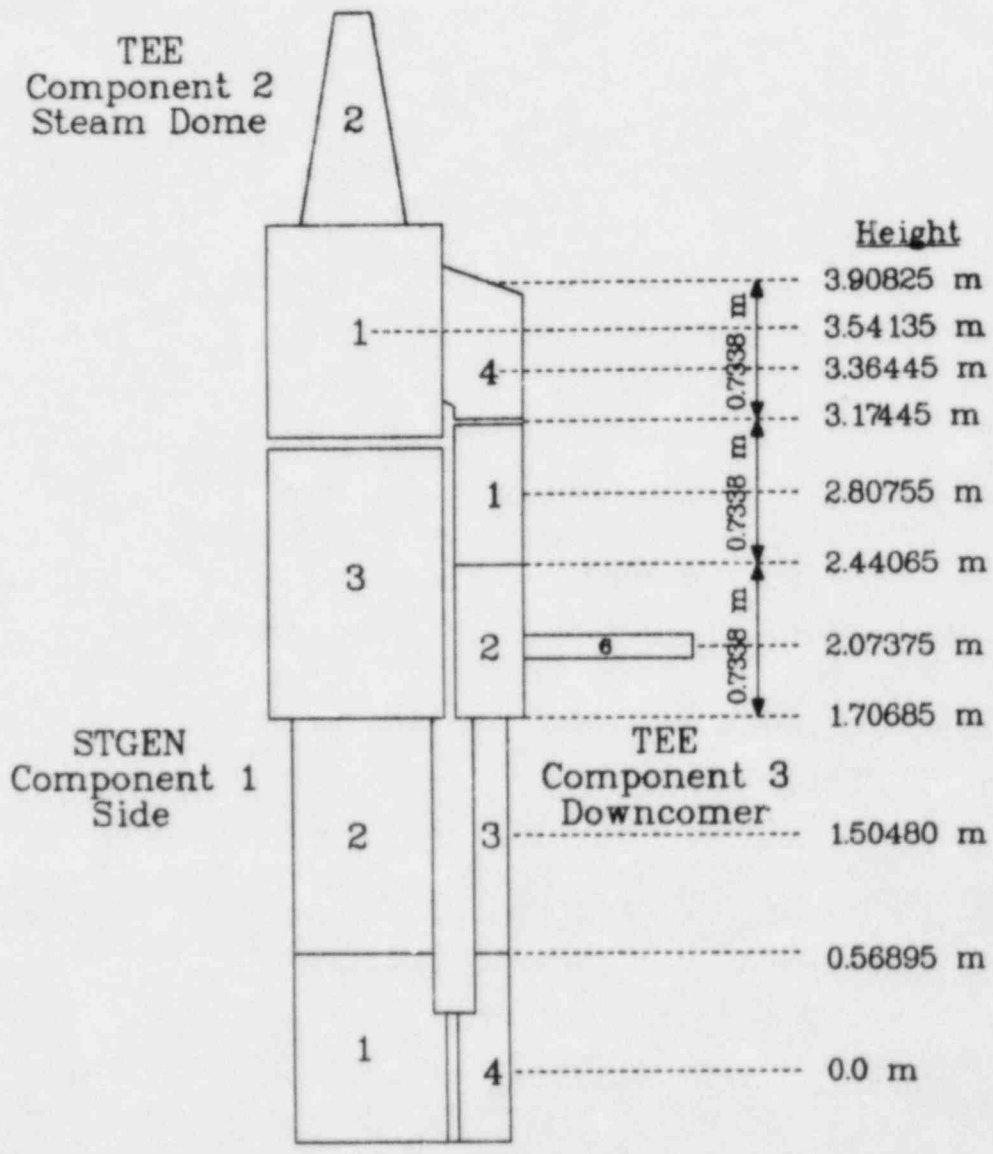


Fig. D-1.
LOFT steam-generator secondary-side model.

There are three components in the LOFT steam generator secondary-side model. The height of vertically collapsed liquid water in cells 1 to 4 of component 3 and cell 4 of component 2 is the water level we wish to define. This can be evaluated from the following signal variables:

<u>ID</u>	<u>Signal Variable</u>	<u>Component Number</u>	<u>Cell Numbers</u>
1	L	3	4 to 1
2	α	2	4

Signal-variable parameter L is the summed length of component 3's primary side cells 4 to 1 having liquid water from the primary side vertically collapsed into them. Vapor water that is present is assumed to occupy component 3's primary side volume above that. L needs to have 0.56895 m subtracted from it to define the liquid water height because the lower half of cell 4 is modeled to have no vertical height. Signal-variable parameter α is the vapor volume fraction in cell 4 of component 2. It is used to define the liquid in cell 4 that needs to be vertically collapsed into component 3. Cell 4 of component 2 has the same volume, vertical height, and horizontal cross section area as cells 1 and 2 of component 3. The horizontal cross section area does change in going from cell 2 to cell 3 in component 3. Because of this area change, we will assume that if the water level in component 3 lies below 1.70685 m (below cell 2), there is no liquid water in cell 4 of component 2 ($\alpha = 1$). This simplifies the combined water level definition because liquid in cell 4 maintains the same cross section area when vertically collapsed into component 3. Thus, the height of liquid water in cell 4 of component 2, $(1 - \alpha) * 0.7338$ m, is added to the height of liquid water in component 3, $L - 0.56895$ m, to define the combined liquid level. This is done by the following signal-variable expression:

Subexpression J	Operator ISE(1,J)	1st Argument ISE(2,J)	2nd Argument ISE(3,J)	Subexpression
1	2	1	801	$L-0.56895$
2	3	2	802	$\alpha*0.7338$
3	2	802	902	$(1-\alpha)*0.7338$
4	1	901	903	$L-0.56895+(1-\alpha)*0.7338$

where $SCN(1) = 0.56895$ and $SCN(2) = 0.7338$.

The third type of trip signal is the combined set status of trips assigned to a trip-controlled trip. An addition or multiplication arithmetic operator is used to combine the set status values ($-1 = ON_{reverse}$, $0 = OFF$, $+1 = ON$ and $ON_{forward}$) of the assigned trips. These arithmetic operations on set status values achieve logical operations on the status of trips. The summed set status values achieve an AND logical operation on trips having an ON status. The resulting trip-controlled trip is commonly referred to as a coincidence trip. Multiplication of the set status values achieves an OR logical operation on trips having an OFF status. This trip-controlled trip is commonly referred to as a blocking trip. An example of each type follows.

Example 3. Coincidence Trip: A nuclear reactor is to have its control rods inserted (by evaluating a trip-controlled power reduction or negative reactivity insertion table) when two of three trips are set ON. Define a coincidence trip that activates the evaluation of the power-reactivity table when the above criterion is satisfied.

The three trips to be tested are assumed to have IDs 1, 2, and 3. Assignment of these trips to a trip-controlled trip that sums their set status values for defining its trip signal gives the desired coincidence trip. The trip-signal-range type 2 trip with constant set point values between 1 and 2 in Fig. D-2 has an OFF set status when none or one of the three trips is ON and an ON set status when two or three of the three trips are ON. The power-reactivity table is evaluated when this controlling trip-controlled trip is ON.

Example 4. Blocking Trip: Evaluate a pump coastdown table when any one of four trips is set OFF. Among the four trips, an $ON_{reverse}$ and ON and $ON_{forward}$ set status are possible.

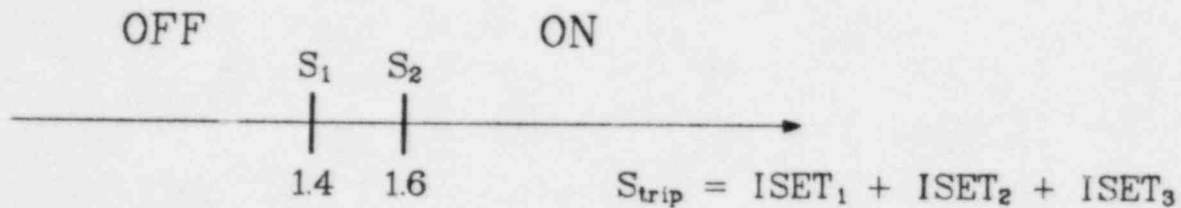


Fig. D-2.
Coincidence trip for controlling the power-reactivity table.

Assume the four trips to be tested have IDs 1, 2, 3, and 4. Assignment of these trips to a trip-controlled trip that multiplies their set status values for defining its trip signal gives the desired blocking trip. The trip-signal-range type 5 trip is needed with constant set point values S_1 and S_2 between -1 and 0 and S_3 and S_4 between 0 and 1 in Fig. D-3. When any one of the four trips is OFF, the trip-controlled trip signal value is 0 , which lies within the ON set status subrange. Otherwise, the trip signal value is -1 when an odd number of the four trips are in $ON_{reverse}$ or $+1$ when an even number of the four trips are in $ON_{reverse}$ with the remaining trips having ON or $ON_{forward}$ set status. These latter trip signal values correspond to OFF set status subranges. Control of the pump coastdown table with this trip-controlled trip results in evaluation of the table when the trip signal value is 0 and the trip is ON. This example shows how activation of a component action can be accomplished when a trip is set OFF with a trip-controlled trip.

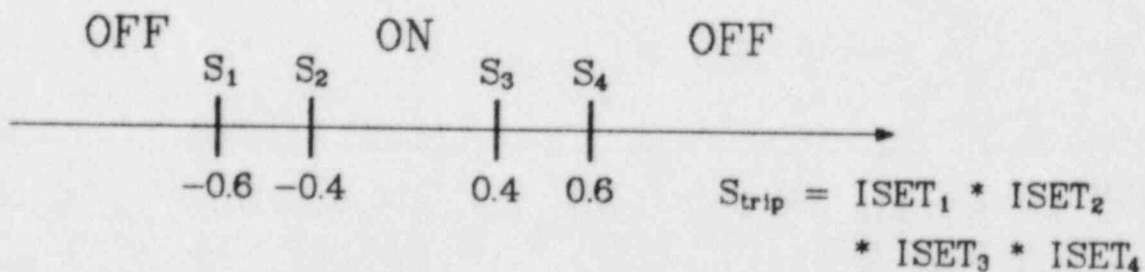


Fig. D-3.
Blocking trip for controlling the pump speed table.

The previous two examples defined a trip-controlled trip with an AND or OR logical expression. The next example defines an AND logical expression with OR logical subexpressions to show how trip-controlled trips also can be assigned to a trip-controlled trip. In this way, a logical expression trip signal can be defined with several levels of logical subexpressions.

Example 5. A component action table is controlled by one of three trips. Figure D-4 defines the trip to be used based on where a signal value lies within the subranges. When the signal is less than S_{12} , use the trip with ID = 1. When the signal is greater than or equal to S_{12} but less than S_{23} , use the trip with ID = 2. When the signal is greater than or equal to S_{23} , use the trip with ID = 3.

In this example the signal could be any one of the three trip signal types. A very common situation, however, is where the signal is problem time. During different time intervals of a problem, different trip criteria should be used to control a component action.

To define the component action controlling trip, start by defining the three trips in Fig. D-5 so that each is set ON only during one of the signal's three subranges. Then define the three blocking trips in Fig. D-6 that combine by multiplication the set status value of each of the above three trips with the trip to be used during the above trip's ON subrange. These three trip-controlled blocking trips then are assigned to the trip-controlled coincidence trip in Fig. D-7 for control of the component action.

Two of the ISET₇, ISET₈, and ISET₉ set status values are zero. The other value is the set status of trip 1, 2, or 3, which controls the component action while the signal lies within its assigned subrange.

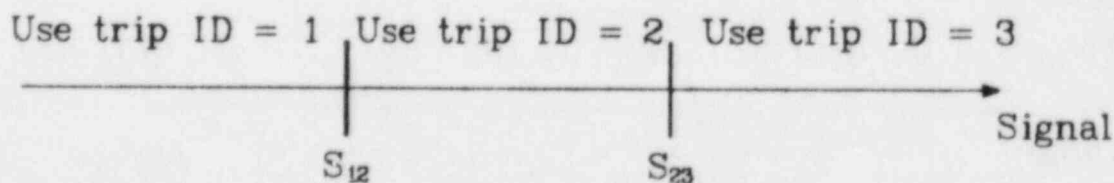
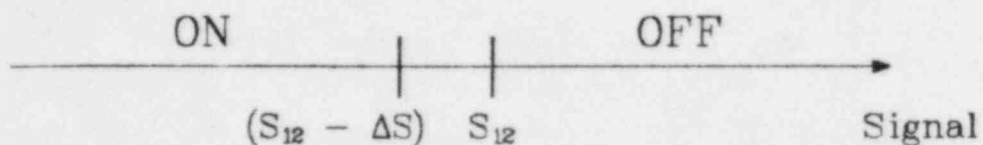


Fig. D-4.
The controlling trip is based on the signal subrange.

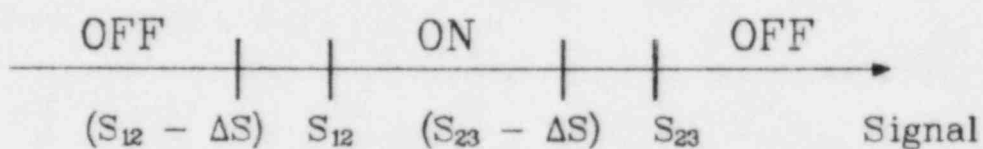
Trip ID = 4

Trip-signal-range type 1



Trip ID = 5

Trip-signal-range type 5



Trip ID = 6

Trip-signal-range type 2

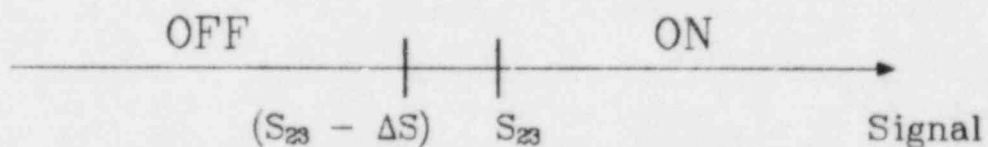


Fig. D-5.

Trips with ON set status for a specific subrange of the signal.

Trip ID = 7, 8, and 9

Trip-signal-range type 3

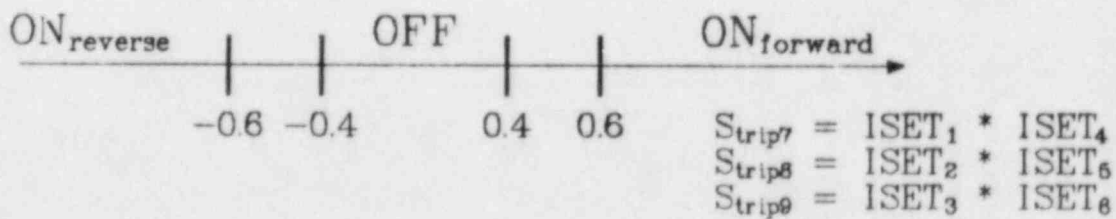


Fig. D-6.

Blocking trips for specific subranges of a signal.

Trip ID = 10

Trip-signal-range type 3

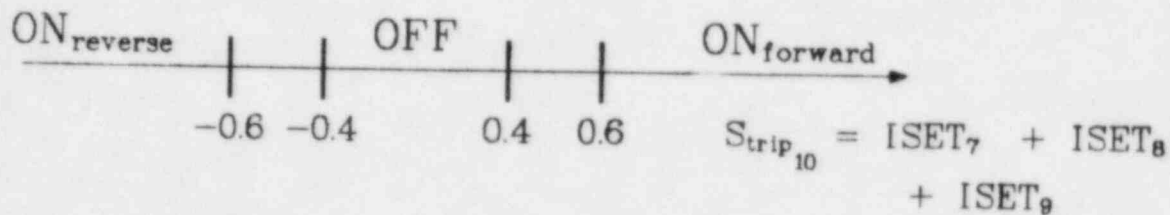
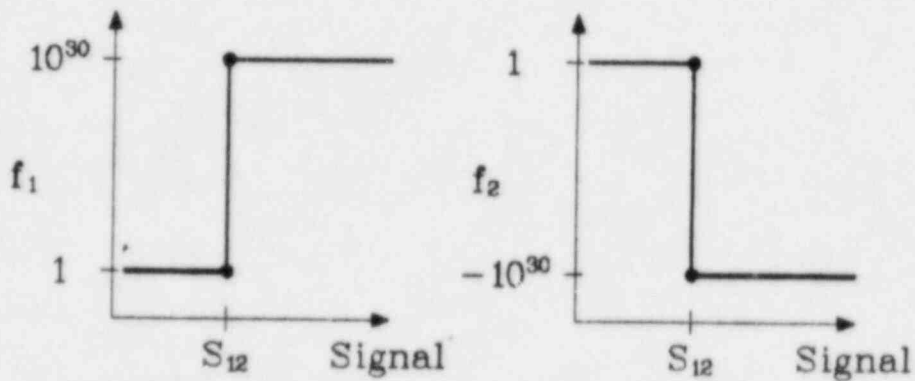


Fig. D-7.

Coincidence trip for controlling the component action.

If the signal in the previous example is a signal-variable parameter, the same control function can be accomplished using set-point factor tables for the set points of trip IDs 1, 2, and 3. By doing so, trip IDs 4 through 9 need not be defined.

Example 6. In the control scenario of Example 5, the signal is defined by a signal-variable parameter. Define the set points of trip IDs 1, 2, and 3 to have set-point table factors applied to them. The signal-variable parameter signal is specified to be the independent variable for those tables. For each trip, the set-point factors are defined to be unity for signal values in the subrange where the trip is to control the component action. Outside of that subrange, the set-point factors are defined to be very large, small, positive, or negative values so that the OFF set status subrange of the trip expands to cover the entire trip signal range. For example, if trip ID = 1 has a trip-signal-range type 3, the set-point factor tables in Fig. D-8 are applied to its set points. If S_1 and S_2 are positive, apply f_2 to their set-point values. If S_1 and S_2 are negative, apply f_1 to them. If S_3 and S_4 are positive, apply f_1 to their set-point values. If S_3 and S_4 are negative, apply f_2 to them. Then, when the signal is greater than or equal to S_{12} , the OFF set status subrange of trip ID = 1 expands to cover the trip signal value range from roughly -10^{30} to $+10^{30}$. As a result, trip ID = 1 is forced to be OFF whenever the signal is greater than or equal to S_{12} . After proceeding to apply in a similar fashion other set-point table factors to the set points of trip IDs 2 and 3, the coincidence trip in Fig. D-9 is defined to control the



Trip ID = 1

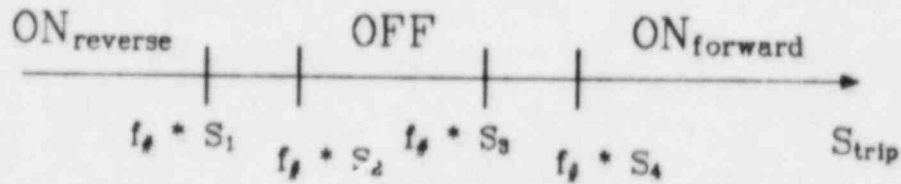


Fig. D-8.
Set point factor tables for trip ID = 1.

Trip ID = 10

Trip-signal-range type 3

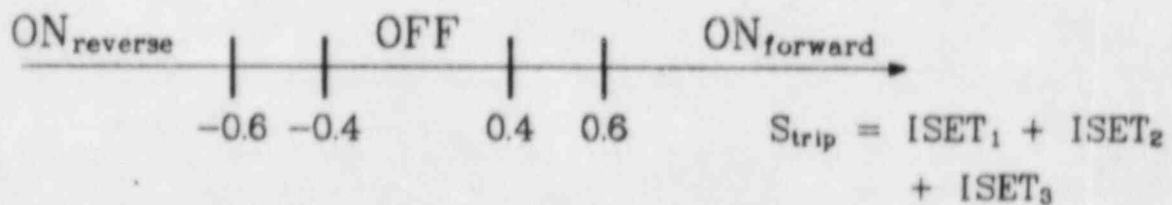


Fig. D-9.
Coincidence trip for controlling the component action.

component action. $ISET_1$, $ISET_2$, and $ISET_3$ have the same values as $ISET_7$, $ISET_8$, and $ISET_9$, respectively, in Example 5.

In the examples thus far, zero delay times for each set point have been assumed. The delay time is the time interval that passes after the set-point criterion is met before the trip set status is changed. Delay times model the actual interval after a trip signal is sent out from the detector to when the trip-controlled component hardware begins its action. In the following example, delay times are used another way to avoid spurious trip signals that would momentarily change the trip set status.

Example 7. Define a trip that requires the set-point criterion for setting the trip ON to be satisfied continuously for 0.1 s before setting the trip ON. If at any moment during that interval the set-point criterion is violated, do not set the trip ON.

For the trip-signal-range type 2 trip in Fig. D-10, define the delay time for set point S_1 to be zero and the delay time for set point S_2 to be 0.1 s. As the trip signal S_{trip} increases to equal or exceed S_2 , the ON set status criterion is met. A delay time of 0.1 s then must pass before the trip is set ON. If, during this time, S_{trip} decreases to equal or lie below S_1 , the OFF set status criterion is met. Then is added to the list of pending trips whose criteria have been met but whose delay times have not elapsed. The criterion for changing to ON would be first in the list; the criterion for changing to OFF would be second. A maximum of five pending criteria can be stacked up in this way. Then TRAC-PF1 checks to see if the delay time for any of the pending criteria has elapsed. Finding one, TRAC-PF1 then deletes all pending criteria earlier in the list and defines the new set status of the criterion whose delay

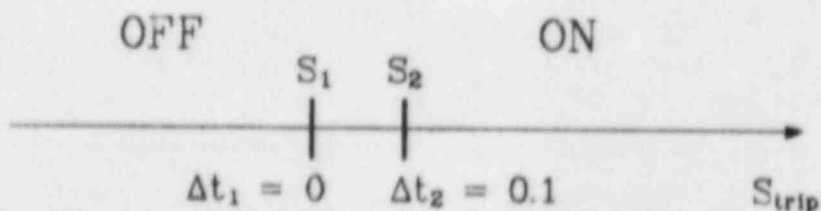


Fig. D-10.

A trip that avoids spurious signals for ON set status.

time has elapsed. In our example, the pending OFF set-status-criterion delay time would be met in that same time step, the pending ON set status criterion would be deleted, and the trip that was OFF would be set to OFF. While the trip set status never changes, TRAC-PF1 edits the fact that the set status is set to OFF. This might be confusing if it were not for the earlier edit that both the trip's ON and OFF set status criteria were met.

TRAC-PF1 allows the user to choose a trip-signal-range type having two or three set status subranges over the trip signal range. The next example shows how this situation can be extended to four or more subranges by combining several trips with a trip-controlled coincidence trip.

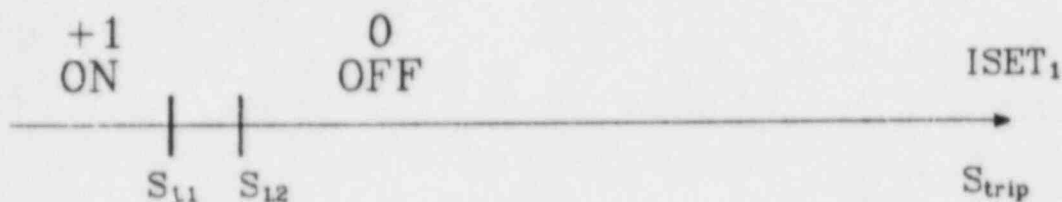
Example 8. Define a trip with five set-status subranges for the trip signal. As the trip signal value increases, define the subrange set status to be ON_{forward}, OFF, ON_{reverse}, OFF, and ON_{forward}.

Two trips with trip-signal-range type 1 and one trip with trip-signal-range type 3 are defined with the same trip signal, S_{trip} , in Fig. D-11. Their set-point values are chosen to give the desired five subranges when later combined. By summing the set status values of these three trips with the trip-controlled coincidence trip in Fig. D-12, the five desired set status subranges for S_{trip} shown in Fig. D-13 are obtained. This is possible with a three-subrange trip because the trip signal for the coincidence trip is $ISET_1 + ISET_2 + ISET_3$ and not S_{trip} .

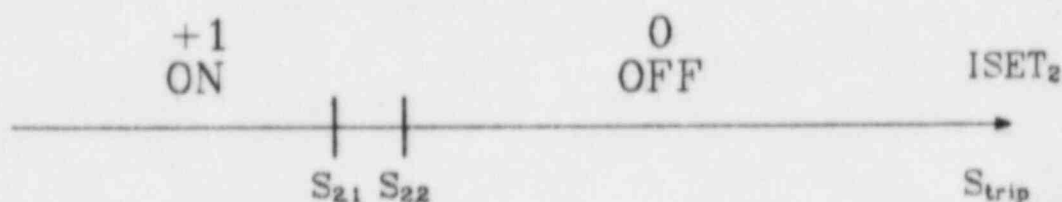
Trip-controlled component actions can be perturbing enough to require a shorter time step for accurate evaluation of the resulting transient. TRAC-PF1 is programmed to adjust the time step automatically when the rate of change varies in the solution. When that change is abrupt and large, as a trip-controlled component action might be, the procedure for automatically reducing the time step size becomes inefficient. The same time step may have to be recalculated a number of times with a progressively smaller time step size before a stable time step solution is achieved. Even then, it may not be small enough to prevent discretization error from entering the solution. A better alternative is provided in the following example by assigning special time step data to the controlling trip.

Example 9. A trip-controlled valve adjustment perturbs the fluid system so severely that TRAC-PF1 needs to reduce the time step size by three decades to continue the calculation. We would like to avoid the inefficiency of the

Trip ID = 1



Trip ID = 2



Trip ID = 3

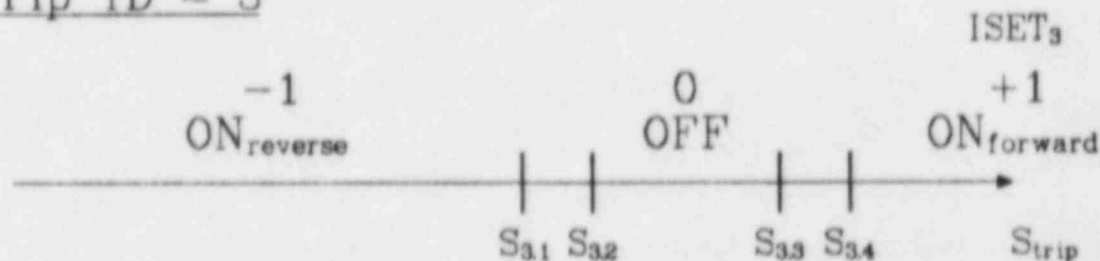


Fig. D-11.

Trips for defining five sub:anges to the trip signal.

automatic time step reduction procedure and would like to get more edits of the fluid-state condition during the rapid transient that follows.

This is possible by assigning a special time-step data set to the controlling trip. When the trip is set to ON , $ON_{forward}$, or $ON_{reverse}$, its assigned special time-step data set replaces for a specified interval of time the normal sequence of time step data. The current time step size is redefined or multiplied by a factor (10^{-3} for this example) to obtain a new time step

Trip ID = 4

Trip-signal-range type 3

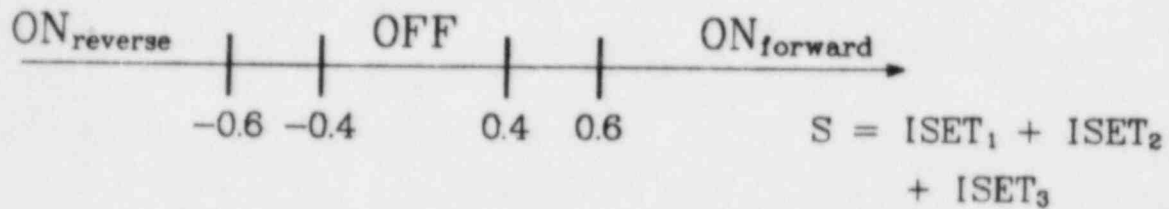


Fig. D-12.
Coincidence trip which behaves like a trip with five subranges.

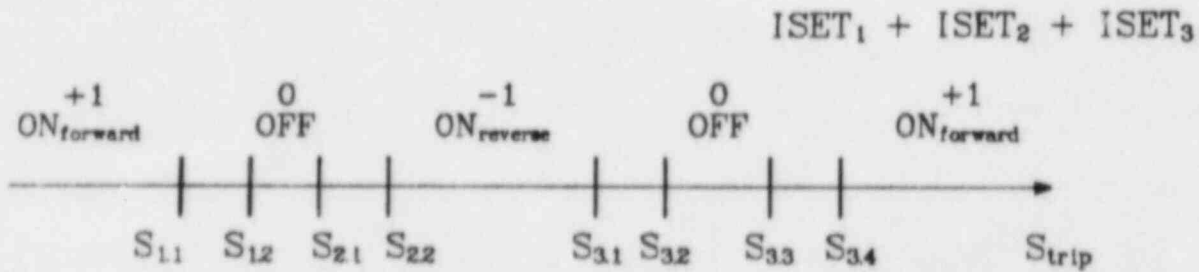


Fig. D-13.
The five subranges of the trip signal.

size. New minimum and maximum time steps, as well as time intervals for editing the fluid state, are assigned. After the specified interval for the special time step data, the time step data that normally would be applied at that time are restored.

The examples thus far have defined trips. Now let us turn our attention to specific component actions that are trip controlled. These actions are normally defined by a component action table specified as part of the component data. The table defines the component action as a function of a signal-variable parameter. A model of component action that is trip controlled involve evaluating its table when the assigned trip has an ON , $ON_{forward}$, or $ON_{reverse}$ set status. When the trip is OFF , no evaluation of the component

action table occurs. Its last defined state is held constant. Thus, when a controlling trip is OFF, it means that no change occurs in the adjustable action of the component. When the trip is ON, any change in the adjustable action depends on the table evaluation. The following example is a trip-controlled mass flow boundary condition defined by a FILL component.

Example 10. Feedwater is to be supplied initially at a mass flow of 50 kg/s to the secondary side of a steam generator. If at any time the water level in the steam-generator secondary-side downcomer falls below 1.7 m, define feedwater mass flow from Fig. D-14 until the water level increases to 3.1 m. Thereafter, supply feedwater at a mass flow of 75 kg/s unless the water level again falls to 1.7 m and the above procedure needs to be repeated.

Assume the steam-generator secondary-side model we are working with is that of Example 2 shown in Fig. D-1. The required feedwater mass flow will be defined by a FILL component joined to cell 6 on the secondary side of TEE component 3. FILL-type option IFTY = 8 is chosen where the FILL component defines constant mass flow until trip, then mass flow vs signal-variable form from a FILL table. The initial constant mass flow is specified to be 50 kg/s, and the mass flow is specified to be 75 kg/s when the FILL table-controlling trip is OFF after being ON. Figure D-14 defines the FILL table with the

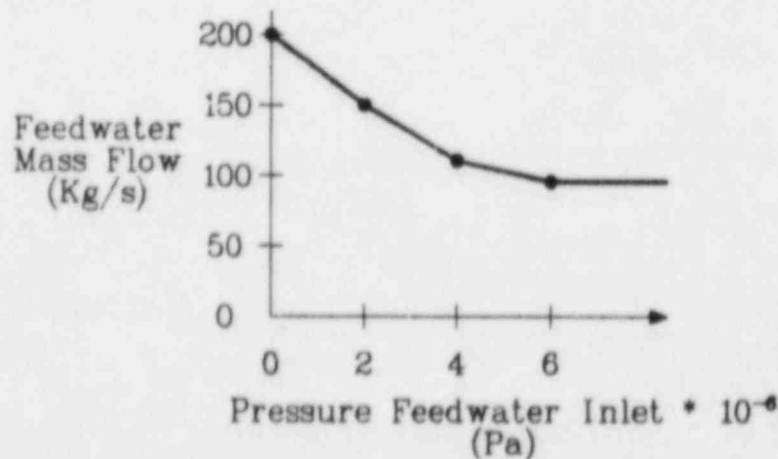


Fig. D-14.
Steam generator secondary-side feedwater mass flow table.

signal-variable form being the absolute value of the signal-variable parameter pressure in cell 6 on the secondary side of TEE component 3. The trip for controlling evaluation of mass flow from the FILL table is assigned the trip signal from Example 2. That trip is shown in Fig. D-15 as having a trip-signal-range type 1 with set points $S_1 = 1.7$ and $S_2 = 3.1$ and zero delay times.

The next trip-controlled component action example will be trip control of pump speed to achieve a desired mass flow.

Example 11. In a steady-state calculation, use trip control to regulate pump speed to obtain a 500 kg/s mass flow through the pump. Activate trip control after 30 s of problem time.

Start by defining the trip-signal-range type 3 trip in Fig. D-16 to decide when increasing or decreasing the pump speed is needed to obtain a mass flow of 500 ± 0.5 kg/s through the PUMP component. The trip ID is negative to indicate that the trip is to be evaluated during steady-state as well as transient calculations. When $\dot{m}_{\text{pump}} \leq 499.5$ kg/s, the trip is set to ON_{reverse} to indicate that the pump speed is to be increased; when $\dot{m}_{\text{pump}} \geq 500.5$ kg/s, the trip is set to ON_{forward} to indicate that the pump speed is to be decreased. This is accomplished by applying trip ID = -1 to the pump speed table defined in Fig. D-17.

In Fig. D-17: Ω_{MIN} , Ω_0 , and Ω_{MAX} are the minimum, initial, and maximum pump speeds, respectively. Δt_{TOTAL} is the total time required to vary the pump speed over its Ω_{MIN} to Ω_{MAX} range. Δt_{TOTAL} should be large enough to allow

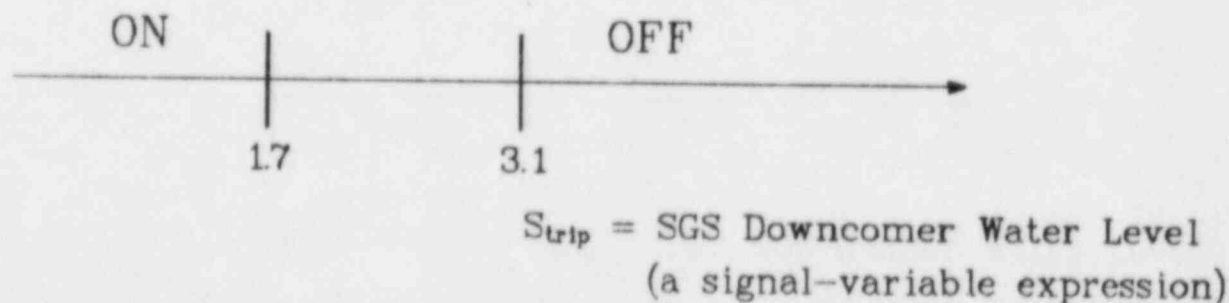


Fig. D-15.
Trip for controlling the FILL mass flow table.

Trip ID = -1

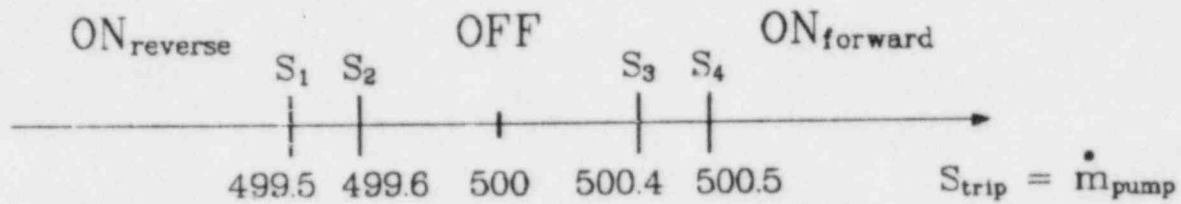


Fig. D-16.
Trip for controlling the pump speed table.

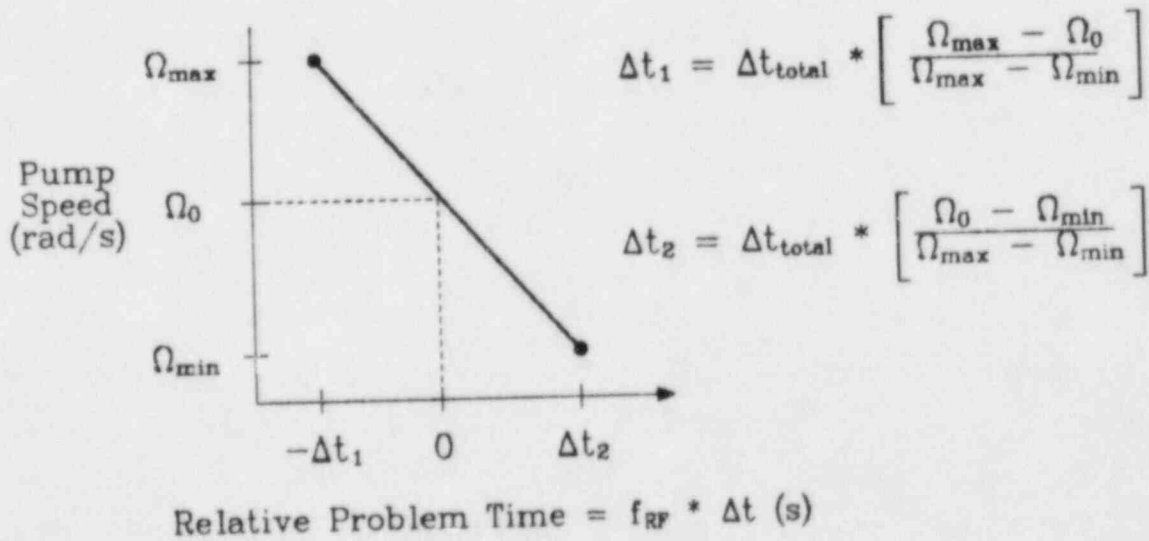


Fig. D-17.
Pump speed table.

feedback from changing the pump speed to effect the trip signal \dot{m}_{pump} so that pump speed over adjustment can be prevented by the trip. The pump speed table's abscissa coordinate is the time step size with a rate factor f_{RF} applied to it.

At this point there are two ways to proceed in defining the control model: (a) define a trip that is OFF until 30 s and a trip-controlled blocking trip that combines that trip and trip ID = -1 to override any ON set status during the initial 30 s, or (b) define set point factors for trip ID = -1 to expand the OFF set status subrange to cover the physical range of the trip signal \dot{m}_{pump} during the initial 30 s.

A similar situation was considered earlier in examples 5 and 6. The first approach has the disadvantage of requiring the definition of two more trips. However, in this example, it has an additional disadvantage in that the rate factor table (defining the rate factor for the pump speed table abscissa coordinate) would be dependent on the blocking trip's signal because the blocking trip would control the pump speed table. Instead, we would like trip ID = -1 to control the pump speed table so that the rate factor table would be a function of \dot{m}_{pump} .

The second approach does this for us. With trip ID = -1 controlling the pump speed table, the rate factor table is a function of the trip signal \dot{m}_{pump} minus the set point value whose criterion changes the trip's set status. When trip ID = -1 is in $\text{ON}_{\text{forward}}$, the rate factor table is a function of $\dot{m}_{\text{pump}} - 500.4$, a positive value; when trip ID = -1 is in $\text{ON}_{\text{reverse}}$, the rate factor table is a function of $\dot{m}_{\text{pump}} - 499.6$, a negative value. The rate factor is needed only to evaluate the pump speed table's abscissa coordinate when this trip is in either set status.

Now let us define the rate factor table so that it slows the rate of pump speed change as $\dot{m}_{\text{pump}} - \left\{ \begin{matrix} 500.4 \\ 499.6 \end{matrix} \right\}$ approaches zero and the trip is about to be set OFF. This helps prevent overadjustment of pump speed. However, as $\dot{m}_{\text{pump}} - \left\{ \begin{matrix} 500.4 \\ 499.6 \end{matrix} \right\}$ gets large, we would like to increase the rate of pump speed change so that the mass flow discrepancy can be corrected more expediently. The rate factor table in Fig. D-18 does this for us. The slope to use in defining the rate factor in Fig. D-18 depends on the rate of pump-speed adjustment in Fig. D-17, $(\dot{\omega}_{\text{MAX}} - \dot{\omega}_{\text{MIN}})/\Delta t_{\text{TOTAL}}$, and on the optimum acceleration

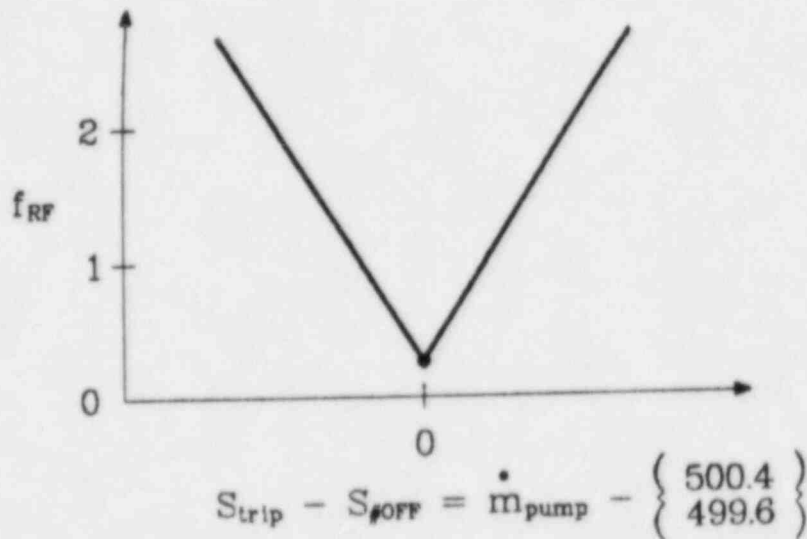


Fig. D-18.

Rate factor table for the pump speed table's abscissa coordinate.

or deceleration of that rate based on the departure of S_{trip} from its set point for setting the trip OFF.

To assure that trip ID = -1 is OFF during the initial 30 s of problem time, apply the set point factors defined in Fig. D-19 to trip ID = -1. Multiply $S_1 = 499.5$ and $S_2 = 499.6$ by f_1 and $S_3 = 500.4$ and $S_4 = 500.5$ by f_2 .

The next three examples consider a VALVE component with an adjustable flow area interface that is trip controlled. Adjustment of the flow area is by a guillotine cut of a circular cross-section pipe. Valve closure is measured by the flow area fraction or the valve stem fractional position of the guillotine blade at the adjustable flow area interface. The first example is a check valve or power-operated relief valve that generally operates in one of two ways.

Example 12. Model a check valve or power-operated relief valve that defines its closure state as a function of the pressure difference across the adjustable flow area interface. Model the valve to operate in each of the following ways:

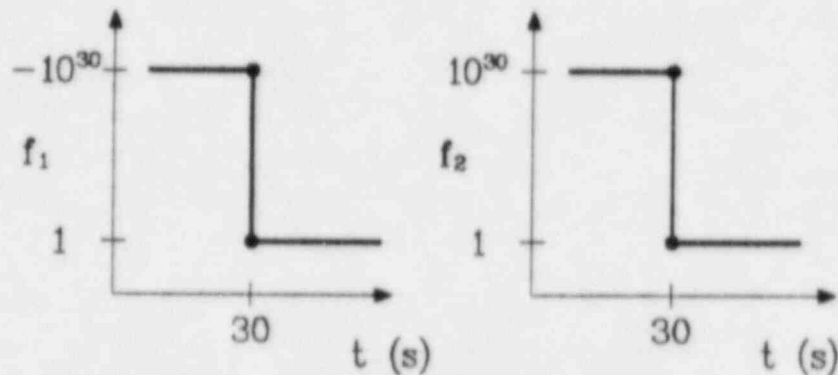


Fig. D-19.
Set point factor tables for trip ID = -1.

(a) The valve is closed with a minimum flow area fraction f_{\min} when the pressure difference is less than or equal to ΔP_{\min} . As the pressure difference increases from ΔP_{\min} to ΔP_{\max} , the valve flow area increases linearly to a maximum flow area fraction f_{\max} at ΔP_{\max} . Any further increase in the pressure difference maintains the f_{\max} open condition of the valve.

(b) The valve is closed initially with a minimum flow area fraction f_{\min} when the pressure difference is less than ΔP_{open} . When the pressure difference increases to or exceeds ΔP_{open} , the valve flow area fraction increases to f_{\max} during the interval Δt_{open} . Thereafter, the valve maintains its f_{\max} open condition until the pressure difference decreases to or lies below ΔP_{close} . When this occurs, the valve closes to f_{\min} during the interval Δt_{open} . ΔP_{close} is less than ΔP_{open} .

The models for a check valve and a power-operated relief valve are similar with only the following major differences: (a) generally ΔP_{\max} and ΔP_{open} are small for a check valve and large for a power-operated relief valve relative to the absolute pressure, (b) the flow area adjustment of a power-operated relief valve is sometimes modeled as a function of the upstream pressure rather than the pressure difference because the downstream pressure is

small in comparison and approximately constant, and (c) check valves generally operate by (a) above and power-operated relief valves by (c) above.

The first way of valve operation only requires the valve table in Fig. D-20 without trip control. The upstream minus downstream pressure difference, ΔP , is definable as a signal variable parameter. For the user to know when the valve reaches its open or closed condition, the trip-signal-range type 2 trip in Fig. D-21 can be defined to indicate when the valve table limits are reached. When ΔP increases to or exceeds ΔP_{\max} , the trip is set to ON,

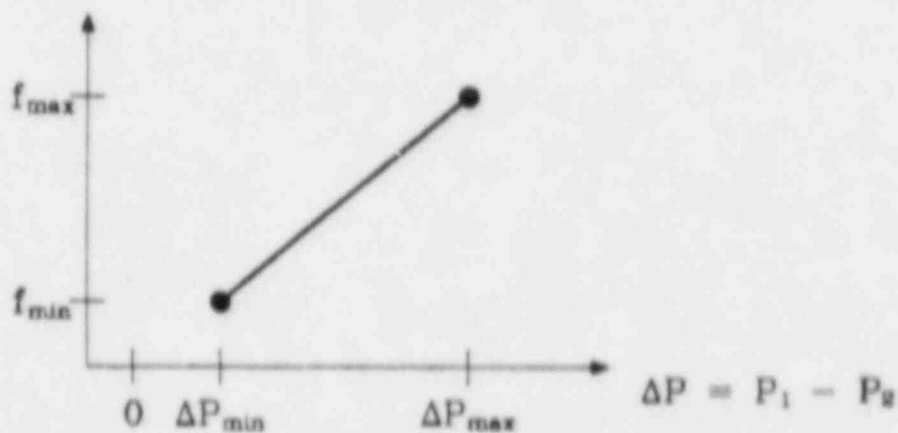


Fig. D-20.
Valve flow area adjustment table.

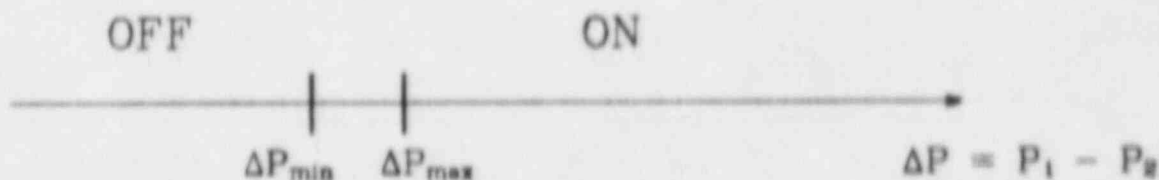


Fig. D-21.
Trip for editing the closure limits of a valve.

indicating the valve is open; when ΔP decreases to or lies below ΔP_{\min} , the trip is set to OFF, indicating the valve is closed.

The second valve operation requires the valve flow area adjustment table to be trip controlled. The trip differentiates which closure state the valve is in when ΔP lies between ΔP_{close} and ΔP_{open} . The trip-signal-range type 3 trip in Fig. D-22 is assigned to control the value table in Fig. D-23. Define the valve table's abscissa coordinate rate factor to unity. The valve table is defined assuming the valve is initially closed. If it is open initially, the

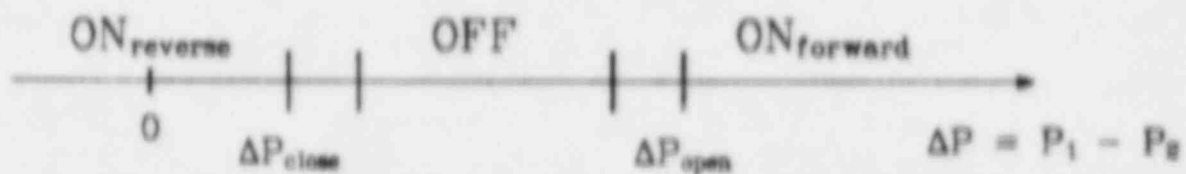


Fig. D-22.
Trip for controlling the valve flow area adjustment table.

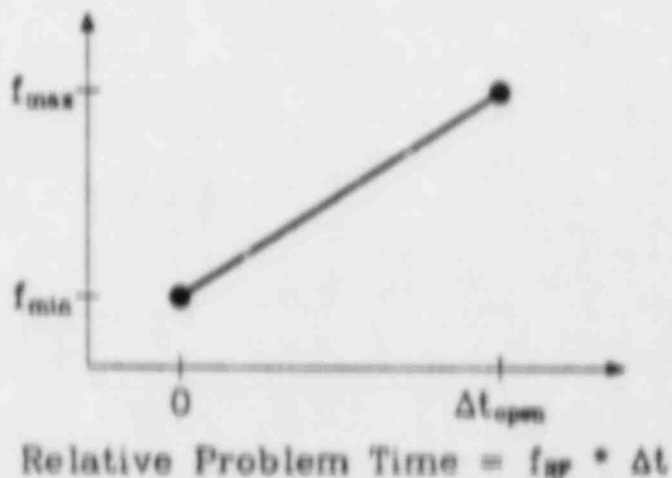


Fig. D-23.
Valve flow area adjustment table.

abscissa coordinate of f_{max} should be zero and the abscissa coordinate of f_{min} should be $-\Delta t_{open}$. During the calculation, TRAC-PFI translates the abscissa coordinate so that zero always corresponds to the last interpolated point in the table. Extrapolation beyond the left or right-most table entries is not allowed. For example, when the trip is set to $ON_{forward}$, the interpolated flow area fraction increases as problem time increases by Δt_{open} . Thereafter, the interpolated point is the right-most entry in the table as long as the trip remains in $ON_{forward}$.

The next example is a regulating valve which adjusts the valve flow area to achieve a desired trip signal value within a specified range.

Example 13. Model a regulating valve that adjusts the flow area of a valve to keep a trip signal value between S_1 and S_4 . The flow area should be decreased when the trip signal exceeds S_4 and increased when the trip signal falls below S_1 .

This can be accomplished when the valve table in Fig. D-23 is controlled by the trip-signal-range type 4 trip in Fig. D-24. A trip-signal-range type 3 trip could be used, but then the slope of the flow area fraction in Fig. D-23 would have to be negative. Rather than using a rate factor of unity, the rate factor form defined in Fig. D-18 provides feedback to control the rate of valve adjustment. A smaller rate of valve adjustment would be performed when the trip signal is slightly out of the desired range. Then, overadjustment might be avoided. As the trip signal further departs from the desired range, the valve adjustment rate gets larger because the trip signal behavior indicates a need for it. Some regulating valves, however, have a constant valve adjustment speed. They should be modeled with a rate factor of unity. Their constant

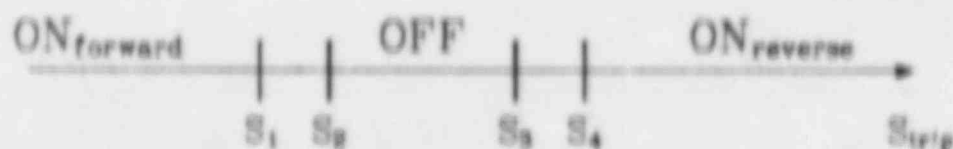


Fig. D-24.
Trip for controlling a regulating valve.

valve adjustment speed would be defined by the slope of the flow area fraction in the Fig. D-23 valve table.

The next valve example considers the hysteresis effect in valve adjustment where the manner of opening a valve differs from that of closing it.

Example 14. Model a valve that opens in five stages with each progressive opening stage taking place when the signal-variable parameter S_v crosses the value S_{o_i} , $i = 1, 2, \dots, 5$ ($S_{o_i} < S_{o_{i+1}}$). Closure occurs in three stages when S_v crosses the values S_{c_i} , $i = 1, 2, 3$ ($S_{c_i} < S_{c_{i+1}}$).

This can be done by defining two valve tables that are controlled by a trip-signal-range type 3 or 4 trip. The first valve table is used when the trip is set to $ON_{forward}$; the second valve table is used when the trip is set to $ON_{reverse}$. The valve tables in Fig. D-25 is controlled by a trip. When defining the valve tables, they both need to increase monotonically or decrease as the abscissa coordinate increases. A valve closure state defined by two or more values of S_v should be avoided in a valve table when there are two tables defined. This is to assure uniqueness when TRAC-PFI interpolates a new valve closure state out of one of the tables, because it translates the abscissa coordinate of the other table so that the value of S_v corresponds to the same

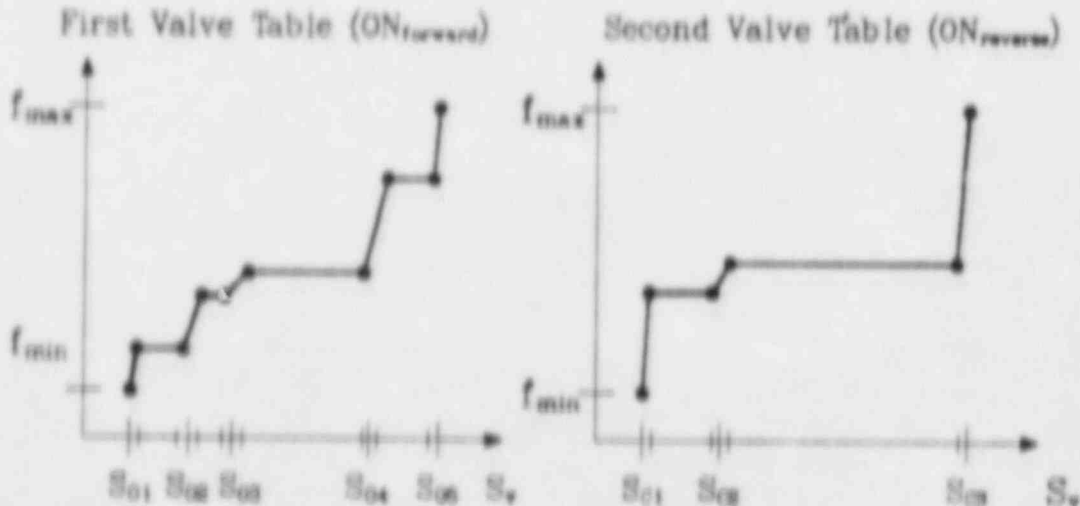


Fig. D-25.
Two valve tables for flow area adjustment.

closure state. When inserting the valve tables, the user needs to assure this as well. If initially the valve is closed with a flow area of f_{\min} , then $S_{O1} \equiv S_V(t=0) \equiv S_{C1}$ is required for both tables to be consistent with each other and with the initial state of the valve.

The final component action table example to be considered involves two component actions controlled by the same trip.

Example 15. Model the reactivity effect and axial power shape distortion from control rod bank movement that under trip control shuts down the reactor core power within 60 s.

This model is applied in a CORE or VESSEL component having fuel rods. The point-reactor kinetics equations, driven by the sum of programmed reactivity from the control rod bank and feedback reactivity, are evaluated to determine reactor power. Programmed reactivity is input vs relative problem time by the power-reactivity table. It defines the negative reactivity worth of the control rod bank as it is continuously inserted into the core at its normal operational rate as shown in Fig. D-26. The $\Delta\rho_{\text{CRB}}$ total reactivity worth of the control rod bank (CRB) is assumed large enough in this example to shut down the reactor power within 60 s for the duration of the calculation. The effect of control-rod-bank movement on distortion of the axial power shape

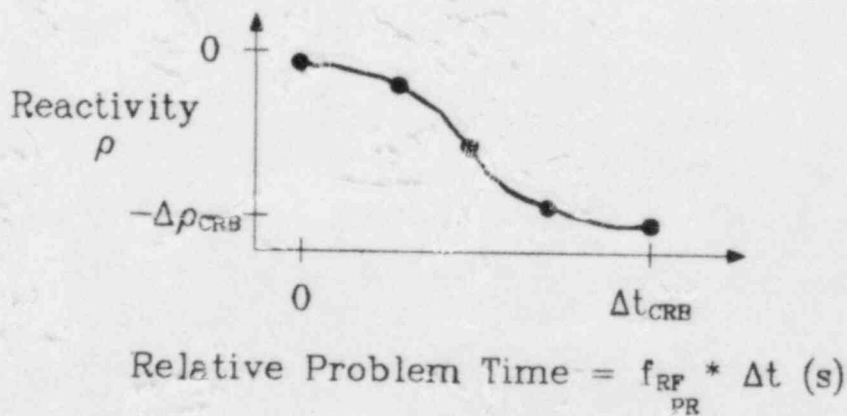


Fig. D-26.
Control-rod-bank programmed reactivity.

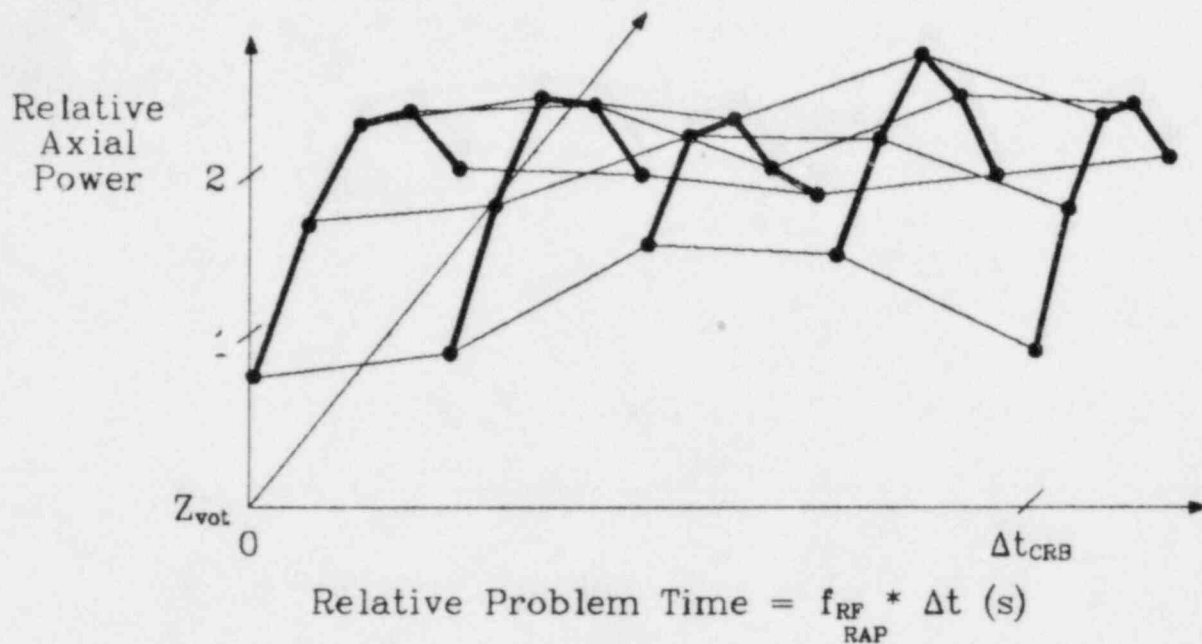


Fig. D-27.
Axial power shape table.

is defined by the axial power shape table in Fig. D-27 as a function of relative problem time.

The behavior in Fig. D-27 is consistent with that of Fig. D-26. A trip is needed to determine when control-rod-bank movement is needed to maintain a 60-s power decay. The trip-signal-range type 3 trip in Fig. D-28 provides that control.

A reactor period greater than 61 s sets the trip to ON_{forward} , while a reactor period less than 59 s sets the trip to ON_{reverse} . Both activate evaluation of the programmed reactivity and axial power shape tables. ON_{forward} moves the interpolation point to the right in both tables, causing negative reactivity to be added and its effect on axial power shape to be made. ON_{reverse} moves the interpolation point to the left with the opposite result. In either case, the effect on reactor power decay is to return it to the desired value of 60 s. If Δt_{CRB} is small or the calculational time step is large, the desired value may be overshoot. This difficulty can be minimized by

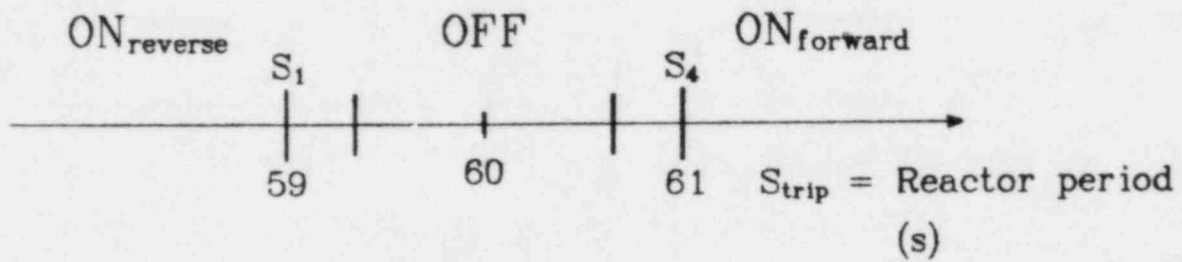


Fig. D-28.
 Trip for controlling programmed reactivity and axial power shape.

defining the rate factor table form in Fig. D-18 to the power-reactivity and axial power shape tables rather than to a rate factor of unity.

APPENDIX E

SAMPLE PROBLEM

This sample problem shows the setup of a large, complicated TRAC problem. Test S-SB-P7 (Ref. 62) conducted in the Semiscale Mod-3 (Ref. 63) facility at INEL was chosen to demonstrate the modeling techniques. Section E-I discusses the Semiscale Mod-3 system briefly. Section E-II summarizes Test S-SB-P7. Section E-III describes the TRAC one-dimensional model. Section E-IV discusses the steady-state calculation. Finally, Secs. E-V.A and E-V.B include listings of the steady-state and transient input decks, respectively. Section E-V.C illustrates use of the free-format input option and describes a three-dimensional TRAC VESSEL configuration that is equivalent to the one-dimensional configuration used in Sec. E-V.A.

I. SEMISCALE MOD-3 SYSTEM DESCRIPTION

The Semiscale Mod-3 system includes an intact loop, a broken loop, an external downcomer assembly, and a pressure vessel to simulate a PWR. An isometric drawing of the system configured for cold-leg break tests is shown in Fig. E-1. The intact loop includes a pressurizer, steam generator, and pump. The broken loop includes a steam generator, pump, and rupture valve assembly. The pressure vessel includes an upper head, an upper plenum, a 25-rod electrically heated core with thermocouples located 0.75 mm beneath the cladding surface, and a lower plenum. The external downcomer assembly includes an inlet annulus and downcomer pipe. Most system components have the same elevations as those in a full-sized PWR.

II. TEST DESCRIPTION

Test S-SB-P7 simulated a 2.5% cold-leg communicative break with delayed pump coastdowns (1099.7 s after the pressurizer pressure reached 12.48 MPa). The simulated core had a flat radial power profile with three unpowered rods in a 5 x 5 matrix.

The initial steady-state operating conditions were: 15.73-MPa system pressure, 1.97-MW core power, 549-K core inlet temperature, and 33-K core temperature differential. Core power decay, pump coastdowns, and steam-generator valve actions were sequenced relative to a trip signal

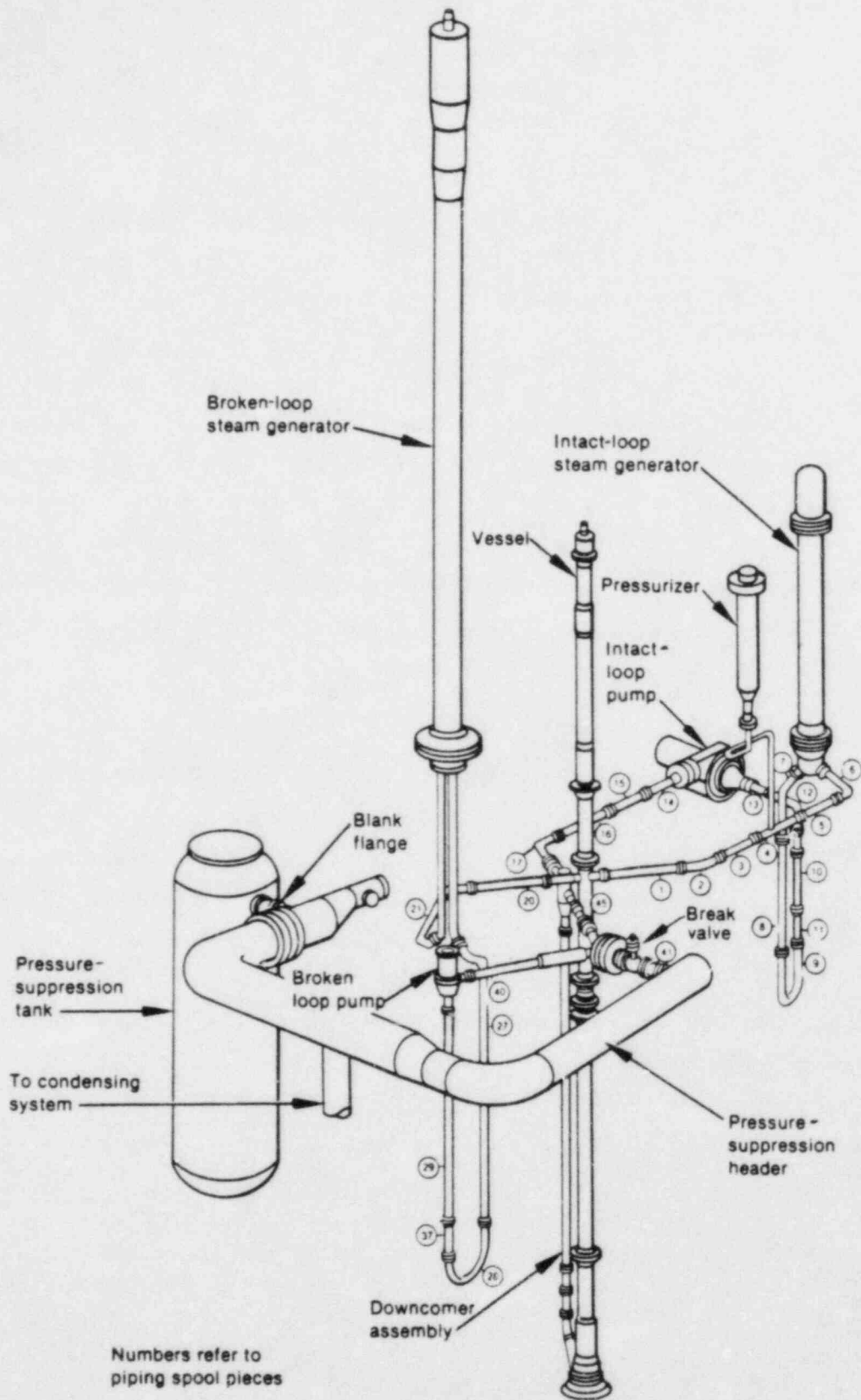


Fig. E-1.

Semiscale Mod-3 system for cold-leg break configuration--isometric (Ref. 62).

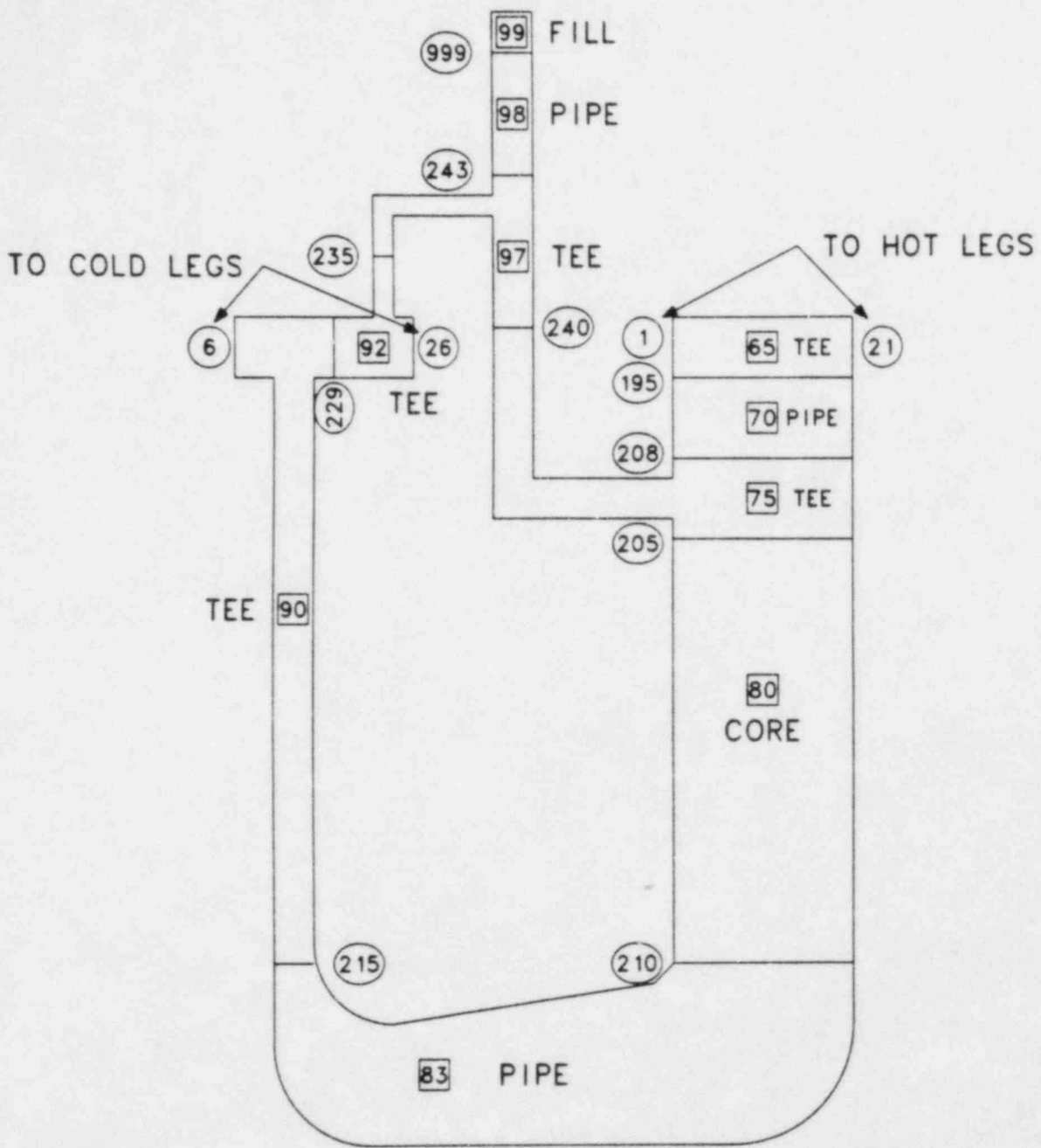
generated by a specified low pressure (12.48 MPa) in the pressurizer. The ECC was provided by the high-pressure injection system (HPIS) only. The accumulators in the intact and broken loops were valved out and the test was terminated before the system pressure fell below the normal low-pressure injection system (LPIS) set point.

The pressure-suppression tank was bypassed for the test and the break discharge was drained through a condensing system into a small catch tank. The catch-tank inventory was measured before and after the test to obtain the total integrated break flow.

A small break was simulated with a bell-mouthed orifice attached to the side of the broken-loop cold-leg piping. A valve was opened to initiate the transient, which lasted for 2465 s. All the trips, except those for the HPIS and the primary pumps, were initiated within ~8 s after the pressurizer pressure dropped to 12.48 MPa. The HPIS was started at 46 s and the primary coolant pumps tripped at 1117 s into the transient. The test was terminated by closing the valve downstream of the break when the system pressure dropped to a predetermined level.

III. TRAC ONE-DIMENSIONAL MODEL

Figures E-2 and E-3 show the loop and vessel arrangement, respectively. The setup includes at least one of every type of TRAC component module except for a three-dimensional vessel. Figure E-4 shows an equivalent vessel-downcomer configuration that uses the TRAC three-dimensional VESSEL. An input listing for this three-dimensional model is given in Sec. E-V.D. The junction and component numbers are shown in circles and squares, respectively. These junctions and component numbers can be used as guides when referring to the input listings in Sec. E-V. The input model consists of 42 components containing a total of 172 cells and 46 junctions. Table E-I lists the components. The input model corresponds to the Semiscale Mod-3 hardware configuration with the following exceptions:



- JUNCTION
- COMPONENT

Fig. E-3.
One-dimensional downcomer and vessel noding for Semiscale Mod-3 facility.

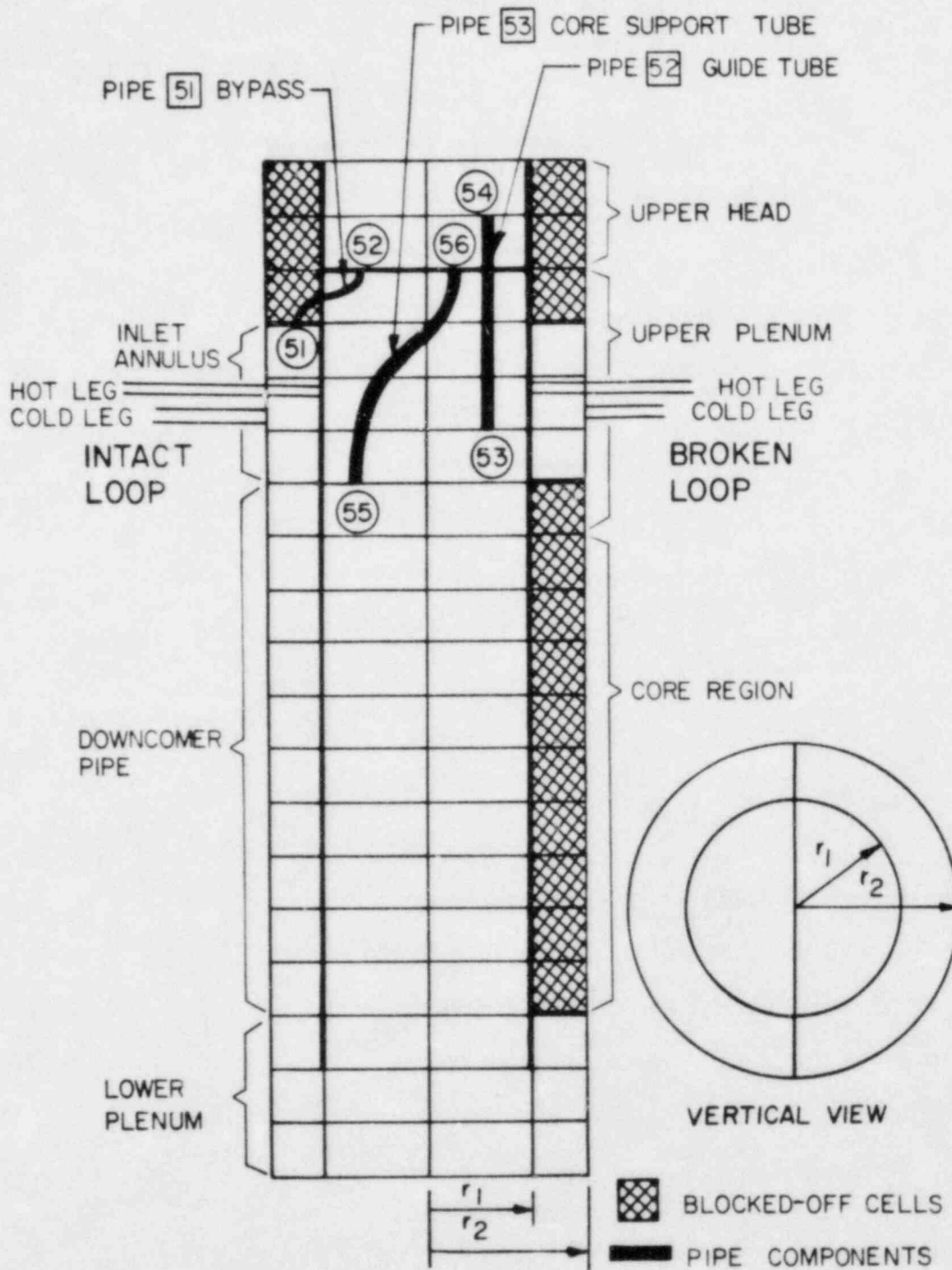


Fig. E-4.
 Three-dimensional VESSEL noding combining all the components shown in Fig. E-3.

TABLE E-I
TRAC MODEL COMPONENTS

<u>Component Number</u>	<u>Component Type</u>	<u>Description</u>	<u>Number of Fluid Cells (Primary Side, Secondary Side)</u>
1	TEE	Intact-loop hot leg	4, 3
2	STGEN	Intact-loop steam generator	10, 5
3	PIPE	Intact-loop pump suction	10
4	PUMP	Intact-loop pump	2
5	TEE	Intact-loop cold leg	4, 1
6	PRIZER	Intact-loop pressurizer	5
7	FILL	Intact-loop steam-generator feedwater	1
8	VALVE	Intact-loop steam line	2
9	BREAK	Intact-loop steam-generator-secondary pressure set point	1
10	TEE	Intact-loop ECC line	2, 1
11	VALVE	Intact-loop accumulator valve	2
12	ACCUM	Intact-loop accumulator	4
13	FILL	Intact-loop HPIS	1
14	TEE	Intact-loop steam-generator-secondary steam dome	2, 1
15	TEE	Intact-loop steam-generator-secondary downcomer	5, 1
16	FILL	Pressurizer inlet	1
21	PIPE	Broken-loop hot leg	3
22	STGEN	Broken-loop steam generator	12, 6
23	PIPE	Broken-loop pump suction	7
24	PUMP	Broken-loop pump	2
25	TEE	Broken-loop cold leg	3, 2
26	FILL	Broken-loop steam-generator feedwater	1
27	VALVE	Broken-loop steam line	2
28	BREAK	Broken-loop steam-generator-secondary pressure set point	1
34	TEE	Broken-loop steam-generator-secondary steam dome	2, 1
35	TEE	Broken-loop steam-generator-secondary downcomer	6, 1
40	FILL, BREAK	Fill for steady-state run, break for transient run	1
41	TEE	Broken-loop cold leg	3, 1
42	TEE	Broken-loop ECC line	2, 1
43	FILL	Broken-loop HPIS	1
44	VALVE	Broken-loop accumulator valve	2
45	ACCUM	Broken-loop accumulator	4

TABLE E-I (cont.)

<u>Component Number</u>	<u>Component Type</u>	<u>Description</u>	<u>Number of Fluid Cells (Primary Side, Secondary Side)</u>
65	TEE	Upper section of upper plenum	1, 1
70	PIPE	Middle section of upper plenum	1
75	TEE	Lower section of upper plenum and guide and core support tubes	1, 1
80	CORE	Core	9
83	PIPE	Lower plenum	3
90	TEE	Intact-loop side downcomer inlet and downcomer	2, 10
92	TEE	Broken-loop side downcomer inlet and upper-head bypass	2, 1
97	TEE	Lower section of upper head and upper-head bypass	3, 2
98	PIPE	Upper section of upper head	2
99	FILL	Upper-head zero-velocity fill	1

The total number of components is 42.

The total number of cells is 172.

The total number of junctions is 46.

1. The pressure-suppression system is not modeled directly. During the steady-state calculation, a zero-velocity FILL (component 40) is introduced at the pressure-suppression system junction. At the beginning of the transient, as shown in the transient restart listing (Sec. E-V.B), this FILL component is replaced by a BREAK component and the pressure and temperature at the break are specified as boundary conditions.
2. The secondary feedwater systems, both main and auxiliary, are represented by FILL components 7 and 26 for the intact and broken loops, respectively.
3. The HPIS is represented by FILL components 13 and 43 for the intact and broken loops, respectively. For tests that have an LPIS also, the same components can represent both the HPIS and the LPIS. Both the accumulators (components 12 and 45) are valved out in the calculation using TRIP 7 because there was no accumulator injection in Test S-SB-P7. The modeling of the accumulators permits generality and allows the model to be adapted easily for tests that have accumulator injection.

The TRAC-PF1 choked-flow model was used to calculate the break flow. The secondary side of the break TEE (component 25) was modeled using two cells, with the second cell representing the break orifice. Because the orifice used in the test had a rounded entrance, the second cell represents the geometric area of the orifice.

The intact-loop pump used the Semiscale pump curves. Revised single-phase curves* for the broken-loop pump were obtained from INEL and incorporated into the input model. Because the radial power profile in Test S-SB-P7 was flat, only the average-power rods were modeled in the core.

The structural heat losses in the Semiscale Mod-3 system were measured experimentally and were shown to be a significant portion of the heat generated in the core during simulated decay heat.⁶⁴ Therefore, the heat losses were incorporated in the TRAC model. Assuming the surrounding air temperature to be 300 K, we calculated a film coefficient based on the outside surface area of the primary system, a primary liquid temperature from a previous TRAC steady-state run, and an 80-kW heat loss.**

* C. B. Davis, Idaho National Engineering Laboratory, personal communication (December 1980).

** T. K. Larson, Idaho National Engineering Laboratory, personal communication (March 1981).

The primary data base for the input model noding is the Semiscale Mod-3 drawings⁶⁵ and the system design description.⁶³ The data base for the initial and boundary conditions incorporated in the TRAC input model includes the experiment operating test specifications,^{66,67} the quick-look report,⁶⁸ and the data report.⁶²

IV. STEADY-STATE CALCULATION

Based on the geometry and the noding described in Sec. E-III, a steady-state calculation was performed using the generalized steady-state TRAC option. The calculation took 777 s of CPU time to simulate 400 s of reactor steady-state time at an average 0.27-s time step. As noted in Sec. E-V, all the initial velocities were zero. At the beginning of the calculation, the reactor power was automatically set to zero. At ~1 s, the system parameters, such as velocities and temperatures, almost reached a zero-power steady state and the power was turned on. The velocities and pressures did not converge to a steady state until ~40 s later. The temperature convergence was much slower because of large system thermal inertia caused by the heat structures. For all practical purposes, the temperatures converged near the end of the run. Table E-II lists the initial conditions and specified test parameters. The TRAC steady-state calculation closely approximates the actual test conditions.

Figures E-5 through E-14 show representative steady-state results for the system pressures, velocities, and temperatures. Figure E-5 shows the upper-plenum pressure history. Figure E-6 shows the velocity in the pressurizer surge line. Note that the pressurizer was treated simply as a constant pressure break during the steady-state calculation to prevent the pressurizer from emptying. Figures E-7 through E-10 show the velocities in the intact-loop hot leg, intact-loop cold leg, broken-loop hot leg, and broken-loop cold leg, respectively. The liquid temperatures at the same locations are presented in Figs. E-11 through E-14, respectively. As mentioned earlier, the temperature convergence is much slower than the convergence of the other system parameters. However, the temperatures are practically converged at ~300 s when the rate of change is only ~0.005 K/s. The oscillations in the broken-loop cold-leg temperature (Fig. E-14) result from erratic steam-generator secondary behavior that causes fluctuations in the secondary-side heat transfer.

TABLE E-II

TEST S-SB-P7 INITIAL CONDITIONS

<u>Parameter</u>	<u>Actual</u>	<u>Calculated</u>
Core power (MW) ^a	1.97	1.97 ^b
Pressurizer pressure (MPa)	15.73	15.73 ^b
Pressurizer liquid volume (m ³)	0.0215	0.0215 ^b
Intact-loop mass flow (kg/s)	8.07	8.14
Intact-loop cold-leg temperature (K)	547.9	547.9
Intact-loop hot-leg temperature (K)	583.8	582.7
Broken-loop mass flow (kg/s)	2.63	2.62
Broken-loop cold-leg temperature (K)	549.8	552.0
Broken-loop hot-leg temperature (K)	581.0	582.6
Intact-loop pump speed (rad/s)	247.	262.
Broken-loop pump speed (rad/s)	1285.	1629.
Intact-loop steam-generator-secondary pressure (MPa)	5.42	4.74
Intact-loop steam-generator-secondary temperature (K)	542.2	533.7
Intact-loop steam-generator-secondary water mass (kg)	127.8	142.9
Intact-loop steam-generator-secondary feedwater temperature (K)	486.3	486.3 ^b
Broken-loop steam-generator-secondary pressure (MPa)	5.09	5.14
Broken-loop steam-generator-secondary temperature (K)	538.2	538.7
Broken-loop steam-generator-secondary water mass (kg)	322.0	324.1
Broken-loop steam-generator-secondary feedwater temperature (K)	486.3	486.3 ^b

^aFlat radial profile.

^bSpecified as input parameter.

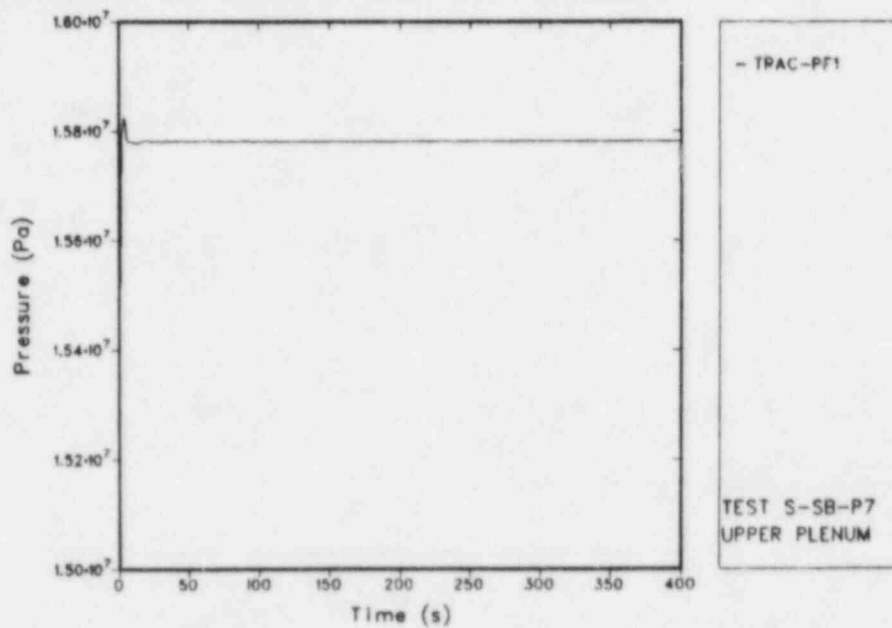


Fig. E-5.
Upper-plenum pressure.

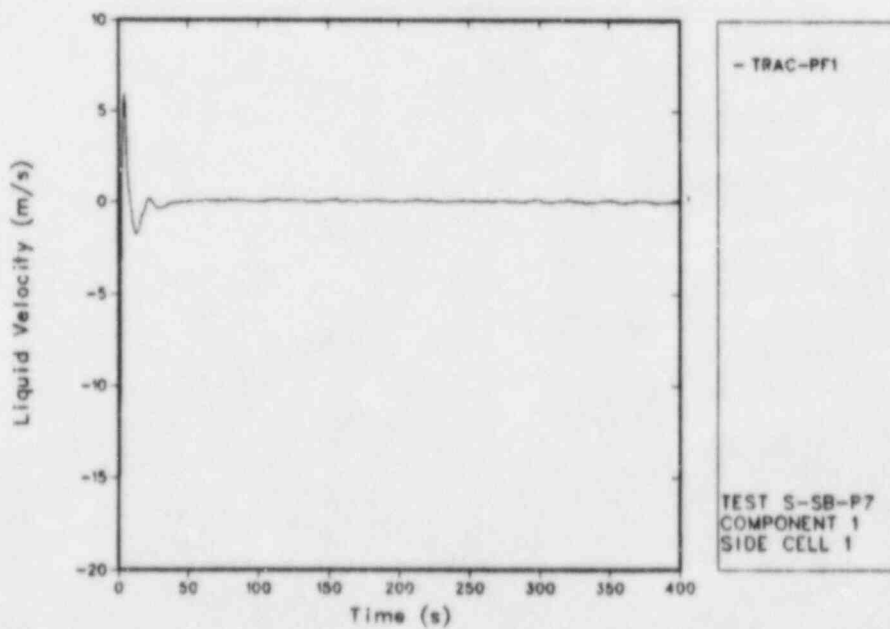


Fig. E-6.
Liquid velocity at the pressurizer outlet.

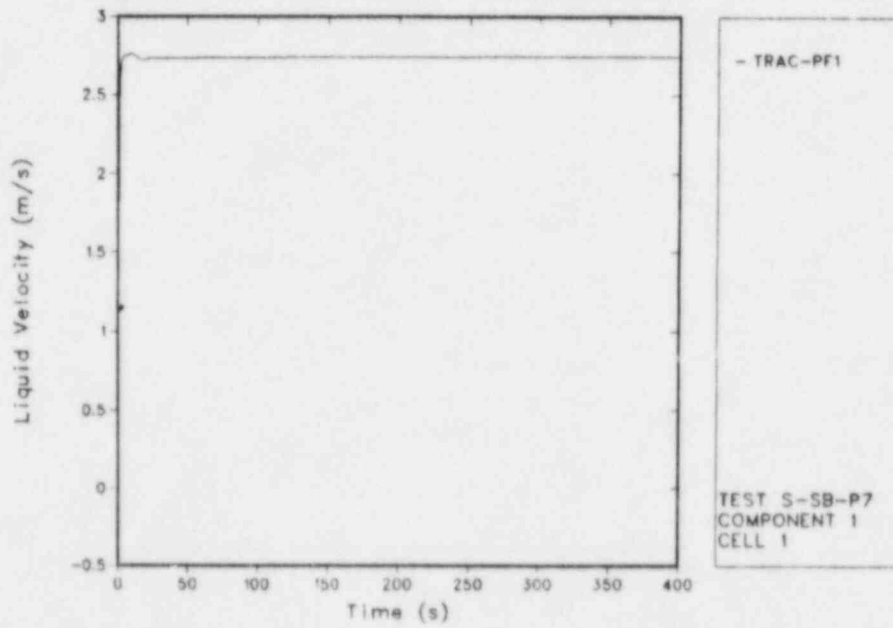


Fig. E-7.
Liquid velocity in the intact-loop hot leg.

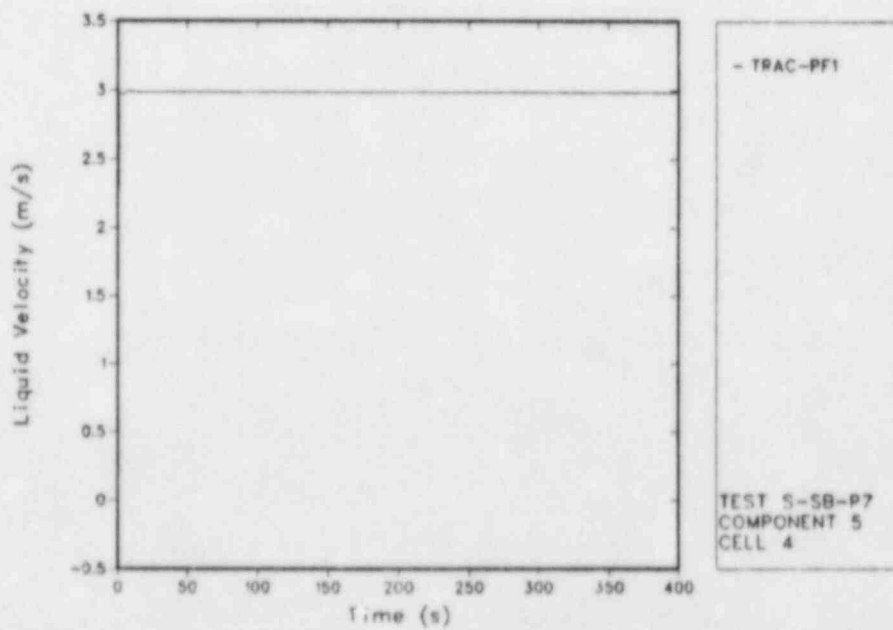


Fig. E-8.
Liquid velocity in the intact-loop cold leg.

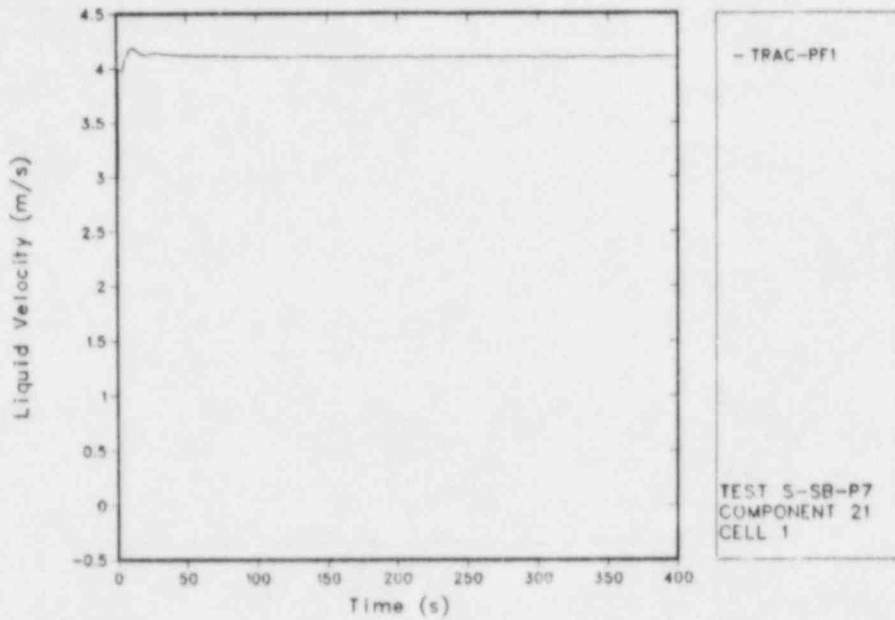


Fig. E-9.
Liquid velocity in the broken-loop hot leg.

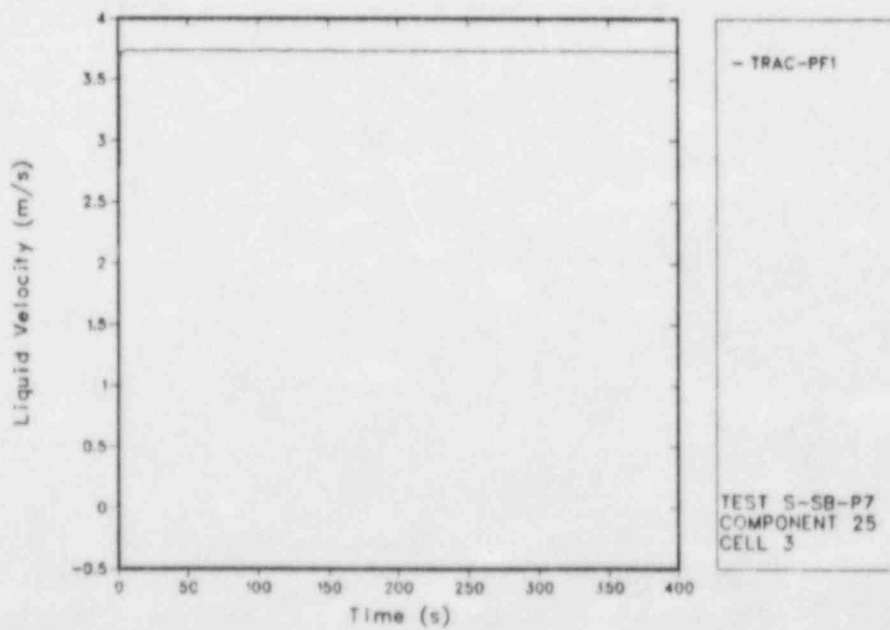


Fig. E-10.
Liquid velocity in the broken-loop cold leg.

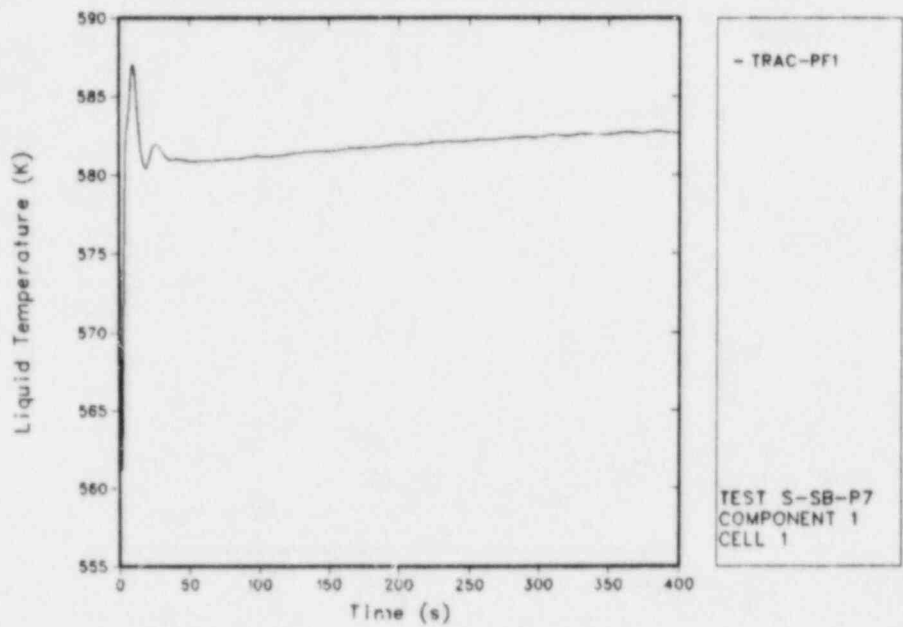


Fig. E-11.
Liquid temperature in the intact-loop hot leg.

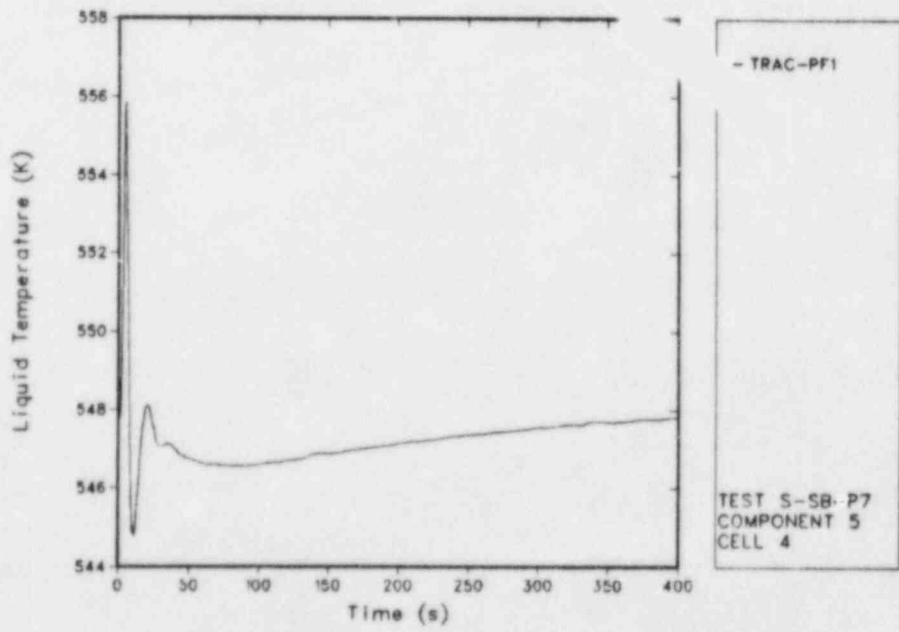


Fig. E-12.
Liquid temperature in the intact-loop cold leg.

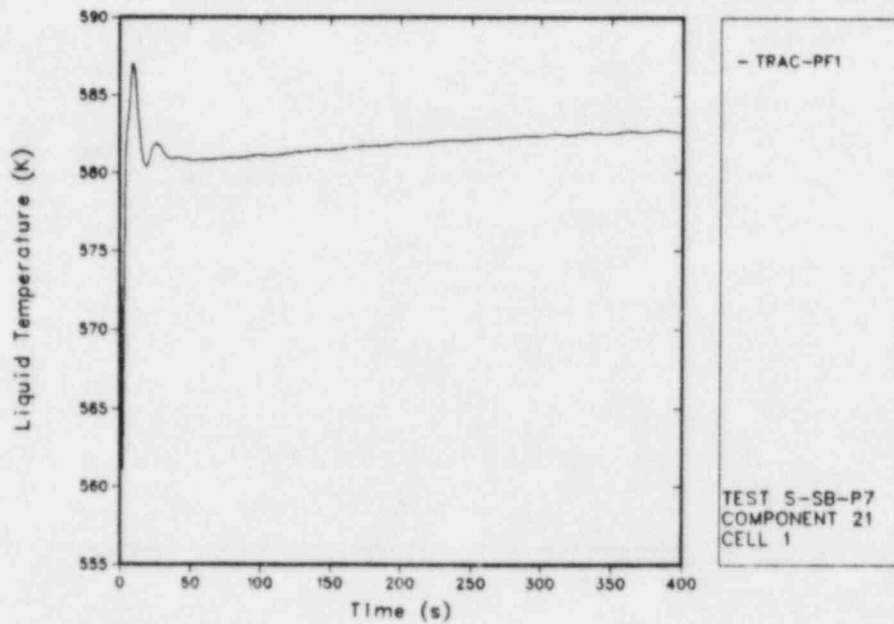


Fig. E-13.
Liquid temperature in the broken-loop hot leg.

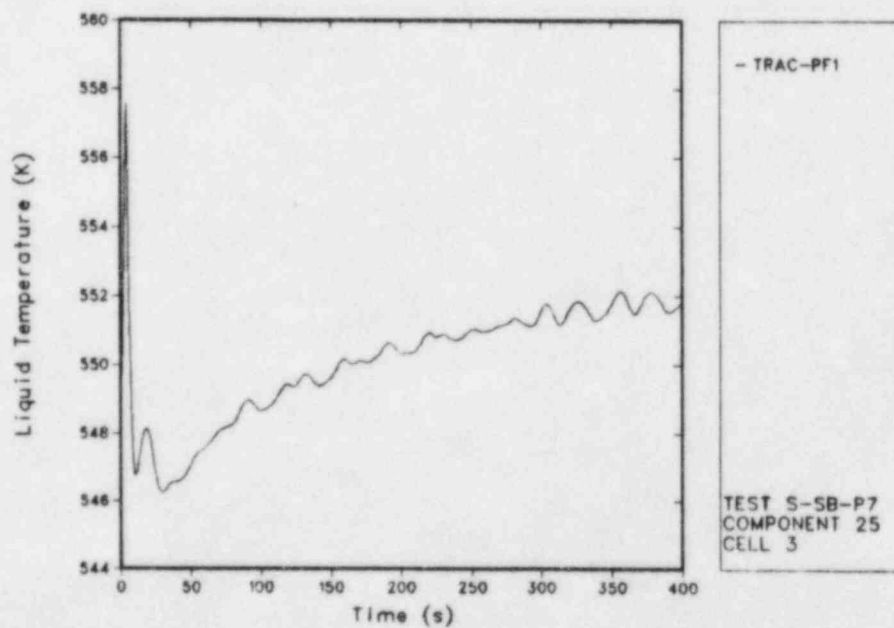


Fig. E-14.
Liquid temperature in the broken-loop cold leg.

V. INPUT LISTINGS

This section contains four separate input listings. The first is a complete steady-state one-dimensional input deck. The second is a restart input deck that begins the transient calculation. The third shows a section of the steady-state input deck recast to illustrate various aspects of the free-format input option. This free format listing is not arranged aesthetically. Rather, it shows the flexibility of a free-format input. Finally, the fourth listing presents a three-dimensional vessel input that is equivalent to the one-dimensional input. This listing demonstrates how the vessel and the downcomer can be modeled using the three-dimensional vessel modeling capability. In this case, all the components shown in Fig. E-3 were combined into a single three-dimensional VESSEL component and three one-dimensional PIPE components, as shown in Fig. E-4. A detailed description of another sample TRAC three-dimensional VESSEL is given in Appendix C of the TRAC-PD2 users' manual.⁶⁹ The geometrical considerations given there also apply to TRAC-PF1.

A. Steady-State One-Dimensional Input Deck

CARD 1234567890123456789012345678901234567890123456789012345678901234567890

1 TRAC

2 43

3 SEMISCALE (MOD3) SMALL BREAK MODEL

4

5 TEST S-SB-P7 (2.5% COLD LEG COMMUNICATIVE BREAK) - DELAYED PUMP TRIP

6

7 DATA BASE

8

9 1. L.L. WEIDERT AND L.B. CLEGG, "EXPERIMENT DATA REPORT FOR SEMISCALE
10 MOD-3 SMALL BREAK TEST SERIES (TESTS S-SB-P1, S-SB-P2 AND
11 S-SB-P7)," EGG-2053, SEPTEMBER 1980.

12

13 2. S.E. DINGMAN, T.J. FAUBLE, AND J.R. HEWITT, "QUICKLOOK REPORT
14 FOR SEMISCALE MOD-3 SMALL BREAK TESTS S-SB-P1, S-SB-P2, AND
15 S-SB-P7," EGG-SEMI-5137, APRIL 1980.

16

17 3. G.W. JOHNSEN, "TRANSMITTAL OF SEMISCALE EOS APPENDIX FOR SMALL
18 BREAK TESTS S-SB-P1 AND S-SB-P2," GWJ-8-80, EG&G IDAHO, INC.,
19 FEBRUARY 1980.

20

21 MODEL INFORMATION

22

23 1. MODEL PREPARATION BEGUN WITH INPUT DECK USED FOR SMALL BREAK TEST
24 S-07-10B.

25

26 2. STEAM GENERATOR COMPONENT 2 REVISED BY ADDING
27 COMPONENTS 14 & 15 TO REPRESENT THE UPPER AND LOWER
28 SECONDARY SHROUDS.

29

30 3. SAME AS ITEM 2 FOR COMPONENT 22 BY ADDING COMPONENTS 34 & 35.

31

32 4. PUMP SUCTION PIPES CONSOLIDATED INTO SINGLE PIPES, COMPONENTS 3 & 23,
33 FOR THE INTACT AND BROKEN LOOPS, RESPECTIVELY.

34

35 5. BROKEN LOOP PUMP COMPONENT 24 CHARACTERISTIC CURVES UPDATED.

36

CARD 12345678901234567890123456789012345678901234567890123456789012345678901234567890

37 6. PIPE COMPONENT 27 REPLACED BY VALVE COMPONENT 27.

38

39 7. TEE COMPONENTS 41 & 42, FILL 43, ACCUM 45 AND VALVE 44 ADDED
40 TO SIMULATE COLD LEG ECCS.

41

42 NOTE *** FILL COMPONENT 40 MUST BE CHANGED TO BREAK COMPONENT
43 40 WHEN RUN TRANSIENT ***

44

45 END OF TITLE CARDS

46	0	0.0				
47	1	0	42	46	1	
48	1.0E-3	1.0E-6	1.0E-5	1.0E-3		
49	10	0	10			
50	5	12	0			
51	1	2	3	4	5	
52	6	7	8	9	10	
53	11	12	13	14	15	
54	16	21	22	23	24	
55	25	26	27	28	34	
56	35	40	41	42	43	
57	44	45	65	70	75	
58	80	83	90	92	97	
59	98	99E				
60	1	21	6	1	0	IDSV 1
61	2	0	0	0	0	IDSV 2
62	3	21	10	4	0	IDSV 3
63	4	21	42	4	0	IDSV 4
64	5	27	25	5	0	IDSV 5
65	0	0	0	0	0	DIMEN
66	1	1	0	1	1	TRIP 1
67	12.480E+6	12.481E+6				IL PUMP
68	1099.7	10000.0				
69	0	0				
70	2	1	0	1	1	TRIP 2
71	12.480E+6	12.481E+6				BL PUMP
72	1099.7	10000.0				

CARD 1234567890123456789012345678901234567890123456789012345678901234567890

73	0	0				
74	3	1	0	1	1	TRIP 3
75	12.480E+6	12.481E+6				CORETRIP
76	3.4	10000.0				
77	0	0				
78	4	1	0	1	1	TRIP 4
79	12.480E+6	12.481E+6				FINE MSH
80	1099.7	10000.0				
81	0	0				
82	5	1	0	1	1	TRIP 5
83	12.480E+6	12.481E+6				IL HPIS
84	28.4	10000.0				
85	0	0				
86	6	1	0	1	1	TRIP 6
87	12.480E+6	12.481E+6				BL HPIS
88	28.4	10000.0				
89	0	0				
90	7	1	0	1	1	TRIP 7
91	12.480E+6	12.481E+6				ACC
92	10000.0	10000.0				
93	0	0				
94	8	1	0	1	1	TRIP 8
95	12.480E+6	12.481E+6				IL SG IN
96	8.4	10000.0				
97	0	0				
98	9	1	0	1	1	TRIP 9
99	12.480E+6	12.481E+6				BL SG IN
100	8.4	10000.0				
101	0	0				
102	10	1	0	1	1	TRIP10
103	12.480E+6	12.481E+6				IL SGOUT
104	0.0	10000.0				
105	0	0				
106	11	1	0	1	1	TRIP11
107	12.480E+6	12.481E+6				BL SGOUT
108	0.0	10000.0				

CARD 123456789012345678901234567890123456789012345678901234567890123456789012345678901234567890

145	V	0.0E								ALP S
146	F	0.0E								VL S
147	F	0.0E								VV S
148		550.0R	2	550.0E						TL S
149		550.0R	2	550.0E						TV S
150		15.730E+6		15.730E+6		15.730E+6E				P S
151	F	0.00E+00E								PA S
152	F	0.0E								QPPP S
153	R 3	550.0R	6	550.0E						TW S
154	FILL			16		16 PRIZER INLET				
155		0		1		0		0		0
156		0								
157		.100000E+01		.100000E+01	0.	0.		.300000E+03		
158		.100000E+06	0.	0.	0.	0.		.300000E+03		
159	PRIZER			6		6 INTACT LOOP PRESSURIZER				
160		5		0		7				
161		0.0		0.0		0.0		0.0		
162		6.03885E-1R	2	2.54000E-1	1.07950E-1	3.83540E-1E				DX
163		1.63682E-2		6.89117E-3	6.93391E-3	2.23618E-3S				VOL
164		9.86256E-4E								VOL
165	R 2	2.71049E-2R	2	2.72989E-2	3.49153E-3	9.07130E-4E				FA
166	F	0.0E								FRIC
167	F	-1.0E								GRAV
168	R 2	4.47310E-2R	2	4.63873E-2	6.66750E-2	3.39852E-2E				HD
169	R 5	1		0E						NFF
170		0.7280		0.0R	3	0.0E				ALP
171	F	0.0E								VL
172	F	0.0E								VV
173	R 3	619.13		600.0	580.0E					TL
174	R 3	619.13		600.0	580.0E					TV
175		15.730E+6		15.730E+6	15.730E+6	15.730E+6S				P
176		15.730E+6E								P
177	F	0.00E+00E								PA
178	STGEN			2		2 IL STEAM GENERATOR				
179		10		3		2		3		12
180		1		0		0		1		

CARD 12345678901234567890123456789012345678901234567890123456789012345678901234567890

217		0	2	15	9		
218		0.1445	0.0079	0.0	0.0	300.0	
219		300.0					
220		0	1	16			
221		0.0859	0.0079	0.0	0.0	300.0	
222		300.0					
223		0.37973	0.59944E				DX P
224		9.79485E-3	3.93081E-1E				VOL P
225	R 2	2.31608E-2	3.14159E-2E				FA P
226	R 2	0.0	1.0E+30E				FRIC P
227	F	1.0E					GRAV P
228	R 2	1.71724E-1	0.2E				HD P
229	F	4E					NFF P
230		0.0	9.85127E-1E				ALP P
231	F	0.0E					VL P
232	F	0.0E					VV P
233	F	542.2E					TL P
234	F	542.2E					TV P
235	F	5.420E+6E					P P
236	F	0.00E+00E					PA P
237		0.37973E					DX S
238		1.54725E-2E					VOL S
239	F	4.07461E-2E					FA S
240	F	0.0E					FRIC S
241		-1.0	-1.0E				GRAV S
242	F	0.11115E					HD S
243	F	4E					NFF S
244	F	0.0E					ALP S
245	F	0.0E					VL S
246	F	0.0E					VV S
247	F	520.0E					TL S
248	F	520.0E					TV S
249	F	5.420E+6E					P S
250	F	0.00E+00E					PA S
251	TEE		15	15 LOWER IL SG SEC SHROUD			
252		5	0	10	0.0	1	

CARD 12345678901234567890123456789012345678901234567890123456789012345678901234567890

253		0	5	17	16	
254		0.1445	0.0079	0.0	0.0	300.0
255		300.0				
256		0	1	8		
257		0.056	0.0079	0.0	0.0	300.0
258		300.0				
259	R 4	6.13341E-1	2.09826E-1E			DX P
260	R 4	9.14122E-3	5.21224E-3E			VOL P
261		3.44878E-2R	4 1.49040E-2	4.07461E-2E		FA P
262	F	0.0E				FRIC P
263		0.0F	1.0E			GRAV P
264		2.71183E-2R	4 3.49504E-2	0.11115E		HD P
265	F	4E				NFF P
266	F	0.0E				ALP P
267	F	0.0E				VL P
268	F	0.0E				VV P
269	F	510.0E				TL P
270	F	510.0E				TV P
271	F	5.420E+6E				P P
272	F	0.00E+00E				PA P
273		1.0E				DX S
274		0.001E				VOL S
275	R 2	0.01E				FA S
276	F	0.0E				FRIC S
277	F	0.0E				GRAV S
278	F	0.11115E				HD S
279	F	4E				NFF S
280	F	0.0E				ALP S
281	F	0.0E				VL S
282	F	0.0E				VV S
283	F	500.0E				TL S
284	F	500.0E				TV S
285	F	5.420E+6E				P S
286	F	0.00E+00E				PA S
287	FILL		7	7 INTACT LOOP SG FEEDWATER		
288		8	8	2	8	7

CARD 12345678901234567890123456789012345678901234567890123456789012345678901234567890

289		2							
290		1.0	0.001	0.0	0.0	0.0	486.3		
291		5.420E+6	0.0	0.650000	0.0	0.0	486.3		
292		1.0							
293		0.0	0.650000	4.0	0.0S			VMTB	
294		55.0	0.0	55.1	0.0S			VMTB	
295		2438.9	0.0	2439.0	0.0S			VMTB	
296		10000.0	0.0E					VMTB	
297		-10000.0	1.0	10000.0	1.0E			RFTB	
298	VALVE		8	8	INTACT LOOP STEAM LINE				
299		2	0	9	10	7			
300		0	1	3	2	10			
301		2	3	0	2				
302		0.05	1.27000E-2	0.0	0.0	300.0			
303		300.0	3.14159E-2	0.2	1.0	1.0			
304	F	2.0E						DX	
305	F	0.004E						VOL	
306	F	3.14159E-2E						FA	
307		1.0E+30	40000.0	0.0E				FRIC	
308		1.0R 2	0.0E					GRAV	
309	F	0.2E						HD	
310	F	0E						NFF	
311	F	1.0E						ALP	
312	F	0.0E						VL	
313	F	0.0E						VV	
314	F	542.2E						TL	
315	F	542.2E						TV	
316		5.420E+6	8.687E+4E					P	
317	F	0.00E+00E						PA	
318		0.00	1.000	4.00	0.000S			VLOTB	
319		10000.00	0.000E					VLOTB	
320		-10000.0	1.0	10000.0	1.0E			VRFTB	
321	BREAK		9	9	IL SG SEC ATM BOUNDARY				
322		10	0	0	3				
323		2.0	0.004	1.0	400.0	8.687E+4			
324		0.00E+00							

CARD 12345678901234567890123456789012345678901234567890123456789012345678901234567890

325	PIPE		3	3	INTACT LOOP PUMP SUCTION	
326		10	3	3	4	7
327		1	0			
328		3.33248E-2	1.11252E-2	0.0	26.76782	300.0
329		300.0				
330		8.16184E-1	5.34100E-1	7.50000E-1	7.50000E-1	5.00000E-1 DX
331		7.50000E-1	7.50000E-1	4.15561E-1	7.64248E-1	7.64248E-1E DX
332		2.84756E-3	2.61665E-3	2.61665E-3	2.61665E-3	1.74444E-3 VOL
333		2.61665E-3	2.61665E-3	1.44984E-3	2.66636E-3	2.66636E-3E VOL
334	F	3.48887E-3E				FA
335		1.570	5.401E-3	8.522E-3	7.295E-3	1.328E-2 FRIC
336		1.328E-2	7.295E-3	6.259E-3	3.091E-3	9.389E-3 FRIC
337		0.0E				FRIC
338		-0.854486R 3	-1.0	-0.895613	0.895613R 3	1.0 GRAV
339		0.441503	0.0E			GRAV
340	F	6.66496E-2E				HD
341	F	4E				NFF
342	F	0.0E				ALP
343	F	0.0E				VL
344	F	0.0E				VV
345	F	547.9E				TL
346	F	547.9E				TV
347	F	15.730E+6E				P
348	F	0.00E+00E				PA
349	F	0.0E				QPPP
350	F	547.9E				TW
351	PUMP		4	4	INTACT LOOP PUMP	
352		2	3	4	5	7
353		1	0	1	1	1
354		2	1	5	2	
355		3.33248E-2	1.11252E-2	0.0	0.0	300.0
356		300.0				
357		1315.17	136.937	1.68577E-2	997.96	366.52
358		1.6140	11.823	0.0	261.71	261.71
359		1				
360		0.0	1.000000	33.0	0.242915S	TSPTBL

CARD 12345678901234567890123456789012345678901234567890123456789012345678901234567890

361		116.0	0.080972	123.0	0.000000S		TSPTBL
362		10000.0	0.000000E				TSPTBL
363		-10000.0	1.0	10000.0	1.0E		RFTBL
364	F	5.84376E-1E					DX
365	F	2.03881E-3E					VOL
366	F	3.48887E-3E					FA
367	F	0.0E					FRIC
368		0.0	0.0	0.0E			GRAV
369	F	6.66496E-2E					HD
370		4	0	4E			NFF
371	F	0.0E					ALP
372	F	0.0E					VL
373	F	0.0E					VV
374	F	547.9E					TL
375	F	547.9E					TV
376	F	15.730E+6E					P
377	F	0.00E+00E					PA
378	F	0.0E					QPPP
379	F	547.9E					TW
380	TEE		5	5	INTACT LOOP COLD LEG		
381		3	3	7	0.0	1	
382		0	4	5	6		
383		3.33248E-2	1.11252E-2	0.0	26.76782	300.0	
384		300.0					
385		0	1	11			
386		1.21539E-2	4.54660E-3	0.0	0.0	300.0	
387		300.0					
388	F	6.14590E-1E					DX P
389	R 3	2.14423E-3	2.16067E-3E				VOL P
390	R 4	3.48887E-3	4.20283E-3E				FA P
391		0.0R 3	3.283E-1	9.566E-2E			FRIC P
392	F	0.0E					GRAV P
393	R 4	6.66496E-2	7.31520E-2E				HD P
394	F	4E					NFF P
395	F	0.0E					ALP P
396	F	0.0E					VL P

CARD 12345678901234567890123456789012345678901234567890123456789012345678901234567890

397	F	0.0E					VV P
398	F	547.9E					TL P
399	F	547.9E					TV P
400	F	15.730E+6E					P P
401	F	0.00E+00E					PA P
402	F	0.0E					QPPP P
403	F	547.9E					TW P
404	F	2.49528E					DX S
405	F	1.15798E-3E					VOL S
406	F	4.64068E-4E					FA S
407		0.504784	0.259133E				FRIC S
408		-1.0	0.0E				GRAV S
409	F	2.43078E-2E					HD S
410	F	1E					NFF S
411	F	0.0E					ALP S
412	F	0.0E					VL S
413	F	0.0E					VV S
414	F	500.0E					TL S
415	F	500.0E					TV S
416	F	15.730E+6E					P S
417	F	0.00E+00E					PA S
418	F	0.0E					QPPP S
419	F	500.0E					TW S
420	TEE		10	10	INTACT LOOP ECC LINE		
421		2	0	7	0.0	1	
422		0	2	12	11		
423		1.21539E-2	4.54660E-3	0.0	0.0	300.0	
424		300.0					
425		0	1	14			
426		1.21539E-2	4.54660E-3	0.0	0.0	300.0	
427		300.0					
428	F	2.49528E					DX P
429	F	1.15798E-3E					VOL P
430	F	4.64068E-4E					FA P
431	F	0.259133E					FRIC P
432	F	0.0E					GRAV P

CARD 12345678901234567890123456789012345678901234567890123456789012345678901234567890

469		1.00E+10	0.00000E				VMTB
470	ACCUM		12	12	INTACT LOOP	ACCUMULATOR	
471		4	13				
472		4.11940E-1	4.0E-1	2.5E-1	2.0E-2E		DX
473		2.66519E-2	2.58794E-2	1.61746E-2	1.29397E-3E		VOL
474	R 4	6.46985E-2	4.64068E-4E				FA
475	R 4	0.0	0.514145E				FRIC
476	R 4	-1.0	-0.618606E				GRAV
477	R 4	2.55550E-1	2.43078E-2E				HD
478	F	1E					NFF
479		0.938019R 3	0.0E				ALP
480	F	0.0E					VL
481	F	0.0E					VV
482	F	300.0E					TL
483	F	300.0E					TV
484	F	2.740E+6E					P
485	F	0.00E+00E					PA
486	VALVE		11	11	INTACT LOOP	ACC VALVE	
487		2	0	13	12	7	
488		1	0	3	2	7	
489		2	3	0	2		
490		1.21539E-2	4.54660E-3	0.0	0.0	300.0	
491		300.0	4.64068E-4	2.43078E-2	0.0	0.0	
492	F	2.49528E					DX
493	F	1.15798E-3E					VOL
494	F	4.64068E-4E					FA
495		0.514145R 2	0.259133E				FRIC
496		-0.618606R 2	0.0E				GRAV
497	F	2.43078E-2E					HD
498	F	1E					NFF
499	F	0.0E					ALP
500	F	0.0E					VL
501	F	0.0E					VV
502		300.0	300.0E				TL
503		300.0	300.0E				TV
504		2.40E+6	15.730E+6E				P

CARD 12345678901234567890123456789012345678901234567890123456789012345678901234567890

505	F	0.00E+00E							PA
506		0.0	0.0	0.2	1.0S				VLOTB
507		10000.0	1.0E						VLOTB
508		-10000.0	1.0	10000.0	1.0E				VRFTB
509	PIPE		21	21	BROKEN LOOP HOT LEG				
510		3	3	21	22			7	
511		1	0						
512		1.69926E-2	7.13740E-3	0.0	26.76782			300.0	
513		300.0							
514	F	8.95182E-1E							DX
515	F	8.12046E-4E							VOL
516	R 3	9.07130E-4	6.13116E-4E						FA
517		7.110E-2R 2	5.802E-3	2.205E-2E					FRIC
518	R 3	0.0	0.79797E						GRAV
519		3.00000E-1R 2	3.39852E-2	2.79400E-2E					HD
520	F	4E							NFF
521	F	0.0E							ALP
522	F	0.0E							VL
523	F	0.0E							VV
524	F	581.0E							TL
525	F	581.0E							TV
526	F	15.730E+6E							P
527	F	0.00E+00E							PA
528	F	0.0E							QPPP
529	F	581.0E							TW
530	STGEN		22	22	BL STEAM GENERATOR				
531		12	3	22	23			12	
532		1	0	0	1				
533		9.86790E-3	1.24460E-3						
534		6	37	35					
535		2.26409R 4	1.84895R 2	1.87076R 4	1.84895	2.26409E			DX P
536		2.99941E-3R 4	1.13124E-3R 2	1.14458E-3R 4	1.13124E-3	2.99941E-3E			VOL P
537		6.13116E-4R11	6.11828E-4	6.13116E-4E					FA P
538		2.205E-2	2.285E-3R 4	0.0	9.180E-4R 4	0.0			FRIC P
539		4.356E-3	2.239E-2E						FRIC P
540		0.79797R 5	1.0	0.0R 5	-1.0	-0.93829E			GRAV P

CARD 12345678901234567890123456789012345678901234567890123456789012345678901234567890

541		2.79400E-2R11	1.97358E-2	2.79400E-2E		HD P
542		4R11	1	4E		NFF P
543	F	0.0E				ALP P
544	F	0.0E				VL P
545	F	0.0E				VV P
546	F	565.4E				TL P
547	F	565.4E				TV P
548	F	15.730E+6E				P P
549	F	0.00E+00E				PA P
550	F	538.2E				TW P
551	R 5	1.84895	1.07730E			DX S
552	R 4	4.92129E-2	4.90267E-2	3.95682E-2E		VOL S
553	R 5	2.66166E-2	3.51514E-2	5.50165E-2E		FA S
554	R 6	0.0	1.202E-2E			FRIC S
555		0.0F	1.0E			GRAV S
556	R 5	4.83783E-2	2.11556E-1	2.64668E-1E		HD S
557	F	1E				NFF S
558	F	0.0E				ALP S
559	F	0.0E				VL S
560	F	0.0E				VV S
561	F	538.2E				TL S
562	F	538.2E				TV S
563	F	5.090E+6E				P S
564	F	0.00E+00E				PA S
565		0.0R 4	2.29277E-1R 2	2.31981E-1R 4	2.29277E-1	0.0E WA1
566	R 4	2.58195E-1	2.61240E-1	0.0E		WA2
567	TEE		34	34 BL SG SEC UPPER SHROUD		
568		2	0	10	1.0	1
569		0	2	35	28	
570		0.1323	0.0042	0.0	0.0	300.0
571		300.0				
572		0	1	36		
573		0.2048	0.0238	0.0	0.0	300.0
574		300.0				
575		1.01270	2.28397E-1E			DX P
576		5.57151E-2	3.00880E-1E			VOL P

CARD 12345678901234567890123456789012345678901234567890123456789012345678901234567890

577	R 2	5.50165E-2	7.85398E-3E							FA P
578	R 2	0.0	1.0E+30E							FRIC P
579	F	1.0E								GRAV P
580	R 2	2.64668E-1	0.1E							HD P
581	F	4E								NFF P
582		8.67319E-1	1.0E							ALP P
583	F	0.0E								VL P
584	F	0.0E								VV P
585	F	538.2E								TL P
586	F	538.2E								TV P
587	F	5.090E+6E								P P
588	F	0.00E+00E								PA P
589		1.01270E								DX S
590		6.69540E-2E								VOL S
591		7.31971E-2	2.06167E-2E							FA S
592	F	0.0E								FRIC S
593		-1.0	-1.0E							GRAV S
594		0.13650	0.04450E							HD S
595	F	4E								NFF S
596	F	9.33751E-1E								ALP S
597	F	0.0E								VL S
598	F	0.0E								VV S
599	F	520.0E								TL S
600	F	520.0E								TV S
601	F	5.090E+6E								P S
602	F	0.00E+00E								PA S
603	TEE		35		35	LOWER	BL	SG	SEC	SHROUD
604		6	0		10			0.0		1
605		0	6		37			36		
606		0.1209	0.0151		0.0			0.0		300.0
607		300.0								
608		0	1		27					
609		0.01905	0.00508		0.0			0.0		300.0
610		300.0								
611	R 4	1.84895	2.08625	8.40001E-1E						DX P
612	R 4	1.59655E-2	1.80146E-2	2.95771E-2E						VOL P

CARD 123456789012345678901234567890123456789012345678901234567890123456789012345678901234567890

649		-10000.0	1.0	10000.0	1.0E		RFTB
650	VALVE		27	27	BROKEN LOOP STEAM LINE		
651		2	0	28	29		7
652		0	1	3	2		11
653		2	3	0	2		
654		0.05	6.35000E-3	0.0	0.0		300.0
655		300.0	7.85398E-3	0.1	1.0		1.0
656	F	2.0E					DX
657	F	0.001E					VOL
658	F	7.85398E-3E					FA
659		1.0E+30	17500.0	0.0E			FRIC
660		1.0R 2	0.0E				GRAV
661	F	0.1E					HD
662	F	0E					NFF
663	F	1.0E					ALP
664	F	0.0E					VL
665	F	0.0E					VV
666	F	538.2E					TL
667	F	538.2E					TV
668		5.090E+6	8.687E+4E				P
669	F	0.00E+00E					PA
670		0.00	1.000	2.80	0.000S		VLOTB
671		10000.00	0.000E				VLOTB
672		-10000.0	1.0	10000.0	1.0E		VRFTB
673	BREAK		28	28	BL SG SEC ATM BOUNDARY		
674		29	0	0	3		
675		2.0	0.001	1.0	400.0	8.587E+4	
676		0.00E+00					
677	PIPE		23	23	BROKEN LOOP PUMP SUCTION		
678		7	3	23	24		7
679		1	0				
680		1.69926E-2	7.13740E-3	0.0	26.76782	300.0	
681		300.0					
682		8.47510E-1	5.34100E-1	7.50000E-1	1.00000	1.00000	DX
683		7.50000E-1	9.03020E-1E				DX
684		7.68802E-4R 2	6.80350E-4R 2	9.07132E-4	6.80349E-4	8.19157E-4E	VOL

004

CARD 1234567890123456789012345678901234567890123456789012345678901234567890

685	6.13116E-4R 7	9.07130E-4E				FA
686	2.239E-2	2.434E-3	3.928E-3	2.883E-3	5.437E-3	FRIC
687	3.843E-3	2.035E-3	0.0E			FRIC
688	-0.93829R 3	-1.0	0.0R 2	1.0	0.86232E	GRAV
689	2.79400E-2R 7	3.39852E-2E				HD
690	R 7	4	0E			NFF
691	F	0.0E				ALP
692	F	0.0E				VL
693	F	0.0E				VV
694	F	549.8E				TL
695	F	549.8E				TV
696	F	15.730E+6E				P
697	F	0.00E+00E				PA
698	F	0.0E				QPPP
699	F	549.8E				TW
700	PUMP	24	24	BROKEN LOOP PUMP		
701		2	3	24	25	7
702		1	0	1	1	1
703		2	2	5	2	
704	1.69926E-2	7.13740E-3	0.0	0.0	300.0	
705	300.0					
706	780.13	2.9828	3.2365E-3	997.96	1597.0	
707	9.2709E-3	2.4811	0.0	1628.92	1628.92	
708	0					
709	9	8	10	5	16	
710	7	19	8	13	13	
711	11	12	2	2	2	
712	2	5	9			
713	-1.0000	1.5000	-0.8000	1.2750S		HHSP1
714	-0.6000	1.3750	-0.4000	1.3750S		HSP1
715	0.0000	1.7821	0.2845	1.7059S		HSP1
716	0.5690	1.6270	0.8535	1.1878S		HSP1
717	1.0000	1.0000E				HSP1
718	-1.0000	0.1750	-0.7500	-0.1500S		HHSP2
719	-0.5500	-0.3000	-0.2750	-0.4000S		HSP2
720	0.0000	-1.6359	0.7130	0.0000S		HSP2

CARD 1234567890123456789012345678901234567890123456789012345678901234567890

721	0.8271	0.2959	1.0000	1.0000E	HSP2
722	-1.0000	1.5000	-0.8000	1.1500S	HHSP3
723	-0.6000	0.9500	-0.4000	0.8300S	HSP3
724	-0.2000	0.7750	0.0000	0.7250S	HSP3
725	0.2000	0.7250	0.4000	0.8000S	HSP3
726	0.6000	1.0250	1.0000	1.9500E	HSP3
727	-1.0000	0.1750	-0.5000	0.6500S	HHSP4
728	0.0000	0.9750	0.5000	1.3500S	HSP4
729	1.0000	1.9500E			HSP4
730	-1.0000	2.6600	-0.9000	2.6000S	HHTP1
731	-0.8000	3.0100	-0.7000	4.7200S	HTP1
732	-0.6000	4.1600	-0.5000	4.1900S	HTP1
733	-0.4000	4.0400	-0.2500	2.9400S	HTP1
734	-0.1000	1.7400	0.0000	1.2200S	HTP1
735	0.1000	0.1200	0.2000	0.1100S	HTP1
736	0.5000	0.1400	0.7000	0.1000S	HTP1
737	0.9000	0.1000	1.0000	0.0000E	HTP1
738	-1.0000	0.1750	0.0000	-0.3500S	HHTP2
739	0.3000	-0.3000	0.4000	-0.3100S	HTP2
740	0.8000	-0.1250	0.9000	-0.0200S	HTP2
741	1.0000	0.0000E			HTP2
742	-1.0000	2.6600	-0.9000	2.1000S	HHTP3
743	-0.8000	1.6500	-0.7000	1.3600S	HTP3
744	-0.6000	1.1200	-0.5000	0.9700S	HTP3
745	-0.3500	0.8200	-0.2000	0.7250S	HTP3
746	-0.1000	0.6700	0.0000	0.6150S	HTP3
747	0.1000	0.5950	0.2500	0.6000S	HTP3
748	0.4000	0.6700	0.5000	0.8500S	HTP3
749	0.6000	1.0650	0.7000	1.4900S	HTP3
750	0.8000	2.0100	0.9000	2.6400S	HTP3
751	1.0000	3.4200E			HTP3
752	-1.0000	0.1750	-0.5000	0.6500S	HHTP4
753	0.0000	0.9750	0.2000	1.4600S	HTP4
754	0.4000	1.9200	0.6000	2.4000S	HTP4
755	0.8000	2.9000	1.0000	3.4200E	HTP4
756	-1.0000	0.6200	-0.8000	0.6800S	TTSP1

CARD 1234567890123456789012345678901234567890123456789012345678901234567890

757	-0.6000	0.5300	-0.4000	0.4600S	TSP1
758	-0.2000	0.4900	0.0000	0.5400S	TSP1
759	0.2000	0.5900	0.4000	0.6500S	TSP1
760	0.6000	0.7700	0.8000	0.9500S	TSP1
761	0.9000	0.9800	0.9500	0.9600S	TSP1
762	1.0000	0.8700E			TSP1
763	-1.0000	-1.4400	-0.8000	-1.1200S	TTSP2
764	-0.6000	-0.7900	-0.4000	-0.5200S	TSP2
765	-0.2000	-0.3100	0.0000	-0.1500S	TSP2
766	0.2000	0.0200	0.4000	0.2200S	TSP2
767	0.6000	0.4600	0.8000	0.7100S	TSP2
768	0.9000	0.8100	0.9500	0.8500S	TSP2
769	1.0000	0.8700E			TSP2
770	-1.0000	0.6200	-0.8000	0.5300S	TTSP3
771	-0.6000	0.4600	-0.4000	0.4200S	TSP3
772	-0.2000	0.3900	0.0000	0.3600S	TSP3
773	0.2000	0.3200	0.4000	0.2700S	TSP3
774	0.6000	0.1800	0.8000	0.0500S	TSP3
775	1.0000	-0.1300E			TSP3
776	-1.0000	-1.4400	-0.8000	-1.2500S	TTSP4
777	-0.6000	-1.0800	-0.4000	-0.9200S	TSP4
778	-0.2000	-0.7700	0.0000	-0.6300S	TSP4
779	0.2000	-0.5100	0.4000	-0.3900S	TSP4
780	0.6000	-0.2900	0.8000	-0.2000S	TSP4
781	0.9000	-0.1600	1.0000	-0.1300E	TSP4
782	-1.0000	0.0000	1.0000	0.0000E	TTTT1
783	-1.0000	0.0000	1.0000	0.0000E	TTTT2
784	-1.0000	0.0000	1.0000	0.0000E	TTTT3
785	-1.0000	0.0000	1.0000	0.0000E	TTTT4
786	0.0000	0.0000	0.0750	0.0000S	HHDM
787	0.2000	1.0000	0.9200	1.0000S	HDM
788	1.0000	0.0000E			HDM
789	0.0000	0.0000	0.0001	0.0000S	TTDM
790	0.0060	0.0000	0.1000	0.0000S	TDM
791	0.1500	0.0500	0.2400	0.5600S	TDM
792	0.8600	0.5600	0.9600	0.4500S	TDM

CARD 12345678901234567890123456789012345678901234567890123456789012345678901234567890

793		1.0000	0.0000E				TDM
794		0.0	1.000000	22.0	0.351751S		TSPTBL
795		61.0	0.336965	66.0	0.000000S		TSPTBL
796		10000.0	0.000000E				TSPTBL
797		-10000.0	1.0	10000.0	1.0E		RFTBL
798	F	7.33573E-1E					DX
799	F	6.65446E-4E					VOL
800	F	9.07130E-4E					FA
801	F	0.0E					FRIC
802		+0.86232R 2	0.0E				GRAV
803	F	3.39852E-2E					HD
804	F	0E					NFF
805	F	0.0E					ALP
806	F	0.0E					VL
807	F	0.0E					VV
808	F	549.8E					TL
809	F	549.8E					TV
810	F	15.730E+6E					P
811	F	0.00E+00E					PA
812	F	0.0E					QPPP
813	F	549.8E					TW
814	TEE		41	41	BROKEN LOOP COLD LEG		
815		2	3	7	0.0	1	
816		1	3	25	60		
817		1.69926E-2	7.13740E-3	0.0	26.76782	300.0	
818		300.0					
819		1	1	61			
820		9.42340E-3	3.91160E-3	0.0	0.0	300.0	
821		300.0					
822		0.500000	0.250000	0.250000C			DX P
823		4.53565E-4	2.26783E-4	2.26783E-4E			VOL P
824	F	9.07130E-4E					FA P
825		0.0	2.098E-1	3.148E-1	3.148E-1E		FRIC P
826	F	0.0E					GRAV P
827	F	3.39852E-2E					HD P
828	F	4E					NFF P

CARD 12345678901234567890123456789012345678901234567890123456789012345678901234567890

865	0.463703R 2	0.408430E				FRIC P
866	-0.207878R 2	0.0E				GRAV P
867	1.38684E-2R 2	1.88468E-2E				HD P
868	F	4E				NFF P
869	F	0.0E				ALP P
870	F	0.0E				VL P
871	F	0.0E				VV P
872	F	400.0E				TL P
873	F	400.0E				TV P
874	F	15.730E+6E				P P
875	F	0.00E+00E				PA P
876	F	8.22960E-1E				DX S
877	F	1.24314E-4E				VOL S
878	F	1.51058E-4E				FA S
879	F	0.0E				FRIC S
880	F	0.0E				GRAV S
881	F	3.39852E-2E				HD S
882	F	4E				NFF S
883	F	0.0E				ALP S
884	F	0.0E				VL S
885	F	0.0E				VV S
886	F	300.0E				TL S
887	F	300.0E				TV S
888	F	15.730E+6E				P S
889	F	0.00E+00E				PA S
890	FILL		43	43 BROKEN LOOP	HPIS	
891		63	8	4	6	15
892		0				
893		8.22960E-1	1.24314E-4	0.0	0.0	300.0
894		5.5E+6	0.0	0.0	0.0	300.0
895		1.0				
896		0.00E+0	0.04293	1.21E+5	0.03750S	VMTB
897		2.61E+5	0.03025	4.23E+5	0.02010S	VMTB
898		6.14E+5	0.01383	7.81E+5	0.00793S	VMTB
899		3.44E+6	0.00658	5.78E+6	0.00548S	VMTB
900		7.39E+6	0.00448	9.01E+6	0.00283S	VMTB

CARD 12345678901234567890123456789012345678901234567890123456789012345678901234567890

901		9.90E+6	0.00155	1.19E+7	0.00093S	VMTB
902		1.30E+7	0.00082	1.40E+7	0.00000S	VMTB
903		1.00E+10	0.00000E			VMTB
904	ACCUM		45	45 BROKEN LOOP ACCUMULATOR		
905		4	64			
906		2.92723E-1	3.0E-1	1.9E-1	2.0E-2E	DX
907		8.46016E-3	8.67048E-3	5.49130E-3	5.78032E-4E	VOL
908	R 4	2.89016E-2	2.78975E-4E			FA
909	R 4	0.0	0.811023E			FRIC
910	R 4	-1.0	-7.14868E-3E			GRAV
911	R 4	1.67005E-1	1.88468E-2E			HD
912	F	1E				NFF
913		0.969249R 3	0.0E			ALP
914	F	0.0E				VL
915	F	0.0E				VV
916	F	300.0E				TL
917	F	300.0E				TV
918	F	4.140E+6E				P
919	F	0.00E+00E				PA
920	VALVE		44	44 BROKEN LOOP ACC VALVE		
921		2	0	64	62	7
922		1	0	3	2	7
923		2	3	0	2	
924		9.42340E-3	3.91160E-3	0.0	0.0	300.0
925		300.0	2.78975E-4	1.88468E-2	0.0	0.0
926	F	2.77772E				DX
927	F	7.74914E-4E				VOL
928	F	2.78975E-4E				FA
929		0.811023R 2	0.408430E			FRIC
930		-7.14869E-3R 2	0.0E			GRAV
931	F	1.88468E-2E				HD
932	F	1E				NFF
933	F	0.0E				ALP
934	F	0.0E				VL
935	F	0.0E				VV
936	F	300.0E				TL

CARD 12345678901234567890123456789012345678901234567890123456789012345678901234567890

937	F	300.0E							TV
938		4.140E+6	15.730E+6E						P
939	F	0.00E+00E							PA
940		0.0	0.0	0.2	1.0S				VLOTB
941		10000.0	1.0E						VLOTB
942		-10000.0	1.0	10000.0	1.0E				VRFTB
943	TEE		25	25	BROKEN LOOP COLD LEG				
944		2	0	7	0.0			1	
945		0	3	60	26				
946		1.69926E-2	7.13740E-3	0.0	0.00000			300.0	
947		300.0							
948		1	2	30					
949		1.69926E-2	9.48690E-3	0.0	0.0			300.0	
950		300.0							
951		0.250000	0.250000	0.791436E					DX P
952		2.26783E-4	2.26783E-4	7.17935E-4E					VOL P
953	F	9.07130E-4E							FA P
954		3.148E-1	3.148E-1	1.511E-1	3.525E-2E				FRIC P
955	F	0.0E							GRAV P
956	F	3.39852E-2E							HD P
957	F	4E							NFF P
958	F	0.0E							ALP P
959	F	0.0E							VL P
960	F	0.0E							VV P
961	F	549.8E							TL P
962	F	549.8E							TV P
963	F	15.730E+6E							P P
964	F	0.00E+00E							PA P
965		1.26500E-2	9.85500E-3E						DX S
966		1.14752E-5	6.04658E-8E						VOL S
967		9.07130E-4R 2	6.13555E-6E						FA S
968		0.0	0.0	0.0E					FRIC S
969	F	0.0E							GRAV S
970		3.39852E-2R 2	2.79500E-3E						HD S
971		4	0	0E					NFF S
972	F	0.0E							ALP S

CARD 12345678901234567890123456789012345678901234567890123456789012345678901234567890

973	F	0.0E								VL S
974	F	0.0E								VV S
975		540.0F	530.0E							TL S
976		540.0F	530.0E							TV S
977	F	15.730E+6E								P S
978	F	0.00E+00E								PA S
979	FILL		40	40 FILL FOR STEADY STATE RUN						
980		30	1	0	0	0				
981		0								
982		9.85500E-3	6.04658E-8	0.0	0.0	530.0				
983		15.730E+6	0.0	0.0	0.0	530.0				
984	TEE		90	90 IL DNCMR INLET AND DNCMR						
985		2	5	7	0.0	1				
986		0	2	6	229					
987		0.1	0.01	0.0	0.0	300.0				
988		300.0								
989		0	10	215						
990		0.1	0.01	0.0	26.76782	300.0				
991		300.0								
992		7.54799E-01	8.12900E-01E							DX P
993		2.6678E-03	3.529E-03E							VOL P
994	R 2	4.20283E-3R 1	4.90998E-3E							FA P
995		9.566E-2	0.0	0.0E						FRIC P
996	F	0.0E								GRAV P
997		7.3152E-02R 2	1.9258E							HD P
998	F	1E								NFF P
999	F	0.0E								ALP i
1000	F	0.0E								VL P
1001	F	0.0E								VV P
1002	F	547.9E								TL P
1003	F	547.9E								TV P
1004	F	15.730E+6E								P P
1005	F	0.0E								PA P
1006	F	0.0E								QPPP P
1007	F	547.9E								TW P
1008		0.3147R 2	0.4572	0.3048	0.6096	0.1524				DX S

CARD 12345678901234567890123456789012345678901234567890123456789012345678901234567890

1045	F	549.8E					TV P
1046	F	15.730E+6E					P P
1047	F	0.0E					PA P
1048	F	0.0E					QPPP P
1049	F	549.8E					TW P
1050	F	0.22265E					DX S
1051	F	1.29774E-4E					VOL S
1052	F	3.705E-4E					FA S
1053	F	0.0E					FRIC S
1054	F	1.0E					GRAV S
1055	F	6.4E-4E					HD S
1056	F	1E					NFF S
1057	F	0.0E					ALP S
1058	F	0.0E					VL S
1059	F	0.0E					VV S
1060	F	548.9E					TL S
1061	F	548.9E					TV S
1062	F	15.730E+6E					P S
1063	F	0.0E					PA S
1064	F	0.0E					QPPP S
1065	F	548.9E					TW S
1066	PIPE		83		83 LOWER PLENUM		
1067		3	5	215	210	7	
1068		1	0				
1069		0.15	0.01	0.0	26.76782	300.0	
1070		300.0					
1071		0.4762	0.2	0.4762E			DX
1072		2.453858E-3	1.34172E-2	2.32522E-3E			VOL
1073		4.19507E-3	7.67759E-3	4.29953E-3	2.8558E-3E		FA
1074	R 3	0.0	7.870E-3E				FRIC
1075	R 2	-1.0R 2	1.0E				GRAV
1076	R 3	0.055	0.0103E				HD
1077	F	1E					NFF
1078	F	0.0E					ALP
1079	F	0.0E					VL
1080	F	0.0E					VV

CARD 12345678901234567890123456789012345678901234567890123456789012345678901234567890

1117		0.4572	0.9144	1.3716	1.6764	1.8288	Z
1118		2.4384	2.7432	3.2004	3.6576E		Z
1119		0.0R 2	1.0R 5	0.0E			RDPWR
1120	F	1.0E					CPOWR
1121		0.0	0.2916	0.5908	0.9949	1.4351	ZPOWR
1122	R 2	1.5499	1.4351	1.0013	0.5908	0.2916E	ZPOWR
1123	F	22.0E					NRDX
1124		0.0	1.588E-03	2.4E-03	3.844E-03	4.368E-03	RADR
1125		4.369E-03	4.699E-03	5.359E-03E			RADR
1126		4	5R 2	4	3R 2	7E	MATR
1127		0.0	1.0000	3.0	0.4000S		PWTB
1128		6.0	0.2500	20.0	0.1000S		PWTB
1129		30.0	0.0520	60.0	0.0440S		PWTB
1130		100.0	0.0400	200.0	0.0350S		PWTB
1131		1000.0	0.0230	3000.0	0.0170E		PWTB
1132		-10000.0	1.0	10000.0	1.0E		RPRF
1133	R 2	5	9	5	9	5	NFAX
1134		9R 2	5E				NFAX
1135	F	0.0E					FPUO
1136	F	1.0E					FTD
1137	F	0.0E					GMIX
1138	F	0.0E					GMLS
1139	F	0.0E					PGAP
1140	F	0.0E					PLVL
1141	F	0.0E					PSLN
1142	F	0.0E					CLNN
1143	F	0.0E					BURN
1144	F	565.6E					RFTN
1145	TEE		75	75	BOTTOM UPPER PLENUM		
1146		1	5	7	-1.	1	
1147		0	1	205	208		
1148		0.061	0.01	0.0	26.76782	300.0	
1149		300.0					
1150		0	1	240			
1151		0.01	0.01	0.0	0.0	300.0	
1152		300.0					

CARD 1234567890123456789012345678901234567890123456789012345678901234567890

1297	F	1E					NFF
1298	F	0.0E					ALP
1299	F	0.0E					VI
1300	F	0.0E					VV
1301	F	548.9E					TL
1302	F	548.9E					TV
1303	F	15.730E+6E					P
1304	F	0.0E					PA
1305	F	0.0E					QPPP
1306	F	548.9E					TW
1307	FILL		99	99	UPPER HEAD ZERO VEL FILL		
1308		999	1	0	0	0	
1309		0					
1310		2.1722	1.1445E-3	0.0	0.0	300.0	
1311		1.000E+6	0.0	0.0	0.0	300.0	
1312		1.0E-3	1.0	200.0	1000.0 0.5		TIME STP
1313		20.0	1.0	20.0	1.0		TIME STP
1314		-1.0					

B. Restart Input Deck for a Transient Calculation

CARD 123456789012345678901234567890123456789012345678901234567890

1 TRAC
2 14
3 SEMISCALE (MOD3) SMALL BREAK MODEL
4
5 TEST S-SB-P7 (2.5% COLD LEG COMMUNICATIVE BREAK) - DELAYED PUMP TRIP
6
7 RESTART DECK
8
9
10 NOTE *** FILL COMPONENT 40 REPLACED BY BREAK COMPONENT 40
11 TO RUN THE TRANSIENT ***
12
13 SEE STEADY STATE INPUT FOR MORE COMMENTS
14
15

CARD 12345678901234567890123456789012345678901234567890123456789012345678901234567890

16	END OF TITLE CARDS					
17	-1	0.0				
18	0	1	42	46	0	
19	1.0E-3	1.0E-6	1.0E-5	1.0E-3		
20	10	0	10			
21	5	12	0			
22	1	2	3	4	5	
23	6	7	8	9	10	
24	11	12	13	14	15	
25	16	21	22	23	24	
26	25	26	27	28	34	
27	35	40	41	42	43	
28	44	45	65	70	75	
29	80	83	90	92	97	
30	98	99E				
31	-1					TD-1
32	0	0	0	0	0	DIMEN
33	-1					TD-2
34	BREAK	40	40 BREAK FOR TRANSIENT RUN			
35	30	0	0	3		
36	9.85500E-3	6.04658E-8	1.0	392.69	2.0E+5	
37	0.0					
38	END					
39	1.0E-3	1.0	2464.8	1.0 0.5		TIME STP
40	20.0	1.0	20.0	1.0		TIME STP
41	-1.0					

C. Section of Input Deck (Appendix C.A) Recast in Free Format

CARD 1234567890123456789012345678901234567890123456789012345678901234567890

1	TRAC-PF1 INPUT DECK IN FREE FORMAT					
2						
3	*NUMTCR*	*IEOS*	*INOPT*			
4	43	0	1			
5	SEMISCALE (MOD3) SMALL BREAK MODEL					
6						
7	TEST S-SB-P7 (2.5% COLD LEG COMMUNICATIVE BREAK) - DELAYED PUMP TRIP					

8
9
10
11
12
13
14
15
16
17
18
19
20
21
22
23
24
25
26
27
28
29
30
31
32
33
34
35
36
37
38
39
40
41
42
43

DATA BASE

1. L.L. WEIDERT AND L.B. CLEGG, "EXPERIMENT DATA REPORT FOR SEMISCALE MOD-3 SMALL BREAK TEST SERIES (TESTS S-SB-P1, S-SB-P2 AND S-SB-P7)," EGG-2053, SEPTEMBER 1980.
2. S.E. DINGMAN, T.J. FAUBLE, AND J.R. HEWITT, "QUICKLOOK REPORT FOR SEMISCALE MOD-3 SMALL BREAK TESTS S-SB-P1, S-SB-P2, AND S-SB-P7," EGG-SEMI-5137, APRIL 1980.
3. G.W. JOHNSEN, "TRANSMITTAL OF SEMISCALE EOS APPENDIX FOR SMALL BREAK TESTS S-SB-P1 AND S-SB-P2," GWJ-8-80, EG&G IDAHO, INC., FEBRUARY 1980.

MODEL INFORMATION

1. MODEL PREPARATION BEGUN WITH INPUT DECK USED FOR SMALL BREAK TEST S-07-10B.
2. STEAM GENERATOR COMPONENT 2 REVISED BY ADDING COMPONENTS 14 & 15 TO REPRESENT THE UPPER AND LOWER SECONDARY SHROUDS.
3. SAME AS ITEM 2 FOR COMPONENT 22 BY ADDING COMPONENTS 34 & 35.
4. PUMP SUCTION PIPES CONSOLIDATED INTO SINGLE PIPES, COMPONENTS 3 23, FOR THE INTACT AND BROKEN LOOPS RESPECTIVELY.
5. BROKEN LOOP PUMP COMPONENT 24 CHARACTERISTIC CURVES UPDATED.
6. PIPE COMPONENT 27 REPLACED BY VALVE COMPONENT 27.
7. TEE COMPONENTS 41 & 42, FILL 43, ACCUM 45 AND VALVE 44 ADDED TO SIMULATE COLD LEG ECCS.

CARD 1234567890123456789012345678901234567890123456789012345678901234567890

```

44          NOTE *** FILL COMPONENT 40 MUST BE CHANGED TO BREAK COMPONENT
45          40 WHEN RUN TRANSIENT ***
46
47      END OF TITLE CARDS
48
49      *AFTER THE NUMTCR (IN THIS CASE, 43) TITLE CARDS THE USER MAY
50      *INSERT ADDITIONAL BLANK CARDS AND LOCAL COMMENTS.
51
52      *NOTE THAT COMMENTS ARE NOT ALLOWED WITHIN THE FOLLOWING NAMELIST
53      *GROUP RECORD, WHICH INCLUDES ALL COLUMNS FROM $ TO $.
54      *THE NAMELIST OPTIONS MAY ALSO BE USED IN TRAC-FORMAT DECKS.
55
56      $INOPTS IELV=0, ICFLOW = 1, NOAIR = 1,
57
58          ISTOPT = 2 ,
59
60      VL = 0.0, VV = 0.0, PA=0.0 $
61      *(THIS NAMELIST RECORD IS ONLY FOR ILLUSTRATION, AS IT SETS SWITCHES TO
62      * DEFAULT VALUES AND DOESN'T CHANGE THE VARIABLES.)
63
64
65
66          *DSTEP*   *TIMET*
67              0       0.0           **MAIN CONTROL CARD 1
68          *DSTEP*   *TIMET*
69
70      *   STDYST   TRANSI   NCOMP   NJUN   IPAK
71          1       0       42      46     1*PACKER ON*
72
73      **EPSO** 1.0E-3   *EPSI** 1.0E-6   *EPSS* 1.0E-5   *EPSP* 1.0E-3
74
75      *OITMAX,IITMAX,SITMAX*** 10 0 10 ***REMEMBER TO EXPLICITLY INCLUDE THE 0
76
77          *SIGNAL VARIABLE, TRIP, AND CONTROLLER TOTALS
78              5           12       0
79

```

80 *** IORDER ARRAY *
 81 1 2 3 4 5
 82 6 7 8 9 10
 83 11 12 13 14 15
 84 16 21 22 23 24
 85 25 26 27 28 34
 86 35 40 41 42 43
 87 44 45 65 70 75
 88 80 83 90 92 97
 89 98 99E

*** SIGNAL VARIABLE DATA***

92 *	IDSV	ISVN	ILCN	ICN1	ICN2	
93	1	21	6	1	0	*PRESSURIZER PRESSURE SIGNAL
94	2	0	0	0	0	*PROBLEM TIME
95	3	21	10	4	0	*ECE-LINE PRESSURE, INTACT LOOP
96	4	21	42	4	0	*ECE-LINE PRESSURE, BKN LOOP
97	5	27	25	5	0	*COLD LEG VOID FR, BKN LOOP

*** TRIP-DIMENSION VARIABLES CARD ***

100 *	NTSE	NTCT	NTSF	NTDP	NTSD
101	0	0	0	0	0

*** TRIP-DEFINING VARIABLES CARDS ***

104 *SETS OF: IDTP(TRIP ID #),IPOS,ISET,ITYP,IDSG(SIG VAR ID)
 105 * SETP(1,2,3,4) (SET POINT VALUES)
 106 * DTSP(1,2,3,4) (DELAY TIMES)
 107 * IFSP(1,2,3,4) (SET-POINT FACTOR TABLE ID'S)

109 **TRIP 1, INTACT LOOP PUMP**

110 1 1 0 1 1
 111 12.480E+6 12.481E+6
 112 1099.7 10000.0
 113 0 0

115 **TRIP 2, BROKEN LOOP PUMP**

CARD 1234567890123456789012345678901234567890123456789012345678901234567890

116 2 1 0 1 1
117 12.480E+6 12.481E+6
118 1099.7 10000.0
119 0 0
120
121 **TRIP 3, CORE TRIP**
122 3 1 0 1 1
123 12.480E+6 12.481E+6
124 3.4 10000.0
125 0 0
126
127 **TRIP 4, FINE MESH**
128 4 1 0 1 1
129 12.480E+6 12.481E+6
130 1099.7 10000.0
131 0 0
132
133 **TRIP 5, INTACT LOOP HPIS**
134 5 1 0 1 1
135 12.480E+6 12.481E+6
136 28.4 10000.0
137 0 0
138
139 **TRIP 6, BROKEN LOOP HPIS**
140 6 1 0 1 1
141 12.480E+6 12.481E+6
142 28.4 10000.0
143 0 0
144
145 **TRIP 7, ACCUMULATORS**
146 7 1 0 1 1
147 12.480E+6 12.481E+6
148 10000.0 10000.0
149 0 0
150
151 **TRIP 8, INTACT LOOP STEAM GEN, IN**

CARD 1234567890123456789012345678901234567890123456789012345678901234567890

```
152      8 1 0 1 1
153      12.480E+6 12.481E+6
154      8.4 10000.0
155      0 0
156
157      **TRIP 9, BROKEN LOOP STEAM GEN, IN**
158      9 1 0 1 1
159      12.480E+6 12.481E+6
160      8.4 10000.0
161      0 0
162
163      **TRIP 10, INTACT LOOP STEAM GEN, OUT**
164      10 1 0 1 1
165      12.480E+6 12.481E+6
166      0.0 10000.0
167      0 0
168
169      **TRIP 11, BROKEN LOOP STEAM GEN, OUT**
170      11 1 0 1 1
171      12.480E+6 12.481E+6
172      0.0 10000.0
173      0 0
174
175      **TRIP 12, VOID FRACTION**
176      12 2 0 1 5
177      0.49 0.50
178      0.0 0.0
179      0 0
180
181
182      ***TRIP SIGNAL-EXPRESSION CARDS***
183          *NONE*
184
185      ***TRIP-CONTROLLED-TRIP CARDS***
186          *NONE*
187
```

CARD 1234567890123456789012345678901234567890123456789012345678901234567890

```

188      ***TRIP SET-POINT FACTOR-TABLE CARDS***
189              *NONE*
190
191      ***TRIP-INITIATED RESTART DUMP PROBLEM TERMINATION CARDS***
192              *NONE*
193
194      ***TRIP-INITIATED TIME-STEP DATA CARDS***
195              *NONE*
196
197
198              ***CONTROLLER DATA***
199              *NONE*
200
201
202              *****
203              *COMPONENT DATA*
204              *****
205
206
207              **COMPONENT 1, TEE - INTACT LOOP HOT LEG**
208
209 TEE 1 1 INTACT LOOP HOT LEG
210 *JCELL* 3 *NODES* 3 *MATID* 7 *COST* 0.0 *ICHF* 1
211 *IHYD1(DUMMY VALUE)* 0 *NCELL1* 4 *JUN1* 1 *JUN2* 2
212
213      3.33248E-2      1.11252E-2      0.0      26.76782      300.0
214 *      RADIN1      TH1      HOUTL1      HOUTV1      TOUTL1
215
216      300.0
217 *      TOUTV1
218
219
220      0 3 7 *IHYD2(DUMMY),NCELL2,JUN3
221
222 4.69900E-3 1.65100E-3 0.0 0.0 300.0*RADIN2,TH2,HOUTL2,HOUTV2,TOUTL2
223

```

CARD 1234567890123456789012345678901234567890123456789012345678901234567890

224 300.0 ****TOUTV2*
225
226 *ARRAY CARDS*
227 F7.54799E-1E *DX-PRIMARY
228 2.66781E-3 R 3 2.63340E-3 E *VOL-PRIMARY
229 4.20283E-3R4 3.48887E-3E *FA-PRIMARY
230 5.589E-1 R 33.717E-2 1.635 E *FRIE-PRIMARY(NOTE \$INOPTS IKFAC)
231 R4 0.0 0.63045E *GRAV-PRIMARY
232 3.0E-1 R 4 6.66496E-2 E *HD-PRIMARY
233 F4E *NFF-PRIMARY
234 FO.OE *ALP-PRIMARY
235 FO.OE *VL-PRIMARY
236 F 0.0 E*VV-PRIMARY
237 F583.8 E *TL-PRIMARY
238 F583.8E *TV-PRIMARY
239 F 15.730E+6E *P-PRIMARY
240 F 0.0E+00 E *FA-PRIMARY
241 F 0.0 E *QPPP-PRIMARY
242 F583.8E *TJ-PRIMARY
243
244 **SECONDARY TUBE**
245
246 R*COMMENT*2 1.34620*COM T*4.76250E-1E*DX
247 *****
248 *VOL* R 2 9.33835E-5 *,* 4.75410E-4 E
249 *****
250
251 *****
252 **FA** R 3 6.93683E-5 *PRIZER INTERFACE* 9.07130E-4 E
253 *****
254
255 *****
256 *FRIC* *1ST*2.98106E-3 *2ND*1.56432E-3 *3RD*2.31106E-3 *4TH*0.0 E
257 *****
258
259 *****

CARD 1234567890123456789012345678901234567890123456789012345678901234567890

260 *GRAV* 0.30954 0.27536 0.46472 1.0 E
261 *****
262
263 *****
264 **HD** R 39.39800E-3 3.39852E-2 E
265 *****
266
267 *****
268 *NFF** FOE
269 *****
270
271 *****
272 *ALP** F 0.0 E
273 *****
274
275 *****
276 **VL** F 0.0 E
277 *****
278
279 *****
280 **VV** F 0.0 E
281 *****
282
283 *****
284 **TL** 550.0R 2 550.0 E
285 *****
286
287 *****
288 **TV** 550.0 R 2 550.0 E
289 *****
290
291 *****
292 **P*** *1ST CELL* 15.730E+6 *2ND CELL* 15.730E+6 *3RD CELL* 15.730E+6 E
293 *****
294
295 *****

CARD 1234567890123456789012345678901234567890123456789012345678901234567890

296 **PA** FO.OE
 297 *****
 298
 299 *****
 300 *QPPP* FO.OE
 301 *****
 302
 303 *****
 304 **TW** R 3 550.0 R 6 550.0 E
 305 *****
 306
 307
 308 FILL 16 16 PRIZER INLET
 309 * .
 310 * .
 311 * .
 312 * .
 313 * .
 314 * .
 315 * .

D. Input Equivalent to the Ten One-Dimensional Downcomer and Vessel
 Components of Input Deck (Appendix C.A), Using Three-Dimensional VESSEL

CARD	1234567890123456789012345678901234567890123456789012345678901234567890	1234567890123456789012345678901234567890123456789012345678901234567890	1234567890123456789012345678901234567890123456789012345678901234567890	1234567890123456789012345678901234567890123456789012345678901234567890	1234567890123456789012345678901234567890123456789012345678901234567890	1234567890123456789012345678901234567890123456789012345678901234567890
1	VESSEL	50	50	DOWNCOMER, VESSEL, U HEAD		
2	19	2	2	10		
3	16	2	1	12	3	
4	1					
5	0	0	0	2		
6	10.0	75.0	0.005			
7	.100000E+10	.133400E+01	0.			
8	8	10	7	3	1	
9	1	1	0	0	0	
10	4	0	0	0	75	
11	0	0	500	2	2	
12	.197000E+07	0.	0.	0.	1.0	

CARD 1234567890123456789012345678901234567890123456789012345678901234567890

13		0.2112	0.3382	0.8144	1.2716	1.7288	Z
14		2.1860	2.4908	2.6432	3.2528	3.5576	Z
15		4.0148	4.4720	4.7867	5.5996	5.8996	Z
16		6.1012	7.1520	8.94280	10.0289E		Z
17		0.061	0.1369E				RAD
18		3.141593	6.283185E				THETA
19		16	3	2	51		BYPASS
20		18	1	-2	52		BYPASS
21		15	3	3	6		ILCL
22		15	4	3	26		BLCL
23		15	1	3	1		ILHL
24		15	2	3	21		BLHL
25		14	2	2	53		GUIDE TB
26		19	2	-2	54		GUIDE TB
27		13	1	2	55		SUP TB
28		18	2	-2	56		SUP TB
29		0.0R 2	1.0R 5	0.0E			RDPWR
30	F	1.0E					CPOWR
31		0.0S					ZPOWR
32		0.2916	0.5908	0.9949	1.4351	1.5499	ZPOWR
33		1.5499	1.4351	1.0013	0.5908	0.2916E	ZPOWR
34	F	11.0E					NRDX
35		0.0	0.1588E-2	0.24E-2	0.3844E-2	0.4368E-2	RADRD
36		0.4369E-2	0.4699E-2	0.5359E-2E			RADRD
37		4	5R 2	4	3R 2	7E	MATRD
38		0.0	1.97000E+6	3.0	7.88000E+5S		PWTB
39		6.0	4.92500E+5	20.0	1.97000E+5S		PWTB
40		30.0	1.02440E+5	60.0	8.66800E+4S		PWTB
41		100.0	7.88000E+4	200.0	6.89500E+4S		PWTB
42		1000.0	4.53100E+4	3000.0	3.34900E+4E		PWTB
43		-10000.0	1.0	10000.0	1.0E		RPRF
44	R 2	5	9	5	9	5	NFAX
45		9R 2	5E				NFAX
46	F	0.0E					FPUO2
47	F	1.0E					FTD
48	F	0.0E					GMIX

CARD 123456789012345678901234567890123456789012345678901234567890123456789012345678901234567890

121	F	0.0E								FA-R
122	R 2	0.0655R 2	0.0229E							HD-T
123	R 2	0.0655R 2	0.0229E							HD-Z
124	R 2	0.0655R 2	0.0229E							HD-R
125	F	565.6E								HSTN
126	F	7E								MATHS
127	F	0.0E								ALPN
128	F	0.0E								VVN-T
129	F	0.0E								VVN-Z
130	F	0.0E								VVN-R
131	F	0.0E								VLN-T
132	F	0.0E								VLN-Z
133	F	0.0E								VLN-R
134	F	565.6E								TVN
135	F	565.6E								TLN
136	F	15.730E+6E								PN
137	F	0.00E+00E								PAN
138	R 2	0.0654	0.3438	0.0E						HSA
139		.17767E-02	.17767E-02	.28990E-02	0.					HSX
140	F	0.0E								CFZL-T
141	F	0.0E								CFZL-Z
142	F	0.0E								CFZL-R
143	F	0.0E								CFZV-T
144	F	0.0E								CFZV-Z
145	F	0.0E								CFZV-R
146	R 2	0.2443	0.1778	0.0E						VOL
147	R 2	0.1468R 2	0.0E							FA-T
148	R 2	0.2443	0.1479	0.0E						FA-Z
149	F	0.0E								FA-R
150	R 2	0.0103R 2	0.0667E							HD-T
151	R 2	0.0103R 2	0.0667E							HD-Z
152	R 2	0.0103R 2	0.0667E							HD-R
153	F	565.6E								HSTN
154	F	7E								MATHS
155	F	0.0E								ALPN
156	F	0.0E								VVN-T

CARD 12345678901234567890123456789012345678901234567890123456789012345678901234567890

157	F	0.0E					VVN-Z
158	F	0.0E					VVN-R
159	F	0.0E					VLN-T
160	F	0.0E					VLN-Z
161	F	0.0E					VLN-R
162	F	565.6E					TVN
163	F	565.6E					TLN
164	F	15.730E+6E					PN
165	F	0.00E+00E					PAN
166	R 2	0.0654	0.06382		0.0E		HSA
167		.17767E-02	.17767E-02	.12978E-01	0.	E	HSX
168	F	0.0E					CFZL-T
169	F	0.0E					CFZL-Z
170	F	0.0E					CFZL-R
171	F	0.0E					CFZV-T
172	F	0.0E					CFZV-Z
173	F	0.0E					CFZV-R
174	R 2	0.2443	0.1778		0.0E		VOL
175	R 2	0.1468R 2	0.0E				FA-T
176	R 2	0.2443	0.1025		0.0E		FA-Z
177	F	0.0E					FA-R
178	R 2	0.0103R 2	0.0667E				HD-T
179	R 2	0.0103R 2	0.0667E				HD-Z
180	R 2	0.0103R 2	0.0667E				HD-R
181	F	565.6E					HSTN
182	F	7E					MATHS
183	F	0.0E					ALPN
184	F	0.0E					VVN-T
185	F	0.0E					VVN-Z
186	F	0.0E					VVN-R
187	F	0.0E					VLN-T
188	F	0.0E					VLN-Z
189	F	0.0E					VLN-R
190	F	565.6E					TVN
191	F	565.6E					TLN
192	F	15.730E+6E					PN

CARD 123456789012345678901234567890123456789012345678901234567890123456789012345678901234567890

193	F	0.00E+00E					PAN
194	R 2	0.0654	0.1063		0.0E		HSA
195		.17767E-02	.17767E-02		.25175E-02	0.	HSX
196	F	0.0E					CFZL-T
197	F	0.0E					CFZL-Z
198	F	0.0E					CFZL-R
199	F	0.0E					CFZV-T
200	F	0.0E					CFZV-Z
201	F	0.0E					CFZV-R
202	R 2	0.2443	0.1219		0.0E		VOL
203	R 2	0.1468R 2	0.0E				FA-T
204	R 2	0.2443	0.1025		0.0E		FA-Z
205	F	0.0E					FA-R
206	R 2	0.01013R 2	0.0555E				HD-T
207	R 2	0.01013R 2	0.0555E				HD-Z
208	R 2	0.01013R 2	0.0555E				HD-R
209	F	565.6E					HSTN
210	F	7E					MATHS
211	F	0.0E					ALPN
212	F	0.0E					VVN-T
213	F	0.0E					VVN-Z
214	F	0.0E					VVN-R
215	F	0.0E					VLN-T
216	F	0.0E					VLN-Z
217	F	0.0E					VLN-R
218	F	565.6E					TVN
219	F	565.6E					TLN
220	F	15.730E+6E					PN
221	F	0.00E+00E					PAN
222	R 2	0.0436	0.05314		0.0E		HSA
223		.17767E-02	.17767E-02		.25192E-02	0.	HSX
224	F	0.0E					CFZL-T
225	F	0.0E					CFZL-Z
226	F	0.0E					CFZL-R
227	F	0.0E					CFZV-T
228	F	0.0E					CFZV-Z

CARD 1234567890123456789012345678901234567890123456789012345678901234567890

229	F	0.0E							CFZV-R
230	R 2	0.2443	0.1025	0.0E					VOL
231	R 2	0.1468R 2	0.0E						FA-T
232	R 2	0.2443	0.1025	0.0E					FA-Z
233	F	0.0E							FA-R
234	R 2	0.01013R 2	0.0555E						HD-T
235	R 2	0.01013R 2	0.0555E						HD-Z
236	R 2	0.01013R 2	0.0555E						HD-R
237	F	565.6E							HSTN
238	F	7E							MATHS
239	F	0.0E							ALPN
240	F	0.0E							VVN-T
241	F	0.0E							VVN-Z
242	F	0.0E							VVN-R
243	F	0.0E							VLN-T
244	F	0.0E							VLN-Z
245	F	0.0E							VLN-R
246	F	565.6E							TVN
247	F	565.6E							TLN
248	F	15.730E+6E							PN
249	F	0.00E+00E							PAN
250	R 2	0.0218	0.10629	0.0E					HSA
251		.17767E-02	.17767E-02	.25177E-02	0.				HSX
252	F	0.0E							CFZL-T
253	F	0.0E							CFZL-Z
254	F	0.0E							CFZL-R
255	F	0.0E							CFZV-T
256	F	0.0E							CFZV-Z
257	F	0.0E							CFZV-R
258	R 2	0.2443	0.1025	0.0E					VOL
259	R 2	0.1468R 2	0.0E						FA-T
260	R 2	0.2443	0.1025	0.0E					FA-Z
261	F	0.0E							FA-R
262	R 2	0.01013R 2	0.0555E						HD-T
263	R 2	0.01013R 2	0.0555E						HD-Z
264	R 2	0.01013R 2	0.0555E						HD-R

CARD 123456789012345678901234567890123456789012345678901234567890123456789012345678901234567890

265	F	565.6E								HSTN
266	F	7E								MATHS
267	F	0.0E								ALPN
268	F	0.0E								VVN-T
269	F	0.0E								VVN-Z
270	F	0.0E								VVN-R
271	F	0.0E								VLN-T
272	F	0.0E								VLN-Z
273	F	0.0E								VLN-R
274	F	565.6E								TVN
275	F	565.6E								TLN
276	F	15.730E+6E								PN
277	F	0.00E+00E								PAN
278	R 2	0.0872	0.0531		0.0E					HSA
279		.17774E-02	.17774E-02		.25211E-02	0.			E	HSX
280	F	0.0E								CFZL-T
281	F	0.0E								CFZL-Z
282	F	0.0E								CFZL-R
283	F	0.0E								CFZV-T
284	F	0.0E								CFZV-Z
285	F	0.0E								CFZV-R
286	R 2	0.2443	0.1025		0.0E					VOL
287	R 2	0.1468R 2	0.0E							FA-T
288	R 2	0.2443	0.1025		0.0E					FA-Z
289	F	0.0E								FA-R
290	R 2	0.01013R 2	0.0555E							HD-T
291	R 2	0.01013R 2	0.0555E							HD-Z
292	R 2	0.01013R 2	0.0555E							HD-R
293	F	565.6E								HSTN
294	F	7E								MATHS
295	F	0.0E								ALPN
296	F	0.0E								VVN-T
297	F	0.0E								VVN-Z
298	F	0.0E								VVN-R
299	F	0.0E								VLN-T
300	F	0.0E								VLN-Z

CARD 12345678901234567890123456789012345678901234567890123456789012345678901234567890

337	F	0.0E								CFZL-Z
338	F	0.0E								CFZL-R
339	F	0.0E								CFZV-T
340	F	0.0E								CFZV-Z
341	F	0.0E								CFZV-R
342	R 2	0.2443	0.1025	0.0E						VOL
343	R 2	0.1468R 2	0.0E							FA-T
344	R 2	0.2443	0.1025	0.0E						FA-Z
345	F	0.0E								FA-R
346	R 2	0.01013R 2	0.0555E							HD-T
347	R 2	0.01013R 2	0.0555E							HD-Z
348	R 2	0.01013R 2	0.0555E							HD-R
349	F	565.6E								HSTN
350	F	7E								MATHS
351	F	0.0E								ALPN
352	F	0.0E								VVN-T
353	F	0.0E								VVN-Z
354	F	0.0E								VVN-R
355	F	0.0E								VLN-T
356	F	0.0E								VLN-Z
357	F	0.0E								VLN-R
358	F	565.6E								TVN
359	F	565.6E								TLN
360	F	15.730E+6E								PN
361	F	0.00E+00E								PAN
362	R 2	0.0654	0.1063	0.0E						HSA
363		.17767E-02	.17767E-02	.25175E-02	0.				E	HSX
364	F	0.0E								CFZL-T
365	F	0.0E								CFZL-Z
366	F	0.0E								CFZL-R
367	F	0.0E								CFZV-T
368	F	0.0E								CFZV-Z
369	F	0.0E								CFZV-R
370	R 2	0.2443	0.1025	0.0E						VOL
371	R 2	0.1468R 2	0.0E							FA-T
372	R 2	0.2443	0.1025	0.0E						FA-Z

CARD 12345678901234567890123456789012345678901234567890123456789012345678901234567890

409	F	0.0E				VVN-Z
410	F	0.0E				VVN-R
411	F	0.0E				VLN-T
412	F	0.0E				VLN-Z
413	F	0.0E				VLN-R
414	F	565.6E				TVN
415	F	565.6E				TLN
416	F	15.730E+6E				PN
417	F	0.00E+00E				PAN
418		0.1723	0.07868R 2	0.1032E		HSA
419		.26160E-02	.16544E-02	.38248E-02	.38248E-02E	HSX
420	F	0.0E				CFZL-T
421	F	0.0E				CFZL-Z
422	F	0.0E				CFZL-R
423	F	0.0E				CFZV-T
424	F	0.0E				CFZV-Z
425	F	0.0E				CFZV-R
426		0.6455	0.1692R 2	0.094E		VOL
427	R 2	0.0438R 2	0.08065E			FA-T
428		0.5997	0.0R 2	0.2081E		FA-Z
429	F	0.0E				FA-R
430		0.08489	0.04087R 2	0.06992E		HD-T
431		0.08489	0.04087R 2	0.06992E		HD-Z
432		0.08489	0.04087R 2	0.06992E		HD-R
433	F	565.6E				HSTN
434	F	7E				MATHS
435	F	0.0E				ALPN
436	F	0.0E				VVN-T
437	F	0.0E				VVN-Z
438	F	0.0E				VVN-R
439	F	0.0E				VLN-T
440	F	0.0E				VLN-Z
441	F	0.0E				VLN-R
442	F	565.6E				TVN
443	F	565.6E				TLN
444	F	15.730E+6E				PN

CARD 12345678901234567890123456789012345678901234567890123456789012345678901234567890

445	F	0.00E+00E					PAN
446	R 2	0.0466R 2	0.1186E				HSA
447		.35519E-02	.35519E-02	.38258E-02	.38258E-02E		HSX
448	F	0.0E					CFZL-T
449	F	0.0E					CFZL-Z
450	F	0.0E					CFZL-R
451	F	0.0E					CFZV-T
452	F	0.0E					CFZV-Z
453	F	0.0E					CFZV-R
454		0.1753	0.2986R 2	0.2031E			VOL
455	R 2	0.2908R 2	0.2803E				FA-T
456	R 2	0.3339R 2	0.2081E				FA-Z
457	F	0.0E					FA-R
458	R 2	0.045R 2	0.0485E				HD-T
459	R 2	0.045R 2	0.0485E				HD-Z
460	R 2	0.045R 2	0.0485E				HD-R
461	F	565.6E					HSTN
462	F	7E					MATHS
463	F	0.0E					ALPN
464	F	0.0E					VVN-T
465	F	0.0E					VVN-Z
466	F	0.0E					VVN-R
467	F	0.0E					VLN-T
468	F	0.0E					VLN-Z
469	F	0.0E					VLN-R
470	F	565.6E					TVN
471	F	565.6E					TLN
472	F	15.730E+6E					PN
473	F	0.00E+00E					PAN
474	R 2	0.0312R 2	0.0796E				HSA
475		.35573E-02	.35573E-02	.38230E-02	.38230E-02E		HSX
476	F	0.0E					CFZL-T
477	F	0.0E					CFZL-Z
478	F	0.0E					CFZL-R
479	F	0.0E					CFZV-T
480	F	0.0E					CFZV-Z

481	F	0.0E								CFZV-R
482		0.1441	0.1753R 2	0.2031E						VOL
483	R 2	0.2908R 2	0.2803E							FA-T
484	R 2	0.3339R 2	0.0E							FA-Z
485	F	0.0E								FA-R
486	R 2	0.045R 2	0.0485E							HD-T
487	R 2	0.045R 2	0.0485E							HD-Z
488	R 2	0.045R 2	0.0485E							HD-R
489	F	565.6E								HSTN
490	F	7E								MATHS
491	F	0.0E								ALPN
492	F	0.0E								VVN-T
493	F	0.0E								VVN-Z
494	F	0.0E								VVN-R
495	F	0.0E								VLN-T
496	F	0.0E								VLN-Z
497	F	0.0E								VLN-R
498	F	565.6E								TVN
499	F	565.6E								TLN
500	F	15.730E+6E								PN
501	F	0.00E+00E								PAN
502	R 2	0.1545R 2	0.0E							HSA
503		.69136E-02	.69136E-02	0.	0.	0.	0.	0.	E	HSX
504	F	0.0E								CFZL-T
505	F	0.0E								CFZL-Z
506	F	0.0E								CFZL-R
507	F	0.0E								CFZV-T
508	F	0.0E								CFZV-Z
509	F	0.0E								CFZV-R
510		0.2965	0.2156R 2	0.0E						VOL
511	R 2	0.2388R 2	0.0E							FA-T
512	F	0.0E								FA-Z
513	F	0.0E								FA-R
514	F	0.0708E								HD-T
515	F	0.0708E								HD-Z
516	F	0.0708E								HD-R

CARD 12345678901234567890123456789012345678901234567890123456789012345678901234567890

589	F	565.6E					RFTN
590	PIPE		52	52	GUIDE TUBE		
591		3	2	53	54	7	
592		0	0				
593		0.00806	0.00147	0.0	0.0	565.6	
594		565.6					
595	F	1.122E					DX
596	F	0.0011450E					VOL
597	F	0.0010200E					FA
598		0.0R 2	1.409E01	0.0E			FRIC
599	F	1.0E					GRAV
600	F	0.03605E					HD
601	F	1E					NFF
602	F	0.0E					ALP
603	F	0.0E					VL
604	F	0.0E					VV
605	F	565.6E					TL
606	F	565.6E					TV
607	F	15.730E+6E					P
608	F	0.00E+00E					PA
609	F	0.0E					QPPP
610	F	565.6E					TW
611	PIPE		53	53	CORE SUPPORT TUBE		
612		3	3	55	56	7	
613		0	0				
614		0.006887	0.002086	0.0	0.0	565.6	
615		565.6					
616	F	0.9530E					DX
617	F	0.0007100E					VOL
618	F	0.0007450E					FA
619		0.0R 2	2.125E00	0.0E			FRIC
620	F	1.0E					GRAV
621	F	0.030791E					HD
622	F	1E					NFF
623	F	0.0E					ALP
624	F	0.0E					VL

CARD 1234567890123456789012345678901234567890123456789012345678901234567890i234567890

625	F	0.0E					VV
626	F	565.6E					TL
627	F	565.6E					TV
628	F	15.730E+6E					P
629	F	0.00E+00E					PA
630	F	0.0E					QPPP
631	F	565.6E					TW
632	PIPE		51	51	INLET ANN. - UPPER HEAD BYPASS		
633		3	2	51	52	7	
634		0	0				
635		0.003581	0.002769	0.0	0.0	565.6	
636		565.6					
637	F	0.7657E					DX
638	F	0.0002870E					VOL
639	F	0.0003705E					FA
640		0.0R 2	1.484E00	0.0E			FRIC
641	F	1.0E					GRAV
642	F	0.016017E					HD
643	F	1E					NFF
644	F	0.0E					ALP
645	F	0.0E					VL
646	F	0.0E					VV
647	F	565.6E					TL
648	F	565.6E					TV
649	F	15.730E+6E					P
650	F	0.00E+00E					PA
651	F	0.0E					QPPP
652	F	565.6E					TW
653		1.0E-3	1.0	200.0	1000.0	0.5	TIME STP
654		20.0	1.0	20.0	1.0		TIME STP
655		-1.0					

APPENDIX F
TRAC SUBPROGRAMS

<u>Name</u>	<u>Overlay</u>	<u>Function</u>
ACCMBD	MAIN	Sets boundary array for the accumulator component.
ACCM1X	PREP	Evaluates accumulator water level.
ACCUM1	PREP	Controls accumulator prepass.
ACCUM2	OUTER	Controls accumulator outer iteration.
ACCUM3	POST	Controls accumulator postpass.
ALLBLK	INPUT	Tests for all blanks in specified substring of string.
ANNSH	OUTER	Calculates interfacial shear for annular flow.
ASIGN	INPUT	Assigns the component LCM pointers according to the iteration number.
AXPOW	PREP	Linearly interpolates the axial power shape for the core and vessel components.
BACIT	OUTER	Initiates back-substitution after direct vessel matrix inversion.
BFALOC	MAIN	Allocates files and buffers for buffered I/O.
BFCLOS	MAIN	Empties buffers and closes file.
BFIN	MAIN	Initiates binary input subroutine.
BFOUT	MAIN	Initiates binary output subroutine.
BITS	MAIN	Manages bit address flags.
BKMOM	PREP	Initiates back-substitution for stabilizing momentum equations.
BKSMOM	PREP	Back-substitution for stabilizing momentum equations.
BKSSTB	POST	Initiates back-substitution for stabilizing mass and energy equations.
BLOCK DATA	MAIN	Initializes common variables.

<u>Name</u>	<u>Overlay</u>	<u>Function</u>
BREAKX	PREP	Evaluates break pressure, temperature, and void fraction.
BREAK1	PREP	Controls break prepass.
BREAK2	OUTER	Controls break outer iteration.
BREAK3	POST	Controls break postpass.
BREBAL	OUTER	Initiates back-substitution after coarse-mesh rebalance in the vessel.
CDTHEX	POST	Calculates the diametral thermal expansion of Zircaloy as a function of temperature.
CHBD	MAIN	Checks boundary data.
CHEN	PREP	Uses Chen correlation to evaluate the forced-convection nucleate-boiling HTC.
CHF	PREP	Evaluates the CHF based on a local-conditions formulation.
CHF1	PREP	Applies Biasi CHF correlation.
CHKSR	INPUT	Checks vessel source locations.
CHOKE	OUTER	Establishes the choked phasic velocities and their derivatives.
CIVSSL	INIT	Transfers vessel data from LCM to SCM so that remaining data can be initialized.
CLEAN	CLEAN	Closes TRAC output files.
CLEAR	MAIN	Sets an array to a constant value.
COMPI	INIT	Performs various A-array loading tasks common to most one-dimensional components.
CONSTB	POST	Drives subroutine STBME.
COREC1	PREP	Controls core prepass.
COREC2	OUTER	Controls core outer iteration.
COREC3	POST	Controls core postpass.
CORE1	PREP	Evaluates rod HTCs and tracks quench fronts.

<u>Name</u>	<u>Overlay</u>	<u>Function</u>
CORE3	POST	Evaluates rod temperature distributions.
CPLL	MAIN	Calculates specific heat of liquid water as a function of enthalpy and pressure.
CPVV	MAIN	Calculates specific heat of water vapor as a function of enthalpy and pressure.
CPVV1	MAIN	Calculates specific heat of water vapor as a function of temperature and pressure.
CTAIN1	PREP	Controls containment prepass.
CTAIN2	OUTER	Controls containment outer iteration.
CTAIN3	POST	Controls containment postpass.
CWSSL	EDIT	Transfers vessel data from LCM to SCM so that it can be printed.
CYLHT	POST	Calculates temperature fields in a cylinder.
DBRK	DUMP	Generates break data dump.
DCODF	INPUT	Calculates a numeric code based on data types.
DCOMP	DUMP	Dumps one-dimensional component data.
DCORE	DUMP	Generates core data dump.
DELTAR	POST	Calculates transient fuel/clad gap spacing (only if NFCI = 1).
DFHT	PREP	Calculates the dispersed flow wall-to-fluid HTC for use in the transition and film-boiling heat-transfer regimes.
DFILL	DUMP	Generates fill data dump.
DMPIT	DUMP	Generates overlay dump.
DPIPE	DUMP	Generates pipe data dump.
DPUMP	DUMP	Generates pump data dump.
DVLVE	DUMP	Generates valve data dump.
DVSSL	DUMP	Generates vessel data dump.
ECOMP	EDIT	Writes hydrodynamic and heat-transfer information for one-dimensional components to output file.

<u>Name</u>	<u>Overlay</u>	<u>Function</u>
EDIT	EDIT	Begins entry routine for overlay edit.
ENDDMP	MAIN	Empties dump buffers and closes dump file.
ENDGRF	MAIN	Empties graphics buffers and closes graphics file.
EOVLY	MAIN	Closes overlay bookkeeping.
ERRGET	MAIN	Sets error trap indicators.
ERROR	MAIN	Processes different kinds of error conditions.
ERRTRP	MAIN	Processes trapped errors.
ESTGEN	OUTER	Evaluates steam-generator tee parameters on explicit pass.
ETEE	POST	Evaluates tee parameters on explicit pass.
EVALDF	POST	Evaluates the absolute difference between XOLD and XNEW.
EXPAND	PREP	Adds rows of conduction nodes within the vessel rods during reflood.
FAXPOS	PREP	Evaluates the flow area fraction, FA, on valve stem position, XPOS for the VLVE component.
FEMOM	PREP	Sets up stabilizing momentum equations.
FF3D	POST	Makes final pass update for all variables in three-dimensional vessel.
FILL1	PREP	Controls fill prepass.
FILL2	OUTER	Controls fill outer iteration.
FILL3	POST	Controls fill postpass.
FILLX	MAIN	Evaluates postpass fill velocity.
FLUX	PREP	Calculates mass flow at boundary of one-dimensional component for use in mass inventory.
FNDLP	INPUT	Catalogs one primary-loop configuration for PWR initialization.

<u>Name</u>	<u>Overlay</u>	<u>Function</u>
FNMESH	PREP	Initializes the supplemental user-specified rows of conduction nodes within the vessel rods at the start of reflood.
FPROP	MAIN	Calculates values for fluid enthalpy, transport properties, and surface tension.
FROD	POST	Calculates temperature profiles in nuclear or electrically heated fuel rods.
FTHEX	POST	Calculates the fuel linear thermal expansion coefficient for uranium dioxide and mixed oxide fuels.
FWALL	PREP	Computes a two-phase friction factor.
GAPHT	POST	Calculates fuel-clad gap HTC.
GETBIT	MAIN	Returns value of bit N of word B.
GETCRV	MAIN	Gets appropriate pump curves from data base.
GRAF	GRAF	Edits graphics data during transient.
GRFGET	MAIN	Returns entries in graphics catalog block.
GRFPUT	INIT	Places entries in graphics catalog block.
GVSSL1	POST	Calculates integrated vessel parameters for graphics purposes.
GVSSL2	POST	Calculates average values for vessel graphics (integrated values calculated in subroutine GVSSL1).
HLS	MAIN	Calculates enthalpy of saturated water as a function of pressure.
HOUT	MAIN	Controls the outer iteration logic for a complete time step.
HTCOR	PREP	Computes HTCs.
HTPIPE	PREP	Averages velocities and generates HTCs for one-dimensional components.
HTVSSL	PREP	Averages velocities and generates HTCs for the vessel.
HUNTS	INPUT	Searches character string for specified search string.

<u>Name</u>	<u>Overlay</u>	<u>Function</u>
HVFILM	PREP	Calculates the vapor HTC that is the maximum of the Bromley, natural-convection, and Dougall-Rohsenow coefficients.
HVS	MAIN	Calculates enthalpy of saturated steam as a function of pressure.
IACCUM	INIT	Initializes the accumulator data arrays that are not input from cards.
IBRK	INIT	Initializes the break data arrays that are not input from cards.
ICHL	INPUT	Returns character at given position in string (left-justified, blank-filled).
ICMPR	MAIN	Compares logically a real variable to an integer.
ICOMP	INIT	Controls the routines that initialize component data.
ICORE	INIT	Initializes the core data arrays that are not input from cards.
IDEL	INPUT	Searches specified substring of string for any one character in a set of specified characters.
IFILL	INIT	Initializes the fill data arrays that are not input from cards.
IGACUM	INIT	Supplies accumulator data for graphics.
IGBRAK	INIT	Supplies break data for graphics.
IGCOMP	INIT	Supplies graphic output information for most one-dimensional components to the graphics COMMON block.
IGCORE	INIT	Specifies graphics data for one-dimensional core.
IGFILL	INIT	Supplies fill data for graphics.
IGPIPE	INIT	Supplies pipe data for graphics.
IGPRZR	INIT	Supplies pressurizer data for graphics.
IGPUMP	INIT	Supplies pump data for graphics.
IGRAF	INIT	Initializes graphics variables and writes header to graphics file.

<u>Name</u>	<u>Overlay</u>	<u>Function</u>
IGSTGN	INIT	Supplies steam-generator data for graphics.
IGTEE	INIT	Supplies tee data for graphics.
IGVLVE	INIT	Supplies valve data for graphics.
IGVSSL	INIT	Supplies vessel data for graphics.
INDEL	INPUT	Searches specified substring of string for first nonoccurrence of any one character in a set of specified characters.
INIT	INIT	Supplies entry routine for overlay INIT.
INNER	OUTER	Performs an inner iteration for a one-dimensional component.
INPUT	INPUT	Supplies entry routine for overlay INPUT.
IOVLY	MAIN	Initializes overlay bookkeeping.
IPIPE	INIT	Initializes the pipe data arrays that are not input from cards.
IPRIZR	INIT	Initializes the pressurizer data arrays that are not input from cards.
IPROP	INIT	Calls subroutines THERMO, FPROP, and MIXPRP for most one-dimensional components.
IPUMP	INIT	Initializes the pump data arrays that are not input from cards.
ISORT	MAIN	Sorts a list of integers in ascending order.
ISTGEN	INIT	Initializes the steam-generator data arrays that are not input from cards.
ITEE	INIT	Initializes the tee data arrays that are not input from cards.
ITRI	OUTER	Gives iterative solution of reduced, linearized three-dimensional finite-difference equations.
IVLVE	INIT	Initializes the valve data arrays that are not input from cards.
IVSSL	INIT	Initializes the vessel data arrays that are not input from cards.
J1D	MAIN	Fills boundary array at component junctions.

<u>Name</u>	<u>Overlay</u>	<u>Function</u>
JFIND	INIT	Locates junctions in junction sequence array.
JUNSOL	INIT	Determines junction parameters for connecting and sequencing components.
JVALUE	INPUT	Converts one character of a string to a binary number; 0-9 returned as binary mode; blank, as binary 0; all others, as less than 0.
LCMOVE	MAIN	Copies data from one part of LCM to another.
LEVEL	OUTER	Calculates water level in pipe during stratified flow.
LININT	MAIN	Performs linear interpolation on arrays.
LOAD	INPUT	Reads in specially formatted input data.
LPCON	PWRSS	Evaluates loop properties.
LPRPL	PWRSS	Replaces pump heads and steam-generator areas and checks for convergence of steady-state calculation.
LPSET	PWRSS	Supplies PWRSS overlay entry point; resets PWR loop parameters for steady state.
MANAGE	MAIN	Performs all level and rod data management operations for the vessel.
MBN	PREP	Calculates values for electrically heated nuclear fuel-rod insulator properties.
MFROD	PREP	Orders fuel-rod property selection and evaluates an average temperature for property evaluation.
MFUEL	PREP	Calculates values for uranium dioxide and uranium-plutonium dioxide properties.
MGAP	POST	Calculates values for the thermal conductivity of the gap gas mixture.
MHTR	PREP	Calculates values for electrically heated fuel-rod heater coil properties.
MIXPRP	MAIN	Calculates mixture properties from those of separate phases.
MPROP	PREP	Orders structure property selection and evaluates an average temperature for property evaluation.

<u>Name</u>	<u>Overlay</u>	<u>Function</u>
MSTRCT	PREP	Calculates properties for certain types of steel.
MWRX	POST	Calculates the Zircaloy steam reaction in the cladding at high temperatures.
MZIRC	PREP	Calculates properties for Zircaloy-4.
NEWDLT	MAIN	Evaluates prospective new time increment.
NXTCMP	INPUT	Finds the beginning of data for the next component.
ORIENT	PWRSS	Determines adjacent junction index given the component number.
OUT1D	OUTER	Controls outer calculation for one-dimensional components.
OUT3D	OUTER	Controls outer calculation for the vessel.
OUTER	OUTER	Controls outer calculation for one time step.
PACKIT	MAIN	Packs data from one array into another.
PATH	INPUT	Catalogs a path beginning at a given junction of a given component.
PIPE1	PREP	Controls pipe prepass.
PIPE1X	PREP	Calculates liquid volume discharged (q_{out}), collapsed liquid level (z), and volumetric flow rate (v_{flow}); assumes vertical component with low-numbered cell at top.
PIPE2	OUTER	Controls pipe outer iteration.
PIPE3	POST	Controls pipe postpass.
PMPP	PWRSS	Calculates pump enthalpy, pressure, and density.
POLY	MAIN	Evaluates a polynomial through successive multiplications.
POST	POST	Controls postpass calculation for one time step.
POST3D	POST	Controls postpass calculation for the vessel.
POSTER	POST	Performs postpass calculation for one-dimensional components.
PREINPT	INPUT	Converts free-format TRACIN deck to format used by TRAC input subroutine.

<u>Name</u>	<u>Overlay</u>	<u>Function</u>
PREP	PREP	Controls prepass calculation for one time step.
PREP1D	PREP	Controls the one-pass calculation for one-dimensional components.
PREP3D	PREP	Controls prepass calculation for three-dimensional components.
PREPER	PREP	Performs prepass calculation for one one-dimensional components.
PRIZR1	PREP	Controls pressurizer prepass.
PRIZR2	OUTER	Controls pressurizer outer iteration.
PRIZR3	POST	Controls pressurizer postpass.
PRZR1X	PREP	Evaluates pressurizer water level and heater/sprayer source.
PRZR3X	POST	Evaluates mass change during steady-state calculation.
PSTEPQ	MAIN	Controls printing, dumping, and graphing of data at the completion of a time step.
PUMP1	PREP	Controls pump prepass.
PUMP2	OUTER	Controls pump outer iteration.
PUMP3	POST	Controls pump postpass.
PUMPD	MAIN	Calculates head and torque from pump curves.
PUMPI	INPUT	Supplies built-in pump characteristics.
PUMPSR	PREP	Evaluates pump momentum and energy source.
PUMPX	PREP	Calculates pump head and torque.
RACCUM	INPUT	Reads accumulator data input file and sets up pointer table for that data.
RBREAK	INPUT	Reads break data from input file and sets up a pointer table for that data.
RCNTL	INPUT	Reads in signal-variable, trip, and controller input data.

<u>Name</u>	<u>Overlay</u>	<u>Function</u>
RCOMP	INPUT	Reads data common to most one-dimensional components from input files and writes these data to output file.
RCORE	INPUT	Reads core data from input file and sets up pointer table for that data.
RDCOMP	INPUT	Controls reading of component data from input file.
RDCRDS	MAIN	Reads time-step cards until DTMIN < 0 is encountered.
RDCRVS	INPUT	Reads pump curves from input file.
RDDIM	INPUT	Reads number of points on pump curves from input file.
RDLCM	MAIN	Moves data from LCM to SCM.
RDLOOP	INPUT	Reads loop data and sets up geometrical data for steady state.
RDREST	INPUT	Controls reading of component data from a restart dump file.
REACCM	INPUT	Reads accumulator data from a restart dump and sets up a pointer table for that data.
READI	INPUT	Reads integer data in I14 format.
READR	INPUT	Reads real data in E14.6 format.
REBRK	INPUT	Reads break data from a restart dump and sets up a pointer table for that data.
RECNTL	INPUT	Reads the signal-variable, trip and controller data from the restart file.
RECOMP	INPUT	Reads data from disk common to most one-dimensional components (used by subroutine RESTART).
RECORE	INPUT	Reads core data from a restart dump and sets up pointer table for that data.
REFILL	INPUT	Reads fill data from a restart dump and sets up a pointer table for that data.
REPIPE	INPUT	Reads pipe data from a restart dump and sets up a pointer table for that data.

<u>Name</u>	<u>Overlay</u>	<u>Function</u>
REPRZK	INPUT	Reads pressurizer data from a restart dump and sets up a pointer table for that data.
REPUMP	INPUT	Reads pump data from a restart dump and sets up a pointer table for that data.
RESTGN	INPUT	Reads steam-generator data from a restart dump and sets up a pointer table for that data.
RETEE	INPUT	Reads tee data from a restart dump and sets up a pointer table for that data.
REVLVE	INPUT	Reads valve data from a restart dump and sets up a pointer table for that data.
REVSSL	INPUT	Reads vessel data from a restart dump and sets up a pointer table for that data.
RFDBK	PREP	Evaluates the reactor core reactivity feedback caused by changes in the fuel temperature, coolant temperature, and coolant void from the beginning of the previous time step.
RFILL	INPUT	Reads fill data from input file and sets up a pointer table for that data.
RHOLIQ	MAIN	Calculates values of liquid density and its derivatives.
RKIN	PREP	Integrates the neutron point-kinetics equations.
RODHT	POST	Calculates the fuel-rod temperature field.
RPIPE	INPUT	Reads pipe data from input file and sets up a pointer table for that data.
RPPH	PWRSS	Tests and replaces pump speed.
RPRIZR	INPUT	Reads pressurizer data from input file and sets up a pointer table for that data.
RPSGA	PWRSS	Tests and replaces steam-generator heat-transfer area.
RPUMP	INPUT	Reads pump data from input file and sets up a pointer table for that data.
RSTGEN	INPUT	Reads steam-generator data from input file and sets up pointer tables for that data.

<u>Name</u>	<u>Overlay</u>	<u>Function</u>
RTEE	INPUT	Reads tee data from input file and sets up a pointer table for that data.
RVLVE	INPUT	Reads valve data from input file and sets up a pointer table for that data.
RVSSL	INPUT	Reads vessel data from input file and sets up a pointer table for that data.
SIDPTR	INPUT	Sets pointers for one-dimensional components.
SAVBD	MAIN	Moves boundary information into component arrays.
SCLTBL	INPUT	Scales input table according to scale factor passed by input routine.
SCMLCM	INPUT	Checks for overflow. Transfers fixed length, variable length, and pointer tables to LCM. Adjusts pointers.
SCMOVE	MAIN	Copies a given number of words from one SCM array into another.
SEDIT	MAIN	Writes short edit to TRCOUT file.
SETBD	MAIN	Stores component information into boundary arrays.
SETLCM	MAIN	Monitors use of LCM dynamic area.
SETNET	INIT	Provides the information needed to set up the network solution matrices.
SETPOW	MAIN	Initializes reactor power.
SETPRP	MAIN	Determines pump speed and steam-generator heat-transfer area.
SETSCM	MAIN	Monitors use of SCM dynamic area.
SGTBC	PREP	Boundary cell calculations for the special case where the tee junction cell is the first or last cell in a main steam-generator pipe. This logic duplicates the logic in subroutine TEEL after the call to BKMOM.
SHRINK	PREP	Removes rows of conduction nodes within the vessel rods during reflood.
SIGMA	MAIN	Returns surface tension of water as a function of pressure.

<u>Name</u>	<u>Overlay</u>	<u>Function</u>
SLABHT	POST	Calculates the slab temperatures.
SLVLP	PWRSS	Solves one primary loop in steady state.
SMOVE	INPUT	Moves a character from one string to another.
SMOVEN	INPUT	Moves a specified number of characters from one string to another.
SOLVE	OUTER	Solves linear system of the form, $A*X = B$.
SPLIT	MAIN	Reads appropriate data from pump curves.
SREBAL	OUTER	Sets up coarse-mesh rebalance in the vessel.
SRTLTP	INPUT	Sorts components into loops and reorders them for the network solution.
STBME	POST	Sets up the stabilizing mass and energy equations.
STDIR	OUTER	Sets up direct inversion of the vessel matrix.
STEADY	MAIN	Generates a steady-state solution.
STGEN1	PREP	Controls steam-generator prepass.
STGN1X	PREP	Evaluates HTC's for steam-generator secondary.
STGEN2	OUTER	Controls steam-generator outer iteration.
STGEN3	POST	Controls steam-generator postpass.
STGN3X	POST	Performs steam-generator heat-transfer calculation.
STGNA	MAIN	Calculates steam-generator primary-side wall area.
STGNP	PWRSS	Calculates thermal properties for steam generator.
STGNTX	PREP	Computes needed quantities on prepass.
SVSET	PREP	Evaluates location-independent ($0 = ISUN < 17$) signal variables.
SVSET1	PREP	Evaluates signal variables with locations defined in the one-dimensional components.
SVSET3	PREP	Evaluates signal variables with locations defined in the three-dimensional vessel component.
TEE1	PREP	Controls tee prepass.

<u>Name</u>	<u>Overlay</u>	<u>Function</u>
TEE1X	PREP	Calculates source for tee side-leg hydrodynamics.
TEE2	OUTER	Controls tee outer iteration.
TEE3	POST	Controls tee postpass.
TEEP	PWRSS	Calculates central cell pressure and enthalpy flow rate for a tee.
TEMPL	PWRSS	Evaluates temperature based on liquid enthalpy and pressure.
TF1D	OUTER	Drives one-dimensional hydrodynamics routines.
TF1DS	OUTER	Solves the hydrodynamic equations for the one-dimensional two-fluid pipe model.
TF1DS1	OUTER	Sets up initial velocity approximations and their pressure derivatives for the one-dimensional two-fluid pipe model.
TF1DS3	OUTER	Performs the back-substitution for the one-dimensional two-fluid pipe model.
TF3DE	OUTER	Evaluates constitutive relations for interfacial shear and heat transfer; makes an evaluation of new time velocities.
TF3DI	OUTER	Sets up the linearized three-dimensional finite-difference equations.
THCL	MAIN	Returns thermal conductivity of water as a function of pressure and enthalpy.
THCV	MAIN	Returns thermal conductivity of steam as a function of pressure and enthalpy.
THERMO	MAIN	Calculates thermodynamic properties of water.
TIMCHK	MAIN	Checks elapsed time to see whether certain functions should be performed.
TIMSTP	MAIN	Sets up time-step and time-edit interval times.
TLOTVO	MAIN	Calculates the liquid and vapor temperatures on the secondary side of steam generators.
TMSFB	PREP	Calculates the minimum stable film boiling temperature (T_{min}).
TRAC	MAIN	Supplies MAIN program.

<u>Name</u>	<u>Overlay</u>	<u>Function</u>
TRANS	MAIN	Controls overall calculation for each time step.
TRCE	INPUT	Traces paths to locate a given component.
TRIP	MAIN	Returns status of a trip.
TRISLV	POST	Solves linear system of the form $A \cdot X = B$ where A is tridiagonal.
TRPSET	MAIN	Sets up trip status flags.
UNPKIT	MAIN	Unpacks data packed by subroutine PACKIT.
VALUE	INPUT	Converts an ascii string to its binary value.
VELCK	OUTER	Checks for incorrect donor-celling in subroutine VSSL caused by velocity sign changes.
VISCL	MAIN	Evaluates viscosity of water as a function of pressure and enthalpy.
VISCV	MAIN	Evaluates viscosity of steam as a function of pressure and enthalpy.
VLVE1	PREP	Controls valve prepass.
VLVE2	OUTER	Controls valve outer iteration.
VLVE3	POST	Controls valve postpass.
VLVEX	PREP	Evaluates the value of the flow area change action.
VOLFA	INIT	Calculates cell volume flow areas.
VOLV	PREP	Calculates cell average phase velocities for one-dimensional components.
VSCON	PWRSS	Evaluates vessel constants and junction properties.
VSSL1	PREP	Performs prepass calculations for vessel dynamics.
VSSL2	OUTER	Performs inner iterations for vessel dynamics.
VSSL3	POST	Performs postpass calculations for vessel dynamics.
WACCUM	EDIT	Writes selected accumulator data to output file TRCOUT.
WARRAY	MAIN	Writes a real array to output file TRCOUT.

<u>Name</u>	<u>Overlay</u>	<u>Function</u>
WBREAK	EDIT	Writes selected break data to output file TRCOUT.
WCOMP	EDIT	Controls the writing of selected component data to output file TRCOUT.
WCORE	EDIT	Writes selected core data to output file TRCOUT.
WFILL	EDIT	Writes selected fill data to output file TRCOUT.
WIARR	MAIN	Writes an integer array to output file TRCOUT.
WPIPE	EDIT	Writes selected pipe data to output file TRCOUT.
WPRIZR	EDIT	Writes selected pressurizer data to output file TRCOUT.
WPUMP	EDIT	Writes selected pump data to output file TRCOUT.
WRCOMP	INPUT	Writes data common to one-dimensional components to output files.
WRLCM	MAIN	Transfers a given number of words from SCM to LCM.
WRSLP	INPUT	Prints out subloop description.
WSTGEN	EDIT	Writes selected steam-generator data to output file TRCOUT.
WTEE	EDIT	Writes selected tee data to output file TRCOUT.
WVLVE	EDIT	Writes selected valve data to output file TRCOUT.
WVSSL	EDIT	Writes selected vessel data to output file TRCOUT.

APPENDIX G

TRAC ERROR MESSAGES

Errors diagnosed by TRAC are handled by subroutine ERROR. The level number associated with each error listed below is used by ERROR to determine its course of action.

<u>Level</u>	<u>Actions</u>
1, 3	Fatal error, stop problem.
2	Nonfatal error, continue problem.
4	Fatal error, add dump to the TRCDMP file, then stop problem.

I. OVERLAY MAIN

<u>Subroutine</u>	<u>Level</u>	<u>Message*</u>	<u>Explanation</u>
MAIN	1	NO SPACE FOR VERSION INFORMATION	Insufficient LCM space is available to store version information.
BFIN	1	DATA SET TYPE ERROR	An error exists in reading data in the binary format.
BFIN	1	DATA SET EOF ERROR	An illegal end-of-file was found when the data were read.
BFOUT	1	DATA SET TYPE ERROR	An error exists in writing the data in a binary format.
BITS	1	ILLEGAL BIT SPECIFIED	An attempt was made to set bit beyond the word length.
CHBD	2	BOUNDARY ERROR DETECTED	Adjacent components have mismatched geometry.
ENDDMP	2	DUMP FILE NOT CLOSED	An I/O error occurred when an attempt was made to close file TRCDMP.

*Each message also identifies the subroutine detecting the error.

<u>Subroutine</u>	<u>Level</u>	<u>Message</u>	<u>Explanation</u>
ENDGRF	2	GRAPHICS FILE NOT CLOSED	An I/O error occurred when an attempt was made to close file TRCGRF.
EOVLY	2	OVERLAY UNLOAD ERROR	An illegal overlay sequence exists.
FILLX	1	FILL TABLE SIGNAL VAR. NOT FOUND	The fill-table signal-variable ID number is not listed in the signal-variable ID numbers.
FILLX	1	ERROR IN RATE-FACTOR TABLE LOOPUP	An error occurred when a linear interpolation was performed for the rate-factor table that is applied to the fill-table independent variable.
FILLX	2	MASS FLOW RATE TOO LARGE FROM ADJACENT CELL	The mass flow specified in a FILL is negative and $ MFLOW *DELT$ exceeds the total mass in the adjacent cell. No action is taken.
FILLX	1	ERROR IN TABLE LOOKUP	There are zero entries in the fill table.
GETBIT	1	ILLEGAL BIT SPECIFIED	The bit position specified is either too small or too large.
HOUT	1	OUTER ITERATION DID NOT CONVERGE	The outer iteration procedure failed three consecutive times.
IOVLY	1	ERROR INITIALIZING SCM	Subroutine SETSCM found an error.
IOVLY	1	SCM SPACE TOO SMALL FOR OVERLAY	Insufficient dynamic SCM space exists for this overlay.
MANAGE	1	SCM MEMORY OVERFLOW	Insufficient dynamic SCM space exists.
MANAG ^r	1	LEVEL PROBLEM	The core level or rod number requested does not exist.
PUMPD	1	CANNOT LOCATE HEAD CURVE	The pump regime is outside the data base.
PUMPD	1	CANNOT LOCATE TORQUE CURVE	The pump regime is outside the data base.

<u>Subroutine</u>	<u>Level</u>	<u>Message</u>	<u>Explanation</u>
SETPOW	2	REACTOR POWER INITIALIZED	The reactor power has been initiated for a steady-state calculation.
STEADY	1	STEADY STATE DID NOT CONVERGE	The problem did not reach a steady state within the specified time domains.
STEADY	1	PWR INITIALIZATION INCOMPLETE	Convergence was not achieved for the PWR initialization and all specified time domains were completed.
THERMO	2	PRESSURE LIMIT EXCEEDED	The pressure in some cell has fallen below 1.0×10^3 or risen above 1.9×10^7 .
THERMO	2	VAPOR TEMPERATURE LIMIT EXCEEDED	The vapor temperature in some cell has fallen below 280 K.
THERMO	2	LIQUID TEMPERATURE LIMIT EXCEEDED	The liquid temperature in some cell has fallen below 280 K or risen above 647 K.
THERMO	1	SATURATION TEMPERATURE TOO LARGE	A temperature above the range of THERMO was encountered.
TIMSTP	4	CANNOT REDUCE TIME STEP FURTHER	The time step was reduced to the minimum allowed and the outer iteration failed to converge.
TRIP	1	TRIP NUMBER NOT DEFINED	The status of an undefined trip was requested.
TRPSET	1	TRIP SIGNAL NOT FOUND	The signal-variable ID number that defines the signal-variable trip signal is not listed in the signal-variable ID numbers.
TRPSET	1	SIGNAL EXP. NOT FOUND	The signal-expression ID number that defines the signal-expression trip signal is not listed in the signal-expression ID numbers.

<u>Subroutine</u>	<u>Level</u>	<u>Message</u>	<u>Explanation</u>
TRPSET	1	EXP. SIGNAL NOT FOUND	A signal-variable ID number that defines a subexpression argument value for the signal-expression trip signal is not listed in the signal-variable ID numbers.
TRPSET	1	TRIP TRIPS NOT FOUND	The trip-controlled trip-signal ID number that defines the trip-controlled trip signal is not listed in the trip-controlled trip-signal ID numbers.
TRPSET	1	TRIP ID NO. NOT FOUND	The trip ID number that defines the trip-controlled trip signal is not listed in the trip ID numbers evaluated previously during this time step.
TRPSET	1	SF FACTOR ID NOT FOUND	The set-point factor-table ID number is not listed in the set-point factor-table ID numbers.
TRPSET	1	FACTOR SIG. NOT FOUND	The signal-variable ID number that defines the set-point factor-table independent variable is not listed in the signal-variable ID numbers.
TRPSET	1	TOO MANY DELAYED TRIPS	After five trip criteria are satisfied and a trip set-status change is pending because of delay time, all subsequent trip criteria that are fulfilled are ignored.

II. OVERLAY INPUT

INPUT	1	FILE TRACIN DOES NOT EXIST	An input deck does not exist.
INPUT	1	VERSION INFORMATION EXCEEDS LCM	The version information exceeds its allocated LCM space.
INPUT	1	INOPTS NAMELIST DATA NOT FOUND	The option that indicates NAMELIST data exist for group INOPTS was selected; however, the data are not in the TRACIN file.

<u>Subroutine</u>	<u>Level</u>	<u>Message</u>	<u>Explanation</u>
INPUT	2	COMPONENT ID.GT.99	A component with an ID number larger than 99 exists in the IORDER array.
INPUT	1	NO SPACE FOR BUFFERS	Insufficient LCM space exists for I/O buffers.
INPUT	1	FATAL INPUT ERROR(S)	A fatal input error occurred when an input or restart file was read.
CHKSR	2	TWO VESSEL SOURCES LOCATED IN ONE CELL	The vessel input specifies two sources in one fluid cell.
CHKSR	2	VESSEL SOURCE POSITION ERROR	The specified source position is impossible.
FNDLP	1	INVALID VESSEL JUNCTION	There is a PWR-initialization input error. A junction that is not connected to the vessel is specified.
FNDLP	1	TEE MISSING FROM JUN ARRAY	There is a PWR-initialization input error. A loop tee is not specified in the JUN array.
FNDLP	1	STGEN MISSING FROM JUN ARRAY	There is a PWR-initialization input error. A loop steam generator is not specified in the JUN array.
FNDLP	1	COMPLEX SECONDARY LOOP	There is a PWR-initialization input error. The steam-generator secondary side must be connected only to pipes, fills, and breaks.
FNDLP	1	LAST COMMON COMPONENT NOT FOUND	There is a PWR-initialization input error. In a two-pump loop, the connecting tee is not specified.
FNDLP	1	LAST COMMON COMPONENT NOT A TEE	There is a PWR-initialization input error. In a two-pump loop, the connecting component is not a tee.
LOAD	2	REPEAT LEVEL CARD	A REPEAT LEVEL data card was found when the array data were read.

<u>Subroutine</u>	<u>Level</u>	<u>Message</u>	<u>Explanation</u>
LOAD	2	OPERATION END ENCOUNTERED BUT INTERPOLATION INCOMPLETE	When the array data were read, operation E was specified before both end points of an interval to be interpolated were read.
LOAD	2	ARRAY FILLED BUT OPERATION END NOT FOUND	When the array data were read, operation E was not specified after the array was filled.
LOAD	2	DATA OVERFLOWED ARRAY REPEAT COUNT RESET TO ONE	When the array data were read, a repeat operation overfilled the array.
LOAD	2	REPEAT COUNT LESS THAN ONE, COUNT RESET TO ONE	When the array data were read, a repeat count of less than one was found.
LOAD	2	INTEGER INTERPOLATION NOT ALLOWED	When an integer array was read, an interpolation operation was specified.
LOAD	2	ZERO OR FEWER INTERPOLATIONS - OPERATION TREATED AS BLANK	When the array data were read, an interpolation count less than one was specified.
LOAD	2	UNDEFINED OPERATION REPEAT COUNT SET TO ONE	When the array data were read, an undefined load operation was specified.
LOAD	2	NOT ENOUGH DATA TO FILL ARRAY	Insufficient data were input to fill an array.
LOAD	2	UNEXPECTED END-OF-FILE REACHED	When the array data were read, an unexpected end-of-file was specified.
LOAD	2	INPUT ERROR - NEW COMPONENT WAS ENCOUNTERED UNEXPECTEDLY	When the array data for a component were loaded, data for an additional component or an "END" card was specified.
LOAD	2	INPUT ERROR - UNEXPECTED NAMELIST DATA ENCOUNTERED	When the array data were loaded, NAMELIST data were specified.
LOAD	2	REAL DATA ENCOUNTERED IN INTEGER ARRAY	When data were loaded into an integer array, real data were specified.

<u>Subroutine</u>	<u>Level</u>	<u>Message</u>	<u>Explanation</u>
NXTCMP	1	END-OF-FILE REACHED WHILE SEARCHING FOR NEXT COMPONENT	An end-of-file was specified when data for an new component were read for a new component.
NXTCMP	2	CARD SKIPPED - DATA FOR NEW COMPONENT OR END CARD WAS EXPECTED	Too many data were encountered for the component being processed.
PATH	1	ADJACENT COMPONENT MISSING	There is a PWR initializa- tion input error. A junction was encountered that is connected only to one component.
PATH	1	COMPONENT NOT FOUND IN IORDER ARRAY	There is a PWR initializa- tion input error. A component was encountered that is not listed in the IORDER array.
PATH	1	PIPE JUNCTIONS NOT ADJACENT	There is a PWR initializa- tion input error. The two entries in JUN for a pipe are not consecutive.
RBREAK	2	ERROR IN TABLE SPECIFICATIONS	Incompatible BREAK options were selected.
RBREAK	2	LCM OVERFLOW	LCM area overflowed during input of data for a break.
RBREAK	2	SCM OVERFLOW	There is insufficient SCM for this break.
RCNTL	2	BAD TRIP ID DEFINITION	A trip ID was read in, the absolute value of which was either zero or greater than 9999.
RCNTL	2	TRIP SET POS. INVALID	The trip set status variable ISET has an invalid input value.
RCNTL	2	BAD SIG. EXP. OPERATOR	The arithmetic operator ID number for a sub- expression within the signal expression definition has an invalid input value less than one or greater than eight.

<u>Subroutine</u>	<u>Level</u>	<u>Message</u>	<u>Explanation</u>
RCORE	2	BAD TRIP ID DEFINITION	A trip ID was read in that was either equal to -1, less than -9999, or greater than 9999.
RCORE	2	LCM OVERFLOW	LCM area overflowed during input of data for a core.
RCORE	2	SCM OVERFLOW	There is insufficient SCM for this core.
RCORE	2	NZ MAX. LT. (NCRZ+1) +SUM OF NFAX(I)	The number of allowable rows of rod conduction nodes is less than the minimum specified by the user for reflood calculations.
RDCOMP	1	COMPONENT TYPE NOT RECOGNIZED	An invalid component type was encountered.
RDCOMP	1	DUPLICATE COMPONENT NUMBERS	At least two components were assigned the same No. during input.
RDDIM	2	ILLEGAL PUMP CURVE OPTION	Illegal pump option was specified on pump card 9.
RDLOOP	1	VESSEL NOT FOUND IN JUN ARRAY	There is a PWR initialization input error. The vessel is not listed in the JUN array.
RDLOOP	1	VESSEL NOT FOUND IN IORDER ARRAY	There is a PWR initialization input error. The vessel is not listed in the IORDER array.
RDREST	1	FILE TRCRST DOES NOT EXIST	Component data was omitted from the input deck, but a restart dump file to initialize missing components cannot be found.
RDREST	1	RESTART FILE OPEN ERROR	An I/O error was made while attempting to open the restart file.
RDREST	1	RESTART FILE INCOMPATIBLE WITH THIS PROBLEM	The restart file cannot be used with this TRAC version.

<u>Subroutine</u>	<u>Level</u>	<u>Message</u>	<u>Explanation</u>
RDREST	1	DUMP TIME NOT FOUND ON RESTART FILE	Restart dump at time indicated on input file is not on the restart file.
RDREST	1	NO DUMPS ON FILE	There are no complete dumps on the TRCRST file.
RDREST	1	COMPONENT DATA NOT FOUND	Data for a particular component were not found in either input or restart file.
RDREST	1	TYPE NOT RECOGNIZED IN RESTART	An invalid component type was encountered.
REACCM	2	POINTER TABLE MISMATCH	Accumulator pointer table does not match restart file.
READI	1	UNEXPECTED END-OF-FILE REACHED	End-of-file was encountered while trying to read integer data (I14).
READI	2	REPEAT LEVEL CARD MISPLACED	A repeat level card was encountered while trying to read integer data (I14).
READI	1	INPUT ERROR - ENCOUNTERED UNEXPECTED LOAD DATA	A load operation was encountered while trying.
READI	1	INPUT ERROR - REAL DATA ENCOUNTERED IN INTEGER FIELD	Real data was encountered while trying to read integer data in I14 format.
READI	1	INPUT ERROR - NEW COMPONENT WAS ENCOUNTERED UNEXPECTEDLY	Data for a new component was encountered before all of the data for the current component was read in.
READI	2	INPUT ERROR - UNEXPECTED NAMELIST DATA ENCOUNTERED	NAMELIST data was encountered while trying to read integer data in I14 format.
READR	1	UNEXPECTED END-OF-FILE REACHED	End-of-file was encountered while trying to read real data (E14.6).
READR	2	REPEAT LEVEL CARD MISPLACED	A REPEAT LEVEL card was encountered while trying to read real data (E14.6).

<u>Subroutine</u>	<u>Level</u>	<u>Message</u>	<u>Explanation</u>
READR	1	INPUT ERROR - ENCOUNTERED UNEXPECTED LOAD DATA	A load operation was encountered while trying to read non-array real data in E14.6 format.
READR	1	INPUT ERROR - NEW COMPONENT WAS ENCOUNTERED UNEXPECTEDLY	Data for new component was encountered before all of the data for the current component was read in.
READR	2	INPUT ERROR - UNEXPECTED NAMELIST DATA ENCOUNTERED	NAMELIST data was encountered while trying to read real data in E14.6 format.
REBRK	2	LCM OVERFLOW	LCM area overflowed while reading break data from restart file.
REBRK	2	SCM OVERFLOW	There is insufficient SCM for this break.
REBRK	1	ERROR IN TABLE SPECIFICATIONS	Processing of input data stopped because of a previous error.
REBRK	2	POINTER TABLE MISMATCH	Break pointer table does not match restart file.
REBRK	1	FATAL ERROR	Processing of input data stopped because of a previous error.
RECNTL	1	CNTL STORAGE TOO SMALL	The variable storage for signal variables, trips, and controllers that was dimensioned on input data is too small to contain the remaining data from the restart file.
RECNTL	1	SIGNAL VAR. EXCEED DIM	The number of signal variables with different ID numbers from input and the restart file exceeds the input data dimension.

<u>Subroutine</u>	<u>Level</u>	<u>Message</u>	<u>Explanation</u>
RECNTL	1	TRIP VAR. EXCEED DIM.	The number of trips with different ID numbers from input and the restart file exceeds the input data dimension.
RECNTL	1	TOO MANY SIGNAL EXPRS.	The number of signal expressions on the restart file exceeds the input data dimension.
RECNTL	1	SIGNAL EXP. EXCEED DIM.	The number of signal expression ID numbers from input and from the restart file exceeds the input data dimension.
RECNTL	1	TOO MANY TRIP-CON. TRIP	The number of trip-controlled trips on the restart file exceeds the input data dimension.
RECNTL	1	TRIP-TRIPS EXCEED DIM.	The number of trip-controlled trip ID numbers with different ID numbers from input and from the restart file exceeds the input data dimension.
RECNTL	1	TOO MANY FACTOR TABLES	The number of set-point factor tables on the restart file exceeds the input data dimension.
RECNTL	1	FACT. TABLES EXCEED DIM.	The number of set-point factor table ID numbers with different ID numbers from input and the restart file exceeds the input data dimension.
RECNTL	1	TOO MANY DUMP TRIP IDS	The number of trip ID numbers that generated restart dumps when they are set to ON exceeds the input data dimension.

<u>Subroutine</u>	<u>Level</u>	<u>Message</u>	<u>Explanation</u>
RECNTL	1	TOO MUCH TIME STEP DAT	The number of trip-controlled time-step data sets on the restart file exceeds the input data dimension.
RECNTL	1	TIME STEP DATA EXC. DIM.	The number of trip-controlled time-step data sets with different ID numbers from input and from the restart file exceeds the input data dimension.
RECORE	2	POINTER TABLE MISMATCH	CORE pointer table does not match restart file.
RECORE	2	LCM OVERFLOW	LCM area overflowed during input of data for a core.
RECORE	2	SCM OVERFLOW	There is insufficient SCM for this core.
REFILL	2	LCM OVERFLOW	LCM area overflowed while reading fill data from restart file.
REFILL	2	SCM OVERFLOW	There is insufficient SCM for this fill.
REFILL	2	POINTER TABLE MISMATCH	Fill pointer table does not match restart file.
REFILL	1	FATAL ERROR	Processing of input data stopped because of a previous error.
REPIPE	2	POINTER TABLE MISMATCH	Pipe pointer table does not match restart file.
REPRZR	2	POINTER TABLE MISMATCH	Pressurizer pointer table does not match restart file.
REPUMP	2	POINTER TABLE MISMATCH	Pump pointer table does not match restart file.
REPUMP	1	SCM OVERFLOW	SCM area overflowed while reading pump data from restart file.

<u>Subroutine</u>	<u>Level</u>	<u>Message</u>	<u>Explanation</u>
RESTGN	2	POINTER TABLE MISMATCH	Steam-generator pointer table does not match restart file.
RETEE	2	POINTER TABLE MISMATCH	Tee pointer table does not match restart file.
REVLVE	2	POINTER TABLE MISMATCH	Valve pointer table does not match restart file.
REVSSL	2	POINTER TABLE MISMATCH	Vessel pointer table does not match restart file.
REVSSL	2	LCM OVERFLOW	LCM area overflowed while reading vessel data from restart file.
REVSSL	2	SCM OVERFLOW	SCM area overflowed while reading vessel data from restart file.
RFILL	2	LCM OVERFLOW	LCM area overflowed while reading fill data from input file.
RFILL	2	ILLEGAL FILL TYPE OPTION	An illegal fill-type option was read in from fill card 2.
RFILL	2	NFTX .LT. 1	FILL type options 4 to 9 require at least one FILL table pair.
RFILL	2	IFSV .LT. 1	The signal-variable ID number for FILL type options 4 to 9 must be greater than zero.
RFILL	2	BAD TRIP ID DEFINITION	A trip ID was read in that was either equal to -1, less than -9999, or greater than 9999.
RFILL	2	SCM OVERFLOW	SCM area overflowed while reading fill data from input file.
RPUMP	2	PUMP TYPE NOT RECOGNIZED	IPMPTY is allowed to be only 1 or 2.

<u>Subroutine</u>	<u>Level</u>	<u>Message</u>	<u>Explanation</u>
RPUMP	2	NCELLS .LT. 2	Number of fluid cells in the pump must be at least two.
RPUMP	2	BAD TRIP ID DEFINITION	A trip ID was read in that was either equal to -1, less than -9999, or greater than 9999.
RPUMP	2	SPEED TABLE PARAM. BAD	The signal variable ID number for the pump type 1 rotational-speed table's independent variable is invalid.
RPUMP	2	RATE FACTOR NPMPRF BAD	The signal variable ID number for the rate factor table's independent variable is invalid.
RPUMP	2	IPMPV.NE.0	The signal variable ID number defining the pump speed table's independent variable should not be defined for pump type 2.
RPUMP	2	NPMPV.NE.0	The number of pump speed table pair entries input should be zero for pump type 2, which is defined internally in TRAC.
RPUMP	2	NPMPRF.NE.0	No rate factor table can be applied to the pump speed table's independent variable for pump type 2.
RPUMP	2	FRIC(2) .NE. 0.	FRIC(2) must be input 0.0 in PUMP.
RSTGEN	2	STGEN MUST HAVE HEAT-TRANSFER NODES	No nodes were specified for a STGEN.

<u>Subroutine</u>	<u>Level</u>	<u>Message</u>	<u>Explanation</u>
RSTGEN	2	ERROR IN S/G TEE INPUT	There is an inconsistency or error in one or more of the following steam-generator tee nodding input: JCELLS, JCELLP, NCELL3, NCELL4. An error results for the following input combinations: (1) JCELLP >0 and JCELLS ≤0 (2) JCELLP >0 and NCELL4 ≤0 (3) JCELLS >0 and NCELL3 ≤0
RSTGEN	2	STEAM GENERATOR WALL AREAS INCONSISTANT. SECONDARY CELL NO. XXX.	Secondary-side wall area is not consistent with primary side {WA2 = WA1 * [1.+(TH/RADIN)]}.
RVLVE	2	FAVLVE AND XPOS INVALID	The input values of FAVLVE and XPOS are both outside their 0 to 1 physical range.
RVLVE	2	BAD VALVE TYPE OPTION	The valve option parameter IVTY has an input value outside the 0 to 4 defined range.
RVLVE	2	BAD VALVE TABLE SIZE	The number of pair entries in the first valve table is inconsistent with the valve option IVTY value.
RVLVE	2	BAD VALVE TABLE SIGNAL	The signal variable ID number defining the valve table's independent variable is inconsistent with the valve option IVTY value.
RVLVE	2	BAD TRIP ID DEFINITION	The trip ID number that controls valve table usage is either equal to -1, less than -9999, or greater than 9999.

<u>Subroutine</u>	<u>Level</u>	<u>Message</u>	<u>Explanation</u>
RVLVE	2	BAD 2ND VALVE TAB. SIZE	The number of pair entries in the second valve table is invalid. A first valve table must be input before the second valve table can be input.
RVLVE	2	BAD RATE FACT. TAB. SIZE	The number of pair entries in the rate factor table is invalid. A rate factor table is input only when the valve table usage is trip controlled.
RVLVE	2	INVALID VALVE POSITION	The input location of the adjustable valve cell interface is invalid.
RVSSL	2	BAD TRIP ID DEFINITION	A trip ID number was either input equal to -1, less than -9999, or greater than 9999.
RVSSL	2	INCONSISTENT CORE INPUT	An error was made in specifying the core positional parameters, ICRU, ICRL, ICRR, or the number of heat-transfer nodes.
RVSSL	2	INCONSISTENT DOWNCOMER INPUT	An error was made in specifying the downcomer positional parameters, IDCU, IDCL, and IDCR.
RVSSL	2	NRODS IS LESS THAN NCRX	Number of computational fuel rods necessary to perform the fluid-dynamics analysis is less than the number of fluid-dynamics segments (r,θ).
RVSSL	2	LCM OVERFLOW	LCM area overflowed while reading vessel data from an input file.
RVSSL	2	SCM OVERFLOW	SCM area overflowed while reading vessel data from an input file.

<u>Subroutine</u>	<u>Level</u>	<u>Message</u>	<u>Explanation</u>
RVSSL	2	VESSEL CONVERGENCE CRITERIA TOO LOOSE	The convergence criterion for vessel iteration (EPSI) was set to a value greater than 1.0×10^{-05} .
RVSSL	2	VESSEL ITERATION MAX SHOULD BE AT LEAST 50	The maximum number of vessel iterations (IITMAX) is less than 50.
RVSSL	2	NZMAX.LT.NCRZ+1 + SUM OF NFAX(I)	The number of allowable rows of rod conduction nodes is less than the minimum specified by the user for reflood calculations.
RVSSL	2	ILLEGAL REPEAT LEVEL NUMBER	An illegal level number was read off a REPEAT LEVEL card.
RVSSL	2	INCONSISTENT SLAB INTERFACE INPUT	An incorrect value for INHSMX was input.
RVSSL	1	UNEXPECTED END-OF-FILE	An end-of-file was encountered while reading VESSEL level data.
SCMLCM	2	LCM OVERFLOW	Insufficient LCM space is available for storing component data.
SCMLCM	2	SCM OVERFLOW	Insufficient SCM space is available for reading in component array data.
TRCE	1	TOO MANY NESTED TEES	There is a PWR initializa- tion input error. More than 5 tees are connected.
TRCE	1	COMPONENT TYPE NOT LOCATED	There is a PWR initializa- tion input error. A steam generator, pump, or vessel hot leg is not connected to the vessel cold leg.
TRCE	1	TEE JUNCTIONS NOT ADJACENT	There is a PWR initializa- tion input error. The entries in the JUN array for a tee are not consecutive.

<u>Subroutine</u>	<u>Level</u>	<u>Message</u>	<u>Explanation</u>
TRCE	1	COMPONENT JUNCTIONS NOT ADJACENT	There is a PWR initialization input error. The entries in the JUN array for a component are not adjacent.
III. OVERLAY INIT			
CIVSSL	1	JUNCTION PROBLEM	A component adjacent to the vessel cannot be found.
CIVSSL	1	IORDER PROBLEM	The calculational sequence must compute the component connected to the vessel before it calculates the vessel.
CIVSSL	1	CONNECTIONS COMPUTED AFTER VESSEL	The component calculational sequence must compute the connections before the vessel.
CIVSSL	1	VESSEL CONNECTED TO BREAK	A vessel cannot be connected to a break.
CIVSSL	1	VESSEL CONNECTED TO A FILL	A vessel cannot be connected to a fill.
GRFPUT	2	ERROR IN GRAPHICS OUTPUT	Integer is too large to be packed into a 15-bit word.
ICOMP	1	JUNCTION COUNT ERROR	The number of junctions specified is inconsistent with the number found.
ICOMP	1	INCONSISTENT JUNCTION NUMBERS	Inconsistent specification of junction numbers was made.
ICOMP	1	JUNCTION NUMBERS WRONG	The junctions are assigned incorrectly.
ICOMP	1	UNRECOGNIZED COMPONENT	The component type was not recognized.

<u>Subroutine</u>	<u>Level</u>	<u>Message</u>	<u>Explanation</u>
ICORE	1	ROD POWER PROBLEM	The input parameters for the fuel rod geometry, number, and power distribution are invalid. A nonpositive unnormalized power from a fuel rod was evaluated.
IGRAF	1	GRAPHICS FILE ALLOCATION FAILURE	An I/O error occurred while attempting to allocate space for graphics file.
IGRAF	1	COMPONENT TYPE NOT RECOGNIZED	An invalid component type was encountered.
IGRAF	1	NO LCM SPACE FOR GRAPH CATALOG	Insufficient LCM is available.
IGRAF	1	SCM OVERFLOW	Insufficient SCM is available.
IVLVE	1	INVALID VALVE LOCATION	The valve interface where the flow area is adjustable doesn't lie between two cells within the valve component.
IVSSL	1	ROD POWER PROBLEM	The reactor power option specified is not within allowable limits.
JFIND	1	JUNCTION PROBLEM	A junction number could not be located in the junction sequence array.

IV. OVERLAY DUMP

<u>Subroutine</u>	<u>Level</u>	<u>Message</u>	<u>Explanation</u>
DMPIT	3	TYPE NOT RECOGNIZED	An invalid component type was encountered.
DMPIT	3	DUMP FILE DEFINE ERROR	File TRCDMP could not be created.

V. OVERLAY PWRSS

<u>Subroutine</u>	<u>Level</u>	<u>Message</u>	<u>Explanation</u>
LPCON	1	NO PUMP IN PRINCIPAL LOOP	No pump was found in the loop description.

<u>Subroutine</u>	<u>Level</u>	<u>Message</u>	<u>Explanation</u>
LPCON	1	NO STGEN IN PRINCIPAL LOOP	No steam generator was found in the loop description.
LPCON	1	MISSING VESSEL JUNCTION	An invalid vessel junction number was found in the vessel junction data area.
LPSET	1	ZERO FLOW OR POWER FOUND AT PWR INITIALIZATION	The reactor power and flow rate must be nonzero.
LPSET	1	ILLEGAL LOOP PARAMETER	The PWR initialization calculated a negative value for the steam-generator area or pump speed.
ORIENT	1	NO JUNCTION MATCH	A junction connected to a tee or steam generator in the JUN array was not found.
RPPH	1	CONVERGENCE FAILURE EVALUATING PUMP SPEED	The pump speed to achieve the needed head could not be calculated.
TEMPL	1	TOO MANY ITERATIONS	The temperature cannot be evaluated from values of the enthalpy and pressure.

VI. OVERLAY PREP

<u>Subroutine</u>	<u>Level</u>	<u>Message</u>	<u>Explanation</u>
PREP	1	COMPONENT TYPE NOT RECOGNIZED	An invalid component type was encountered.
BREAKX	1	ERROR IN TABLE LOOKUP	An error exists in interpolating a break table.
CHF	1	TCHF FAILED TO CONVERGE	The calculation failed to converge on a unique critical heat-flux wall temperature.
CORECI	1	REACTOR POWER INITIALIZED	The reactor core's total power is turned on to its input initial value.
CTAIN1	1	CONTAINMENT MODULE NOT YET IMPLEMENTED	The containment component will be in a future TRAC version.

<u>Subroutine</u>	<u>Level</u>	<u>Message</u>	<u>Explanation</u>
PIPE1	1	ERROR IN TABLE LOOKUP	There is an error in interpolating pipe power table.
PREP3D	1	COMPONENT TYPE NOT RECOGNIZED	An invalid component type was encountered.
PUMPSR	1	PUMP TABLE SIGNAL VAR. NOT FOUND	The signal variable ID number defining the pump speed table's independent variable was not found in the list of signal variable ID numbers.
PUMPSR	1	RATE FACTOR TABLE LOOKUP ERROR	An error was encountered while interpolating in the rate factor table that is applied to the pump speed table's independent variable.
PUMPSR	1	PUMP SPEED TABLE LOOKUP ERROR	An error was encountered while interpolating in the pump speed table.
PUMPSR	1	INSUFFICIENT SCM SPACE	There is insufficient dynamic SCM for pump since calculations.
PUMPSR	1	ERROR IN ROUTINE PUMPX	An error was encountered while evaluating a pump head or torque.
RKIN	1	POWER-REACT.TABLE SIGNAL NOT FOUND	There was an error in interpolating the reactor kinetics table.
RKIN	1	ERROR IN RATE FACTOR TABLE LOOKUP	An error was encountered while interpolating in the rate factor table that is applied to the power or reactivity table's independent variable.

<u>Subroutine</u>	<u>Level</u>	<u>Message</u>	<u>Explanation</u>
RKIN	1	ERROR IN POWER REACT. TABLE LOOKUP	An error was encountered while interpolating in the power or reactivity table.
SVSET3	1	LOCAL DIM. GT. 50 NEEDED	There are more than 50 signal variables defined in the vessel component that require local variable storage in subroutine SVSET3 while searching over two or more axial levels to evaluate their signal variable value.
VLVEX	1	VALVE TABLE SIGNAL VARIABLE NOT FOUND	The signal variable ID number defining the valve table's independent variable was not found in the list of signal variable ID numbers.
VLVEX	1	ERROR IN RATE FACTOR TABLE LOOKUP	An error was encountered while interpolating in the rate factor table that is applied to the valve table's independent variable.
VLVEX	1	FIRST VALVE TABLE LOOKUP ERROR	An error was encountered while interpolating in the first valve table.
VLVEX	1	SECOND VALVE TABLE LOOKUP ERROR	An error was encountered while interpolating in the second valve table.
VSSL1	2	REACTOR POWER INITIALIZED	The reactor core's total power is turned on to its input initial value.

VII. OVERLAY OUTER

<u>Subroutine</u>	<u>Level</u>	<u>Message</u>	<u>Explanation</u>
OUTER	1	FATAL ERROR	A fatal error has occurred.
CTAIN2	1	CONTAINMENT MODULE NOT YET IMPLEMENTED	Containment component will be in a future TRAC version.
OUT1D	1	COMPONENT TYPE NOT RECOGNIZED	Invalid component type was encountered.

<u>Subroutine</u>	<u>Level</u>	<u>Message</u>	<u>Explanation</u>
OUT3D	1	COMPONENT TYPE NOT RECOGNIZED	Invalid component type was encountered.

VIII. OVERLAY POST

<u>Subroutine</u>	<u>Level</u>	<u>Message</u>	<u>Explanation</u>
POST	1	COMPONENT TYPE NOT RECOGNIZED	An invalid component type was encountered.
CORE3	1	POWER SHAPE TABLE SIGNAL NOT FOUND	The signal variable ID number defining the axial power shape table's independent variable was not found in the list of signal variable ID numbers.
CORE3	1	ERROR IN RATE FACTOR TABLE LOOKUP	An error was encountered while interpolating in the rate table that is applied to the axial power shape table's independent variable.
COREC3	1	INSUFFICIENT SCM SPACE	There is insufficient SCM space.
COREC3	1	POWER SHAPE TABLE SIGNAL NOT FOUND	The signal variable ID number defining the axial power shape table's independent variable was not found in the list of signal variable ID numbers.
COREC3	1	ERROR IN RATE FACTOR TABLE LOOKUP	An error was encountered while interpolating in the rate factor table that is applied to the axial power shape table's independent variable.
CTAIN3	1	CONTAINMENT MODULE NOT YET IMPLEMENTED	Containment component will be in a future TRAC version.
POST3D	1	COMPONENT TYPE NOT RECOGNIZED	An invalid component type was encountered.
POSTER	1	NO SCM SPACE FOR CYLHT	There is insufficient dynamic SCM space.

<u>Subroutine</u>	<u>Level</u>	<u>Message</u>	<u>Explanation</u>
STGN3X	1	INSUFFICIENT SPACE FOR CYLHT	There is insufficient dynamic SCM space.
IX. OVERLAY GRAF			
<u>Subroutine</u>	<u>Level</u>	<u>Message</u>	<u>Explanation</u>
GRAF	1	DATA TYPE ERROR	There is an invalid data type in the graphics catalog.
GRAF	1	SCM OVERFLOW	There is insufficient SCM for packing graphics data.
INPUT	1	INOPTS NAMLIST DATA NOT FOUND	The option that indicates NAMELIST data exist for group INOPTS was selected; however, the data are not in the TRACIN file.
LOAD	2	REPEAT LEVEL CARD MISPLACED	A REPEAT LEVEL data card was found when the array data were read.
READI	2	REPEAT LEVEL CARD MISPLACED	A REPEAT LEVEL data card was encountered when trying to read integer data (I14).
READR	2	REPEAT LEVEL CARD MISPLACED	A REPEAT LEVEL data card was encountered while trying to read real data in E14.6 format.
RVSSL	1	ILLEGAL REPEAT LEVEL NUMBER	An illegal level number was read from a REPEAT LEVEL card.
RVSSL	1	UNEXPECTED END-OF-FILE	An end-of-file was encountered when reading VESSEL level data.
RKIN	1	POWER-REACT.TABLE SIGNAL NOT FOUND	There was an error in interpolating the reactor- kinetics table.
COREC3	1	INSUFFICIENT SCM SPACE	There is insufficient SCM space available to solve the ROD conduction equations.

APPENDIX H

DESCRIPTION OF COMMON BLOCK VARIABLES

COMMON A(20000)

A(20000)Dynamic SCM storage area.

COMMON/ALP10/NMSAL/FMSLQ/FMSVP

NMSAL: Variable not implemented.

FMSLQ: Variable not implemented.

FMSVP: Variable not implemented.

COMMON/BKCNTRL/LREIT,LREITV,LBCKV,IPREIT,IPBCKV

LREIT: If .TRUE., then variable forces a reiteration.

LREITV: If .TRUE., then variable forces a reiteration.

LBCKV: If .TRUE., then variable forces a time-step back-up.

IPREIT: Flag to print messages on forced reiteration.

IPBCKV: Flag to print messages on forced back-up.

COMMON/DONR/IDON,ITDON,NCOMDP,JDONP

IDON: Variable not implemented.

ITDON: If flow reversals occur for OITNO > ITDON the time step is backed up.

NCOMDP: Component number of flow reversal forcing back-up.

JDONP: Cell number in NCOMDP.

COMMON/BKPOST/LBKPST,IBKPST,JBKPST

LBKPST: Logical variable. If .TRUE., then a time-step back-up is forced from POST.

IBKPST: Component forces back-up.

JBKPST: Cell number.

COMMON/CHGALP/DAU,DAL,OAU,OAL,XDAU,XDAL,XOAU,XOAL,JDAU,JDAL,JOAU,JOAL,NDAU,
NDAL,NOAU,NOAL

DAU: Maximum increase in void fraction over the time step.
DAL: Maximum decrease in void fraction.
OAU: Maximum increase in void immediately following a decrease.
OAL: Maximum decrease in void immediately following an increase.
XDAU: Limit on DAU beyond which the time step is reduced.
XDAL: Limit on DAL beyond which the time step is reduced.
XOAU: Limit on OAU beyond which the time step is reduced.
XOAL: Limit on OAL beyond which the time step is reduced.
JDAU: Cell where DAU occurred.
JDAL: Cell where DAL occurred.
JOAU: Cell where OAU occurred.
JOAL: Cell where OAL occurred.
NDAU: Component where DAU occurred.
NDAL: Component where DAL occurred.
NOAU: Component where OAU occurred.
NOAL: Component where OAL occurred.

COMMON/CODEBK/CBNAM(5),ILEV,MAXLEN,MAXLN3, MAX1LV,MLNVMT

CBNAM: Array containing the names of the overlays currently in core.
ILEV: The number of overlays currently in core.
MAXLEN: Maximum amount of SCM storage needed to process any one-dimensional component.
MAXLN3: Maximum amount of SCM storage needed to process any three-dimensional component.
MAX1LV: Maximum amount of SCM storage needed for three-dimensional components when only one level of data is required.

MLNVMT: The amount of SCM space required to solve the vessel matrix.

COMMON/CONST/PI,GC,ZERO,ONE,EPSALP

PI: Constant π .

GC: Gravitational constant.

ZERO: Real constant zero.

ONE: Real constant one.

EPSALP: Void-fraction cutoff for thermodynamic vapor properties.

COMMON/CONTRL/STDYST,TRANSI,DSTEP,ICP,LCMPTR,ETIME,DELT,TIMET,EPSO,EPSI,EPSS,
OITMAX,IITMAX,SITMAX,IEOS,VMAXT,DAMX,VARER,ICMP,DTMIN,DTMAX,
ISTDY,TEND,IPAK,EPSP,ICCMX,KCCMX,NITMX,NITMN,NITAV,NSTP,NCMX,
NCMN,NSMN,NSMX,VCMX,VCMN,NSVSMX,NSVSMN,NIVSMX,NIVSMN,VMOLD,
VMNEW,VMCON,DTLMX,DTVMX,DTSMX,DTRMX,DAMMC,NSEO,VMAXO,DELHT,
ITMIN,DTO,DIFMIN,DPRMX,ODELT,IM100,ISSFLG,IACCMD,IPAKON,ITPAKO,
NSEND,NSPL,NSPU,IPKMP,IFPREP,ISTTC,HTLOST,HTLOSO.

INTEGER STDYST,TRANSI,DSTEP,OITMAX,SITMAX

STDYST: Steady-state calculation indicator.

TRANSI: Transient calculation indicator.

DSTEP: Time-step number of dump to be used for restart.

ICP: Temporary pointer to next free location in the dynamic storage area for component data.

LCMPTR: Pointer to end of component data for last component read in.

ETIME: Current calculation time used for edits.

DELT: Current time increment for advancement of finite-difference equations.

TIMET: Current calculation time.

EPSO: Convergence criterion for outer iteration.

EPSI: Convergence criterion for vessel iteration.

EPSS: Convergence criterion for steady-state calculation.

OITMAX: Maximum number of outer iterations.

IITMAX: Maximum number of vessel iterations.

SITMAX: Maximum number of outer iterations for steady-state calculation.

IEOS: Flag to indicate either steam-air-water (0) or air-water (1).

VMAXT: Maximum Courant number.

DAMX: Error caused by relative change in void fraction.

VARER: Variable error.

ICMP: Component indicator.

DTMIN: Minimum allowable time-step size for time interval.

DTMAX: Maximum allowable time-step size for time interval.

ISTDY: Flag to indicate type of calculation (0 = transient; 1 = steady state).

TEND: End of time domain.

IPAK: Flag to indicate water packer option (0 = off; 1 = on).

EPSP: Convergence criteria for PWR-initialization calculation.

ICCMX: Component number in the IORDER array with the most severe time-step limit for stability.

KCCMX: Cell in above component that limits stability.

NITMX: Maximum number of outer iterations taken since the last edit.

NITMN: Minimum number of outer iterations since the last edit.

NITAV: Average number of outer iterations since the last edit.

NSTP: Number of time steps since the last edit.

NCMX: Position in IORDER array for component that was last to converge at step NSMX.

NCMN: Position in IORDER array for component that was last to converge at step NSMN.

NSMN: Last step at which NITMN outer iterations occurred.

NSMX: Last step at which NITMX outer iterations occurred.

VCMX: Final convergence for component NCMX at step NSMX.

VCMN: Final convergence for component NCMN at step NSMN.

NSVSMX: Last time step at which NIVSMX vessel iterations occurred.
 NSVSMN: Last time step at which NIVSMN vessel iterations occurred.
 NIVSMX: Maximum number of vessel iterations required since the last edit.
 NIVSMN: Minimum number of vessel iterations required since the last edit.
 VMOLD: Vessel water mass (liquid + vapor) at (t^n).
 VMNEW: Vessel water mass (liquid + vapor) at (t^{n+1}).
 VMCON: Net water mass (liquid + vapor) convected into vessel during time interval ($t^{n+1} - t^n$).
 DTLMX: Maximum liquid temperature change during time step.
 DTVMX: Maximum vapor temperature change during time step.
 DTSMX: Maximum metal temperature change during time step.
 DTRMX: Maximum rod temperature change during time step.
 DAMMC: Maximum void fraction change during time step.
 NSEO: Time-step number of last completed edit.
 VMAXO: Maximum Courant number found during time step.
 DELTHT: Heat-transfer time-step size.
 ITMIN: Minimum stable film boiling option flag.
 DTO: Previous time-step size.
 DIFMIN: Minimum diffusion number required for stability of the nod conduction solution.
 DPRMX: Maximum pressure change during the current time step.
 ODELT: Time increment for previous time-step.
 IM100: Flag to indicate that back-up occurred on previous time-step (used for mass check on logic).
 ISSFLG: Flag for controlling editing in steady state.
 IACCMD: Variable not currently implemented.

IPAKON: Flag to indicate that water-packer logic is on during time-step.
 ITPAKO: Iteration number for which water-packing was detected.
 NSEND: End the calculation at this step number.
 NSPL: Print if NSPL < NSTEP < NSPU.
 NSPU: Print if NSPL < NSTEP < NSPU.
 IPKMP: 0 = (default) do not do water packing corrections at a pump source.
 1 = do water packing corrections at a pump source.
 IFPREP: Flag indicating sections of preper to be executed (nonzero only for 1-D cores).
 ISTTC: Static check flag.
 0 = normal mode.
 1 = a static balance check has been requested by inputting STDYST = 5.
 HTLOSI Inside system heat loss-1D component only (total system heat loss to the inside walls-1D component only).
 HTLOSO Outside system heat loss-1D components only (total heat loss from the outside of the heat structures to the surroundings-1D component only).

COMMON/CTRLDP/ICTRLD(8),DMPFLG,TDUMP,DMPINT,LTDUMP,LDMPTR,NDMPTR,NSDO

INTEGER DMPFLG

REAL LTDUMP

ICTRLD(8): Array that contains buffering information about the dump output file.
 DMPFLG: Flag that signals whether the dump output file has been initialized (0 = uninitialized; 1 = initialized).
 TDUMP: Calculation time at which next dump is to be taken.
 DMPINT: Dump interval for time domain.
 LTDUMP: CPU time when last dump was taken.
 LDMPTR: Pointer to dump trip data.
 NDMPTR: Number of trips when a dump is to be taken.

NSDO: Time-step number of last completed dump.

COMMON/DEFVAL/ISTOPT,ALP,VL,VV,TL,TV,P,PA,QPPP,TW,HSTN

ISTOPT: Default value input option. Option is off when ISTOPT = 0, or when ISTOPT = 1 or 2.

ALP: Default value for initial void fractions used during input when ISTOPT = 0.

VL: Default value for initial liquid velocities used during input when ISTOPT = 0.

VV: Default value for initial vapor velocities used during input when ISTOPT = 0.

TL: Default value for initial liquid temperatures used during input when ISTOPT = 0.

TV: Default value for initial vapor temperatures used during input when ISTOPT = 0.

P: Default value for initial pressures used during input when ISTOPT = 0.

PA: Default value for initial air pressures used during input when ISTOPT = 0.

QPPP: Default value for volumetric heat sources in Pipe wall used during input when ISTOPT = 0.

TW: Default value for initial wall temperatures used during input when ISTOPT = 0.

HSTN: Default value for initial heat slab temperatures used during input when ISTOPT = 0.

COMMON/DF1DC/IDF1D,ISRB,ISLB,JSTART,IL,ICME,IBKS,SSMC2,SSMC,SSVE,SSVC,
SSMOM,SSE,VJS,DVJP,SSAC,SRHE,SRHVC,SRHEV,R1V,R1L,R2V,R2L,SAVT,
SALT,VVJS,VLJS,DVVJP,DVLJP,SRHAC,MSC,I01,I02,I03,S01,S02,I101,
I102,I103,NTEE,NSTG,FL1,FV1,FL2,FV2,CT,C1A,C2A,ISLBP,ISRBP,IACC2,
CTP,C1AV,C2AV,NC2.

IDF1D: Hydrodynamics trigger.

ISRB: Right-hand boundary switch.

ISLB: Left-hand boundary switch.

JSTART: Cell number at left end of one-dimensional segment.

IL: Loop number index.
 ICME: Component index for referencing IOU array.
 IBKS: Indicator for network solution.
 SSMC2: Momentum source to right-hand cell boundary.
 SSMC: Mass source.
 SSVE: Vapor energy source.
 SSVC: Vapor mass source.
 SSMOM: Momentum source to left-hand cell boundary.
 SSE: Energy source.
 VJS: Source velocity.
 DVJP: Pressure derivative of source velocity.
 SSAC: Air source.
 SRHE: Variable not implemented.
 SRHVC: Variable not implemented.
 SRHEV: Variable not implemented.
 R1V: Coefficient for the vapor momentum source term at the left edge of the tee junction cell.
 R1L: Coefficient for the liquid momentum source term at the left edge of the tee junction cell.
 R2V: Coefficient for the vapor momentum source term at the right edge of the tee junction cell.
 R2L: Coefficient for the liquid momentum source term at the right edge of the tee junction cell.
 SAVT: Source term to vapor for compressible work.
 SALT: Source term to liquid for compressible work.
 VVJS: Variable not implemented.
 VLJS: Variable not implemented.
 DVVJP: Variable not implemented.

DVLJP: Variable not implemented.
 SRHAC: Variable not implemented.
 MSC: Cell number for source terms.
 IO1: ABS(IOU(1,current component)).
 IO2: ABS(IOU(2,current component)).
 IO3: IOU(3,current component)(always positive).
 SO1: Sign of IOU(1,current component).
 SO2: Sign of IOU(2,current component).
 II01: IO1 plus a displacement for the current loop.
 II02: IO2 plus a loop displacement.
 II03: IO3 plus a loop displacement.
 NTEE: Counter for tees.
 NSTG: Counter for steam generators.
 FL1: Temporary storage for liquid mass flow corrections for mass conservation checks at low-numbered cell face.
 FV1: Temporary storage for vapor mass flow corrections for mass conservation checks at low-numbered cell face.
 FL2: Temporary storage for liquid mass flow corrections for mass conservation checks at high-numbered cell face.
 FV2: Temporary storage for vapor mass flow corrections for mass conservation checks at high-numbered cell face.
 CT: Momentum source coefficient.
 C1A: Fraction of liquid velocity at the left face of the tee junction cell contributing to the momentum transfer into the tee side leg.
 C2A: Fraction of liquid velocity at the right face of the tee junction cell contributing to the momentum transfer into the tee side leg.
 ISLBP: Variable not implemented.
 ISRBP: Variable not implemented.

IACC2: Flag for pipe used to model accumulator.
CTP: Momentum source coefficient.
C1AV: Vapor velocity fraction at the left face of the tee junction cell contributing to the momentum transfer into the tee side leg.
C2AV: Vapor velocity fraction at the right face of the tee junction cell contributing to the momentum transfer into the tee side leg.
NC2: Cell number which begins a tee and steam generator tee secondary.

COMMON/DIDDLE/ALPSHL,ALPSHU,ENFAC1,ENFAC2,ENMIN,IAV,IAVA,AFCT,ENCUT,NIFSLB,VWALLW,VWALUP,FMD1,FMD2

ALPSHL: Void below which the interface sharpener is off.
ALPSHU: Void above which the interface sharpener is completely on.
ENFAC1: Scaling factor for minimum entrainment velocity.
ENFAC2: Scaling factor for entrainment correlation exponent.
ENMIN: Variable not implemented.
IAV: Variable not implemented.
IAVA: Variable not implemented.
AFCT: Area scaling for waves on inverted annular interface.
ENCUT: Minimum droplet entrainment fraction.
NIFSLB: If nonzero then slabs should be used to test for inverted annular flow.
VWALLW: Variable not implemented.
VWALUP: Variable not implemented.
FMD1: Factor scaling the gravity void-fraction adjustment. If both are zero, there is no manometer damping.
FMD2: Factor scaling the gravity void-fraction adjustment. If both are zero, there is no manometer damping.

COMMON/DIDDLH/ALP2,ALPCUT,ALP3,PDFHL,IHTCN,NSHTCN,IHTAV,CFWH

ALP2: Void above which vapor is in forced convection.

ALPCUT: Void above which nucleate boiling is not permitted (if other criteria are met).

ALP3: Void above which there is no liquid heat-transfer.

PDFHL: Time averaging factor for heat-transfer.

IHTCN: Variable is normally 0. If set to 1, then heat-transfer coefficients are forced to remain constant.

NSHTCN: Variable is normally 10 000 000. If NSTEP > NSHTCN, then IHTCH is set to 1 (for debugging only).

IHTAV: Variable is normally 1. If IHTAV is 0, then there is no time averaging of heat transfer coefficients.

CFWH: Variable not used.

COMMON/DIMEN/NUMTCR,NCOMP,NJUN,LENTBL,IFREE,LAST,LFREE,LLAST,LENBD,
NTHM,NJNT,NMVSSL,NJNMX,NLOOPS,JNVSSL,NVCON,LVER,NTHM1D,NTHM3D.

NUMTCR: Number of title cards.

NCOMP: Number of components.

NJUN: Number of junctions.

LENTBL: Length of fixed length table.

IFREE: First free word in the dynamic storage area.

LAST: Last word in the dynamic storage area.

LFREE: First free location in LCM.

LLAST: Last location in LCM.

LENBD: Length of boundary data array for each junction.

NTHM: Number of elements per cell in the DRIV array.

NJNT: Total number of network junctions for all loops.

NMVSSL: Number of vessels.

NJNMX: Maximum number of network junctions.

DDVV: Measure of the maximum difference in V_g between the basic and stabilizer steps.

DDVL: Measure of the maximum difference in V_g between the basic and stabilizer steps.

JDARV: Cell where DARV occurred.

IDARV: Component where DARV occurred.

JDARL: Cell where DARL occurred.

IDARL: Component where DARL occurred.

JDDVV: Cell where DDVV occurred.

IDDVV: Component where DDVV occurred.

JDDVL: Cell where DDVL occurred.

IDDVL: Component where DDVL occurred.

IPTEST: Component with maximum $|\delta p/p|$.

JPTEST: Cell with maximum $|\delta p/p|$.

NSDL: If $NSDL \leq NSTEP \leq NSDU$, a detailed diagnostic should be printed to TRCMSC of DARV, etc.

NSDU: If $NSDL \leq NSTEP \leq NSDU$, a detailed diagnostic should be printed TRCMSC of DARV, etc.

TIMDL: If $TIMDL \leq TIMET \leq TIMDU$ details of DARV, etc., should be printed.

TIMDU: If $TIMDL \leq TIMET \leq TIMDU$ details of DARV, etc., should be printed.

ILREIT: Flag to allow reiteration messages when equation set changes.

ICHGA: Flag to print maximum void fraction changes to the message file.

DARA: Maximum change in ap_g .

JDARA: Cell location for DARA.

IDARA: Component location for DARA.

DTVL: Largest decrease in vapor temperature in a given iteration.

JDTVL: Cell location of DTVL.

IDTVL: Component location of DTVL.
 DTVU: Largest increase in T_g for current iteration.
 JDTVU: Cell location for DTVU.
 IDTVU: Component location for DTVU.
 DTLL: Largest decrease in T_g for current iteration.
 JDTLL: Cell location of DTLL.
 IDTLL: Component location of DTLL.
 DTLU: Largest increase in T_g for current iteration.
 JDTLU: Cell location of DTLU.
 IDTLU: Component location of DTLU.
 CTVL: Largest decrease in vapor temperature on a given time step.
 JCTVL: Cell location of CTVL.
 ICTVL: Component location of CTVL.
 CTVU: Largest increase in T_g for current time.
 JCTVU: Cell location for CTVU.
 ICTVU: Component location for CTVU.
 CTLL: Largest decrease in T_g for current time step.
 JCTLL: Cell location for CTLL.
 ICTLL: Component location for CTLL.
 CTLU: Largest increase in T_g for current time step.
 JCTLU: Cell location for CTLU.
 ICTLU: Component location for CTLU.
 DTVLM: DTVLM and DTLLM are limits on DTVL and DTLL beyond which another iteration must be performed.
 DTVUM: DTVLM and DTLLM are limits on DTVL and DTLL beyond which another iteration must be performed.
 DTLLM: DTVLM and DTLLM are limits on DTVL and DTLL beyond which another iteration must be performed.

DTLUM: DTVLM and DTLLM are limits on DTVL and DTLL beyond which another iteration must be performed.

CTVLM: CTVLM and -CTLLM are limits on CTVL-CTLL beyond which the time step is reduced.

CTVUM: CTVLM and CTLLM are limits on CTVL-CTLL beyond which the time step is reduced.

CTLLM: CTVLM and CTLLM are limits on CTVL-CTLL beyond which the time step is reduced.

CTLUM: CTVLM and CTLLM are bounds on CTVL-CTLL beyond which the time step is reduced.

COMMON/ELVKF/IELV,IINL,IKFAC

IELV: Input option switch to allow user to input cell centered elevations for gravity term.

IINL: Index for the two passes through INIT.

IKFAC: Input option switch to allow user to input K factors for additive loss coefficients.

COMDECK,ERRCON

COMMON/ERRCON/DALPC,DALPCA,DARV,DARL,DDVV,DDVL,JDARV,IDARV,JDARL,
 1 IDARL,JDDVV,1DDVV,JDDVL,IDDVL,IPTEST, 'TEST,NSDL,NSDU,TIMDL,TIMDU
 2,ILREIT,ICHGA
 2 ,DARA,JDARA,IDARA,DTVL,JDTVL, IDTVL,DTVU,JDTVU, IDTVU
 3 ,DTLL,JDTLL, IDTLL,DTLU,JDTLU, IDTLU,CTVL,JCTVL, ICTVL
 4 ,CTVU,JCTVU, ICTVU,CTLL,JCTLL, ICTLL,CTLU,JCTLU, ICTLU
 5 ,DTVLM,DTVUM,DTLLM,DTLUM,CTVLM,CTVUM,CTLLM,CTLUM

DALPC: Not used.

DALPCA: Not used.

DARV: Measure of the maximum difference in αg between the basic and stabilizer steps.

DARL: Same as DARV but $(1 - \alpha)\rho g$.

DDVV: Same as DARV but V_g .

DDVL: Same as DARV but V_g .

JDARV: CELL where DARV occurred.

IDARV: Component where DARV occurred.

JDARL: CELL where DARL occurred.
 IDARL: Component where DARL occurred.
 JDDVV: CELL where DDVV occurred.
 IDDVV: Component where DDVV occurred.
 JDDVL: CELL where DDVL occurred.
 IDDVL: Component where DDVL occurred.
 IPTTEST: Component with maximum $|\frac{\delta\rho}{\rho}|$.
 JPTEST: CELL with maximum $|\frac{\delta\rho}{\rho}|$.
 NSDL: If $NSDL \leq NSTEP \leq NSDU$ do a detailed diagnostic print to TRCMMSG of DARV etc.
 NSDU: If $NSDL < NSTEP < NSDU$ do a detailed diagnostic print to TRCMMSG of DARV etc.
 TIMDL: If $TIMDL \leq TIMET \leq TIMDU$ print details of DARV etc.
 TIMDU: If $TIMDL < TIMET < TIMDU$ print details of DARV etc.
 ILREIT: Flag to allow reiteration messages when equation set changes.
 ICHGA: Flag to imprint maximum void fraction changes to the message file.
 DARA: Maximum change in $\alpha\rho_a$.
 JDARA: Cell location for DARA.
 IDARA: Component location for DARA.
 DTVL: Largest decrease in vapor temperature on a given iteration.
 JDTVL: Cell location of DTVL.
 IDTVL: Component location of DTVL.
 DTVU: Largest increase in T_g for current iteration.
 JDTVU: Cell location for DTVU.
 IDTVU: Component location for DTVU.
 DTL: Largest decrease in T_l for current iteration.

JD TLL: Cell location of DTLL.
 ID TLL: Component location of DTLL.
 DT LU: Largest increase in T_g for current iteration.
 JD TLU: Cell location of DTLU.
 ID TLU: Component location of DTLU.
 CT VL: Largest decrease in vapor temperature on a given time step.
 JCT VL: Cell location of CTVL.
 ICT VL: Component location of CTVL.
 CT VU: Largest increase in T_g for current time step.
 JCT VU: Cell location for CTVU.
 ICT VU: Component location for CTVU.
 CT LL: Largest decrease in T_g for current time step.
 JCT LL: Cell location of CTLL.
 ICT LL: Component location of CTLL.
 CT LU: Largest increase in T_g for current time step.
 JCT LU: Cell location of CTLU.
 ICT LU: Component location of CTLU.
 DT VLM:
 DT VUM: DT VLM-DT LLM are bounds on
 DT VL-DT LL beyond which another
 DT LLM: iteration must be taken.
 DT LUM:
 CT VLM: CT VLM-CT LLM are bounds on CT VL-CT LL beyond which the time step
 is reduced.
 CT LLM: Not currently used.
 CT LUM: Not currently used.

COMMON/FIXUM/NTHRMC,NSMEC,NVTC,NVTCP,NOAIR

NTHRMC: Variable that turns off (debugs) basic equation set.

NSMEC: Variable that turns off stabilizer mass and energy equations.
NVTC: Variable that turns off stabilizer motion equations.
NVTCP: Variable not implemented.
NOAIR: Variable that turns off air field calculations.

COMMON/GRAPH/IBUFF,LCMGCT,NCTX,NWTX,KLENTH,KP,LCAT,TEDIT,EDINT,TGRAF,GFINT,
IPKG,ICTRLG(8),NSGO,TSEDIT,SEDINT,LENCAT

IBUFF: Length of graphics buffer.
LCMGCT: Address of graphics catalog in LCM.
NCTX: Number of graphics catalog entries.
NWTX: Number of words written to disk per graphics edit.
KLENTH: Length of the graphics disk file.
KP: Pointer in graphics catalog block.
LCAT: Address of graphics catalog in SCM.
TEDIT: Time of next print edit.
EDINT: Print edit interval for time domain.
TGRAF: Time of next graphics edit.
GFINT: Graphics edit interval for time domain.
IPKG: Graphics file packing density.
ICTRLG(8): Array that contains buffering information about the graphics
output file.
NSGO: Time-step number of last completed graphics edit.
TSEDIT: Time for next short edit.
SEDINT: Interval for short edits.
LENCAT: Number of words of each catalog entry.

COMMON/HOLL/PIPEH,PUMPH,TEEH,VALVEH,BREAKH,FILLH,CTAINH,PRIZRH,STGENH,ACCUMH,
VSSLH,COREH

INTEGER PIPEH,PUMPH,TEEH,VALVEH,BREAKH,FILLH,CTAINH,PRIZRH,STGENH,ACCUMH,VSSLH,CORE

PIPEH: Hollerith representation of word "PIPE."
PUMPH: Hollerith representation of word "PUMP."
TEEH: Hollerith representation of word "TEE."
VALVEH: Hollerith representation of word "VALVE."
BREAKH: Hollerith representation of word "BREAK."
FILLH: Hollerith representation of word "FILL."
CTAINH: Hollerith representation of word "CTAIN."
PRIZRH: Hollerith representation of word "PRIZER."
STGENH: Hollerith representation of word "STGEN."
ACCUMH: Hollerith representation of word "ACCUM."
VSSLH: Hollerith representation of word "VESSEL."
COREH: Hollerith representation of word "CORE."

COMMON/ISTAT/NSTEP,OITNO,IITNO,VERR,VARERM,IIBIG,IIFAIL,IITV,IOTT

INTEGER OITNO

NSTEP: Number of time steps taken.
OITNO: Outer iteration number.
IITNO: Inner iteration number.
VERR: Velocity error at component junction.
VARERM: Maximum variable error.
IIBIG: Maximum number of inner iterations per outer iteration.
IIFAIL: Flag to indicate failure of hydrodynamics to converge.
IITV: Variable passes the vessel inner iteration count.
IOTT: Temporary storage for IITNO.

COMMON/NMFAIL/NFLMX,ITFL1,NFL1,NFL3,IFTP,ICMPF,JCFL,S1,S2,S3,S4

NFLMX: Variable not implemented.

ITFL1: Stores iteration number of last TFID failure.

NFL1: Count of total number of TFID failures in the current time step.

NFL3: Total number of TFID failures in the current time step.

IFTP: Flag to prevent thermo failure messages if a message has come from TFID3 or FF3D.

ICMPF: Variable not implemented.

JCFL: Variable not implemented.

S1: Variable not implemented.

S2: Limit on interfacial heat-transfer coefficient.

S3: Offset on liquid super heat used in interfacial area adjustment.

S4: Variable not implemented.

COMMON/PSE/NPSE,NPSE1,NPSE3,NPICMP,NPSJ,NPSIZ,NPSK,NPSV1

NPSE: Pause in TRANS if NSTEP = NPSE.

NPSE1: Pause in TFIDS if NSTEP = NPSE1. The cell number is NPSJ, and the component number is NPICMP.

NPSE3: Pause in TF3DI if NSTEP = NPSE3. The cell index K is NPSK, and the second level is NPSIZ.

NPICMP: Component number in TFIDS (pause) if NSTEP = NPSE1.

NPSJ: Cell number in TFIDS (pause) if NSTEP = NPSE1.

NPSIZ: Level in TF3DI (pause) if NSTEP = NPSE3.

NPSK: Cell index in TF3DI (pause) if NSTEP = NPSE3.

NPSV1: Pause in TF1DS1 if NSTEP = NPSE1. The cell number is NPSJ, and the component number is NPICMP.

COMMON/PTRS/LTITL, LORDER, LILCMP, LNBR, LCOMPT, LIITNO, LJUN, LJSEQ, LVSI, LBD, LCNL, LIJVS, LJOUT, LNVCL, LLOOPN, LNSIGP, LNSIG, LIVCON, LNJN, LIOU, LVRH, LDVB, LAOU, LIVLJN, LDPVC, LDPVCV, LIDPCV, LMSCT, LMCMSH, LLCON, LDRV, LDRL, LDREV, LDREL, LAOV, LAOL, LOD, LFXD, LENFXD, LVMAT, LVSSC, LVSSIP, NVCELL, NPX, LDRA

LDRV: Variable to rework solution of ARV and VVT (contains right-hand side of linear equations).

LDRL: Variable to rework solution of ARL and VLT (contains right-hand side of linear equations).

LAOV: Variable to rework solution of ARV, AREV, and VVT (contains rework matrix).

LAOL: Variable to rework solution of ARL, AREL, and VLT (contains rework matrix).

LVMAT: Vessel matrix storage for coarse-mesh rebalance or direct inversion.

LVSSC: Right-hand side of equation associated with LVMAT.

LVSSIP: Pivoting information for LVMAT.

NVCELL: Total number of coarse regions when iteration is used on the vessel or total number of cells in all vessels if direct solution is used.

NPX: Number of pointers in the PTRS COMMON block.

(The remaining elements of this common block are pointers to the fixed segment TB dynamic SCM. These are described in Table IX of Sec. VI.B).

COMMON/PWRS/NLOOP, LENLDP, LENLPP, LENSLEP, LLOOP, LVJN, NITPWR, QV, QVS, FLOW, FLOWS, W, W1, W2, TVIS, AREA, PH1, PH2, PVO, TVI, MTD, RHOP1, RHOP2, RS, RP1, RP2, RV1, RV2, DHS, USG, ISGK, DHP1, DHP2, DHV1, DHV2, RELX

REAL MTD

NLOOP: Number of primary coolant loops.

LENLDP: Length of overall loop data area prologue.

LENLPP: Length of loop prologue.

LENSLEP: Length of subloop prologue.

LLOOP: Pointer to beginning of loop data area.

LVJN: Pointer to vessel junction data area within loop data area.

NITPWR: Parameter iteration counter for PWR initialization.

QV: Total energy entering fluid through the vessel.

QVS: Desired total energy entering fluid through the vessel.

FLOW: Total mass flow through the vessel.

FLOWS: Desired total mass flow through the vessel.

W: Mass flow through the loop hot leg.

W1: Mass flow through the first loop pump.

W2: Mass flow through the second loop pump.

TVIS: Desired temperature at vessel inlet.

AREA: Steam-generator heat-transfer area.

PH1: Head for first loop pump.

PH2: Head for second loop pump.

PVO: Pressure at vessel hot-leg junction.

TVI: Current temperature at VESSEL inlet.

MTD: Steam-generator mean temperature difference.

RHOP1: Fluid density at first loop pump source cell.

RHOP2: Fluid density at second loop pump source cell.

RS: Flow resistance of steam generator.

RP1: Flow resistance of first loop pump.

RP2: Flow resistance of second loop pump.

RV1: Flow resistance of vessel as seen by first loop pump.

RV2: Flow resistance of vessel as seen by second loop pump.

DHS: Specific enthalpy differential for steam generator.

USG: Overall heat-transfer coefficient for steam generator.

ISGK: Steam-generator type flag.

DHP1: Specific enthalpy differential for first loop pump.

DHP2: Specific enthalpy differential for second loop pump.
DHV1: Specific enthalpy differential for vessel as seen by first loop pump.
DHV2: Specific enthalpy differential for vessel as seen by second loop pump.
RELX: A relaxation factor for changes in pump speed and steam generator area that are automatically made during the PWR steady-state initialization.

COMMON/JUNCT/JPTR

JPTR: Number of junction-component pairs.

COMMON/LCMSP/ALCM(131071)

ALCM(131071) Dynamic LCM storage area.

COMMON/RESTART/ICTRLR(8),DDATE,DDTIME,DNCOMP,DLNFLT

INTEGER DNCOMP,DLNFLT

ICTRLR(8): Array that contains buffering information about the restart file.

DDATE: Date restart file was created.

DDTIME: Time restart file was created.

DNCOMP: Number of components in the restart file.

DLNFLT: Length of fixed length tables read from restart file.

COMMON/SIGNAL/ISVF(100),CPV(42),DSV(2)

ISVF(100): ISVF(I) is the flag vector for one or more signal variables being defined in the Ith component evaluated by TRAC.

CPV(42): Control Panel Vector for storing the values of signal variable parameter numbers 1 through 6 and 7 through 15 for up to four coolant loops.

DSV(2): Dummy Signal Variable vector for storing the values of signal variable parameter numbers 16 and 17.

COMMON/SSCON/FMAX,LOK,RTWFP,MCELL,FMX,FMXLVZ,MAXFLO,MAXFLN,STIME,NEF,EPS,IPOWR.

REAL MAXFLO,MAXFLN

FMAX(7): Maximum normalized errors.

LOK(7,2): Location of maximum normalized errors.

RTWFP: Ratio of heat-transfer to fluid-dynamics time-step sizes.

MCELL(7): Cell numbers of maximum normalized rates of change for a component.

FMX(7): Maximum normalized rates of change for a component.

FMXLVZ: Maximum normalized rate of change for axial vessel velocities.

MAXFLO: Maximum one-dimensional mass flow at last steady-state convergence test times 10^{-3} .

MAXFLN: Maximum one-dimensional mass flow at this steady-state convergence test.

STIME: Current calculation time for steady state.

NEF: Number of time steps between steady state checks.

EPS: Convergence criterion.

IPOWR: FLAY for turning on power in steady state.

COMMON/TF3DC/KU,KL,ORG,IZ,INSCT,KABSO,KCMSH

KU: Displacement of level (IZ+1) from level (IZ) in A3D array.

KL: Displacement of level (IZ-1) from level (IZ) in A3D array.

ORG: Origin of level (IZ) data A3D array.

IZ: Vessel level number currently being used.

INSCT: Variable used to obtain a displacement into network arrays involving vessel junctions when there is more than one vessel.

KABSO: Storage offset to obtain an absolute cell number when there are multiple vessels.

KCMSH: Offset for coarse-mesh indexing with multiple vessels.

COMMON/TSATCN/C1,C2,C3,A14

C1: Constant in expression for saturation temperature, set in routine THERMO.
C2: Constant in expression for saturation temperature.
C3: Constant in expression for saturation temperature.
A14: Constant in expression for saturation temperature.

COMMON/TWOSTP/CORPOW,NUMCOR,NTSPRN,NPSFE,NPSME

CORPOW: Variable not implemented.
NUMCOR: Variable not implemented.
NTSPRN: Flag for printing extra stabilizer step information to TRCOUT.
NPSFE: Pause in FEMOM if NSTEP = NPSEL. The cell number is NPSJ, and the component number is NPICMP.
NPSME: Pause in STBME if NSTEP = NPSEL. The cell number is NPSJ, and the component number is NPICMP.

COMMON/UNITS/IN,IOUT,ITTY,IGOUT,IDOUI,IRSTRT,IMOUT,IBFADG,IBFADR,IBFADD,IBFLNG,IBFLNR,IBFLND,IODONE,IOERR,IOSKIP,CARD(9),INPROC.

INTEGER CARD(9)

IN: I/O unit number for input data file.
IOUT: I/O unit number for output data file.
ITTY: I/O unit number for terminal output.
IGOUT: I/O unit number for graphics output file.
IDOUI: I/O unit number for dump output file.
IRSTRT: I/O unit number for restart input file.
IMOUT: I/O unit number for warning messages.
IBFADG: Pointer to beginning of graphics LCM buffer.
IBFADR: Pointer to beginning of restart LCM buffer.
IBFADD: Pointer to beginning of dump LCM buffer.
IBFLNG: Length of graphics buffer.

IBFLNR: Length of restart buffer.
IBFLND: Length of dump buffer.
IOERR: Input error flag.
IOSKIP: Flag to turn on and turn off input processing.
IODONE: Flag indicating whether the current input card has been read.
CARD(9): Variable contains the current input card in character format.
INPROC: Flag used during input that indicates whether component data is being processed.

COMMON/VCKDAT/ISKIP, IPRVCK, ITVKMX, DONTOL

ISKIP: Flag to skip re-donor-cell logic in VESSEL component (normally set to 0 for no skip).
IPRVCK: Flag to print information about re-donor-celling in VESSEL (normally set to 0 for no print).
ITVKMX: Maximum iteration count to check for need to re-donor-cell in VESSEL.
DONTOL: Tolerance for density difference requiring re-donor-celling in VESSEL.

COMMON/WEBNUM/WEB, WED, WEDU, CNDFC, DMIN, BMIN

WEB: Bubble Weber number.
WED: Droplet Weber number.
WEDU: Droplet Weber number during core upflow (not implemented).
CNDFC: Condensation rate scaling factor.
DMIN: Minimum allowed drop size.
BMIN: Minimum allowed bubble size.

COMMON/XVAR/SX1, SX2, SX3, SX4, SX5, SX6, SX7, SX8, NX1, NX2, NX3, NX4, NX5

SX1: The SX1-NX5 variables are reserved for code testing purposes.
SX2: The SX1-NX5 variables are reserved for code testing purposes.
SX3: The SX1-NX5 variables are reserved for code testing purposes.

SX4: The SX1-NX5 variables are reserved for code testing purposes.
SX5: The SX1-NX5 variables are reserved for code testing purposes.
SX6: The SX1-NX5 variables are reserved for code testing purposes.
SX7: The SX1-NX5 variables are reserved for code testing purposes.
SX8: The SX1-NX5 variables are reserved for code testing purposes.
NX1: The SX1-NX5 variables are reserved for code testing purposes.
NX2: The SX1-NX5 variables are reserved for code testing purposes.
NX3: The SX1-NX5 variables are reserved for code testing purposes.
NX4: The SX1-NX5 variables are reserved for code testing purposes.
NX5: Variable set to 1 to bypass coarse-mesh rebalance in the VESSEL.

COMMON/XVOL/DAXVL,DAXVU,LDAX,FREV,DGSS,BGSS,DAWL,DAWU,IFVT

DAXVL: Bypass switches on special TFIDS flux logic.
DAXVU: Bypass switches on special TFIDS flux logic.
LDAX: Bypass switches on special TFIDS flux logic.
FREV: Sensitivity level for reiteration on flow reversal.
DGSS: Limits on special void-fraction prediction logic.
BGSS: Limits on special void-fraction prediction logic.
DAWL: Weighting factors in special TFIDS flux logic.
DAWU: Weighting factors in special TFIDS flux logic.
IFVT: Flag for setting velocities passed to TFIDS for special flux logic.

APPENDIX I
COMPONENT DATA TABLES

I. FIXED-LENGTH TABLES

The structure of the fixed-length data tables is shown below and is identical for all the TRAC components. Refer to Sec. VI for a detailed discussion of the TRAC data base.

<u>Position(s)</u>	<u>Parameter</u>	<u>Description</u>
1	NUM	Component number.
2	TYPE	Component type.
3	ID	Component identification.
4	NCELLT	Total number of cells.
5	LENVLT	Length of variable-length table.
6	LENPTR	Length of pointer table.
7	LENARR	Length of array block.
8	LFV	Relative position of old fundamental variables.
9	LFVN	Relative position of new fundamental variables.
10	LENFV	Length of fundamental variables.
11	LTDVO	Relative position of time-dependent variables in variable-length table (old time).
12	LTDVN	Relative position of time-dependent variables in variable-length table (new time).
13	LENTDV	Number of time-dependent variables in the variable-length table.
14	IREST	Component restart indicator.
15	LEXTRA	Length of nonstandard dump for components.
16-18	CTITLE(3)	Component description.
19	LENFV2	Length of fundamental variables for which old time and new time values are the same at the start of the OUTER code block.

<u>Position(s)</u>	<u>Parameter</u>	<u>Description</u>
20-50	FLTDUM(31)	Dummy variable.

II. GENERAL POINTER TABLES

The pointer tables for one-dimensional components (described below) use four general sets of pointers, DUALPT, HYDROPT, INTPT, and HEATPT.

A. DUALPT

These pointers refer to variables whose value is stored at both old and new time values.

<u>Word</u>	<u>Name</u>	<u>Array</u>	<u>Dimension</u>	<u>Description</u>
1	LALP	ALP	NCELLS	Old vapor fractions.
2	LALPD	ALPD	0	Variable not currently implemented.
3	LALV	ALV	NCELLS	Old interfacial surface area.
4	LARA	ARA	NCELLS	Old stabilizer value for $\alpha\rho_a$.
5	LAREL	AREL	NCELLS	Old stabilizer value for $(1 - \alpha)\rho_l e_l$.
6	LAREV	AREV	NCELLS	Old stabilizer value for $\alpha\rho_v e_v$.
7	LARL	ARL	NCELLS	Old stabilizer value for $(1 - \alpha)\rho_l$.
8	LARV	ARV	NCELLS	Old stabilizer value for $\alpha\rho_v$.
9	LBIT	BIT	NCELLS+1	Bit flags from previous time step.
10	LVLTO	VLTO	NCELLS+1	Old stabilizer liquid velocity (\bar{V}_l^n).
11	LVVTO	VVTO	NCELLS+1	Old stabilizer vapor velocity (\bar{V}_g).
12-14	LD(3)		0	Variable not currently implemented.
15	LEA	EA	NCELLS	Old air internal energy.
16	LEL	EL	NCELLS	Old liquid internal energy.

<u>Word(s)</u>	<u>Name</u>	<u>Array</u>	<u>Dimension</u>	<u>Description</u>
17	LEV	EV	NCELLS	Old vapor internal energy.
18	LHILO	HILO	NCELLS	Old HTC between inside wall and liquid.
19	LHIVO	HIVO	NCELLS	Old HTC between inside wall and vapor.
20	LHLV	HLV	NCELLS	Old interfacial HTC.
21	LP	P	NCELLS	Old pressure.
22	LPA	PA	NCELLS	Old air partial pressure.
23	LROA	ROA	NCELLS	Old air densities.
24	LROL	ROL	NCELLS	Old liquid densities.
25	LROV	ROV	NCELLS	Old vapor densities.
26	LTD	TD	0	Variable not currently implemented.
27	LTL	TL	NCELLS	Old liquid temperature.
28	LTV	TV	NCELLS	Old vapor temperature.
29	LCIF	CIF	2(NCELLS+1)	Old interfacial drag coefficients.
30	LVM	VM	NCELLS+1	Initial mixture velocities.
31	LTW	TW	NCELLS*NODES	Old wall temperatures.
32	LVL	VL	NCELLS+1	Old liquid velocities.
33	LVV	VV	NCELLS+1	Old vapor velocities.
34	LALPN	ALPN	NCELLS	New vapor fraction.
35	LALPDN	ALPDN	0	Variable not currently implemented.
36	LALVN	ALVN	NCELLS	New interfacial surface area.
37	LARAN	ARAN	NCELLS	New stabilizer value for $\alpha \rho_a$.
38	LARELN	ARELN	NCELLS	New stabilizer value for $(1 - \alpha) \rho_l e_l$.

<u>Word(s)</u>	<u>Name</u>	<u>Array</u>	<u>Dimension</u>	<u>Description</u>
39	LAREVN	AREVN	NCELLS	New stabilizer value for $\alpha_p e_v$.
40	LARLN	ARLN	NCELLS	New stabilizer value for $(1 - \alpha)p_g$.
41	LARVN	ARVN	NCELLS	New stabilizer value for $\alpha_p v$.
42	LBITN	BITN	NCELLS+1	Bit flags for current time step.
43	LVLT	VLT	NCELLS+1	New stabilizer liquid velocity (\tilde{v}_e^{n+1}).
44	LVVT	VVT	NCELL+1	New stabilizer vapor velocity (\tilde{v}_g^{n+1}).
45-47	LDN(3)	DN	0	Variable not currently implemented.
48	LEAN	EAN	NCELLS	New air internal energy.
49	LELN	ELN	NCELLS	New liquid internal energy.
50	LEVN	EVN	NCELLS	New vapor internal energy.
51	LHIL	HIL	NCELLS	New HTC between inside wall and liquid.
52	LHIV	HIV	NCELLS	New HTC between inside wall and vapor.
53	LHLVN	HLVN	NCELLS	New interfacial HTC.
54	LPN	PN	NCELLS	New pressure.
55	LPAN	PAN	NCELLS	New air partial pressure.
56	LROAN	ROAN	NCELLS	New air density.
57	LROLN	ROLN	NCELLS	New liquid density.
58	LROVN	ROVN	NCELLS	New vapor density.
59	LTDN	TDN	0	Variable not currently implemented.
60	LTLN	TLN	NCELLS	New liquid temperature.
61	LTVN	TVN	NCELLS	New vapor temperature.
62	LCIFN	CIFN	2(NCELLS+1)	New interfacial drag coefficients.

<u>Word(s)</u>	<u>Name</u>	<u>Array</u>	<u>Dimension</u>	<u>Description</u>
63	LVMN	VMN	NCELLS+1	New mixture velocity.
64	LTWN	TWN	NCELLS*NODES	New wall temperatures.
65	LVLN	VLN	NCELLS+1	New liquid velocities.
66	LVVN	VVN	NCELLS+1	New vapor velocities.

B. HYDROPT

These pointers refer to variables associated with the hydrodynamic calculations.

<u>Word(s)</u>	<u>Name</u>	<u>Array</u>	<u>Dimension</u>	<u>Description</u>
1	LB	B	IHYDRO* 30*NCELLS	Variable not currently implemented.
2	LCFZ	CFZ	0	Variable not currently implemented.
3	LCL	CL	NCELLS	Liquid conductivity.
4	LCPL	CPL	NCELLS	Liquid specific heat at constant pressure.
5	LCPV	CPV	NCELLS	Vapor specific heat at constant pressure.
6	LCV	CV	NCELLS	Vapor conductivity.
7	LDRIV	DRIV1	19*(NCELLS+1)	Storage array for thermodynamic derivatives and enthalpies.
8	LDX	DX	NCELLS	Cell length in flow direction.
9	LFA	FA	NCELLS+1	Cell-edge flow area.
10	LFRIC	FRIC	NCELLS+1	Additive friction factors.
11	LGRAV	GRAV1	NCELLS+1	Gravitation terms (cosine theta).
12	LALPO	ALPO	NCELLS	Void fraction from previous step (α^{n-1}).
13	LH(1)	WFHF	NCELLS+1	Weighting factor for stratified flow regime.
14	LH(2)	SI*DX	NCELLS+1	Stratified interfacial area.

<u>Word(s)</u>	<u>Name</u>	<u>Array</u>	<u>Dimension</u>	<u>Description</u>
15	LH(3)	DHLDZ	NCELLS+1	Gravitational head force caused by alpha gradient.
16	LH(4)	--	0	Variable currently not implemented.
17	LHD	HD	NCELLS+1	Hydraulic diameters.
18	LHFG	HFG	NCELLS	Latent heat of vaporization.
19	LQPPP	QPPP	NCELLS	Wall heat source.
20	LRMEM	RMEM	NCELLS	Variable not currently implemented.
21	LRMVM	RMVM	NCELLS+1	Mixture density times mixture velocity.
22	LROM	ROM	NCELLS	Mixture density.
23	LRHS	RHS	NCELLS	Right side for vapor continuity and energy equations.
24	LSIG	SIG	NCELLS	Surface tension.
25	LTRID	TRID	6*(NCELLS+1)	Storage for stabilizer linear system.
26	LTSAT	TSAT	NCELLS	Saturation temperature.
27	LTSSN	TSSN	NCELLS	Saturation temperature for steam pressure.
28	LVISL	VISL	NCELLS	Liquid viscosity.
29	LVISV	VISV	NCELLS	Vapor viscosity.
30	LVOL	VOL	NCELLS	Cell volumes.
31	LVR	VR	NCELLS+1	Relative velocity.
32	LWA	WA	NCELLS	Wall areas.
33	LDFVDP	DFVDP	NCELLS+1	Derivative of vapor velocity with respect to pressure.
34	LDFLDP	DFLDP	NCELLS+1	Derivative of liquid velocity with respect to pressure.
35	LVLX	VLX	0	Variable not currently implemented.
36	LVVX	VVX	0	Variable not currently implemented.
37	LWFL	WFL	NCELLS+1	Wall friction factor for liquid.

<u>Word(s)</u>	<u>Name</u>	<u>Array</u>	<u>Dimension</u>	<u>Description</u>
38	LWFV	WFV	NCELLS+1	Wall friction factor for vapor.
39	LELEV	ELEV	NCELLS*IELV	The pointer for the array containing cell-centered elevations. This is used only if IELV is set to 1 in the namelist input.
40	LFAVOL	FAVOL	NCELLS+1	Cell flow area used in choked flow model.
41	LVVVOL	VVOL	NCELLS+1	Cell vapor velocity used in choked flow model.
42	LVLVOL	VLVOL	NCELLS+1	Cell liquid velocity used in choked flow model.

C. INTPT

These pointers refer to variables with integer values.

<u>Word(s)</u>	<u>Name</u>	<u>Array</u>	<u>Dimension</u>	<u>Description</u>
1	LIDR	IDR	NCELLS	Heat-transfer regime.
2	LMATID	MATID	NODES-1	Material identifications.
3	LNFF	NFF	NCELLS+1	Friction correlation options.

D. HEATPT

These pointers refer to variables associated with the wall heat-transfer calculations.

<u>Word(s)</u>	<u>Name</u>	<u>Array</u>	<u>Dimension</u>	<u>Description</u>
1	LCPW	CPW	(NODES-1) *NCELLS	Specific heat of wall.
2	LCW	CW	(NODES-1) *NCELLS	Wall conductivity.
3	LDR	DR	NODES-1	Radial mesh size.
4	LEMIS	EMIS	NCELLS	Wall emissivity.
5	LHOL	HOL	NCELLS	HTC between outside wall and liquid.
6	LHOV	HOV	NCELLS	HTC between outside wall and vapor.

<u>Word(s)</u>	<u>Name</u>	<u>Array</u>	<u>Dimension</u>	<u>Description</u>
7	LQPPC	QPPC	NCELLS	Critical heat flux.
8	LRN	RN	NODES	Radii at nodes.
9	LRN2	RN2	NODES-1	Radii at node centers.
10	LROW	ROW	(NODES-1) *NCELLS	Wall density.
11	LTOL	TOL	NCELLS	Liquid temperature outside wall.
12	LTOV	TOV	NCELLS	Vapor temperature outside wall.

III. ACCUMULATOR MODULE

A. ACCUM Variable-Length Table

<u>Position(s)</u>	<u>Parameter</u>	<u>Description</u>
1	NODES	Number of heat-transfer nodes (= 0).
2	NCELLS	Number of fluid cells.
3	JUN2	Junction number at discharge from the accumulator.
4	QINT	Initial water volume in accumulator.
5	QOUT	Volume of liquid that has been discharged from the accumulator.
6	TYPE2	Adjacent component type.
7	IGJ	Iteration index of adjacent component.
8	IUV1	Indicator for velocity update at junction 1 (= 0).
9	IUV2	Indicator for velocity update at junction 2.
10	JS2	Junction sequence number at accumulator discharge.
11	Z	Water height above discharge.
12	FLOW	Volume flow rate at discharge.
13	ISTOP	Indicator that accumulator has emptied.
14	BSMASS	Time-integrated mass flow out of component.

<u>Position(s)</u>	<u>Parameter</u>	<u>Description</u>
15-16	FL(2)	Liquid mass flow corrections for mass conservation checks.
17-18	FL(2)	Vapor mass flow corrections for mass conservation checks.
19-175	VLTDUM(157)	Dummy variable.

B. ACCUM Pointer Table

<u>Word(s)</u>	<u>Name</u>	<u>Array</u>	<u>Dimension</u>	<u>Description</u>
1-66	DUALPT	--	--	General pointer table.
67-108	HYDROPT	--	--	General pointer table.
109-111	INTPT	--	--	General pointer table.
112	LBD1	BD1	LENBD	Dummy BD1 array.
113	LQPPL	QPPL	NCELLS	Heat flux from wall to liquid.
114-300	PLTDUM	PLTDUM	187	Dummy variable.

IV. BREAK MODULE

A. BREAK Variable-Length Table

<u>Position(s)</u>	<u>Parameter</u>	<u>Description</u>
1	NODES	Number of heat-transfer nodes (= 0).
2	JUN1	Junction number where break is located.
3	ICJ	Iteration index of adjacent component.
4	TYPE1	Type of component adjacent to break.
5	JS1	Junction sequence number.
6	BXMASS	Current mass flow out of break.
7	BSMASS	Time-integrated flow rate out of break.
8	IBROP	Break table read options.
9	NBTB	Number of pairs for each break table.
10	KPOINT	Pointer to last used interval in the break velocity table.

<u>Position(s)</u>	<u>Parameter</u>	<u>Description</u>
11	ISAT	Break table use option.
12	TIN	Fluid temperature at the BREAK.
13	INEXTI	Implicitness level of adjacent component.
14-175	VLTDUM(162)	Dummy variable.

B. BREAK Pointer Table (For BREAKS, NCELLS = 1)

<u>Word(s)</u>	<u>Name</u>	<u>Array</u>	<u>Dimension</u>	<u>Description</u>
1-66	DUALPT	--	--	General pointer table.
67-108	HYDROPT	--	--	General pointer table.
109	LPTB	PTB	2*NBTB	Pressure table.
110	LTLTB	TLTB	2*NBTB	Liquid temperature table.
111	LTVTB	TVTB	2*NBTB	Vapor temperature table.
112	LALPTB	ALPTB	2*NBTB	Void fraction table.
113	LPATB	PTAB	2*NBTB	Air partial pressure table.
114-300	PTDUM	PTDUM	187	Dummy variable.

V. CORE MODULE

A. Core Variable-Length Table

<u>Position(s)</u>	<u>Parameter</u>	<u>Description</u>
1	NODES	Number of wall heat-transfer nodes.
2	NCELLS	Total number of fluid cells.
3	JUN1	Junction number of junction adjacent to cell 1.
4	JUN2	Junction number of junction adjacent to cell NCELLS.
5	MAT	Material Identification.
6	TYPE1	Type of adjacent component at JUN1.
7	TYPE2	Type of adjacent component at JUN2.

<u>Position(s)</u>	<u>Parameter</u>	<u>Description</u>
8	JS1	Junction sequence number at low-numbered core end.
9	JS2	Junction sequence number at high-numbered core end.
10	ISOLLB	Indicator for velocity update at JUN1.
11	ISOLRB	Indicator for velocity update at JUN2.
12	ICHF	CHF calculation option.
13	IHYDRO	One-dimensional hydrodynamics option.
14	BSMASS	Total fluid mass for core.
15	RADIN	Inner radius of core wall.
16	TH	Thickness of core wall.
17	HOUTL	Heat-transfer coefficient between outer boundary of core wall and liquid.
18	HOUTV	Heat-transfer coefficient between outer boundary of core wall and vapor.
19	TOUTL	Liquid temperature outside core.
20	TOUTV	Vapor temperature outside core.
21	ICJ1	Iteration index of adjcent component at JUN1.
22	ICJ2	Iteration index of adjcent component at JUN2.
23	ICRU	Core upper boundary segment number, Z(ICRU).
24	ICRL	Core lower boundary segment number, Z(ICRL).
25	LNPTRR	Number of pointers of rod data.
26	LENGEN	Length of the general data.
27	LENRD	Length of rod data.
28	LFVG	Relative postion of old time power data.
29	LFVGN	Relative position of new time power data.

<u>Position(s)</u>	<u>Parameter</u>	<u>Description</u>
30	LENFVG	Length of power data stored at both the old and new times.
31	LFVR	Relative position of old time rod data.
32	LFVRN	Relative position of new time rod data.
33	LNFVR	Length of rod data stored at both old and new times.
34	LFVS	Relative position of old time slab data (unused).
35	LFVSN	Relative position of new time slab data (unused).
36	LNFVS	Length of slab data at both old and new times.
37	NCRZ	Number of axial mesh cell.
38	HGAPO	Rod gap-conductance coefficient (MATRD = 3).
39	NFUEL	number of nodes in fuel pellet.
40	NMWRX	Metal-water reaction flag. (0 = no calculation; 1 = calculation.)
41	NINT	Number of interfaces between dissimilar materials in rods.
42	NRODS	Number of computational rods.
43	NSLBS	Number of computational slabs (unused).
44	NDSLBS	Number of slab heat transfer nodes (unused).
45	NDRDS	Number of rod heat transfer nodes.
46	NFCI	Fuel-clad interaction (FCI) flag. (0 = no calculation; 1 = calculation.)
47	NFCIL	Upper limit on number of FCI calculations per time step.
48	PLDR	Pellet dish radius. (PLDR = 0.0, no calculation of pellet dishing).
49	PDRAT	Rod pitch-to-diameter ratio.

<u>Position(s)</u>	<u>Parameter</u>	<u>Description</u>
50	NRFDS	Rod fine-mesh status flag. (0 = coarse-mesh flag; 1 = fine-mesh flag.)
51	NRFD	Reflood flag. (0 = no action; 1 = turn on fine-mesh flag.)
52	NRFDI	Rod fine-mesh flag trip identification.
53	NDGX	Number of delayed neutron groups.
54	NDHX	Number of decay heat group.
55	TNEUT	Neutron generation time.
56	BEFF	Total delayed neutron fraction.
57	ENEFF	Total decay heat fraction.
58	REACT	Total reactivity at the beginning time of the present time step.
59	NPWX	Number of power table entries.
60	IRPOP	Reactor kinetics option flag.
61	IRPTR	Reactor kinetics trip identification number.
62	RPOWR	Old reactor power.
63	RPOWRN	New reactor power.
64	RPOWRI	Initial reactor power.
65	NRAMAX	Cell number of the average-rod peak clad temperature (always 1).
66	TRAMAX	Average-rod peak clad temperature.
67	NRHMAX	Cell number of the supplemental rod peak clad temperature.
68	TRHMAX	Maximum supplemental rod temperature.
69-70	DTNHT(2)	Delta T_{\min} used in reflood calculation.
71-72	DTXHT(2)	Delta T_{\max} used in reflood calculation.
73	DZNHT	Delta Z_{\min} used in reflood calculation.

<u>Position(s)</u>	<u>Parameter</u>	<u>Description</u>
74	NZMAX	Maximum number of rows of heat-transfer nodes used in reflood calculation.
75	QSLTOT	Total slab heat flux.
76	QRDTOT	Total rod heat flux.
77	FUCRAC	Fraction of uncracked fuel.
78	AMH2	Hydrogen mass generated from metal-water reaction.
79-80	FL(2)	The liquid mass flux correction for use in checking mass conservation.
81-82	FV(2)	The vapor mass flux correction for use in checking mass conservation.
83-85	RCFORM(3)	The form number for the reactivity coefficient type.
86-88	RCA(3)	The zeroth order polynomial term coefficient defining the reactivity coefficient.
89-91	RCB(3)	The first order polynomial term coefficient defining the reactivity coefficient.
92-94	RCC(3)	The second order polynomial term coefficient defining the reactivity coefficient.
95-97	XO(3)	The old time value of the independent variable of the second order polynomial defining the reactivity coefficient.
98-100	XN(3)	The new time value of the independent variable of the second order polynomial defining the reactivity coefficient.
101	RMCKO	The reactor multiplication constant at the beginning time of the previous time step.
102	RMCK	The reactor multiplication constant at the beginning time of the present time step.
103	RMCKN	The reactor multiplication constant estimate at the ending time of the present time step.
104	REACTN	The total reactivity estimate at the ending time of the present time step.

<u>Position(s)</u>	<u>Parameter</u>	<u>Description</u>
105	REAC	The reactivity feedback at the beginning of the previous time step.
106	REACE	The reactivity feedback at the beginning of the present time step.
107	REACN	The reactivity feedback estimate at the end of the present time step.
108	STIMET	The problem time at which the last reactivity change was summed to variable storage for late printout(s).
109	SDT	The time interval since the last reactivity change printout(s).
110-121	SRP(12)	The summed programmed reactivity and feedback reactivity changes since the last printout, the last table printout, and the beginning of the problem. (NBTB equals the number of pairs for each break table.)
122	NRTS	The number of time steps the programmed reactivity and reactivity feedback changes are summed over for printout.
123	NPSZ	The number of axial power shape table entries.
124	IPSTR	The axial power shape trip ID number.
125	IPSSV	The signal variable ID number defining the axial power shape table's independent variable.
126	NPSRF	The number of axial power shape rate factor table entries.
127	IRPSV	The signal variable ID number defining the power or reactivity tables independent variable.
128	NRPRF	The number of power or reactivity rate factor table entries.
129	KPOINT	The previous power or reactivity table entry point where the power or reactivity value was linearly interpolated.
130	NPOINT	The previous power or reactivity rate factor table entry point where the rate factor value was linearly interpolated.

<u>Position(s)</u>	<u>Parameter</u>	<u>Description</u>
131	NSET	The previous reflood fine-mesh trip set position status value.
132	NSHP	The previous axial power shape table entry point where the axial power shape was linearly interpolated.
133-300	VLTDUM(43)	Dummy variable.

B. Core Pointer Table

<u>Word(s)</u>	<u>Name</u>	<u>Array</u>	<u>Dimension</u>	<u>Description</u>
1-66	DUALPT			General pointer table.
67-108	HYDROPT			General pointer table.
109-111	INTPT			General pointer table.
112-123	HEATPT			General pointer table.
124	LRDA	RDA	NCELLS	Total rod area.
125	LICRN	ICRN	NCELLS	Core volume number.
126	LRDTL	RDTL	NCELLS	Average rod temperature to liquid.
127	LRDTV	RDTV	NCELLS	Average rod temperature to vapor.
128	LRDHL	RDHL	NCELLS	Average rod HTC (liquid).
129	LRDHV	RDHV	NCELLS	Average rod HTC (vapor).
130	LZ	Z	NCELLS	Axial segment upper elevation.
131	LRDPWR	RDPWR	NDRDS	Rod relative radial power density.
132	LCPOWR	CPOWR	1	Relative rod power density.
133	LRPKF	RPKF	NRODS	Rod power peaking factor.
134	LZPOWR	ZPOWR	NCRZP2 *NPSZ	Relative axial power shape table.
135	LPSRF	PSRF	NRSRF*2	Power shape rate factor table.
136	LNRDX	NRDX	1	Number of rods in volume.
137	LRADRD	RADRD	NDRDS	Rod node radius (cold).
138	LMATRD	MATRD	NDMI	Rod material identification.

<u>Word(s)</u>	<u>Name</u>	<u>Array</u>	<u>Dimension</u>	<u>Description</u>
139	LPWTB	PWTB	NPWX*2	Power or reactivity table.
140	LRPRF	RPRF	NRPRF*2	Power or reactivity rate factor table.
141	LBETA	BETA	NDGX	Delayed group neutron.
142	LLAMDA	LAMDA	NDGX	Delay constant of neutron delayed groups.
143	LLAMDH	LAMDH	NDHX	Delay constant of decay heat groups.
144	LEDH	EDH	NDHX	Energy yield fraction of decay heat groups.
145	LNFAH	NFAH	NCRZ	Rod fine-mesh nodding factor.
146	LFPUO2	FPUO2	1	Fraction of plutonium oxide in mixed oxide fuel fraction.
147	LFTD	FTD	1	Fuel theoretical density.
148	LGMIX	GMIX	7	Mole fraction of gap gas constituents.
149	LGMLG	GMLG	1	Moles of gap gas.
150	LPGAPT	PGAPT	1	Gap total gas pressure.
151	LPLVOL	PLVOL	1	Rod plenum volume.
152	LPSLEN	PSLEN	1	Pellet stack length.
153	LCDG	CDG	NDGX	Old concentration of delayed neutron groups.
154	LCDH	CDH	NDHX	Old concentration of decay heat groups.
155	LCLEN	CLEN	1	Old total cladding length.
156	LCDGN	CDGN	NDGX	New concentration of delayed neutron groups.
157	LCDHN	CDHN	NDHX	New concentration of decay heat groups.
158	LCLENN	CLENN	1-1	New total cladding length.
159	LBURN	BURN	NCRZ+1	Fuel burnup.

<u>Word(s)</u>	<u>Name</u>	<u>Array</u>	<u>Dimension</u>	<u>Description</u>
160	LCND	CND	NDRDS (NCRZ+1)	Rod conductivity.
161	LCPND	CPND	NDRDS (NCRZ+1)	Rod specific heat.
162	LZHT	ZHT	NZMAX	Axial location of heat transfer node.
163	LEMISR	EMISR	NDRDS NCRZ+1	Rod emissivity.
164	LHDR	HDR		Rod bundle hydraulic diameter.
165	LHGAP	HGAP	NCRZ+1	Gap conductance.
166	LHLVR	HLVR	NCRZ	Interfacial HTC.
167	LRDTLR	RDTLR	NCRZ	Average rod wall temperature seen by liquid.
168	LRDTVR	RDTVR	NCRZ	Average rod wall temperature seen by vapor.
169	LHRFL	HRFL	NZMAX	Fine mesh liquid HTC.
170	LHRFV	HRFV	NZMAX	Fine mesh vapor HTC.
171	LHRLI	HRLI	NCRZ+1	Liquid heat transfer coefficient.
172	LHRLV	HRLV	NCRZ+1	Vapor heat transfer coefficient.
173	LIDRGR	IDRGR	NCRZ	Flow regime flag.
174	LIHTF	IHTF	NXMAX	Fine mesh heat transfer regime flag.
175	LPGAP	PGAP	NCRZ+1	Gap local gas pressure.
176	LPINT	PINT	NCRZ+1	Pellet-clad contact pressure.
177	LPLDV	PLDV	NCRZ	Pellet dish volume.
178	LQWRX	QWRX	NCRZ+1	Metal-water reaction heat source.
179	LRND	RND	NDRDS (NCRZ+1)	Rod density.
180	LRPOWF	RPOWF	NDRDS	Rod power density.
181	LTCHFR	TCHFR	NCRZ	Wall temperature at CHF point.

<u>Word(s)</u>	<u>Name</u>	<u>Array</u>	<u>Dimension</u>	<u>Description</u>
182	LTCHFF	TCHFF	NZMAX	Fine-mesh wall temperature at CHF point.
183	LTLEID	TLEID	NZMAX	Leiden frost temperature.
184	LIDHT	IDHT	NZMAX	Heat-transfer cell identifier.
185	LNOHT	NOHT	1	Number of rows of heat-transfer nodes for each rod.
186	LRADR	RADR	NDRDS (NCRZ+1)	Old radial node positions.
187	LDRVDT	DRVDT	NCRZ	Derivative of vapor density with respect to vapor temperature.
188	LDRLDT	DRLDT	NCRZ	Derivative of liquid density with respect to liquid temperature.
189	LRFT	RFT	NDRDS NZMAX	Old fine-mesh rod temperature.
190	LRDHLO	RDHLO	NCRZ	Variable not currently implemented.
191	LRDHVO	RDHVO	NCRZ	Variable not currently implemented.
192	LDRZ	DRZ	NCRZ+1	Old zirconium dioxide reaction depth.
193	LRFTN	RFTN	NDRDS NZMAX	New fine-mesh rod temperatures.
194	LRDHLR	RDHLR	NCRZ	Liquid HTC.
195	LRDHVR	RDHVR	NCRZ	Vapor HTC.
196	LDRZN	DRZN	NCRZ+1	New zirconium dioxide reaction depth.
197	LCNDR	CNDR	NINT* NCRZ+1	Rod heat conductivity at right of interface.
198	LCPDR	CPDR	NINT* (NCRZ+1)	Rod heat capacity at specific heat.
199	LRNDR	RNDR	NINT (NCRZ+1)	Rod density at right of interface.
200-300	PTDUM	PTDUM	101	Dummy variable.

VI. FILL MODULE

A. FILL Variable-Length Table

<u>Position(s)</u>	<u>Parameter</u>	<u>Description</u>
1	NODES	Number of heat-transfer nodes (= 0).
2	JUN1	Junction number where fill is located.
<u>Position(s)</u>	<u>Parameter</u>	<u>Description</u>
3	IGJ	Iteration index of adjacent component.
4	TYPE1	Type of component adjacent to fill.
5	JS1	Junction sequence number at junction 1.
6	FXMASS	Current mass flow rate out of fill.
7	FSMASS	Time-integrated mass flow rate out of fill.
8	IFTY	FILL type.
9	IFTR	FILL trip number.
10	NFTX	Number of FILL table pairs.
11	KPOINT	Pointer to last utilized interval in the FILL velocity table.
12	INEXTI	Implicitness level of adjacent component.
13	FLOWIN	Initial mass flow into or from adjacent component.
14	IFSV	The signal variable ID number that defines the fill table independent variable.
15	NFRF	The number of rate factor table pairs whose rate factor is applied to the fill table independent variable.
16	NPOINT	The rate factor table's previous pair number where interpolation was evaluated.
17	TWTOLD	The fraction of a previous fill fluid dynamic state parameter that is averaged with the fill-table-defined parameter in defining the fill parameter value for this time step ($0.0 \leq \text{TWTOLD} < 1.0$).
18-175	VLTDUM(158)	Dummy variable.

B. FILL Pointer Table (For FILLS, NCELLS = 1)

<u>Word(s)</u>	<u>Name</u>	<u>Array</u>	<u>Dimension</u>	<u>Description</u>
1-66	DUALPT	--	--	General pointer table.
67-108	HYDROPT	--	--	General pointer table.
109	LPTB	PTB	2*NFTX	Pressure table.
110	LTLTB	TLTB	2*NFTX	Liquid temperature table.
111	LTVTB	TVTB	2*NFTX	Vapor temperature table.
112	LALPTB	ALPTB	2*NFTX	Void fraction table.
113	LVMTB	VMTB	2*NFTX	Liquid velocity table.
114	LVVTB	VVTB	2*NFTX	Vapor velocity table.
115	LPATB	PATB	2*NFTX	Air partial pressure table
116	LRFTB	RFTB	2*NFRF	The pointer for the fill-rate-factor table.
117-300	PTDUM	PTDUM	184	Dummy variable.

(NFTX equals number of FILL table pairs.)

VII. PIPE MODULE

A. PIPE Variable-Length Table

<u>Position(s)</u>	<u>Parameter</u>	<u>Description</u>
1	NODES	Number of wall heat-transfer nodes.
2	NCELLS	Number of fluid cells.
3	JUN1	Junction number of low-numbered pipe end.
4	JUN2	Junction number of high-numbered pipe end.
5	MAT	Material identification.
6	RADIN	Inner radius of pipe wall.
7	TH	Thickness of pipe wall.
8	HOUTL	HTC between outer boundary of pipe wall and liquid.

<u>Position(s)</u>	<u>Parameter</u>	<u>Description</u>
9	HOUTV	HTC between outer boundary of pipe wall and vapor.
10	TOUTL	Liquid temperature outside pipe.
11	TOUTV	Vapor temperature outside pipe.
12	ICJ1	Iteration index of adjacent component at junction 1.
13	ICJ2	Iteration index of adjacent component at junction 2.
14	TYPE1	Type of adjacent component at junction 1.
15	TYPE2	Type of adjacent component at junction 2.
16	JS1	Junction sequence number at low-numbered pipe end.
17	JS2	Junction sequence number at high-numbered pipe end.
18	ISOLLB	Indicator for velocity update at junction 1.
19	ISOLRB	Indicator for velocity update at junction 2.
20	ICHF	CHF calculation option.
21	IHYDRO	One-dimensional hydrodynamics option.
22	BSMASS	Time-integrated mass flow out of pipe.
23-24	FL(2)	Liquid mass flow corrections for mass constructive checks.
25-26	FV(2)	Vapor mass flow corrections for mass constructive checks.
27	CPOW	Special pipe power input.
28	KPOINT	Current position in pipe power table.
29	NPOWTB	Length of pipe power table.
30	IACC	Pipe accumulator option switch.
31	QINT	Initial water volume in pipe.
32	QOUT	Volume of liquid that has been discharged from pipe used as accumulator.

<u>Word(s)</u>	<u>Name</u>	<u>Description</u>
33	VFLOW	Volume flow rate at discharge from pipe used as accumulator.
34	Z	Water height above discharge.
35	TDPOW	Time delay for pipe power table.
36-175	VLTDUM(140)	Dummy variable.

B. PIPE Pointer Table

<u>Word(s)</u>	<u>Name</u>	<u>Description</u>
1-66	DUALPT	General pointer table.
67-108	HYDROPT	General pointer table.
109-111	INTPT	General pointer table.
112-123	HEATPT	General pointer table.
124-300	PTDUM(177)	Dummy variable.

VIII. PRESSURIZER MODULE

A. PRIZER Variable-Length Table

<u>Position(s)</u>	<u>Parameter</u>	<u>Description</u>
1	NODES	Number of heat-transfer nodes (= 0).
2	NCELLS	Number of fluid cells.
3	JUN2	Junction number at pressurizer discharge (high-numbered end).
4	QHEAT	Total heater power.
5	PSET	Pressurizer pressure set point for heater-spray control.
6	DPMAX	Differential pressure at which heaters have maximum power.
7	QINT	Initial water volume in pressurizer.
8	ZHTR	Water height for heater cutoff.
9	QOUT	Volume of liquid that has discharged from the pressurizer.

<u>Position(s)</u>	<u>Parameter</u>	<u>Description</u>
10	TYPE2	Adjacent component type.
11	ICJ	Iteration index of adjacent component.
12	IUV1	Indicator for velocity update at junction 1 (= 0).
13	IUV2	Indicator for velocity update at junction 2.
14	JS2	Junction sequence number at pressurizer discharge.
15	Z	Water height above discharge.
16	QIN	Heater power being input to water.
17	FLOW	Volume flow rate at discharge.
18	BXMASS	Current mass flow during steady state.
19	BSMASS	Time-integrated mass flow out of pressurizer.
20	BSMSSP	Current mass flow rate during transient.
21-22	FL(2)	Liquid mass flow corrections for mass conservation checks.
23-24	FV(2)	Vapor mass flow corrections for mass conservation checks.
25	JUN1	Junction number of low-numbered pressurizer end.
26	JS1	Junction sequence number of low-numbered pressurizer end.
27	TYPE1	Type of component.
28	ICT1	The sequence number (position in the IORDER array) of the component next to junction / of the pressurizer. This variable is computed but not used.
29-175	VLTDUM(147)	Dummy variable.

B. PRIZER Pointer Table

<u>Word(s)</u>	<u>Name</u>	<u>Array</u>	<u>Dimension</u>	<u>Description</u>
1-66	DUALPT	--	--	General pointer table.
67-108	HYDROPT	--	--	General pointer table.

<u>Word(s)</u>	<u>Name</u>	<u>Array</u>	<u>Dimension</u>	<u>Description</u>
109-111	INTPT	--	--	General pointer table.
112	LBD1	BD1	LENBD	Dummy BD1 array.
113	LQPPL	QPPL	NCELLS	Heat flux from wall to liquid.
114-300	PTDUM	PTDUM	187	Dummy variable.

IX. PUMP MODULE

A. PUMP Variable-Length Table

<u>Position(s)</u>	<u>Parameter</u>	<u>Description</u>
1	NODES	Number of radial heat-transfer nodes.
2	NCELLS	Number of fluid cells.
3	JUN1	Junction number of low-numbered end of pump.
4	JUN2	Junction number of high-numbered end of pump.
5	IPMPTY	Pump type (1 or 2).
6	IRP	Reverse speed indicator. (1 = reverse allowed; 0 = reverse not allowed.)
7	IPM	Two-phase indicator. (1 = use two-phase curves; 0 = use single-phase curves.)
8	RHEAD	Rated head.
9	RTORK	Rated torque.
10	RFLOW	Rated flow.
11	RRHO	Rated density.
12	EFFMI	Moment of inertia.
13	TFR1	Frictional torque constant 1.
14	TFR2	Frictional torque constant 2.
15	ROMEGA	Rated angular velocity.
16	INDXHM	Index on head degradation multiplier curve.
17	INDXTM	Index on torque degradation multiplier curve.

<u>Position(s)</u>	<u>Parameter</u>	<u>Description</u>
18	NHDM	Number of points on the head degradation multiplier curve.
19	NTDM	Number of points on the torque degradation multiplier curve.
20	ICJ1	Iteration index of adjacent component at junction 1.
21	ICJ2	Iteration index of adjacent component at junction 2.
22	TYPE1	Type of adjacent component at junction 1.
23	TYPE2	Type of adjacent component at junction 2.
24	ISOL1	Indicator for velocity update at junction 1.
25	ISOL2	Indicator for velocity update at junction 2.
26	OMEGA	Angular velocity at old time.
27	OMEGAN	Angular velocity at new time.
28	RHO	Pump mixture density.
29	FLOW	Pump volumetric flow rate.
30	ALPHA	Pump void fraction.
31	HEAD	Pump head.
32	TORQUE	Pump torque.
33	SMOM	Momentum source.
34	DELP	Delta P across pump.
35	MAT	Wall material identification.
36	RADIN	Inner radius of wall.
37	TH	Wall thickness.
38	HOUTL	HTC between outer boundary of pump wall and liquid.
39	HOUTV	HTC between outer boundary of pump wall and vapor.

<u>Position(s)</u>	<u>Parameter</u>	<u>Description</u>
40	TOUTL	Liquid temperature outside wall.
4	TOUTV	Vapor temperature outside wall.
42	JS1	Junction sequence number at low-numbered pump end.
43	JS2	Junction sequence number at high-numbered pump end.
44	ICHF	CHF calculation option.
45	IHYDRO	One-dimensional hydrodynamics option.
46	NDMAX	Size of scratch storage array.
47	MFLOW	Pump mass flow rate.
48	IPMPTR	Pump trip identification.
49	NPMPTX	Number of pump-speed table entries.
50	ISAVE	The pump speed table's previous pair number where interpolation was evaluated.
51	ICOND	Trip condition.
52	OPTION	Pump curve option.
53	BSMASS	Time-integrated mass flow out of pump.
54	DSMOM	Derivative of pump head with velocity.
55-56	FL(2)	Liquid mass flow corrections for mass conservation checks.
57-58	FV(2)	Vapor mass flow corrections for mass conservation checks.
59	ALPHAO	Void fraction used on previous time step for pump head calculation.
60	IPMPSV	The signal variable ID number that defines the pump speed table independent variable.
61	NPMPRF	The number of rate factor table pairs whose rate factor is applied to the pump speed table independent variable.

<u>Position(s)</u>	<u>Parameter</u>	<u>Description</u>
62	NSAVE	The rate factor table's previous pair number where interpolation was evaluated.
63-175	VLTDUM(113)	Dummy variable.

B. PUMP Pointer Table

<u>Word(s)</u>	<u>Name</u>	<u>Array</u>	<u>Dimension</u>	<u>Description</u>
1-66	DUALPT	--	--	General pointer table.
67-108	HYDROPT	--	--	General pointer table.
109-111	INTPT	--	--	General pointer table.
<u>Word(s)</u>	<u>Name</u>	<u>Array</u>	<u>Dimension</u>	<u>Description</u>
112-123	HEATPT	--	--	General pointer table.
124	LSPTBL	SPTBL	NPMTX*2	Pump-speed table.
125	LRFTBL	RFTBL	NPMPRF*2	The pointer variable for the rate factor table which is applied to the pump speed table independent variable.
126	LNDATA	NDAATA	16	Number of sets of points in head and torque curves.
127	LHSP1	HSP1	2*NDAATA(1)	Single-phase head curve 1.
128	LHSP2	HSP2	2*NDAATA(2)	Single-phase head curve 2.
129	LHSP3	HSP3	2*NDAATA(3)	Single-phase head curve 3.
130	LHSP4	HSP4	2*NDAATA(4)	Single-phase head curve 4.
131	LHTP1	HTP1	2*NDAATA(5)	Two-phase head curve 1.
132	LHTP2	HTP2	2*NDAATA(6)	Two-phase head curve 2.
133	LHTP3	HTP3	2*NDAATA(7)	Two-phase head curve 3.
134	LHTP4	HTP4	2*NDAATA(8)	Two-phase head curve 4.
135	LTSP1	TSP1	2*NDAATA(9)	Single-phase torque curve 1.
136	LTSP2	TSP2	2*NDAATA(10)	Single-phase torque curve 2.
137	LTSP3	TSP3	2*NDAATA(11)	Single-phase torque curve 3.

<u>Word(s)</u>	<u>Name</u>	<u>Array</u>	<u>Dimension</u>	<u>Description</u>
138	LTSP4	TSP4	2*NDATA(12)	Single-phase torque curve 4.
139	LTP1	TTP1	2*NDATA(13)	Two-phase torque curve 1.
140	LTP2	TTP2	2*NDATA(14)	Two-phase torque curve 2.
141	LTP3	TTP3	2*NDATA(15)	Two-phase torque curve 3.
142	LTP4	TTP4	2*NDATA(16)	Two-phase torque curve 4.
143	LHDM	HDM	NHDM	Head degradation multiplier curve.
144	LTDM	TDM	NTDM	Torque degradation multiplier curve.
145	LIDXCS	IDXCS	16	Curve set index array.
146	LBD4	BD4	LENBD	Dummy variable.
147-300	PTDUM	PTDUM	154	Dummy variable.

X. STEAM GENERATOR MODULE

A. STGEN Variable-Length Table

<u>Position(s)</u>	<u>Parameter</u>	<u>Description</u>
1	NODES	Number of wall temperature nodes.
2	NCELL1	Number of fluid cells on tube side (primary side).
3	NCELL2	Number of fluid cells on shell side (secondary side).
4	JUN11	Junction number adjacent to cell 1 on primary side.
5	JUN12	Junction number adjacent to cell NCELL1 on primary side.
6	JUN21	Junction number adjacent to cell 1 on secondary side.
7	JUN22	Junction number adjacent to cell NCELL2 on secondary side.
8	MAT	Material identification for tubes.
9	RADIN	Inner radius of a tube wall.

<u>Position(s)</u>	<u>Parameter</u>	<u>Description</u>
10	TH	Tube wall thickness.
11	NFF1	Friction-factor correlation option for primary side.
12	NFF2	Friction-factor correlation option for secondary side.
13	ICJ11	Iteration index of adjacent component at JUN11.
14	ICJ12	Iteration index of adjacent component at JUN12.
15	ICJ21	Iteration index of adjacent component at JUN21.
16	ICJ22	Iteration index of adjacent component at JUN22.
17	TYPE11	Type of adjacent component at JUN11.
18	TYPE12	Type of adjacent component at JUN12.
19	TYPE21	Type of adjacent component at JUN21.
20	TYPE22	Type of adjacent component at JUN22.
21	ISVLB1	Indicator for velocity update at JUN11.
22	ISVRB1	Indicator for velocity update at JUN12.
23	ISVLB2	Indicator for velocity update at JUN21.
24	ISVRB2	Indicator for velocity update at JUN22.
25	KIND	STGEN type. (1 = U-tube; 2 = once through.)
26	JS11	Junction sequence number at primary-side inlet.
27	JS12	Junction sequence number at primary-side discharge.
28	JS21	Junction sequence number at secondary-side inlet.
29	JS22	Junction sequence number at secondary-side discharge.
30	IHYDRO	Type of hydrodynamics. (0 = partially implicit; 1 = fully implicit.)
31	ICHF1	Indicator for CHF calculation on primary side.
32	ICHF2	Indicator for CHF calculation on secondary side.

<u>Position(s)</u>	<u>Parameter</u>	<u>Description</u>
33	BSMSS1	Time-integrated mass flow out of primary side.
34	BSMSS2	Time-integrated mass flow out of secondary side.
35-42	FL(8)	Liquid mass flow corrections for mass conservation checks.
43-50	FV(8)	Vapor mass flow corrections for mass conservation checks.
51	RT1LS	Coefficient for the liquid momentum source term at the left edge of the secondary tee junction cell.
52	RT1VS	Coefficient for the vapor momentum source term at the left edge of the secondary tee junction cell.
53	RT2LS	Coefficient for the liquid momentum source term at the right edge of the secondary tee junction cell.
54	RT2VS	Coefficient for the upper momentum source term at the right edge of the secondary tee junction.
55	CAS	Fraction of liquid velocity at the left face of the secondary tee junction cell.
56	CA1S	Fraction of liquid velocity at the right face of the secondary tee junction cell contributing to the momentum transfer into the secondary tee-side leg.
57	CAVS	Fraction of vapor velocity at the left face of the secondary tee-junction cell contributing to the momentum transfer into the secondary tee-side leg.
58	CA1VS	Fraction of vapor velocity at the right face of the tee-junction cell contributing to the momentum transfer into the secondary tee-side leg.
59	ISLBTS	Variable not currently implemented.
60	ISRBTS	Variable not currently implemented.
61	RT1LP	Coefficient for the liquid momentum source term at the left edge of the primary junction cell.

<u>Position(s)</u>	<u>Parameter</u>	<u>Description</u>
62	RT1VP	Coefficient for the vapor momentum source term at the left edge of the primary tee-junction cell.
63	RT2LP	Coefficient for the liquid momentum source term at the right edge of the primary tee-junction cell.
64	RT2VP	Coefficient for the upper momentum source term at the right edge of the primary tee junction.
65	CAP	Fraction of liquid velocity at the left face of the primary tee-junction cell contributing to the momentum transfer into the tee-side leg.
66	CALP	Fraction of liquid velocity at the right face of the primary tee-junction cell contributing to the momentum transfer into the primary tee-side leg.
67	CAVP	Fraction of vapor velocity at the left face of the primary tee-junction cell contributing to the momentum transfer into the primary tee-side leg.
68	CALVP	Fraction of vapor velocity at the right face of the primary tee-junction cell contributing to the momentum transfer into the primary tee-side leg.
69	ISLBTP	Variable not currently implemented.
70	ISRBTP	Variable not currently implemented.
71	JCELLS	Junction cell index of a secondary tee connection.
72	IHYD3	Hydrodynamics option of secondary tee.
73	NCELL3	Number of cells in secondary tee.
74	JUN3	Junction number of the high-numbered end of a secondary tee.
75	COSTS	Cosine of the angle from the low-numbered segment to the secondary side.
76	NCELLS	Total number of fluid cells. NCELL1 + NCELL2+1.
77	ICJ3	Iteration index of adjacent component at JUN3.

<u>Position(s)</u>	<u>Parameter</u>	<u>Description</u>
78	TYPE3	Type of adjacent component at JUN3.
79	ISOL3	Indicator for velocity update at JUN3.
80	JS3	Junction sequence number at JUN3.
81	JCELLP	Junction cell index of a primary tee connection.
82	IHYD4	Hydrodynamics option of a primary tee.
83	NCELL4	Number of cells in primary tee.
84	JUN4	Junction number of the high-numbered end of a primary tee.
85	COSTP	Cosine of the angle of a primary tee.
86	NCELST	NCELL1 + NCELL2 + NCELL3 + 2.
87	ICJ4	Iteration index of adjacent component at JUN4.
88	TYPE4	Type of adjacent component at JUN4.
89	ISOL4	Indicator for velocity update at JUN4.
90	JS4	Junction sequence number at JUN4.
91-175	VLTDUM(85)	Dummy variable.

B. STGEN Pointer Table (For STGEN, NCELLS = NCELL1 + NCELL2 + NCELL3 + NCELL4 + 3NCELLT = NCELL1 + NCELL2 + 1)

<u>Word(s)</u>	<u>Name</u>	<u>Array</u>	<u>Dimension</u>	<u>Description</u>
1-66	DUALPT	--	--	General pointer table.
67-108	HYDROPT	--	--	General pointer table.
109-111	INTPT	--	--	General pointer table.
112-123	HEATPT	--	--	General pointer table.
124	LHLEFF	HLEFF	NCELL2	Effective wall-to-liquid HTC. (Stored within HIL array.)
125	LHVEFF	HVEFF	NCELL2	Effective wall-to-vapor HTC. (Stored within HIV array.)
126	LTWEFF	TWEFF	NODES*NCELL2	Effective wall temperature. (Stored within TW array.)

<u>Word(s)</u>	<u>Name</u>	<u>Array</u>	<u>Dimension</u>	<u>Description</u>
127	LHLO	HLO	NCELL1	Wall-to-liquid HTC secondary side (SS).
128	LHVO	HVO	NCELL1	Wall-to-liquid HTC (SS).
129	LTLO	TLO	NCELL1	Liquid temperature (SS).
130	LTVO	TVO	NCELL1	Vapor temperature (SS).
131	LQPPL	QPPL	NCELLT	Heat flux from wall to liquid.
132	LQPPV	QPPV	NCELLT	Heat flux from wall to vapor.
133	LBD4	BD4	LENBD	Array for dummy boundary cell between main pipe and side tube for secondary cell.
134	LBD5	BD5	LENBD	Array for dummy boundary cell between main pipe and side tube for primary tee.
135-300	PTDUM	PTDUM	166	Dummy variable.

XI. TEE MODULE

A. TEE Variable-Length Table

<u>Position(s)</u>	<u>Parameter</u>	<u>Description</u>
1	NODES	Number of heat-transfer nodes.
2	NCELLS	NCELL1 + NCELL2 + 1.
3	NCELL1	Number of fluid cells in the primary tube of the tee.
4	NCELL2	Number of fluid cells in the side tube of the tee.
5	JCELL	Index of the junction cell within the primary tube.
6	JUN1	Junction number of the low-numbered end of the primary tube.
7	JUN2	Junction number of the high-numbered end of the primary tube.
8	JUN3	Junction number of the high-numbered end of the secondary tube.

<u>Position(s)</u>	<u>Parameter</u>	<u>Description</u>
9	MATID	Material identification for tee.
10	COST	Cosine of the angle from the low-numbered segment to the secondary tube.
11	RADIN1	Inner radius of the primary tube.
12	RADIN2	Inner radius of the secondary tube.
13	TH1	Wall thickness of the primary tube.
14	TH2	Wall thickness of the secondary tube.
15	HOUTL1	HTC to liquid at the outer boundary of the primary tube wall.
16	HOUTV1	HTC to vapor at the outer boundary of the primary tube wall.
17	HOUTL2	HTC to liquid at the outer boundary of the secondary tube wall.
18	HOUTV2	HTC to vapor at the outer boundary of the secondary tube wall.
19	TOUTL1	Temperature of liquid outside the primary tube wall.
20	TOUTV1	Temperature of vapor outside the primary tube wall.
21	TOUTL2	Temperature of liquid outside the secondary tube wall.
22	TOUTV2	Temperature of vapor outside the secondary tube wall.
23	ICJ1	Iteration index of adjacent component to tee at JUN1.
24	ICJ2	Iteration index of adjacent component to tee at JUN2.
25	ICJ3	Iteration index of adjacent component to tee at JUN3.
26	TYPE1	Type of adjacent component at JUN1.
27	TYPE2	Type of adjacent component at JUN2.
28	TYPE3	Type of adjacent component at JUN3.

<u>Position(s)</u>	<u>Parameter</u>	<u>Description</u>
29	JS1	Junction sequence number at JUN1.
30	JS2	Junction sequence number at JUN2.
31	JS3	Junction sequence number at JUN3.
32	ISOL1	Indicator for velocity update at JUN1.
33	ISOL2	Indicator for velocity update at JUN2.
34	ISOL3	Indicator for velocity update at JUN3.
35	ICHF	CHF calculation option.
36	IHYD1	One-dimensional hydrodynamics option in primary tube.
37	IHYD2	One-dimensional hydrodynamics option in side tube.
38	ITRP	Variable not currently implemented.
39	ALSEP	Phase-separation void fraction.
40	ISEP	Flag for phase-separation option in tee.
41	BSMASS	Time-integrated mass flow out of tee.
42	RTL1	Coefficient for the liquid momentum source term at the left edge of the junction cell.
43	RTL1V	Coefficient for the vapor momentum source term at the left edge of the tee-junction cell.
44	RT2L	Coefficient for the liquid momentum source term at the right edge of the tee-junction cell.
45	RT2V	Coefficient for the upper momentum source term at the right edge of the tee junction.
46	CA	Fraction of liquid velocity at the left face of the tee-junction cell contributing to the momentum transfer into the tee-side leg.
47	CA1	Fraction of liquid velocity at the right face of the tee-junction cell contributing to the momentum transfer into the side leg.
48-51	FL(4)	Liquid mass flow corrections for mass conservation checks.

<u>Position(s)</u>	<u>Parameter</u>	<u>Description</u>
52-55	FV(4)	Vapor mass flow corrections for mass conservation checks.
56	ISLBT	Variable not currently implemented.
57	ISRBT	Variable not currently implemented.
58	CAV	Fraction of vapor velocity at the left face of the tee-junction cell contributing to the momentum transfer into the tee-side leg.
59	CAV	Fraction of vapor velocity at the right face of the tee-junction cell contributing to the momentum transfer into the tee-side leg.
60-175	VLTDUM(116)	Dummy variable.

B. TEE Pointer Table (For TEE, NCELLS = NCELL1 + NCELL2 + 1)

<u>Word(s)</u>	<u>Name</u>	<u>Array</u>	<u>Dimension</u>	<u>Description</u>
1-66	DUALPT	--	--	General pointer table.
67-108	HYDROPT	--	--	General pointer table.
109-111	INTPT	--	--	General pointer table.
112-123	HEATPT	--	--	General pointer table.
124	LBD4	BD4	LENBD	Dummy BD4 array.
125-300	PTDUM	PTDUM	176	Dummy variable.

XII. VALVE MODULE

A. VALVE Variable-Length Table

<u>Position(s)</u>	<u>Parameter</u>	<u>Description</u>
1	NODES	Number of heat-transfer nodes.
2	NCELLS	Number of fluid cells.
3	JUN1	Junction number of low-numbered valve end.
4	JUN2	Junction number of high-numbered valve end.
5	MAT	Material identification.
6	RADIN	Inner radius of pipe wall.

<u>Position(s)</u>	<u>Parameter</u>	<u>Description</u>
7	TH	Thickness of pipe wall.
8	HOUTL	HTC between outer boundary of valve wall and liquid.
9	HOUTV	HTC between outer boundary of valve wall and vapor.
10	TOUTL	Liquid temperature outside valve.
11	TOUTV	Vapor temperature outside valve.
12	ICJ1	Iteration index of adjacent component at JUN1.
13	ICJ2	Iteration index of adjacent component at JUN2.
14	TYPE1	Type of adjacent component at JUN1.
15	TYPE2	Type of adjacent component at JUN2.
16	JS1	Junction sequence number at low-numbered valve end.
17	JS2	Junction sequence number at high-numbered valve end.
18	ISOLLB	Indicator for velocity update at JUN1.
19	ISOLRB	Indicator for velocity update at JUN2.
20	ICHF	CHF calculation option.
21	IHYDRO	Variable not currently implemented.
22	IVTY	Valve type index.
23	IVSV	The signal variable ID number that defines the valve table's independent variable.
24	IVTR	Valve trip identification.
25	IVPS	Valve position.
26	NVOTB	The number of valve table pairs defining the valve table used when NVCTB < 1 or when the trip controlling the valve table is set to ON or ON forward and NVCTB > 1.

<u>Position(s)</u>	<u>Parameter</u>	<u>Description</u>
27	NVCTB	The number of valve table pairs defining the valve table used when the trip controlling the valve table is set to ON reverse.
28	NVRF	The number of rate factor table pairs whose rate factor is applied to the valve table's independent variable.
29	AVLVE	Valve open flow area.
30	HVLVE	Valve open hydraulic diameter.
31	FAVLVE	The fraction of the fully open flow area AVLVE to which the adjustable valve cross section is set.
32	XPOS	Variable flag for valve operation in progress, (0 = no movement, +1 = opening movement, -1 = closing movement)
33	BSMASS	Time-integrated mass flowout of valve.
34-35	FL(2)	Liquid mass flow corrections for mass.
36-37	FV(2)	Vapor mass flow corrections for mass conservation checks.
38	MODE	The indicator for valve movement over the previous time step (-1 = closing, 0 = no movement, 1 = opening).
39	KPTO	The previous pair number in the valve table with NVOTB pairs where interpolation was evaluated.
40	KPTC	The previous pair number in the valve table with NVCTB pairs where interpolation was evaluated.
41	NPT	The rate factor table's previous pair number where interpolation was evaluated.
42-175	VLTDUM(134)	Dummy variable.

B. VALVE Pointer Table

<u>Word(s)</u>	<u>Name</u>	<u>Array</u>	<u>Dimension</u>	<u>Description</u>
1-66	DUALPT	--	--	General pointer table.

<u>Word(s)</u>	<u>Name</u>	<u>Array</u>	<u>Dimension</u>	<u>Description</u>
67-108	HYDROPT	--	--	General pointer table.
109-111	INTPT	--	--	General pointer table.
112-123	HEATPT	--	--	General pointer table.
124	LVL0TB	--	--	The pointer variable for the valve table with NV0TB pairs.
125	LVLCTB	--	--	The pointer variable for the valve table with NVCTB pairs.
126	LVRFTB	--	--	The pointer variable for the rate factor table that is applied to the valve table independent variable.
127-300	PTDUM	PTDUM	173	Dummy variable.

XIII. VESSEL MODULE

A. VESSEL Variable-Length Table

<u>Position(s)</u>	<u>Parameter</u>	<u>Description</u>
1	NODES	Number of rod heat-transfer nodes.
2	NCELLS	Total number of fluid cells.
3	NCLX	Number of fluid cells per level.
4	NASX	Number of axial segments (levels).
5	NRSX	Number of radial segments.
6	NTSX	Number of theta segments.
7	IDCU	Downcomer upper boundary segment number, Z(IDCUC).
8	IDCL	Downcomer lower boundary segment number, Z(IDCL).
9	IDCR	Downcomer radial boundary segment number, RAD(IDCR).
10	ICRU	Core upper boundary segment number, Z(ICRU).
11	ICRL	Core lower boundary segment number, Z(ICRL).

<u>Position(s)</u>	<u>Parameter</u>	<u>Description</u>
12	ICRR	Core outer radial boundary segment number, RAD(ICRR).
13	LNPTRL	Number of level data pointers.
14	LENLD	Length of level data.
15	LFVL	Relative position of old fundamental variables of level data.
16	LFVNL	Relative position of new fundamental variables of level data.
17	LNFVL	Length of fundamental variables of level data.
18	LNPTRR	Number of pointers of rod data.
19	IITOT	Inner iteration counter.
20	LENRD	Length of rod data.
21	LFVR	Relative position of old fundamental variables of rod data.
22	LFVNR	Relative position of new fundamental variables of rod data.
23	LNFVR	Length of fundamental variables of rod length.
24	NCSR	Number of cell sources (connections).
25	INHSMX	Number of interfaces between dissimilar materials in the vessel slabs.
26	NCRXX	Total number of core volumes.
27	NCRX	Maximum number of core volumes per level.
28	NCRZ	Number of core levels.
29	NDM1	NODES - 1.
30	HGAPO	Rod gap-conductance coefficient (MATRD = 3).
31	NFUEL	Number of nodes in fuel pellet.
32	NMWRX	Metal-water reaction flag. (0 = no calculation; 1 = calculation.)
33	NINT	Number of interfaces between dissimilar materials in rods.

<u>Position(s)</u>	<u>Parameter</u>	<u>Description</u>
34	NRODS	Number of computational rods.
35	NFCI	Fuel-clad interaction (FCI) flag. (0 = no calculation; 1 = calculation.)
36	NFCIL	Limit on FCI calculations per time step.
37	PLDR	Pellet dish radius (= 0.0, no calculation of pellet dishing).
38	PDRAT	Rod pitch-to-diameter ratio.
39	NRFDS	Rod fine-mesh status flag. (0 = coarse-mesh flag; 1 = fine-mesh flag.)
40	NRFD	Reflood flag. (0 = no action; 1 = turn on fine-mesh flag if it is off.)
41	NRFDT	Rod fine-mesh flag trip identification.
42	NFFA	Axial friction-factor correlation option.
43	NFFR	Radial friction-factor correlation option.
44	NFFT	Theta friction-factor correlation option.
45	NDGX	Number of delayed neutron groups.
46	NDHX	Number of decay heat groups.
47	TNEUT	Neutron generation time.
48	BEFF	Total delayed neutron fraction.
49	ENEFF	Total decay heat fraction.
50	REACT	Total reactivity.
51	NPWX	Number of absolute power entries.
52	IRPOP	Reactor kinetics option flag.
53	IRPTR	Reactor kinetics trip identification.
54	RPOWR	Old reactor power.
55	RPOWRN	New reactor power.
56	RPOWRI	Initial reactor power.
57	NRAMAX	Location of average-rod peak clad temperature.

<u>Position(s)</u>	<u>Parameter</u>	<u>Description</u>
58	TRAMAX	Average-rod peak clad temperature.
59	VLQMS	Total liquid mass in the VESSEL.
60	VDCLQ	Total liquid mass in the downcomer.
61	VLPLQ	Total liquid mass in the lower plenum.
62	VCORE	Total liquid mass in the core.
63	CIMFR	Core inlet mass flow rate.
64-65	DTNHT(2)	Delta T_{MINs} used in reflood calculation.
66	DZNHT	Delta Z_{MIN} .
67	NZMAX	Maximum number of rows of heat-transfer nodes used in reflood calculation.
68	DCLQVL	Downcomer liquid volume fraction.
69	VOLDC	Downcomer volume.
70	VOLLP	Lower plenum volume.
71	VLPLM	Lower plenum liquid mass.
72	TLP	Lower plenum average temperature.
73	PLP	Lower plenum average pressure.
74	VLPLIQ	Lower plenum liquid volume fraction.
75	IZBK	Switch for backup on water pack.
76	IZNX	Variable used in water pack logic.
77	BSMASS	Integrated fluid flow from vessel at start of time step.
78	QSLTOT	Total slab heat flux.
79	QRDTOT	Total rod heat flux.
80	VSFLOW	Vessel mass flow.
81	DCFLOW	Downcomer mass flow rate.
82	FUCRAC	Fraction of uncracked fuel.

<u>Position(s)</u>	<u>Parameter</u>	<u>Description</u>
83	AMH2	Hydrogen mass generated from metal-water reaction.
84-85	DTXHT(2)	Delta T_{MAXS} used in reflood calculation.
86	VUPLIQ	Upper plenum liquid volume fraction.
87	VOLUP	Upper plenum volume.
88	VUPLM	Upper plenum liquid mass.
89	COMFR	Core outlet mass flow rate.
90	PUP	Upper plenum average pressure.
91	ILCSP	Lower core support plate axial segment number.
92	IUCSP	Upper core support plate axial segment number.
93	IUHP	Upper head plate axial segment number.
94	PCORE	Average core pressure.
95	VLCORE	Core liquid mass.
96	CORELQ	Core liquid volume fraction.
97	CIMFRL	Core inlet liquid mass flow rate (MFR).
98	CIMFRV	Core liquid volume fraction.
99	COMFRL	Core outlet liquid MFR.
100	COMFRV	Core outlet vapor pressure MFR.
101	TUP	Upper plenum average liquid temperature.
102	PDC	Downcomer average pressure.
103	TDC	Downcomer average liquid temperature.
104	TSDC	Downcomer average saturation temperature.
105	TSLP	Lower plenum average saturation temperature.
106	TSUP	Upper plenum average liquid temperature.
107	TCORE	Average core temperature.
108	TSCORE	Average core saturation temperature.

<u>Position(s)</u>	<u>Parameter</u>	<u>Description</u>
109	NRHMAX	Location of supplemental rod peak clad temperature.
110	TRHMAX	Maximum supplemental rod temperature.
111	IZBK2	Switch for re-donor cell logic.
112	BSMSSN	Integrated fluid flow from vessel at end of time step.
113	NVENT	Number of cells with vent valves in outer radial surface.
114-116	RCFORM(3)	The form number for the reactivity coefficient type.
117-119	RCA(3)	The zeroth order polynomial term coefficient defining the reactivity coefficient.
120-122	RCB(3)	The first order polynomial term coefficient defining the reactivity coefficient.
123-125	RCC(3)	The second order polynomial term coefficient defining the reactivity coefficient.
126-128	XO(3)	The old time value of the independent variable of the second order polynomial defining the reactivity coefficient.
129-131	XN(3)	The new time value of the independent variable of the second order polynomial defining the reactivity coefficient.
132	RMCKO	The reactor multiplication constant at the beginning of the previous time step.
133	RMCK	The reaction multiplication constant at the beginning time of the present time step.
134	RMCKN	The reactor multiplication constant estimate at the ending time of the present time step.
135	REACTN	The total reactivity estimate at the ending time of the present time step.
136	REAC	The reactivity feedback at the beginning of the previous time step.
137	REACE	The reactivity feedback at the beginning of the present time step.

<u>Position(s)</u>	<u>Parameter</u>	<u>Description</u>
138	REACN	The reactivity feedback estimate at the end of the present time step.
139	STIMET	The problem time at which the last reactivity change was summed to variable storage for later printout(s).
140	SDT	The time interval since the last reactivity change printout(s).
141-152	SRP(12)	The summer programmed reactivity and feedback reactivity changes since the last printout, the last table printout, and the beginning of the problem.
153	NRTS	The number of time steps the programmed reactivity and reactivity feedback changes are summed over for printout.
154	NODHS	Number of nodes in the heat slab.
155	NPSZ	The number of axial power shapes in the axial power shape table.
156	IPSTR	The axial power shape trip ID number.
157	IPSSV	The signal variable ID number that defines the axial power shape table independent variable.
158	NPSRF	The number of rate factor table pairs whose rate factor is applied to the axial power shape table independent variable.
159	IRPSV	The signal variable ID number that defines the power or reactivity table independent variable.
160	NRPRF	The number of rate factor table pairs whose rate factor is applied to the power or reactivity table independent variable.
161	KPOINT	The power or reactivity table's previous pair number where interpolation was evaluated.
162	NPOINT	The rate factor table's previous pair number where the rate factor applied to the power or reactivity table independent variable was interpolated.

<u>Position(s)</u>	<u>Parameter</u>	<u>Description</u>
163	NSET	The absolute value of the reflood fine axial mesh trip set status number during the previous time step.
164	NSHP	The rate factor table's previous pair number where the rate factor applied to the axial-power-shape-table independent variable was interpolated.
165	SHELV	Added to the input vessel Z coordinates to get elevations for computing GRAV in one dimension.
166	TCOLMF	Integrated core outlet liquid mass flow (kg).
167	TCOVMF	Integrated core outlet vapor mass flow (kg).
168	TCILMF	Integrated core inlet liquid mass flow (kg).
169	TCIVMF	Integrated core inlet vapor mass flow (kg).
170-175	VLTDUM(6)	Dummy variable.

B. VESSEL Pointer Table

<u>Word(s)</u>	<u>Name</u>	<u>Array</u>	<u>Dimension</u>	<u>Description</u>
1	LZ	Z	NASX	Axial segment upper elevation.
2	LDZ	DZ	NASX	Axial segment lengths (delta Z).
3	LRAD	RAD	NRSX	Radial segment outer radii.
4	LDR	DR	NRSX	Radial segment lengths (delta R).
5	LTH	TH	NTSX	Theta segment angle.
6	LDTH	DTH	NTSX	Theta segment length (delta theta).
7	LISRL	ISRL	NCSR	Level number associated with source.
8	LISRC	ISRC	NCSR	Relative cell number associated with source.
9	LISRF	ISRF	NCSR	Face number associated with source.
10	LJUNS	JUNS	NCSR	Junction number associated with source.

<u>Word(s)</u>	<u>Name</u>	<u>Array</u>	<u>Dimension</u>	<u>Description</u>
11	LJSN	JSN	NCSR	Junction sequence number associated with source.
12	LIGJ	IGJ	NCSR	Adjacent component associated with source.
13	LMSC	MSC	NCSR	Absolute cell number of source.
14	LNSRL	NSRL	NASX	Number of sources on level.
15	LISOLB	ISOLB	NCSR	Indicator for velocity update.
16	LIZREP	IZREP	NASX	Indicator for levels to be re-donor celled.
17	LSVC	SVC	NCSR*2	Vapor continuity source.
18	LSAC	SAC	NCSR*2	Air continuity source.
19	LSLC	SLC	NCSR*2	Liquid continuity source.
20	LSVE	SVE	NCSR*2	Vapor energy source.
21	LSLE	SLE	NCSR*2	Liquid energy source.
22	LDVVDP	DVVDP	NCSR	Derivative of vapor source velocity for pressure.
23	LDVLDP	DVLDP	NCSR	Derivative of liquid source velocity for pressure.
24	LSMOMV	SMOMV	NCSR*6	Vapor momentum source.
25	LSMOML	SMOML	NCSR*6	Liquid momentum source.
26	LVELSV	VELSV	NCSR	Vapor source velocity.
27	LVELSL	VELSL	NCSR	Liquid source velocity.
28	LPSOLD	PSOLD	NCSR	Old source pressure.
29	LPSNEW	PSNEW	NCSR	New source pressure.
30	LRDPWR	RDPWR	NODES	Rod relative radial power density.
31	LCPOWR	CPOWR	NCRX	Relative power per rod.
32	LZPOWR	ZPOWR	NCRZ+1	Relative axial power density.
33	LNRDX	NRDX	NCRX	Number of rods in volume.

<u>Word(s)</u>	<u>Name</u>	<u>Array</u>	<u>Dimension</u>	<u>Description</u>
34	LRPKF	RPKF	NRODS	Rod power peaking factor.
35	LIDROD	IDROD	NRODS	Cell identifier for rods.
36	LRADRD	RADRD	NODES	Rod node radius (cold).
37	LMATRD	MATRD	NODES-1	Rod material identification.
38	LNFAK	NFAK	NCRZ	Rod fine-mesh noding factor.
39	LBETA	BETA	NDGX	Delayed group neutron fraction.
40	LLAMDA	LAMDA	NDGX	Decay constant of delayed groups.
41	LLAMDH	LAMDH	NDHX	Decay constant of decay heat groups.
42	LEDH	EDH	NDHX	Energy yield fraction of decay heat groups.
43	LPWTB	PWTB	NPWX*2	Power table.
44	LFPUO2	FPUO2	NCRX	Fraction of plutonium oxide in mixed oxide fuel fraction.
45	LFTD	FTD	NCRX	Fuel density (fraction of theoretical).
46	LGMIK	GMIK	NCRX*7	Mole fraction of gap gas constituents.
47	GMLES	GLES	NCRX	Moles of gap gas.
48	LPGAPT	PGAPT	NCRX	Gap total gas pressure.
49	LPLVOL	PLVOL	NCRX	Rod plenum volume.
50	LPSLEN	PSLEN	NCRX	Pellet stack length.
51	LCDG	CDG	NDGX	Old concentration of delayed neutron groups.
52	LCDH	CDH	NDHX	Old concentration of decay heat groups.
53	LCLEN	CLEN	NCRX	Old total cladding length.
54	LCDGN	CDGN	NDGX	New concentration of delayed neutron groups.

<u>Word(s)</u>	<u>Name</u>	<u>Array</u>	<u>Dimension</u>	<u>Description</u>
55	LCDHN	CDHN	NDHX	New concentration of decay heat groups.
56	LPSRF	PSRF	NPSZ* (NCRZ12)	The pointer variable for the rate factor table that is applied to the axial power shape table independent variable.
57	LRPRF	RPRF	NPSRF*2	The pointer variable for the rate factor table that is applied to the power or reactivity table independent variable.
58	LCLENN	CLENN	NCRX	New total cladding length.
59	LAVENT	AVENT	NTSX	Pointer for vent valve AEARS.
60	LDPCVN	DPCVN	NVENT	Pointer for vent valve maximum DP to be closed.
61	LDPOVN	DPOVN	NVENT	Pointer for vent valve minimum DP to be open.
62	LFRCVN	FRCVN	NVENT	Pointer for vent valve FRIC value when closed.
63	LFROVN	FROVN	NVENT	Pointer for vent valve FRIC value when open.
64	LLOCVN	LOCVN	NVENT	Pointer for vent valve location.

--Items below are repeated for each level--

65	LDRIV	DRIV	NCLX*27	Storage array for thermodynamic derivatives, enthalpies, and temporary storage for matrix inversions.
66	LISRN	ISRN	NCSR	Source numbers on level.
67	LDROP	DROP	NCLX*4	Droplet field storage area.
68	LGCOND	GCOND	NCLX	Vapor condensation rate.
69	LGEVAP	GEVAP	NCLX	Liquid evaporation rate.
70	LSIG	SIG	NCLX	Surface tension.
71	LICMSH	ICMSH	NCLX	Index to associated coarse-mesh region.

<u>Word(s)</u>	<u>Name</u>	<u>Array</u>	<u>Dimension</u>	<u>Description</u>
72	LICRN	ICRN	NCLX	Core volume number.
73	LTCHF	TCHF	NCRX	Rod critical temperature.
74	LIDRG	IDRG	NCRX	Flow-regime flag.
75	LRDHL	RDHL	NCRX	Average-rod HTC (liquid).
76	LRDHV	RDAV	NCRX	Average-rod HTC (vapor).
77	LRDA	RDA	NCRX	Total rod area.
78	LIHSN	IHSN	NCLX	Heat-slab number.
79	LHSA	HSA	NCLX	Heat-slab area.
80	LHSX	HSX	NCLX*NODHS	Spacing of heat transfer nodes in the slabs.
81	LTCHFS	TCHFS	NCLX	Slab critical temperature.
82	LIDRGS	IDRGS	NCLX	Slab heat-transfer regime flag.
83	LHSHL	HSHL	NCLX	Slab HTC (liquid).
84	LHSHV	HSHV	NCLX	Slab HTC (vapor).
85	LARV	ARV	NCLX	Product of void fraction and vapor density.
86	LRMEM	RMEM	NCLX	Mixture internal energy.
87	LROM	ROM	NCLX	Mixture density.
88	LVM	VM	NCLX*3	Mixture velocity.
89	LVLC	VLC	NCLX	Liquid cross-flow velocity.
90	LVVC	VVC	NCLX	Vapor cross-flow velocity.
91	LQRD	QRD	NCLX	Rod heat flux.
92	LQSL	QSL	NCLX	Slab heat flux.
93	LCFZL	CFZL	NCLX*3	Total friction factors (liquid).
94	LCFZV	CFZV	NCLX*3	Total friction factors (vapor).
95	LFRICL	FRICL	NCLX*3	Friction multipliers (liquid).
96	LFRICV	FRICV	NCLX*3	Friction multipliers (vapor).

<u>Word(s)</u>	<u>Name</u>	<u>Array</u>	<u>Dimension</u>	<u>Description</u>
97	LDVV	DVV	NCLX*3	Derivative used in momentum update (liquid).
98	LDLL	DLL	NCLX*3	Derivative used in momentum update (vapor).
99	LVOL	VOL	NCLX	Cell fluid volumes.
101	LVOLG	VOLG	NCLX	Cell geometric volumes.
102	LFA	FA	NCLX*3	Cell-edge fluid areas.
103	LFAG	FAG	NCLX*3	Cell-edge geometric areas.
104	LGRAV	GRAV	NCLX	Gravitation terms.
105	LMFRL	MFRL	NCLX	Liquid mass flow.
106	LMFRV	MFRV	NCLX	Vapor mass flow.
107	LHD	HD	NCLX*3	Hydraulic diameters.
108	LCPL	CPL	NCLX	Liquid specific heat at constant pressure.
109	LCPV	CPV	NCLX	Vapor specific heat at constant pressure.
110	LTSAT	TSAT	NCLX	Saturation temperature.
111	LTSSN	TSSN	NCLX	Saturation temperature corresponding to steam partial pressure.
112	LCL	CL	NCLX	Liquid conductivity.
113	LCV	CV	NCLX	Vapor conductivity.
114	LVISL	VISL	NCLX	Liquid viscosity.
115	LVISV	VISV	NCLX	Vapor viscosity.
116	LHFG	HFG	NCLX	Latent heat of vaporization.
117	LRDTL	RDTL	NCRX	Average-rod temperature to liquid.
118	LRDTV	RDTV	NCRX	Average-rod temperature to vapor.
119	LHLV	HLV	NCLX	Old interfacial HTC.

<u>Word(s)</u>	<u>Name</u>	<u>Array</u>	<u>Dimension</u>	<u>Description</u>
120	LALV	ALV	NCLX	Old interfacial area.
121	LFRICI	FRICI	NCLX*3	Old interfacial friction factors.
122	LALD	ALD	NCLX	Old droplet fraction.
123	LAND	AND	NCLX	Reserved for a droplet field.
124	LPA	PA	NCLX	Old air partial pressure.
125	LROA	ROA	NCLX	Old air density.
126	LEA	EA	NCLX	Old air energy.
127	LVD	VD	NCLX*3	Storage currently not implemented.
128	LHST	HST	NCLX	Old heat-slab temperatures.
129	LROHS	ROHS	NCLX*NODHS	SLAB densities.
130	LCPHS	CPHS	NCLX*NDHS	SLAB specific heats.
131	LCNHS	CNHS	NCLX*NODHS	SLAB conductivities.
132	LEMHS	EMHS	NCLX*NODHS	SLAB enmissivities.
133	LMATHS	MATHS	NCLX*NHSM1	SLAB material ID numbers.
134	LALP	ALP	NCLX	Old vapor fraction.
134	LHSHLO	HSHLO	NCLX	Variable not currently implemented.
135	LHSHVO	HSHVO	NCLX	Variable not currently implemented.
136	LBIT	BIT	NCLX	Bit flag.
137	LROV	ROV	NCLX	Old vapor density.
138	LROL	ROL	NCLX	Old liquid density.
139	LVV	VV	NCLX*3	Old vapor velocity.
140	LVL	VL	NCLX*3	Old liquid velocity.
141	LEV	EV	NCLX	Old vapor internal energy.
142	LEL	EL	NCLX	Old liquid internal energy.

<u>Word(s)</u>	<u>Name</u>	<u>Array</u>	<u>Dimension</u>	<u>Description</u>
143	LTV	TV	NCLX	Old vapor temperature.
144	LTL	TL	NCLX	Old liquid temperature.
145	LP	P	NCLX	Old pressure.
146	LHLVN	HLVN	NCLX	New interfacial HTC.
147	LALVN	ALVN	NCLX	New interfacial area.
148	LFRGIN	FRCIN	NCLX*3	New interfacial friction factors.
149	LALDN	ALDN	NCLX	New droplet fraction.
150	LANDN	ANDN	NCLX	Reserved for a droplet field.
151	LPAN	PAN	NCLX	New air partial pressure.
152	LROAN	ROAN	NCLX	New air density.
153	LEAN	EAN	NCLX	New air energy.
154	LVDN	VDN	NCLX*3	Variable not currently implemented.
155	LHSTN	HSTN	NCLX	New heat-slab temperatures.
156	LALPN	ALPN	NCLX	New vapor fraction.
157	LBITN	BITN	NCLX	Bit flag.
158	LROVN	ROVN	NCLX	New vapor density.
159	LROLN	ROLN	NCLX	New liquid density.
160	LVVN	VVN	NCLX*3	New vapor velocity.
161	LVLN	VLN	NCLX*3	New liquid velocity.
162	LEVN	EVN	NCLX	New vapor internal energy.
163	LELN	ELN	NCLX	New liquid internal energy.
164	LTVN	TVN	NCLX	New vapor temperature.

--Items Below are Repeated for Each Rod--

165	LTLN	TLN	NCLX	New liquid temperature.
166	LPN	PN	NCLX	New pressure.

<u>Word(s)</u>	<u>Name</u>	<u>Array</u>	<u>Dimension</u>	<u>Description</u>
167	LROHSN	ROHSN	INHSMX*NCLX	Slab density at a material interface.
168	LCPHSN	CPHSN	INHSMX*NCLX	Slab specific heat at a material interface.
169	LCNHSN	CNHSN	INHSMX*NCLX	Slab conductivities at a material interface.
170	LALPR	ALPR	NCRZ+2	Vapor fraction.
171	LALVR	ALVR	NCRZ+2	Interfacial area.
172	LBURN	BURN	NCRZ+1	Fuel burnup.
173	LCLR	CLR	NCRZ+2	Liquid conductivity.
174	LCND	CND	NODES* (NCRZ+1)	Rod conductivity.
175	LCNDR	CNDR	NINT* (NCRZ+1)	Rod heat conductivity at right of interface.
176	LCPLR	CPLR	NCRZ+2	Liquid specific heat.
177	LCPND	CPND	NODES* (NCRZ+1)	Rod specific heat.
178	LCPDR	CPDR	NINT* (NCRZ+1)	Rod heat capacity at specific heat.
179	LCPVR	CPVR	NCRZ+2	Vapor specific heat.
180	LCVR	CVR	NCRZ+2	Vapor conductivity.
181	LZHT	ZHT	NZMAX	Axial location of heat-transfer node.
182	LEMIS	EMIS	NODES* (NCRZ+1)	Rod emissivity.
183	LHDR	HDR	NCRZ+2	Rod-bundle hydraulic diameter.
184	LHFGR	HFGR	NCRZ+2	Latent heat of vaporization.
185	LHGAP	HGAP	NCRZ+1	Gap conductance.
186	LHLVR	HLVR	NCRZ+2	Interfacial HTC.
187	LRDHLR	RDHLR	NCRZ	Liquid HTC.

<u>Word(s)</u>	<u>Name</u>	<u>Array</u>	<u>Dimension</u>	<u>Description</u>
188	LRDHVR	RDHVR	NCRZ	Vapor HTC.
189	LHRFL	HRFL	NZMAX	Fine-mesh liquid HTC.
190	LHRFV	HRFV	NZMAX	Fine-mesh vapor HTC .
191	LHRLI	HRLI	NCRZ+1	Liquid heat-transfer coefficient.
192	LHRLV	HRLV	NCRZ+1	Vapor heat-transfer coefficient.
193	LIDRGR	IDRGR	NCRZ+2	Flow-regime flag.
194	LIHTF	IHTF	NZMAX	Fine-mesh heat-transfer regime flag.
195	LPR	PR	NCRZ+2	Coolant pressure.
196	LPGAP	PGAP	NCRZ+1	Gap local gas pressure.
197	LPINT	PINT	NCRZ+1	Pellet-clad contact pressure.
198	LPLDV	PLDV	NCRZ+1	Pellet dish volume.
199	LQWRX	QWRX	NCRZ	Metal-water reaction heat source.
200	LRDTLR	RDTLR	NCRZ	Average-rod wall temperature seen by liquid.
201	LRDTVR	RDTVR	NCRZ	Average-rod wall temperature seen by vapor.
202	LRND	RND	NODES* (NCRZ+1)	Rod density.
203	LRNDR	RNDR	NINT (NCRZ+1)	Rod density at right of interface.
204	LROLR	ROLR	NCRZ+2	Liquid density.
205	LROVR	ROVR	NCRZ+2	Vapor density.
206	LROMR	ROMR	NCRZ+2	Mixture density.
207	LRPOWF	RPOWF	NODES* (NCRZ+1)	Rod power density.
208	LSIGR	SIGR	NCRZ+2	Surface tension.
209	LTCHFR	TCHFR	NCRZ	Wall temperature at CHF point.

<u>Word(s)</u>	<u>Name</u>	<u>Array</u>	<u>Dimension</u>	<u>Description</u>
210	LTCHFF	TCHFF	NZMAX	Fine-mesh wall temperature at CHF point.
211	LTLEID	TLEID	NZMAX	Leidenfrost temperature.
212	LTLR	TLR	NCRZ+2	Liquid temperature.
213	LTSATR	TSATR	NCRZ+2	Saturation temperature.
214	LTVR	TVR	NCRZ+2	Vapor temperature.
215	LVISLR	VISLR	NCRZ+2	Liquid viscosity.
216	LVISVR	VISVR	NCRZ+2	Vapor viscosity.
217	LVLCR	VLCR	NCRZ+2	Liquid cross-flow velocity.
218	LVLZR	VLSR	NCRZ+2	Axial liquid velocity.
219	LVVCR	VVCR	NCRZ+2	Vapor cross-flow velocity.
220	LVVZR	VVZR	NCRZ+2	Axial vapor velocity.
221	LVMZR	VMZR	NCRZ+2	Axial mixture velocity.
222	LIDHT	IDHT	NZMAX	Heat-transfer cell identifier.
223	LNOHT	NOHT	1	Number of rows of heat-transfer nodes for each rod.
224	LDRZ	DRZ	NCRZ+1	Old zirconium dioxide reaction depth.
225	LBITR	BITR	0	Variable not currently implemented.
226	LRADR	RADR	NODES* (NCRZ+1)	Old radial node positions.
227	LRFT	RFT	NODES*NZMAX	Old fine-mesh rod temperatures.
228	LDRZN	DRZN	NCRZ+1	New zirconium dioxide reaction depth.
229	LBITRN	BITRN	0	Variable not currently implemented.
230	LRADRN	RADRN	NODES* (NCRZ+1)	New radial node positions.
231	LRFTN	RFTN	NODES*NZMAX	New fine-mesh rod temperatures.

<u>Word(s)</u>	<u>Name</u>	<u>Array</u>	<u>Dimension</u>	<u>Description</u>
232	LRDHLO	RDHLO	NCRZ	Variable not currently implemented.
233	LRDHVO	RDHVO	NCRZ	Variable not currently implemented.
234	LELR	ELR	NCRZ+2	Old liquid internal energy.
235	LEVR	EVR	NCRZ+2	Old vapor internal energy.
236	LDRVDT	DRVDT	NCRZ+2	Derivative of vapor density for vapor temperature.
237	LDRLDT	DRLDT	NCRZ+2	Derivative of liquid density for liquid temperature.
238	LVOLR	VOLR	NCRZ+2	The pointer variable for the fluid volume in axial mesh cells associated with the fuel rod.
239-300	PTDUM	PTDUM	62	Dummy variable.

AUTHORS AND ACKNOWLEDGMENTS

Many people contributed to the TRAC-PF1 code development and to this report. Because it was a team effort, there was considerable overlap in responsibilities and contributions. The participants are listed according to their primary activity. Those with the prime responsibility for each area are listed first.

PRINCIPAL INVESTIGATORS:	Dennis R. Liles and John H. Mahaffy
FLUID DYNAMICS:	John H. Mahaffy, Dennis R. Liles, Susan B. Woodruff, and Manjit S. Sahota
HEAT TRANSFER:	Frank L. Addressio and David A. Mandell
CODE DEVELOPMENT AND PROGRAMMING:	Ronald P. Harper, Paul T. Giguere Jennie R. Netuschil, and Terry F. Bott
TRIPS AND CONTROLS:	Robert G. Steinke
GRAPHICS:	Michael R. Turner
SAMPLE PROBLEM:	Manjit S. Sahota and Paul T. Giguere
REPORT COMPILATION:	John H. Mahaffy, Dennis R. Liles, and Vera B. Metzger
REPORT EDITING:	Nancy N. Sheheen
REPORT TYPING:	Nancy Warnes

In addition to those listed above, acknowledgment is made of all others who contributed to earlier versions of TRAC. In particular, Richard Pryor and James Sicilian's major contributions to the code architecture still are used in the code. We also acknowledge useful discussions and technical exchanges from: Louis Shotkin, Novak Zuber, and Stan Fabric, US Nuclear Regulatory Commission; Tony Hirt, Dan Butler, Frank Harlow, William Rivard, and Burton Wendroff, Los Alamos National Laboratory; John Meyer and Peter Griffith, Massachusetts Institute of Technology; George Bankoff, Northwestern University; and Garrett Birkhoff, Harvard University. Thanks also are due to all Los Alamos users who supplied comments and corrections to this document, particularly Charles Watson, Gordon Willcutt, and James Lime.

REFERENCES

1. G. Kocomustafaogullari, "Thermo-Fluid Dynamics of Separated Two-Phase Flow," Ph.D. Thesis, School of Mechanical Engineering, Georgia Institute of Technology, Atlanta, Georgia (December 1971).
2. M. Ishii, Thermo-Fluid Dynamic Theory of Two-Phase Flow, Collection de la Direction des Etudes et Recherches D'Electricite de France, Eyrolles, Paris (1975).
3. F. H. Harlow and A. A. Amsdem, "A Numerical Fluid Dynamics Calculation Method for All Flow Speeds," *J. Comp. Phys.* 8, 197 (1971).
4. F. H. Harlow and A. R. Amsdem, "KACHINA: An Eulerian Computer Program for Multifield Fluid Flows," Los Alamos Scientific Laboratory report LA-5680 (1975).
5. D. R. Liles and W. H. Reed, "A Semi-Implicit Method for Two-Phase Fluid Dynamics," *J. of Comp. Physics* 26, No. 3, 390-407 (1978).
6. J. H. Mahaffy, "A Stability-Enhancing Two-Step Method for One-Dimensional Two-Phase Flow," Los Alamos Scientific Laboratory report LA-7951-MS (1979).
7. J. H. Mahaffy, "A Stability-Enhancing Two-Step Method for Fluid Flow Calculations," submitted to *J. Comp. Phys.* [Los Alamos National Laboratory report LA-UR-81-1398 (October 1981)].
8. J. G. Collier, Convective Boiling and Condensation (McGraw-Hill Book Company, New York, New York, 1972).
9. W. M. Rohsenow and H. Y. Choi, Heat, Mass, and Momentum Transfer (Prentice-Hall Inc., Englewood Cliffs, New Jersey, 1961).
10. C. W. Hirt and N. C. Romero, "Application of a Drift-Flux Model To Flashing In Straight Pipes," Los Alamos Scientific Laboratory report LA-6005-MS (1975).
11. G. W. Govier and A. Aziz, The Flow of Complex Mixtures in Pipes (Van Nostrand-Rheinhold Co., New York, New York, 1972).
12. B. S. Massey, Mechanics of Fluids (D. Van Nostrand Co., New York, New York, 1968).
13. V. L. Streeter, Fluid Mechanics (McGraw-Hill Book Company, New York, New York, 1966).
14. "Flow of Fluids," Crane Company technical paper 409 (May 1942).
15. S. Lekach, "Development of a Computer Code for Thermal Hydraulics of Reactors (THOR)," Brookhaven National Laboratory Quarterly Progress report BNL-19978 (1975).

16. C. J. Crowley, J. A. Block, and C. N. Cary, "Downcomer Effects in a 1/15-Scale PWR Geometry: Experimental Data Report," Creare, Inc. report NUREG-0281 (May 1977).
17. W. C. Rivard and M. D. Torrey, "Numerical Calculation of Flashing from Long Pipes Using a Two-Field Model," Los Alamos Scientific Laboratory report LA-6104-MS (1975).
18. K. Lee and D. J. Ryley, "The Evaporation of Water Droplets in Superheated Steam," ASME paper 68-HT-11 (1968).
19. A. E. Dukler, "Two Phase Interactions in Countercurrent Flow," U. of Houston, Department of Chemical Engineering annual report Nov. 1978-Oct. 1979 (January 1980).
20. V. G. Levich, Physicochemical Hydrodynamics (Prentice-Hall Inc., New York, New York, 1962), pp. 430-432.
21. V. P. Isachenko, "Heat Transfer in Condensation in Turbulent Jets," *Teploenergetika* No. 2, 7-10 (1976).
22. Y. Taitel and A. E. Dukler, "A Model for Predicting Flow Regime Transitions in Horizontal and Near Horizontal Gas-Liquid Flow," *AIChE Journal* 22, No. 1, 47-55 (1976).
23. P. J. Roache, Computational Fluid Dynamics, (Hermosa Publishers, Albuquerque, New Mexico, 1972).
24. G. Yadigaroglu, "The Reflooding Phase of the LOCA in PWRs. Part I: Core Heat Transfer and Fluid Flow," *Nuclear Safety* 19, 1 (1978).
25. "Reactor Safety Research Program, Quarterly Report for the Period July 1--September 30, 1978," Battelle Pacific Northwest Laboratories report PNL-2653-3, NUREG/CR-0546 (1978).
26. L. S. Tong and J. Weisman, Thermal Analysis of Pressurized Water Reactors, Second Edition (American Nuclear Society, LaGrange Park, Illinois, 1979).
27. P. E. MacDonald and J. Weisman, "Effect of Pellet Cracking on Light Water Reactor Fuel Temperatures," *Nucl. Tech.* 31, 357-366 (1976).
28. B. A. Boley and J. H. Weiner, Theory of Thermal Stresses (John Wiley and Sons, Inc., New York, New York, 1960).
29. J. V. Cathcart, "Quarterly Progress Report on the Zirconium Metal-Water Oxidation Kinetics Program," Oak Ridge National Laboratory report ORNL/NUREG/TM-41 (August 1976).
30. "MATPRO--Version 11: A Handbook of Materials Properties for Use in the Analysis of Light Water Reactor Fuel Rod Behavior," Idaho National Engineering Laboratory report NUREG/CR-0497, TREE-1280 (February 1979).

31. J. C. Chen, "A Correlation for Boiling Heat Transfer of Saturated Fluids in Convective Flow," ASME paper 63-HT-34 (1963).
32. J. P. Holman, Heat Transfer, Third Edition (McGraw-Hill Book Company, New York, New York, 1972).
33. T. A. Bjornard and P. Griffith, "PWR Blowdown Heat Transfer," in Thermal and Hydraulic Aspects of Nuclear Reactor Safety, Vol. 1 (American Society of Mechanical Engineers, New York, New York, 1977), pp. 17-41.
34. R. P. Forslund and W. M. Rohsenow, "Dispersed Flow Film Boiling," J. Heat Trans. 90, 399-407 (November 1968).
35. L. A. Bromley, "Heat Transfer in Stable Film Boiling," Chem. Eng. Prog. 46, 221-227 (May 1950).
36. S. S. Kutateladze, "Heat Transfer During Film Boiling," in Heat Transfer in Condensation and Boiling, Atomic Energy Commission report AEC-TR-3770 (1952).
37. W. H. McAdams, Heat Transmission, Third Edition (McGraw-Hill Book Company, New York, New York, 1954).
38. R. S. Dougall and W. M. Rohsenow, "Film Boiling on the Inside of Vertical Tubes with Upward Flow of the Fluid at Low Qualities," Massachusetts Institute of Technology Mechanical Engineering report 9079-26 (1963).
39. L. Biasi, G. C. Clerici, S. Garribba, R. Sala, and A. Tozzi, "Studies on Burnout: Part 3," Energia Nucleare 14, 530-536 (1967).
40. F. B. Hildebrand, Introduction to Numerical Analysis (McGraw-Hill Book Company, New York, New York, 1974).
41. R. E. Henry, "A Correlation for the Minimum Film Boiling Temperature," AIChE Symposium Series 138, 81-90 (1974).
42. "RELAP4/MOD5: A Computer Program for Transient Thermal-Hydraulic Analysis of Nuclear Reactors and Related Systems," Vol. 1, Idaho National Engineering Laboratory report ANCR-NUREG-1335 (September 1976).
43. "RETRAN--A Program for One-Dimensional Transient Thermal-Hydraulic Analyses of Complex Fluid Flow Systems," Electric Power Research Institute report EPRI-NP-408 (January 1977).
44. S. Gill, "A Process for the Step-by-Step Integration of Differential Equations in an Automatic Digital Computing Machine," Proc. Cambridge Philos. Soc. 47, 96-108 (1951).
45. Robert J. Thompson, "Improving Roundoff in Runge-Kutta Computations with Gill's Method," Communication of the ACM 13, No. 12 (December 1970).

46. D. A. Sharp, "The PWR Steady-State Capability of WRAP--A Water Reactor Analysis Package," Savannah River Laboratory report DPST-NUREG-77-3 (June 1977).
47. V. L. Streeter and E. B. Wylie, Hydraulic Transients (McGraw-Hill Book Company, New York, New York, 1967), pp. 151-160.
48. D. J. Olson, "Experiment Data Report for Single- and Two-Phase Steady-State Tests of the 1-1/2-Loop MOD-1 Semiscale System Pump," Aerojet Nuclear Company report ANCR-1150 (May 1974).
49. G. G. Loomis, "Intact Loop Pump Performance During the Semiscale MOD-1 Isothermal Test Series," Aerojet Nuclear Company report ANCR-1240 (October 1975).
50. D. J. Olson, "Single- and Two-Phase Performance Characteristics of the MOD-1 Semiscale Pump Under Steady-State and Transient Fluid Conditions," Aerojet Nuclear Company report ANCR-1165 (October 1974).
51. Douglas L. Reeder, "LOFT System and Test Description (5.5-Ft. Nuclear Core 1 LOCES)," EG&G Idaho, Inc. report TREE-1208, NUREG/CR-0247 (July 1978), pp. 161-166.
52. W. A. Coffman and L. L. Lynn, "WATER: A Large Range Thermodynamic and Transport Water Property FORTRAN-IV Computer Program," Bettis Atomic Power Laboratory report WAPD-TM-568 (December 1966).
53. D. L. Hagrman, G. A. Reymann, and R. E. Mason, "MATPRO-Version 11 (Revision 1): A Handbook of Material Properties for Use in the Analysis of Light Water Reactor Fuel Rod Behavior," EG&G Idaho, Inc., NUREG/CR-0497, TREE-1280, Rev. 1 (February 1980).
54. "MATPRO-Version 09: A Handbook of Materials Properties for Use in the Analysis of Light Water Reactor Fuel Rod Behavior," Idaho National Engineering Laboratory report TREE-NUREG-1005 (December 1976).
55. Y. S. Touloukian, Editor, Thermophysical Properties of High Temperature Solid Materials (MacMillan Co., New York, 1967).
56. "A Prediction of the SEMISCALE Blowdown Heat Transfer Test S-02-8 (NRC Standard Problem Five)," Electric Power Research Institute report EPRI-NP-212 (October 1976).
57. W. L. Kirchner, "Reflood Heat Transfer In A Light Water Reactor," US Nuclear Regulatory Commission report NUREG-0106, Vols. I and II (August 1976).
58. J. C. Spanner, Editor, "Nuclear Systems Materials Handbook - Vol. 1 Design Data," Hanford Engineering Development Laboratory report TID-26666 (1976).
59. "Properties for LMFBR Safety Analysis," Argonne National Laboratory report ANL-CEN-RSD-76-1 (1976).

60. V. H. Ransom and J. A. Trapp, "The RELAP5 Choked Flow Model and Application to a Large Scale Flow Test," Proceedings of the ANS/ASME/NRC International Topical Meeting on Nuclear Reactor Thermal-Hydraulics, Saratoga Springs, New York, October 5-8, 1980, pp. 799-819.
61. "RELAP5/MOD1 Code Manual, Volume 1: System Models and Numerical Methods," Idaho National Engineering Laboratory report NUREG/CR-1826, EGG-2070 DRAFT, Revision 1 (March 1981).
62. L. L. Weidert and L. B. Clegg, "Experiment Data Report for Semiscale Mod-3 Small Break Test Series (Tests S-SB-P1, S-SB-P2, and S-SB-P7)," Idaho National Engineering Laboratory report NUREG/CR-1640, EGG-2053 (September 1980).
63. "System Design Description for the Mod-3 Semiscale System," Idaho National Engineering Laboratory report, original issue (July 1978), revision A (June 1979).
64. T. K. Larson, J. L. Anderson, and D. J. Shimeck, "Scaling Criteria and an Assessment of Semiscale Mod-3 Scaling for Small Break Loss-of-Coolant Transients," Idaho National Engineering Laboratory report EGG-SEMI-5121 (March 12, 1980).
65. D. J. Olson, "Transmittal of Semiscale Mod-3 Documents" (DJC-129-78), Idaho National Engineering Laboratory letter to R. E. Tiller (October 5, 1978).
66. G. W. Johnsen, "Transmittal of Semiscale EOS Appendix for Small Break Tests S-SB-P1 and S-SB-P2" (GWJ-8-80), Idaho National Engineering Laboratory letter to R. E. Tiller (February 13, 1980).
67. L. P. Leach, "Experimental Operating Specification for Semiscale Small Break Test S-SB-P7" (LPL-33-80), Idaho National Engineering Laboratory letter to R. E. Tiller (March 13, 1980).
68. S. E. Dingman, T. J. Fauble, and J. R. Hewitt, "Quick Look Report for Semiscale Mod-3 Small Break Tests S-SB-P1, S-SB-P2, and S-SB-P7," Idaho National Engineering Laboratory report EGG-SEMI-5137 (April 1980).
69. "TRAC-PD2, An Advanced Best-Estimate Computer Program for Pressurized Water Reactor Loss-of-Coolant Accident Analysis," Los Alamos National Laboratory report LA-8709-MS, NUREG/CR-2054 (April 1981).

DISTRIBUTION

	<u>Copies</u>
Nuclear Regulatory Commission, R4, Bethesda, Maryland	298
Technical Information Center, Oak Ridge, Tennessee	2
Los Alamos National Laboratory, Los Alamos, New Mexico	<u>50</u>
	350

BIBLIOGRAPHIC DATA SHEET

NUREG/CR-3567
LA-9944-MS

3. TITLE AND SUBTITLE

2. LEAVE BLANK

4. RECIPIENT'S ACCESSION NUMBER

TRAC-PF1: An Advanced Best-Estimate Computer Program
for Pressurized Water Reactor Analysis

5. DATE REPORT COMPLETED

MONTH

YEAR

November

1983

6. AUTHOR(S)

Safety Code Development Group
Energy Division

7. DATE REPORT ISSUED

MONTH

YEAR

February

1984

8. PERFORMING ORGANIZATION NAME AND MAILING ADDRESS (Include Zip Code)

Los Alamos National Laboratory
Los Alamos, New Mexico 87545

9. PROJECT TASK/WORK UNIT NUMBER

10. FIN NUMBER

A7016

11. SPONSORING ORGANIZATION NAME AND MAILING ADDRESS (Include Zip Code)

Division of Accident Evaluation
Office of Nuclear Regulatory Research
U.S. Nuclear Regulatory Commission
Washington, DC 20555

12a. TYPE OF REPORT

Informal

12b. PERIOD COVERED (Inclusive dates)

13. SUPPLEMENTARY NOTES

14. ABSTRACT (200 words or less)

The Transient Reactor Analysis Code (TRAC) is being developed at the Los Alamos National Laboratory to provide advanced best-estimate predictions of postulated accidents in light water reactors. The TRAC-PF1 program provides this capability for pressurized water reactors and for many thermal-hydraulic experimental facilities. The code features either a one-dimensional or a three-dimensional treatment of the pressure vessel and its associated internals; a two-phase, two-fluid nonequilibrium hydrodynamics model with a noncondensable gas field; flow-regime-dependent constitutive equation treatment; optional reflood tracking capability for both bottom flood and falling-film quench fronts; and consistent treatment of entire accident sequences including the generation of consistent initial conditions. A new numerical algorithm is used in the one-dimensional hydrodynamics that permits this portion of the fluid dynamics to violate the material Courant condition. This technique permits large time steps and, hence, reduced running time for slow transients.

This report describes the thermal-hydraulic models and the numerical solution methods used in the code. Detailed programming and user information also are provided. A second Los Alamos report, "TRAC-PF1 Developmental Assessment," presents the results of the developmental assessment calculations.

15a. KEY WORDS AND DOCUMENT ANALYSIS

15b. DESCRIPTORS

16. AVAILABILITY STATEMENT

Unlimited

17. SECURITY CLASSIFICATION
(This report)

Unclassified

18. NUMBER OF PAGES

19. SECURITY CLASSIFICATION
(This page)

Unclassified

20. PRICE

\$

Los Alamos

Available from
GPO Sales Program
Division of Technical Information and Document Control
US Nuclear Regulatory Commission
Washington, DC 20555

and
National Technical Information Service
Springfield, VA 22161